

الجمهورية الجزائرية الديمقراطية الشعبية

People's Democratic Republic of Algeria

وزارة التعليم العالي والبحث العلمي

Ministry of Higher Education and Scientific Research

جامعة أبي بكر بلقايد - تلمسان

Abou Bekr Belkaïd University - Tlemcen -

Faculty of TECHNOLOGY

Departement of HYDRAULIC



zef

Zentrum für
Entwicklungsforschung
Universität Bonn

THESIS

Accredited by the MESRS

Supported by the WESA program

Laboratory 25 «Promotion of Water, Mining and Soil Resources, Environmental Legislation and Technological Choices» (Tlemcen),

Center for Development Research ZEF (Bonn, Germany)

University of Bonn, Germany

Presented for obtaining the **Degree** of **DOCTOR of Sciences**

In: **HYDRAULIC**

Specialty: **Water Resources Management**

By:

BOUGARA Hanane

Hydrological modeling in Tafna Basin (North-west Algeria)

Publicly defended, the 23 / 06 / 2022 , in front of the jury composed of:

Mrs. ABDELBAKI Cherifa	M.C.A.	Univ. Tlemcen, Algeria	President
Mrs. BABA HAMED Kamila	Professor	Univ. Tlemcen, Algeria	Supervisor of thesis
Mr. BORGEMEISTER Christian	Professor	ZEF. Bonn, Germany	Co-Supervisor of thesis
Mrs. MEBROUK Naima	Professor	Univ 2. Oran	Examiner
Mr. MEGNOUNIF Abdesselam	Professor	Univ. Tlemcen	Examiner
Mr. TISCHBEIN Bernhard	Doctor	ZEF. Bonn, Germany	Invited member 1
Mr. KUMAR Navneet	Doctor	ZEF. Bonn, Germany	Invited member 2

2021-2022

Acknowledgements

I am very grateful to Allah who gave me the time and opportunity to pursue PhD research.

I consider myself extremely fortunate to have had this opportunity and I am indebted to offer my sincerest gratitude and respect to my supervisors who guided me along the path of my PhD research. My special thanks go to Professor ***Kamila Baba Hamed*** from the University of Tlemcen (Algeria) and to Professor ***Christian Borgemeister***, Director of the research center in Bonn (Germany). They were able to give me the benefit of their knowledge and experience while granting me a certain freedom of development. I value the constructive comments they provided to improve the quality of my papers and my thesis.

I will also not forget Doctor ***Bernhard Tischbein***, and Doctor ***Navneet Kumar***, who supported me a lot during my thesis and for their patience during my stay in Bonn (ZEF).

I would like to express here my gratitude to the members of the jury, for having done me the honor to evaluate my work. My thanks go to Doctor ***Cherifa Abdelbaki***, from the University of Tlemcen, who accepted to preside over the jury and to the examiners Professor ***Naima Mebrouk*** from University of Oran and Professor ***Abdesselam Megnounif*** from University of Tlemcen, who were kind enough to judge this work and to enrich my thesis with their instructive remarks.

I convey my thanks to the Pan African University Institute of Water and Energy Sciences (PAUWES) for planning continuous meetings and colloquiums that contributed to the progress of PhD research. I also thank the Center for Development Research (ZEF) for providing the disciplinary courses and for sponsoring my PhD research as well as the University of Tlemcen. The National Agency of Hydraulic Resources (ANRH) of Algeria is thanked for providing data used in this research.

I would like to express my gratitude to all the faculty and staff members of the Department of Hydraulics, Faculty of Technology, Tlemcen for their continuous support and moral inspiration.

I will probably not forget to thank and extend my gratitude to Professor ***Mustapha Bensalah***, the Director of the Research Laboratory in Tlemcen, who facilitated my access to the laboratory and offered me the best working conditions for where I met my supervisor and my colleagues.

My sincere thanks also go to the German Federal Ministry of Education and Research (BMBF), in the frame of Water and Energy Security in Africa (WESA) Project, for funding this research project.

I wish to express my sincere thanks to Professor ***Abderrazak Bouanani*** for the valuable suggestions and instructions in my work.

I am also thankful to my friends, of the hydraulic Department and WESA project for their helping hands during the project. I would like to thank all the doctoral students for having maintained a friendly and studious atmosphere in the laboratory 25.

Last but not the least; I am especially indebted to my parents, my sisters for their unwavering support, love, and invariable source of motivation. Finally, thank you to everyone who helped me complete my thesis work.

Abstract

The use in this thesis of hydrological models provides a correct estimate of the amount of water. The statistical tests and the drought indices are applied as the drought monitoring tools allowing it to be described quantitatively. This approach could facilitate decision-making by managers and help them to develop strategies for better management of water resources. The new insights of this research for the five Tafna sub basins located in northwestern of Algeria is the analysis of the hydrological response (runoff) following climate variability (temporal change) and in different sub basins (spatial change). The objectives of this work are:

- Selection of the type of climate (wet, dry) in different time series (Annual, seasonal, and monthly) based on statistical analyses aiming at the detection of breakpoint and trends (magnitude and their directions), and evaluation of drought of hydrological variables.
- Simulate the hydrological behavior of the study area (sub basins) based on the lumped models under different climate (wet and dry) conditions.
- Compare the results of the hydrological response of the models in different climates and different sub basins.

Synthetic results of the homogeneity test for the variability hydro-climatic mostly indicate the year break of 2007, and the increase at the end of the rainfall time series. In addition evaluation of drought indices (meteorological and hydrological drought) concluded that the wet periods are in the early of 2000, and the dry periods were between 1990 to 1999. The period between 1990 to 2005 was determined to assess the model performance. The results of application of the two lumped models (GR4J, HBV light), showed that the two models give a good performance for the two calibration periods, and a degradation of the performance in the validation phase relative to the HBV light compared to the GR4J. These differences in the hydrological model response provide insight into factors affecting hydrological processes, furthermore the effect of the hydrological model structure and parameter sets. It is likely that the reason for not seeing a considerable variation despite the different climate conditions of the sub basins is that the hydrological response (runoff) is mostly influenced by the flux from groundwater storage or by infiltration into the groundwater network due to the geology of the region (karstic), leading to be inconsistent with a variation of rainfall time series which represents the wet and dry climate. These models can be a useful tool for predictions of water availability under different climatic conditions for further water management studies in the study area and in other areas with similar conditions.

Keywords: Hydro-climatic variability, Trend analysis, drought index, GR4J, HBV light, hydrological modeling.

Résumé

L'utilisation dans cette thèse de modèles hydrologiques fournit une estimation correcte de la quantité d'eau. Les tests statistiques et les indices de sécheresse sont appliqués comme outils de suivi de la sécheresse permettant de la décrire de manière quantitative. Cette approche pourrait faciliter la prise de décision des gestionnaires et les aider à développer des stratégies pour une meilleure gestion des ressources en eau. La nouvelle perspective de cette recherche pour les cinq sous-bassins de la Tafna situés au Nord ouest algérien réside dans l'analyse de la réponse hydrologique (Débit) suite à la variabilité du climat (changement temporel) et dans différents sous-bassins (changement spatial). Les objectifs de ce travail sont:

- Sélection du type de climat (humide, sec) dans différentes séries chronologiques (annuelles, saisonnières et mensuelles) sur la base d'analyses statistiques visant la détection des points de rupture et des tendances (ampleur et leurs directions) ainsi que l'évaluation de la sécheresse des variables hydrologiques.
- Simuler le comportement hydrologique de la zone d'étude (sous-bassins) à partir des modèles globaux sous différentes conditions climatiques (humides et sèches).
- Comparer les résultats de la réponse hydrologique des modèles dans différents climats et différents sous-bassins.

Les résultats synthétiques du test d'homogénéité de la variabilité hydro-climatique indiquent majoritairement la rupture de l'année 2007, et l'augmentation à la fin de la série chronologique des précipitations. De plus, l'évaluation des indices de sécheresse (sécheresse météorologique et hydrologique) a conclu que les périodes humides se situaient au début de 2000 et que les périodes sèches se situaient entre 1990 et 1999. La période entre 1990 et 2005 a été déterminée pour évaluer les performances du modèle. Les résultats d'application des deux modèles globaux (GR4J, HBV light), ont montré que les deux modèles donnent de bonnes performances pour les deux périodes d'étalonnage, et une dégradation de la performance en phase de validation relative au modèle HBV light par rapport au GR4J. Ces différences dans la réponse du modèle hydrologique donnent un aperçu des facteurs affectant les processus hydrologiques, en plus de l'effet de la structure du modèle hydrologique et des ensembles de paramètres. Il est probable que la raison de ne pas voir une variation considérable malgré les différentes conditions climatiques des sous bassins est que la réponse hydrologique (Débit) est principalement influencée par le flux provenant du stockage des eaux souterraines ou par l'infiltration dans le réseau d'eaux souterraines en raison de la géologie de la région (karstique), ce qui conduit à être incompatible avec une variation de la série chronologique des précipitations qui représente des séquences humides et sèches. Ces modèles peuvent être un outil utile pour prédire la disponibilité de l'eau dans différentes conditions climatiques pour d'autres études de gestion de l'eau dans la zone d'étude et dans d'autres zones présentant des conditions similaires.

Mots clés: variabilité hydro-climatique, analyse des tendances, indice de sécheresse, GR4J, HBV light, modélisation hydrologique.

ملخص

يوفر استخدام النماذج الهيدرولوجية في هذه الأطروحة تقديرا صحيحا لكمية المياه. يتم تطبيق الاختبارات الإحصائية ومؤشرات الجفاف كأدوات لرصد الجفاف مما يتيح وصفه كميا. هذا النهج يمكن أن يسهل إتخاذ القرار من قبل المديرين ومساعدتهم على تطوير استراتيجيات لإدارة أفضل للموارد المائية. الرؤى الجديدة لهذا البحث لأحواض التافنة الفرعية الخمسة الواقعة في شمال غرب الجزائر هي تحليلات الإستجابة الهيدرولوجية (الجريان السطحي) بعد التقلبات المناخية (التغير الزمني) وفي الأحواض الفرعية المختلفة (التغير المكاني). أهداف هذا العمل هي:

- إختيار نوع المناخ (الرطب و الجاف) في سلاسل زمنية مختلفة (سنوي، موسمي، شهري) بناء على التحليلات الإحصائية التي تهدف إلى الكشف عن نقاط الانقطاع والاتجاهات (الحجم و اتجاهاتهم) ، وتقييم الجفاف من المتغيرات الهيدرولوجية.

- محاكاة السلوك الهيدرولوجي لمنطقة الدراسة (الأحواض الفرعية) بناء على النماذج المجمع تحت ظروف مناخية مختلفة (رطبة وجافة).

- قارن نتائج الإستجابة الهيدرولوجية للنماذج في مناخات مختلفة وأحواض فرعية مختلفة.

تشير النتائج التركيبية لإختبار التجانس للتغير المناخي المائي في الغالب إلى الإنقطاع في العام 2007، و الزيادة في نهاية السلسلة الزمنية لهطول الامطار. با لإضافة إلى ذلك، خلص تقييم مؤشرات الجفاف (الجفاف الجوي و الهيدرولوجي) إلى أن الفترات الرطبة كانت في أوائل عام 2000، وأن فترات الجفاف كانت بين عامي 1990 و 1999. وقد تم تحديد الفترة بين 1990 و 2005 لتقييم أداء النموذج. أظهرت نتائج تطبيق النموذجين المجمعين (GR4J, HBV light) أن النموذجين يقدمان أداء جيدا لفترتي المعايرة، وتدهورا في الأداء في مرحلة التحقق بالنسبة إلى HBV light مقارنة ب GR4J.

توفر هذه الإختلافات في إستجابة النموذج الهيدرولوجي نظرة ثاقبة للعوامل التي تؤثر على العمليات الهيدرولوجية، علاوة على تأثير بنية النموذج الهيدرولوجي ومجموعات المعلمات. من المحتمل أن سبب عدم رؤية إختلاف كبير على الرغم من الظروف المناخية المختلفة للأحواض الفرعية هو أن الإستجابة الهيدرولوجية (الجريان السطحي) تتأثر في الغالب بالتدفق من تخزين المياه الجوفية أو بالتسلل إلى الشبكة المياه الجوفية بسبب جيولوجيا المنطقة (الكارستية) ، مما يؤدي إلى عدم الإتساق مع تباين في السلاسل الزمنية لسقوط الأمطار و التي تمثل المناخ الرطب و الجاف. يمكن أن تكون هذه النماذج أداة مفيدة للتنبؤ بتوافر المياه في ظل ظروف مناخية مختلفة لمزيد من دراسات إدارة المياه في المنطقة الدراسة وفي مناطق أخرى ذات ظروف مماثلة.

الكلمات المفتاحية : التقلبات الهيدرولوجية، تحليل الاتجاهات، مؤشر الجفاف ، GR4J ، HBV light، النمذجة الهيدرولوجية.

TABLE OF CONTENTS

Acknowledgements

Abstract

Résumé

ملخص

Abbreviations List

List of Figures

List of Tables

GENERAL INTRODUCTION	1
I.1. Introduction and Problem statement.....	2
I.2. State-of-the-art and scientific questions.....	5
I.3. Aims and Objectives of the research.....	5
I.4. Structure of the thesis.....	6
CHAPTER I GENERAL LITERATURE REVIEW	7
I.1. Introduction.....	8
I.2. Components of the hydrological cycle.....	9
I.2.1.Precipitation.....	9
I.2.2. Factors influencing precipitation.....	9
I.2.3.Evapotranspiration.....	10
I.2.4.Factors influencing evapotranspiration.....	10
I.2.5. Infiltration and percolation.....	10
I.2.6.Runoff.....	10
I.2.7.Factors affecting runoff.....	11
I.3.Scales for study of hydrologic cycle.....	11
I.4. Hydrological modeling.....	12
I.4.1. Choosing a model.....	14
I.4.2. Model calibration methods.....	14
I.5. Classification of hydrological models.....	15

I.6. Rainfall-runoff modeling.....	18
I.6.1. The purpose of a rain - runoff model.....	19
I.7. Uncertainties in hydrology.....	19
I.7.1. Typology of uncertainties in hydrological modeling.....	20
I.7.2. Objectives of the uncertainty analysis.....	20
I.7.3. Uncertainty analysis techniques.....	20
I.7.3.1. A local approach to uncertainty analysis.....	20
I.7.3.2. Global approach.....	21
I.7.4. Modeling evaluation criteria.....	21
I.7.4.1. Nash-Sutcliffe criterion.....	21
I.7.4.2. Coefficient of determination r^2	21
I.7.4.3. Root-mean-square error (RMSE).....	22
I.7.4.4. Mean absolute error (MAE).....	22
I.7.4.5. Bilan.....	22
I.8. The rainfall-runoff models selected.....	22
I.8.1. GR4J: A daily four-parameter rainfall-runoff model.....	23
I.8.1.1. Introduction.....	23
I.8.1.2. Model parameters.....	24
I.8.1.3. Mathematical Description.....	25
I.8.1.4. Calibration and validation.....	28
I.8.2. The HBV light model.....	28
I.8.2.1. Introduction.....	28
I.8.2.2. Mathematical Description.....	29
I.8.2.3. Parameters of the HBV light model.....	33
I.8.2.4. Calibration and validation.....	34
CHAPTER II PRESENTATION OF THE STUDY AREA.....	35
II.1. Introduction.....	36
II.2. Presentation of the study area.....	36
II.2.1. Tafna basin.....	36

II.2.2. Geomorphologic context.....	37
II.2.2.1. Mountainous areas.....	38
II.2.2.2. The plains and plateaus areas.....	38
II.2.3. Geology.....	39
II.2.4. Hydrographic network.....	42
II.2.5. Altitude, dams, and Hydro- climate stations.....	42
II.2.6. Presentation of studied sub basin of the Tafna basin.....	43
II.2.6.1. Geographic situation.....	43
II.2.6.1.1. Upstream Sebdou sub basin.....	43
II.2.6.1.2. Khemis sub basin.....	44
II.2.6.1.3. Wadi Boumessaoud sub basin.....	44
II.2.6.1.4. Chouly sub basin.....	44
II.2.6.1.5. Isser sub basin.....	44
II.2.6.2. Geology preview.....	45
II.2.6.2.1. Upstream Sebdou.....	45
II.2.6.2.2. Khemis.....	45
II.2.6.2.3. Wadi Boumessaoud.....	45
II.2.6.2.4. Chouly.....	46
II.2.6.2.5. Isser.....	46
II.2.6.3. Potential Aquifer	46
II.2.6.4. Morphometry.....	47
II.2.6.4.1. Shape characteristics.....	48
II.2.6.4.1.1. Gravelius compactness index (Kc).....	48
II.2.6.4.1.2. Equivalent rectangle	48
II.2.6.5. Relief.....	50
II.2.6.5.1. Distribution and hypsometric curve.....	50
II.2.6.5.2. Characteristic altitudes.....	53
II.2.6.5.3. Slope indices.....	55
II.2.6.5.4. Hydrographic network	59

II.2.6.5.4.1. Network Hierarchisation.....	59
II.2.6.5.4.2. Long profile.....	62
II.2.6.5.4.3. Average slope of the main thalweg.....	64
II.2.6.5.4.4. Hydrographic Network features.....	66
II.2.7. Land Use.....	71
II.3. Conclusion.....	73
CHAPTER III VARIABILITY AND TREND ANALYSIS OF HYDRO-CLIMATIC VARIABLES.....	75
III.1. Introduction.....	76
III.2. Station presentations.....	77
III.3. Preliminary analysis of rainfall.....	79
III.3.1. Missing data details of rainfall stations.....	79
III.3.2. Annual rainfall analysis.....	81
III.3.3. Monthly rainfall analysis.....	84
III.3.4. Seasonal rainfall analysis.....	87
III.3.5. Daily rainfall analysis.....	89
III.4. Preliminary analysis of runoff.....	91
III.4.1. Annual depth of runoff analysis.....	91
III.4.2. Monthly depth of runoff analysis.....	93
III.4.3. Seasonal depth of runoff analysis.....	95
III.4.4. Daily depth of runoff analysis.....	96
III.5. Preliminary analysis of temperature.....	98
III.5.1. Annual temperature analysis.....	98
III.5.2. Monthly temperature analysis.....	99
III.5.3. Seasonal temperature analysis.....	100
III.5.4. Daily temperature analysis.....	102
III.6. Preliminary analysis of evapotranspiration.....	102
III.6.1. Annual evapotranspiration analysis.....	103
III.6.2. Monthly evapotranspiration analysis.....	103
III.6.3. Seasonal evapotranspiration analysis.....	104

III.6.4. Daily evapotranspiration analysis.....	104
III.7. Water balance.....	105
III.8. Correlation.....	106
III.8.1. Pearson’s correlation.....	106
III.8.2. Spearman’s rho correlation.....	107
III.8.3. Annual correlation.....	107
III.8.4. Monthly correlation.....	107
III.8.5. Daily correlation.....	108
III.9. Statistical test for distribution.....	108
III.9.1. Chi-square Test.....	108
III.9.2. Statistical distribution for annual rainfall and runoff.....	109
III.10. Statistical test for Normality.....	110
III.10.1. Kolmogorov-Smirnov test.....	110
III.10.2. Shapiro-Wilk test.....	110
III.10.3. Normality test for annual rainfall.....	110
III.10.4. Normality test for annual runoff.....	112
III.11. Variability analysis of Hydro - climatic variables.....	113
III.11. 1. Tests for change point detection (homogeneity)	114
III.11.1. 1. Pettitt Test.....	115
III.11.1.2. Buishand Test.....	115
III.11.1.3. Hubert Test.....	116
III.11.1.4. Lee and Heghinian Test.....	116
III.11.2. Trend analysis.....	116
III.11.2.1. Mann-Kendall (MK) Trend Test.....	117
III.11.2.2. Sen’s slope estimator.....	117
III.11.3. Results and discussion of variability analysis.....	118
III.11.3.1. Results and discussion of change point detection (homogeneity)	118
III.11.3.2. Results and discussion of Trend analysis.....	132
III.12. Conclusion.....	152

CHAPTER IV COMPARISON DIFFERENT INDICES OF METEOROLOGICAL DROUGHT AND HYDROLOGICAL DROUGHT	154
IV. 1. Introduction.....	155
IV.2. Methodology.....	157
IV.2.1. Meteorological drought index.....	158
IV.2.1.1. Standardized Precipitation Index (SPI).....	158
IV.2.1.2. Percent of Normal Index (PN).....	159
IV.2.1.3. Decile index (DI).....	159
IV.2.1.4. Rainfall Anomaly Index (RAI)	159
IV.2.2. Hydrological drought index.....	160
IV.3. Results and discussion.....	161
IV.3.1. Comparison of meteorological drought categories.....	161
IV.3.2. Meteorological indices temporal evolution.....	163
IV.3.3. Relationship between SPI AND RAI,DI,PN.....	165
IV.3.4. Comparative evaluation of meteorological drought indices.....	167
IV.3.5. Correlations between drought indices.....	169
IV.3.6. Trend analysis of meteorological drought indices.....	171
IV.3.7. Comparison of hydrological drought categories.....	172
IV.3.8. Comparative evaluation of hydrological drought index.....	173
IV.3.9. Relationship of SDI between the study stations.....	177
IV.3.10. Relationship between hydrological drought (SDI) and meteorological drought (SPI, RAI, DI, PN).....	178
IV.3.11. Trend analysis of hydrological drought indices.....	181
IV.4. Conclusion.....	182
CHAPTER V COMPARISON OF THE PERFORMANCE OF TWO HYDROLOGICAL MODELS (GR4J, AND HBV LIGHT)	184
V.1. Introduction.....	185
V.2. The data used for the application of GR4J, and HBV light models.....	185
V.2.1. Input data.....	185
V.2.2. Output data.....	186
V.3. Modeling methodology	186

V.3.1. GR4J daily model.....	186
V.3.2. HBV light daily model.....	186
V.3.3. Validation period (GR4J, HBV light)	186
V.4. Application of GR and HBV light models.....	187
V.4.1. GR4J.....	187
V.4.1.1. Simulation for first period (Dry/Wet).....	187
V.4.1.2. Simulation for second period(Dry/Dry).....	193
V.4.2. HBV light.....	199
V.4.2.1. Simulation for first period (Dry/Wet).....	199
V.4.2.2. Simulation for second period(Dry/Dry).....	205
V.5. Comparison of models performance.....	212
V.6. Comparison between two validation period for GR4J	213
V.7. Comparison between parameters and performance of HBV light.....	214
V.8. Comparison the correlations between the simulated runoff of the GR, and HBV light models.....	215
V.8.1. Comparison the correlations between the simulated runoff of the GR, and HBV light models for calibration.....	215
V.8.2. Comparison the correlations between the simulated runoff of the GR, and HBV light models for validation.....	218
V.9. Estimating the exceedance probability and cumulative observed runoff compared with simulated runoff from GR4J, HBV light.....	220
V.9.1. Estimating the exceedance probability and cumulative observed runoff compared with simulated runoff from GR4J, HBV light for both the calibration periods.....	220
V.9.2. Estimating the exceedance probability and cumulative observed runoff compared with simulated runoff from GR4J, HBV light for both the validation periods.....	225
V.10. Conclusion.....	230
GENERAL CONCLUSIONS AND RECOMMENDATIONS.....	231
REFERENCES.....	236
APPENDICES.....	265

Abbreviations List

ABH Hydrographic basin agency of Oran

ANAT National Agency for Regional Planning of Algeria

ANRH National Agency of Hydraulic Resources

ArcGis Arc Geographic Information Systems

ASTER Advanced Spaceborne Thermal Emission and Reflection

CDF Cumulative distribution function

CEMAGREF National Center for Agricultural Machinery, Rural Engineering and Water and Forests

DEM Digital elevation model

ENSO El Nino Southern Oscillation

FAO Food and Agriculture Organisation

GR Rural Genie

HBV Hydrologiska Byråns Vattenbalansavdelning

HEC-HMS Hydrologic Modeling System

INSID National Institute for Irrigation and Drainage

IPCC Intergovernmental Panel on Climate Change

NAO North Atlantic oscillation

O.R.S.T.O.M Overseas Scientific and Technical Research Office

TOPMODEL Topography based hydrological model

SMHI Swedish Meteorological and Hydrological Institute

SST Sea Surface Temperature

WeMOI Western Mediterranean Oscillation Index

WMO World Meteorological Organization

List of Figures

Figure I.1. Water cycle Diagram.....	9
Figure I.2. A global schematic of the hydrologic cycle.....	12
Figure I.3. A schematic of the hydrologic cycle of the earth system.....	12
Figure I.4. Schematic representation of a hydrologic model application	14
Figure I.5. General classification of the Components of hydrological models	17
Figure I.6. Schematics of three different models, lumped, semi-lumped and semi-distributed.....	17
Figure I.7. Diagram of the structure model GR4J rainfall-runoff	24
Figure I.8. Illustration of the behavior of the production functions (E_s/E_n : solid line; P_s/P_n : dashed line) as a function of storage rate S/x_1 for different values of E_n/x_1 or P_n/x_1 (Perrin et al., 2003).....	26
Figure I.9. Example of the ordinates of UH1 and UH2 for parameter x_4 $\frac{1}{4}$ 3:8 days.....	27
Figure I.10. Illustration of the outflow Q_r from the routing reservoir as a function of the level in the store after the introduction of input Q_9	28
Figure I.11. Schematic structure of the HBV model.....	29
Figure I.12. Example of simulations with different values for CFMAX and TT.....	30
Figure I.13. Soil routine: Left: Reduction of potential evapotranspiration depending on soil moisture storage. Right: Contribution from rainfall to soil moisture storage and groundwater recharge. Response routine	30
Figure I.14. Response function	31
Figure I.15. Routing routine (Example of runoff transformation with MAXBAS=5).....	31
Figure II.1. Geographical location of the Tafna basin:(a) Large Northern basins in Algeria, (b) Tafna basin.....	37
Figure II.2. Geomorphologic context of the Tafna basin.....	39
Figure II.3. Geological context of the Tafna basin.....	40
Figure II.4. Hydrographic network of The Tafna basin.....	41
Figure II.5. DEM, and Dams, Hydro-Climate stations in the Tafna basin.....	42
Figure II.6. Geographic Situations of the study area sub basins.....	45

Figure II.7. Geologic map of the study sub basins of the Tafna	46
Figure II.8. Potential aquifers of the study area sub basins	47
Figure II.9. Hypsometric curves of the study sub basins.....	53
Figure II.10. Altimetric maps of the study sub basins.....	54
Figure II.11. Slope maps of the study sub basins of the Tafna basin.....	58
Figure II.12. The hydrographic network of the sub basins studied.....	60
Figure II.13. Long profile of the studied sub basins.....	64
Figure II.14. Representation of the number of thalwegs according to the ordre.....	67
Figure II.15. Line representative of the ratio of the lengths as a function of the order.....	69
Figure II.16. Land use map of the studied basins of the Tafna basin.....	72
Figure II.17. Traditional agriculture of Sebdou.....	73
Figure II.18. Traditional agriculture of Ouled Mimoun.....	73
Figure III.1. Location of climatic and hydrometric measurement stations on studied sub basins.....	79
Figure III.2. Overall summary of missing data.....	80
Figure III.3. Annual rainfall box plot. The upper and lower limit of the box indicate the 25th and 75th percentiles, respectively. The linear extensions mark the highest and lowest observed values.....	81
Figure III.4. Variability of average rainfall of the study stations.....	83
Figure III.5. Annual evolution of precipitation at study stations in the sub basins (1979/1980 - 2011/2012).....	84
Figure III.6. Variation of average monthly, minimum, maximum and average extremes rainfall (1979/1980-2011/2012).....	86
Figure III.7. Variation of monthly average rainfall of the study stations (1979/1980-2011/2012).	87
Figure III.8. Seasonal variations in rainfall of the studied stations in the Tafna basin.....	88
Figure III.9. Box plot of the seasonal rainfall for the study stations.....	89
Figure III.10. Variation of daily rainfall at the study stations (1979/1980 - 2011/2012).....	90
Figure III.11. Frequency of daily rainfall.....	91
Figure III.12. Variation of average annual runoff at the study station (1985/1986-2010/2011).....	92
Figure III.13. Annual depth of runoff (mm) for the study stations.....	93
Figure III.14. Box plots of average monthly depth of runoff of the study stations.	94

Figure III.15. Variation of monthly average depth of runoff of the study stations.....	95
Figure III.16. Seasonal depth of runoff for the study station.....	96
Figure III.17. Variation of seasonal average depth of runoff of the study runoff station.....	96
Figure III.18. Variation of daily depth of runoff of the study stations.....	97
Figure III.19. Range of daily runoff of the study stations.....	98
Figure III.20. Variation of average annual temperature of the study stations.....	99
Figure III.21. Box plots of monthly average temperature of the study stations.....	99
Figure III.22. Variation of monthly average temperature of the study stations.....	100
Figure III.23. Variation of seasonal average temperature at the study stations.....	100
Figure III.24. Seasonal evolution of average temperatures of Beni Bahdel station.....	101
Figure III.25. Seasonal evolution of average temperature of Zenata station.....	101
Figure III.26. Variation of daily average temperature of Beni Bahdel station.....	102
Figure III.27. Variation of daily average temperature of Zenata station.....	102
Figure III.28. Variation of annual average evapotranspiration of the study stations.....	103
Figure III.29. Variation of monthly average evapotranspiration of the study stations.....	104
Figure III.30. Variation of seasonal average evapotranspiration of the study stations.....	104
Figure III.31. Variation of daily average evapotranspiration of the study stations.	105
Figure III.32. Mean annual water balance (Rainfall, Depth of runoff, and evapotranspiration during the study period (1985/1986 - 2010/2011).....	106
Figure III.33. Q-Q plot for normality of annual rainfall to the log normal distribution.....	112
Figure III.34. Q-Q plot for normality of annual runoff to the log normal distribution.....	113
Figure III.35. Khronostat results of annual rainfall at Sebdou station: (a) Pettitt test; (b) Buishand test; (c) Lee and Heghinian test.....	120
Figure III.36. Khronostat results of annual rainfall at Khemis station: (a) Pettitt test; (b) Buishand test; (c) Lee and Heghinian test.....	120
Figure III.37. Khronostat results of annual rainfall at Djebel Chouachi station: (a) Pettitt test; (b) Buishand test; (c) Lee and Heghinian test.....	121
Figure III.38. Khronostat results of annual rainfall at Hennaya station: (a) Pettitt test; (b) Buishand test; (c) Lee and Heghinian test.....	122
Figure III.39. Khronostat results of annual rainfall at Chouly: (a) Pettitt test; (b) Buishand test; (c) Lee and Heghinian test.....	122

Figure III.40. Khronostat results of annual rainfall at Meurbah station: (a) Pettitt test; (b) Buishand test; (c) Lee and Heghinian test.....	123
Figure III.41. Khronostat results of annual rainfall at Ouled Mimoun station: (a) Pettitt test; (b) Buishand test; (c) Lee and Heghinian test.....	124
Figure III.42. Khronostat results of annual rainfall at Sidi Bounakhla station: (a) Pettitt test; (b) Buishand test; (c) Lee and Heghinian test.....	124
Figure III.43. Pettitt results of annual runoff at the stations: (a) Sebdou; (b) Zahra; (c) Zenata; (d) Chouly; (e) Sidi Aissa.....	127
Figure III.44. Khronostat results of annual temperature at Beni Bahdel station: (a) Pettitt test; (b) Buishand test; (c) Lee and Heghinian test.....	130
Figure III.45. Khronostat results of annual temperature at Zenata station: (a) Pettitt test; (b) Buishand test; (c) Lee and Heghinian test.....	131
Figure III.46. Annual time series and significant trend statistics of rainfall.....	133
Figure III.47. Seasonal time series and significant trend statistics of rainfall at Khemis.....	135
Figure III.48. Seasonal time series and significant trend statistics of rainfall at Djebel Chouachi station.....	136
Figure III.49. Seasonal time series and significant trend statistics of rainfall at Hennaya station.	136
Figure III.50. Seasonal time series and significant trend statistics of rainfall at Chouly station.....	137
Figure III.51. Seasonal time series and significant trend statistics of rainfall at Meurbah station.....	137
Figure III.52. Seasonal time series and significant trend statistics of rainfall at Ouled Mimoun station.....	138
Figure III.53. Seasonal time series and significant trend statistics of rainfall at Sidi Bounakhla station.....	138
Figure III.54. Seasonal time series and significant trend statistics of rainfall at Sebdou station.....	139
Figure III.55. Annual time series and significant trend statistics of runoff.	140
Figure III.56. Seasonal time series and significant trend statistics of runoff at Zahra station.....	142
Figure III.57. Seasonal time series and significant trend statistics of runoff at Zenata station.....	143
Figure III.58. Seasonal time series and significant trend statistics of runoff at Chouly station.....	144
Figure III.59. Seasonal time series and significant trend statistics of runoff at Sidi Aissa station.....	144
Figure III.60. Seasonal time series and significant trend statistics of runoff at Sebdou station.....	145
Figure III.61. Annual time series and significant trend statistics of temperature.....	146

Figure III.62. Seasonal time series and significant trend statistics of temperature at Beni Bahdel station.....	148
Figure III.63. Seasonal time series and significant trend statistics of temperature at Zenata station.....	149
Figure IV.1. Drought categories percentage for SPI, RAI, DI, PN for different time scale (annual, seasonal, monthly).....	163
Figure IV.2. SPI index at annual scale for all stations.....	164
Figure IV.3. RAI index at annual scale for all stations.....	164
Figure IV.4. DI index at annual scale for all stations.....	165
Figure IV.5. PN index at annual scale for all stations.....	165
Figure IV.6. The spider chart displays the timescale variations of Pearson correlation between SPI and other indices.....	167
Figure IV.7. The spider chart displays the timescale variations of Spearman's correlation between SPI and other indices.....	167
Figure IV.8. Average time series of all indices and Rainfall at annual scale.....	168
Figure IV.9. Average time series of all indices and rainfall at seasonal.....	169
Figure IV.10. Average time series of all indices and rainfall at monthly scale.....	169
Figure IV.11. Average Pearson correlations of all indices with a different time scale from all stations.....	171
Figure IV.12. Average Spearman's rho correlations of all indices with a different time scale from all stations.....	171
Figure IV.13. Drought categories percentage for SDI for different time scale (annual, seasonal,monthly).....	173
Figure IV.14.Evaluation of SDI on annual scale.....	174
Figure IV.15. Evaluation of SDI on monthly scale.....	175
Figure IV.16. Evaluation of SDI on autumn season.....	175
Figure IV.17. Evaluation of SDI on winter season.	176
Figure IV.18. Evaluation of SDI on spring season.....	176
Figure IV.19. Evaluation of SDI on summer scale.....	176
Figure V .1. Results of simulation and correlation for the calibration during the period (1990-1999).....	190
Figure V.2. Results of simulation and correlation for the validation during the period (2002-2005).....	193
Figure V.3. Results of simulation and correlation for the calibration during the period (1990-1996).....	196

Figure V.4: Results of simulation and correlation for the validation during the period (1997-1999).....	199
Figure V.5. Results of simulation and correlation for the calibration during the period (1990-1999).....	202
Figure V.6. Results of simulation and correlation for the validation during the period (2002-2005).....	205
Figure V.7. Results of simulation and correlation for the calibration during the period (1990-1996).....	20
8	
Figure V.8. Results of simulation and correlation for the validation during the period (1997-1999).....	212
Figure V.9. Validation results for wet and dry periods for GR4J.....	213
Figure V.10. Comparison of parameter FC, SFCF, K2 and Nash for the wet and the dry periods for HBV light.....	215
Figure V.11. Correlation between the simulated runoff of the two models in the calibration(1990-1999).....	216
Figure V.12. Correlation between the simulated runoff of the two models in the calibration(1990-1996).....	217
Figure V.13. Correlation between the simulated runoff of the two models in the validation(2002-2005).....	219
Figure V.14. Correlation between the simulated runoff of the two models in the validation(1997-1999).....	220
Figure V.15. Exceedance probability curve for observed and simulated runoff from GR4J, HBV light for calibration (1990-1999).....	221
Figure V.16. Exceedance probability curve for observed and simulated runoff from GR4J, HBV light for calibration (1990-1996).....	222
Figure V.17. Cumulative runoff for observed and simulated runoff from GR4J, HBV light for calibration (1990-1999).....	223
Figure V.18. Cumulative runoff for observed and simulated runoff from GR4J, HBV light for calibration (1990-1996).....	224
Figure V.19. Exceedance probability curve for observed and simulated runoff from GR4J, HBV light for validation (2002-2005).....	226
Figure V.20. Exceedance probability curve for observed and simulated runoff from GR4J, HBV light for validation (1997-1999).....	227
Figure V.21. Cumulative runoff for observed and simulated runoff from GR4J, HBV light for validation (2002-2005).....	228
Figure V.22. Cumulative runoff for observed and simulated runoff from GR4J, HBV light for validation (1997-1999).....	229

List of Tables

Table I.1. List of different of models, with the code and number of parameters.....	18
Table I.2. Value of the parameters of the GR4J model	24
Table I.3. Catchment parameters..	33
Table I.4. Vegetation parameters	34
Table II.1. Rainfall stations of Tafna basin.....	43
Table II.2. Dams of the Tafna basin	43
Table II.3. Shape characteristic of the study sub basins of the Tafna.....	49
Table II.4. Classes of basin shapes according to the values of the Gravelius index	49
Table II.5. Altimetric distribution of the Upstream Sebdou sub basin.....	50
Table II.6. Altimetric distribution of the Khemis sub basin.....	50
Table II.7. Altimetric distribution of the Wadi Boumessaoud sub basin.....	51
Table II.8. Altimetric distribution of the Chouly sub basin.....	51
Table II.9. Altimetric distribution of the Isser sub basin.....	52
Table II.10. Results of the characteristic altitudes of the studied sub basins.....	55
Table II.11. Classification of reliefs according to Ig by O.R.S.T.O.M.....	56
Table II.12. Classification of relief according to Ds (ORSTOM).....	56
Table II.13. Results of Indices of slopes for the study sub basins of the Tafna basin.....	57
Table II.14. Classes of the slopes of the study sub basins.....	58
Table II.15. Classification of thalweg of Upstream Sebdou sub basin.....	61
Table II.16. Classification of thalweg of Khemis sub basin.....	61
Table II.17. Classification of thalweg of Wadi Boumessaoud sub basin.....	61
Table II.18. Classification of thalweg of Chouly sub basin.....	61
Table II.19. Classification of thalweg of Isser sub basin.....	61
Table II.20. Length of main thalweg of the sub basins studied.....	62
Table II.21. Distance and slope of main thalweg of Upstream Sebdou basin.....	65
Table II.22. Distance and slope of main thalweg of Khemis basin.....	65

Table II.23. Distance and slope of main thalweg of Wadi Boumessaoud basin.....	65
Table II.24. Distance and slope of main thalweg of Chouly basin.	65
Table II.25. Distance and slope of main thalweg of Isser basin.....	66
Table II.26. Confluence report of the study sub basins.....	66
Table II.27. Length ratio of the studied sub basins.....	68
Table II.28. Characteristics Hydrographic of the studied sub basins.....	71
Table II.29. Distribution of land in the different zones of the studied basins.....	73
Table III.1. Descriptive information of rainfall stations of the study area.....	78
Table III.2. Descriptive information of runoff stations of the study area.....	78
Table III.3. Descriptive information of Temperature stations of the study area.	78
Table III.4. Descriptive information of Missing data of rainfall station.	80
Table III.5. Regression correlation between study rainfall stations.....	81
Table III.6. Results of Chi-square Test.	84
Table III.7. Range of daily rainfall.....	91
Table III.8. Frequency of different range of daily runoff of the study stations.....	98
Table III.9. Correlation coefficients between annual rainfall and runoff of the study sub basins.	107
Table III.10. Correlation coefficients between monthly rainfall and runoff of the study sub basins.....	108
Table III.11. Correlation coefficients between daily rainfall and runoff of the study sub basins.....	108
Table III.12. Results of Chi-square Test at annual rainfall.....	109
Table III.13. Results of Chi-square Test at annual runoff.	109
Table III.14. Results of normality on annual rainfall to the log normal distribution.....	111
Table III.15. Results of normality on annual runoff to the log normal distribution.....	112
Table III.16. Summary of statistical tests.	114
Table III.17. Results of change point detection on annual rainfall.....	119
Table III.18. Results of homogeneity test on monthly rainfall.....	125
Table III.19. Results of homogeneity test on annual runoff.....	126
Table III.20. Results of homogeneity test on monthly runoff.....	127
Table III.21. Results of homogeneity test on annual temperature.	129

Table III.22. Results of homogeneity test on monthly temperature.....	131
Table III.23. Results of Mann-Kendall test and Sen's method on annual rainfall.....	132
Table III.24. Results of Mann-Kendall test and Sen's method on monthly rainfall.....	134
Table III.25. Results of Mann-Kendall test and Sen's method on seasonal rainfall.....	135
Table III.26. Results of Mann-Kendall test and Sen's method on annual runoff.....	139
Table III.27. Results of Mann-Kendall test and Sen's method on monthly runoff.	141
Table III.28. Results of Mann-Kendall test and Sen's method on seasonal runoff.....	142
Table III.29. Results of Mann-Kendall test and Sen's method on annual temperature.....	145
Table III.30. Results of Mann-Kendall test and Sen's method on monthly temperature.....	147
Table III.31. Results of Mann-Kendall test and Sen's method on seasonal temperature.....	148
Table IV.1. Classification of meteorological drought indices range	160
Table IV.2. Definition of states of hydrological drought based on the SDI classes	161
Table IV.3. The correlation coefficients between SPI and DI, PN, and RAI respectively at different time scale.....	166
Table IV.4. Average correlation coefficients of indices from all stations with different time scale.....	170
Table IV.5. Mann Kendall test results of all indices at all stations in different time sale.....	172
Table IV.6. The correlation coefficients between SDI for all stations at annual time scale..	177
Table IV.7. The correlation coefficients between SDI for all stations at monthly time scale.....	177
Table IV.8. The correlation coefficients between SDI for all stations at seasonal time scale.....	178
Table IV.9. The correlation coefficients between SDI and meteorological drought indices for Upstream sub basin at different time scale.....	179
Table IV.10. The correlation coefficients between SDI and meteorological drought indices for Khemis sub basin at different time scale.....	180
Table IV.11. The correlation coefficients between SDI and meteorological drought indices for Wadi Boumessaoud sub basin at different time scale.....	180
Table IV.12. The correlation coefficients between SDI and meteorological drought indices for Chouly at different time scale.....	180
Table IV.13. The correlation coefficients between SDI and meteorological drought indices for Isser sub basin at different time scale.....	181
Table IV.14. Mann Kendall test results of SDI at all stations in different time sale.....	181
Table V.1. Results of simulation and optimize parameters for the calibration during the period (1990-1999).....	188

Table V.2. Results of simulation for the validation during the period (2002-2005).....	191
Table V.3. Results of simulation and optimize parameters for the calibration during the period (1990-1996).....	194
Table V.4. Results of simulation for the validation during the period (1997-2000).....	197
Table V.5. Results of simulation and optimize parameters for the calibration during the period (1990-1999).....	199
Table V.6. Results of simulation for the validation during the period (2002-2005).....	203
Table V.7. Results of simulation and optimize parameters for the calibration during the period (1990-1996).....	206
Table V.8. Results of simulation for the validation during the period (1997-1999).....	209

GENERAL INTRODUCTION

I.1. Introduction and Problem statement

Water is a key resource known as the most complex and unique natural resource on the earth and highly uneven in space and time. Its availability is important to determine the rate of social and economic development, and essential for almost all activities related to the production of food and energy, to a necessary resource for supply of drinking water, where natural surface freshwater resources account for only a minimal share of the total water resources of the Earth.

Due to the increasing growth in population, economy, industrial activities, urbanization, agricultural and livestock production, demand for water has increased in recent decades (demand for water for domestic, industrial, and agriculture sectors have risen roughly at 2.4 % per annum in the world) (Gleick, 2003; Lombha, 2017), they were become one of the most resources exposed to challenges among the natural resources. And these challenges become even worse in arid and semi arid areas, where the associated risks of catastrophic drought, flood, extreme climate change, and limited means of managing water resources have dominated in these regions, will lead to water scarcity by 2025 (Seckler et al., 1999) threatening so food security, human health, and natural ecosystems than requires efforts in decision making processes on conserving water in term of the amount which their information is important to view the state of water resource. These objectives require hydrological estimates (river flows) and models are simplified representations of hydrology, and conceptualized the water fluxes in different climate conditions for understanding the hydrological behavior, and this is reason to include the hydrological models which are indispensable tools for calculating flows at a fixed time step in the outlet of the basins and most operational systems choose the model that contribute in developing the basic relationships between the different hydrologic systems like rainfall, evapotranspiration, and runoff and to be used in several practical and essential purposes based on the availability of long time-series of historical data from different sources (e.g. automatic rain gauges, radar, satellite) to produce the discharge hydrographs from basins (Ficchi, 2017). The performance evaluation of hydrological models is required to estimate their parameter values by calibration, validation based on comparison to the observed and simulated runoff of basins, and this does not guarantee proper representation of all hydrological processes within the basin (Güntner, 2008). Where hydrologic processes in different basins vary because of the difference in basin characters (the type of soil, land cover..etc), hydrologic models are commonly used as forecasting of flood due to change in factors governing the surface water flux, droughts anticipation (Lobligeois, 2014). The model is therefore an essential tool for water resources management, water allocation, and water balance, and/ or one of the various face to the flood protection, hydrological and ecological management of the catchment under study (Bouadila, 2015).

Nowadays, the models have become standard tools to address many issues of the hydrological system, so it is important for researchers to have the ability to manipulate hydrological models and to use which requires the initiator to understand in general the notions of hydrology and understanding of hydrological variables and their variations which

are considered as input (factor of running the model) (Wagener and McIntyre, 2007; Seibert, 2012).

Water is a resource that is regularized domestic activities, agricultural and most economic activities, and their development. It is for this reason that we can notice that populations are generally grouped around water points. The demand for water has increased with the increase of the population, where the population reach 432 million in 2007 and is projected to reach nearly 700 million by 2050 in the Middle East and North Africa (Roudi-Fahimi and Kent, 2007), this will lead to a 40% drop in per capita water availability in the region by 2050 (Terink et al., 2013).

The existence of water resource is related to the rainfall, which represents approximately 75% of surface water resource in Algeria, and it is considered as a generator to a runoff, where the rainfall rate of 327.2 mm can produce 203 Hm³ per year of runoff as entries in the Tafna basin (Northwestern of Algeria). North of Algeria experienced runoff deficits ranging from 37 to over 70% of the east towards the west of the country (Meddi, H., and Meddi, M., 2004), and more than 20% of annual rainfall amount starting from the mid-1970s (Meddi et al., 2010; Hasanean, 2004; Knippertz et al., 2003; Zeroual et al., 2017) in Tafna basin, which led to a drastic decrease of streamflow by almost 55% in this region, and fluctuates from 61 to 71 % decline in streamflow in the extreme northwest (Meddi & Hubert, 2003) as the trend of 50% reduction in surface resources and 30% in underground resources in the Tafna basin. Where the decrease of rainfall amount affected by the drought phenomenon caused a deficit in the water resource which affected the agriculture, the stopping of some water-consuming plants (Ghenim and Megnounif, 2011), this resource often over-exploited and poorly managed, controlling the agricultural and industrial use of water evenly distributed have become major issues (Belarbi et al., 2015).

For all these reasons, the quantification of water resources becomes important to better manage and exploit it in order to meet the demand for water in the sector of domestic, agricultural, and other activities that are related to the water in future studies. The model by using the software to improve the estimation of water quantity (runoff) was considered in the current study. Hydrological models are essential tools for all studies and research in the field of water resource estimation, valuation, and management (Bouanani et al, 2011; Boldetti, 2012). However, the lack a lack of data availability, particularly in North Africa make limitation in choosing models. Several hydrological models exist that are capable to simulate hydrological processes from low to high objective, the input data, model structures, and the concept of the model to quantify runoff are different from model to model (Döll et al., 2015), this was a major factor for selecting the models in the current study. The data of rainfall, runoff, temperature, or evapotranspiration are used to produce the output simulated flows, these variables show a considerable shift throughout the last century, where are considered as critical variables of climate and hydrological studies and the change that they are faced will affect the hydrological cycle, streamflow (Jain and Kumar 2012; Kumar et al., 2019). Therefore, the knowledge of the characteristics, behavior, and interactions of the hydrological systems is important, especially when the hydrological behavior variability of the basins, although contiguous, is noticed (Karlsen et al., 2014; Oudin et al., 2010; Lyon et al., 2012; Teutschbein et al., 2015) under different climate conditions which also part of the variability in the hydrological behavior (Bloschl and Montanari, 2010), even in nearby and seemingly similar basins. To assess the hydrological responses of this region in the different climate periods (wet, dry), we resorted to using the hydrological models, where the model parameters characterize the hydrology of the basin representing it in a simplified way (Thirel

et al., 2015; Wang et al., 2018), where it is sensitive to changes in climate conditions (Nauditt et al., 2017). Understanding the response of these parameters to different climate condition, will give a more clear view about affected of some hydrological properties and processes of the basin by climate conditions. The common approach to reach this point is to perform a comparative study of the impact of different climate condition on parameters to a certain model and connect them with the model performance. The previous study in our region has not been conducted for the sensitivity of model parameters with different climate conditions, the new insights in this research for the study area is the study the hydrological response (runoff) in the variability of climate (temporal change) and in different sub basins (spatial change) which has not been processed before in our region. To choose an appropriate model for current research, we took look at some studies that made comparisons between distributed, semi-distributed, and lumped conceptual models. Their results reported that distributed models may or may not provide improvements compared with lumped models (Refsgaard and Knudsen, 1996; Reed et al., 2004), and the studies of (Tegegne et al., 2017b; Anshuman et al., 2019; Srivastava et al., 2020) encouraged to use lumped model than a complex model for hydrological modeling in data-limited basins, and in some cases, the performance of complex models does not necessarily yield significantly better performance, where the lumped model is commonly used due to its simplicity and low computational costs. The application of hydrological models provide a proper estimation of the water quantity, this approach could give confidence to decision-makers to develop water resource strategies and provision which their dimensions must be adapted to different climate conditions, and potentially transferable to other Mediterranean regions for the sustainable management of water resources. Therefore, the aim of this study is to assess the hydrological responses for different sub basins in the different climate periods (wet, dry) in lumped model.

There are a lot of research activities going on in the North of Algeria undertaking the hydrological modeling (rainfall-runoff) which is currently often used in the research works in assessing the runoff for evaluating and quantify the water resource in small to a large basin to improve the planning, protection, and exploitation of water resources and are considered as a standard tool that is routinely used for the investigations and applications in hydrology. Research works conducted in the hydrological modeling in Algeria, we mention the study of (Bouguerne, 2016) which applied two models GR4J and HBV light. The results obtained by the two approaches diverge for a semi-arid region, especially for the Rhumel watershed, where the simulation of runoff through the use of the HBV light is more satisfactory, especially for sub basins at high altitudes. The results on the daily outlet specific simulated runoff are very adequate for the small and ungauged sub-basins. And the study of (Gherissi, 2017) showed that the rainfall and runoff trends in the Wadi Lakhdar basin have generally been in deficit. The hydric analysis results obtained by the rainfall-runoff found this change's impact on water resources. Indeed, the climatic variability manifestations have had repercussions on the water resources of the basin which has also experienced a rainfall reduction and an increase in temperature. While the study of (Bendjema, 2020) tried to understand the hydrological functioning of the Wadi Mellah (Northeastern) using the models (GR1A, GR2M and GR4J, GARDENIA, HBV light). The results obtained indicate that these models have good predictive power and that the use of these methods therefore constitutes a fully justified and privileged alternative in the field of surface water resource management. In this regard, comparative studies in modeling would enable the identification of suitable models for understanding hydrological processes better and the prediction of water resources.

I.2.State-of-the-art and scientific questions

Hence the comparison between the hydrological models is the best option for making decisions on the performance of the model in several basins and climate conditions:

- What's the relationship between the observed hydro-climate variables used as input in the hydrological model?
- Which methodology can be used to determine the climate conditions of the time series in the study?
- Which model can be selected in the study based on data availability?
- What are the best calibration parameters for each of the models?
- Is there a best model that can accurately predict runoff in the different sub basins in study area?
- How different are the optimized performance of the simulations runoff by the two models given in the two different calibrations?
- Which model performs better in simulating the runoff in different climates (dry, wet) and different sub basins in the study area?

I.3.Aims and Objectives of the research

The aim of this study is to assess the hydrological responses by using a lumped models for different sub basins during different climate periods (wet, dry) in the Tafna basin (located in Northwestern Algeria) which is characterized by temporal variability of rainfall from the 1950s until the 1990s and reflected a significant decline of more than 20% of annual rainfall amount starting from the mid-1970s. This region suffered by drought years with the return of rising rainfall between 2001 and 2007.

To reach this objective, we resort to:

1. To asses variability (homogeneity) and trend analysis of hydro-climatic variables of the basins based on available data to defined the break point in time series for selection homogeneity period,
2. Comparison of different indices for meteorological drought and hydrological drought,
3. Select the type of climate (wet, dry) in time periods series based on the results of statistical analyses.
4. Set-up different hydrological model for different level of data condition,
5. To identify which parameters in each of the two models influence the simulated runoff in calibration phase,
6. Simulate the hydrological behavior (Validation) of the lumped model (GR4J, HBV light) under different climate conditions,

7. To compare the performance of different hydrological models under different levels of data in different climates and different sub basins, and identify the best of the two models for predicting runoff.

I.4. Structure of the thesis

In order to achieve the above objectives, the thesis is organized into 5 chapters (including the introduction the context of our work, providing a review of the problem, describes the objective) as follows:

Chapter 1 presents a literature review of hydrology, hydrological modeling concept, with particular emphasis on rainfall-runoff models selected including the structure, parameters, and performance criteria in current research.

Chapter 2 presents an introduction to the study area includes geographical location, morphometric, geological, and hydro climatic study.

Following this, chapter 3 presents the historic hydro-climatic data and studies the variability, homogeneity, and trend analysis.

Chapter 4: Comparison of different indices of meteorological and hydrological to identify the drought or wet periods.

Chapter 5: Comparison of the performance of two hydrological models (GR, and HBV light) in order to assess the impact of drought and wet conditions on the hydrological models' response, which is also followed by conclusions and recommendations for future research areas.

CHAPTER ONE
GENERAL LITERATURE REVIEW

I.1. Introduction

Hydrology is quantifying the water cycle in the continental part i.e. the movement of masses of water in the hydrosphere. The major physical processes (fig.I.1) considered in continental hydrology include precipitation, interception, evaporation, transpiration, infiltration, percolation, runoff (from overland, sub-surface, and groundwater flow), and open-channel flow (Ficchi, 2017). This is a representative part of the cycle that still covers meteorological phenomena, flows with a free surface, porous medium, mass, and energy transfers in the biosphere, etc.(Moine, 2008). The basin is defined at any point or cross-section of a river, as the entire topographical and geological area drained by the river and its tributaries upstream of this section (Ficchi, 2017).

The hydrological model can be used to describe the observed behavior of the basin from precipitation to runoff (Fouchier, 2010; Chaponniere, 2005; Reed et al., 2007), and it is a simplified representation of a complex or natural system. Physical phenomena are quantified by equations or the logical operations in a program algorithm (Bessière, 2008; Ramos et al., 2009; Musy and Higy, 1998; Maref, 2019) with the aim of analysing of the system behavior such explaining hydrological processes and for hydrological forecasting (Haan et al., 1982). Hydrologic models can be classified into the category of deterministic models(Lumped model, semi-distributed model, and distributed model) based on the presence of random variables, their distribution in space, and temporal variation (Chow, Maidment, & Mays, 1988), and stochastic models based on whether random variables in space influence each other, and also into the process description (conceptual, empirical, and physical)(Dwarakish and Ganasri, 2015). Several scientific and operational applications to hydrological models are represented in hypothesis testing, improving our understanding of the system and extrapolating measured data in time and space(Götzinger, 2007). All of these applications contribute to some extent to the decision making in water management (Beven, 2012; Pool, 2018). The fluxes of water and the storage illustrated the hydrological functioning of the basin, and it is estimated by calibration of parameters, this allows a conceptual approximation to reality, and on the other case, there is the approximation in a physical way but for much larger scale (Beven, 2012). Through the calibration, the estimation of the parameter was by minimizing the difference between observed and simulated discharge using an error metric (Mean absolute error (MAE), mean squared error(MSE)...etc) (Pool, 2018). In the current research, the rainfall-runoff models are used in operational hydrology. These models are estimating the forecast of the runoff from amount of rainfall by this basin (Donnelly-Makowecki and Moore, 1999). A literature review of the concept and the types of models that are used in this research are given in the following section.

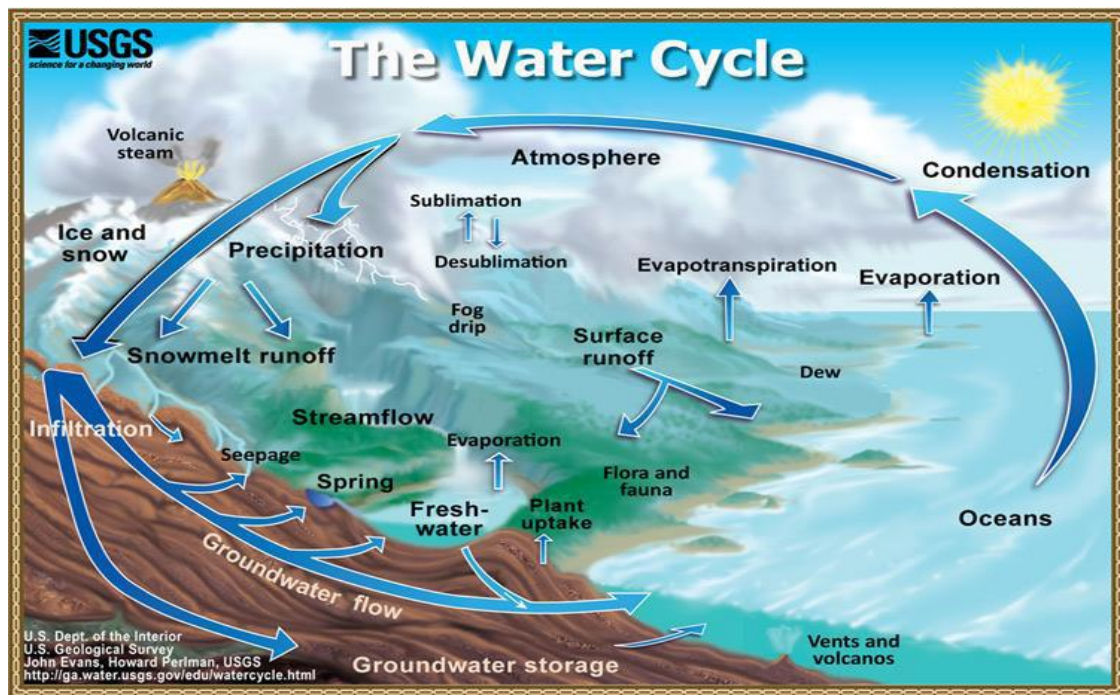


Figure I.1. Water cycle Diagram (Evans and Perlman, 2015).

I.2. Components of the hydrological cycle

The hydrologic cycle can be subdivided into three major systems: The oceans being the major reservoir and source of water, the atmosphere functioning as the carrier and deliverer of water, and the land as the user of water. The major components of the hydrologic cycle are precipitation, interception, depression storage, evaporation, transpiration, infiltration, percolation, moisture storage in the unsaturated zone, and runoff (surface runoff, interflow, and baseflow).

I.2.1. Precipitation

Precipitation is moisture that falls from the atmosphere as rain, snow, sleet, or hail to the land surface, and it varies in amount, intensity, and form by the season and geographic location which impact whether the water flows into streams or infiltrate into the ground. Precipitation is one of the main inputs in the water balance but is the most difficult variable to measure due to temporal and spatial variability in an area (Jiang, 2004; Zhang and Srinivasan, 2010; Jeniffer et al., 2010).

I.2.2. Factors influencing precipitation

The factors contributing in difference of precipitation, especially at watersheds are mainly topographical such as altitude, aspect, direction of mountain ranges (Basist et al., 1994; Daly, 2006; Cukur, 2011), global ocean currents, relative continental position, and orographic enhancement which is affected by wind speed and direction (Johansson and Chen, 2003; Daly, 2006) and it has minimal influence on precipitation in arid and semi-arid areas Augustine (2010) stated that orographic variation has minimal influence on precipitation in arid and semi-arid areas (Mengistu, 2019).

I.2.3. Evapotranspiration

It is the transformation of natural liquid water into vapor. Evaporation happens in surface waters, while transpiration is the process of vaporization of water contained in plant tissues and loss to the atmosphere (Allen et al., 1998). Therefore, evapotranspiration term describing the two processes mostly occur simultaneously, and is difficult to separate them (Jovanovic and Israel, 2012).

Evapotranspiration uses a large portion of precipitation related to other processes associated with the hydrological cycle.

I.2.4. Factors influencing evapotranspiration

There are two factors that influence evapotranspiration (Hillel, 1977; Rasheed et al., 1989; Hillel, 2004):

- A continual supply of heat to meet the latent heat requirement of water, which can be influenced by meteorological factors such as radiation, air temperature, humidity and wind velocity, which together determine atmospheric evaporability.
- A continual supply of water to the site of evaporation depends on the properties of water in the evaporating body which determine the maximal rate at which the body can transmit water to the evaporation site (Hillel, 1977; Rasheed et al., 1989; Hillel, 2004; Rose et al., 2005).

Therefore, evapotranspiration is affected by the complex interaction between topography, soil characteristics, vegetation, and climatic factors (Mo et al., 2004; Western et al., 2004; Wenzhi and Xibin, 2016). These factors determine the rate of evapotranspiration by influencing the availability of water, energy and vegetation type of the area (Mengistu, 2019).

I.2.5. Infiltration and percolation

Infiltration refers to the movement of water entering the surface layers of the soil and the flow of this water in the soil and subsoil, under the action of gravity and the effects of pressure. The rate of infiltration is influenced by the physical characteristics of soil, soil cover, the water content of the soil, and rainfall intensity. Rather, percolation is the downward movement of water through soil and rock. Groundwater percolates through the soil much as water fills a sponge, and move from space to space along fractures in the rock, through sand and gravel, or through channels in formations such as cavernous limestone. The terms infiltration and percolation are often used interchangeably.

I.2.6. Runoff

Runoff is a natural phenomenon of water flowing freely to stream channels, lakes, ocean, or low points on the earth's surface. Four types of runoff may occur (Mockus, 2004; Wagener et al., 2004), (i) when rain falls directly on a flowing stream and appears in the hydrograph (a graph showing the rate of flow versus time), (ii) when the rate of water application or rainfall exceeds the soil's rate of infiltration, (iii) when infiltrated rainfall saturates a subsurface horizon with poor drainage and travels laterally above the subsurface

zone, (iv) or in form base flow is a steady flow that comes from an aquifer replenished by percolation after a rainfall event (Mockus, 2004, Mengistu,2019).

I.2.7.Factors affecting runoff

Apart from rainfall characteristics, there are a number of other factors influencing the occurrence and volume of runoff such as:

- Soil type

The infiltration capacity is dependent on the porosity of a soil which is based on soil type. The highest infiltration capacities are observed in loose, sandy soils; this factor determines the water storage capacity and affects the resistance of water to flow into deeper layers

- Vegetation

The amount of rain lost to interception storage on the foliage depends on the kind of vegetation and its growth stage. Whereas what affects the surface flow is a dense vegetation cover on low slopes, giving the water more time to infiltrate and evaporate, yields less runoff than bare ground.

- Slope and watersheds size

Investigations on experimental runoff plots (Sharma et al. 1986) have shown that steep slope plots yield more runoff than those with low slopes, in addition, the quantity of runoff decreased with increasing slope length. The runoff efficiency (volume of runoff per unit of area) increases with the decreasing size of the watersheds, where the size of the watersheds is larger, the time of concentration is increased, and runoff efficiency decrease.

I.3. Scales for study of hydrologic cycle

There, two scales are readily distinct from the point of view of hydrologic studies (fig.I.2; fig.I.3):

- Global scale

The hydrologic cycle can be considered to be comprised of three major systems; the oceans, the atmosphere, and the landsphere. Precipitation, runoff and evaporation are the principal processes that transmit water from one system to the other. In general, the hydrologic cycle shows the interactions between the earth (lithosphere), the oceans (hydrosphere), and the atmosphere, which is necessary to understand the global fluxes and global circulation patterns.

- Watersheds Scale

On a watersheds scale, the spatial scale can range from a few square km to thousands of square km, and the time scale could be a storm lasting for a few hours to a study spanning many years. The water movement can follow three systems: the land (surface) system, the

subsurface system, and the aquifer (or geologic) system. When the attention is focused on the hydrologic cycle of the land system, the dominant processes are precipitation, evapotranspiration, infiltration, and surface runoff. The land system itself comprises of three subsystems: vegetation subsystem, structural subsystem and soil subsystem. These subsystems subtract water from precipitation through interception, depression and detention storage.

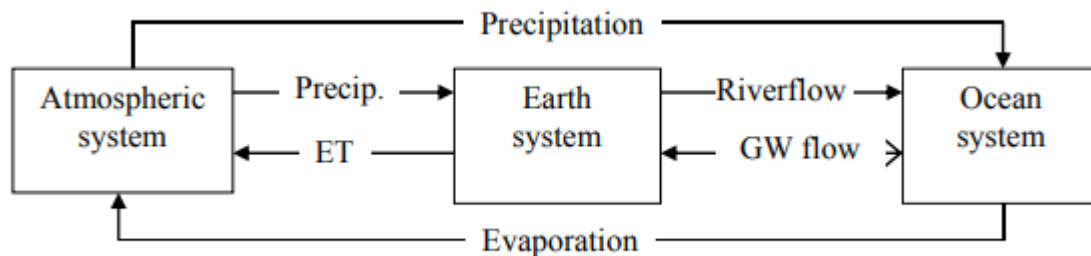


Figure I.2. A global schematic of the hydrologic cycle.

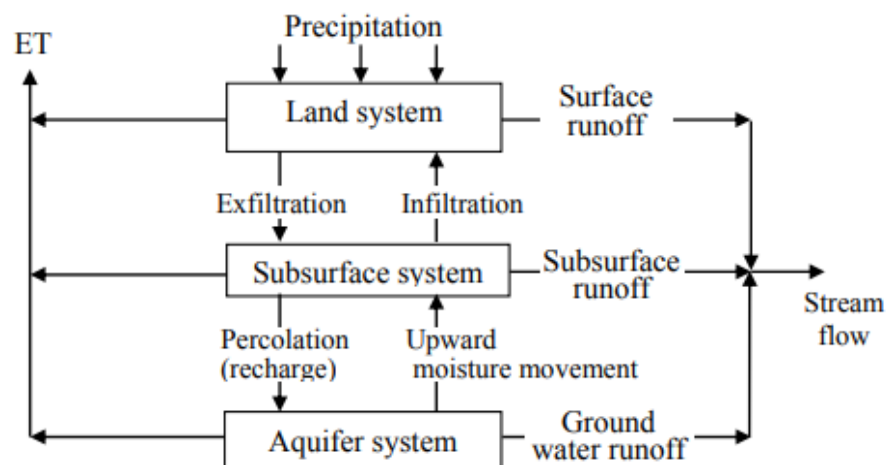


Figure I.3. A schematic of the hydrologic cycle of the earth system.

I.4. Hydrological modeling

The model is defined as a simplified system representing the schema to a physical phenomenon, the equations, or the logical operations in a program algorithm (Bessière, 2008; Ramos *et al.*, 2009; Musy and Higy, 1998; Maref, 2019) aim of simplifying the study and the analysing of the system process. each model has a numeric measure of a feature, which is defined as parameters (Beven, 2001) can be classified into physical and process parameters (Sorooshian and Gupta, 1995). Physical parameters can be measured directly, such as, measures soil permeability, while, the process parameters cannot be measured directly and must be deduced indirectly (Gupta *et al.*, 1998), such as the effective depth of soil moisture storage, etc.

Among these models, the hydrological model that depends on modeling the water cycle in a basin (infiltration, runoff, evaporation, evapotranspiration, snowmelt, etc.) (Fouchier, 2010;

Chaponniere, 2005) through a mathematical and physical relation that studies the relationship between rainfall and runoff and the comprehension of frequency flows (Reed *et al.*, 2007) and explain hydrological processes and for hydrological forecasting (Haan *et al.*, 1982). There several applications of hydrological models such as simulation, predetermination (evaluation of project data), reconstruction, or extrapolation of data, and forecasting (Bessièrè, 2008; Ramos *et al.*, 2009) for the objective such as: Study of the interaction between surface water and groundwater; the short-term flood simulations, prediction of floods and sizing of structures, this represents the most common operational use of hydrological models., and water resource management under affected by climate change, management of water tanks for drinking water supply and irrigation (Singh and Frevert, 2006), the impact of agricultural (Rousseau *et al.*, 2011; 2013) and urban (Mailhot *et al.*, 2002) discharges on water quality.

The approach of modeling contains specific steps:

- Choosing a suitable model based on the general problem and the availability and quality of hydrological data (Abushandi, 2011) and the objective of the study, all types of models have their own domain of efficiency (Dooge, 1977) and adaptability.
- The entry of the data collected and the Sensitivity analysis of a model. There are two different stages of the sensitivity analysis in modeling: first, perform a sensitivity analysis before the calibration step to identify the most important parameters and reduce the dimensionality of the calibration process (Bastidas *et al.*, 1999), and second after the calibration step to assess whether the parameters are correctly or poorly identified (Clarke, 1973).
- Calibration of the model, where the parameters are adjusted to reduce the error between simulated and observed values (Refsgaard and Storm, 1996; Bessièrè, 2008) in order to obtain a conceptually realistic set of parameters that reflects the understanding of the physical system (Sorooshian, 1983) and identify and recognize certain hydrological properties of the watershed (Gerard, 2010). The success of any model calibration process depends on the observed data, the structure of the model, the calibration conditions, and the optimization procedure (Abouabdillah, 2009).
- Validation is following a process of the calibration for verification is a step often included in the modeling procedures, and it must be used to test the divergence of a model over a wide range of hydrological conditions (Todini and Wallis, 1977). Validation tests should be used to test the model's ability to give results for input data other than that used to calibrate the model (Refsgaard and Storm, 1996). The phases of hydrological modeling can be summarized in the diagram below (fig.I.4) (Refsgaard and Henriksen, 2004).

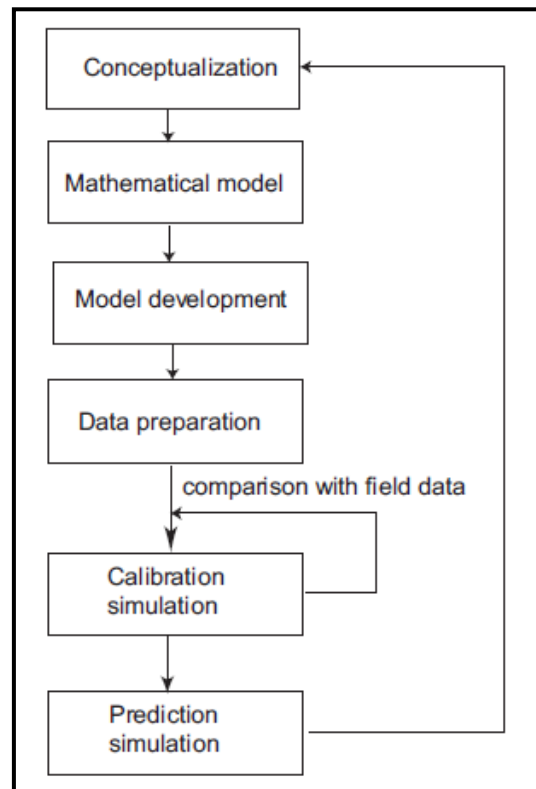


Figure I.4. Schematic representation of a hydrologic model application (Yu, 2015).

Hydrological models are classified based on the following criteria:

- Description of hydrological processes;
- The representation of space;
- Temporal discretization (Bessière, 2008).

I.4.1. Choosing a model

The choice of a hydrological model is based on the following elements:

- It includes a well-developed user interface where all parameters, inputs, and outputs easily could be controlled,
- Easily perform runs from the command line for simulation,
- Data needed were readily available (Kloosterman, 2012; Masih et al., 2010),
- It has been widely used world-wide in particular in Mediterranean region (Dakhlaoui et al., 2012; Ouatiki et al., 2020).
- The choosing certain parameters in the modeling is based on the objectives of the hydrological study;
- Calibration methods of rainfall-runoff models.

I.4.2. Model calibration methods

The model calibration can be classified into three different methods:

- Manual calibration

This method is based on evaluating manually the error between the output values and the observed values and the sample of reference for giving values to the parameters of the model.

- Automatic calibration

This method is based on using of a numerical algorithm to find an extreme of a given numerical criterion to optimize the model parameters in order to determine the set of parameters that will satisfy a given precision criterion through different possible combinations (Kingumbi, 2006).

- Mixed calibration

Mixed calibration consists of combining the manual setting and automatic setting. We determine the parameter variation interval manually, and then the automatic method is used to find the optimal parameter values.

I.5. Classification of hydrological models

According to the approach of the hydrological modeling used, it can differentiate between the models (tab.I.1). The classification was summarized (Kauark Leite, 1990) into three groups:

- According to the model approach, models can be classified into two different types (fig.I.5):

Deterministic models: they are based on physical processes (Chow *et al.*, 1988), which represent a real system similar system that has similar properties (Audrey, 2013). And they associate with each set of forcing variables, state variables, parameters, and unique realization value of the output variables (Maftai, 2002).

Stochastic models: they deal with state variables or parameters which are random variables, using statistical distributions. Thus, the output variable or variables are random variables. When the phenomenon studied is random, it could use the probabilistic approach (Chocat, 1997).

- According to the description of processes that determine the transformation of rain into flow at the level of the watershed, the models can be classified into three different types:

Empirical models: they are based on the stochastic time series (Ambroise, 1999), containing parameters that may have little direct physical significance and not give the internal structure and the response of the basin into account (Bessière, 2008). Empirical models applied a less number of parameters and data (Abushandi, 2011). And they are useful to decision-making due to the accuracy of its answer (Hsu *et al.*, 1995), this appears in the time series models. An example of these models is the GR (Fr. Génie Rural) models (Loumagne, 1988; Edijanto and Michel, 1989).

A physical-based model: it uses a system that similarity to a logical structure of the real system, and it can be classified as scale models that have a physical similarity to the real system, and analog models that are using a physical system with properties similar to that of reality. Physical models are useful for understanding a complex phenomenon and carried experiments under favorable conditions (Maref, 2019). Physics-based models include runoff models (Bessière, 2008), infiltration models (Morel-Seytoux, 1978), evaporation models (Freezb, 1971). An example of these models is the SHE model (Abbott *et al.*, 1986).

Conceptual models: they are intermediate between physical and empirical models. Conceptual models transformed of rain into a runoff in the reservoirs as a cascading structure (Furusho, 2008; Moussu, 2011) which drain into each other. These models are close to the reality of hydrological and less complex than physical models (Maref, 2019). An example of these models is TOPMODEL(TOPography based hydrological MODEL) (Obled *et al.*, 2009).

- According to the spatial discretization, the model can be classified into three different types (fig.I.6):

Global models: the model treat the basin as a homogeneous set, which requests the limited amount of input data expressed by mean values o the basin: average rain, average slope, etc. The elementary processes of transformation of rain into flow are described in the form of simplified equations or equations from experience (Singh, 1995). An example of these models is the HEC-1 model, GR (HEC, 1998; Perrin *et al.*, 2003).

A semi-distributed model: this model adopts partition of the basin into separate sub-basins that are treated as homogenous in themselves, where it is entering the separate input data to each sub-basin (rain, flow, slope, etc.). The best example of these models is the HEC-HMS, HBV light model (Bergström and Forman, 1973; Scharffenberg and Flemin, 2010).

Distributed models: In this model, the whole basin is divided into elementary unit sub-basins (meshes) which is considered as a homogeneous unit. For run this model requires a large amount of hydrological and physical data (Batelaan *et al.*, 1996), where the number of parameters estimated increases (Beven and Binley, 1992; Senarath *et al.*, 2000). Distributed models are frequently used as tools for the detailed description and simplifying of hydrological processes which can fluctuate in time and space (Abushandi, 2011). An example of these models is HYDROTEL, SWAT (Soil and water assessment tool) (Fortin *et al.*, 1995; Arnold *et al.*, 2012).

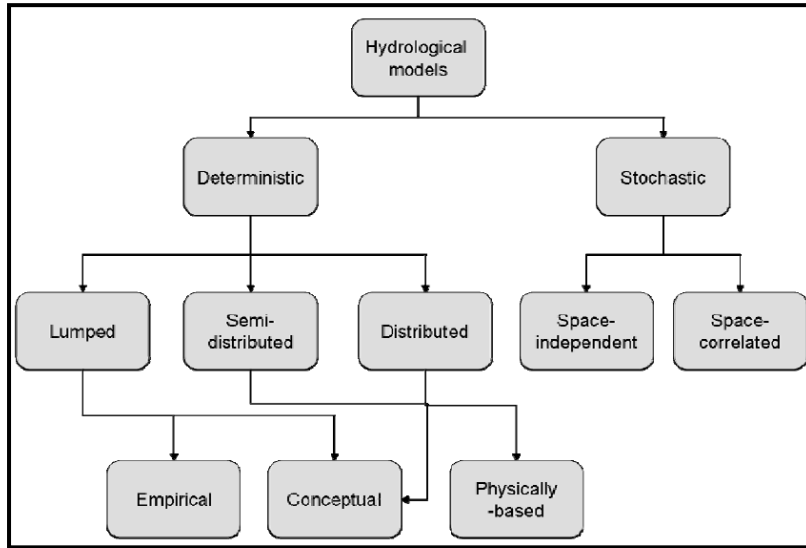


Figure I.5. General classification of the Components of hydrological models (Chow *et al.*, 2005).

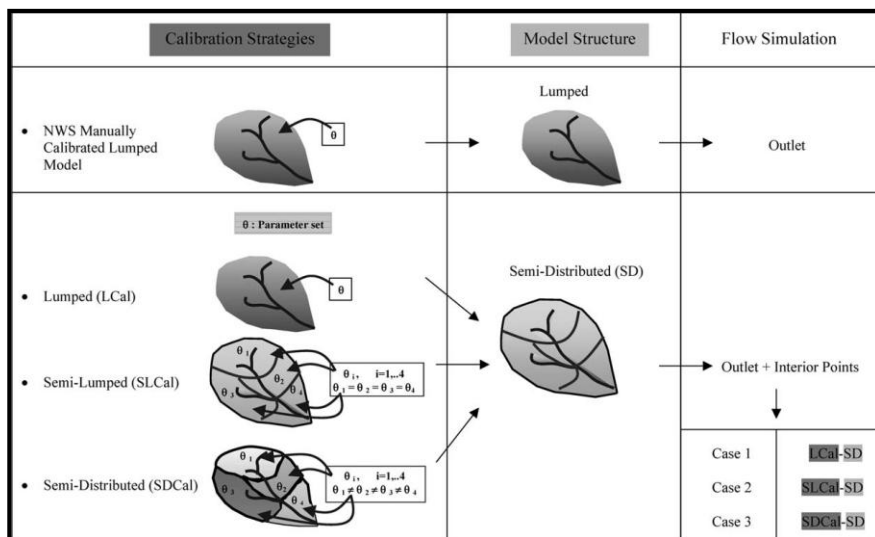


Figure I.6. Schematics of three different models, lumped, semi-lumped and semi-distributed (Newsha *et al.*, 2004).

Table I.1. List of different of models, with the code and number of parameters (Perrin *et al.*, 2000).

N°	Modèle	Code structure	Paramètres
0	Tsykin (1985)	TSYK	5
1	GR3J (Edijatno <i>et al.</i> , 1999)	GR3J	3
2	GR4J (Nascimento, 1995)	GR4J	4
3	GR3J à 4 paramètres (Edijatno <i>et al.</i> , 1999)	GR4K	4
4	MHR (Leviandier, 1993)	MHR0	4
5	Modèle C (Bonvoisin et Boorman, 1992)	BOOC	5
6	ABCD (Thomas, 1981)	ABCD	6
7	Modèle B (Bonvoisin et Boorman, 1992)	BOOB	6
8	Bucket (Thomthwaite et Mather, 1955)	BUCK	6
9	CREC (Comary et Guilbot, 1973)	CREC	6
10	Gardenia (Thiery, 1982)	GARD	6
11	GR5J (Ma <i>et al.</i> , 1990)	GR5J	6
12	PDM (Moore et Clarke, 1981)	PDM0	6
13	IHACRES (Jakeman <i>et al.</i> , 1990)	IHAC	7
14	Martine (Mazenc <i>et al.</i> , 1984)	MART	7
15	MODALP (Arikan, 1988)	MODA	7
16	TANK (Sugawara, 1979)	TANK	7
17	TOPMODEL (Beven et Kirkby, 1979)	TOPM	7
18	mSFB (Summer <i>et al.</i> , 1997)	BOUG	8
19	CATPRO (Raper et Kuczera, 1991)	CATP	8
20	Haan (1972)	HAAN	8
21	MODGLO (Servat, 1986)	MODG	8
22	SIXPAR (Gupta et Sorooshian, 1983)	SIXP	8
23	SMAR (O'Connell <i>et al.</i> , 1970)	SMAR	8
24	TMWAM (Bobba et Lam, 1985)	TMWA	8
25	Wageningen (Warmerdam <i>et al.</i> , 1997)	WAGE	8
26	Xinanjiaog (Zhao <i>et al.</i> , 1980)	XINA	8
27	Arno (Todini, 1996)	ARNO	9
28	Cequeau (Girard <i>et al.</i> , 1972)	CEQU	9
29	Georgakakos et Baumer (1996)	GEOR	9
30	GRHUM (Loumagne <i>et al.</i> , 1996)	GRHU	9
31	HBV (Bergström et Forsman, 1973)	HBV0	9
32	HMS (Morel-Seytoux, 1999)	HMS0	9
33	Institute of Hydrology Lumped Model (Blackie et Eeles, 1985)	IHLM	9
34	MODHYDROLOG (Porter et McMahon, 1971)	MODH	9
35	NAM (Nielsen et Hansen, 1973)	NAM0	9
36	Dawdy et O'Donnell (1985)	ODON	9
37	Sacramento (Burnash <i>et al.</i> , 1973)	SACR	9
38	SDI (Langford et O'Shaughnessy, 1977)	SDI0	9

I.6. Rainfall-runoff modeling

Rainfall-runoff models describe the behavior of hydrological systems in a simplified and usable form that can be used for practical purposes by generating streamflow time series. And these models attempt to interpret by mathematical expression (Eykhoff, 1974; Ficchi, 2017) the rainfall in a certain time and space into a discharge at the outlet of the basin. In addition to rainfall, there are other variables used to produce the output flows, such as temperature or evapotranspiration. Several models are currently used and some still to be improved to be close to reality despite the complexity levels (Chkir, 1994). To deal with this complexity, there is a variety of approaches that can be summarized in two general complementary strategies:

- The reductionist approach: this approach is based on the division of the study system (basin) into a number of interconnected elementary units of smaller spatial dimensions (grid elements) where some elementary physical laws can be applied.
- The lumped approach: it analyses the system at a large spatial scale, and define the rainfall-runoff relationship with some conceptual or empirical relationships.

Rainfall-runoff model is defined by:

Input variables (independent variables): defined also as forcing variables that playing a role in a large number of processes. These variables are usually represented by rain and evapotranspiration or temperature.

- The state variables: describe the state of the internal variables of the system.
- The output variables (dependent variables): These generally represent the response of the system, in addition to variables of interest to the modeller.
- The mathematical equations: these allow connect the output variables to the input variables and to the state variables and involving the function of the system process.
- The parameters: it may (or not) represent a physical significance to adopt the relationships governing the model to functioning actually observed (Perrin et al, 2000).

I.6.1. The purpose of a rain - runoff model

a) Simulation of flows: the reconstruction of historical flows (rain data is often available for periods much longer than flows), for filling gaps in data series or to allow statistical processing.

b) Forecast of floods and low water: This involves assessing in advance the state of the basin, the flood flows likely to present risks (flooding) and the occurring number of floods and how long. The low water flows may require special management of the resource (Example: reservoir dams) to ensure water supply and the arrangements in the bed of the watercourse.

c) Influence of developments on hydrology: the analysis of the changes and predict it under the human origin or environmental changes to highlight two important aspects, that of risk assessment and that of resource management. The response of these issues can relate to the suitability of the model in its representation of the basin and the objectives set (Perrin *et al.*, 2000).

I.7. Uncertainties in hydrology

Definition of uncertainty:

Uncertainty is the result of the lack of information in the modeling of physical phenomena. According to (Mailhot and Villeneuve, 2003), uncertainty is defined as the probability of exceeding a given threshold (or probability of system failure).

I.7.1. Typology of uncertainties in hydrological modeling

For hydro-systems, (Refsgaard and Storm, 1996) identify the following sources of uncertainty:

- **Uncertainties on forcing variables:** This uncertainty is present in data acquisition techniques (weather stations, radar, etc.), where it is difficult to identify the variability and the local complexity of the data through a few measurement points.
- **Uncertainties linked to nature:** this is the spatio-temporal variability of the modeled processes thus generating variability in the outputs of the model.
- **Uncertainties linked to the structure of the model:** this type of uncertainty is the result of the fact that the model is a rough representation of the complex natural system.
- **Uncertainties linked to the parameters of the model:** they are associated with the use of imperfect techniques for estimating parameters of the calibration of the model.
- **Uncertainties on the states of the watershed over time;** no simulation time, in particular the initial state.
- **Uncertainties on the flow observations used both in calibration and validation.**

I.7.2. Objectives of the uncertainty analysis

All the potential sources of uncertainties should be evaluated. The estimation of the uncertainty on the model must be realised (Beck, 1987) to characterize the main ones, combine them and propagate them to have the total uncertainty on the output of the model in order to succeed the model in better reproducing the real behavior of a watershed and for hydrological modeling to achieve its objectives (assess the dynamics of the different flows and stocks, for example, spatial interpolation of precipitation, evapotranspiration, surface runoff, water flows and contents in saturated and unsaturated zones, stream flows) and identify the parameters whose uncertainties contribute the most to uncertainties on simulated flows. The analysis of the uncertainty makes it possible to estimate the probability of obtaining a certain flow rate value, depending on the uncertainty on the parameters of the model (Melching *et al.*, 1990).

I.7.3. Uncertainty analysis techniques

There are two main approaches for estimating model parameter uncertainties (Muleta and Nicklow, 2005):

I.7.3.1. A local approach to uncertainty analysis

This approach is based on the Taylor series development of the model response as a function of the parameters and analysis according to the local approach in the parametric hyperspace of the model and around an optimal operating point (reference point) (Turanyi *et al.*, 2006). This approach involves the analysis of partial derivatives of the response. In the case where these derivatives are complex to solve analytically, the resolution is done numerically.

I.7.3.2. Global approach

Global approaches are based on the principle of a random sampling of parameter sets and the estimation of the statistical characteristics of the response of the model from sets of random parameters (Griensven *et al.*, 2006; Turanyi *et al.*, 2006). The advantage of the global approach is that it takes account of the whole of parametric space and the interdependencies between the parameters.

I.7.4. Modeling evaluation criteria

The evolution and efficiency of a hydrological model relate to criteria which are analytical or graphic criteria depending on the objectives of the study and provide more information on the systematic and dynamic errors present in the model simulation, these criteria are as follows:

I.7.4.1. Nash-Sutcliffe criterion

The Nash coefficient is defined as one minus the sum of the absolute squared differences between the predicted and observed values (Nash & Sutcliffe, 1970), and it provides information on the differences between the values calculated by the model and the values observed. The Nash coefficient is commonly used by hydrologists to assess the relevance of the modeling results. It is calculated as:

$$Nash = \left[1 - \frac{\sum_{i=1}^n (Q_{obs} - Q_{cal})^2}{\sum_{i=1}^n (Q_{obs} - \bar{Q}_{obs})^2} \right] \quad \text{Eq.I.1}$$

$Q_{cal,i}$: Calculated value,

$Q_{obs,i}$: Observed value,

\bar{Q}_{obs} = Average of the observed values (i = 1 to n).

The range of the Nash coefficient between $-\infty$ and 100 % (perfect fit). A Nash coefficient lower than zero indicates that the mean value of the observed time series would have been a better predictor than the model (Lavabre *et al.*, 2003).

I.7.4.2. Coefficient of determination r^2

The coefficient of determination r^2 is defined as the squared value of the coefficient of correlation according to Bravais-Pearson, and it can be defined as the squared ratio between the covariance and the multiplied standard deviations of the observed and predicted values. It is calculated as:

$$r^2 = \left(\frac{\sum_{i=1}^n (Q_{obs} - \bar{Q}_{obs})(Q_{cal} - \bar{Q}_{cal})}{\sqrt{\sum_{i=1}^n (Q_{obs} - \bar{Q}_{obs})^2} \sqrt{\sum_{i=1}^n (Q_{cal} - \bar{Q}_{cal})^2}} \right)^2 \quad \text{Eq.I.2}$$

The range of r^2 lies between 0 and 1 which describes the dispersion between a fitted line and all of the data points that are scattered throughout the diagram. A value of zero means no

correlation at all whereas a value of 1 means that the dispersion is equal to that of the observation (Krause et al.,2005).

I.7.4.3. Root-mean-square error (RMSE)

It represents the differences between the observed values and the calculated values. It varies with the variability within the distribution of error magnitudes and with the square root of the number of errors ($n/2$) (Cort and Kenji, 2005), where:

$$RMSE = \sqrt{\frac{\sum_{i=1}^n (Q_{cal} - Q_{obs})^2}{n}} \quad \text{Eq.I.3}$$

I.7.4.4. Mean absolute error (MAE)

It defined by the average of the differences between the observed values and the calculated values (Cort and Kenji, 2005):

$$MAE = \frac{1}{n} \sum_{i=1}^n (Q_{Cal} - Q_{obs}) \quad \text{Eq.I.4}$$

I.7.4.5. Bilan

This criterion compares the performance of the model from one period to another.

$$Bilan = \frac{\sum_{i=1}^n Q_{cal}}{\sum_{i=1}^n Q_{obs}} \quad \text{Eq.I.5}$$

I.8.The rainfall-runoff models selected

In this study, we have chosen two rainfall-runoff models which are simple and quick to use, and theoretically adapted to any type of climate which encouraged us to apply this models, not very data-needful, it required the rainfall, temperature, and flow inputs to simulate flows, in facing the situation of lack of data and the insufficient data spatially distributed in each one of the sub basins, where the available data reflect only part of the sub basin. The comparison method that focuses on two models is an approach that we have chosen in order to obtain satisfactory results and limit the volume of the results presented and draw general conclusions where each model has different levels of the complexity and the parameters used. The lumped models are superior when it comes to simulating flows at the outlet of watersheds (Bormann *et al.*, 2009).

The first model (GR4J)(Perrin, 2000, Perrin *et al.*, 2003) is a simple model with 4 parameters to calibrate with the advantage of having relatively different formulations of their production function, which obtained reliability results in Mediterranean watersheds (Tafna (Baba Hamed, 2001; Bouanani, 2010; Gherissi, 2018), Mekerra (Otmane, 2015), Tunisia (Boudahraa, 2007), Morocco (Ahbari, 2013)).

The second model HBV light (Bergström and Forman, 1973; Bergström, 1992) is a more complex model with 14 calibration parameters, it was applied to a watershed in eastern Algeria (Bouguerne, 2017, Bendjema, 2020), and a Tunisian basin (Dakhlaoui, 2014; Ouachani, 2003, 2004). The use of two hydrological models is important to compare the outputs of the models which ensure that the results do not depend on a specific feature of a single hydrological model. The structure of the two lumped models is presented below:

I.8.1. GR4J: A daily four-parameter rainfall-runoff model

I.8.1.1. Introduction

The GR4J model (Fr. "Génie Rural") is a daily lumped rainfall-runoff model that is based on four parameters:

X1: the maximum capacity of the production tank (mm),

X2: the groundwater exchange coefficient (mm), which influences the routing store, water infiltrates to the aquifer when X2 has a negative value, while water exits the aquifer and adds to the routing storage when it has a positive value,

X3: the maximum capacity of the routing tank (mm), it depends upon the type and the humidity of the soil,

X4: the time peak ordinate of hydrograph unit UH1 (day), the ordinate of this hydrograph is generated based on runoff, where 90% of the flow is a slow flow that infiltrates into the ground, and 10% of the flow is a fast flow along the soil surface.

The production tank (X1) is stored at the surface of the soil that holds rainfall (Perrin *et al.*, 2003, Tegegne *et al.*, 2017). The GR4J model is the last modified version of the GR3J model originally, it was developed at the French CEMAGREF (Perrin *et al.*, 2003) in early 1980 and had several versions proposed by (Edijatno *et al.*, 1999; Perrin and Michel, 2002; Perrin, 2002; Perrin *et al.*, 2003; Michel *et al.*, 2003; Oudin *et al.*, 2005). The transformation from the rain into a runoff through the GR4J model by means of two reservoirs and a routing production, using an empirical and comparative approach (fig.I.7). It aims to ensure robust rainfall-runoff simulations to be reliable to use for resource management applications.

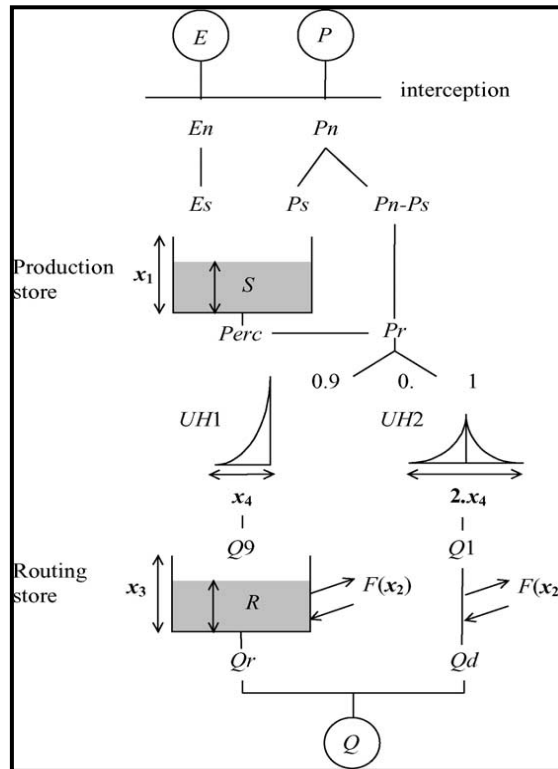


Figure I.7. Diagram of the structure model GR4J rainfall-runoff (Perrin *et al.*, 2003).

I.8.1.2. Model parameters

In the GR4J model, four parameters have to be optimised for yielding the best model results. Where the optimisation algorithms applied to calibrate the model parameters require knowledge of an initial parameters set, which can capable of identifying parameter values yielding satisfactory results. The confidence interval is approximately 90%. The four parameters to calibrate (tab.I.2) are described in detail by (Perrin *et al.*, 2003):

Table I.2. Value of the parameters of the GR4J model (Ficchi, 2017).

Parameter	Signification	Theoretical transformation From Δt_1 [s] to Δt_2 [s]	90% confidence interval	Unit
X1	Production tank capacity	$\beta_{(\Delta t_2)} = \beta_{(\Delta t_1)} \left(\frac{\Delta t_1}{\Delta t_2} \right)^{\frac{1}{4}}$	100 - 1200	mm
X2	Coefficient of underground exchanges	$x_{2(\Delta t_2)} = x_{2(\Delta t_1)} \left(\frac{\Delta t_1}{\Delta t_2} \right)^{-\frac{1}{8}}$	-5 - 3	-
X3	Routing tank capacity	$x_{3(\Delta t_2)} = x_{3(\Delta t_1)} \left(\frac{\Delta t_1}{\Delta t_2} \right)^{\frac{1}{4}}$	20 - 300	mm
X4	Basic time of the unit hydrograph	$x_{4(\Delta t_2)} = x_{4(\Delta t_1)} \left(\frac{\Delta t_1}{\Delta t_2} \right)$	1.1 - 2.9	j

I.8.1.3. Mathematical Description

The discrete equations of the GR4J model derive from the integration of the continuous equations over a time step Δt and are expressed in mm. In the following, the equations of different functions of GR4J:

First, the determination of the evaporation from intercepted water (E_i) through a neutralisation function of the precipitation P by the potential evapotranspiration E to determine either a net rainfall P_n or a net evapotranspiration capacity E_n .

$$E_i = \min(P, E) \quad \text{Eq.I.6}$$

$$P_n = P - E_i \quad \text{Eq.I.7}$$

$$E_n = E - E_i \quad \text{Eq.I.8}$$

if $P \geq E$ then, E_n

if $P \leq E$ then, P_n

The production store is filled by part P_s of the net rainfall which the part of it infiltrating in the soil moisture accounting store, the remaining part passes the production store and reaches directly the routing part of the model. And E_s is the actual rate of evaporation of water in the tank. The two functions of P_s and E_s are determined as:

$$P_s = \frac{x_1 \left(1 - \left(\frac{S}{x_1}\right)^2\right) \tanh\left(\frac{P_1}{x_1}\right)}{1 + \frac{S}{x_1} \tanh\left(\frac{P_1}{x_1}\right)} \quad \text{Eq.I.9}$$

$$E_s = \frac{S \left(2 - \frac{S}{x_1}\right) \tanh\left(\frac{E_1}{x_1}\right)}{1 + \left(1 - \frac{S}{x_1}\right) \tanh\left(\frac{E_1}{x_1}\right)} \quad \text{Eq.I.10}$$

Where S [mm] is the level of the production store at the beginning of the time step, and is updated with: $S = S_k - E_s + P_s$; x_1 is the maximum capacity of the production store. The rating curves obtained with equations of (P_s) and (E_s) is shown in Figure I.8.

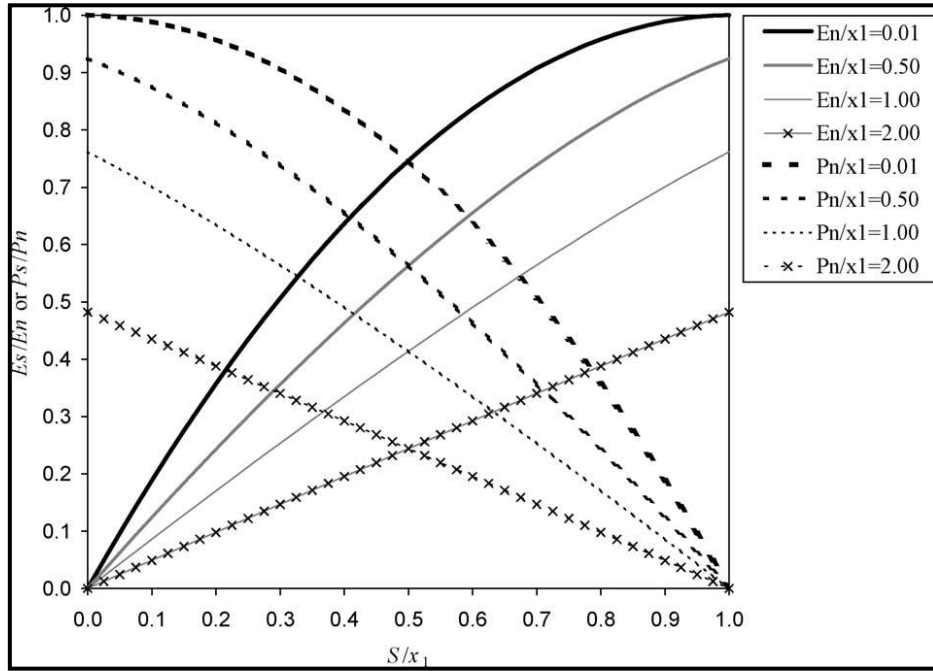


Figure I.8. Illustration of the behavior of the production functions (E_s/E_n : solid line; P_s/P_n : dashed line) as a function of storage rate S/x_1 for different values of E_n/x_1 or P_n/x_1 (Perrin *et al.*, 2003).

The percolation leakage $Perc$ is removed from the production store. It is calculated as:

$$Perc = S \left\{ 1 - \left[1 + \left(\frac{4S}{9x_1} \right)^4 \right]^{-\frac{1}{4}} \right\} \quad \text{Eq.I.11}$$

The amount of water is divided into two parts and is expressed by the function, $Pr = Perc + (Pn - Ps)$:

- 90% of Pr is routed by a unit hydrograph (UH1), it denoted HU1 and a routing tank.
- 10% of Pr is routed only by a single unit hydrograph (UH2).

The ordinates of the unit hydrographs are determined as:

$$UH1(j) = SH1(j) - SH1(j-1) \quad \text{Eq.I.12}$$

$$UH2(j) = SH2(j) - SH2(j-1) \quad \text{Eq.I.13}$$

The ordinates of the unit hydrographs are derived from the corresponding S-curves (SH1 and SH2). These curves are calculated as:

$$\text{For } 0 \leq t \leq x_4 : \quad SH1(t) = \left(\frac{t}{x_4} \right)^{\frac{5}{2}} \quad \text{Eq.I.14}$$

$$\text{For } 0 < t \leq x_4 : \quad SH2(t) = \frac{1}{2} \left(\frac{t}{x_4} \right)^{\frac{5}{2}} \quad \text{Eq.I.15}$$

$$\text{For } x_4 \leq t \leq 2x_4 : \quad \text{SH2}(t) = 1 - \frac{1}{2} \left(2 - \frac{t}{x_4} \right)^2 \quad \text{Eq.I.16}$$

Where j is an integer between 1 and the maximum number of ordinates, n and m , for $UH1$ and $UH2$, respectively. If $0.5 \leq x_4 \leq 1$; $UH1$ has a single ordinate equal to one and $UH2$ has only two ordinates. Figure I.9 shows an example of unit hydrograph ordinates for $x_4 = 3.8$ days.

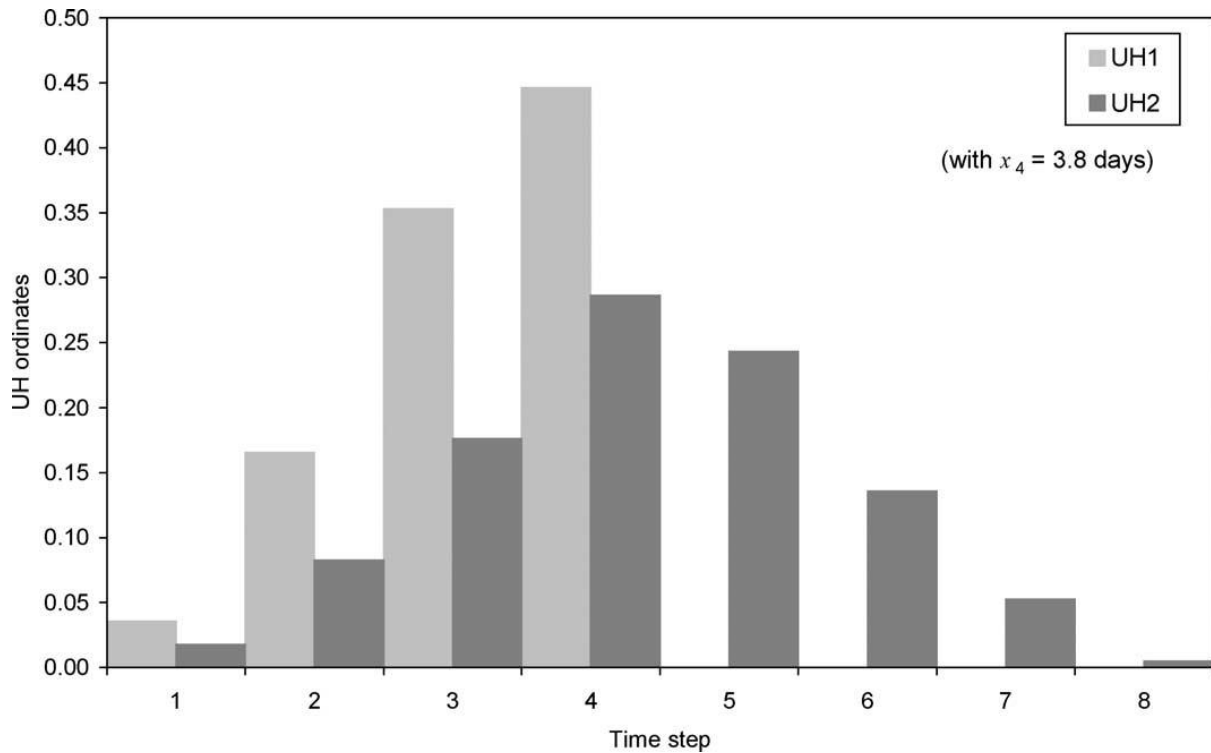


Figure I.9. Example of the ordinates of $UH1$ and $UH2$ for parameter $x_4 = 3.8$ days (Perrin *et al.*, 2003).

A groundwater exchange is highlighted by F which is determined by:

$$F = x_2 \left(\frac{R}{x_3} \right)^{3.5} \cdot \Delta t \quad \text{Eq.I.17}$$

Where R [mm] is the level in the routing store at the beginning of the time step.

The outflow from the routing store gives the first flow component Q_r , and is calculated as:

$$Q_r = R \left\{ 1 - \left[1 + \left(\frac{R}{x_3} \right)^4 \right]^{\frac{1}{4}} \right\} \quad \text{Eq.I.18}$$

Q_r is always lower than R ; as shown in Figure I.10.

The hydrograph $UH2$ output provides the direct flow component Q_d , and it calculated as:

$$Q_d = \max(0; Q_1 + F) \quad \text{Eq.I.19}$$

The total streamflow is the sum of the two flow components ($Q_r + Q_d$) (Ficchi, 2017).

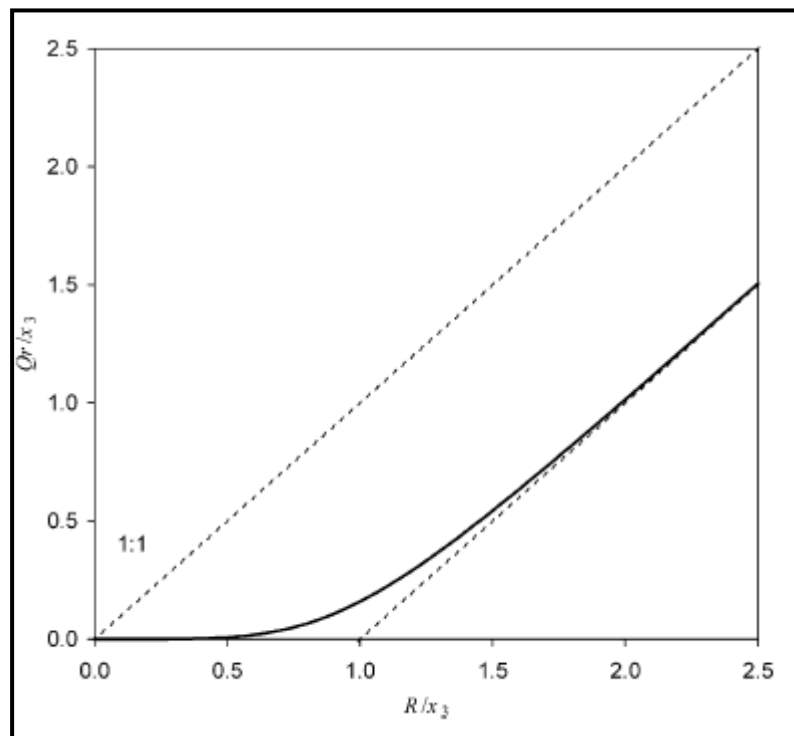


Figure I.10. Illustration of the outflow Q_r from the routing reservoir as a function of the level in the store after the introduction of input Q_9 (Perrin *et al.*, 2003).

I.8.1.4. Calibration and validation

The calibration performance is based on choosing best sets of model parameters which has better response at the outlet (Madsen *et al.*, 2002), where their numerical values are adjusting manually or automatically within a range of selected values on based the knowledge of the hydrology in the respective area, literature values or measurements (Fischer, 2013; Xu, 2002). Which is leading to an optimal match between modeled variables and concurrent observations, with the estimation of the error between this two variables (Legates and McCabe, 1999). In the beginning of the calibration, One year for model warm-up can be used (Chiew and McMahon, 1994). The evaluation of the calibration is done by the validation process by checking the reproducibility of the results by the calibrated parameters, with new data set not used for the calibration phase of the same basin. The validation of models is also based on some statistical evaluation criteria (Nash and Barsi, 1983) such as the Nash-Sutcliffe, r^2 , and bilan. The application of hydrologic model can be successful depends on better performance of the both calibration and the validation (Kumar, 2011).

I.8.2. The HBV light model

I.8.2.1. Introduction

The HBV-model (Hydrologiska Byrans Vattenbalansavdelning)(Bergström, 1976; Linde, 2008) has several versions, the developed version was at Uppsala University in 1993 and has become widely used in education at several universities and for many researches (Konz & Seibert, 2010; Seibert & Beven, 2009; Steele-Dunne *et al.*, 2008; Seibert & Marc,

2012), The newest version of HBV light was reprogrammed in collaboration with M. Vis (2010) to transfer the software from the programming language VB6 to VB.NET (Seibert und Vis, 2012). HBV light model is a lumped conceptual rainfall-runoff model and was developed by the SMHI (Swedish Meteorological and Hydrological Institute) in 1972. It has become widely used for runoff simulations in such different climatic conditions as for example Sweden (Bergström, 1990, 1992). Moreover, the model has been applied in more than 30 countries all over the world such as (Normand et al., 1970; Seibert, 2005; Grillakis et al., 2010; Masih et al., 2010; Dakhlaoui et al., 2012; Nauditt et al., 2017; Reynolds et al., 2017; Reynolds et al., 2017). This model is normally run with input data on daily values of rainfall and air temperature, and daily or monthly estimates of potential evapotranspiration (Seibert, 2002). The HBV light version 2.0 which is used in the current research provides two options, the first one is the possibility to include observed groundwater levels into the analysis and the second is the possibility to use a different response routine with a delay parameter. As shown in (fig.I.11), the model can be distinguished as four components: snow, soil, groundwater (or response) and routing routine.

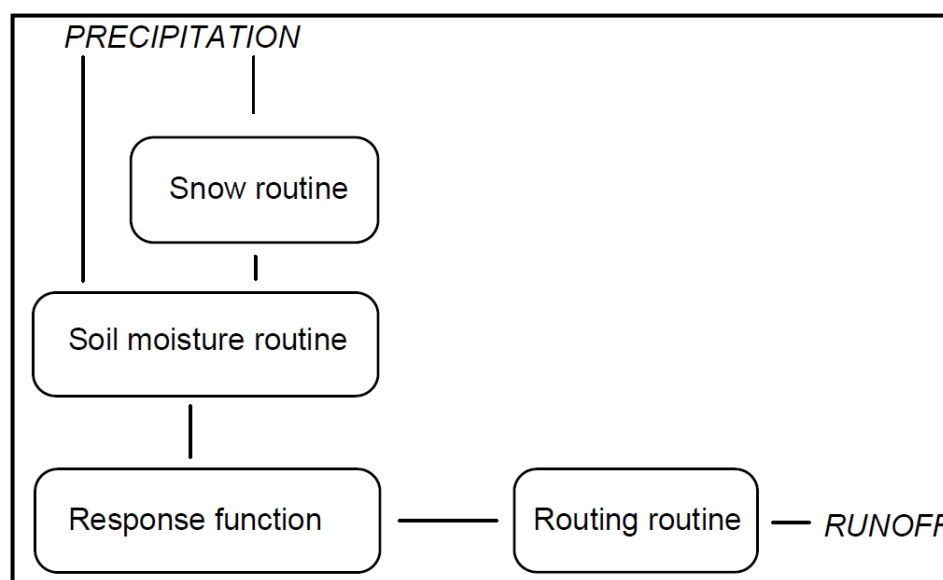


Figure I.11. Schematic structure of the HBV model (Seibert, 2005).

I.8.2.2. Mathematical Description

The model consists of different routines as follow:

- The snow routine snow accumulation and snowmelt are computed by a degree-day method and it was calculated as:

$$\text{meltwater} = \text{CFMAX} (T - \text{TT}) \text{ (mm day-1)} \quad \text{Eq.I.20}$$

Where CFMAX is degree-day factor ($\text{mm } ^\circ\text{C}^{-1} \text{ day}^{-1}$), TT is threshold temperature ($^\circ\text{C}$). CFMAX varies normally between 1.5 and 4 $\text{mm } ^\circ\text{C}^{-1} \text{ day}^{-1}$ (in Sweden), and between 2 and 3.5 in forested and open landscape respectively (fig.I.12).

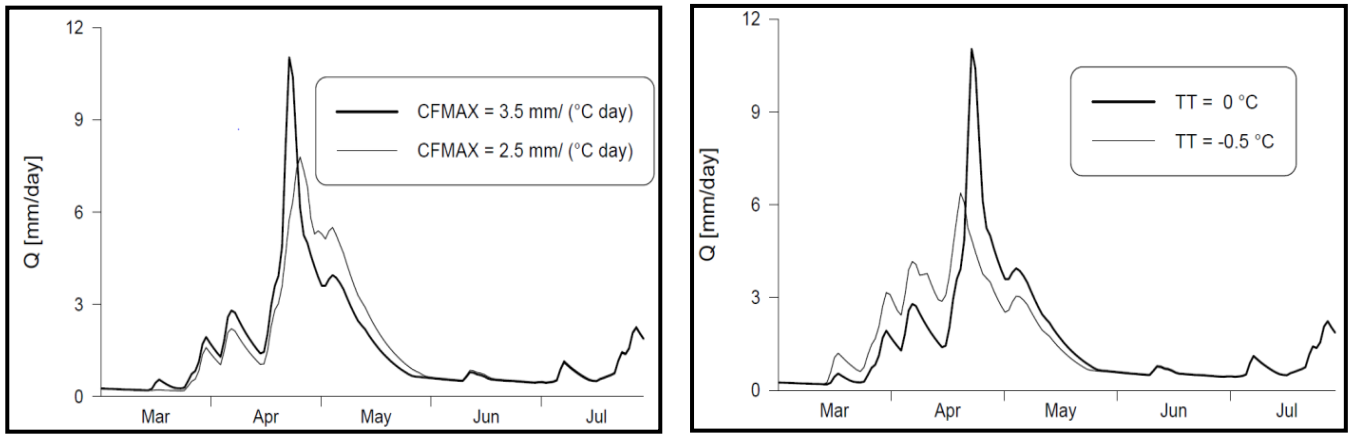


Figure I.12. Example of simulations with different values for CFMAX and TT (Seibert, 2005).

- The soil routine groundwater recharge and actual evaporation are simulated as functions of actual water storage (fig.I.13), and explained as:

$$\frac{recharge}{P} = \left(\frac{S_{Sm}}{FC}\right)^{BETA} \quad \text{Eq.I.21}$$

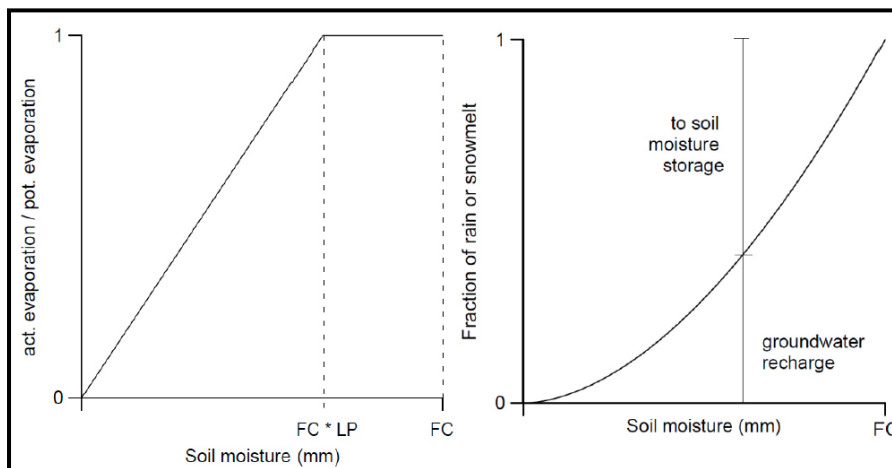


Figure I.13. Soil routine: Left: Reduction of potential evapotranspiration depending on soil moisture storage. Right: Contribution from rainfall to soil moisture storage and groundwater recharge. Response routine (Seibert, 2005).

Where FC is maximum soil moisture storage (mm), LP is soil moisture value above which ET_{act} reaches ET_{pot} (mm), and BETA is parameter that determines the relative contribution to runoff from rain or snowmelt.

- The response (or groundwater) routine, runoff is computed as a function of water storage. And the simple description of a function is as follow:

$$Q(t) = k \cdot S(t) \quad \text{Eq.I.22}$$

S is storage (mm), Q is outflow (mm day⁻¹), t is time (day), k is storage (or recession) coefficient (day⁻¹) (fig.I.14).

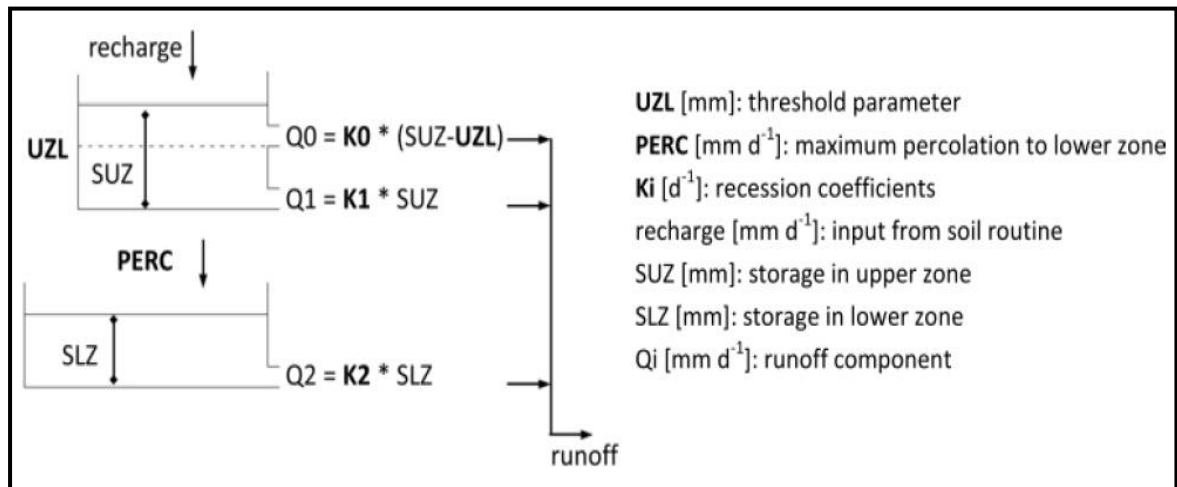


Figure I.14. Response function (Seibert, 2005).

- The routing routine a triangular weighting function is used to simulate the routing of the runoff to the catchment outlet. And it is defined by the parameter MAXBAS to give the simulated runoff $Q_{Sim}(t)$ [mm d⁻¹], where Q_{GW} is groundwater runoff (fig.I.15):

$$\left\{ \begin{array}{l} Q_{Sim}(t) = \sum_i^{MAXBAS} C_i Q_{GW}(t - i - 1) \\ C(i) = \int_{i-1}^i \frac{2}{MAXBAS} - \left| u - \frac{MAXBAS}{2} \right| \frac{4}{MAXBAS^2} du \end{array} \right\} \quad \text{Eq.I.23}$$

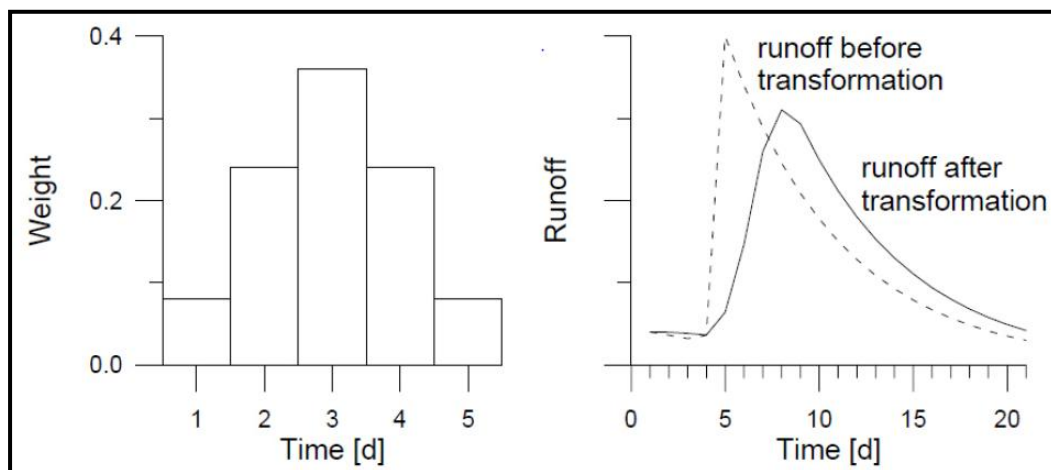


Figure I.15. Routing routine (Example of runoff transformation with MAXBAS=5)(Seibert, 2005).

HBV light uses one year of warm-up period which is sufficient for evolving from standard initial values to their appropriate values according to meteorological conditions and parameter values(Seibert and Vis, 2012; Bouguerne, 2017, Seibert, 2005).

They are various of fundamental parameters in the HBV model, which are threshold temperature TT, maximum soil moisture storage capacity (FC), evapotranspiration limitation (LP), snowfall correction factor (SFCF), Meltwater and rainfall is retained within the snowpack until it exceeds a certain fraction(CWH), threshold value (UZL), the velocity of water flowing up through the soil due to capillarity force (CFLUX), the velocity of water flowing down due to the natural percolation process (PERC), the coefficient for subsurface discharge (Kf), the coefficient for groundwater discharge (K4), the power coefficient for subsurface discharge (a), and the power coefficient for recharge and percolation (b), If different elevation zones are used the changes precipitation and temperature with elevation are calculated using the two parameters (PCALT) and (TCALT), and a correction factor(CET), and for the parameter(MAXBAS), which is transformed the runoff to give the simulated runoff by a triangular weighting function. These parameter are useful due to their physical based (Rusli *et al.*, 2015, Seibert, 2005). The general water balance is described as in Equation I.24:

$$P - E - Q = \frac{d}{dt} [SP + SM + UZ + LZ + Lakes] \quad \text{Eq.I.24}$$

Where; P = precipitation, E = evapotranspiration, Q = runoff, SP = snow pack, SM = soil moisture, UZ= upper groundwater zone, LZ =lower groundwater zone, Lakes = lake volume (Wilk *et al.*, 2001).

The variables in the soil box are calculated with the following equations:

$$EA = \frac{SM}{LP} EP \quad \text{Eq.I.25}$$

$$R = P \frac{SM_0^\beta}{FC} \quad \text{Eq.I.26}$$

$$CF = CFLUX \frac{FC - SM}{FC} \quad \text{Eq.I.27}$$

$$SM = SM_0 + P + EA + FC \quad \text{Eq.I.28}$$

Where EA is the actual evapotranspiration (mm), EP is the potential evapotranspiration (mm).

The upper response box equations are calculated as follows:

$$PC = PERC \frac{SM^\beta}{FC} \quad \text{Eq.I.29}$$

$$Q_{uz} = K_f h_{uz}^{\alpha+1} \quad \text{Eq.I.30}$$

$$h_{uz} = h_{uz0} + R - CF - PC + Q_{uz} \quad \text{Eq.I.31}$$

Where R is recharge from the soil box, CF is capillarity (output) to the soil box, huz0 is an initial water depth, PC is percolation of the outflows from the upper response box, Quz is sub-surface discharge of the lower response box, where huz is the water depth in the upper layer.

The formulas involved in the lower response box are as follows:

$$Q_{lz} = K_4 h_{lz} \quad \text{Eq.I.32}$$

$$h_{lz} = h_{lz0} + PC - Q_{lz} \quad \text{Eq.I.33}$$

$$Q_t = Q_{uz} + Q_{lz} \quad \text{Eq.I.34}$$

Where Q_{lz} Groundwater discharges, Q_t is total flow at the basin outlet (Rusli *et al.*, 2015).

I.8.2.3. Parameters of the HBV light model

The tables I.3, I.4 show the parameters and their ranges used for sensitivity analysis and calibration as follow.

Table I.3. Catchment parameters (Rusli *et al.*, 2015).

Name	Unit	Valid range	Description
PERC	mm/d	[0,inf)	Threshold setting
Alpha	-	[0,inf)	Coefficient of non-linearity
UZL	mm	[0,inf)	Threshold setting
K0	1/d	[0,1)	Storage (or recession) coefficient 0
K1	1/d	[0,1)	Storage (or recession) coefficient 1
K2	1/d	[0,1)	Storage (or recession) coefficient 2
MAXBAS	Δt	[1,100]	Triangular function weighting length
Cet	1/°C	[0,1]	Potential correction factor for evaporation
PCALT	%/100m	(-inf,inf)	Changes in precipitation with altitude Variables
TCALT	°C/100m	(-inf,inf)	Variation of temperature with altitude Variables
Pelev	m	(-inf,inf)	Elevation of precipitation data in PTQ files
Telev	m	(-inf,inf)	Elevation of temperature data in PTQ files
PART	-	[0,1]	Part of the recharge that is added to the groundwater box
DELAY	d	[0,inf)	Period of time during which the recharge is distributed

Table I.4. Vegetation parameters (Rusli *et al.*, 2015).

Name	Unit	Valid range	Description
TT	°C	(inf,inf)	Threshold temperature
CFMAX	mm/d°C	[0,inf)	Degree factor- Δt
SFCF	-	[0,inf)	Snowfall correction factor
CFR	-	[0,inf)	Freeze coefficient
CWH	-	[0,inf)	Water retention capacity
CFGlacier	-	[0,inf)	Glacier correction factor
CFSlope	-	(0,inf)	Slope correction factor
FC	mm	(0, inf)	Maximum soil storage humidity
LP	-	[0,1]	Soil moisture value above which AET reaches PET
BETA	-	(0,inf)	parameter which determines the contribution relative to runoff from rain or snowmelt

The goal of the HBV model is to provide an easy to use and educational tool to for research purposes and hydrological problems (Seibert, 2005) such as compute hydrological forecasts, for the computation of design floods or for climate change studies.

I.8.2.4. Calibration and validation

The calibration of the HBV model is usually done manually by adjusting the values of the model parameters: The selection of the model parameters is based on the approaching the hydrological behavior of the basin by the model simulation, through achieving the best possible agreement between the calculated flow and observed flow, which is based on different criteria like visual inspection of plots with Q_{Sim} (simulated flow) and Q_{Obs} (observed flow) and appraise the adjustment (the Nash-Sutcliffe efficiency coefficient (NSE), Coefficient of determination). Validation of model is confirmation of the goodness-of-fit of the model, which is basically a test of model performance with calibrated parameters for an independent time period (Rusli *et al.*, 2015; Seibert, 2005).

CHAPTER TWO
PRESENTATION OF THE STUDY AREA

II.1. Introduction

Hydrology deals with the occurrence, movement, and storage of water in the earth system, where the rainfall plays important role in alimentary rivers and groundwater, and it is transported through other processes, such as the atmosphere, land surface, and the subsurface, and part somewhat is temporarily stored in soil, vegetation cover, lakes, and oceans.

Hydrology uses physical sciences (meteorology, physics of the globe), natural sciences (geology, geomorphology), mathematics (statistics, operational calculation, computer science) and technology (measuring device, remote sensing) for understanding the complex processes involved and estimating the quantity and quality of water in the various phases and stores. Where the hydrology studies are important science for researchers in the exploitation and control of natural waters or for any implementation of any development or hydraulic projects. The response of a basin is based on several factors such as geology, topography, and land use. For this purpose, in this chapter, we present a comprehensive view of the geography, geology, hydrogeology, and the main physical characteristics of the five sub basins of the Tafna basin.

II.2. Presentation of the study area

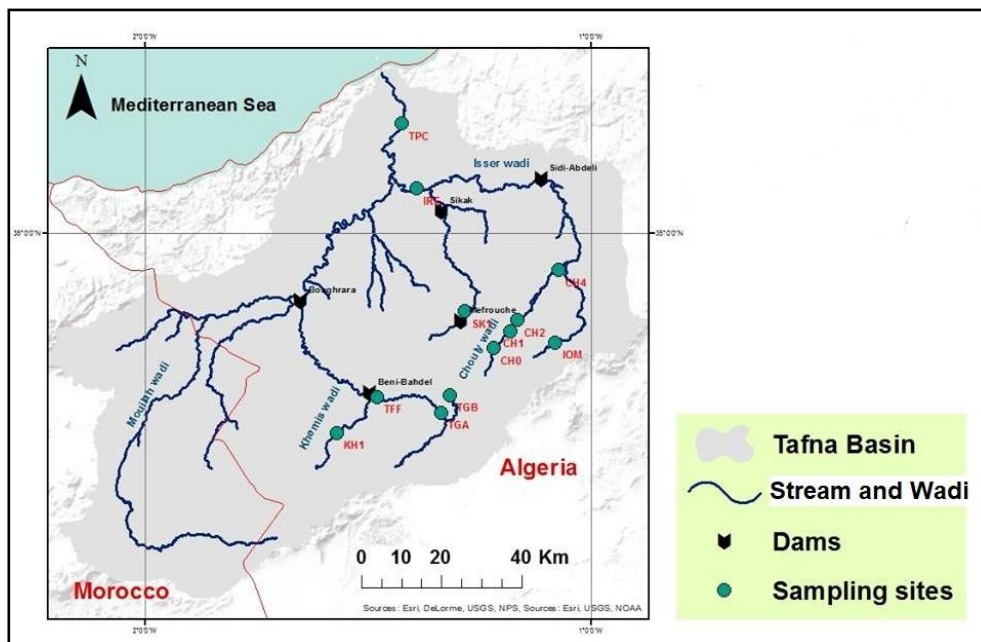
II.2.1. Tafna basin

The Tafna basin is a transboundary basin covering an area of 7245 km². The biggest part of its area is located in the Northwest of the Algerian territory (Wilaya of Tlemcen) and the upper part on the territory of Morocco. According to the new structure of Hydro geological units in Algeria, the Tafna basin belongs to the entire Oranie-Chott-Chergui (Bouanani, 2004). It bears the code 16 of the 17 basins of Algeria (fig.II.1).

It extends between 1° to 2° west longitude and 34° 5' to 35° 3' north latitude (Bouanani, 2004) and consists of eight sub basins in which two are located upstream in the Moroccan territory (2007 km² which is around 27.7% of the total area) (Ketrouti et al., 2012). The Tafna basin features a very rugged terrain with an average altitude of 780 m above the mean sea level (a.m.s.l.) and a maximum altitude exceeding 1800 m (a.m.s.l.).



a)



b)

Figure II.1. Geographical location of the Tafna basin:(a) Large Northern basins in Algeria, (b) Tafna basin(Mekhloufi, 2014; Benhadji et al., 2020).

II.2.2. Geomorphologic context

The Tafna basin is delimited in the South by the main relief of the Tlemcen Mountains which characterized by an abrupt relief with slopes greater than 25%, and in the North by the Mediterranean Sea and the high Oran plains and valley, and to the West by the Moroccan Middle Atlas,Traras mountains, and Plain of Maghnia, While in the East by the plain of Sidi Bel Abbes.

The Geomorphologic maps of the Tafna basin are taken from the Hydrographic basin agency of Oran (ABH) (Map N° 07) at scale 1 / 500 000 (fig.II.2). This study is based on research carried out by Bouanani (2004) and Adjim (2004):

II.2.2.1. Mountainous areas

The Tafna is occupied in its center by plains and depressions and is surrounded in the north, south, and north west by mountainous areas. These areas are represented by:

- The Traras Mountains: it is a coastal mountain range located in the northwest of the basin with area around 1250 km². This area is characterized by steep slopes, and they correspond to the series of ridges in a NE-SW direction, its average altitude varies from 500 to 1000 m with height level at Djebel Fillaoucène which is characterized by the forest cover. This mountains area constitutes a barrier between the basin and the sea.
- The mountains of Tlemcen: it is a mountain range located in the southern border of basin with area of 3000 km² to extend west of Moroccan and east to the Tessala Mountains (Sidi Bel Abbas). They have a very rugged relief with steep slopes and its average altitude varies between 1200 and 1500 m with the culminate at 1843 m in Djebel Tenouchfi. It is relatively well watered with rainfall varying from 500 to 700 mm / year.
- The Sebâa Chioukh Mountains: This is mountain range located in the Northeast of the basin with area 250 km² with an average altitude of between 600 and 800 m. It forms the extension of the east side of the Traras Mountains; its reliefs have slopes exceeding 25%.

II.2.2.2. The plains and plateaus areas

The interior plains and plateaus occupy the central part of the basin, surrounded by mountainous areas. We distinguish:

- The Maghnia plain: It is limited in the north and northeast by the Traras Mountains and the south by the Tlemcen mountains, while in the west by a natural extension of the plain of the Angad (Morocco), which is largely covered with very fertile silts. The soils of the plain are limited in depth by limestone crusts.
- The Hennaya plain: it is bounded to the south by the northern foothills of Tlemcen and to the north by the Zenata plateau; its deposits are formed from recent alluvium.
- Zenata - Ouled Riah plateau: it is located northwest of the Hennaya Plain. It consists of red Mediterranean soils resting on crusts or sometimes on the limestone shell; the texture of the soil is clayey-silty.
- Sidi Abdelli - Ain Nahala plateau: it is made up of brown limestone soils containing clay, and it is located on the right bank of the Oued Isser north of Ouled Mimoun. In the summer, the structure of the soil experiences an elevation of large cracks due to the variation in humidity.

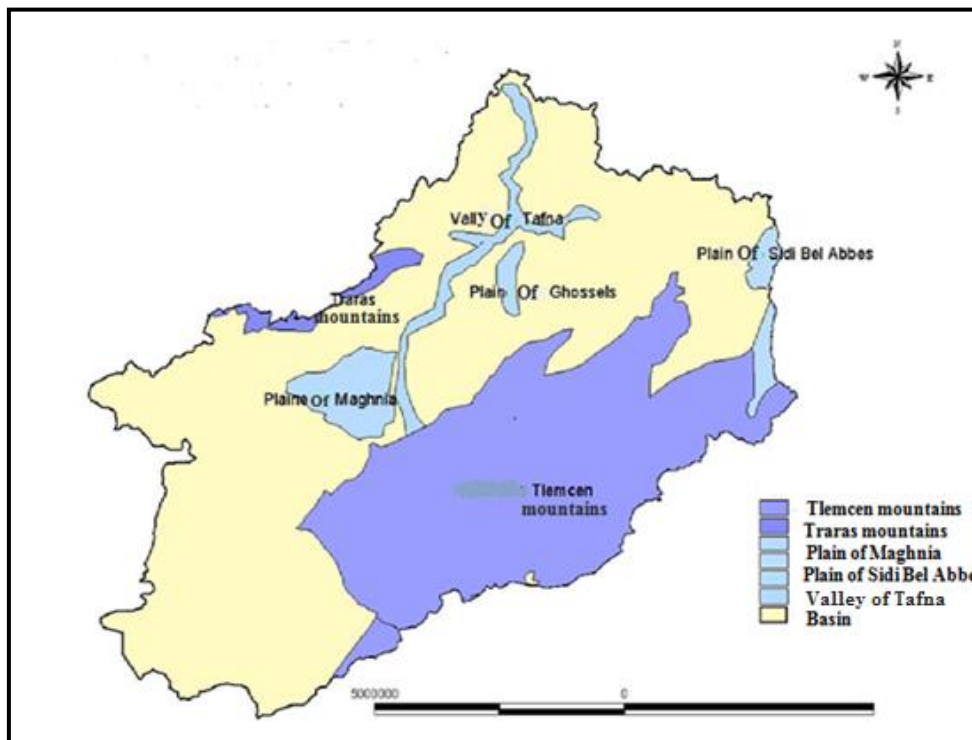


Figure II.2. Geomorphologic context of the Tafna basin (ABH, 2006).

II.2.3. Geology

The Tafna basin is characterized by two large plains which are the plain of Maghnia in the west and those of the Ghossels in the east surrounded by high mountains, such as the Traras massif including the Fillaoucène chain, and the Tlemcen mountains, which its western part is occupied by the Rhar Roubane mountains, and it is crossed between the aquifers in north, and the high Oran plains in the south.

The basin is characterized by a very complex geology and great tectonics, which is evaluated from Primary to Plio-Quaternary (Bouanani, 2004).

a) The primary: the land in this section is characterized by the presence of a schisto-quartzite formation of Silurian to Devonian age, which appear in the basin of the Oued Mouilah at Ghar-Roubane Mountains to the west and the Fellaoucene to the east.

b) The secondary: It is occupying a large part of the basin and the Tlemcen Mountains. The lithostratigraphic series is represented by:

Trias: it is located mainly north of Aïn Tellout and at Beni Bahdel and to the east in the Oued Mouilah basin.

Jurassic: it is composed of the lower and middle Jurassic and which appear in Ghar-Roubane. The Upper Jurassic is represented by the limestones of Zarifet and Lato, the dolomites of Tlemcen and Terny and finally the marl-limestones of Ouled Mimoun, Raourai and Hariga;

Cretaceous: the Lower Cretaceous series is forming the clays of Ouled Mimoun and Sebdu, the clays of Lamoricière and the sandstones of Berthelot.

c) The Tertiary sector: It comprises:

Eocene: this formation is composed by the siliceous sandstones, yellow to reddish with greenish clay marls and occupying the valley of the Isser, near the confluence with the Oued Tafna in the Sebâa Chioukh massif.

The lower Miocene: it is composed of very resistant dolomitic limestone elements with calcareous-sandstone cement. The formation is located between the valley of the Oued Zitoune and the Djebel Fellaoucène.

Middle Miocene: It consists essentially of a thick series of gray or bluish marly clays, well represented at 4 km east of Hammam Boughrara.

Upper Miocene: the formation is located between Tlemcen and Remchi, in the Sikkak basin, and in the north and south of the Maghnia plain in the Mouilah basin. It consists by deposits of hard sandstone, golden yellow or lemon, poorly consolidated.

d) The Plio-Quaternary: This series is a complex and consists discontinuous deposits formed from heterometric and heterogeneous elements, represented by villafranchian travertines located in the Tlemcen mountains, and the silts, sands and gravels which extend between wadi Mehaguène and Chaâbet El Arneb in the North East of the Algerian-Moroccan border, while marl with little or no pebbles is appear in the wadi Mouilah basin, and old alluvium from greenish alluvial marls to pebbles is exist in the main valleys of the basin (Bouanani, 2004). The Geology maps of the Tafna basin (fig.II.3) is taken from National Agency of Hydraulic Resources (ANRH) (2nd edition) at scale 1 / 500 00 and Bouanani thesis, 2004.

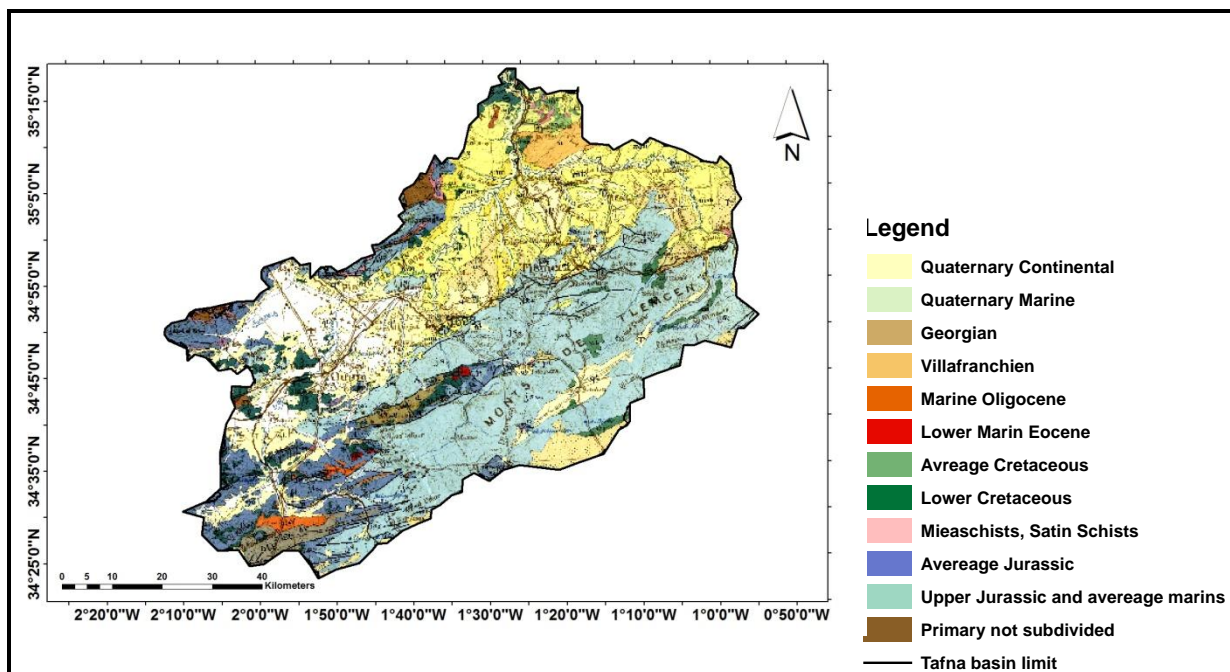


Figure II.3. Geological context of the Tafna basin.

II.2.4. Hydrographic network

The Tafna hydrographic network is characterized by a large set of valley and Permanent or temporary wadi (fig.II.4).

Overall, the geomorphologic of the Tafna basin is subdivided into three main parts:

- Eastern part with as main tributaries the valley of Isser and valley of Sikkak,
- Western part including the upper Tafna (wadi Sebdu and wadi Khemis) and wadi Mouilah,
- Northern part which begins at the village of Tafna and continues until its outlet at Rechgoune. The Boukiou, Boumessaoud and Zitoun valleys are the main tributaries of this part.

The plains of the Tafna basin extend to the piedmont of the Tlemcen mountains in front of the Traras and Tessala massifs; they are surrounded by massifs with high reliefs forming a regular edifice consisting mainly by Mesozoic and Cenozoic formations.

The Traras Mountains in the North West constitutes a barrier between the basin and the sea, they correspond to a series of NE - SW direction ridges culminating at 1136 m at Jebel Fillaoucène.

The main stream of the Tafna measuring 170 km has its source in the Tlemcen mountains (Sebdu region).

Geomorphologically the Tafna basin can be subdivided into three parts:

The Upper Tafna: (western part) includes wadi Sebdu, wadi Khemis and wadi Mouilah.

The middle Tafna: (eastern part) including the main tributaries wadi Isser and wadi Sikkak.

The lower Tafna: it started from the village of Tafna and extends to the outlet of the Tafna on the sea (Rechgoune beach). The Boukiou, Boumessaoud and Zitoun wadis are the the important tributaries of this part.

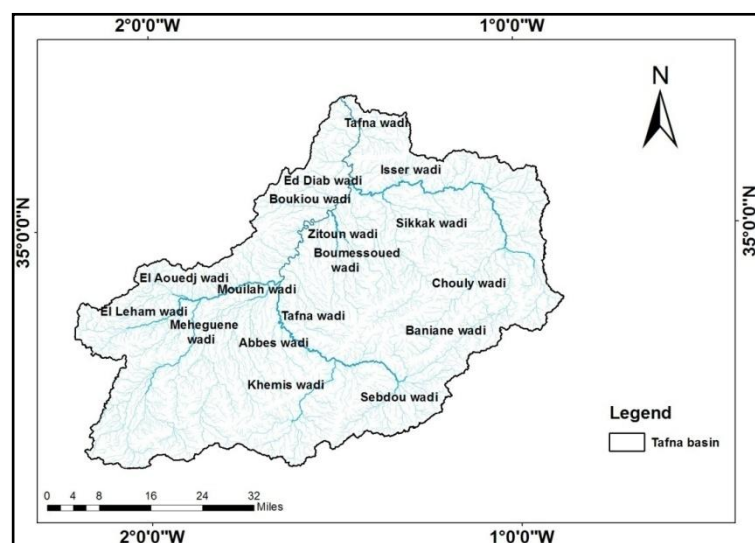


Figure II.4. Hydrographic network of The Tafna basin.

II.2.5. Altitude, dams, and Hydro- climate stations

The topography of Tafna basin is described by modeling the altitude through the processing of the digital terrestrial model (MNT) with an accuracy of 30 m in ArcGIS and obtaining a map of the altitude with variation in the western north to eastern north between 4 to 450 m, and altitude is occupying with 680 to 1773 m in the south area.

The basin is characterized by a semi arid climate with two predominant seasons. A wet season runs from October to May with fairly irregular rains, the dry season runs from June to September with low rainfall. It has 27 rainfall stations distributed across the sub basins included in our region, and 17 Hydrometric stations (fig.II.5) (tab.II.1).

The Tafna basin contains five large dams in service: Beni Bahdel dam, Meffrouche dam, Sidi Abdelli dam, Hammam Bouhrara dam, and Sikkak dam. The Souani dam reserve is intended to receive the excess of the Beni Bahdel dam estimated overtime at around 14 Hm³. With a capacity of 13.8 Hm³ (tab.II.2) (ANAT, 2000; Rouissat, 2016).

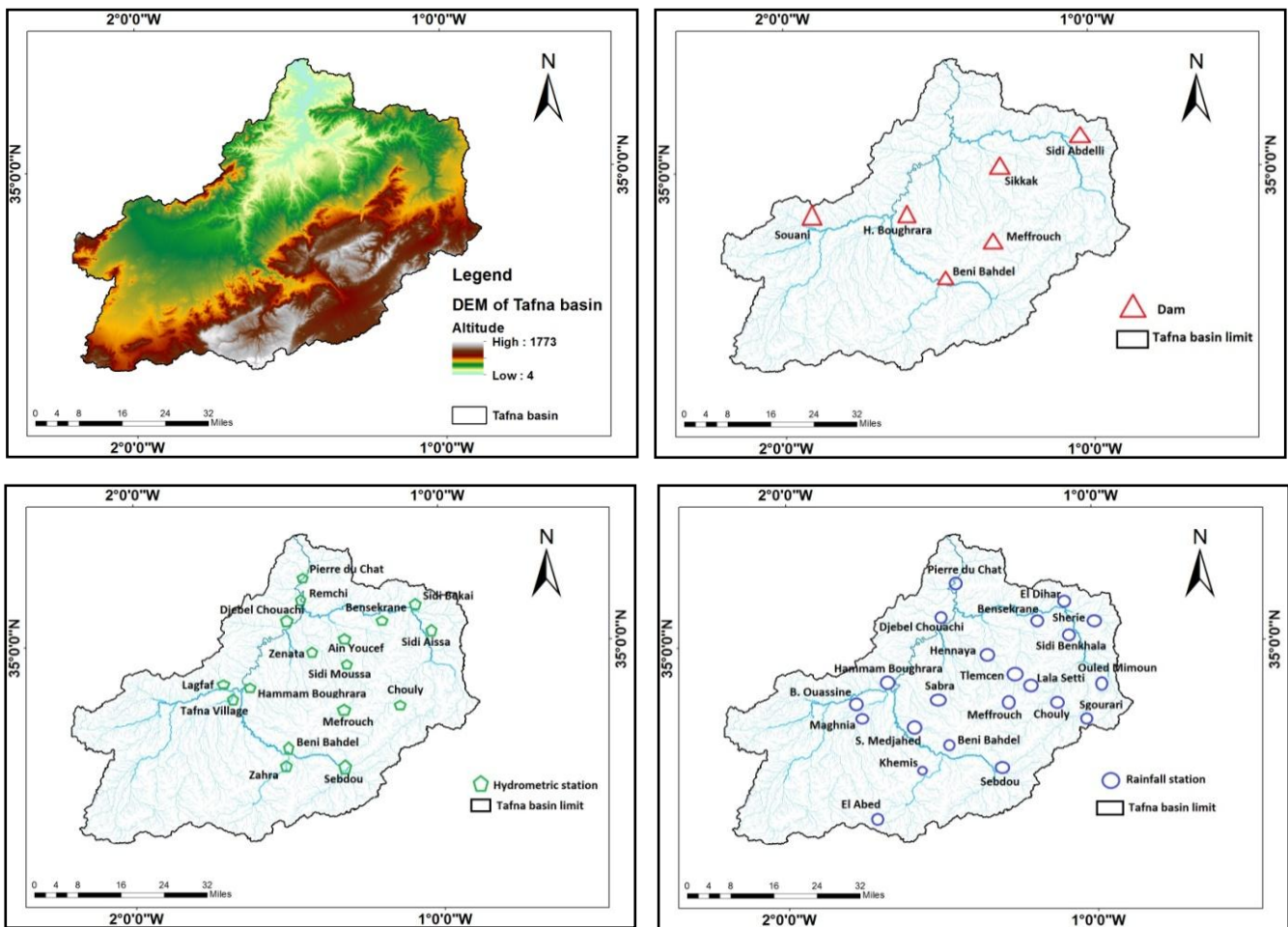


Figure II.5. DEM, and Dams, Hydro-Climat stations in the Tafna basin.

Table II.1. Rainfall stations of Tafna basin.

Code S/B	Denomination	Number of rainfall stations
1603	Mehaguène valley	4
1604	Tafna Upstream	7
1605	Tafna Boukiou	4
1606	Isser Cedra	8
1607	Isser Sikkak	3
1608	Tafna Maritime	1
Total	-	27

Table II.2. Dams of the Tafna basin (Rouissat, 2016).

Dam	Notations	Valley	Year of service	Total volume (Hm ³)
Beni Bahdel	BBB	Tafna	1952	63
Meffrouch	BM	El Nachef	1963	20
Sidi Abdelli	BSA	Isser	1988	106
Hammam Boughrara	BHB	Tafna	1999	175
Sikkak	BS	Sikkak	2004	30
Souani	BRS	-	1992	13.8
Total = 394 Hm³				

Our study area consists of five sub basins belonging to part of the Tafna basin located only in the Algerian territory (fig.II.6).

II.2.6. Presentation of Study sub basin of the Tafna basin

II.2.6.1. Geographic situation

The Geographic analysis of the sub basins of the Tafna basin is taken from map of the National Agency of Hydraulic Resources (ANRH) at scale 1/ 200, 000 which established by the National Geographical Institute, Paris, France (1961).

II.2.6.1.1. Upstream Sebdou sub basin

The Upstream Sebdou sub basin is part of the upper Tafna basin which also considered as important source to supply the basin (under code N° 1604, according to subdivision of the National Agency for Water Resources ANRH), it is limited in North by the

Titmokhen plateau, and to South by Djebel Lato, Si Abdellah, Maiter, Zninia, Toumiet and Koudiat el Harcha, and in the East, by Djebel Mazoudjène, Djebel El Ahmer, and Djebel el Arbi, to the West by the Azails plateau. It extends between the North latitude $34^{\circ} 7'$ and $34^{\circ} 5'$ and the East longitude $1^{\circ} 1'$ and $1^{\circ} 9'$. At its end, it flows into Beni Bahdel valley, taking in consideration the only basin controlled by hydrometric station of Seb Dou.

II.2.6.1.2. Khemis sub basin

The Khemis sub basin is part of the upper Tafna basin (under code N° 1604, according to subdivision of the National Agency for Water Resources ANRH), it extends between the North latitude $34^{\circ} 7'$ and $34^{\circ} 5'$ and the East longitude $1^{\circ} 5'$ and $1^{\circ} 8'$. The main tributaries in this sub basin is Khemis wadi. It delimited in south to East by Djebel Tenouchfi and Djebel Kerrouch, and in West by Djebel Tissefsafine, and in the North by Beni Bahdel Dam.

II.2.6.1.3. Wadi Boumessaoud sub basin

Wadi Boumessaoud sub basin is located in the northernmost part of the Tafna between longitudes $1^{\circ} 3'$ and $1^{\circ} 4'$ W, and latitudes $34^{\circ} 8' 15''$ and 35° N. The sub basin is limited to the east by the sub-basin of the Sikkak, to the west by the Mouilah sub-basin, to the south by Djebel Taksemt and Djebel Tefatisset (867 m). The small valleys which fuel the sub basin are occupying the heights of the Terny plateau to the east of the Zarifet forest, at Djebel Tamesguida (1154m), and Djebel Fernane (1150m).

II.2.6.1.4. Chouly sub basin

The Chouly sub basin is a part of the middle Tafna with the presence of a series of mountain ranges (Djebel Dar Cheich 1616 m, Djebel Tazkminet 1606m). It is located upstream of Isser wadi between $34^{\circ} 49'$ and $34^{\circ} 7'$ N latitude and between $1^{\circ} 1'$ and $1^{\circ} 3'$ W longitude. It is bounded to the south west by Djebel Rhenndas, Djebel Mehalla and Djebel Diar Ouled Yahia, and to the north east by Djebel Boulaâdour, Djebel Beni Yahia, Djebel Gaât El Hakoud.

II.2.6.1.5. Isser sub basin

The Isser sub basin is a part of the middle Tafna between $34^{\circ} 7'$ and 35° N latitude and between 1° and $1^{\circ} 2'$ W longitude. Its boulder from the south to east by Djebel Asses, and Djebel Bel Alatene, and in the North by Sidi Abdelli dam, while the west by Djebel Er Ramlya.

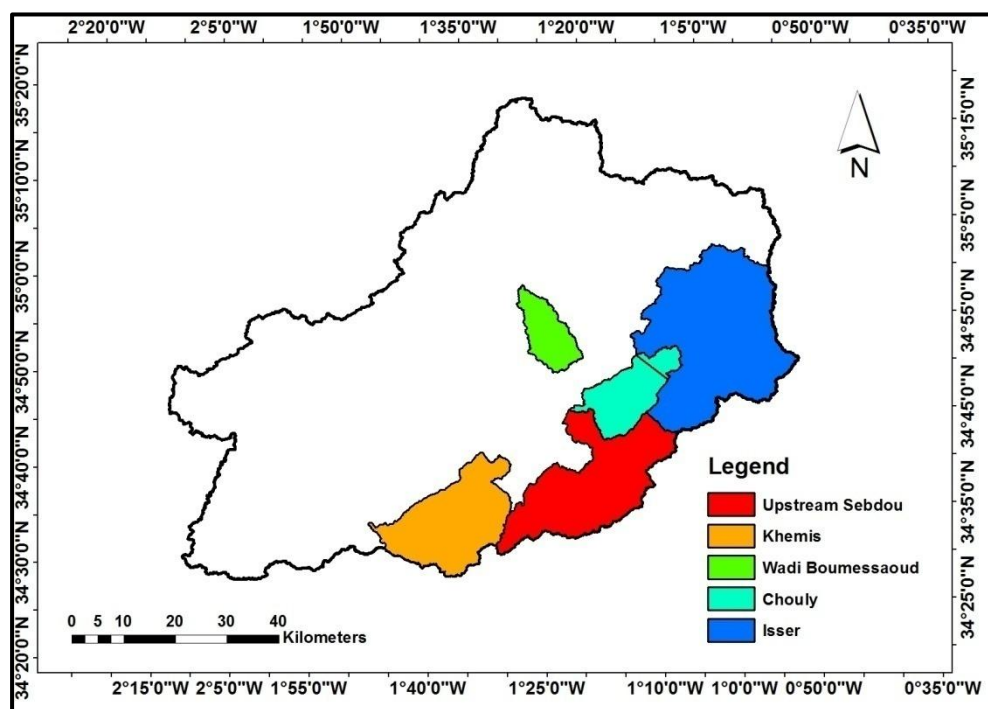


Figure II.6. Geographic Situations of the study area sub basins.

II.2.6.2. Geology preview

The Geology analysis of the study sub basins of the Tafna basin is based on observation of the geology map from National Agency of Hydraulic Resources (ANRH) (2 edition) at scale 1 / 500,00, and the thesis of Bouanani (2004)(fig.II.7).

II.2.6.2.1. Upstream Sebdoou

The Tlemcen Mountains occupy a large area in this sub basin. They are constituted by Mesozoic and Cenozoic formations. We note the predominance of sedimentary formations. Where the sedimentary layers is characterized with highest percentage of average cretaceous with small rate of Upper Jurassic which is mainly made up of limestone marl from Lamoricière and sandstones from Berthelot formations occupying the south part of the basin. The continental Quaternary outcrops in the extreme south.

II.2.6.2.2. Khemis

This area represent the end of Tlemcen mountains range in the south western, such as Djebel Tissefsafine (1484 m), Djebel Maroui (1424 m), and Djebel Moudjahadine (1623 m).

The upper and middle Jurassic appears in the region with Tlemcen dolomites constituting the cliffs. These are crystalline dolomites with cavities filled with calcite like that of Djebel Tefatisset.

II.2.6.2.3. Wadi Boumessaoud

In the south of the basin, the formations of the upper and middle Jurassic emerge, mainly formed by carbonate rocks.

In the North, the Miocene formations rest in discordance on the Mesozoic formations represented by limestones, clays and silts.

II.2.6.2.4. Chouly

The northern part of the basin is occupied by the upper Jurassic formations of the Tlemcen Mountains. They are represented by the limestones of Zarifet, Lato and the dolomites of Tlemcen.

In the southwest, outcrops the middle Cretaceous formed mainly of clay. To the east, the continental Quaternary is represented by alluvial terraces.

II.2.6.2.5. Isser

The upper Jurassic occupies a large part of the basin represented by the limestones of Zarifet and Lato, the dolomites of Tlemcen and Terny.

The Cretaceous appears with the marl-limestones of Ouled Mimoun. While in North, the Villafranchien is represented by alluvium, terraces and greenish clays which occupy the Isser valley.

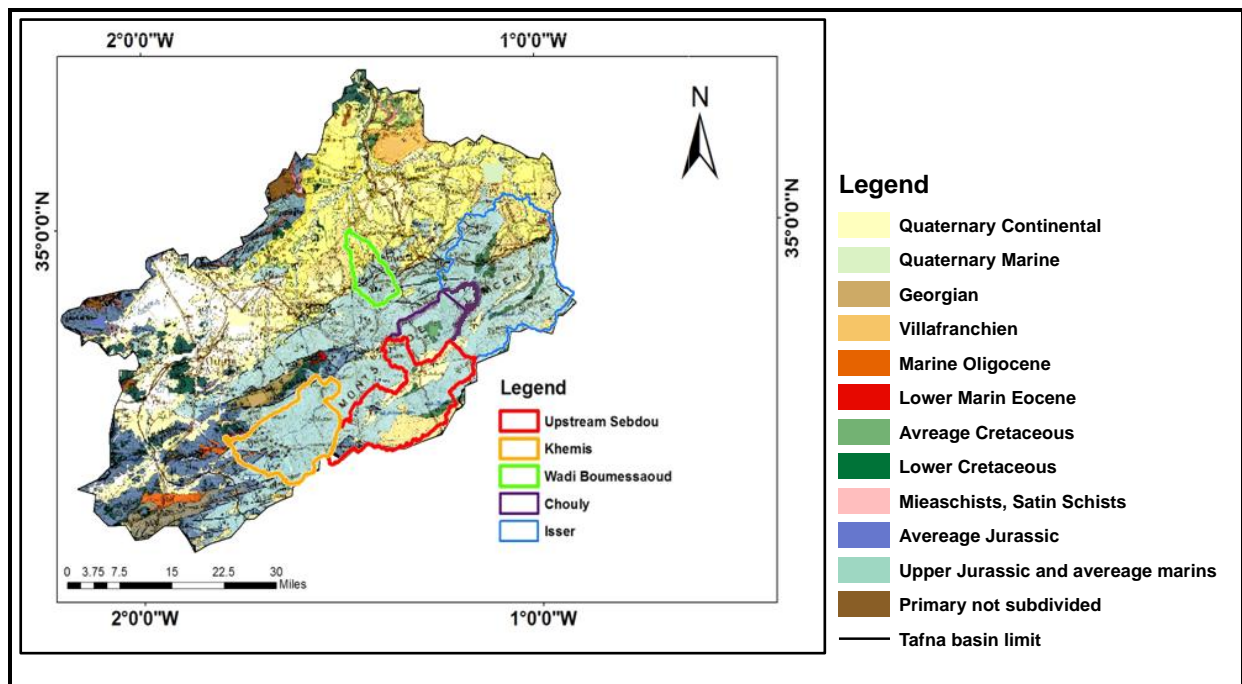


Figure II.7. Geologic map of the study sub basins of the Tafna (ABH, 2006).

II.2.6.3. Potential Aquifer

The limestones and dolomites of the upper Jurassic are the most widespread formations which occupy vast areas in the Tafna basin, offering the best properties and which conceal very important potential aquifers.

The intensity of karstification and cracks, as well as the numerous sources located at the extreme northwest and south of the basin, give these formations a great hydrogeological interest.

The Plio-Quaternary formations which appear along the valley as well the terraces and limestone crusts which fill the Sebdoou ditch and Sidi Aissa (Isser sub basin) show great aquifer capacities (fig.II.8).

The study of the hydrogeological properties of the different formations of aquifers of the study sub basins defined two main types:

- Aquifers drained by a Valley such as Chouly, and Isser Valleys.
- Ante Miocene aquifers located in the North of the Tlemcen mountains. The karstic aquifers are numerous and isolated from each other by formations with low permeability (Jurassic sandstones and Miocene marls), they are defined at Wadi Boumessoued sub basin (Collignon, 1986).

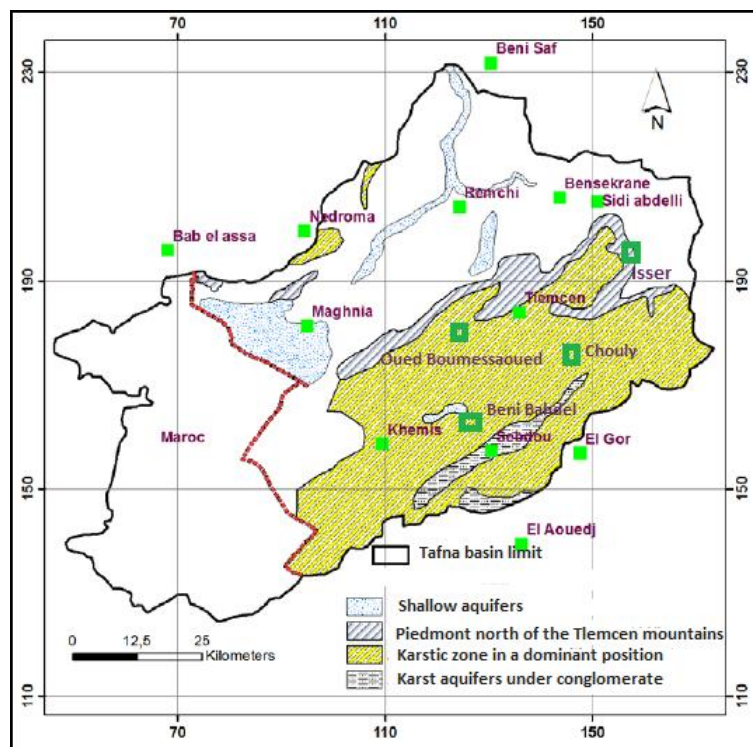


Figure II.8. Potential aquifers of the study area sub basins (Collignon, 1986).

II.2.6.4. Morphometry

The physical characteristics of a watershed play a significant role in understanding flow.

The morphometric analysis is based on the shape, the order of the thalwegs, the relief, and the drainage density, the frequency of the streams, the elongation ratio, and the profile of the streams.

II.2.6.4.1. Shape characteristics

A watershed is the area of reception of the rainfalls and of supplying the watercourse, the outlet flows depending thus on its surface. The surface of a watershed can be measured using a variety of methods: superposing a grid over the watershed map, using a planimeter or digitalizing methods.

The shape characteristics make it possible to determine the physical environment of a basin and facilitate the comparison of several basins between them (tab.II.3).

II.2.6.4.2. Gravelius compactness index (K_c)

The Gravelius coefficient K_c , is defined as the relation between the perimeter of the watershed and that of a circle having a surface equal to that of a watershed (Roche, 1963):

$$K_c = 0.28 \frac{P}{\sqrt{A}} \quad \text{Eq.II.1}$$

K_c : Gravelius compactness index,

P: Basin perimeter (Km),

A: Basin area (Km²).

II.2.6.4.3. Equivalent rectangle

The equivalent rectangle is defined as the rectangle of length (L) and width (I) which has the same area and the same perimeter as the basin, it allows to compare the influence of shape on the flow in the different basins (Roche, 1963).

The dimensions of the equivalent rectangle are given as follow:

- **Length (L)**

$$L = \frac{K_c \sqrt{A}}{1.12} \left[1 + \sqrt{1 - \left(\frac{1.12}{K_c} \right)^2} \right] \quad \text{Eq.II.2}$$

- **Width (I)**

$$I = \frac{K_c \sqrt{A}}{1.12} \left[1 - \sqrt{1 - \left(\frac{1.12}{K_c} \right)^2} \right] \quad \text{Eq.II.3}$$

L: Length of the rectangle (km),

I: Width of the rectangle (km),

K_c : Compactness coefficient.

The area of the study sub basins was measured by digitalization techniques with basin delineation using ASTER Global Digital Elevation Model V003 maps (N36W02W03, and N35W02W03). The area and perimeter of the sub basins was calculated using the ArcGis 10.

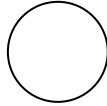

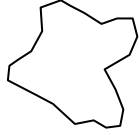


The values of the coefficient of compactness for Khemis, wadi Boumessaoued, and Chouly sub basins are between 1.4 and 1.7 showing elongated basins. On the other hand, for the Upstream Sebdou, and Isser wadi, K_c is greater than 1.7, so their shape is more stretched than the previous ones. They often present amoeboid tendency, which consequently implies a slower response in runoff water.

Table II.3. Shape characteristic of the study sub basins of the Tafna.

Sub Basins	Area (km ²)	Perimeter (m)	K_c	Length (Km)	Width (Km)
Upstream Sebdou	439.30	153.88	2.06	70.73	6.21
Khemis	342.22	104.35	1.58	44.48	7.69
Wadi Boumessaoud	108.76	57.16	1.53	24.06	4.52
Chouly	176.39	78.80	1.66	34.25	5.15
Isser	696.10	164.26	1.74	72.53	9.6

In order to define classes of compactness or shape, Karimou Barké et al. 2017, retained five values of K_c (tab.II.4):

Table II.4. Classes of basin shapes according to the values of the Gravelius index (Karimou Barké et al., 2017).

Shape	Index values	Definition	Stylized diagram
Circular	1 à 1.03	Basin having a circular shape	
Ovoid	1.03 à 1.3	Ovoid basin	
Amoeboid	1.3 à 1.4	Basin characterized by an association of irregular, lobed, amoeboid looking areas, with clear contours very contrasted.	
Stretched	1.4 à 1.7	Elongated basin.	
Very stretched with amoeboid tendency	> 1.7	Basin more stretched than the previous ones. Often presents amoeboid fragments, i. e. lobed contours.	

II.2.6.5. Relief

The relief is an essential factor on understanding the hydrological behavior of a basin. It influences the flow velocity, the infiltration and the evaporation, where many hydrological variables change with altitude (Gherissi, 2018). The relief of the Tafna sub basins is determined by different characteristics.

II.2.6.5.1. Distribution and hypsometric curve

Hypsometric analysis is the study of distribution of the cross-sectional areas of ground surface with respect to its elevations (Strahler, 1952), and it is used to characterize the erosional landforms at their different stages of erosion (Schumn, 1956).

The hypsometric curve allows indicating the stage of erosional cycle for landforms in a watershed where the convex upward hypsometric curve reflects a young basin, S-shaped curve for mature basin and concave upward curve for peneplains (Strahler, 1952).

The curve is presents the distribution of the cumulative area (%) based on the distribution by altitude ranges, thus defining the percentage of the area which represents a certain altitude for each of the sub basins. (tab.II.5, II.6, II.7, II.8, II.9).

Table II.5. Altimetric distribution of the Upstream Sebdou sub basin.

Altitude (m)	Partial Areas		Cumulative areas	
	(km ²)	(%)	(km ²)	(%)
1616-1600	0.01	0.002	0.01	0.002
1600-1500	1.11	0.25	1.12	0.25
1500-1400	8.32	1.89	9.44	2.15
1400-1300	39.64	9.02	49.08	11.17
1300-1200	67.59	15.39	116.67	26.56
1200-1100	124.23	28.28	240.9	54.83
1100-1000	127.38	28.99	368.28	83.83
1000-900	67.8	15.43	436.08	99.26
900-852	3.24	0.74	439.32	100

Table II.6. Altimetric distribution of the Khemis sub basin.

Altitude (m)	Partial Areas		Cumulative areas	
	(km ²)	(%)	(km ²)	(%)
1773-1700	0.12	0.04	0.12	0.04
1700-1600	8.3	2.42	8.42	2.46
1600-1500	28.87	8.43	37.29	10.89
1500-1400	80.85	23.62	118.14	34.51
1400-1300	107.15	31.3	225.29	65.81
1300-1200	53.23	15.55	278.52	81.36

1200-1100	20.29	5.93	298.81	87.29
1100-1000	13.26	3.87	312.07	91.17
1000-900	11.22	3.28	323.29	94.44
900-800	11.12	3.25	334.41	97.69
800-700	6.7	1.96	341.11	99.65
700-654	1.2	0.35	342.31	100

Table II.7. Altimetric distribution of the Wadi Boumessaoud sub basin.

Altitude (m)	Partial Areas		Cumulative areas	
	(km ²)	(%)	(km ²)	(%)
1265-1200	2.22	2.04	2.22	2.04
1200-1100	6	5.52	8.22	7.56
1100-1000	5.43	4.99	13.65	12.55
900-1000	4.59	4.22	18.24	16.77
900-800	13.58	12.48	31.82	29.25
800-700	19.58	18	51.4	47.25
700-600	10.32	9.49	61.72	56.74
600-500	9.28	8.53	71	65.27
500-400	15.13	13.91	86.13	79.18
400-300	18.34	16.86	104.47	96.04
300-212	4.31	3.96	108.78	100

Table II.8. Altimetric distribution of the Chouly sub basin.

Altitude (m)	Partial Areas		Cumulative areas	
	(km ²)	(%)	(km ²)	(%)
1623-1600	0.1	0.06	0.1	0.06
1600-1500	4.58	2.6	4.68	2.65
1500-1400	22.06	12.51	26.74	15.16
1400-1300	57.52	32.61	84.26	47.77
1300-1200	34.62	19.63	118.88	67.4
1200-1100	22.33	12.66	141.21	80.06
1100-1000	14.61	8.28	155.82	88.35
1000-900	9.11	5.17	164.93	93.51
900-800	7.86	4.46	172.79	97.97
800-713	3.58	2.03	176.37	100

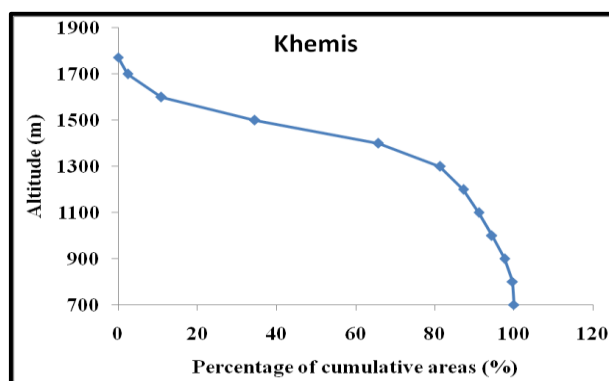
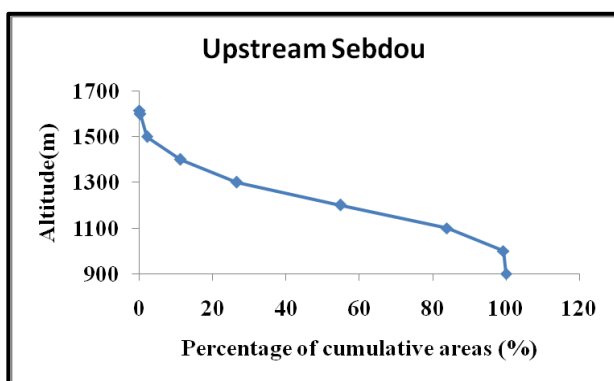
Table II.9. Altimetric distribution of the Isser sub basin.

Altitude (m)	Partial Areas		Cumulative areas	
	(km ²)	(%)	(km ²)	(%)
1623-1600	0.15	0.02	0.15	0.02
1600-1500	2.51	0.36	2.66	0.38
1500-1400	8.25	1.19	10.91	1.57
1400-1300	23.32	3.35	34.23	4.92
1300-1200	45.32	6.51	79.55	11.43
1200-1100	66.8	9.6	146.35	21.03
1100-1000	75.92	10.91	222.27	31.93
1000-900	87.75	12.61	310.02	44.54
900-800	80.74	11.6	390.76	56.14
800-700	91.3	13.12	482.06	69.25
700-600	121.93	17.52	603.99	86.77
600-500	67.48	9.69	671.47	96.47
500-400	23.46	3.37	694.93	99.84
400-359	1.14	0.16	696.07	100

The hypsometric curves (fig.II.9) of the Upstream Sebdo, and Isser basins show clearly steep slopes upstream (towards high altitudes) indicating the presence of a plateau surrounded by mountainous reliefs.

While for, Khemis, and Chouly basins we note that the high altitudes occupy large areas and the slopes are more accentuated downstream of the two basins.

As for, Wadi Boumessaoud, the low altitude dominate indicating the presence of a deep valley (212 m).



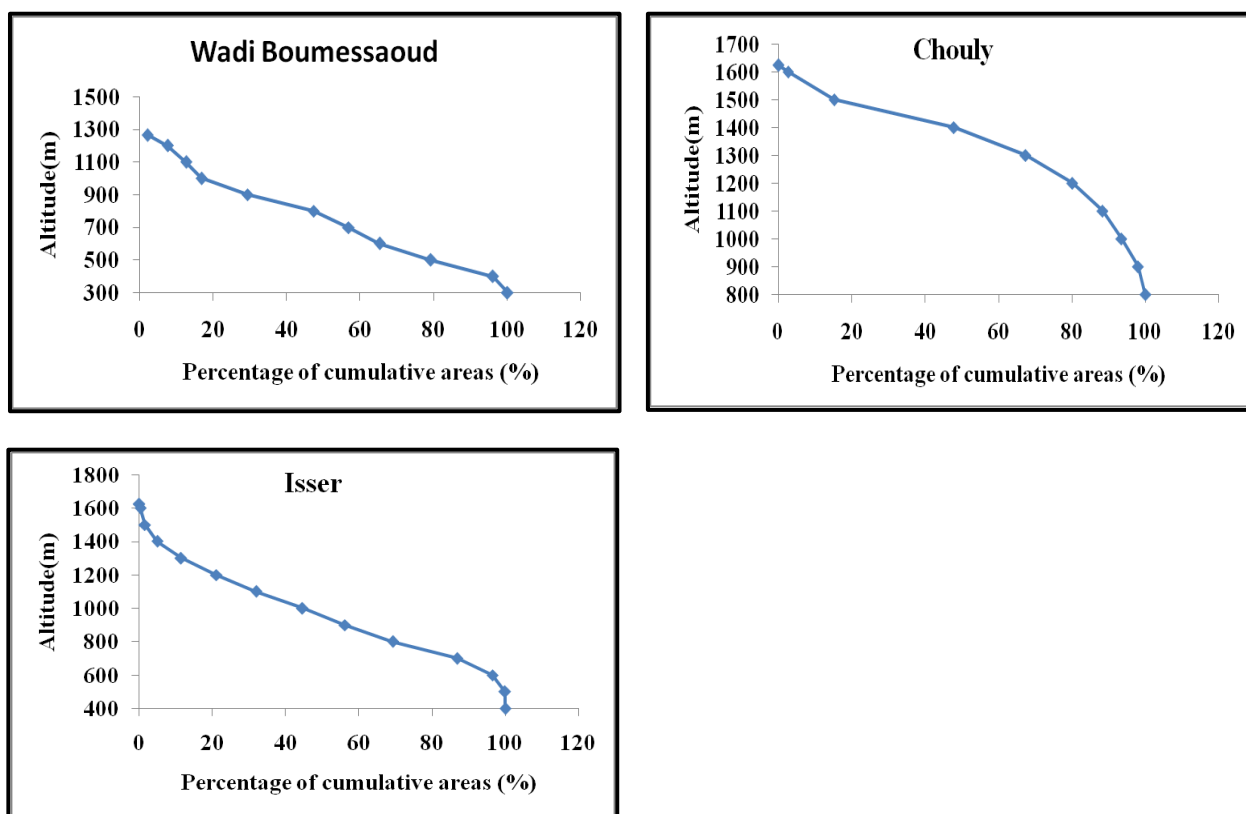


Figure II.9. Hypsometric curves of the study sub basins.

The high altitudes observed upstream in all the basins vary between 1265 m (Wadi Boumessaoud) (Djebel Tefatisset) to 1773 m for wadi Khemis represented by a series of mountains (Djebel Toumziyet, Djebel Moudjahadine, Djebel Mderba, and Djebel Tenouchfi), while the low altitudes are defined in the downstream part and vary between 212 m (Wadi Boumessaoud) and 852 m (Upstream from Sebdou city).

The altitudes ranges in the sub-basins are between (852-1616) for wadi Sebdou, (654-1773) for wadi Khemis and (713-1623) for wadi Chouly. The difference between the maximum and minimum altitudes varies between 764 to 1119 m. The analysis shows that the valleys of these sub basins belong to fairly high relief.

II.2.6.5.2. Characteristic altitudes

- **Maximum and minimum altitudes**

The analysis of figure II.10 makes it possible to see the maximum and minimum of the Study sub-basins. We can also identify the characteristics altitudes from the preceding hypsometric curves.

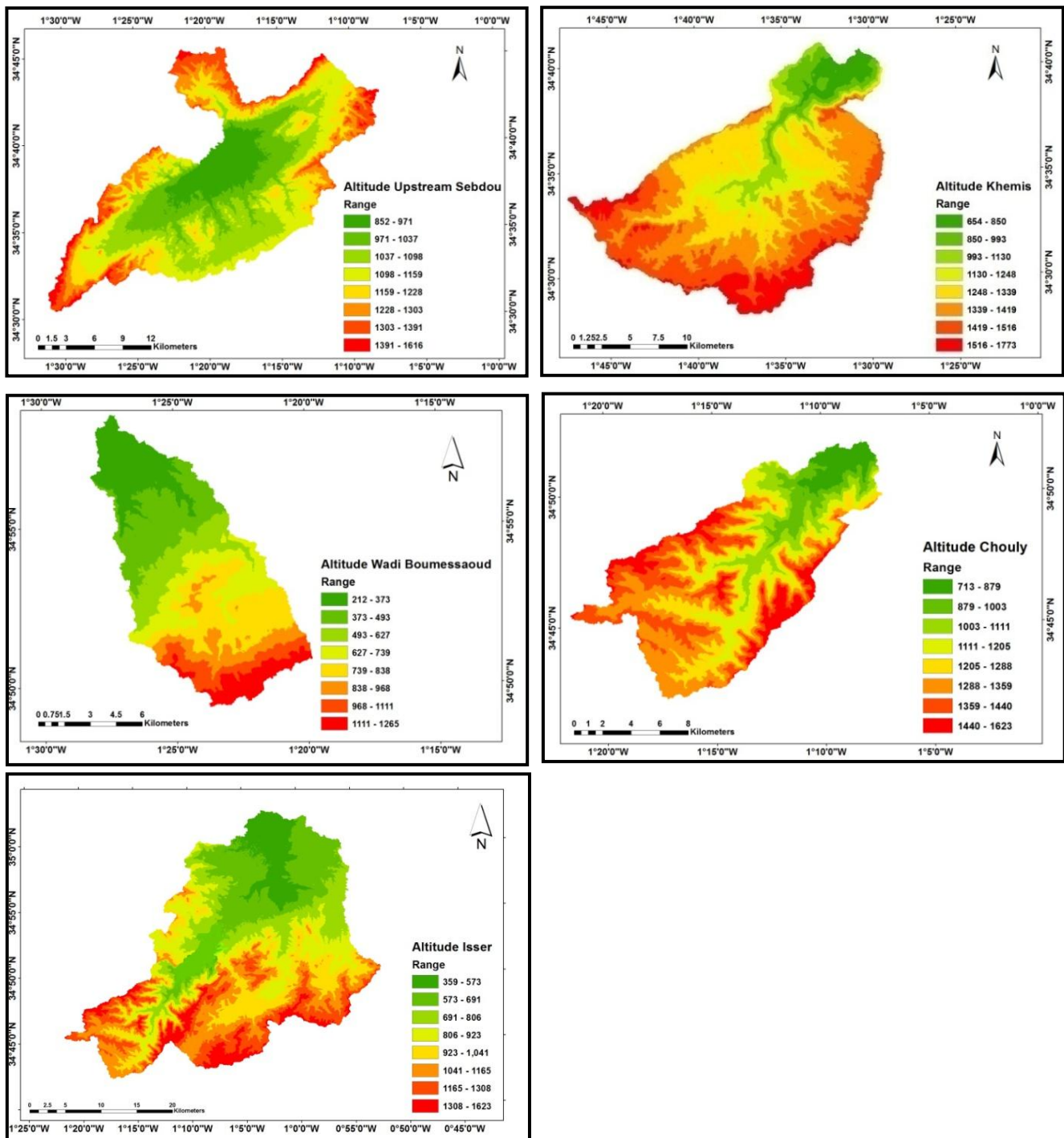


Figure II.10. Altimetric maps of the study sub basins.

- **Average altitude**

The average altitude is determined from the formula as follow:

$$H_{Average} = \frac{\sum_{i=1}^n H_i A_i}{A_T} \quad \text{Eq.II.4}$$

$A_{Average}$: Average altitude of the sub basin (m),

A_T : Total area of the sub basin (Km²),

A_i : Area between the two heights H_i and $H_i + 1$ (Km²),

H_i and H_{i+1} : Altitudes of two alternating contour lines (m).

- **Median, 5%, and 95% of area altitude (H50%, H5%, H95%)**

The hypsometric curve allows us to derive the altitudes which corresponding 5, 50, 95 % of the total surface of the sub basins.

The results of the characteristic altitudes of sub basins are presented in the table II.10 as following:

Table II.10. Results of the characteristic altitudes of the Study sub basins.

Sub basins	H_{Max}	H_{Min}	$H_{average}$	$H_{5\%}$	$H_{50\%}$	$H_{95\%}$
Upstream Sebdou	1616	852	1128.25	1460	1210	1020
Khemis	1773	654	1315.41	1660	1450	980
Wadi Boumessaoud	1265	212	637.37	1230	770	370
Chouly	1623	713	1243.06	1580	1380	960
Isser	1623	359	874.32	1390	950	610

II.2.6.5.3. Slope indices

The slope indices make it possible, as for certain geometric characteristics, to compare the basin with each other.

- **Roche slope index (I_p)**

The slope index I_p also defined by (Roche, 1963) from the equivalent rectangle. It is expressed as a percentage:

$$I_p = \frac{1}{\sqrt{L}} \sum_{n=1}^n \sqrt{A_i (H_i - H_{i-1})} \quad \text{Eq.II.5}$$

I_p : Roche slope index,

A_i : Fraction of the total surface between the altitudes H_i and H_{i-1} (%),

L : Length of the equivalent rectangle (m),

H_i and H_{i-1} : Difference in height between two neighboring curves (m).

- **Global slope index (I_g)**

This slope index is the ratio of the difference between the altitude of 5%, 95% of the percentage surface cumulative (D) over the length of the equivalent rectangle (Dubreuil, 1966). The formula is as follow:

$$I_g = \frac{H_{5\%} - H_{95\%}}{L} = \frac{D}{L} \quad \text{Eq.II.6}$$

I_g : Global slope index,

D : Height difference (m): $H_{5\%}$, $H_{95\%}$ ($H_{5\%}$ and $H_{95\%}$ are the altitudes between which 90% of the surface) (m),

L : Length of the equivalent rectangle (m).

The Overseas Scientific and Technical Research Organization (O.R.S.T.O.M.) provided a first classification of the relief based on the global slope index (Ig). It is represented in table II.11:

Table II.11. Classification of reliefs according to Ig by O.R.S.T.O.M.

Type of relief	Ig (m/km)
Very low relief	$Ig < 0.002$
Low relief	$0.002 < Ig < 0.005$
Fairly low relief	$0.005 < Ig < 0.01$
Moderate relief	$0.01 < Ig < 0.02$
Fairly strong relief	$0.02 < Ig < 0.05$
strong relief	$0.05 < Ig < 0.5$
Very strong relief	$0.5 < Ig$

- **Average slope index (Im)**

It is defined by the formula as follow:

$$I_m = \frac{H_{max} - H_{min}}{L} \quad \text{Eq.II.7}$$

Im: Average slope index,

H_{Max} and H_{Min} : Maximum and minimum altitude of the sub basin (m),

L: Length of the equivalent rectangle (m).

- **Specific height difference (Ds)**

It is the product of the global slope index (Ig) by the square root of the basin area. The Ig decreases when L and Kc increase which makes difficult to compare two different sizes of basins. The Ds defined as follow:

$$D_s = I_g \sqrt{A} \quad \text{Eq.II.8}$$

Ds: Specific height difference (m);

Ig: Global slope index (m / km);

A: Area of the basin (km²).

The classification of the O.R.S.T.O.M based on the specific height difference (Ds) is as follow (tab.II.12):

Table II.12. Classification of relief according to Ds (ORSTOM).

Type of relief	Ds(m)
Very low relief	$Ds < 10$
Low relief	$10 < Ds < 25$
Fairly low relief	$25 < Ds < 50$
Moderate relief	$50 < Ds < 100$

Fairly strong relief	$100 < D_s < 250$
strong relief	$250 < D_s < 500$
Very strong relief	$D_s > 500$

These indices show the relief character and the importance of slopes of the studied sub basins (tab.II.13):

Table II.13. Results of Indices of slopes for the study sub basins of the Tafna basin.

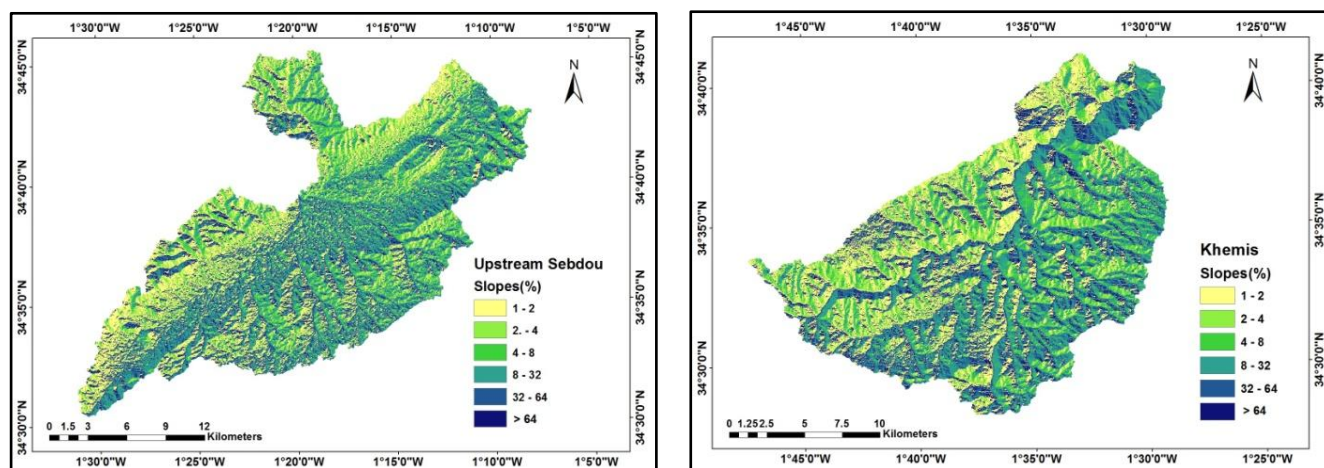
Sub basins	Ip	Ig	Im	Ds (m)
Upstream Sebdou	0.09	0.01	0.10	439.31
Khemis	0.14	0.02	0.25	342.23
Wadi Boumessaoud	0.2	0.04	0.44	108.77
Chouly	0.15	0.02	0.27	176.37
Isser	0.12	0.01	0.17	696

The specific difference in height (DS) is greater than 500 m at Isser sub basin representing very strong relief. While Ds is between 250 and 500 at Upstream Sebdou, and Khemis sub basins representing strong relief. We can note the importance of the mountainous volume and the strong incision of the relief. While Wadi Boumessaoud sub basin has fairly strong relief representing plain area.

The value Ig found between 0.02 and 0.04 at Khemis, Chouly, and Wadi Boumessaoud sub basins according to the classification of the O.R.S.T.O.M. (tab.II.11) indicating to fairly strong relief. While Moderate relief at Upstream Sebdou, and Isser sub basins which adequacy with the morphology of these sub basins.

- **Spatial analysis of slopes**

The spatial analysis of slopes is determined from ASTER Global Digital Elevation Model V003 maps (N36W02W03, and N35 W02W03) using ArcGis 10.3.1 software to represent the topography the terrain of the study area (fig.II.11).



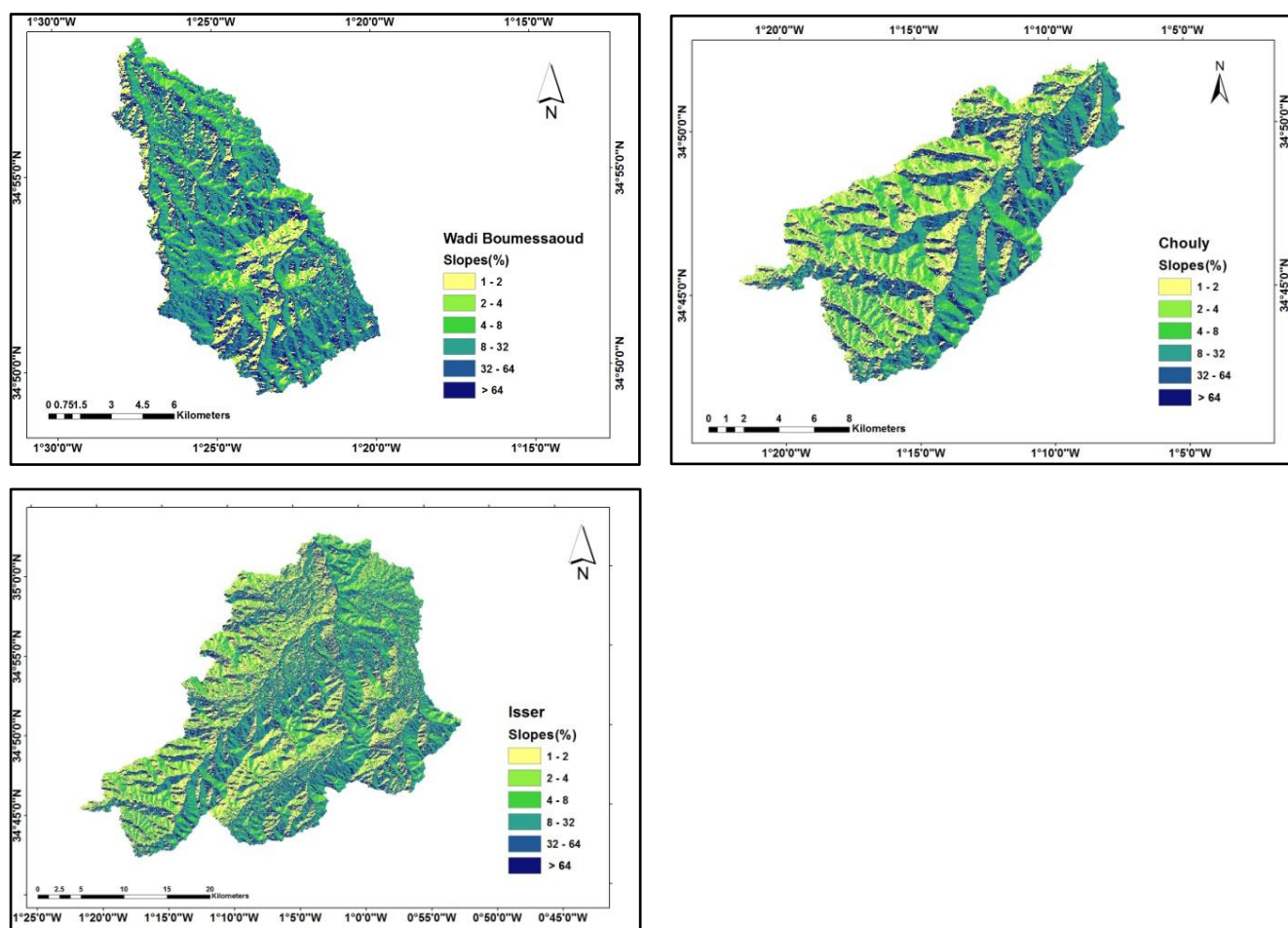


Figure II.11. Slope maps of the study sub basins of the Tafna basin.

The area of spatial distribution of the slope classes in km^2 and percentage is defined in table II.14.

Table II.14. Classes of the slopes of the study sub basins.

Slope (%)	1 - 2		2 - 4		4 - 8		8 - 32		32 - 64		> 64	
	Ai (km^2)	Ai (%)	Ai (km^2)	Ai (%)	Ai (km^2)	Ai (%)	Ai (km^2)	Ai (%)	Ai (km^2)	Ai (%)	Ai (km^2)	Ai (%)
Upstream Seb Dou	62.65	14.26	40.31	9.18	70.11	15.96	113.81	25.91	40.81	9.29	111.63	25.41
Khemis	50.61	14.79	31.51	9.21	48.57	14.19	83.65	24.44	32.6	9.53	95.29	27.84
Wadi Boumessaoud	10.97	10.08	4.04	3.71	7.8	7.17	30.88	28.39	17.1	15.72	37.99	34.92
Chouly	27.32	15.49	15.28	8.66	25.3	14.34	40.19	22.78	16.34	9.26	51.97	29.46
Isser	106.51	15.3	53.76	7.72	84.81	12.18	164.85	23.68	72.76	10.45	213.38	30.65

The slope class between 8 to 32 % and > 64 % is representing a large area in all sub basins of the study area covering surface of 22% (Chouly) to 34% (Wadi Boumessaoud) corresponding to the reliefs of the Tlemcen mountains located in the southern zone of the

Tafna basin which is mainly characterized by the Upper Jurassic (the Zarifet and Lato limestones).

The 1 to 2 %, 4-8 %, and 32 to 64% class covers between 7 to 16 % of the total area representing the percentage of Quaternary continental which is mainly formed by alluvium, terraces.

The slope class between 2 and 4% is representing less area in all sub basins with percentage of 3% (Wadi Boumessaoud) and more than 9% (Upstream Sebdou, Khemis) distributing over entire sub basins area.

II.2.6.5.4. Hydrographic network

The hydrographic network is represented by natural drainage channels which represents the runoff path coming from precipitation or recharge from temporary or continuous groundwater (Roche, 1963).

The geology and the reliefs have a significant impact in the layout of the hydrographic network and its evolution.

- The important tributary of Upstream Sebdou sub basin is wadi Sebdou (controlled by Sebdou hydrometric station).
- The important tributaries of Khemis are Khemis, and Boulefran wadis.
- The important tributaries of Wadi Boumessaoud are Boumessaoud, Bou Ennag, and Bou Madjmar.
- The important tributaries of Chouly are Chouly, El Fernane, and Ougarene.
- The important tributaries of Isser are Isser, Beniane, and Bou Hadi.

II.2.6.5.4.1. Network Hierarchisation

The classification of the hydrographic network reflects the branching of the drainage network. There are several classifications, the method used in our work is that of Strahler (1957) which assumes that any thalweg without tributaries is of order 1, and the stream formed by the confluence of two rivers of different order takes the higher order of the two, and if the two streams have the same order, they are increased by 1 (fig.II.12).

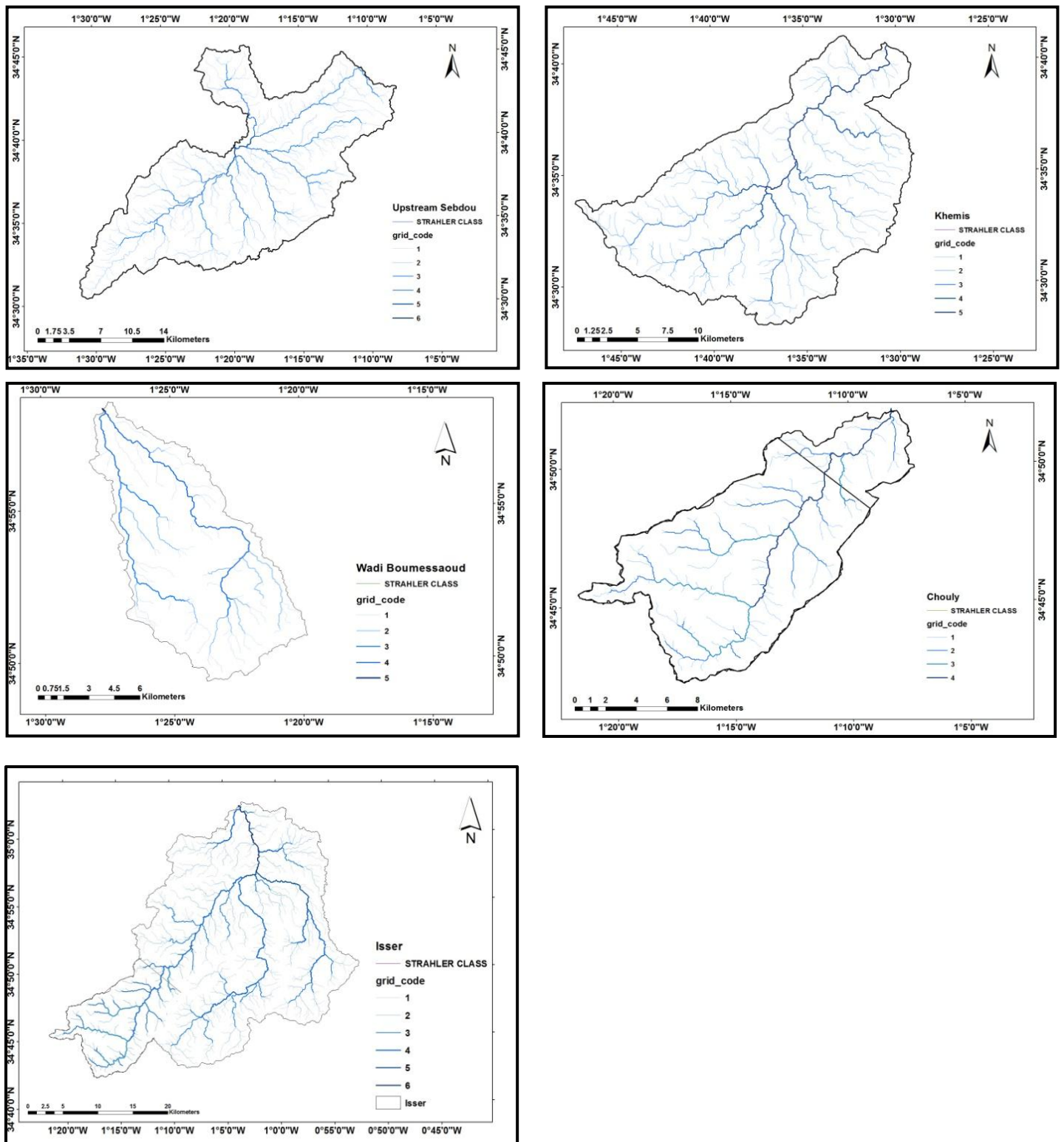


Figure II.12. The hydrographic network of the studied sub basins.

The average length of each order of the hydrographic networks of the studied sub basins are shown in tables II.15, II.16, II.17, II.18, and II.19:

Table II.15. Classification of thalweg of Upstream Sebdou sub basin.

Order (i)	Number (Ni)	Cumulative length (Li) (km)	Average length (La) (km)
1	589	291.62	0.5
2	215	141.82	0.66
3	114	72.84	0.64
4	113	56.53	0.5
5	30	7.07	0.24
6	1	0.26	0.26

Table II.16. Classification of thalweg of Khemis sub basin.

Order (i)	Number (Ni)	Cumulative length (Li) (km)	Average length (La) (km)
/	/	(km)	(km)
1	359	209.29	0.58
2	174	82.56	0.47
3	96	56.82	0.59
4	51	25.74	0.5
5	38	22.35	0.59

Table II.17. Classification of thalweg of Wadi Boumessaoud sub basin.

Order (i)	Number (Ni)	Cumulative length (Li) (km)	Average length (La) (km)
1	121	71.69	0.59
2	53	32.16	0.61
3	16	15.71	0.98
4	34	23.8	0.7
5	1	0.39	0.39

Table II.18. Classification of thalweg of Chouly sub basin.

Order (i)	Number (Ni)	Cumulative length (Li) (km)	Average length (La) (km)
1	154	92.44	0.6
2	84	47.19	0.56
3	67	28.82	0.43
4	50	20.49	0.41

Table II.19. Classification of thalweg of Isser sub basin.

Order (i)	Number (Ni)	Cumulative length (Li) (km)	Average length (La) (km)
1	766	457.05	0.6
2	457	227.71	0.5
3	165	89.12	0.54
4	179	80.2	0.45
5	23	15.04	0.65

6	21	11.45	0.55
---	----	-------	------

II.2.6.5.4.2. Long profile

The longitudinal profile of sub basins (fig.II.13) showed the distance distribution of main thalweg on different altitudes range. The length of the main thalweg of Upstream Sebdo, Khemis, Wadi Boumessaoud, Chouly, Isser sub basins are ranging 24.85, 34.27, 20.47, 26.41, 53.97 Km (tab.II.20), respectively. It is divided into sections from upstream to downstream.

Table II.20. Length of main thalweg of the studied sub basins.

Sub basin	Upstream Sebdo	Khemis	Wadi Boumessaoud	Chouly	Isser
Main thalweg Length (Km)	24.85	34.27	20.47	26.41	53.97

Upstream Sebdo sub basin originates from the mountains of Hariga, Lato with altitude 1300 m and length of 1.31 km, and slope of 0.96% (tab.II.21) to flows into the Tafna Valley at outlet at altitude 852 m with very strong slope of 9.08 %.

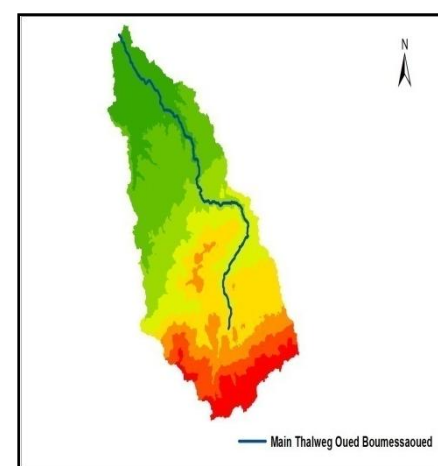
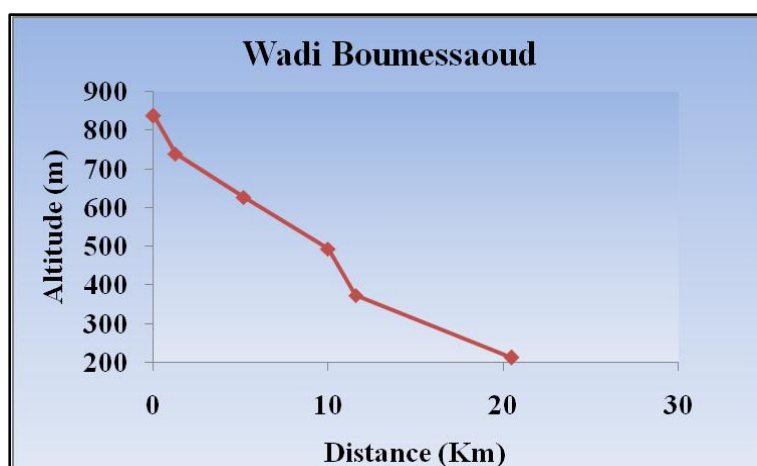
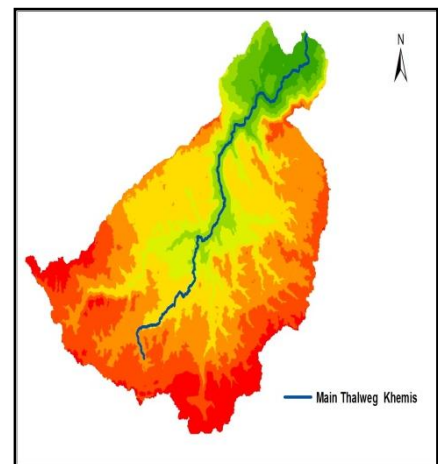
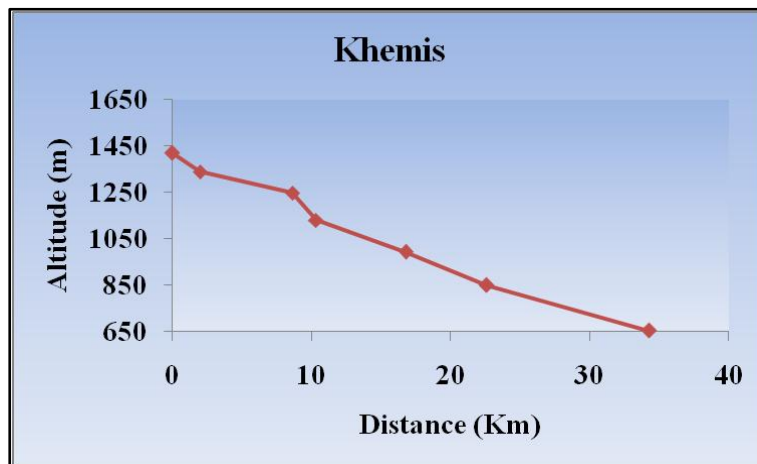
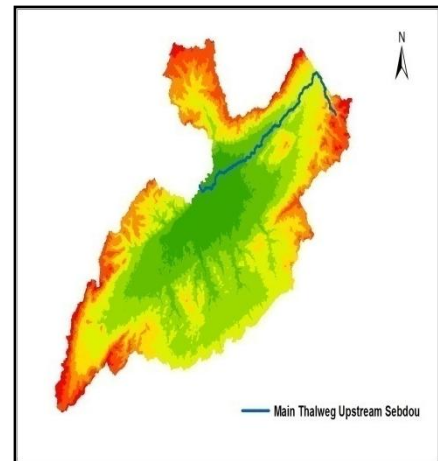
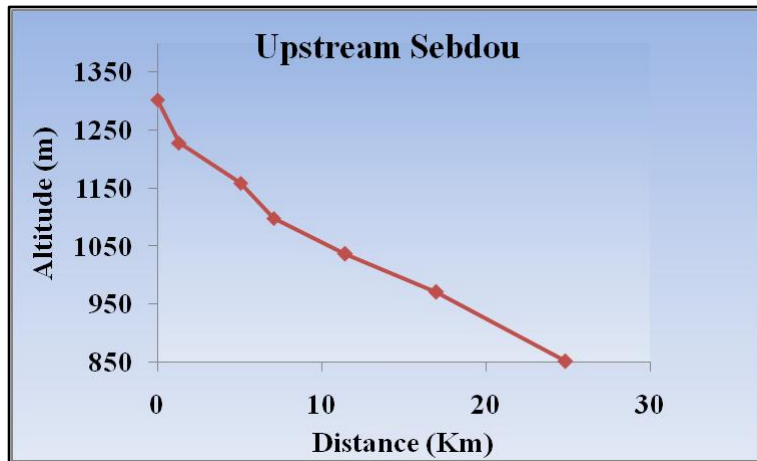
Khemis sub basin (tab.II.22) originates from Boulefrane valley coming from Sidi Moh Senoussi with length 1.97 km between altitudes 1339 to 1419 km and very strong slope of 4.06%, and this sub basin has more source coming from Maroui, Kerrouch, and Moudjahadine mountains to fuel thalweg with length 6.65 Km between altitudes 1248 to 1339 and slopes of 1.37 % to continues its course and flows at the end in Beni Bahdel dam.

Wadi Boumessaoud sub basin (tab.II.23) originates from Ennag valley with length 3.89 Km between altitudes 627 to 739 m and strong slope of 2.88 % coming from Tefatisset mountain between altitudes 739 to 838 m, to be connected in its following path with Bou Madjmar to flows at outlet with altitude 212 after slope of 1.81 %. The tributaries of Wadi Boumessaoud are united with Zitoune tributaries to flow at Tafna valley that is coming from Maghnia region.

Chouly basin (tab.II.24) is originate from Ougarene valley located between the two mountains Dar Cheikh and Rhenndas, the length of the valley is 3.62 Km between altitudes 1205 to 1288 m with strong slope of 2.29 % to flow into El Fernane valley and Chouly valley respectively, before flowing into Isser valley at the outlet with altitude 713 m after strong slope of 2.61 %.

The origin of Isser sub basin (tab.II.25) comes from El Asses, and Bel Khia mountains to fuel Beniane valley with length 10.72 km between altitude 923 to 1041 m with slope of 1.1 % to flow at Isser valley which is most important tributaries and lengthiest in this sub basin, and it also alimented from Bou Hadi valley in north to continues its flow to Sidi Abdelli Dam, the outlet of the principle valley at altitude 359 m after slope of 1.5 %.

The main thalweg is characterized by regular slope at Chouly, and Isser sub basins, and very strong slope at Seb dou, Khemis, and Wadi Boumessaoued sub basins which showed rupture in slope probably due to the geology formation (the Upper Jurassic), or the existence of fractures in the area and that can involve strong flows caused the erosion.



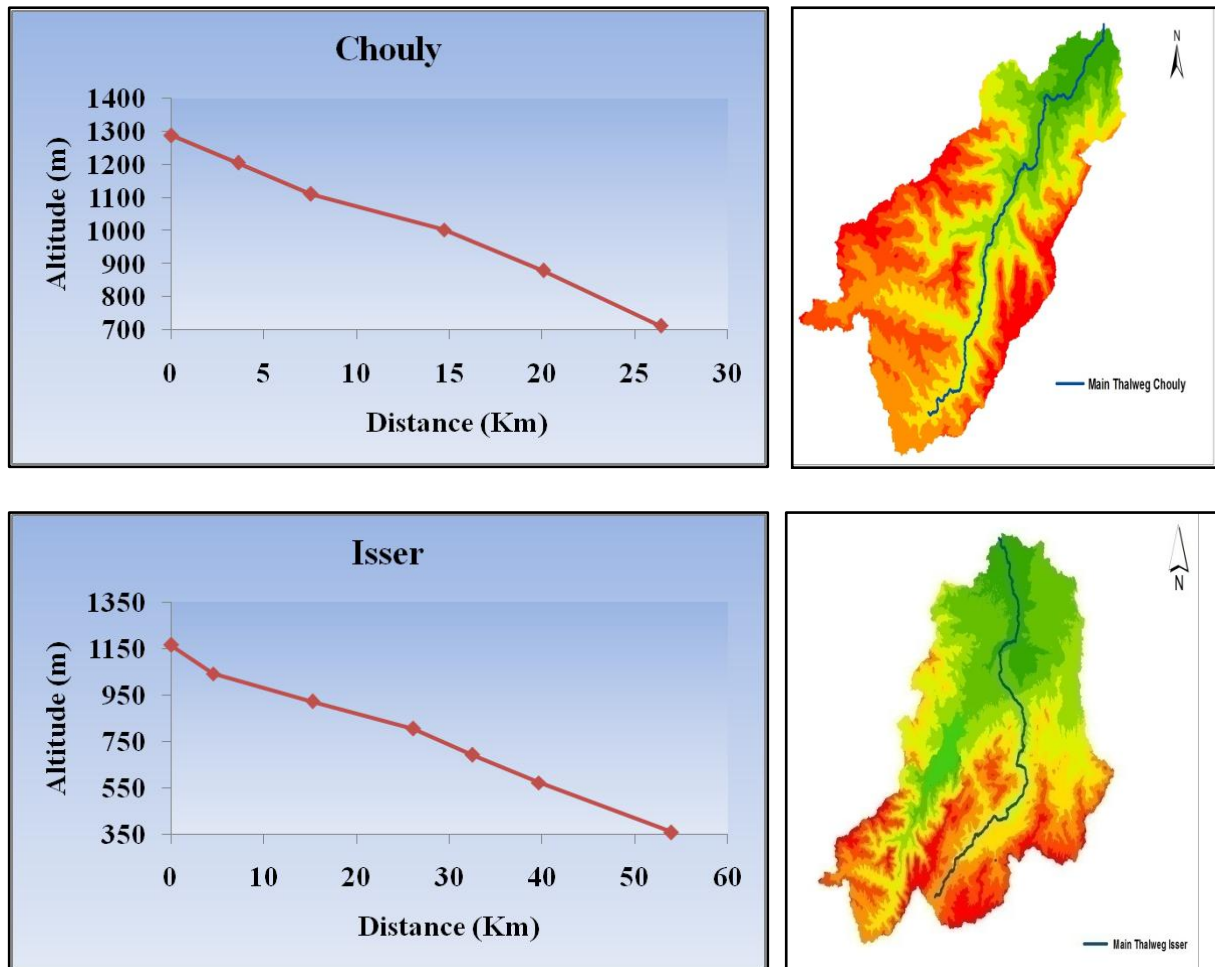


Figure II.13. Long profile of the studied sub basins.

II.2.6.5.4.3. Average slope of the main thalweg

It is defined by the ratio of the difference in altitude (ΔH) to the total length of the main thalweg (ΔL), a steep slope favors surface flow, while a low slope favors infiltration:

$$I_a = \frac{\Delta H}{\Delta L} \quad \text{Eq.II.9}$$

Ia: Average slopes (%),

ΔH : Difference of the altitude (Km),

ΔL : Length of main thalweg (Km).

Table II.21. Distance and slope of main thalweg of Upstream Sebdou basin.

Altitude (m)	Distance (Km)	Slope (%)
[852 - 971]	7.85	9.08
[971 - 1037]	5.55	1.76
[1037 - 1098]	4.38	3.05
[1098 - 1159]	2	1.39
[1159 - 1228]	3.75	1.24
[1228 - 1303]	1.31	0.96

Table II.22. Distance and slope of main thalweg of Khemis basin.

Altitude (m)	Distance (Km)	Slope (%)
[654 - 850]	11.67	1.68
[850 - 993]	5.81	2.46
[993 - 1130]	6.47	2.12
[1130 - 1248]	1.7	6.94
[1248 - 1339]	6.65	1.37
[1339 - 1419]	1.97	4.06

Table II.23. Distance and slope of main thalweg of Wadi Boumessaoud basin.

Altitude (m)	Distance (Km)	Slope (%)
[212 - 373]	8.91	1.81
[373 - 493]	1.59	7.55
[493 - 627]	4.82	2.78
[627 - 739]	3.89	2.88
[739 - 838]	1.26	7.86

Table II.24. Distance and slope of main thalweg of Chouly basin.

Altitude (m)	Distance (Km)	Slope (%)
[713 - 879]	6.35	2.61
[879 - 1003]	5.36	2.31
[1003 - 1111]	7.16	1.51
[1111 - 1205]	3.92	2.4
[1205 - 1288]	3.62	2.29

Table II.25. Distance and slope of main thalweg of Isser basin.

Altitude (m)	Distance (Km)	Slope (%)
[359 - 573]	14.3	1.5
[573 - 691]	7.17	1.65
[691 - 806]	6.37	1.81
[806 - 923]	10.9	1.07
[923 - 1041]	10.72	1.1
[1041 - 1165]	4.51	2.75

II.2.6.5.4.4. Hydrographic Network features

The important parameters which govern the hydrological regime of a watershed are: the drainage density (D_d), the confluence ratio (R_c) and the length ratio (R_L) and the torrentiality coefficient. The determination of these parameters is based on the classification of Strahler (1957) under a geographic information system (ArcGIS).

- **Confluence report (R_c)**

This is an important element to consider in establishing correlations from one region to another. It is defined by the following relation:

$$R_c = \frac{N_i}{N_{i+1}} \quad \text{Eq.II.10}$$

R_c : Confluence report,

N_i : Number of thalwegs of order i ,

N_{i+1} : Number of thalwegs of order $i + 1$.

Table II.26. Confluence report of the study sub basins.

Order	Upstream Sebdou	Khemis	Wadi Boumessaoued	Chouly	Isser
1	2.74	2.06	2.28	1.83	1.68
2	1.89	1.81	3.31	1.25	2.77
3	1.01	1.88	0.47	1.34	0.92
4	3.77	1.34	34	/	7.78
5	30	/	/	/	1.1
6	/	/	/	/	/

R_c shows that the network is well organized and constitutes a geometric series (tab.II.26, fig.II.14).

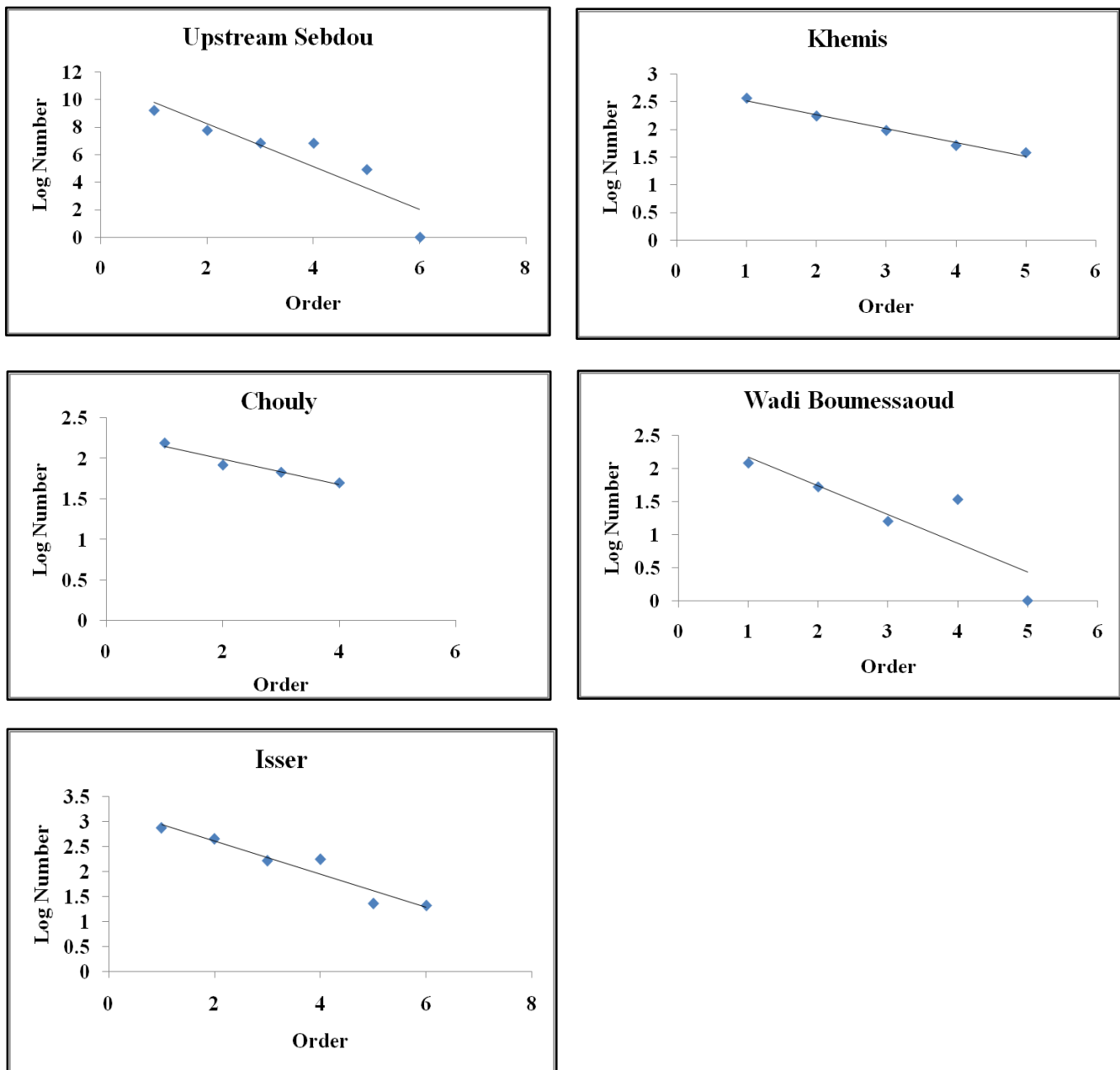


Figure II.14. Representation of the number of thalwegs according to the ordre.

- **Length ratio (R_L)**

The definition is as follows:

$$R_L = \frac{L_{i+1}}{L_i} \quad \text{Eq.II.11}$$

R_L : Length ratio,

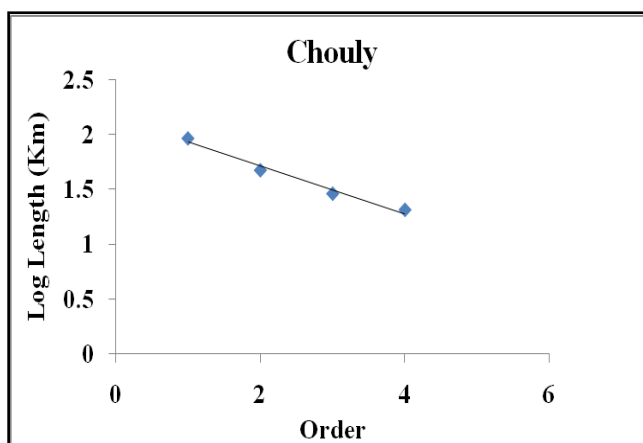
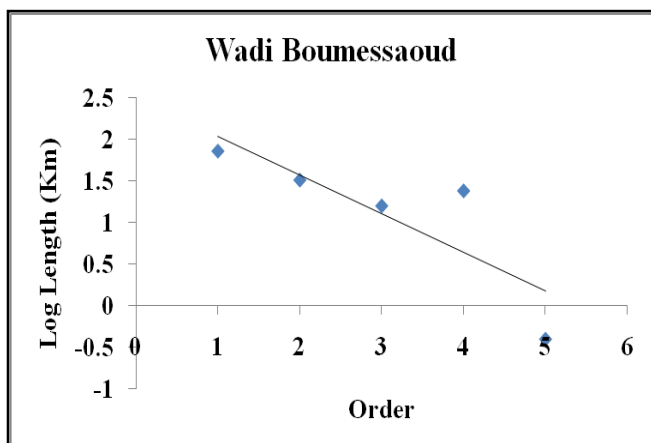
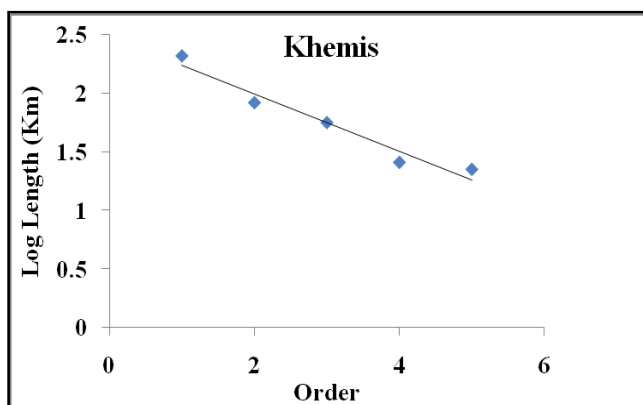
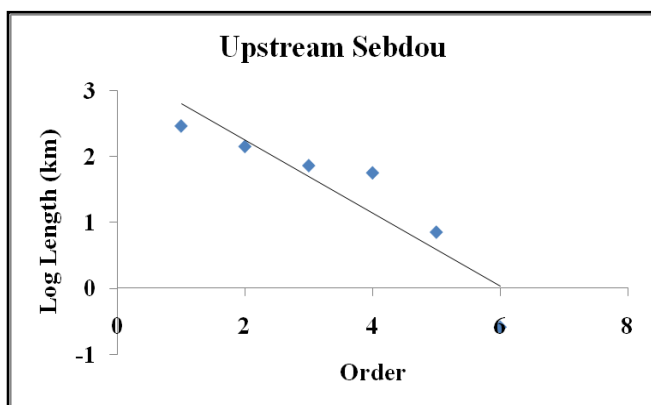
L_i : Length of thalwegs of order I,

L_{i+1} : Length of thalwegs of order $i + 1$.

The values of the length ratio (tab.II.27) showed that the hydrographic networks of sub basins are well organized and distributed with successive thalwegs forming an inverse geometric series (fig.II.15).

Table II.27. Length ratio of the studied sub basins.

Order	Upstream Sebdou	Khemis	Wadi Boumessaoud	Chouly	Isser
1	/	/	/	/	/
2	0.49	0.39	0.45	0.51	0.5
3	0.51	0.69	0.49	0.61	0.39
4	0.78	0.45	1.51	0.71	0.9
5	0.13	0.87	0.02	/	0.19
6	0.04	/	/	/	0.76



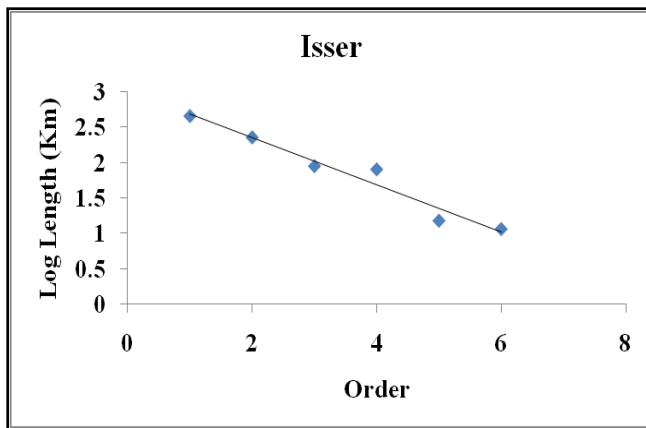


Figure II.15. Line representative of the ratio of the lengths as a function of the order.

- **Drainage density**

Drainage density is based on the geology of the topographical characteristics of the basin and climatologically and anthropogenic conditions to maintain the hydrological conditions in a unit hydrographic vector by representing the area of the basin. It is defined as the sum of the lengths of the thalwegs draining the surface of the basin (Horton, 1932, 1945). Drainage density is defined by:

$$D_d = \frac{\sum_{i=1}^n L_i}{A} \quad \text{Eq.II.12}$$

D_d : Drainage density (km / km²),

L : Cumulative length of all thalwegs in the basin (km),

A : Basin area (km²).

- **Hydrographic density (F_t)**

Hydrographic density represents the number of thalweg per unit area.

$$F_t = \frac{N_t}{A} \quad \text{Eq.II.13}$$

F : Hydrographic density (km⁻²),

N_t : Number total of thalweg,

A : Basin area (km²).

- **Hydrographic density for order 1 (F_1)**

It is the ratio of the total number of thalweg of order 1 to the area of the basin.

$$F_1 = \frac{N_1}{A} \quad \text{Eq.II.14}$$

F_1 : Hydrographic density of order 1 (km⁻²),

N_1 : Total number of thalweg of order 1,

A : Basin area (km²).

- **Torrentiality coeffiient (C_t)**

It is a coefficient which takes into account both the drainage density and that of the elementary thalwegs of order 1:

$$C_t = D_d \cdot F_1 \quad \text{Eq.II.15}$$

C_t : Torrentiality coefficient,
 D_d : Drainage density (Km/Km²),
 F_1 : Frequency of thalweg of order 1 (Km⁻²).

- **Elongation coefficient (E)**

It is given by the following relation:

$$E = \frac{2\sqrt{A}\pi}{L_0} \quad \text{Eq.II.16}$$

$$L_0 = \frac{\sum L_m}{n} \quad \text{Eq.II.17}$$

A : Area of the basin (Km²),
 n : Order number,
 L_m : Average length of main thalweg (km),
 L_0 : Average length of each thalweg (Km).

- **Concentration time (T_C)**

It is the time it takes for a water particle coming from the most distant part of the basin to reach the outlet, it depends on several factors: the shape of the basin, the vegetation cover, the lithology. The concentration time is defined by the formula of Giandotti which has been approved in North Africa as follow (Giandotti, 1934):

$$T_C = \frac{4\sqrt{A}+1.5L_p}{\sqrt{H_{av}-H_{min}}} \quad \text{Eq.II.18}$$

T_C : Concentration time (hours),
 A : Area of basin (km²),
 L : Length of the main thalweg (km),
 $H_{average}$: Average altitude (m),
 H_{min} : Minimum altitude (m).

- **Concentration speed (V_C)**

It defined as being the average speed of propagation of a flood as formula follow:

$$V_C = \frac{L_M}{T_C} \quad \text{Eq.II.19}$$

V_C : Concentration speed (Km/h),
 L_M : Length of the main thalweg (Km),
 T_C : Concentration time (hours).
 Hydrographic Network features are presented as follow (tab.II.28):

Table II.28. Characteristics Hydrographic of the Study sub basins.

Sub basin	Hydrographic Characteristic						
	D_d	F_t	F_1	C_t	E	T_c	V_c
	Km/Km ²	Km ⁻²	Km ⁻²	/	/	hours	Km/h
Upstream Seb dou	1.3	2.42	1.34	1.74	159.55	9.11	32.02
Khemis	1.16	2.1	1.05	1.22	119.54	6.1	34.34
Wadi Boumessaoud	1.32	2.07	1.11	1.47	56.54	4.39	16.33
Chouly	1.07	2.01	0.87	0.93	94.04	5.03	18.36
Isser	1.26	2.31	1.10	1.39	170.93	10.27	44.51

The results of drainage density of the Study basins seem homogeneous over the whole of the Tafna basin, showing good drainage.

The density was relatively higher in Wadi Boumessaoud sub basin due to his small area and it is supplied from the main tributary (Tafna valley).

The values of the hydrographic density (F_1) of Upstream Seb dou, Wadi Boumessaoud and Isser sub basins are respectively 1.34, 1.11, 1.10 km⁻². These results show that these sub basin has a greater number of thalwegs of order 1 compared to their density of hydrograph of all order of thalweg respectively 2.42, 2.07, 2.31 km⁻².

These sub basins have a high torrentiality coefficient ranging from 1.39 (Isser) to 1.74 (Seb dou). We note a runoff concentration time of approximately 9 hours for Seb dou corresponding to an average speed of 32.02 km / h. While the runoff concentration times of the Wadi Boumessaoud and Isser are 4 and 10 hours, respectively, with respective flow speeds of 16.33 and 44.51 km / h.

II.2.7. Land Use

The study of land use in the Study basins is taken from the land use map that the INSID (National Institute for Irrigation and Drainage) had produced at a scale of 1/50 000 and data collected from the ANRH document "The Environmental Atlas of Tlemcen Wilaya".

Land cover represents a determining and regulator factor of the runoff regime, where its resistance is increased due to the severity of the topography and the density of vegetation cover which affects the climatic factor (evaporation rate), and the retention capacity of the basin.

The main agricultural characteristic of the Tafna basin lies in the diversity of the natural sets which allows a diversity of activities according to the different climatic stages and the nature of the soils.

According to the numerous studies carried out by the A.N.A.T. (National Agency for Regional Planning of Algeria), there are four (04) large natural spaces that make it possible to draw up a sketch of the different agricultural potentials in the study area:

- A coastal area was characterized by market gardening, in particular, legumes and various fruit trees due to the absence of frost. It is represented by the Traras Mountains range - a set of plains and plateaus crossed by large wadis (Isser and Tafna) with excellent soil quality. These cover areas are located in the north-eastern Boumessaoued and Isser sub basins.

Concerning the region of the Traras Mountains, the phenomenon of soil erosion is still worrying and it is more than necessary to reflect on an ambitious program of water and soil conservation. While in the plains zone, the programs are modest and have not made it possible to slow down the process of degradation of natural resources and desertification in this area.

- On the plateaus and in the Piedmonts, agricultural activity is oriented towards cereals, and it adapts to all dry or irrigated crops distributed in the Isser basin in the valleys and quaternary filling plains (Ouled Mimoun - Ain Tellout) characterized by a soil formed of alluvial deposits.

- The Tlemcen mountain range: this zone with fairly uneven relief is occupied by forests and maquis which cover a large area of the study basins.

- North of the Tlemcen Mountains: we can see the high steppe plains, it is an arid zone with shallow soils, very poor in organic matter and the vegetation cover consists of steppe species such as the alpha covering a part of the northeast, and the extreme northwest of the Isser sub basin. The main activity remains sheep farming in the North at Wadi Boumessaoud.

The Tafna basin experienced degradation in the landscape by extensive small-scale agriculture, where the traditional cropping system such as fallow cereal (47.26% cereal cultivation) extensively dominates land use, which is not a better economic choice considering the quality of the soil in the basin. Intensive crops are limited to the perimeter of Maghnia, the Hennaya plain, and some valleys (Tafna, Khemis, Isser, and Sikkak) (fig.II.16)(tab.II.29).

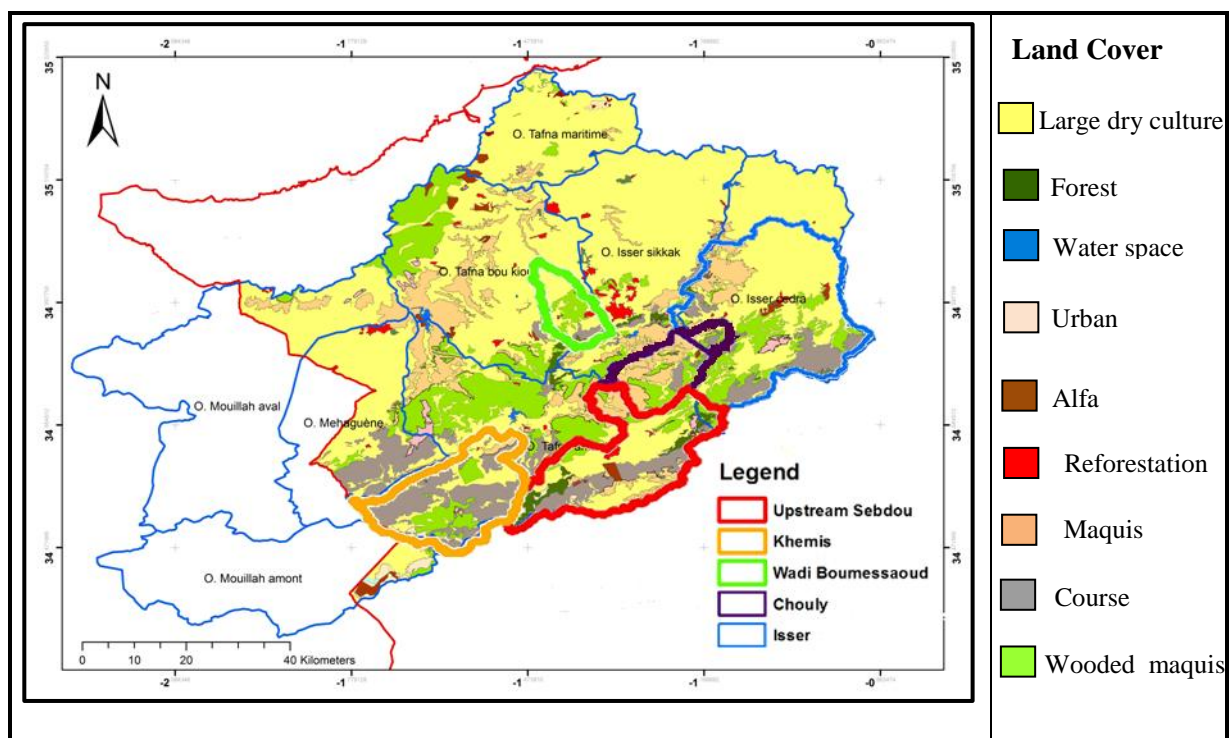


Figure II.16. Land use map of the study sub basins of the Tafna basin.

Table II.29. Distribution of land in the different zones of the Study basins (ABH, 2006).

Sub basin	Town	Area occupied (Ha)		
		Market gardening	Arboreal culture	cereals
Upstream Seb dou	Seb dou	108	489	3682
Khemis	Beni snous	176	221	1360
Wadi Boumessaoud	Beni Mester	100	320	1177
Chouly	Wadi Lakhdar	254	137	750
Isser	Ouled Mimoun	374	352	2250
	Ain Tellout	145	163	7800
	Ben Smiel	212	157	1360
	Ain Yousef	107	448	2996
	El – Fhoul	600	638	



Figure II.17. Traditional agriculture of Seb dou.



Figure II.18. Traditional agriculture of Ouled Mimoun.

II.3. Conclusion

This chapter describes the main geographical, geological, hydrogeological and morphometric characteristics as well as the land use of the study sub basins (Seb dou, Khemis, Wadi Boumessaoued, Chouly, Isser) of the Tafna basin. These characteristics have a definite influence on the response of the surface flow.

The geological study showed that the sub basins are essentially occupied by the formations of the upper Jurassic, mainly formed by very karstic Tlemcen dolomites, favoring the infiltration of surface water.

While the study of physical factors such as slope has shown that the Study basins belong to two classes:

- A fairly strong relief reflecting the mountains zone responsible for the high drainage density,
- and Moderate relief which according to the morphology of the sub basins.

The values of the coefficient of compactness for the Sebdou and Isser sub basins greater than 1.7 demonstrate their elongated shape, which consequently implies a slower response in runoff with a water concentration time of more than 9 hours.

The study of the land use showed that:

- in the sub basins located upstream dominates the forest character covering the chain of the Tlemcen Mountains,
- The vegetation cover is directly involved in the process of filtration, runoff and soil loss, where the silvopastoral and pastoral areas can provide low erosion when the land is protected.

CHAPTER THREE
VARIABILITY AND TREND ANALYSIS OF
HYDRO-CLIMATIC VARIABLES

III.1. Introduction

The hydrological cycle is greatly experienced fluctuations of hydro-climatic variables such as temperature, wind speed, precipitation, soil moisture, and evapotranspiration (Teng et al., 2012; Guo et al., 2020), particularly in the Mediterranean basins, and in semi-arid regions are characterized by high temporal and spatial variability of extreme rainfall, low runoff, high evapotranspiration (Romero et al., 1998; Mehta and Yang, 2008; Schilling et al., 2012; Touazi and Laborde, 2004), Increasing temperature has a consequence on rainfall, which its variation raises the uncertainty of predictions on rainfall in terms of its trend as well as the spatial distribution (Ramos and Martínez-Casasnovas, 2006; Batisani and Yarnal, 2010). High temperatures also affect water availability (Modal et al., 2015) , and strongly affecting the streamflow regime (Zamoum and Souag-Gamane, 2019; Meddi and Hubert, 2003, Meddi et al., 2010a), and increasing pressures on water resources (Sellami et al., 2016; Barbé, 2002; Bekele et al., 2019), which may enhance the process of desertification (Lopez-Bermudez et al., 1998). Around 13% of Algeria has a Mediterranean climate, and the watersheds of this region contribute to approximately 75% of the annual surface water flow (Belarbi e al., 2016) with a situation of water scarcity in dry periods (Benblidia and Thivet, 2010). A reducing trend of rainfall with order 20 % in the northern center of Algeria was observed, which led to a drastic decrease of streamflow by almost 55% in this region and fluctuates from 61 to 71 % decline in streamflow in the extreme northwest (Meddi and Hubert, 2003) due to a reduction of more than 36% of rainfall (Meddi, H. and Meddi, M, 2009). Northwest Algeria has experienced fluctuations in rainfall between the two decades 1940s and 1990s from positive to negative anomalies, which reflected a significant decline in rainfall during the mid-1970s.

Therefore, the comprehensive analysing of the hydro-climatological variable such as rainfall, runoff, the temperature and its variations is important to understand and analyze the hydrological behavior of the basin, and to assess the response of rivers to these variations, and improving water management, understanding the variation of climate and the problems associated with floods, droughts, and their impact on water resources (Traore et al., 2017; Dash and Kumar, 2017; Ndiaye et al., 2016; Tossou et al., 2017), in addition to being the major input data into any hydrological system. However, long-term time series data is not available in several regions of the world especially in the African continent, and may affect the accuracy and impact of the results of trend analysis. The importance of analyzing the complexity and variability of the space–time hydro-climatological variable patterns has clearly revealed the need for expanding the actual hydrometeorological -monitoring networks and improving the quality control and maintenance of databases. These improvements in monitoring networks and data pre-processing will increase the options to detect possible changes in climate and improve the understanding of the climate and the water cycle (Celleri et al., 2007). The analysis of climate variables needs to be based on homogeneous data (Conrad and Pollak, 1995; Longobardi and Villani, 2009) which are not affected by non-climate factors such as changes in instrumentation and the location of meteorological stations as well as their surrounding and the other disturbing factors (Peterson et al., 1998).

The study on climate change requires several tools for statistical analyses (Hubert, 2000) aimed at the detection of breakpoints and trends (magnitude and their directions) (Traore et al., 2017). There are several parametric and non-parametric tests available for detecting the

trend in climate variables. However, several studies have been given high attention in detecting trend in climate and hydrologic variables (mainly rainfall and temperature) world-wide (Garbrecht et al., 2004; Jiang et al., 2007; Donald et al., 2008; Jain and Kumar, 2012; Yang et al., 2014; Kisi and Ay, 2014; Da Silva et al., 2015; Liuzzo et al., 2016; Pal et al., 2017; Lappas et al., 2017; Wu and Qian, 2017; Qin et al., 2017; Kale and Sönmez, 2018; Kumar et al., 2019; Panda and Sahu, 2019), and several studies in Northern Algeria (Touazi et al. 2011; Hamlaoui-Moulai et al. 2013; Baahmed et al. 2015; Djellouli et al. 2017; Mrad et al. 2018; Otmane et al., 2018; Hallouz et al., 2019; Kadir et al., 2020; Khedimallah et al., 2020; Charifi Bellabas et al., 2020; Zekouda et al., 2020).

Therefore, further analyzing hydro-climatological in the Northwestren of Algeria region is required for improving the strategies on water resource management. In this study, we complement previous studies by dealing with sub basins that were not previously addressed in Tafna basin. The aim objectives of this chapter is to analyse the different hydrological and climatic variables of the five sub basins of the Tafna basin (Upstream Sebdou, Khemis, Wadi Boumessaoud, Chouly, Isser) on a different time scales are:

- (1) Preliminary analysis of hydrometeorological variables (rainfall, runoff, temperature, potential evapotranspiration) on an annual, monthly, seasonal, and daily scale.
- (2) Statistical analysis of homogeneity on hydrometeorological variables (rainfall, runoff, and temperature) on an annual, and monthly, and detecting of breakpoints.
- (3) Analysing the trend (magnitude and their directions) of hydrometeorological variables (rainfall, runoff, and temperature) on an annual, monthly, and seasonal scale.

III.2. Station presentations

Daily rainfall data were collected from eight climate stations from (Sebdou, Khemis, Hennaya, Djebel Chouachi, Chouly, Meurbah, Ouled Mimoun, and Sidi Bounakhla) located in different parts of five sub basins of Tafna basin for a time period of 32 years (1979/1980-2011/2012), and daily flow data collected from five hydrometric stations from (Sebdou, Zahra, Zenata, Chouly, Sidi Aissa) located in the outlet of sub basin for a time period of 26 years (1985/1986–2010/2011), and which is provided by National Agency of Hydraulic Resources (ANRH) of Algeria. And daily temperature data were collected from two climatic stations (Beni Bahdel, Zenata) for a time period of 32 years (1979/1980–2010/2011), which is provided by the National Agency of Hydraulic Resources (ANRH) of Algeria, and the Hydrographic basin agency of Oran (ABH). The period of the study was selected based on the compatible duration in the start and the end of the time series of all stations, as well as the quality of the recordings. The major characteristics of the stations (name, code, coordinates, and database periods) presented in table III.1, table III.2, and table III.3.

Table III.1. Descriptive information of rainfall stations of the study area.

N	Sub basin	Name of station	Code of station	Longitude (W)	Latitude (N)	Elevation (m)	Period of Data
1	Upstream Sebdou	Sebdou	16-04-01	1°33'	34°65'	875	1975-2011
2	Khemis	Khemis	16-04-06	1°56'	34°64'	920	1970-2011
3	Wadi Boumessaoud	Hennaya	16-05-16	1°39'	34°92'	515	1973-2011
		Djebel Chouachi	16-05-18	1°50'	34°94'	110	1974-2014
4	Chouly	Chouly	16-06-01	1°14'	34°83'	700	1970-2013
		Meurbah	16-06-02	1°17'	34°79'	1100	1970-2013
5	Isser	Ouled Mimoun	16-06-07	1°03'	34°90'	705	1979-2012
		Sidi Bounakhla	16-06-10	1°05'	35°03'	430	1973-2011

Table III.2. Descriptive information of runoff stations of the study area.

N	Sub basin	Name of station	Code of station	Longitude (W)	Latitude (N)	Elevation (m)	Period of Data
1	Upstream Sebdou	Sebdou	16-04-01	1°20'	34°39'	875	1980-2010
2	Khemis	Zahra	16-04-09	1°30'	34°40'	660	1972-2011
3	Wadi Boumessaoud	Zenata	16-04-07	1°27'	34°58'	380	1985-2011
4	Chouly	Chouly	16-06-01	1°8'	34°51'	205	1970-2010
5	Isser	Sidi Aissa	16-06-14	1°3'	35°2'	720	1985-2011

Table III.3. Descriptive information of Temperature stations of the study area.

N	Name of station	Code of station	Longitude (W)	Latitude (N)	Elevation (m)	Period of Data
1	Beni Bahdel	16-04-02	1°27'	34°41'	665	1979-2010
2	Zenata	60531	1°27'	35°01'	247	1979-2010

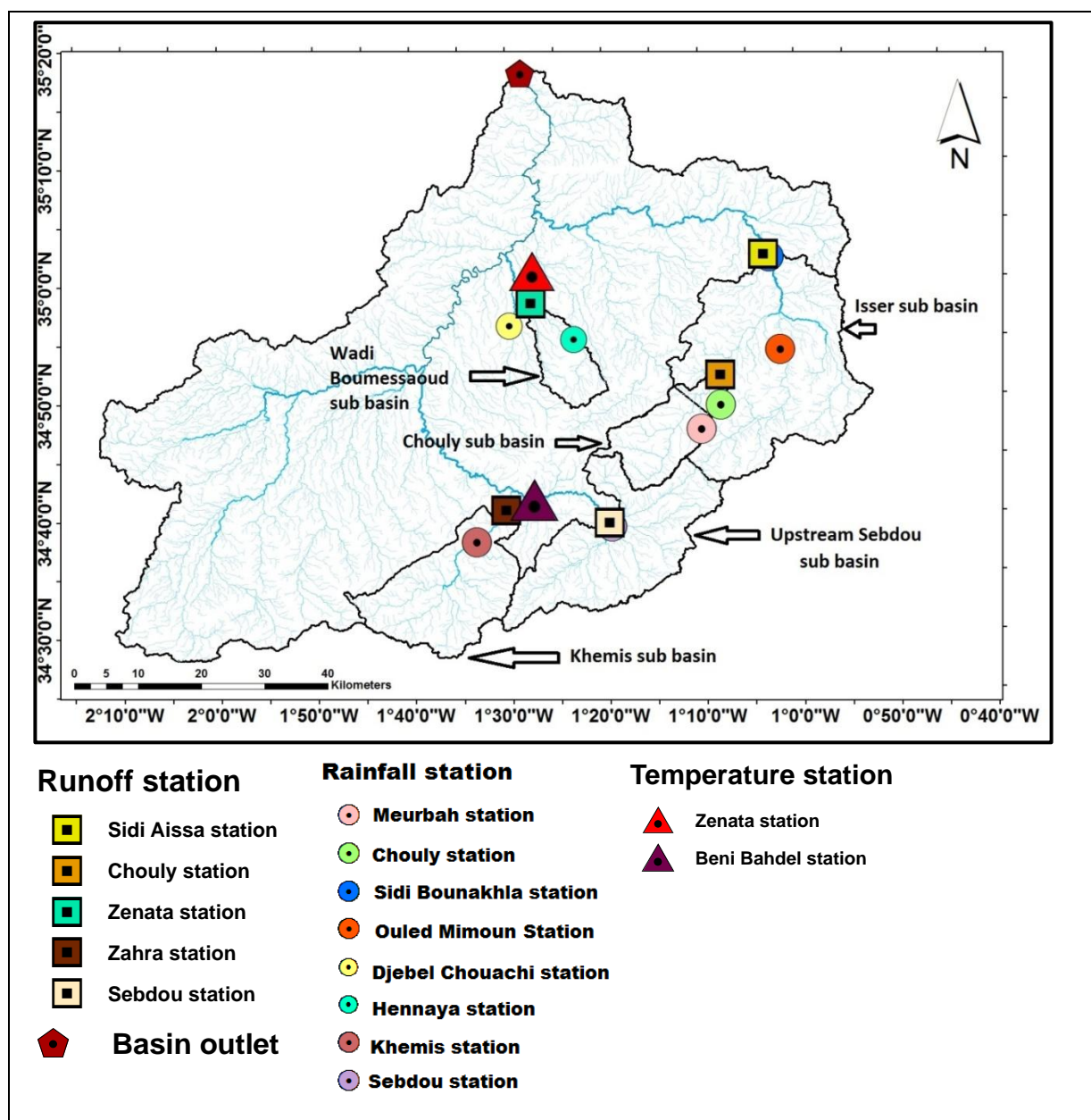


Figure III.1. Location of climatic and hydrometric measurement stations on studied sub basins.

III.3. Preliminary analysis of rainfall

III.3.1. Missing data details of rainfall stations

The amount of missing daily rainfall (tab.III.4, fig.III.2) data was about 0.8% for Sebdo, Khemis, was about 1.5% and 0.8% for Hennaya and Djebel Chouachi stations, respectively, with a standard error of estimation not exceeding a value of 7%. The amount of missing data reported to be 1.6% and 6.1% for Chouly and Meurbah stations and about 1.6% and 1.2% for Ouled Mimoun and Sidi Bounakhla stations with a standard error of estimation not exceeding the value of 6%, respectively. Overall, in general, the average missing daily rainfall data of the nine rainfall stations were 2.27% only.

We filled the missing data in the eight stations by a linear regression method as well as considering the data from the other adjacent stations (Beni Bahdel, Meffrouch, Sebra, Zaouia

Ben Amer, and Smala Sidi stations). The equations of the linear regression method is based on checking the correlation coefficient between the complete time series for the number of adjacent stations with the study area rainfall stations separately (tab. III.5).

Table III.4. Descriptive information of Missing data of rainfall station.

	Station	Std. Deviation	Missing	
			Count	Percent
Stations of the Study	Sebdou	4.13	94	0.8
	Khemis	4.83	91	0.8
	Hennaya	4.43	180	1.5
	Djebel Chouachi	4.44	92	0.8
	Chouly	4.39	197	1.6
	Meurbah	3.96	739	6.1
	Ouled Mimoun	3.55	190	1.6
	Sidi Bounakhla	3.86	150	1.2
Nearest stations	Meffrouch	5.98	1031	8.6
	Smala Sidi	3.62	244	2.0
	Sebra	4.54	218	1.8
	Zaouia Ben Amer	4.9	59	0.5

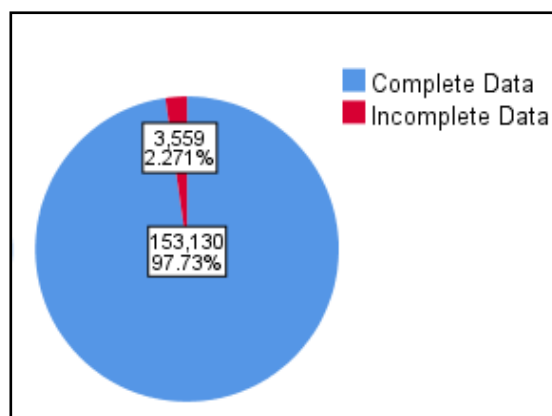


Figure III.2. Overall summary of missing data.

Table III.5. Regression correlation between study rainfall stations.

Station	Sebdou	Khemis	Beni Bahdel	Hennaya	Djebel Chouachi	Chouly	Meurbah	Ouled Mimoun	Sidi Bounakhla	Meffrouch	Smala Sidi Sebra	Zaouia Ben Amer	
Sebdou	1												
Khemis	0.52	1											
Hennaya	0.55	0.57	0.46	1									
Djebel Chouachi	0.4	0.4	0.3	0.5	1								
Chouly	0.6	0.56	0.44	0.73	0.5	1							
Meurbah	0.56	0.49	0.4	0.57	0.4	0.62	1						
Oued Mimoun	0.54	0.52	0.43	0.7	0.41	0.75	0.6	1					
Sidi Bounakhla	0.54	0.52	0.44	0.73	0.46	0.74	0.58	0.75	1				
Meffrouch	0.63	0.58	0.5	0.79	0.42	0.74	0.65	0.69	0.68	1			
Smala Sidi Sebra	0.5	0.52	0.42	0.68	0.4	0.59	0.5	0.6	0.57	0.62	1		
Sebra	0.55	0.53	0.4	0.77	0.43	0.66	0.55	0.6	0.62	0.75	0.68	1	
Zaouia Ben Amer	0.54	0.55	0.43	0.79	0.5	0.7	0.55	0.63	0.69	0.72	0.67	0.72	1

III.3.2. Annual rainfall analysis

As visualized in (fig.III.3), it is clear through the Box plot that the station of the highest length of the box (range) and the presence of the outliers are the station of the highest variability and station of the lowest range. Absence of the outliers is the station of least variability.

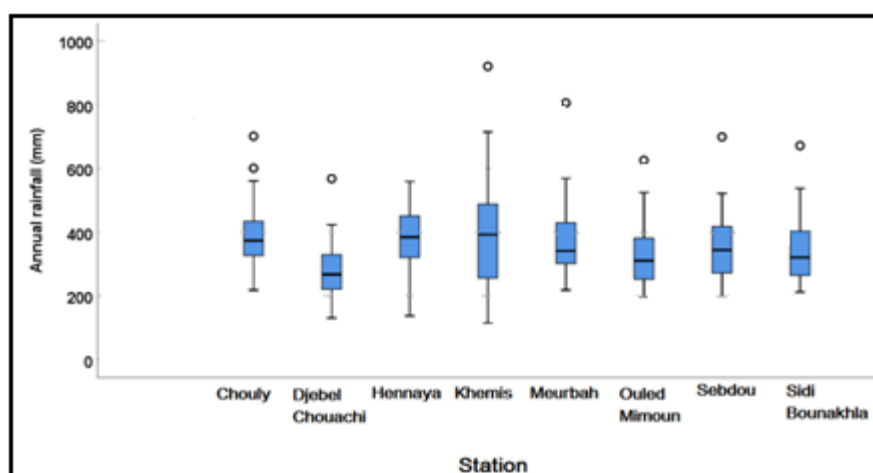
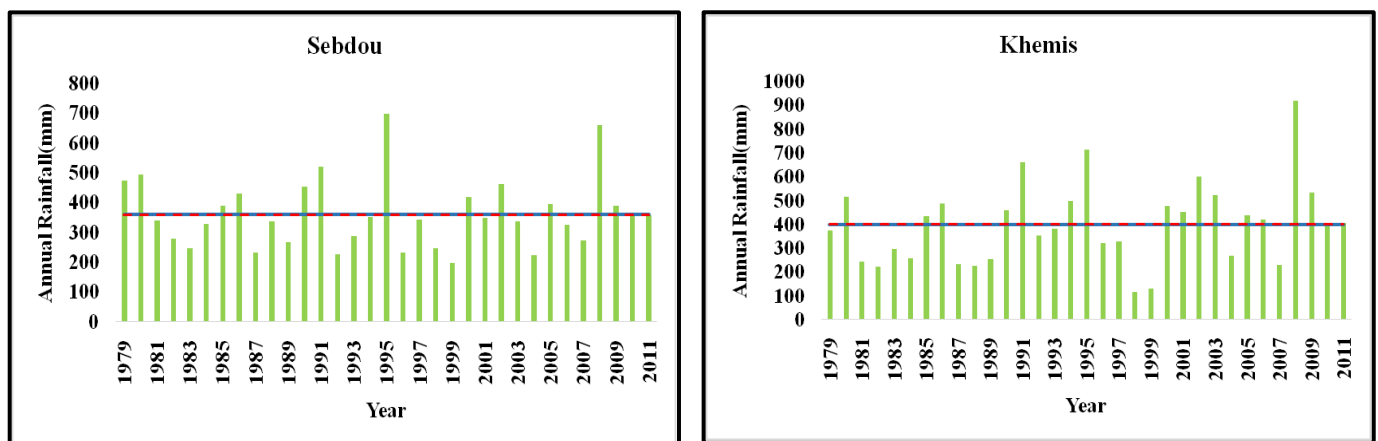


Figure III.3. Annual rainfall box plot. The upper and lower limit of the box indicate the 25th and 75th percentiles, respectively. The linear extensions mark the highest and lowest observed values.

The annual series of rainfall over a period of 32 years (fig.III.4) showed significant irregularity from year to year for rainfall station distributed over the entire study sub basins, where the average of rainfall for each 5 years range is between 288.6 mm to 417.26 mm for Sebdou station, and for Khemis station, the rainfall varies between 274.78 mm to 521.58 mm, all these stations are located in the Haute area of the Tafna basin. While the average rainfall for these stations is above 360.49 mm. The average rainfall of 5 years range in the center area of the basin is between 216 mm to 341.7 mm for Djebel Chouachi station, and between 354.27 mm to 409.74 mm for Hennaya station with the annual average of two stations is above 278.68. In the Est area of the average basin, the 5 years range of rainfall is between 329.56 - 454 mm, 326.43 - 443.87, 275.76 - 401.46 mm, and 310 - 390.75 mm for Chouly, Meurbah, Ouled Mimoun, and Sidi Bounakhla stations respectively, where the average rainfall is above 313.4 mm.

The highest average of rainfall was detected between 1994-1995 for Khemis, and Sebdou stations with a maximum of 521.58 mm at Khemis station. While during the period 2001-2005 was recorded the highest average of rainfall at Djebel Chouachi and Hennaya stations, and the period 2006-2011 for Chouly, Meurbah, Ouled Mimoun, and Sidi Bounakhla with a maximum of 454.2 mm at Chouly station. The decrease in rainfall was detected in the period 1996-2000 for Sebdou, Khemis, Chouly, Ouled Mimoun, and Sidi Bounakhla stations, and in the period 1979-1985 for Hennaya, and Meurbah stations, and only Djebel Chouachi station showed a decrease in rainfall for period 1986-1990 with the minimum of 216.16 mm. That showed homogeneity in a variation of rainfall in terms of the increase of rainfall for close stations (fig.III.5). In the observation of the time series of annual rainfall, the heighest rainfall was recorded at all stations between 568.3 mm (Djebel Chouachi) to 919.9 mm (Khemis) in 2008 , except Sebdou, and Hennaya stations was recorded in 1995, and 1980 respectively.



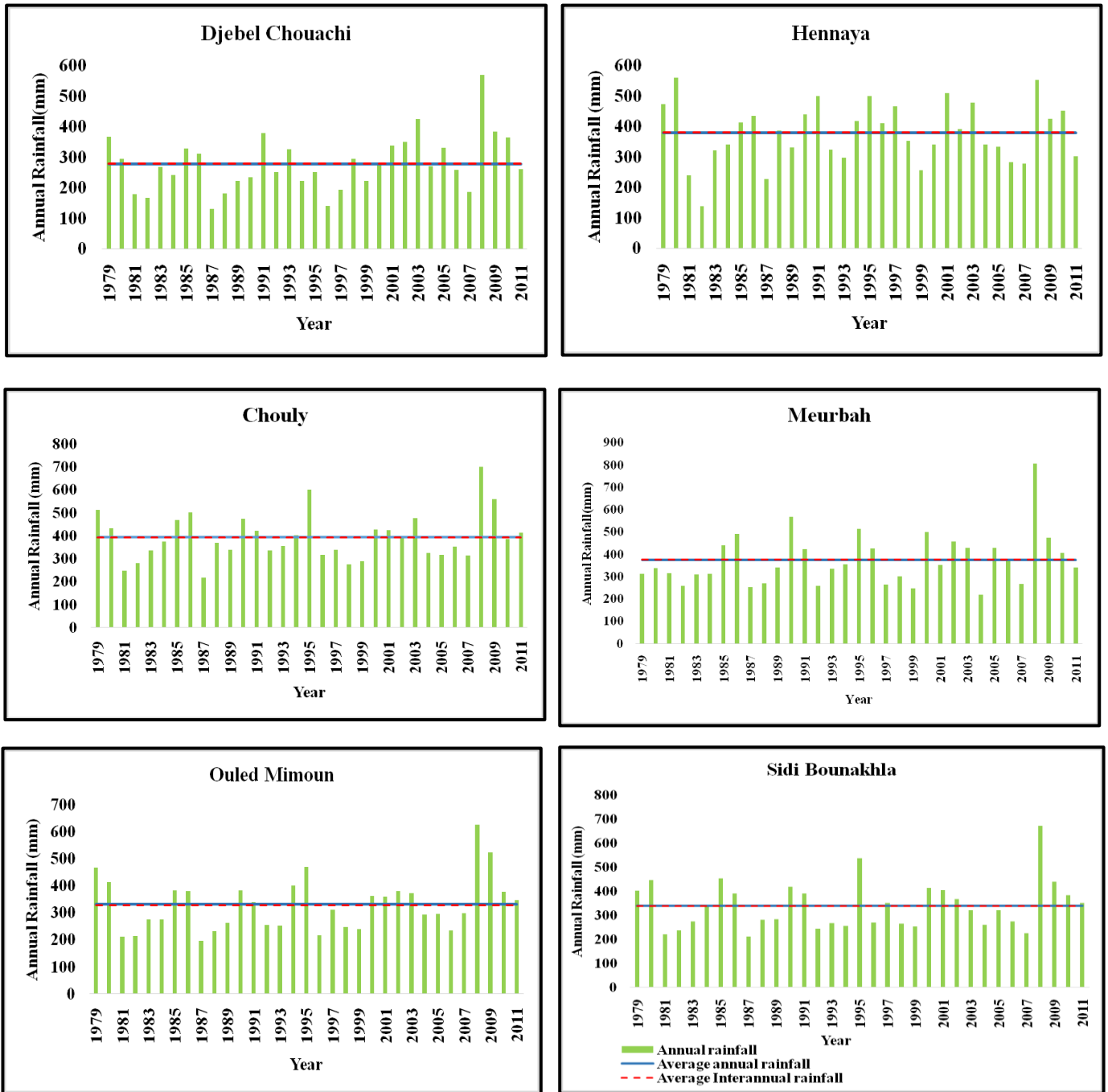


Figure III.4. Variability of average rainfall of the study stations.

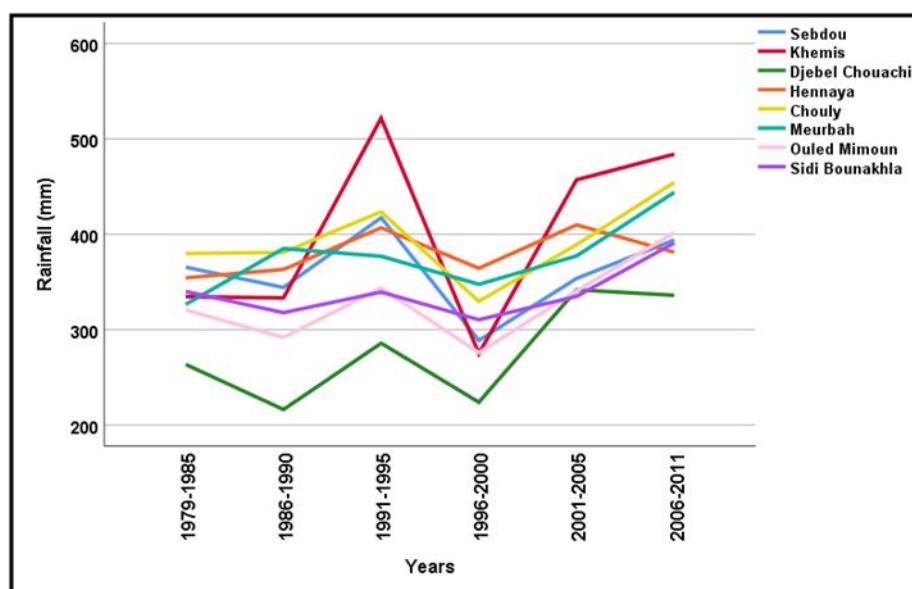


Figure III.5. Annual evolution of precipitation at study stations in the sub basins (1979/1980 - 2011/2012).

The Pearson Chi Square test is used to determine whether a statistically significant relationship exists between the two categorical variables. We used this test to verify for a relation between the number of rainfall days and the rainfall stations featured by location or elevation. The results show a significant level at 5% while the value of the test is 908.309. The assumption of the test has not been violated, which emphasizes the percentage of the cells less than the value of 5 should not be more than 20% (less value of the cells in the data series is 15.33) (tab. III.6).

Table III.6. Results of Chi-square Test.

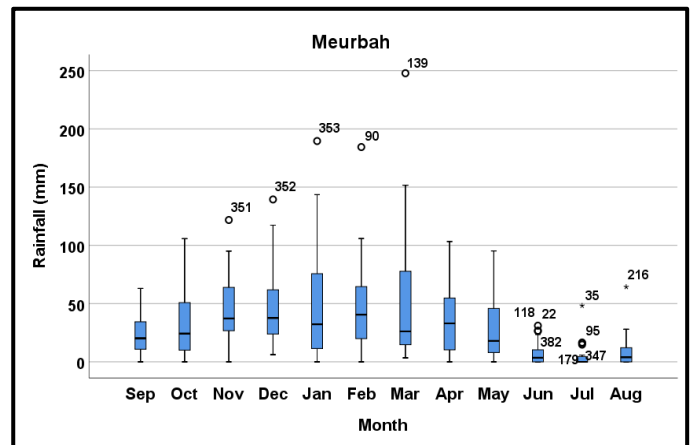
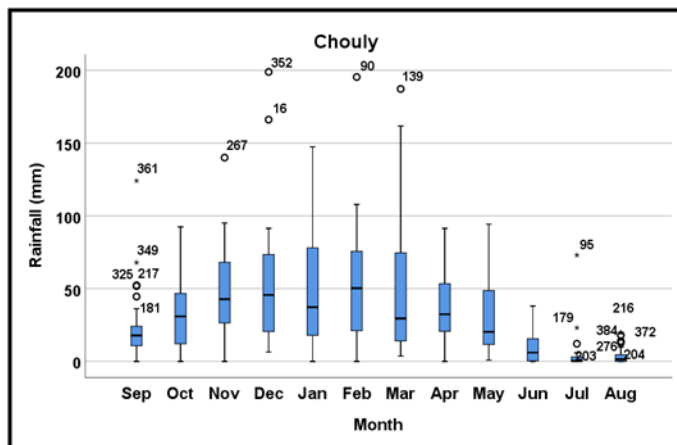
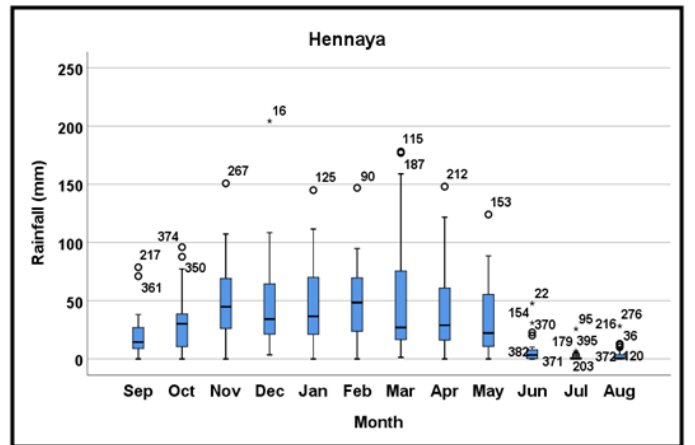
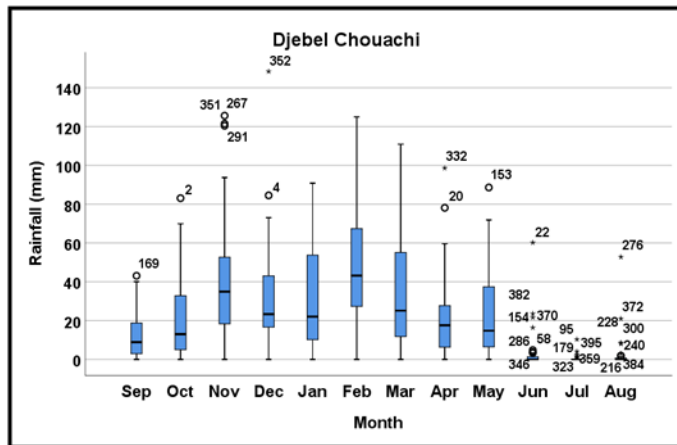
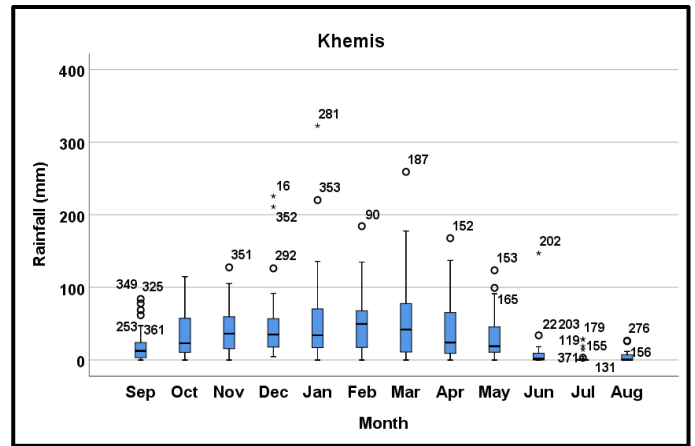
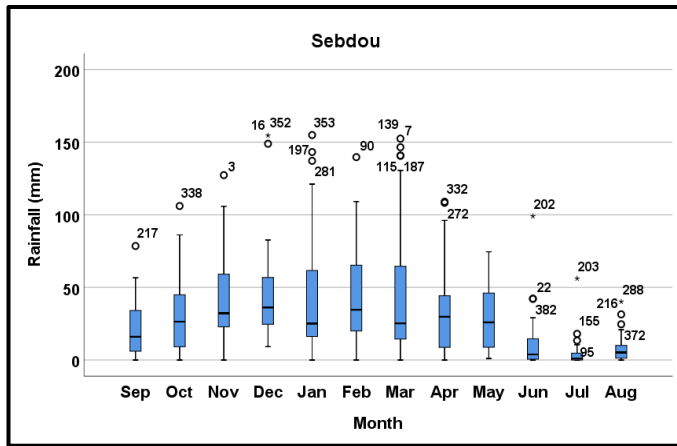
	Value	df	Asymptotic Significance (2-sided)
Pearson Chi-Square	908.309 ^a	33	.000
Likelihood Ratio	973.059	33	.000
N of Valid Cases	108477		

a. 0 cells (.0%) have expected count less than 5. The minimum expected count is 15.33.

III.3.3. Monthly rainfall analysis

The maximum monthly rainfall was in December above 148.4 mm for Djebel Chouachi, Hennaya, and Chouly, and in January with values of 154.9, 322.5 mm for Sebdou and Khemis respectively, and in February with maximum values of 157.3, 182.3 mm for Ouled Mimoun, and Sidi Bounakhla respectively, and only Meurbah station has maximum value (247.8 mm) with March. Box plots show the statistical distribution of data, indicating the maximum, 75 percentile, median, 25 percentile and minimum values, from the top of the graph, respectively. Figure III.6 showed the box plot of March, January, February which has

the highest length of the box, and a few the outliers showing the lowest variability of rainfall. And September has more outliers which indicating the highest variability.



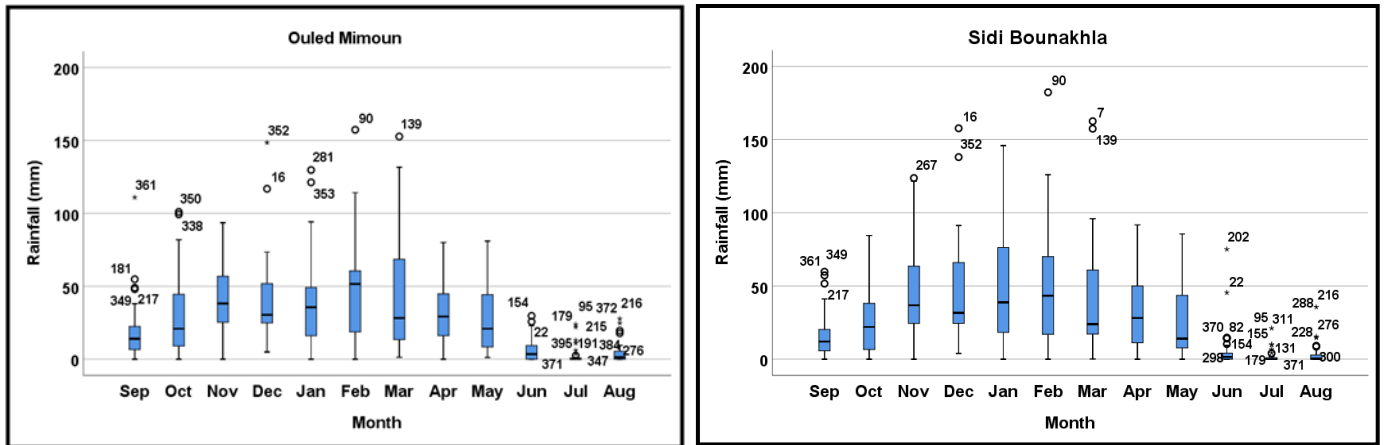
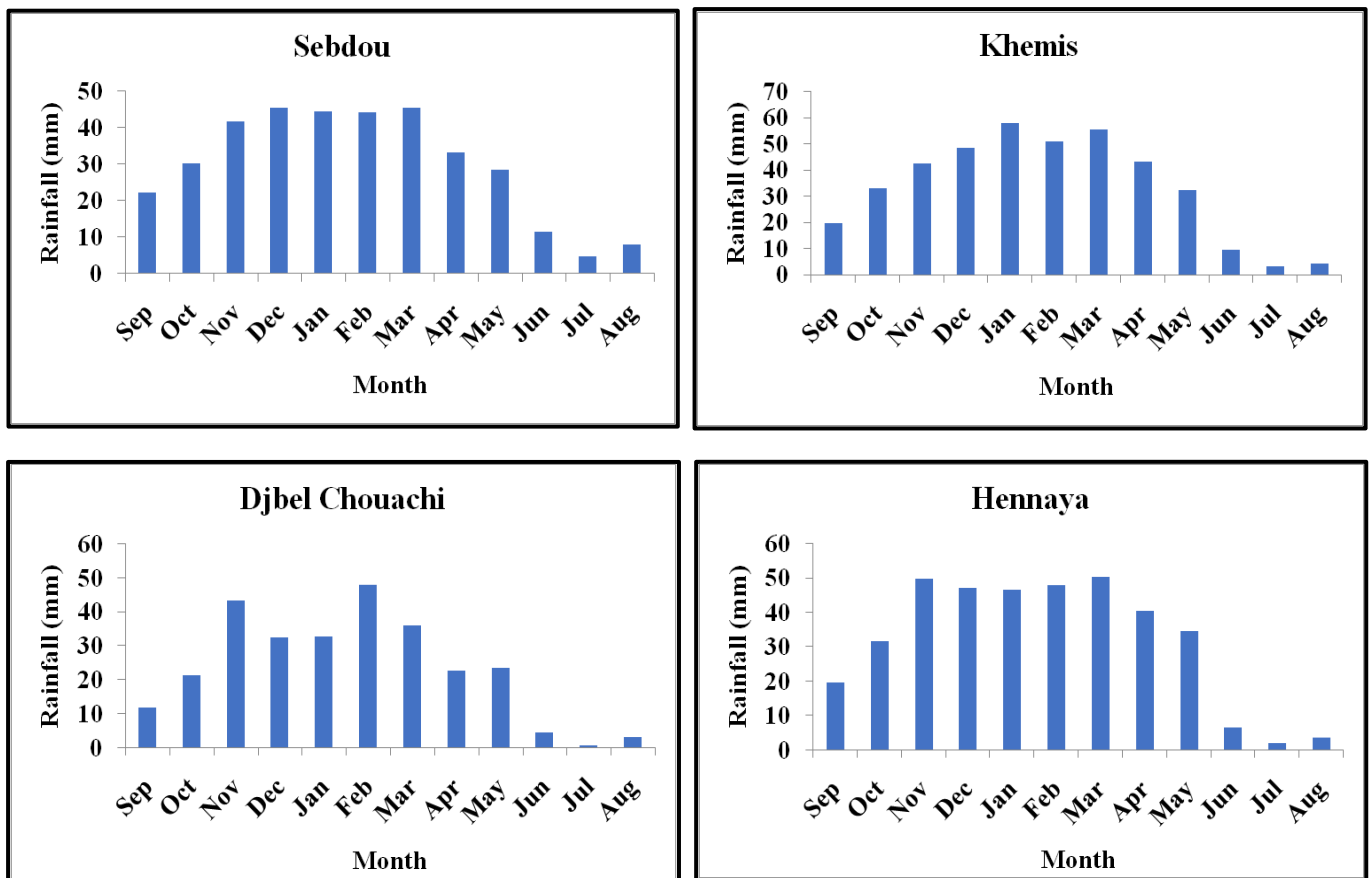


Figure III.6.Variation of average monthly, minimum, maximum and average extremes rainfall (1979/1980-2011/2012).

The average monthly rainfall for the period (1979-2011) of the study stations (fig.III.7) shows the minimum rainfall is mostly observed in July approximately around 0.6 mm (Djebel Chouachi) to 4.7 mm (Sebdou) representing the most dry month, and the maximum in March with range 49.3 mm (Meurbah) to 55.4 mm (Khemis), February with 46.3 mm (Ouled Mimoun) to 51.1mm (Sidi Bounakhla), and December with 45.6, 52.9 mm for Sebdou, Chouly respectively, and that represent the rainiest month.



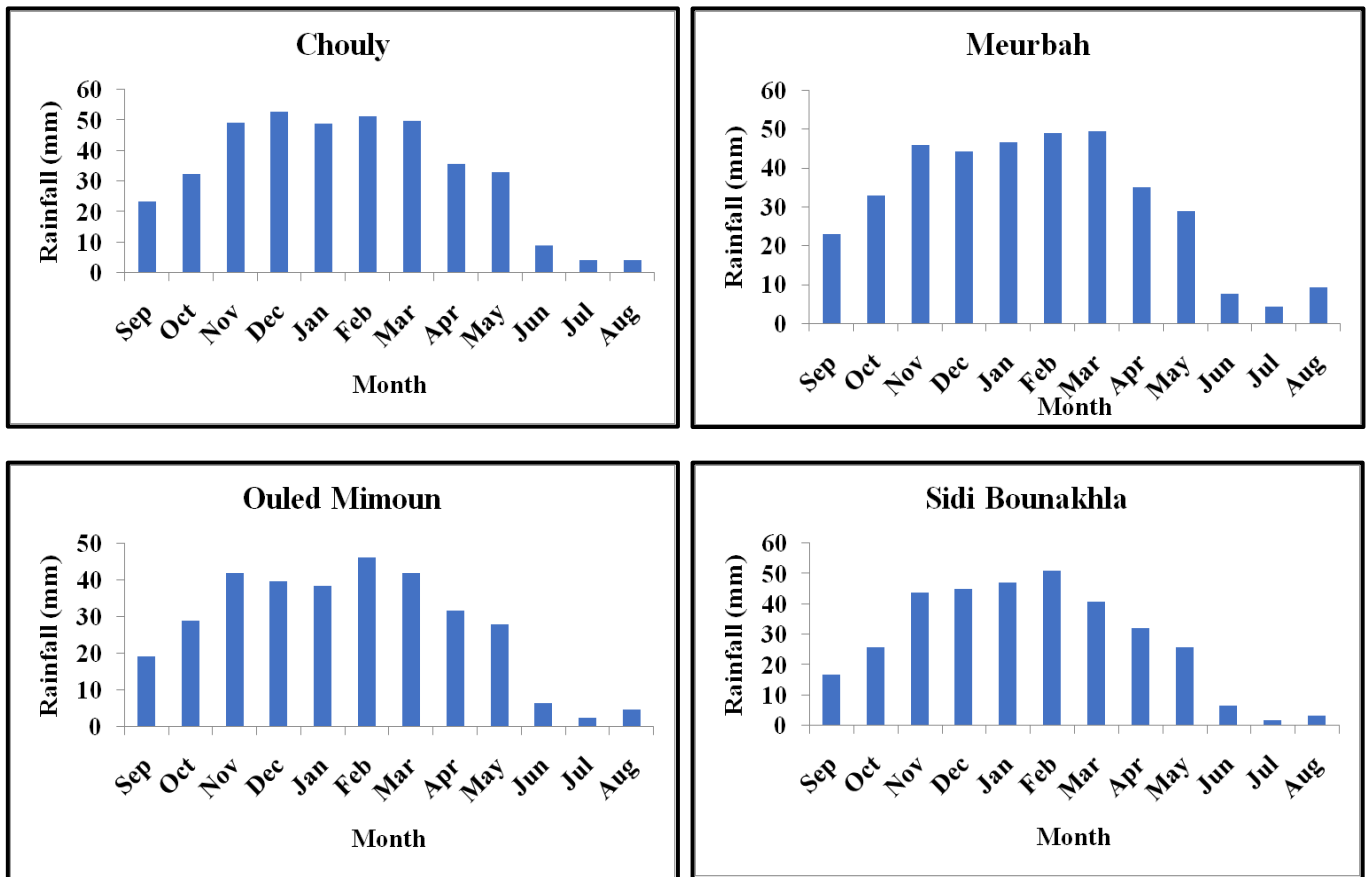


Figure III.7. Variation of monthly average rainfall of the study stations (1979/1980-2011/2012).

III.3.4. Seasonal rainfall analysis

The seasonal analysis is important to define the variability for specific season or to several seasons. The figure III.8 showed that the Winter season (December, January, February) has the highest average rainfall compared to Autumn season (September, October, November), and Spring season (March, April, May) and the highest values was defined at Khemis station (156.8 mm), while the lowest average rainfall was at summer season (June, July, August), where Djebel Chouachi has the lower value 7.96 mm.

The box plots (fig.III.9) show a small range between high and low values in summer for all stations indicates uniformity among the data (the low values close or equivalent to zero). The highest length of the box was defined in Winter and Spring showing the lowest variability of rainfall.

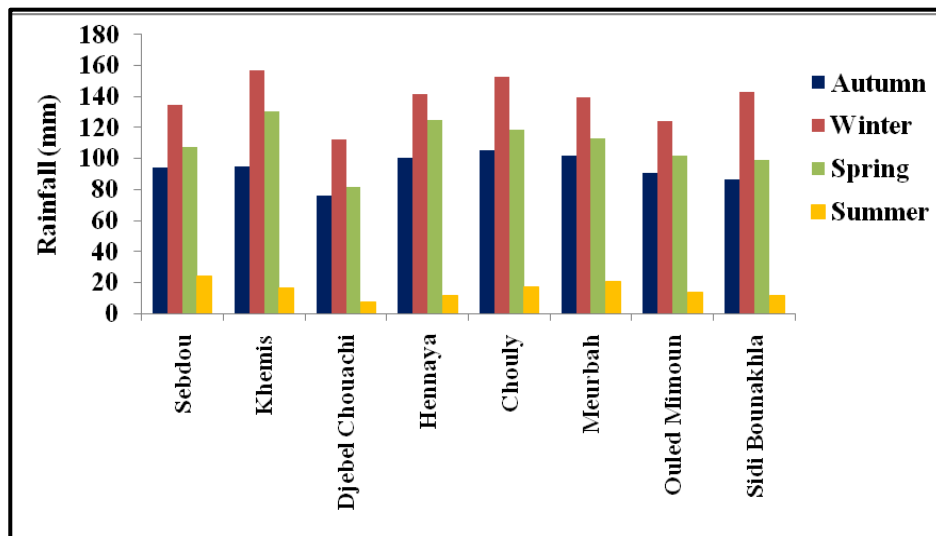
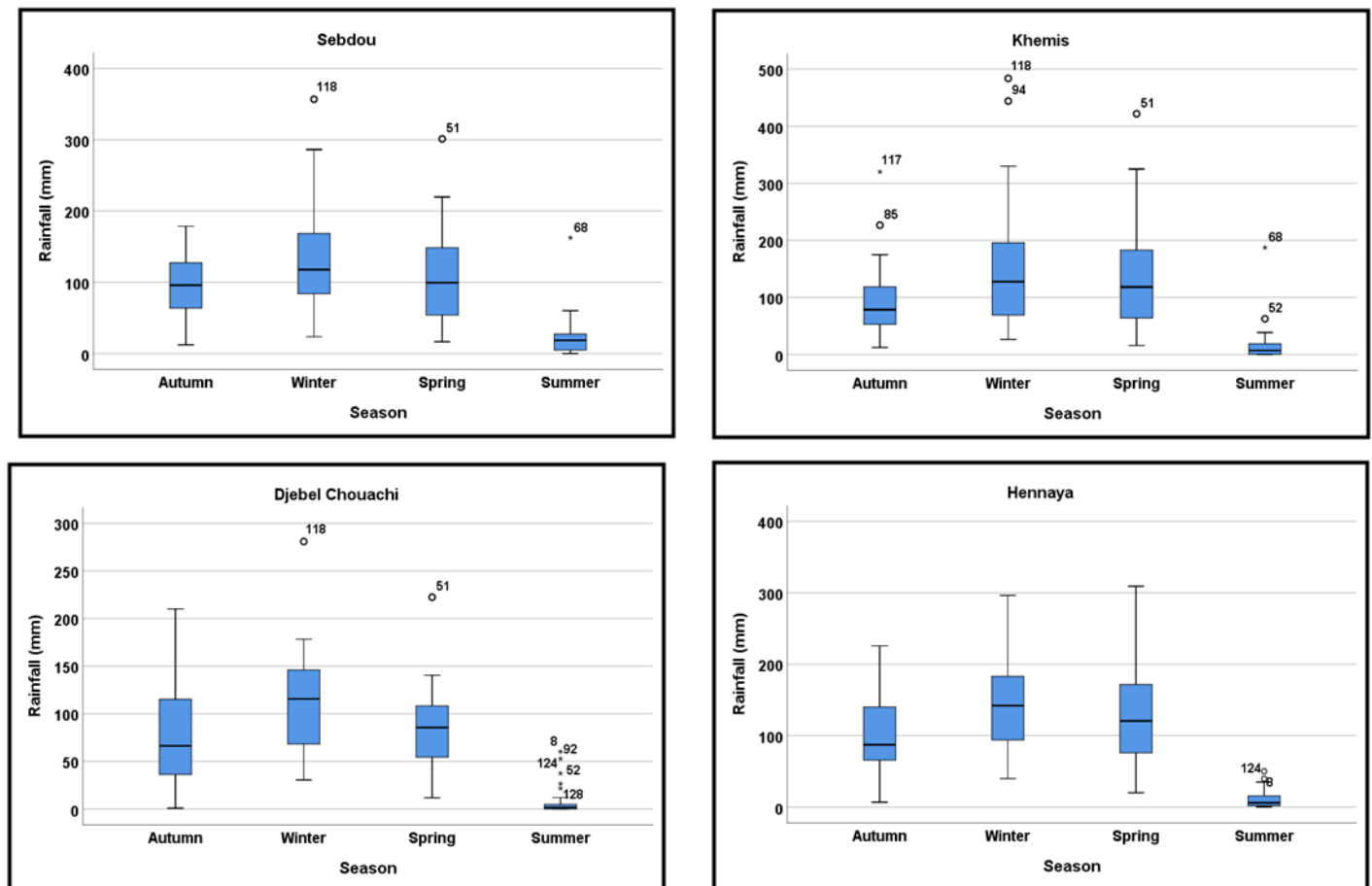


Figure III.8. Seasonal variations in rainfall of the studied stations in the Tafna basin.



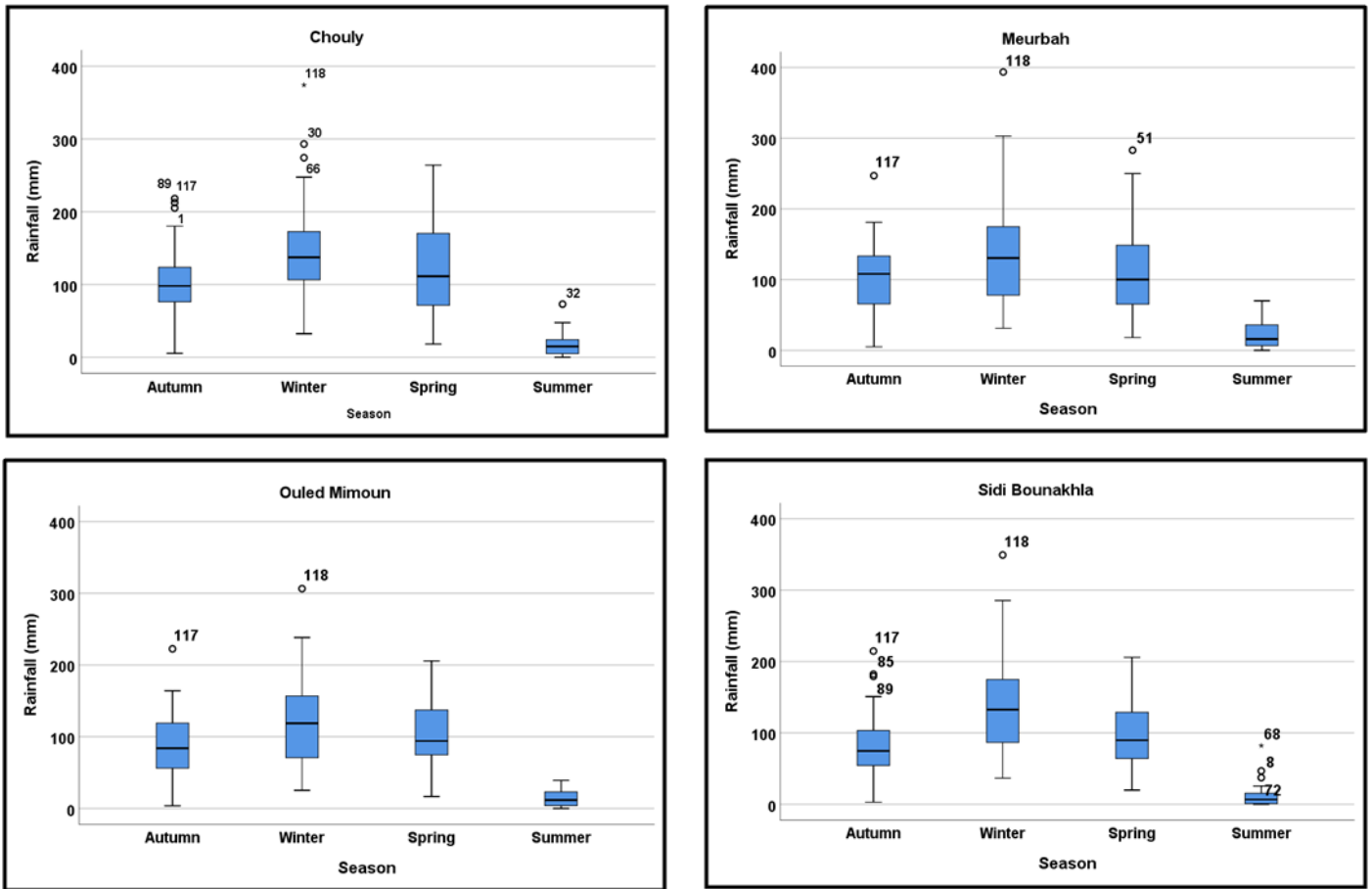
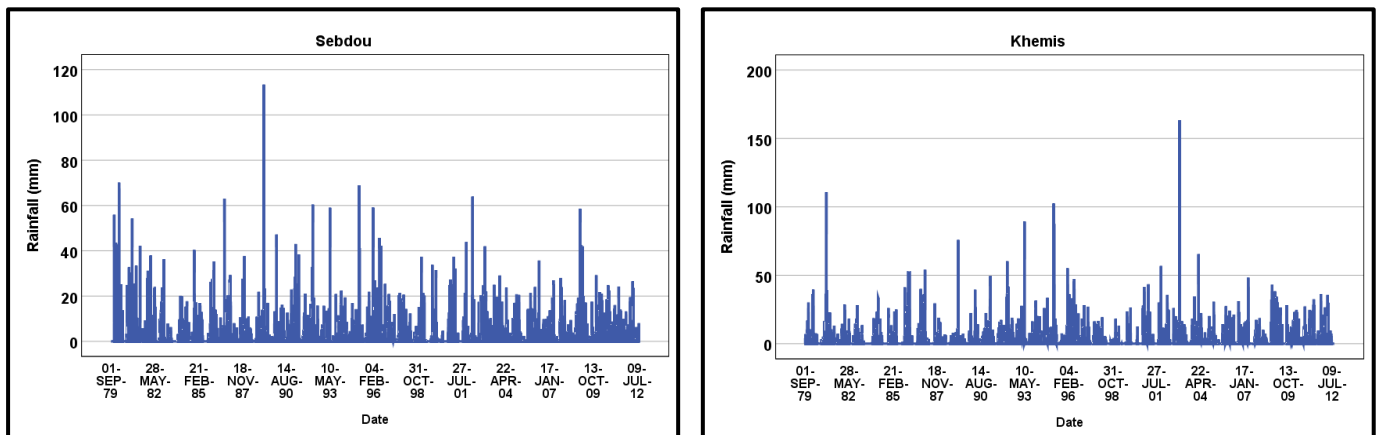


Figure III.9. Box plot of the seasonal rainfall for the study stations.

III.3.5. Daily rainfall analysis

The daily rainfall time series is showed irregularity variation. The visualization graphic (fig.III.10) showed clearly the rainiest period are recorded from 1979 - 1989 at Sebdou station, and from 2000 - 2011, 1989 - 2011 for Khemis and Djebel Chouachi respectively.



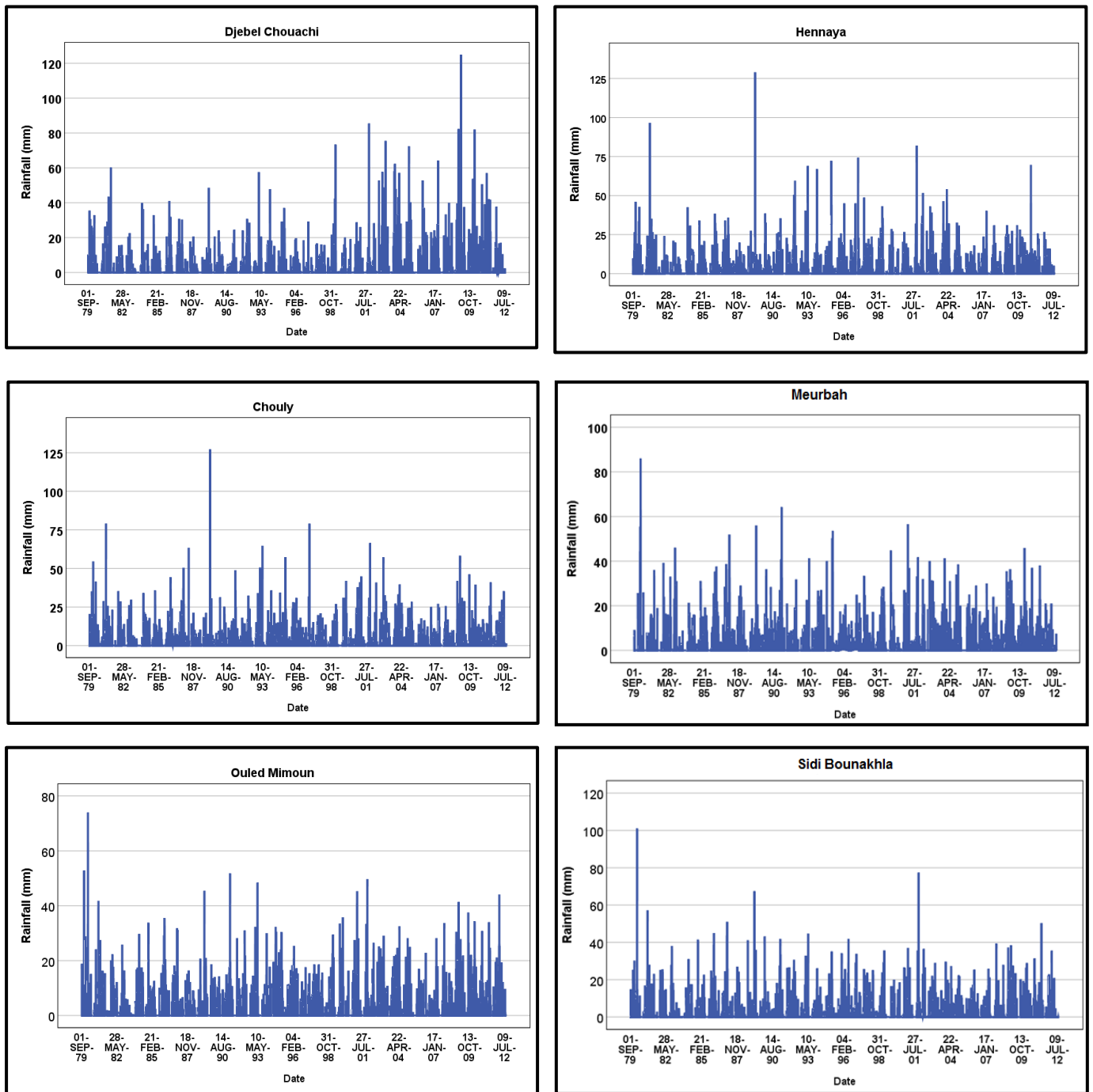


Figure III.10. Variation of daily rainfall at the study stations (1979/1980 - 2011/2012).

The station (location, elevation) and the count of range number of rain days (tab.III.7, fig.III.11) are not independent, where the higher number of non-rain days (10800 days) corresponds to the station of the low altitude (110 m) and near to the sea (Djebel Chouachi), and the lower number of non-rain days (9747 days) corresponds to the higher altitude (1100 m).

Table III.7. Range of daily rainfall.

	[0.1-0.9]	[0]	[1-10]	[10.1-44.9]	>=45
Sidi Bounakhla	788	9789	1129	340	7
Chouly	640	9837	1196	365	15
Djebel Chouachi	356	10800	627	244	26
Hennaya	631	9940	1115	349	18
Khemis	330	10297	987	421	18
Meurbah	760	9747	1179	357	10
Ouled Mimoun	311	10246	1151	338	7
Sebdou	673	9822	1214	330	14

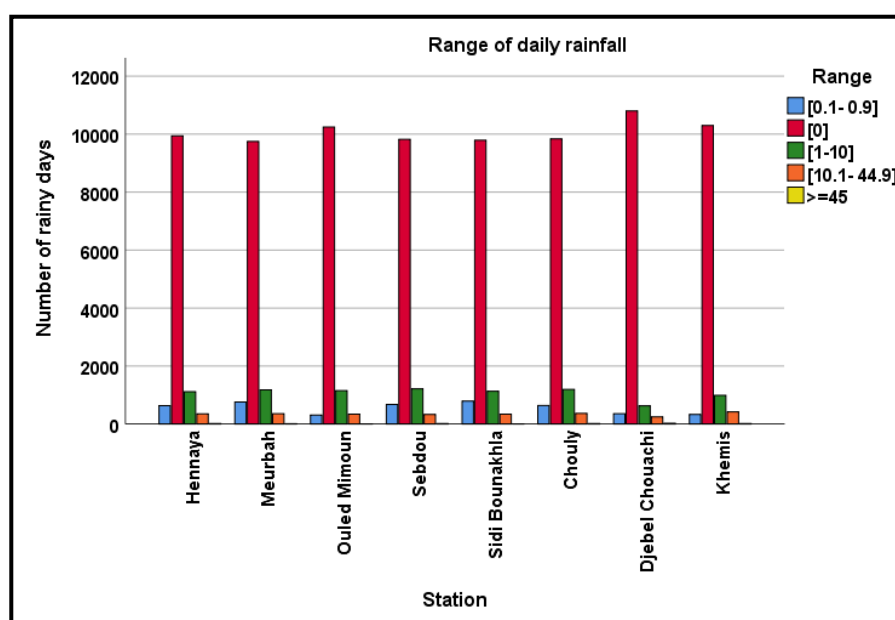


Figure III.11. Frequency of daily rainfall.

III.4. Preliminary analysis of runoff

III.4.1. Annual depth of runoff analysis

The results of the variation of the annual runoff during the study period 1985/1986 - 2010/2011 (fig.III.12), showed irregularity from one period to another period. The minimum average annual runoff was mostly defined in the period 1996 - 2000 with values 0.22, 0.34, 0.13 m³/s at Sebdou, Zahra, and Chouly respectively, and only in the period 2001-2005 at Zenata and Sidi Aissa with values 0.06, and 0.32 m³/s respectively. The maximum average annual runoff was mostly defined in the period 2006-2010 with values 0.25, 1 m³/s at Chouly, and Sidi Aissa respectively, while in the period 2001-2005, 1991-1995, 1996-2000 at Sebdou, Zahra, and Zenata respectively. The visualization of figure III.13 showed that 1989, 1993, 1996 to 1999, and 2004 has the lowest amount of runoff depth for all station, where

Chouly station has the highest values of runoff depth during the study period with a high peak of approximately around 182 mm in 2008, and Zenata has the lowest runoff depth in the study period.

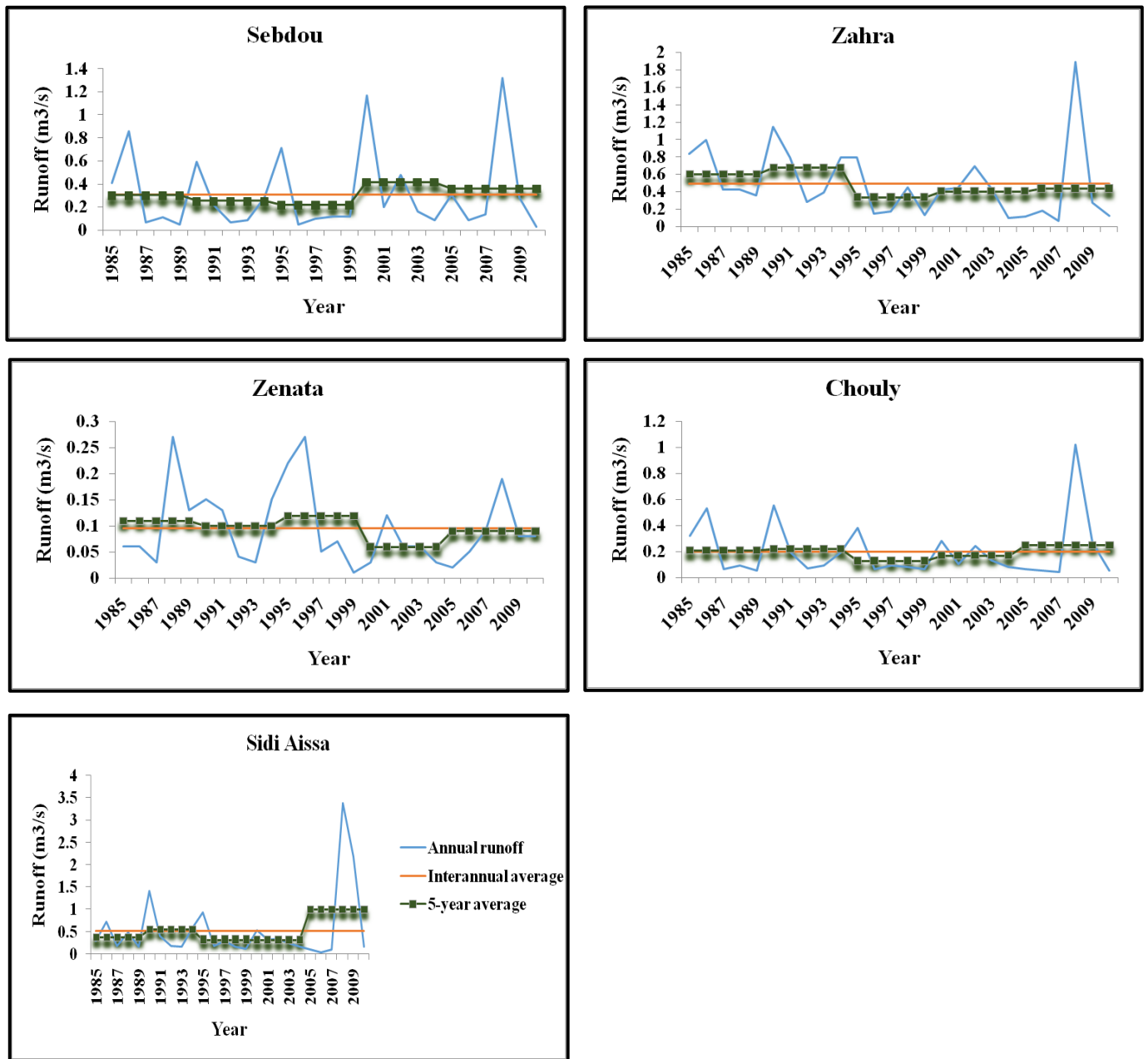


Figure IV.12. Variation of average annual runoff at the study station (1985/1986-2010/2011).

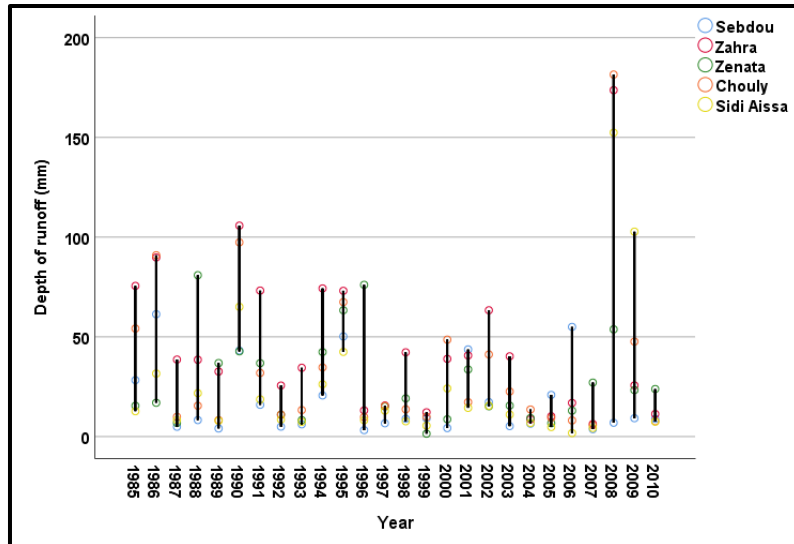
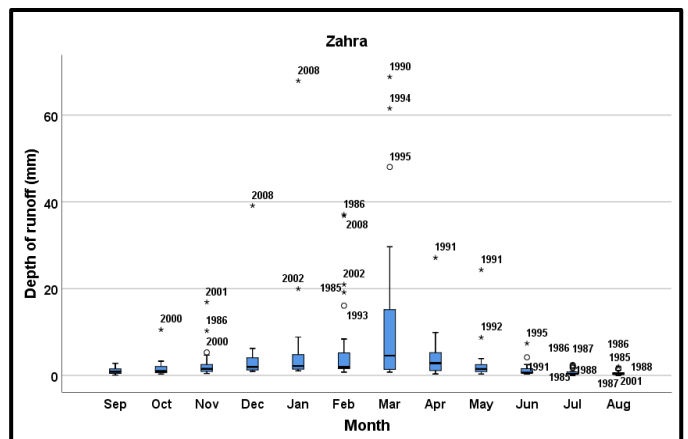
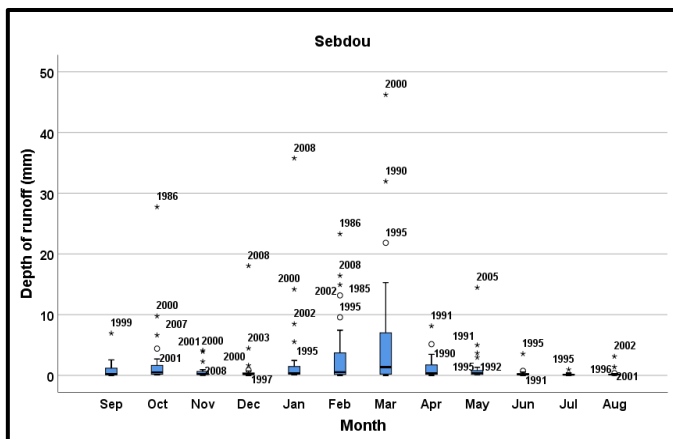


Figure IV.13. Annual depth of runoff (mm) for the study stations.

III.4.2. Monthly depth of runoff analysis

The box plots (fig.III.14) of the average monthly depth of runoff shows the high length of the box was defined in March indicating that the high amount of runoff depth was in this month with high length at Zahra, while the small box plots were defined in June, July, August indicating the lower value for depth of runoff in these months.



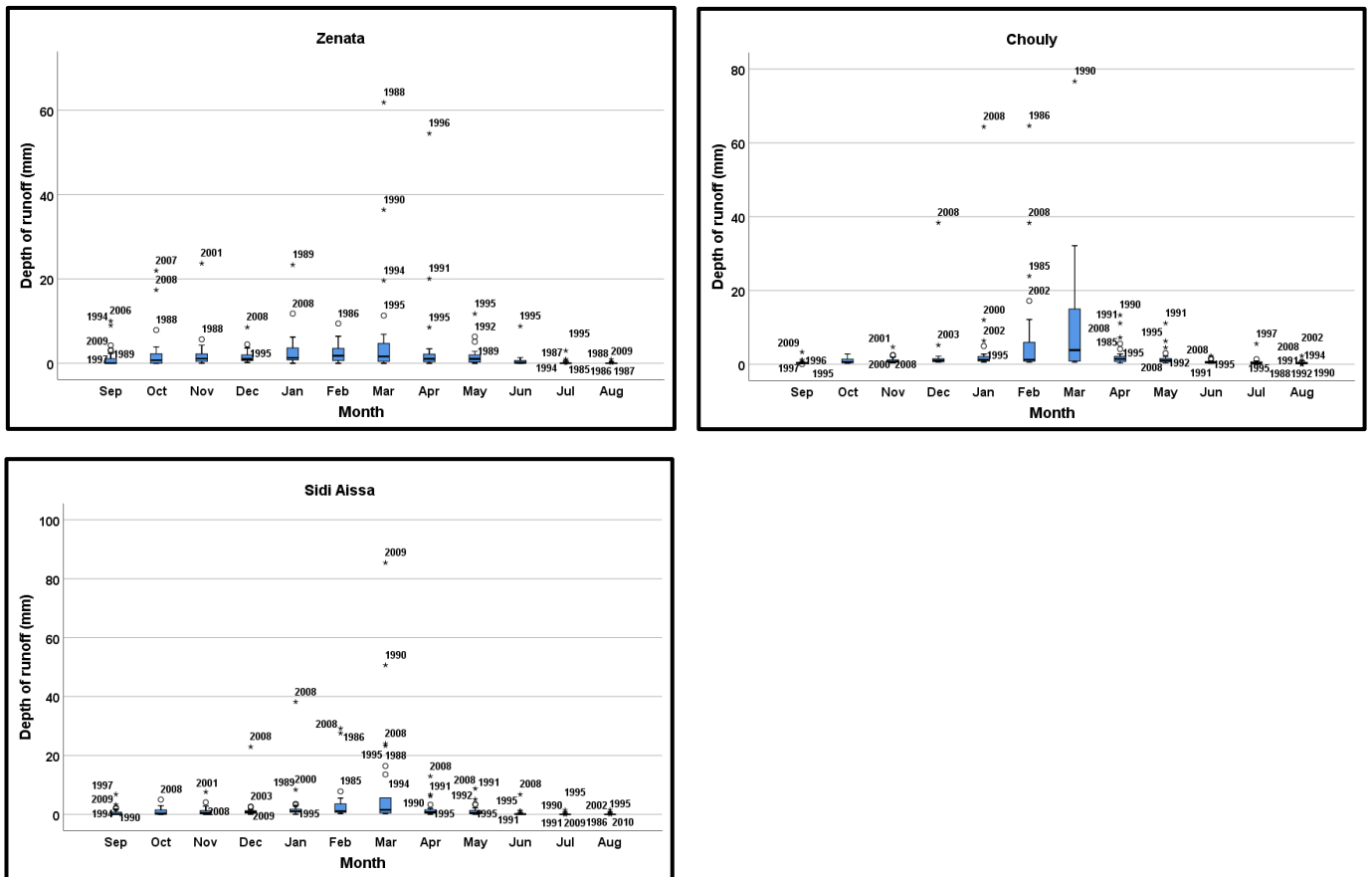
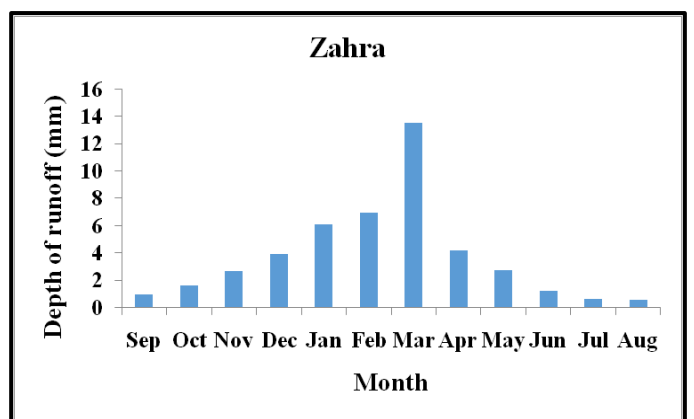
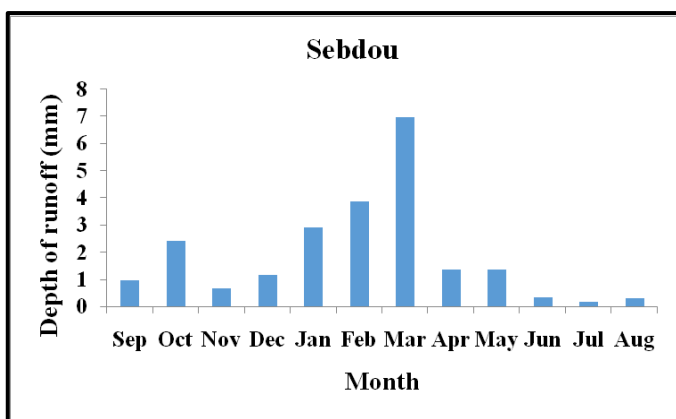


Figure III.14. Box plots of average monthly depth of runoff of the study stations.

The average monthly depth of runoff (fig.III.15) shows a maximum value in March with a range of 6.72 mm (Zenata) to 13.57 (Zahra). The minimum values are mostly observed in July within the values 0.16, 0.11 at Sebdou, and Sidi Aissa, respectively, and also in August with values 0.58, 0.07, and 0.4 at Zahra, Zenata, Chouly, respectively.



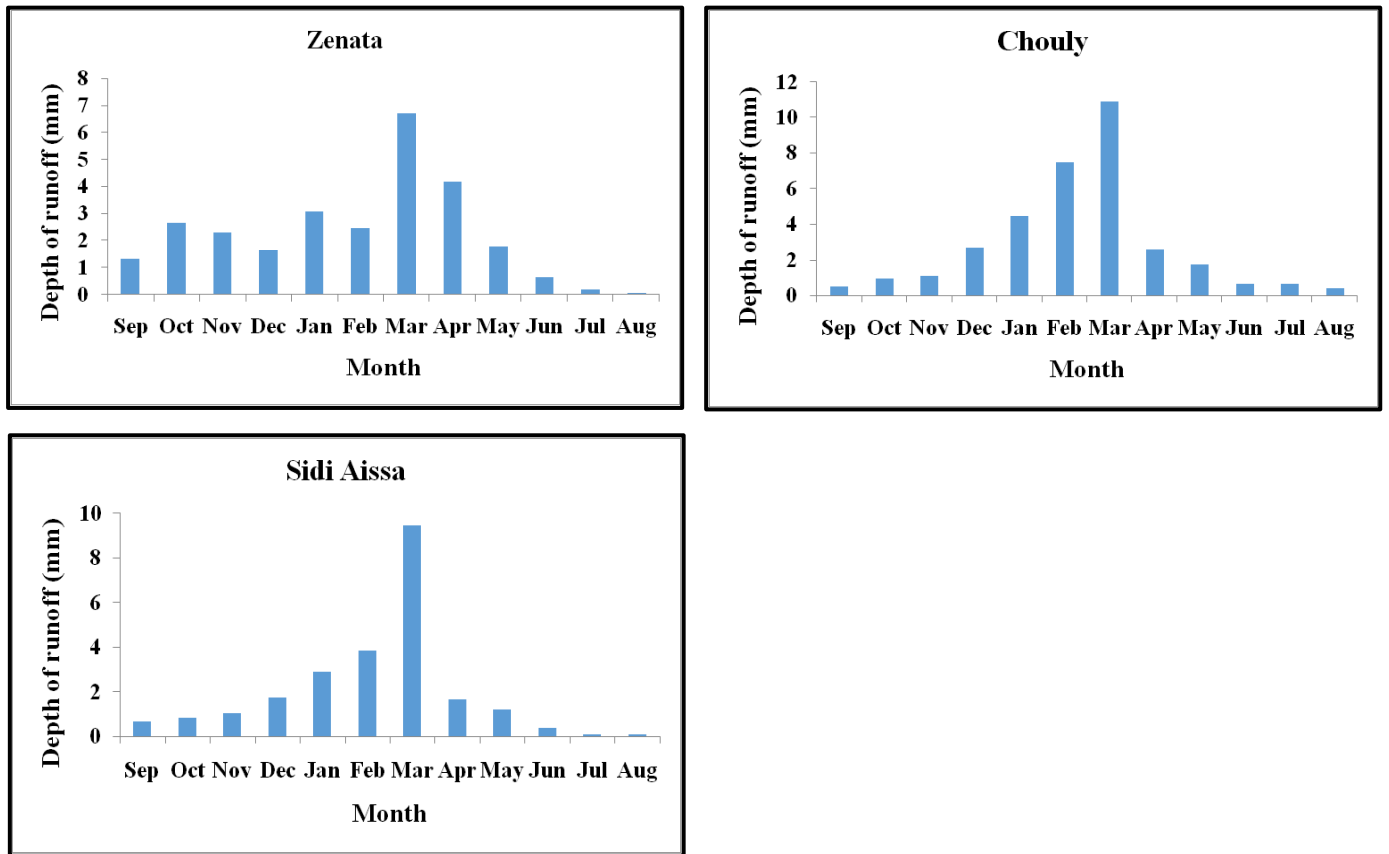
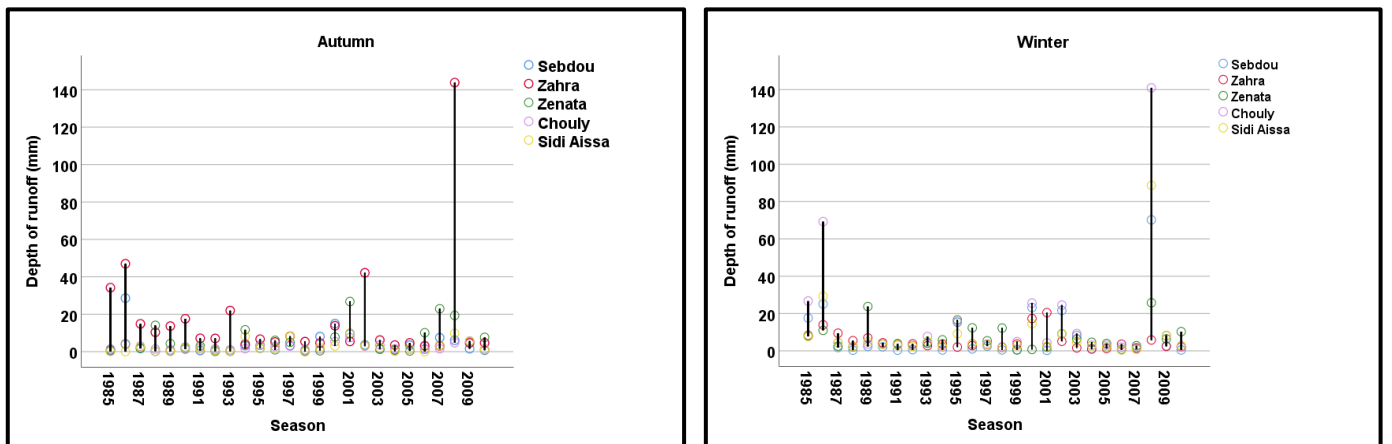


Figure III.15. Variation of monthly average depth of runoff of the study stations.

III.4.3. Seasonal depth of runoff analysis

Figure III.16 showed that amount runoff depth was low in 1988, 1989, 1996, 1998, 2004 in Autumn, and 1987 to 2007 in winter, and in Spring with the year 1987, 1989, 1993, 1997, 2007, and with 1989, 1994, 2000, 2005, 2006, 2007 in summer. the highest depth of runoff was 2008 in Autumn and winter at Zahra and Chouly respectively, and in 1990, 1995 at spring and summer respectively at Chouly, Zenata respectively.



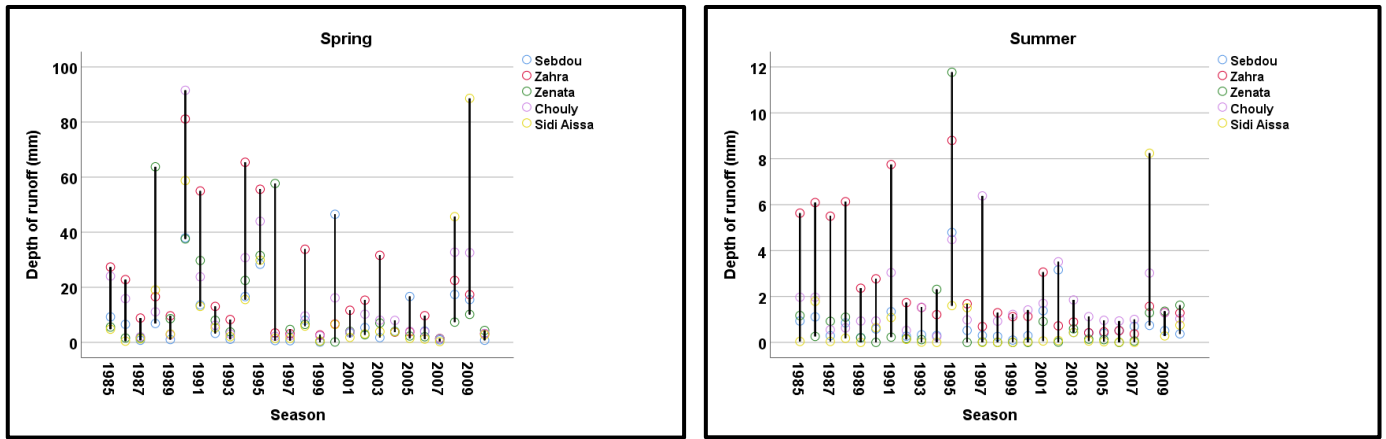


Figure III.16. Seasonal depth of runoff for the study station.

The seasonal average depth of runoff in figure III.17 showed that spring has the highest depth of runoff compared to autumn and winter for all stations, and his peak was defined at Zahra station around 20.52 mm , while the lowest values were at Sidi Aissa station around 0.65 mm in summer. Zahra station showed highest values of seasonal depth of runoff to spring, summer and winter among the study stations, while the highest value runoff depth for autumn was at Zenata stations (6.26 mm).

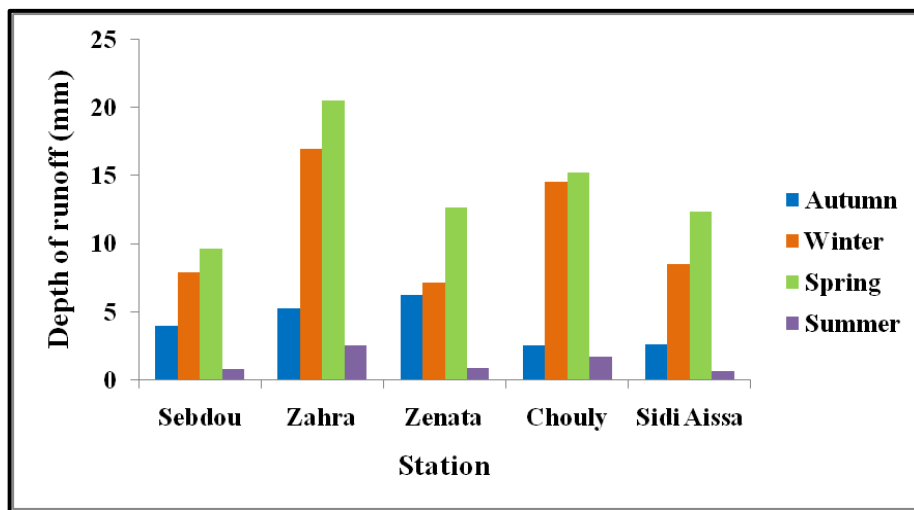


Figure III.17. Variation of seasonal average depth of runoff of the study runoff station.

III.4.4. Daily depth of runoff analysis

The daily depth of runoff time series (fig.III.18) is showed irregularity variation with high peaks approximately around 40, 50 mm at Sebdu and Zenata stations respectively, and is above 30 mm at Zahra station, and above 25, 15 mm for Chouly and Sidi Aissa stations respectively.

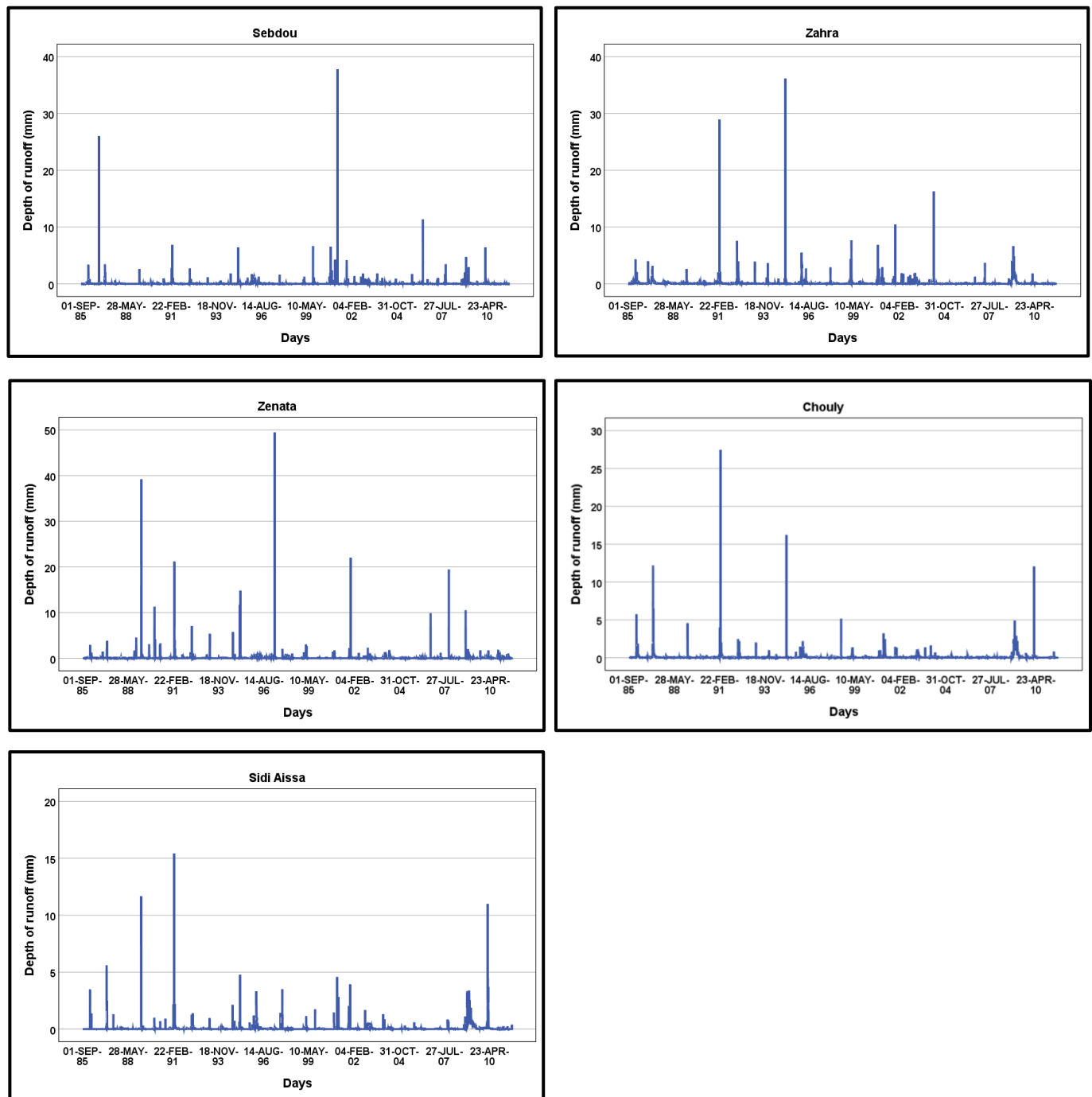


Figure III.18. Variation of daily depth of runoff of the study stations.

The frequency of the different range of daily runoff are presented in table III.8 and figure III.19, the results showed that Zahra station has the range of the highest values of 0.11 to above $0.5 \text{ m}^3/\text{s}$, which means receiving high amounts of runoff compared to other stations, while Zenata has the lowest values in this range Zahra station. And Chouly and Sebdu stations are receiving moderate amount of runoff represented by the high rate of the range 0.02 to $0.06 \text{ m}^3/\text{s}$. Zenata and Sidi Aissa stations receive less amount of runoff illustrated in the high rate of the range of the lowest values of 0 to $0.01 \text{ m}^3/\text{s}$.

Table III.8. Frequency of different range of daily runoff of the study stations.

Station	Classification of Range of the Number of Runoff Days (m^3/s)				
	[0-0.01]	[0.02-0.06]	[0.07-0.1]	[0.11-0.5]	> 0.5
Sebdou	2264	4950	479	925	878
Zahra	440	1733	1231	4641	1451
Chouly	342	5903	1460	1210	581
Zenata	4865	2895	611	938	187
Sidi Aissa	3732	754	662	3215	1133

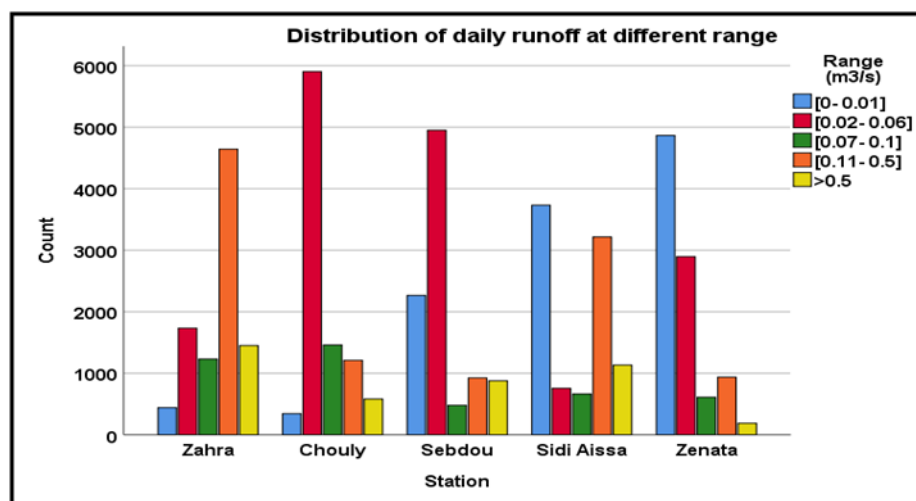


Figure III.19. Range of daily runoff of the study stations.

III.5. Preliminary analysis of temperature

III.5.1. Annual temperature analysis

The average annual temperatures (fig.III.20) are irregular by tending to increase or decrease from one period to another. The low values of temperature were defined in period 1979 - 1985, and 1991 - 1995 with value 21, 20.9 °C respectively at Beni Bahdel, and with the same period with values 18.4, 18.2 °C respectively at Zenata which are below the average 21.62, 18.81 °C at both stations respectively. The high temperature was in the period 2006-2010 with values 22.3, 19.3 °C at both stations respectively.

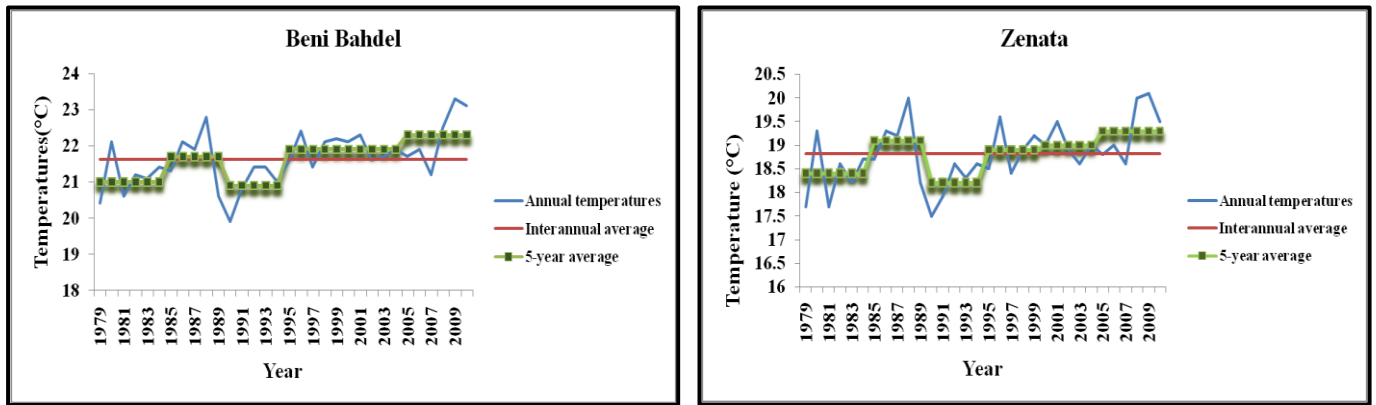


Figure III.20. Variation of average annual temperature of the study stations.

III.5.2. Monthly temperature analysis

The variations of the monthly average temperatures are presented in the figure III.22, the high value was defined in August with values 34.4, 30.1°C at Beni Bahdel and Zenata, respectively which indicate it as the hot month. And January indicates the lower values of temperature 11.2, 9.8 °C at both stations respectively and is defined as the coldest month. The visualized of the box plots (fig.III.21) of two stations showed that the box of September at Beni Bahdel and March at Zenata have a presence the outliers which mean are the month of highest variability.

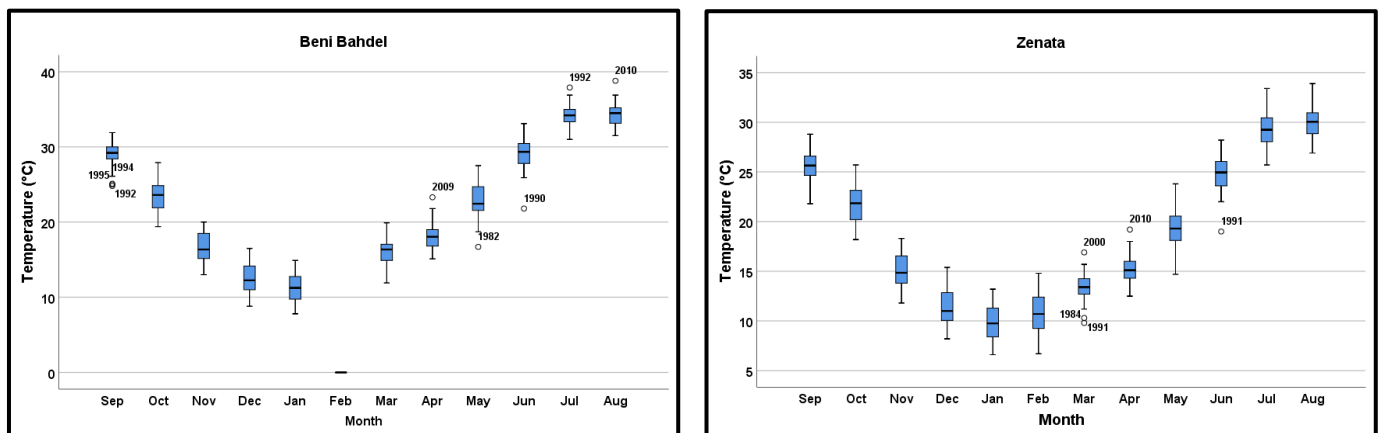


Figure III.21. Box plots of monthly average temperature of the study stations.

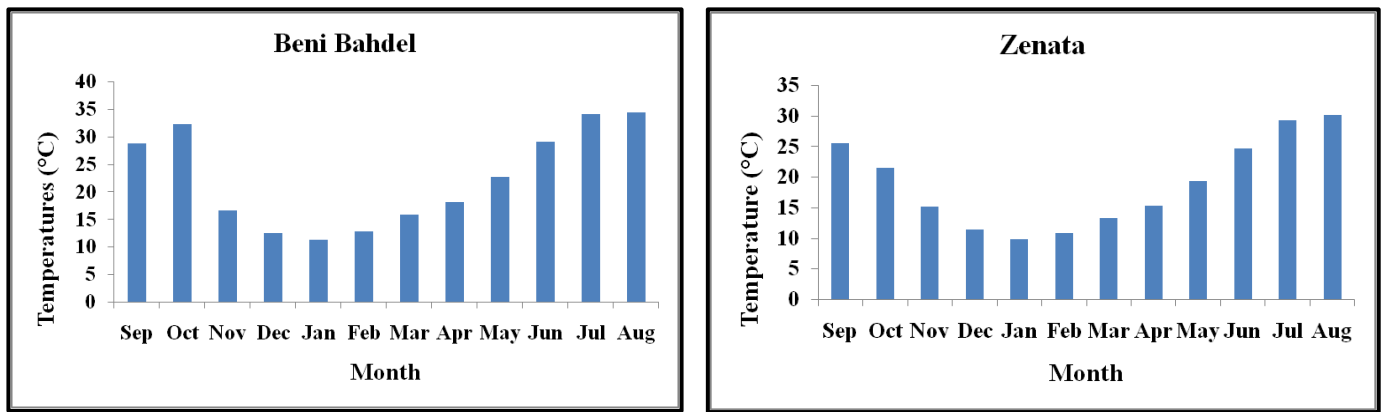


Figure III.22. Variation of monthly average temperature of the study stations.

III.5.3. Seasonal temperature analysis

The variation of the seasonal average of temperatures (fig.III.23) shows that summer and autumn correspond to the hottest seasons, where is recorded the lower values in the period 1991-1995 for Beni Bahdel and Zenata and the higher values in the periods 1986-1990 for Zenata, 2001-2005 for Beni Bahdel in autumn, and 2006-2010 for both stations in summer. And winter and spring as the cold seasons, where is recorded the lower values in the period 1979-1985 for both stations, and the higher values in the periods 1996-2000 in winter, and 2001-2005 in spring for both stations which is presented in figure III.24, and III.25.

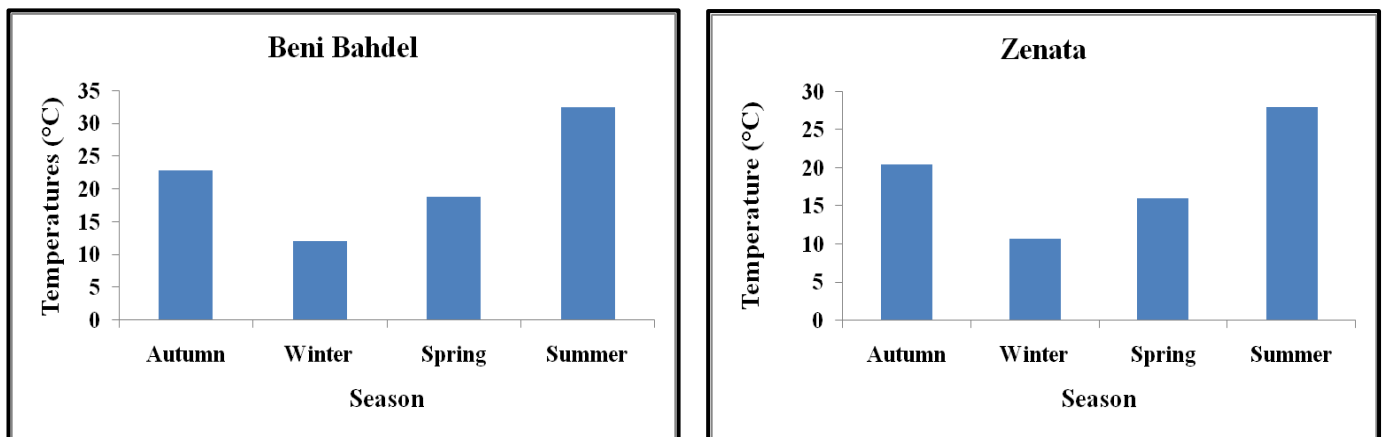


Figure III.23. Variation of seasonal average temperature at the study stations.

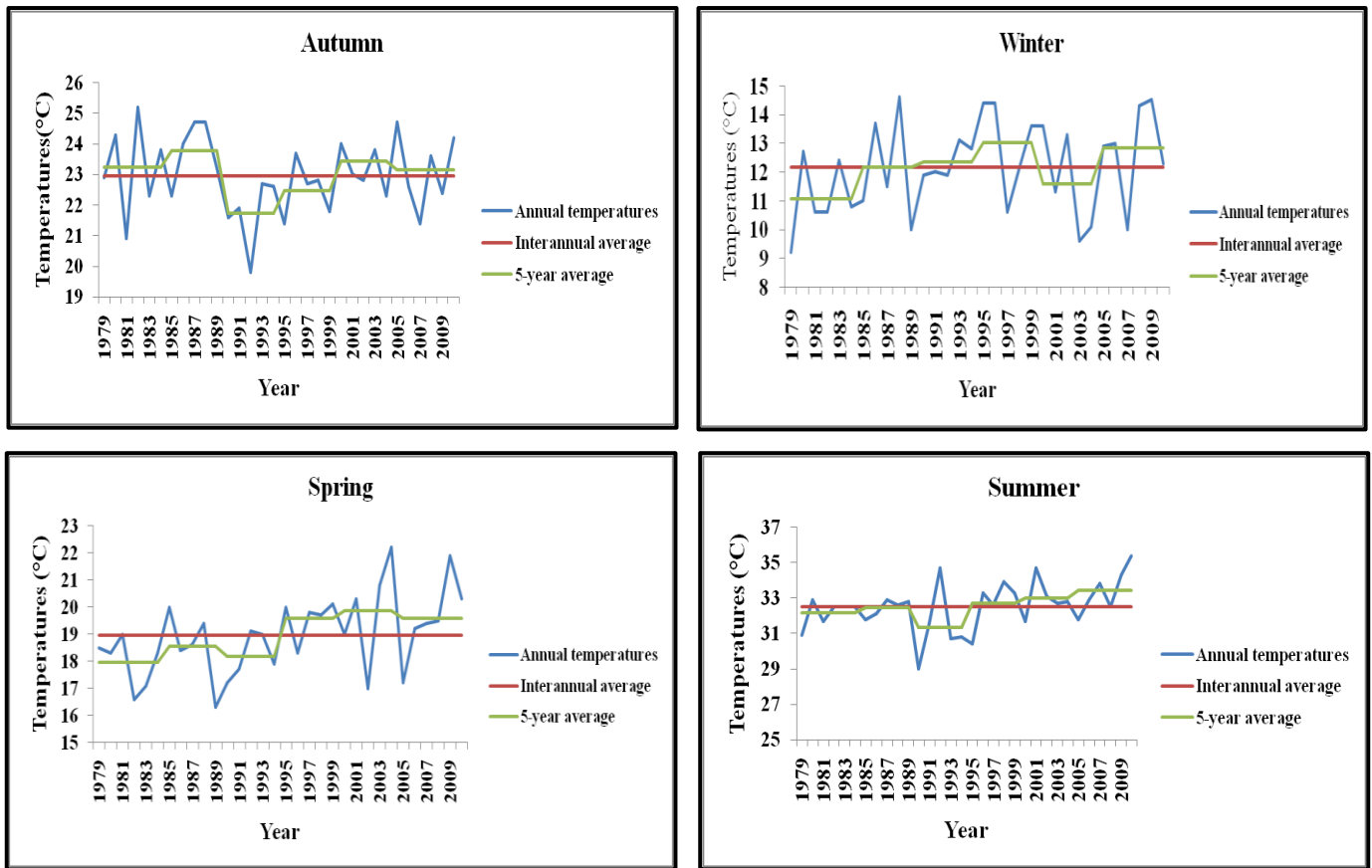


Figure III.24. Seasonal evolution of average temperatures of Beni Bahdel station.

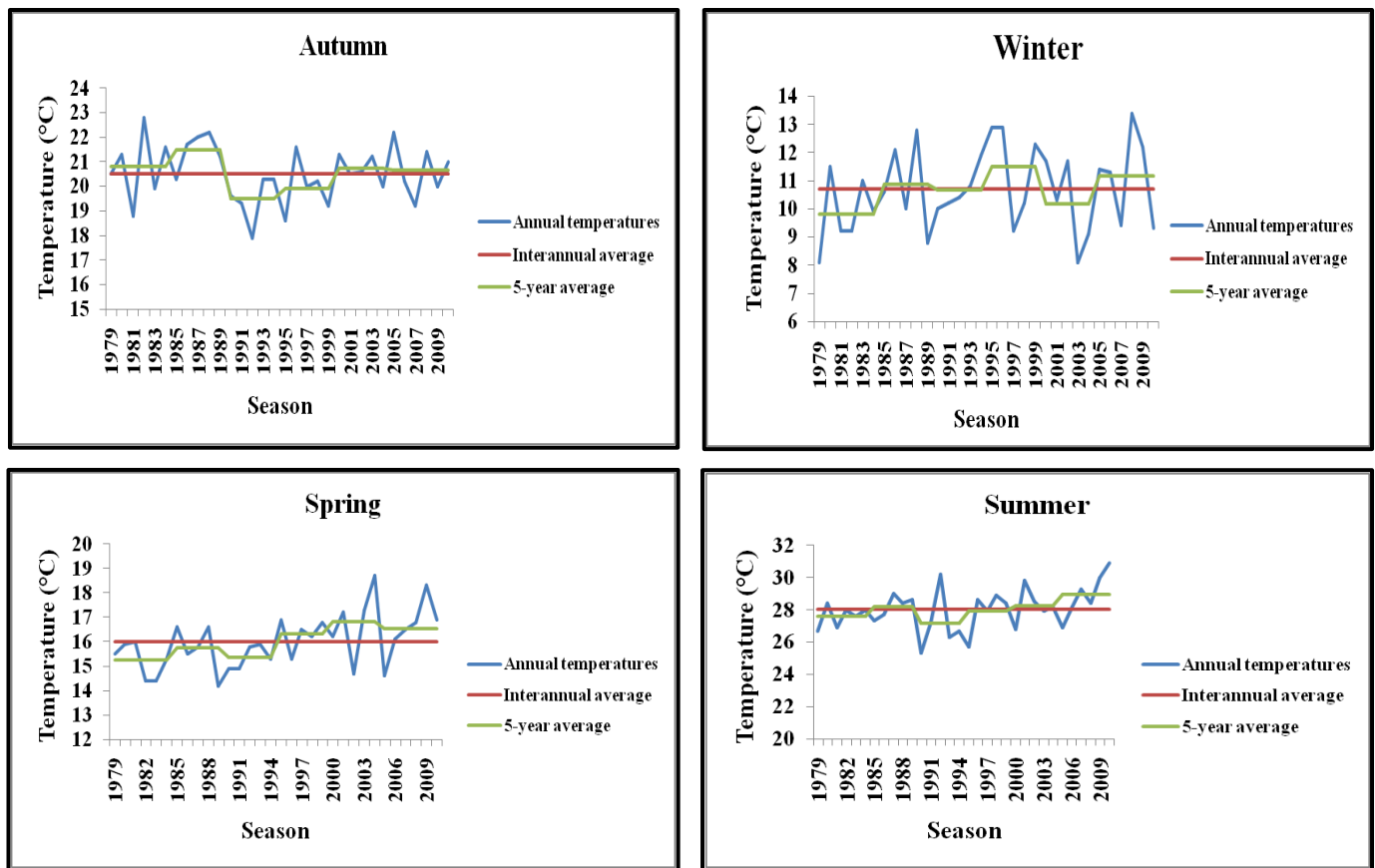


Figure III.25. Seasonal evolution of average temperature of Zenata station.

III.5.4. Daily temperature analysis

The variation of daily average temperatures of both stations is presented in figure III.26 and III.27. There is a gradual decrease in temperatures starting from November to February, and a considerable increase from May until the end of July.

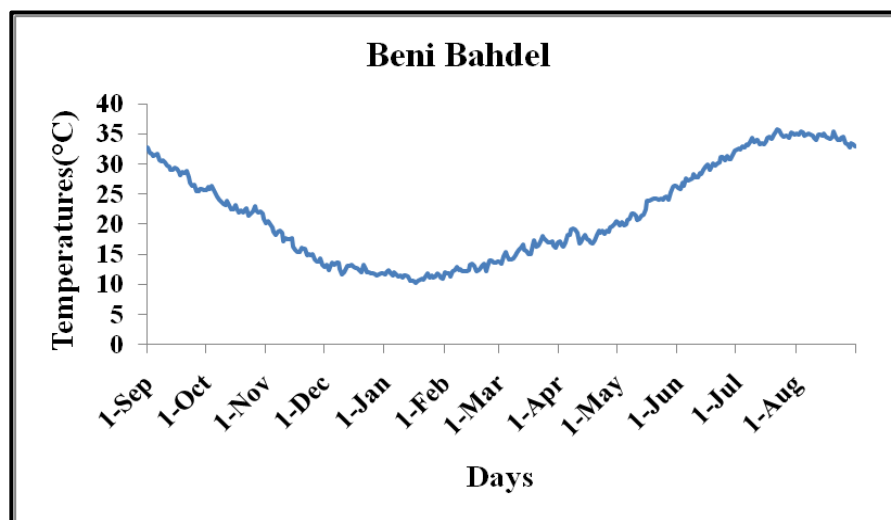


Figure III.26. Variation of daily average temperature of Beni Bahdel station.

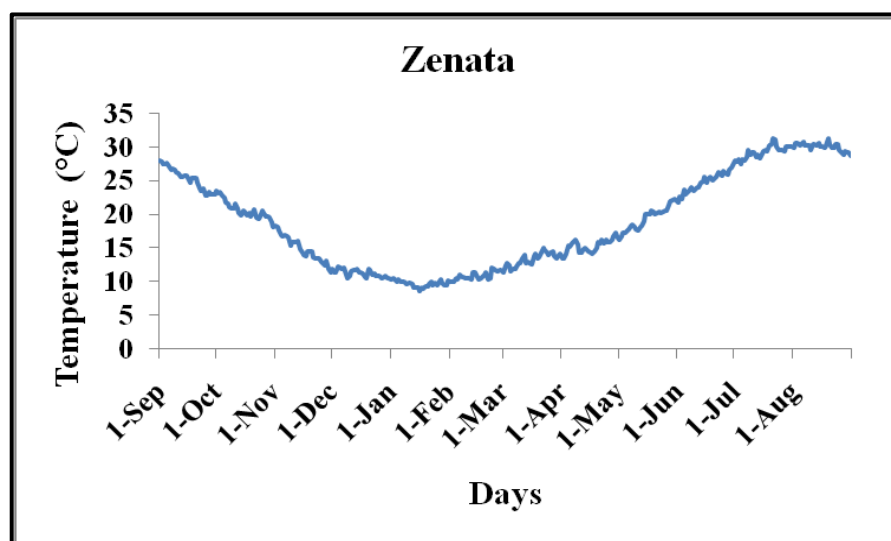


Figure III.27. Variation of daily average temperature of Zenata station.

III.6. Preliminary analysis of evapotranspiration

Evapotranspiration is the transferred amount of water vapor to the atmosphere by transpiration from surface of free water, plants and by evaporation from soil. There are several formulas have been developed to estimate the evapotranspiration and depends on the availability of climate variables such as the Thornthwaite (1944), Turc (1962), Blanney-Criddle (1950), and Penman Monteith-FAO (1998). For our study, we will applied the Oudin method (2004) which required the daily time series, the complex and physically formulas do not necessarily offer the best results (Oudin et al., 2005), where simple formulas are preferred

for current operational modeling. For the calculation of ETP by (Oudin, 2004) method with using that the formulas of (Jensen-Haise, 1963) and (McGuinness-Bordne, 1972) as follow:

$$ETP = \frac{R_e}{\lambda \rho_w} \cdot \frac{T_a + k_2}{k_1} \quad \text{Eq.III.1}$$

If $T_a + k_2 > 0$, If not $ETP = 0$.

ETP: Potential evapotranspiration (mm /d),

k_2 : Threshold on the temperatures which make ETP are not systematically zero when the air temperature is negative ($^{\circ}\text{C}$),

k_1 : Scale factor for adjusting the total volume of ETP in the year ($^{\circ}\text{C}$),

T_a : Average air temperature only according to Julian day ($^{\circ}\text{C}$),

λ : Potential heat of vaporization = $2.45 \cdot 10^6$ (J / kg),

ρ_w : Water density = 1000 (kg / m^3),

R_e : Quantity of solar radiation at the top of the atmosphere ($\text{MJ}/\text{m}^2/\text{d}$) (Djikou, 2006; Belouz, 2009; Kay and Davies, 2008).

III.6.1. Annual evapotranspiration analysis

The variation of average evapotranspiration by the Oudin method during the period 1979 - 2011 (fig.III.28) shows the higher values were defined in period 2006- 2010, 2001-2005 with 1333.45, 1169.54 mm respectively above the average 1303.23 and 1147.91 mm at Beni Bahdel and Zenata respectively, where the higher peak of ETP of 1383.3 mm in 2009 at Beni Bahdel, and 1236 mm in 2007 at Zenata indicating the drought periods. The lower values were defined in period 1991-1995 with values of 1263.6, 1123.04 mm at Beni Bahdel and Zenata respectively, where the lower peak of ETP is 1215, 1091.9 mm respectively indicating wet periods.

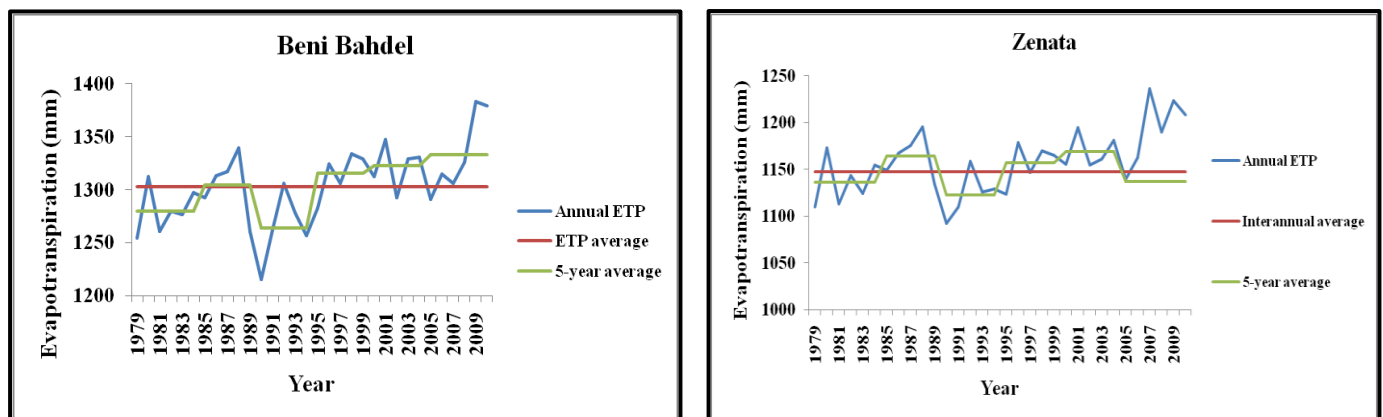


Figure III.28. Variation of annual average evapotranspiration of the study stations.

III.6.2. Monthly evapotranspiration analysis

The variations of the monthly average evapotranspiration are presented in the (fig.III.29) showed that the high value was defined in July with values 204.6, 202.74 mm at Beni Bahdel and Zenata respectively which indicate as the dry month, and the lower values were in

December and January with values of 38.2, 41.76 mm respectively at both stations respectively indicates the two months as the coldest month.

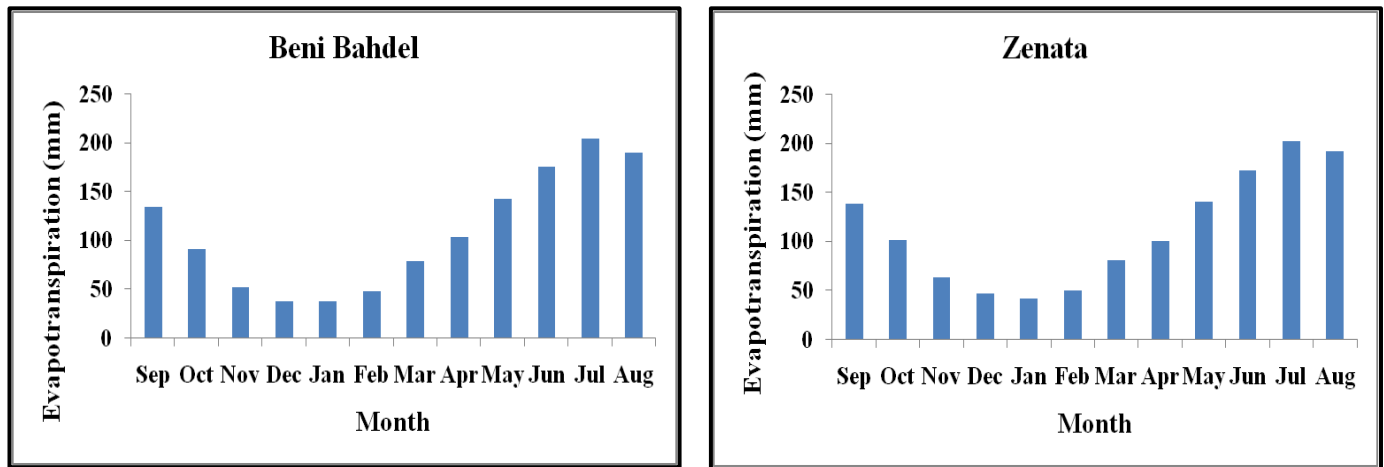


Figure III.29. Variation of monthly average evapotranspiration of the study stations.

III.6.3. Seasonal evapotranspiration analysis

The average seasonal variation (fig.III.30) shows the highest values in Summer with 571.61, 570.57 mm at Beni Bahdel, Zenata represent the drought season, and the lowest values in Winter with 124.70, 140.57 mm which define as the wet season.

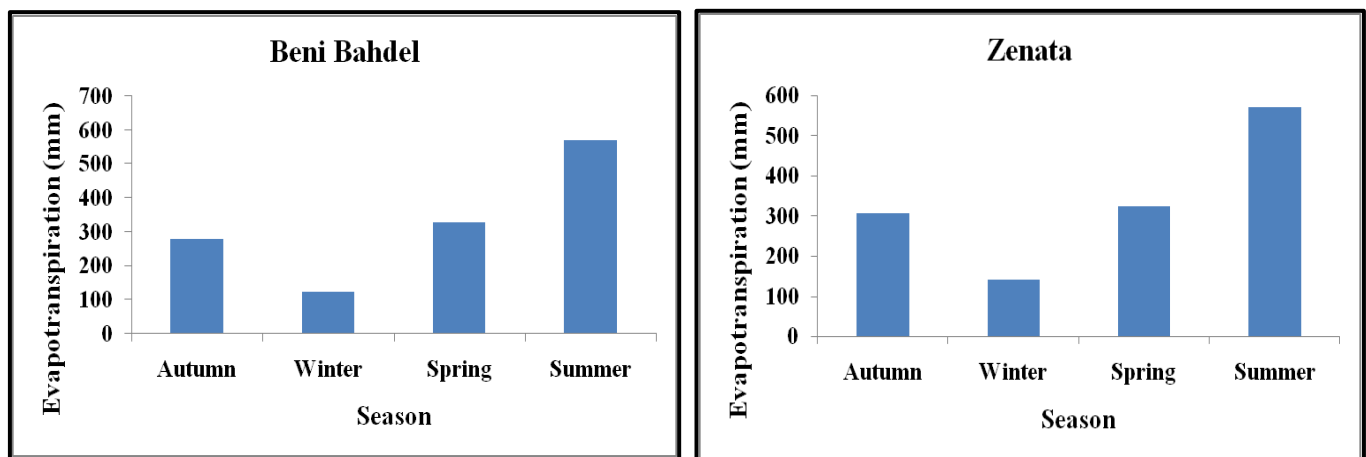


Figure III.30. Variation of seasonal average evapotranspiration of the study stations.

III.6.4. Daily evapotranspiration analysis

The variation of the average daily evapotranspiration (fig.III.31) showed a gradual decrease in evapotranspiration from October to February reaching approximately 1 mm, followed by an impressive increase from May until the end of August reaching approximately 6 mm.

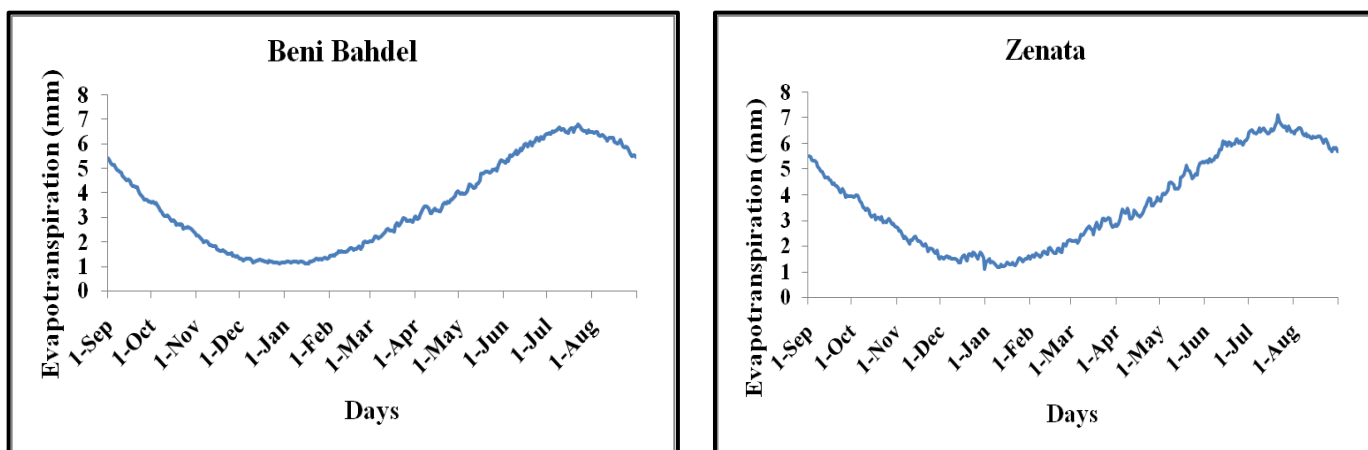
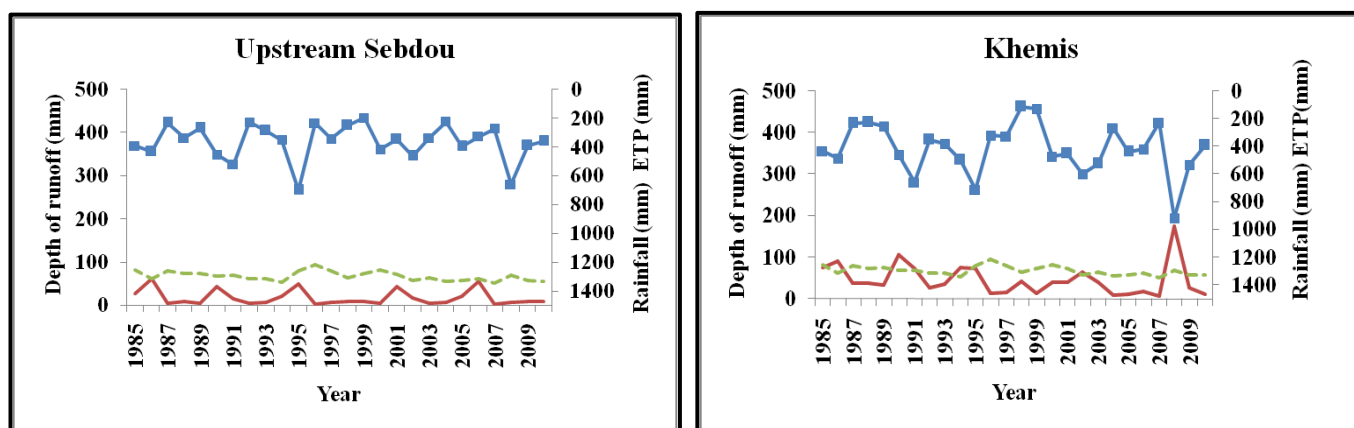


Figure III.31. Variation of daily average evapotranspiration of the study stations.

III.7. Water balance

The study period covers the period 1985/1986-2010/2011 in the 26 available records for the study five sub basins (fig.III.32). The year 2008 was defined as amongst the wettest years on record at all sub basins between a range of rainfall 559.85 mm, and 919.9 mm, a period which was also characterized by above average depth of runoff with a range between 6.39 to 284.02 mm. The year 1987 mostly defined as the dry period with values of rainfall between 197.25 to 269.1 mm, and for the depth of runoff has lower values in 2004 at Upstream Seb dou, and Khemis, and in 2006 at Chouly and Isser, and only in 1999 at Wadi Boumessaoud, which are not correspond to the input amount. The estimated ETP appears quite stable oscillating between 1091.9 and 1347.5 mm, which reflects the energy-limited environment and ETP likely with underestimated rainfall, affected the annual water balance.



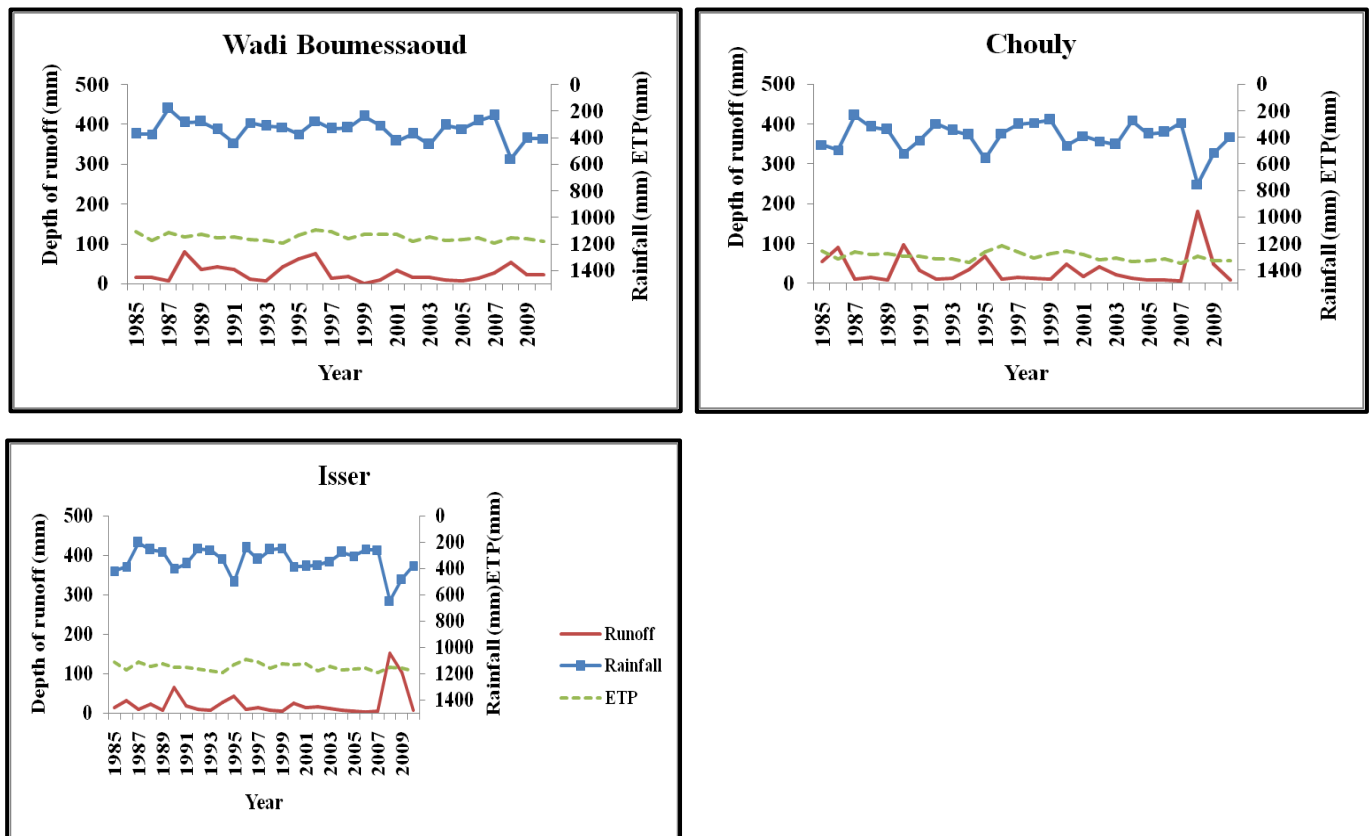


Figure III.32. Mean annual water balance (Rainfall, Depth of runoff, and evapotranspiration during the study period (1985/1986 - 2010/2011).

III.8. Correlation

Rainfall is considered as the driving force in a rainfall-runoff relationship, where is always the runoff that comes after rainfall at a particular period of time. The basis of the analysis comprises of determination of the relationship between the rainfall and runoff by plotting a regression line between rainfall and runoff at annual, monthly, daily steps, and to evaluate the dependability in determining the correlation between the two, the Pearson coefficient, and the Spearman's rho correlation will be used, which are well known and widely used internationally at annual, monthly, daily steps.

III.8.1. Pearson's correlation

The Pearson's coefficient of correlation was described by Karl Pearson in 1896, it is the standard method of his calculation which he called the "product-moments" method (or the Galton function for the coefficient of correlation r). An important assumption in Pearson's 1896 contribution is the normality of the variables analyzed, which could be true only for quantitative variables. Pearson's correlation coefficient is a measure of the strength of the linear relationship between two variables that cannot be measured quantitatively (Pearson, 1896; Pearson, 1900; Hauke and Kossowski, 2011).

III.8.2. Spearman's rho correlation

Spearman's rank correlation coefficient is a nonparametric (distribution-free) rank statistic proposed as a measure of the strength of the association between two variables. Spearman's coefficient is not a measure of the linear relationship between two variables; It is a measure of a monotone association, where It assesses how well an arbitrary monotonic function can describe the relationship between two variables, without making any assumptions about the frequency distribution of the variables. Unlike Pearson's product-moment correlation coefficient, it does not require the assumption that the relationship between the variables is linear. In principle, Spearman's rho coefficient is simply a case of Pearson's product-moment coefficient in which the data are converted to ranks before calculating the coefficient (Spearman, 1910; Hauke and Kossowski, 2011).

III.8.3. Annual correlation

Table III.9 shows the correlation coefficients performed on the rainfall and depth of runoff at annual time series (1985/1986 - 2010/2011) for five sub basins. The results show that the correlation coefficient of Pearson and Spearman's rho values are above 0.7 at a significant level ($p=0.01$) for Chouly, and Isser sub basins, it signifies that both variables move in the same direction, and that the rainfall and runoff variables have a perfect positive relationship; that means annual rainfall and annual runoff are strongly related. And Khemis only showed a great correlation (0.71) with Pearson. While Upstream Sebdou showed average correlation 0.55 with Spearman's rho and weak correlation with Pearson 0.43, and Wadi Boumessaoud showed a weak correlation with both coefficients 0.19, 0.29 respectively due to the presence of points that move away from the line.

Table III.9. Correlation coefficients between annual rainfall and runoff of the study sub basins.

Correlations (Rainfall -Depth of runoff)		Upstream Sebdou	Khemis	Wadi Boumessaoud	Chouly	Isser
Pearson	Correlation Coefficient	0.43*	0.71**	0.19	0.89**	0.82**
Spearman's rho	Correlation Coefficient	0.55**	0.59**	0.29	0.75**	0.71**

** . Correlation is significant at the 0.01 level (2-tailed).

* . Correlation is significant at the 0.05 level (2-tailed).

III.8.4. Monthly correlation

The results of the table III.10 gave an average correlation for Sebdou, Khemis, and Chouly between 0.53 - 0.66 for both Pearson and Spearman's rho coefficients. This means that there existed a strong relationship between rainfall and runoff. Wadi Boumessaoud showed a strong correlation 0.71 with Spearman's rho and an average of 0.54 with Pearson, while Isser showed an average correlation with both coefficients 0.47, 0.65.

Table III.10. Correlation coefficients between monthly rainfall and runoff of the study sub basin.

Correlations (Depth of runoff - Rainfall)		Upstream Sebdou	Khemis	Wadi Boumessaoud	Chouly	Isser
Pearson	Correlation Coefficient	0.53**	0.64**	0.54**	0.62**	0.47**
Spearman's rho	Correlation Coefficient	0.66**	0.57**	0.71**	0.55**	0.65**

** . Correlation is significant at the 0.01 level (2-tailed).

III.8.5. Daily correlation

As shown in table III.11, the correlation coefficient of Pearson and Spearman's rho between daily rainfall and runoff for all sub basins is less than 0.35 indicating that there is a weak relationship between rainfall and runoff and means an insignificant relationship. The weak correlation may due to minimum values of runoff presence despite the higher rainfall values while other minimum values of runoff in the same time series are corresponding to a high rainfall made inconsistency between the two variables.

Table III.11. Correlation coefficients between daily rainfall and runoff of the study sub basins.

Correlations (Depth of runoff - Rainfall)		Upstream Sebdou	Khemis	Wadi Boumessaoud	Chouly	Isser
Pearson	Correlation Coefficient	0.2**	0.17**	0.32**	0.20**	0.15**
Spearman's rho	Correlation Coefficient	0.19**	0.16**	0.26**	0.23**	0.22**

** . Correlation is significant at the 0.01 level (2-tailed).

III.9. Statistical test for distribution

Distribution test is used to determine the variation fit the dataset, the test that has been conducted is chi-square test at significance level ($\alpha=0.05$) for choosing the best probability distribution (Sharma and Singh, 2010).

III.9.1. Chi-square Test

Chi-Square test is used to compares how well theoretical distribution fits the empirical distribution (PDF) of variables dataset, and determines if sample data comes from a population with a specific distribution (Sharma and Sing, 2010). The Chi-squared statistic is defined as:

$$\chi^2 = \sum_{i=1}^k \frac{(O_i - E_i)^2}{E_i} \quad \text{Eq.III.2}$$

Where:

O_i = Observed frequency

E_i = Expected frequency, the formula of E_i : $E_i = F(X_2) - F(X_1)$

i = Number of observations (1, 2,k)

F = CDF of the probability distribution.

III.9.2. Statistical distribution for annual rainfall and runoff

The results of chi-Square are presented in table III.12, and III.13. The value of the test is 20 at a significant level ($p=0.05$). Since the p-value is greater than our chosen significance level ($\alpha = 0.05$), we do not reject the null hypothesis, which that emphasizes the percentage of the cells less than the value 5 should not be more than 20% (the less value of the cells in the data series is 20), and the assumption of the test allows a normal distribution of annual rainfall to be accepted for all stations of the sub basins.

Table III.12. Results of Chi-square Test at annual rainfall.

Station	Pearson Chi-Square			N of Valid Cases
	Value	df	Asymptotic Significance (2-sided)	
Sebdou	20 ^a	16	0.220	5
Khemis	20 ^a	16	0.220	5
Djebel Chouachi	20 ^a	16	0.220	5
Hennaya	20 ^a	16	0.220	5
Chouly	20 ^a	16	0.220	5
Meurbah	20 ^a	16	0.220	5
Ouled Mimoun	20 ^a	16	0.220	5
Sidi Bounakhla	20 ^a	16	0.220	5

a. 25 cells (100.0%) have expected count less than 5. The minimum expected count is .20.

Table III.13. Results of Chi-square Test at annual runoff.

Station	Pearson Chi-Square			N of Valid Cases
	Value	df	Asymptotic Significance (2-sided)	
Sebdou	20 ^a	16	0.220	5
Zahra	20 ^a	16	0.220	5
Zenata	20 ^a	16	0.220	5
Chouly	20 ^a	16	0.220	5
Sidi Aissa	20 ^a	16	0.220	5

a. 25 cells (100.0%) have expected count less than 5. The minimum expected count is .20.

III.10. Statistical test for Normality

The normality tests in the annual time series were selected with two non parametric: Kolmogorov-Smirnov and Shapiro-Wilk.

III.10.1. Kolmogorov-Smirnov test

The Kolmogorov-Smirnov test (Chakravart, Laha, and Roy, 1967) is used to decide whether a random sample followed a specific distribution. The statistic (D) is defined as the largest vertical difference between the theoretical and the empirical cumulative distribution function (ECDF):

$$D = \max_{1 \leq i \leq n} \left(F(x_i) - \frac{i-1}{n}, \frac{i}{n} - F(x_i) \right) \quad \text{Eq.III.3}$$

Where X_i = random sample, $i = 1, 2, \dots, n$,

$$\text{ECDF} = E_n = \frac{n(i)}{N} \quad \text{Eq.III.4}$$

Where $n(i)$ is the number of points. The function increases by $1/N$ at the value of each ordered data point.

F is the theoretical cumulative distribution of the distribution being tested which must be a continuous distribution.

III.10.2. Shapiro-Wilk test

The Shapiro-Wilk test (Shapiro and Wilk, 1965) has been used to investigate whether a random sample follows a normal distribution. The formula of the test as follows:

$$W = \frac{(\sum_{i=1}^n a_{n-i+1}(x_{n-i+1} - x_1))^2}{\sum_{i=1}^n (x_i - \bar{x})^2} \quad \text{Eq.III.5}$$

Where:

$i = 1, 2, \dots, n$: Sample size,

x_i = Ordered values of the sample,

\bar{x} = Mean value of the sample,

a_{n-i+1} = Constants generated from mean, variances, and covariates of the statistical order of a sample of size N and a normal distribution.

The conditions for the two tests to meet a normal distribution at the significance level ($p=0.05$) are defined as follows:

For $W_{\text{cal}} \leq W_{\text{tab}}$ rejects H_0 and accepts H_1 for p value $\alpha < 0.05$.

For $W_{\text{cal}} \geq W_{\text{tab}}$ accepts H_0 for p value $\alpha > 0.05$.

III.10.3. Normality test for annual rainfall

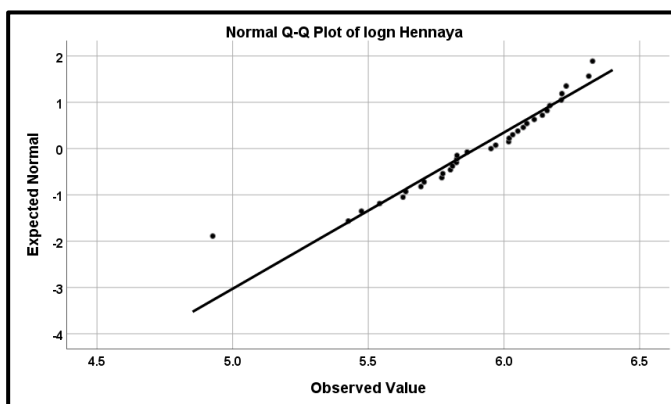
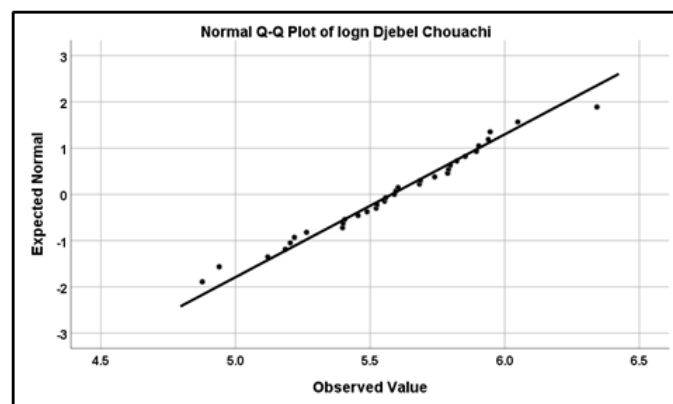
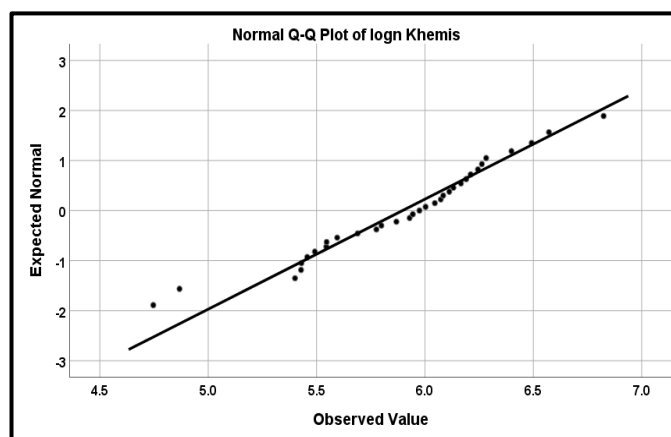
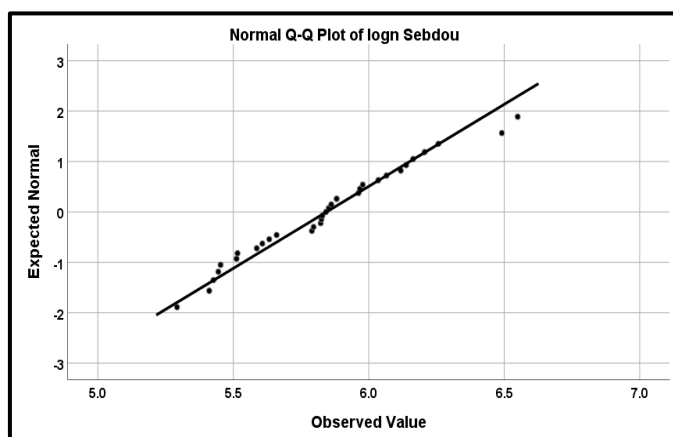
We applied Log normal on data series for all stations. Both tests accepted the normality except Hennaya with Shapiro-Wilk test ($p=0.04$) as shown in table III.14 which

indicates that the data of log-normal follows the normal distribution. The Q-Q (fig.III.33) shows that the Log normal distribution provides good alignment of the points within the envelope curves.

Table III.14. Results of normality on annual rainfall to the log normal distribution.

Station	Tests of Normality			
	Kolmogorov-Smirnov		Shapiro-Wilk	
	Statistic	Sig.	Statistic	Sig.
Sebdou	0.1	0.2 [*]	0.97	0.58
Khemis	0.11	0.2 [*]	0.97	0.42
Djebel Chouachi	0.08	0.2 [*]	0.99	0.93
Hennaya	0.11	0.2 [*]	0.93	0.04
Chouly	0.07	0.2 [*]	0.99	0.1
Meurbah	0.09	0.2 [*]	0.97	0.37
Oued Mimoun	0.1	0.2 [*]	0.97	0.45
Sidi Bounakhla	0.15	0.06	0.96	0.21

* This is lower bound of the true significance.



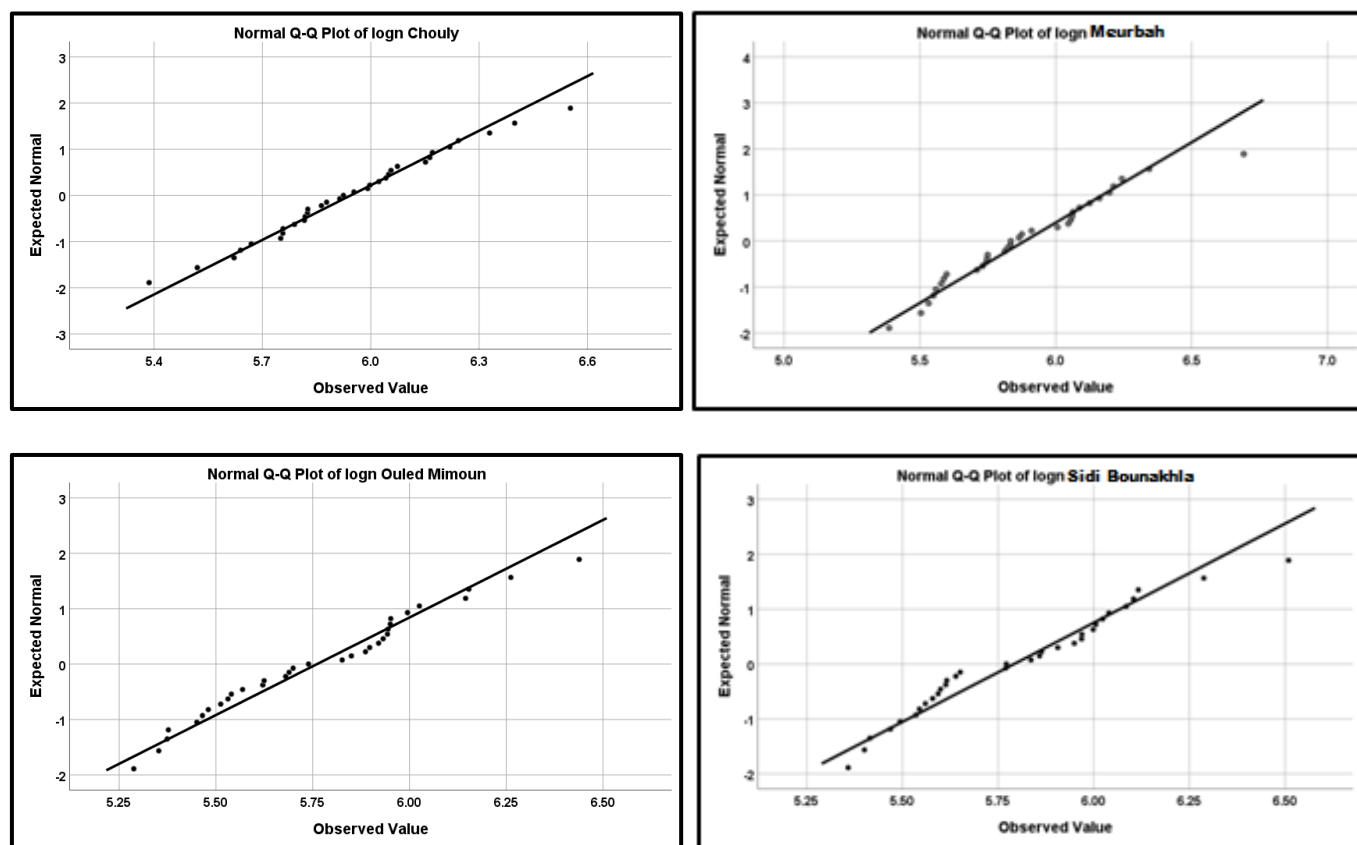


Figure III.33. Q-Q plot for normality of annual rainfall to the log normal distribution.

III.10.4. Normality test for annual runoff

The two normality tests are applied with log normal of annual runoff (tab.III.15). The results show that the p-values of the two tests are above $p=0.05$ at Zahra, Chouly, and Sidi Aissa stations with Kolmogorov-Smirnov, and with Shapiro-Wilk at Chouly, Zenata, and Sidi Aissa stations which shows that the annual time series data are normally distributed.

The Q-Q plot (fig.III.34) compares the quantile of observation with a quantile of a standardized theoretical dataset and showed that the log runoff data of Chouly station meet the criteria of normal distribution where the values are close to the line.

Table III.15. Results of normality on annual runoff to the log normal distribution.

Station	Tests of Normality			
	Kolmogorov-Smirnov		Shapiro-Wilk	
	Statistic	Sig.	Statistic	Sig.
Sebdou	0.21	0.006	0.91	0.03
Zahra	0.17	0.07	0.91	0.02
Chouly	0.08	0.20*	0.95	0.28
Zenata	0.18	0.04	0.93	0.07
Sidi Aissa	0.14	0.19	0.96	0.32

* This is lower bound of the true significance.

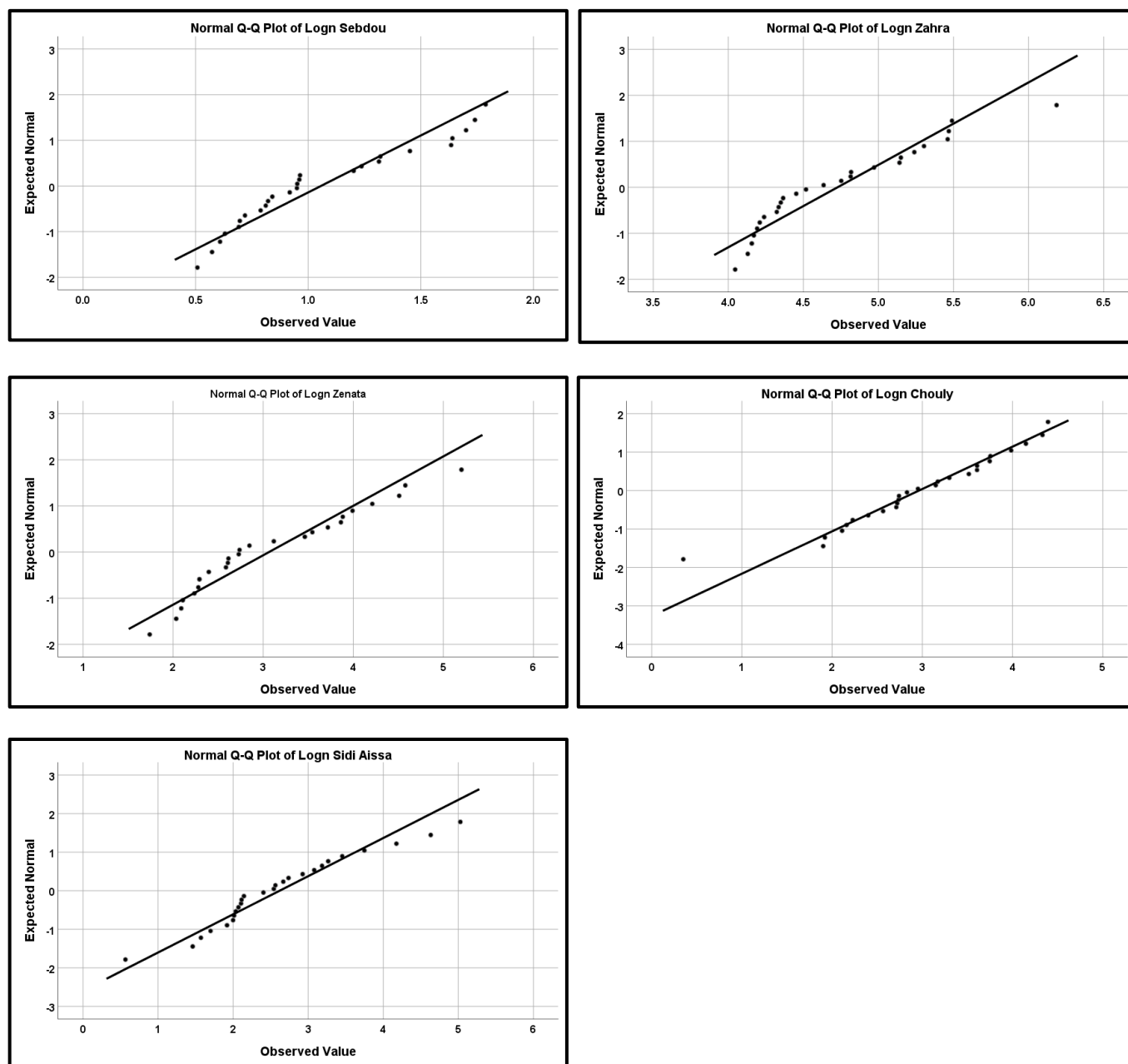


Figure III.34. Q-Q plot for normality of annual runoff to the log normal distribution.

III.11. Variability analysis of Hydro - climatic variables

Non-parametric tests (also known as distribution-free inferential statistical methods) do not require the data to be normally distributed. Since most of the hydro-meteorological time series data are not normally distributed. Hence, non-parametric methods have been widely used (Kumar et al., 2018; Huth and Pokorn, 2004). In this study, we have applied several non parametric tests (tab.III.16) for trend detection, and homogeneity analysis (monthly and annual time scale) of rainfall (8 stations) over period 1979/1980 and 2011/2012, runoff (5 stations) over period 1985/1986 and 2010/2011, and temperature (2 stations) over period 1979/1980 and 2010/2011 distributed in five sub basins of the Tafna basin.

Four tests (Pettit's test, Buishand test, Hubert test, Lee and Heghinian test) were applied to study homogeneity on an annual and monthly time scale. These tests analyse the time series and detect the break point, which is defined as a change of distribution of the variable in time series (i.e., change in the mean). The Khronostat software (version 1.01) was used to perform these tests.

The Mann-Kendall test with Theil-Sen's slope method was employed for detecting a rainfall trend on monthly, seasonal (Autumn (September, October, November), Winter (December, January, February), Spring (March, April, May), Summer (June, July, August)), and annual time scale.

The applied tests mentioned above have been widely used for evaluating the trend in climatic and hydrological data.

Table III.16. Summary of statistical tests.

Statistical Method	Statistical Test Types	Description
Change point detection test	Pettitt Test	Detects a single change-point in hydrological or climate data with continuous long-term time series
	Buishand Test	Detects a change in variables according to any distribution.
	Hubert Test	Detects multiple breaks in time series.
	Lee and Heghinian Test	Detects change of means in the data with a continuous time series.
Trend analysis	Mann-Kendall (MK)	Non-parametric test, which is commonly employed to detect monotonic trends in series of data for mainly climate or hydrological data.
	Sen's Slope Estimator	Computes the linear rate of change (slopes) by choosing the median of the slopes of all lines through pairs of points also computes the upper and lower confidence limits for Sen's slope.

III.11. 1. Tests for change point detection (homogeneity)

The change point detection test is the analysis of variance for data distribution, i.e., the shift in the mean of the variable in the time series. These methods assume a null hypothesis that there is no change in the variance of the series studied (Maftei et al., 2011), do not require the data to be normally distributed. We have applied four tests to study homogeneity on the annual and monthly scale: Pettit's test, Buishand test, Hubert test, Lee & Heghinian test. These tests may help to detect breaks which are defined as a change of distribution of the variable in time series (change in the mean) at different significance levels ($p=0.01, 0.05, 0.1$).

III.11.1. 1. Pettitt Test

The Pettitt test is non-parametric test developed by Pettitt (Pettitt, 1979) for detecting point change (Wijngaard et al., 2003). The statistic, $U_{t,N}$ is defined using the two sums thus obtained in order to assess whether the two samples belong to the same population by the equation (L'Hôte et al., 2002; Traore et al., 2017):

$$U_{t,N} = \sum_{i=1}^t \sum_{j=t+1}^N \text{sgn}(x_i - x_j) \quad \text{Eq.III.6}$$

N: Size of time series,

t: Time,

Sgn: Coefficient given by the equation as follows:

$$\text{Sgn} = \begin{cases} +1 & \text{if } (x_j - x_i) > 0 \\ 0 & \text{if } (x_j - x_i) = 0 \\ -1 & \text{if } (x_j - x_i) < 0 \end{cases} \quad \text{Eq.III.7}$$

Under the null hypothesis, the statistic of the variable to be test is K given as:

$$K = \text{Max}|U_t| \quad \text{Eq.III.8}$$

The exceedance probability of the k as:

$$\text{Prob} (k_N > k) \approx 2 \exp\left(\frac{-6k^2}{N^2 + N^3}\right) \quad \text{Eq.III.9}$$

When the exceedance probability is smaller than α , the null hypothesis is rejected for a significance level α (Traore et al., 2017, Fossou et al., 2014).

III.11.1.2. Buishand Test

Buishand Test has the same hypotheses as the Lee and Heghinian test, the statistic U of the test is given as follow:

$$U = \frac{\sum_{k=1}^{N-1} (S_k / \sigma_x)^2}{N(N+1)} \quad \text{Eq.III.10}$$

$$S_k = \sum_{i=1}^k (X_i - \bar{X}) \quad \text{Eq.III.11}$$

Where S_k is partial sum and σ_x is standard deviation (calculated using equation III.12)

$$\sigma_x^2 = \frac{1}{N} \sum_{i=1}^N (X_i - \bar{X})^2 \quad \text{Eq.III.12}$$

The null hypothesis stands for no break point in time series. The rejection of null hypothesis means a break point in the time series. In addition to these different procedures, the building of a control ellipse makes it possible to analyze the homogeneity of the (xi) series (Traore,

2014; Hubert and Carbonnel, 1993).

III.11.1.3. Hubert Test

Hubert's segmentation procedure detects multiple breaks in the time series (Pettitt, 1979; Maftai et al., 2011; Hubert and Carbonnel, 1989). The principle is to cut the time series into m segments ($m > 1$) such that the calculated means of the neighboring sub-series should differ significantly. To limit the segmentation, the mean of two contiguous and the point of satisfying Scheffe's test should be different. The procedure gives the timing of the shifts. Giving a m^{th} order segmentation of the time series, $i_k, k = 1, \dots, m$, the rank in the initial series of extreme end of the k^{th} segment (with $i_0 = 0$), we defined the following by two equations:

$$\bar{X}_k = \frac{\sum_{i=i_{k-1}+1}^{i=i_k} X_i}{n_k} \quad \text{Eq.III.13}$$

$$D_m = \sum_{k=1}^m \sum_{i=i_{k-1}+1}^{i_k} (X_i - \bar{X}_k)^2 \quad \text{Eq.III.14}$$

D_m is the quadratic deviation between the series and the segmentation. For a given segmentation order, the algorithm determines the optimal segmentation of a series in such a way that the deviation D_m is minimal. This procedure can also be interpreted as a stationary test, the null hypothesis being the studied series should be non-stationary. If the procedure doesn't produce acceptable segmentations of order bigger or equal to two, the null hypothesis is accepted (Traore, 2014; Hubert and Carbonnel, 1993).

III.11.1.4. Lee and Heghinian Test

The Lee and Heghinian test is based on the assumption that the series is normally distributed; the tests are Bayesian procedures based on equation which supposes a change in the series as follow:

$$x_i = \begin{cases} \mu + \varepsilon_i, & i = 1, \dots, \tau \\ \mu + \sigma + \varepsilon_i, & i = \tau + 1, \dots, N \end{cases} \quad \text{Eq.III.15}$$

where ε_i are independent and normally distributed, with a mean equal to zero and a variance equal to σ^2 . τ is the position in time and σ is the scope of the possible change in the mean (Traore, 2014, Hubert and Carbonnel, 1993).

III.11.2. Trend analysis

Trend is a direction of a phenomenon through a fixed period. It can be discovered by statistical tests which is applied to further investigate whether the trend is upward or downward of the data during a time period while considering the level of statistical significance (Longobardi and Villani, 2009; Tabari, 2011; Kisi and Ay, 2014; Da Silva et al., 2015; Gedefaw et al., 2018; Mrad et al., 2018).

III.11.2.1. Mann-Kendall (MK) Trend Test

The non-parametric MK trend test is the rank-based test (Sneyers, 1975; Hamlaoui-Moulai et al., 2013) used to assess the significance of a trend in hydro-meteorological time series (Gocic and Trajkovic, 2013). The statistic S of MK test is calculated as follows:

$$S = \sum_{i=1}^{n-1} \sum_{j=i+1}^n \text{sgn}(x_j - x_i) \quad \text{Eq.III.16}$$

Where n is the number of data points, x_i and x_j are the data values in the time series i and j ($j > i$), respectively, the positive value of S indicates an increasing and the negative indicates decreasing trend. The data values of each X_i is used as a reference point to compare with the data values of X_j , and $\text{sgn}(x_j - x_i)$ is the sign function given as:

$$\text{sgn}(x_j - x_i) = \begin{cases} +1 & \text{if } x_j - x_i > 0 \\ 0 & \text{if } x_j - x_i = 0 \\ -1 & \text{if } x_j - x_i < 0 \end{cases} \quad \text{Eq.III.17}$$

The variance is calculated as:

$$\text{Var}(s) = \frac{n(n-1)(2n+5) - \sum_{i=1}^P t_i(t_i-1)(2t_i+5)}{18} \quad \text{Eq.III.18}$$

Where n is the number of data points, P is the number of tied groups, and t_i is the number of data values in the Pth group. The standardized test statistic Z is calculated as:

$$Z_s = \begin{cases} \frac{S - 1}{\sqrt{\text{Var}(s)}} & \text{if } S > 0 \\ 0 & \text{if } S = 0 \\ \frac{S + 1}{\sqrt{\text{Var}(s)}} & \text{if } S < 0 \end{cases} \quad \text{Eq.III.19}$$

Positive values of Z_s indicate increasing trends while negative Z_s values show decreasing trends. The null hypothesis (H_0) stands for a significant trend, and the alternative hypothesis (H_1) represents no statistically significant trend (Sneyers, 1975; Hamlaoui-Moulai et al., 2013).

III.11.2.2. Sen's slope estimator

Sen's method was used for estimating the slope of detected significant trends, and the variance of the residuals should be constant in time. It is calculated as:

$$Q_i = \frac{x_j - x_k}{j - k} \quad \text{for } i = 1, \dots, n \quad \text{Eq.III.20}$$

Where X_j and X_k are the data values in the times series j and k respectively; n is the number of time periods.

$N = n(n - 1)/2$ If there is only one data in each time period

$N < n(n - 1)/2$ If there are multiple observations in one or more time periods.

The median of Sen's slope estimator is calculated as follows:

$$Q_{\text{med}} = \begin{cases} Q[(n + 1)/2] & \text{if } n \text{ is odd} \\ \frac{Q[\frac{n}{2}] + Q[(n + 2)/2]}{2} & \text{if } n \text{ is even} \end{cases} \quad \text{Eq.III.21}$$

The Q_{med} sign reflects data trend, while its value indicates the steepness of the trend. To determine whether the median slope is statistically different than zero, it is necessary to obtain the confidence interval of Q_{med} at specific probability. The confidence interval about the time slope can be computed as follows:

$$c_{\alpha} = Z_{1-\alpha/2} \sqrt{\text{Var}(s)} \quad \text{Eq.III.22}$$

Where $\text{Var}(S)$ is variance and $Z^{1-\alpha/2}$ is obtained from the standard normal distribution table (Sen, 1968; Gocic and Trajkovic, 2013; Da Silva et al., 2015).

III.11.3. Results and discussion of variability analysis

III.11.3.1. Results and discussion of change point detection (homogeneity)

We present in table III.17 the results of the break detection tests (Pettitt, Hubert, Buishand, Lee and Heghinian) for nine rainfall stations on annual scale at $p = 0.01$ & 0.05 levels of statistical significance. The results showed that the Lee and Heghinian test rejected the null hypothesis (no break in time series) for all the stations and indicating the break point corresponds to 1980 for Sebduou, and Hennaya and for remaining stations in 2007. Pettitt's test did not detect any change except for Djebel Chouachi station in 1999 which is also confirmed by Buishand test that detected a change in 1999 and 2007 and a change was revealed in 2007 by Hubert test. The application of the segmentation method of Hubert leads to reject the null hypothesis for three stations: Djebel Chouachi, Ouled Mimoun, Sidi Bounakhla in 2007 and accepted the null hypothesis for other stations.

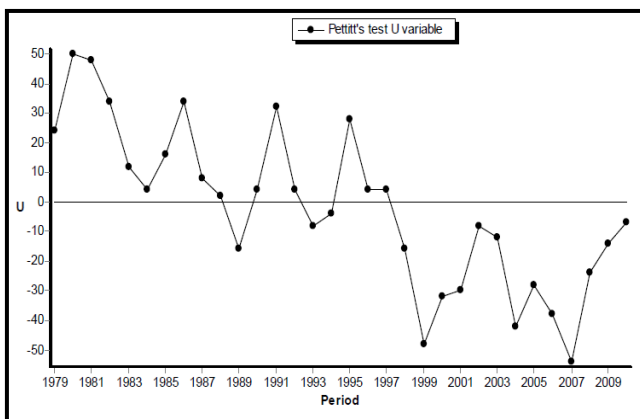
Most changes (break) of the distribution in annual time series is detected for Djebel Chouachi station. This seems to be caused by the effect of characteristics of the zone where the station is located (such as the altitude). Djebel Chouachi station has the lowest altitude (110 m) and may impact the measurements representing the actual amount of rainfall in the area. The study of Hamlaoui-Moulai et al., 2013 has already demonstrated the relationship between the characterization of the zones in northwest of Algeria such as the altitude with rainfall on annual basis.

Table III.17. Results of change point detection on annual rainfall.

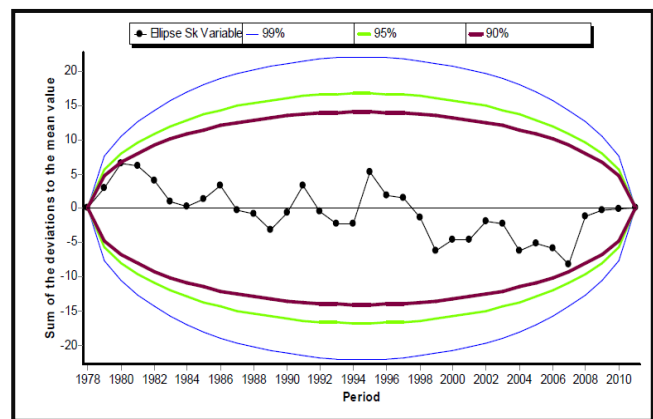
Test	Investigative work	Sebdou	Khemis	Djebel Chouachi	Hennaya	Chouly	Meurbah	Ouled Mimoun	Sidi Bounakhla
Pettitt	Conclusion on H0	Accepted	Accepted	Rejected	Accepted	Accepted	Accepted	Accepted	Accepted
	Break date	/	/	1999*	/	/	/	/	/
Hubert	Conclusion on H0	Accepted	Accepted	Rejected	Accepted	Accepted	Accepted	Rejected	Rejected
	Break date	/	/	2007**	/	/	/	2007**	2007**
Buishand	Conclusion on H0	Accepted	Accepted	Rejected	Accepted	Accepted	Accepted	Accepted	Accepted
	Break date	/	/	1999,2007	/	/	/	/	/
Lee and Heghinian	Break probability	0.1267	0.1380	0.2345	0.2473	0.3842	0.2183	0.5171	0.3505
	Conclusion on H0	Rejected	Rejected	Rejected	Rejected	Rejected	Rejected	Rejected	Rejected
	Break date	1980	2007	2007	1980	2007	2007	2007	2007

** at p=0.01 significant level, * at p=0.05 significant level.

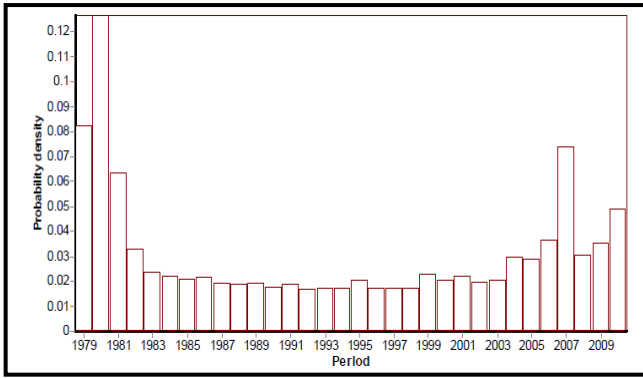
Figures III.35 (a, b, c), III.36 (a, b, c), III.37 (a, b, c), III.38 (a, b, c), III.39 (a, b, c), III.40 (a, b, c), III.41 (a, b, c), and III.42 (a, b, c), respectively are uses to represent graphical results obtained by the khronostat software of some tests such as the Pettitt, Buishand, and Lee & Heghinian tests on the annual time scale. As depicted in figure III.37(a), Pettitt test rejected the null hypothesis at Djebel Chouachi station and indicated the date of break corresponding to year 1999 with the direction of rupture representing an upward for rainfall trend. The Lee and Heghinian test in (fig.III.35b, III.36b, III.37b, III.38b, III.39b, III.40b, III.41b, III.42b) showed the date of break in 2007 at Khemis, Djebel Chouachi, Chouly, Meurbah, Ouled Mimoun, and Sidi Bounakhla stations, and two stations Sebdou, and Hennaya have the date of the break in 1980. While Buishand confirmed with Djebel Chouachi station, the same date of break in 1999 as indicated by Pettitt test and is proposing 2007 as a further year of break, the two break points are followed by an upward trend of rainfall. This results lead to the conclusion that the rainfall time series are not homogeneous and can therefore be divided into three sub-series: 1979-1999, 1999-2007 and 2007-2011.



(a)

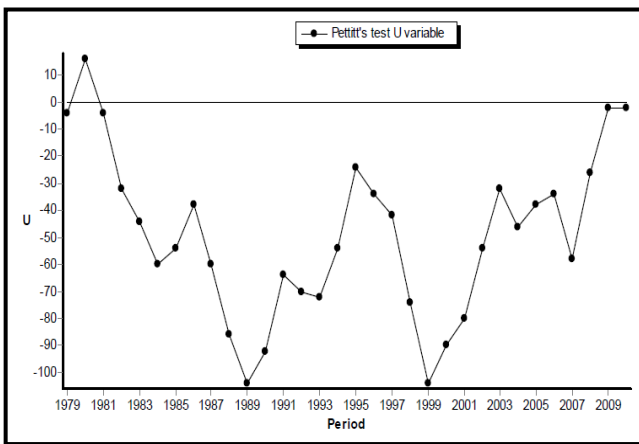


(b)

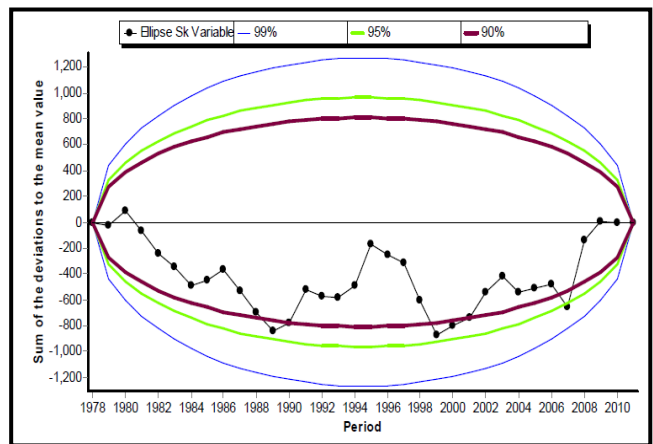


(c)

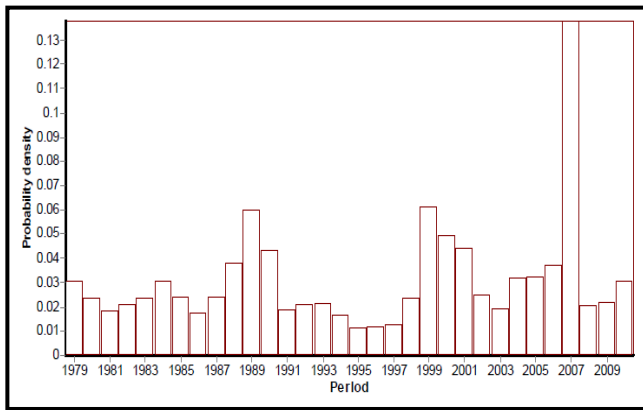
Figure III.35. Khronostat results of annual rainfall at Sebdou station: (a) Pettitt test; (b) Buishand test; (c) Lee and Heghinian test.



(a)

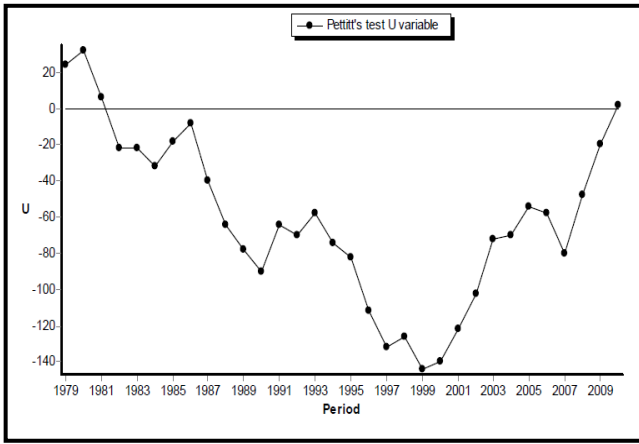


(b)

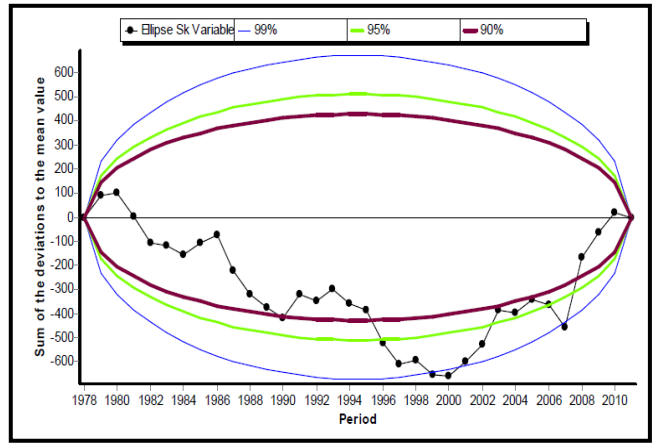


(c)

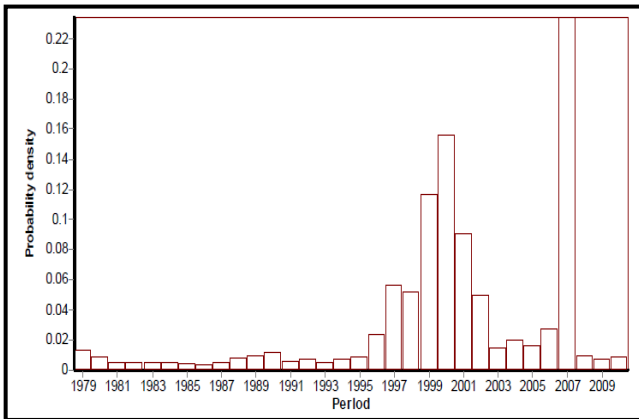
Figure III.36. Khronostat results of annual rainfall at Khemis station: (a) Pettitt test; (b) Buishand test; (c) Lee and Heghinian test.



(a)

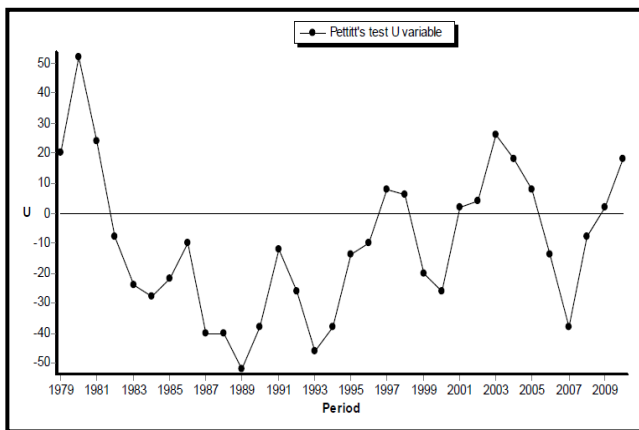


(b)

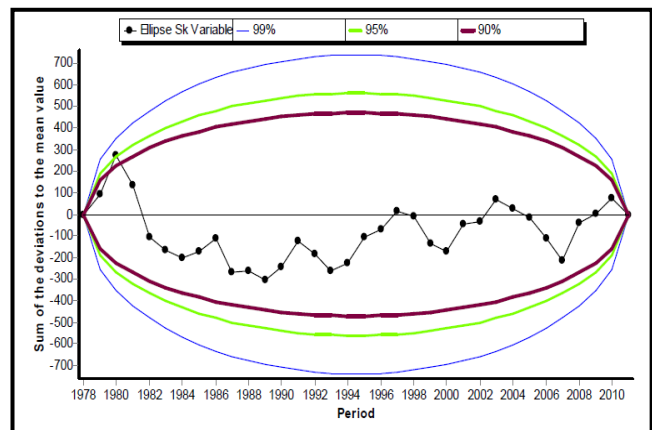


(c)

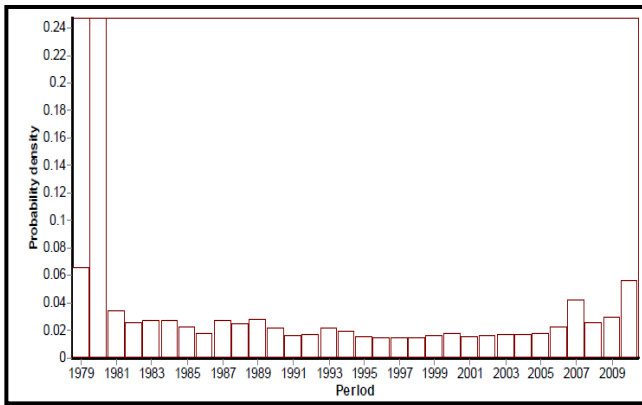
Figure III.37. Khronostat results of annual rainfall at Djebel Chouachi station: (a) Pettitt test; (b) Buishand test; (c) Lee and Heghinian test.



(a)

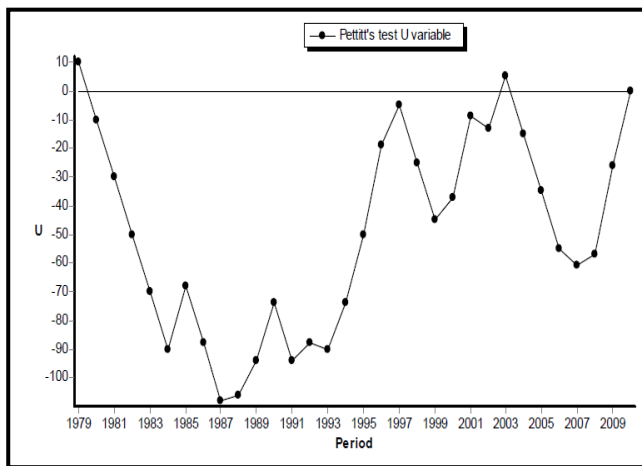


(b)

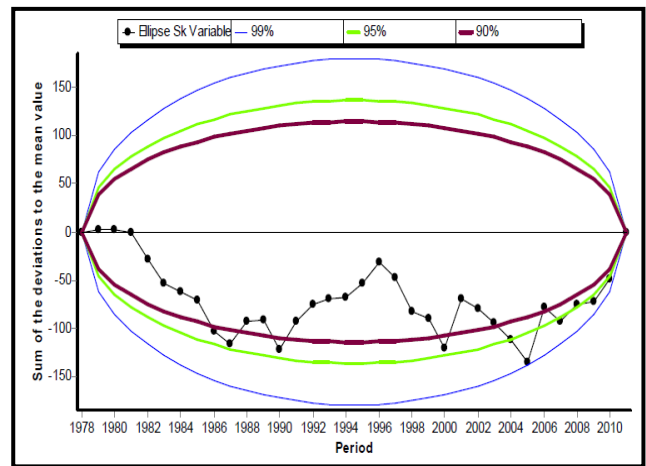


(c)

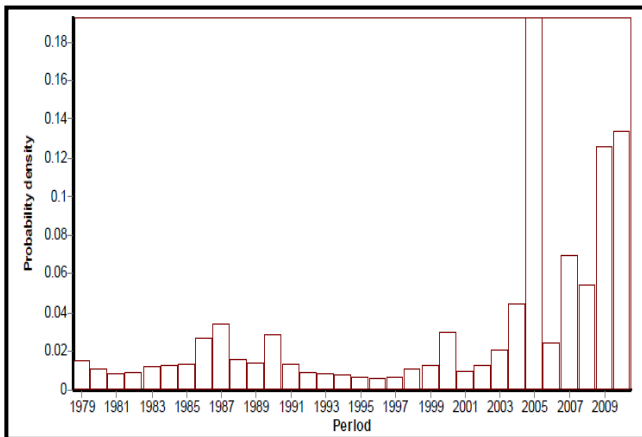
Figure III.38. Khronostat results of annual rainfall at Hennaya station: (a) Pettitt test; (b) Buishand test; (c) Lee and Heghinian test.



(a)

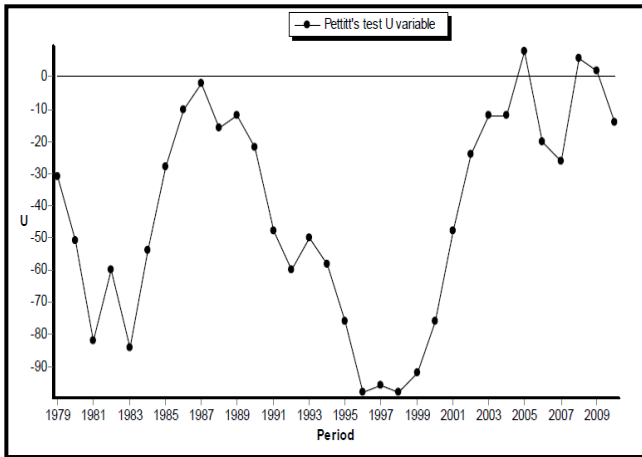


(b)

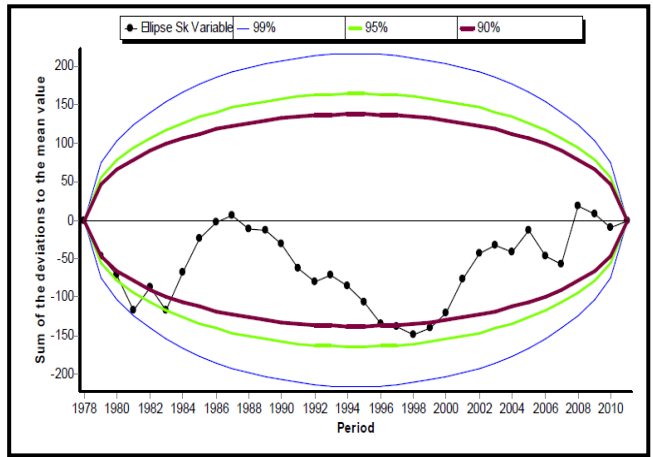


(c)

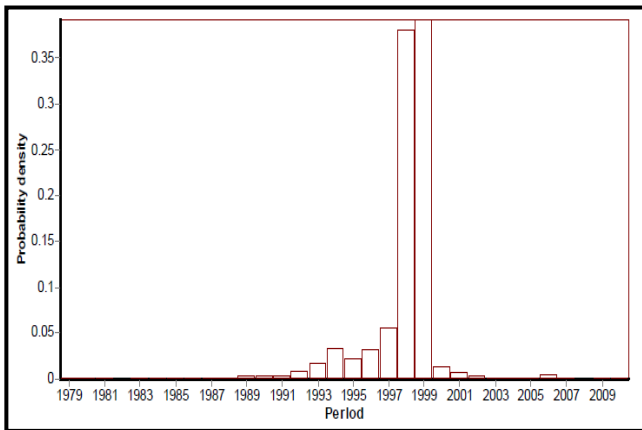
Figure III.39. Khronostat results of annual rainfall at Chouly: (a) Pettitt test; (b) Buishand test; (c) Lee and Heghinian test.



(a)

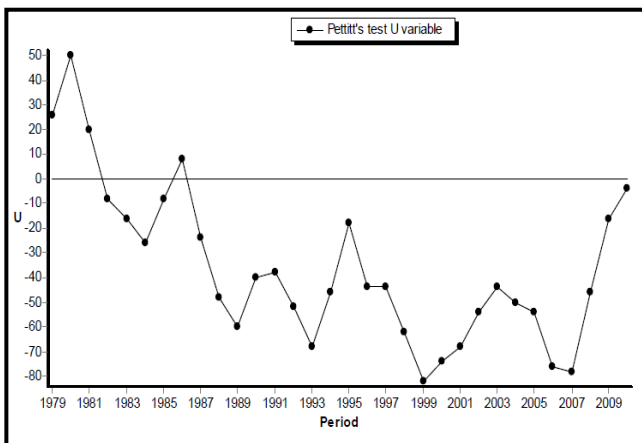


(b)

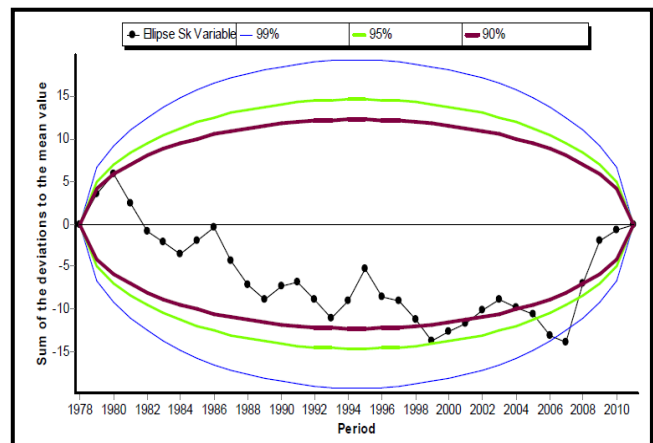


(c)

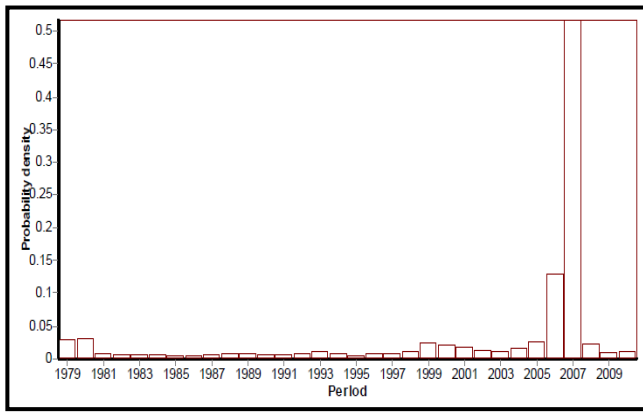
Figure III.40. Chronostat results of annual rainfall at Meurbah station: (a) Pettitt test; (b) Buishand test; (c) Lee and Heghinian test.



(a)

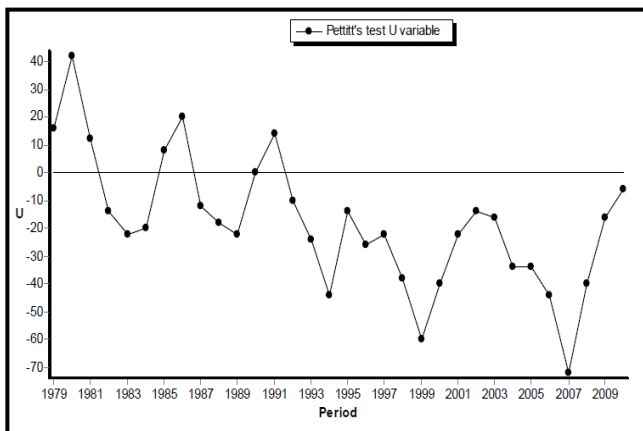


(b)

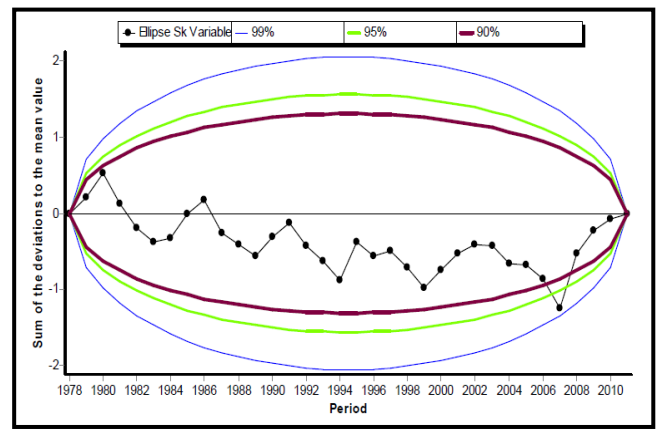


(c)

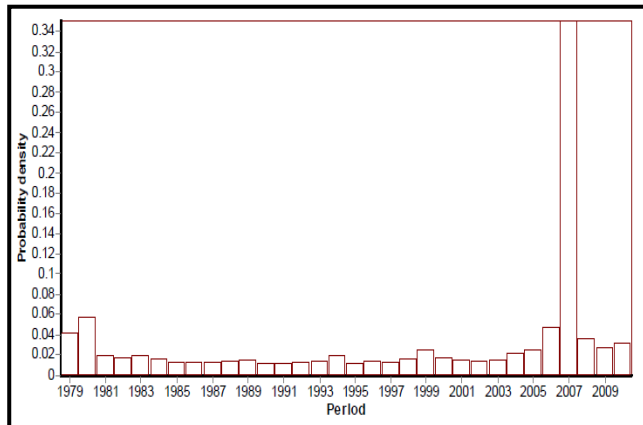
Figure III.41. Khronostat results of annual rainfall at Ouled Mimoun station: (a) Pettitt test; (b) Buishand test; (c) Lee and Heghinian test.



(a)



(b)



(c)

Figure III.42. Khronostat results of annual rainfall at Sidi Bounakhla station: (a) Pettitt test; (b) Buishand test; (c) Lee and Heghinian test.

Analyzing at monthly time scale (tab.III.18) indicates rejection of the null hypothesis (no break) and also acceptance of null hypothesis in different months as detected by all the applied tests (Pettitt, Buishand, Hubert, Lee & Heghinian) leading to break points in monthly time series. Only the months of June, July and August with Buishand and Lee & Heghinian tests has not affirmed the acceptance or the rejection of the hypothesis in detecting breaks for all stations at any statistical significance level due to the sensitivity of the two tests by dealing

with level of the data variability for these months (extreme values). Except Sebdou station rejected the null hypothesis in August month. We conclude that the time series on rainfall are not homogenous because a break point was detected.

Table III.18. Results of homogeneity test on monthly rainfall.

Monthly	Sebdou			Khemis			Djebel Chouachi			Hennaya			Chouly			Meurbah			Ouled Mimoun			Sidi Bounakhta		
	Sep	Oct	Nov	Sep	Oct	Nov	Sep	Oct	Nov	Sep	Oct	Nov	Sep	Oct	Nov	Sep	Oct	Nov	Sep	Oct	Nov	Sep	Oct	Nov
Pettitt	R	A	A	R	R	A	A	A	A	A	R	A	A	A	A	R	R	A	A	A	A	A	R	A
Hubert	A	R	R	R	R	A	A	R	A	A	R	A	R	A	A	R	R	A	R	A	A	A	A	A
Buishand	R	R	A	R	R	A	A	A	A	A	R	A	R	R	A	R	R	A	R	R	A	R	R	A
Lee and Heghinian	R	R	R	R	R	R	R	R	R	R	R	R	R	R	R	R	R	R	R	R	R	R	R	R
Test	Dec	Jan	Feb	Dec	Jan	Feb	Dec	Jan	Feb	Dec	Jan	Feb	Dec	Jan	Feb	Dec	Jan	Feb	Dec	Jan	Feb	Dec	Jan	Feb
Pettitt	A	A	A	A	A	A	A	A	A	A	A	A	A	A	A	A	A	A	A	A	A	A	A	A
Hubert	R	A	A	R	A	A	A	A	A	R	A	A	A	A	A	A	A	A	R	A	A	R	A	A
Buishand	A	A	A	NT	A	A	A	A	A	A	A	A	A	A	A	A	A	A	NT	A	A	A	A	A
Lee and Heghinian	R	R	R	R	R	R	R	R	R	R	R	R	R	R	R	R	R	R	NT	R	R	R	R	R
Test	Mar	Apr	May	Mar	Apr	May	Mar	Apr	May	Mar	Apr	May	Mar	Apr	May	Mar	Apr	May	Mar	Apr	May	Mar	Apr	May
Pettitt	A	A	A	A	A	A	A	A	A	A	A	A	A	A	A	A	A	A	A	A	A	A	A	A
Hubert	A	A	A	A	A	A	A	A	A	A	A	A	A	R	A	A	A	A	A	A	A	R	A	A
Buishand	A	A	A	A	A	A	A	A	A	A	A	A	A	A	A	A	A	A	A	A	A	A	A	A
Lee and Heghinian	R	R	R	R	R	R	R	R	R	R	R	R	R	R	R	R	R	R	R	R	R	R	R	R
Test	Jun	Jul	Aug	Jun	Jul	Aug	Jun	Jul	Aug	Jun	Jul	Aug	Jun	Jul	Aug	Jun	Jul	Aug	Jun	Jul	Aug	Jun	Jul	Aug
Pettitt	A	A	A	A	A	A	A	A	A	A	A	A	A	A	A	A	A	A	A	A	R	A	A	A
Hubert	A	A	A	A	A	A	R	A	A	A	A	A	R	A	A	A	A	A	A	A	R	A	A	A
Buishand	NT	NT	R	NT	NT	NT	NT	NT	NT	NT	NT	NT	NT	NT	NT	NT	NT	NT	NT	NT	NT	NT	NT	NT
Lee and Heghinian	NT	NT	R	NT	NT	NT	NT	NT	NT	NT	NT	NT	NT	NT	NT	NT	NT	NT	NT	NT	NT	NT	NT	NT

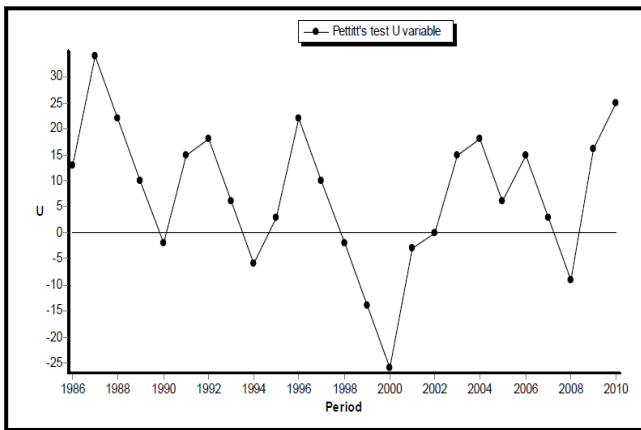
A: accepted null hypothesis, R: rejected null hypothesis, NT: No Test.

To complete the Hydro climatic - analysis, we applied change point detection tests (Pettitt and Hubert) on annual and monthly runoff. The results in table III.19 showed that there was a break in homogeneity of runoff time series only in Zahra station (Khemis sub basin) with Pettitt test on annual scale in the date break 2007 at significance level ($p=0.1$). Les results of Pettitt obtained by the khronostat software are presented in figure III.43, the Pettitt test rejected the null hypothesis at Zahra station and indicated the date of break corresponding to year 2007 with the direction of rupture representing an downward for rainfall trend, this break points at Zahra station lead to conclude that the runoff time series are not homogeneous and can therefore be divided into two sub-series: 1979-2007, and 2007-2011.

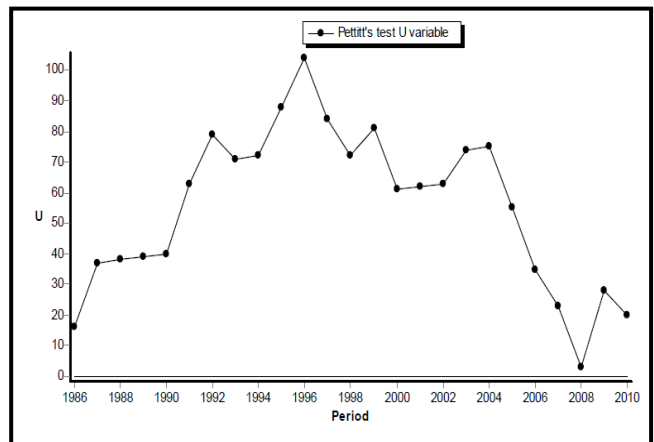
Table III.19. Results of homogeneity test on annual runoff.

Test	Investigative work	Sebdou	Zahra	Zenata	Chouly	Sidi Aissa
Pettitt	Conclusion on H0	Accepted	Rejected	Accepted	Accepted	Accepted
	Break date	/	2007**	/	/	/
Hubert	Conclusion on H0	Accepted	Accepted	Accepted	Accepted	Accepted
	Break date	/	/	/	/	/

** at $p=0.01$ significant level, * at $p=0.05$ significant level



(a)



(b)

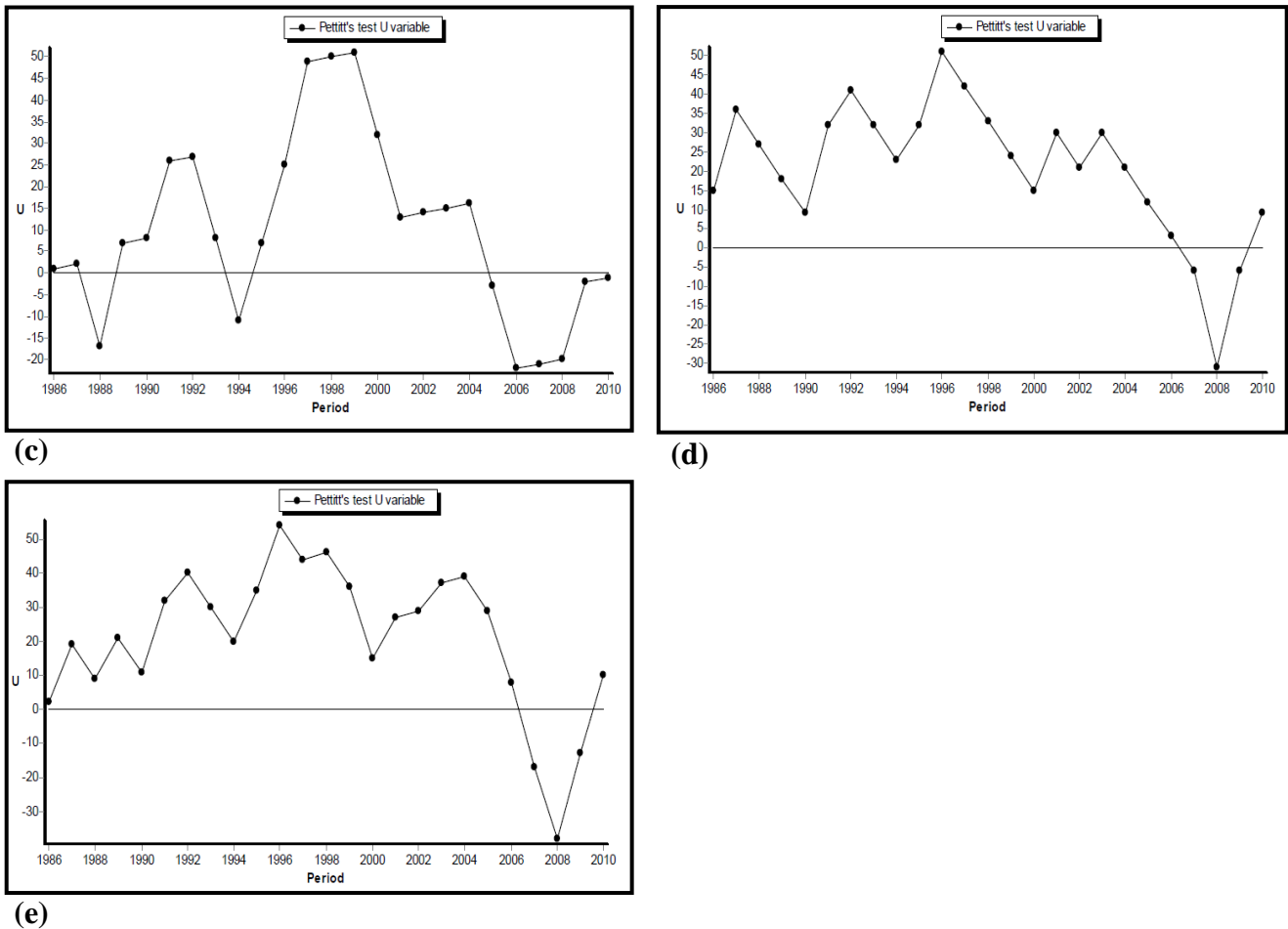


Figure III.43. Pettitt results of annual runoff at the stations: (a) Sebdou; (b) Zahra; (c) Zenata; (d) Chouly; (e) Sidi Aissa.

For monthly time step, the application of the tests of Pettitt and Hubert (tab.III.20) on runoff are indicating the date of break of October in 1986 and 1987 at Sebdou station, and 2007 and 2009 at Zenata station with Hubert test, while on December detect two break points in 2008 and 2009 at Chouly. The month of February indicates common break point in 1987 with Hubert at all stations except Sidi Aissa. The date of break 2007 was detected with Pettitt on May, June, and July at Zahra. At the same station, the data of break 1994 was detected with both tests on August, while multi break points for the months of April in 1991 and 1992, June in 1995 and 1996, and July in 1989 and 1997. The both tests on the month of September, November, January, and March accepted the null hypothesis, we conclude that the time series on runoff are homogenous because no break point was detected.

Table III.20. Results of homogeneity test on monthly runoff.

Month	Test	Investigative work	Sebdou	Zahra	Zenata	Chouly	Sidi Aissa
September	Pettitt	Conclusion on H0	Accepted	Accepted	Accepted	Accepted	Accepted
		Break date	/	/	/	/	/
	Hubert	Conclusion on H0	Accepted	Accepted	Accepted	Accepted	Accepted
		Break date	/	/	/	/	/

October	Pettitt	Conclusion on H0	Accepted	Accepted	Accepted	Accepted	Accepted
		Break date	/	/	/	/	/
	Hubert	Conclusion on H0	Rejected	Accepted	Rejected	Accepted	Accepted
		Break date	1986*** 1987***	/	2007*** 2009***	/	/
November	Pettitt	Conclusion on H0	Accepted	Accepted	Accepted	Accepted	Accepted
		Break date	/	/	/	/	/
	Hubert	Conclusion on H0	Accepted	Accepted	Accepted	Accepted	Accepted
		Break date	/	/	/	/	/
December	Pettitt	Conclusion on H0	Accepted	Accepted	Accepted	Accepted	Accepted
		Break date	/	/	/	/	/
	Hubert	Conclusion on H0	Accepted	Accepted	Accepted	Rejected	Accepted
		Break date	/	/	/	2008*** 2009***	/
January	Pettitt	Conclusion on H0	Accepted	Accepted	Accepted	Accepted	Accepted
		Break date	/	/	/	/	/
	Hubert	Conclusion on H0	Accepted	Accepted	Accepted	Accepted	Accepted
		Break date	/	/	/	/	/
February	Pettitt	Conclusion on H0	Accepted	Accepted	Accepted	Accepted	Accepted
		Break date	/	/	/	/	/
	Hubert	Conclusion on H0	Rejected	Rejected	Rejected	Rejected	Accepted
		Break date	1987***	1987***	1987***	1986*** 1987*** 2008*** 2009***	/
March	Pettitt	Conclusion on H0	Accepted	Accepted	Accepted	Accepted	Accepted
		Break date	/	/	/	/	/
	Hubert	Conclusion on H0	Accepted	Accepted	Accepted	Accepted	Accepted
		Break date	/	/	/	/	/
April	Pettitt	Conclusion on H0	Accepted	Accepted	Accepted	Accepted	Accepted
		Break date	/	/	/	/	/
	Hubert	Conclusion on H0	Accepted	Rejected	Accepted	Accepted	Accepted
		Break date	/	1991,1992***	/	/	/
May	Pettitt	Conclusion on H0	Accepted	Rejected	Accepted	Accepted	Accepted
		Break date	/	2007**	/	/	/
	Hubert	Conclusion on H0	Accepted	Accepted	Accepted	Accepted	Accepted
		Break date	/	/	/	/	/
June	Pettitt	Conclusion on H0	Accepted	Rejected	Accepted	Accepted	Accepted
		Break date	/	2007**	/	/	/
	Hubert	Conclusion on H0	Accepted	Rejected	Accepted	Accepted	Accepted

		Break date	/	1995*** 1996 ***	/	/	/
July	Pettitt	Conclusion on H0	Accepted	Rejected	Accepted	Accepted	Accepted
		Break date	/	2007**	/	/	/
	Hubert	Conclusion on H0	Accepted	Rejected	Accepted	Accepted	Rejected
		Break date	/	1989*** 1997***	/	/	1986*** 1987***
August	Pettitt	Conclusion on H0	Accepted	Rejected	Accepted	Accepted	Accepted
		Break date	/	1994***	/	/	/
	Hubert	Conclusion on H0	Accepted	Rejected	Accepted	Accepted	Accepted
		Break date	/	1994***	/	/	/

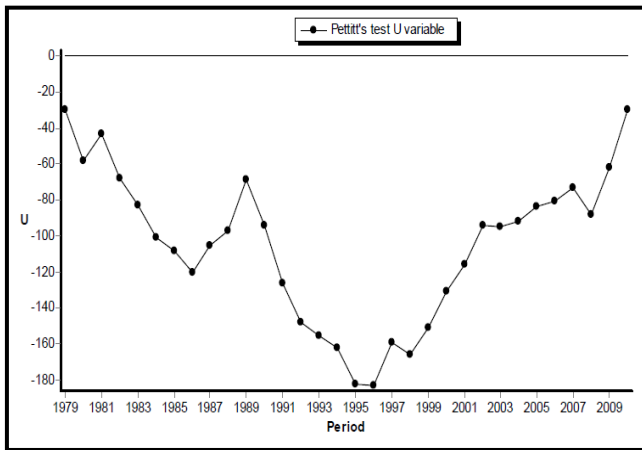
** at p=0.1 significant level, * at p=0.05 significant level, *** at p=0.01 significant level

The tests (Pettitt, Buishand, Lee and Heghinian, Hubert) are applied on annual temperature and presented in table III.21 and figure III.44, III.45. The date of break in 1996 was detected with Pettitt, Hubert, and Buishand tests at Beni Bahdel, and at Zenata with Pettitt and Buishand. Only Lee & Heghinian has detected the date of 2008 as break point at Beni Bahdel and Zenata, while the same date was detected only with Hubert at Zenata. The results showed that the rejection of the null hypothesis with all tests at both stations indicated that the time series on temperature are not homogenous because a break point was detected (1996 and 2008), thus the annual time series of temperature can be divided into two sub series: 1979-1996, 1996-2010, or 1979-2008, 2008-2010.

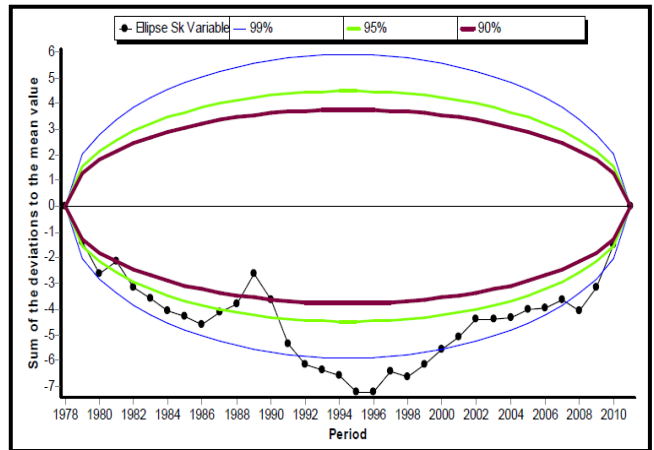
Table III.21. Results of homogeneity test on annual temperature.

Station	Investigative work	Test			
		Pettitt	Hubert	Buishand	Lee and Heghinian
Beni Bahdel	Conclusion on H0	Rejected	Rejected	Rejected	Rejected
	Break date	1996***	1996***	1996***	2008
Zenata	Conclusion on H0	Rejected	Rejected	Rejected	Rejected
	Conclusion on H0	1996*	2008***	1996***	2008***

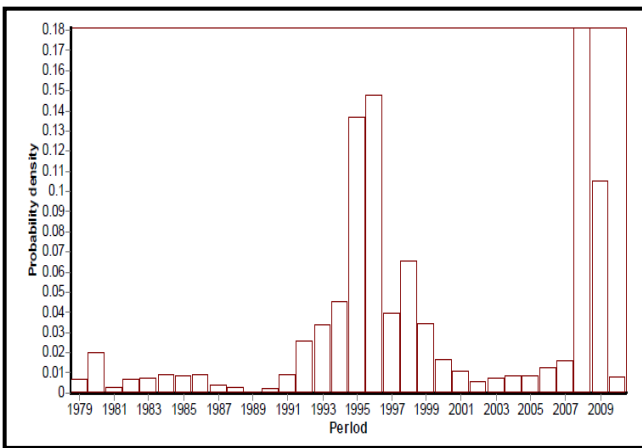
** at p=0.1 significant level, * at p=0.05 significant level, *** at p=0.01 significant level



(a)

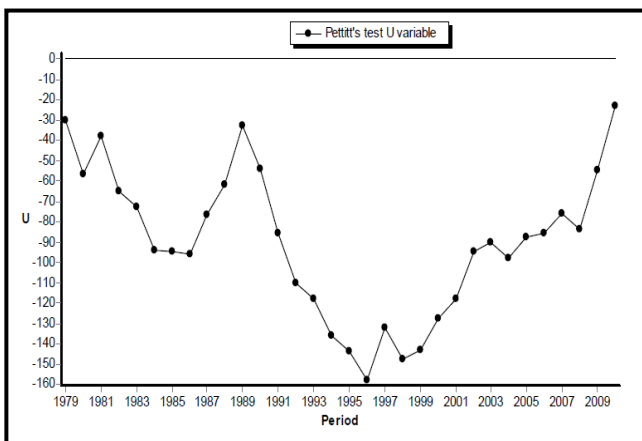


(b)

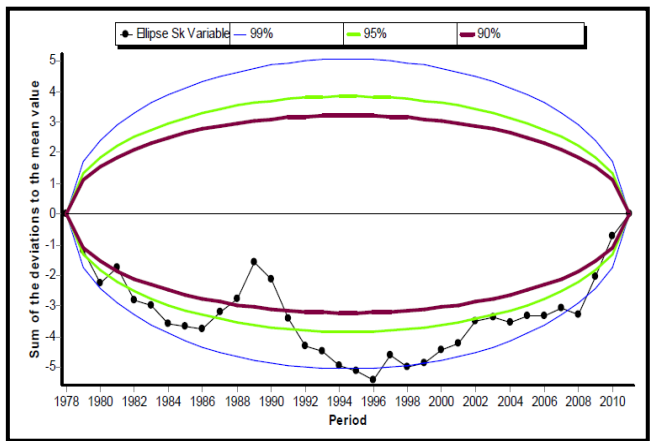


(c)

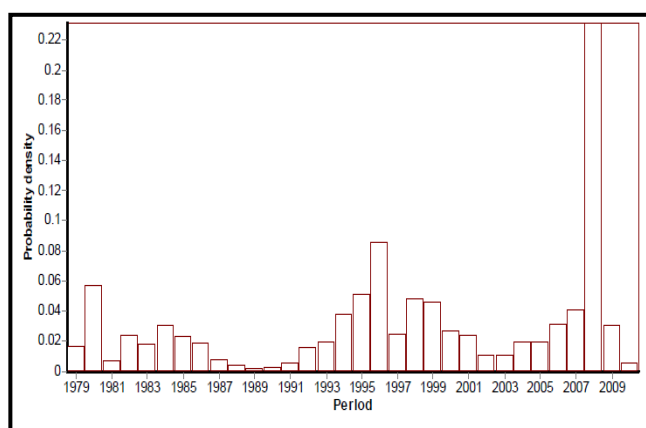
Figure III.44. Khronostat results of annual temperature at Beni Bahdel station: (a) Pettitt test; (b) Buishand test; (c) Lee and Heghinian test.



(a)



(b)



(c)

Figure III.45. Khronostat results of annual temperature at Zenata station: (a) Pettitt test; (b) Buishand test; (c) Lee and Heghinian test.

The application of the tests on monthly temperature (tab.III.22) showed different results between the rejection of the null hypothesis (no break) or the acceptance with different dates of break from test to test of each month may due to the data variability of these months a during the time series indicating inhomogeneity (existence of the extreme values).

Table III.22. Results of homogeneity test on monthly temperature.

Stations	Test	Investigative work	Sep	Oct	Nov	Dec	Jan	Feb	Mar	Ap	May	Jun	Jul	Aug
Beni Bahdel	Pettitt	Conclusion on H ₀	R	A	A	A	A	A	R	A	A	R	R	A
		Conclusion on H ₀	1992**	/	/	/	/	/	1995	/	/	1996	2001	/
	Hubert	Conclusion on H ₀	R	A	A	A	A	A	R	R	R	R	R	R
		Conclusion on H ₀	1992***	/	/	/	/	/	1995***	2008**	1984**	1990	2001**	2009**
		Conclusion on H ₀	1996***	/	/	/	/	/	1995***	2008*	1984*	1991**	2001*	2009*
	Buishand	Conclusion on H ₀	A	A	A	A	R	A	R	R	R	R	R	R
		Conclusion on H ₀	/	/	/	/	1994	/	1995**	2008	1984**	1996**	2001*	2009**
	Lee and Heghinian	Conclusion on H ₀	A	R	R	R	R	R	R	R	R	R	R	R
		Conclusion on H ₀	/	2000	1979	2008	2009	2010	1995	2008	1984	1996	2001	2009
	Zenata	Pettitt	Conclusion on H ₀	R	A	A	A	A	A	R	A	A	R	A
Conclusion on H ₀			2009	/	/	/	/	/	1995	/	/	1996**	/	/
Hubert		Conclusion on H ₀	R	A	A	A	A	A	A	R	R	R	R	R

	Conclusion on H0	1992 ***	/	/	/	/	/	/	2008** *	2003** *	1996** *	2008** *	2009** *
	Conclusion on H0	1996 ****											
Buishand	Conclusion on H0	R	A	A	A	A	A	R	R	R	R	A	A
	Conclusion on H0	2009 **	/	/	/	/	/	1995 **	2008*	2003**	1996**	/	/
Lee and Heghinian	Conclusion on H0	R	R	R	R	R	R	R	R	R	R	R	R
	Conclusion on H0	2000	2000	1979	2008	1994	2010	1995	2008	1984	1996	2008	2009

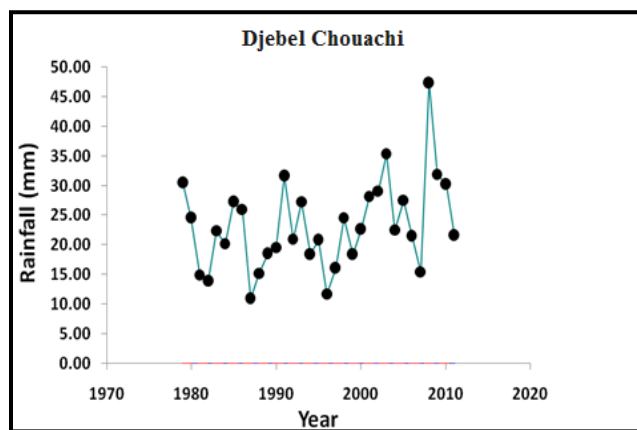
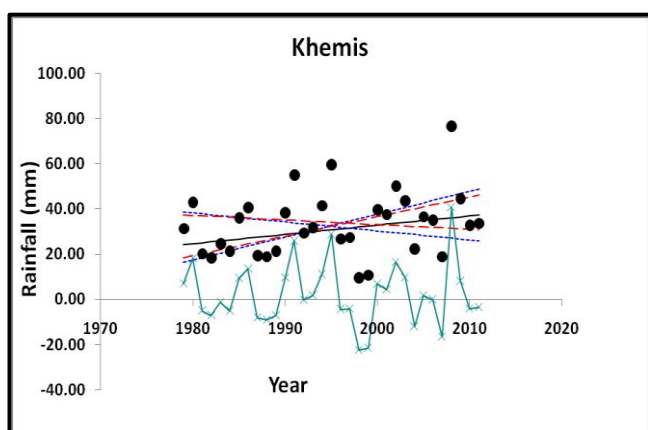
III.11.3.2. Results and discussion of Trend analysis

The results of the MK test presented by table III.23 on the annual time scale at different levels of statistical significance ($p=0.01, 0.05$ and 0.1) over period 1979/1980-2011/2012 show no statistically significant trend for all the rainfall stations, suggesting that the distribution evolution of rainfall totals has not changed over time, which is similar to the results of the study by (Zeroual et al., 2017). The theil-Sen’s estimator, the magnitudes of the insignificant trends were determined to be in the range between $- 0.038$ mm/year at Seb dou station to 0.403 mm/year at Khemis station.

Table III.23. Results of Mann-Kendall test and Sen's method on annual rainfall.

Test	Time series	Seb dou	Khemis	Djebel Chouachi	Hennaya	Chouly	Meurbah	Ouled Mimoun	Sidi Bounakhla
Test Z	Annual	-0.20	1.35	/	0.26	0.39	1.26	1.04	0.54
Q	Annual	-0.038	0.403	/	0.049	0.061	0.199	0.175	0.090

Z: Mann-Kendall test, Q: Sen's slope estimator



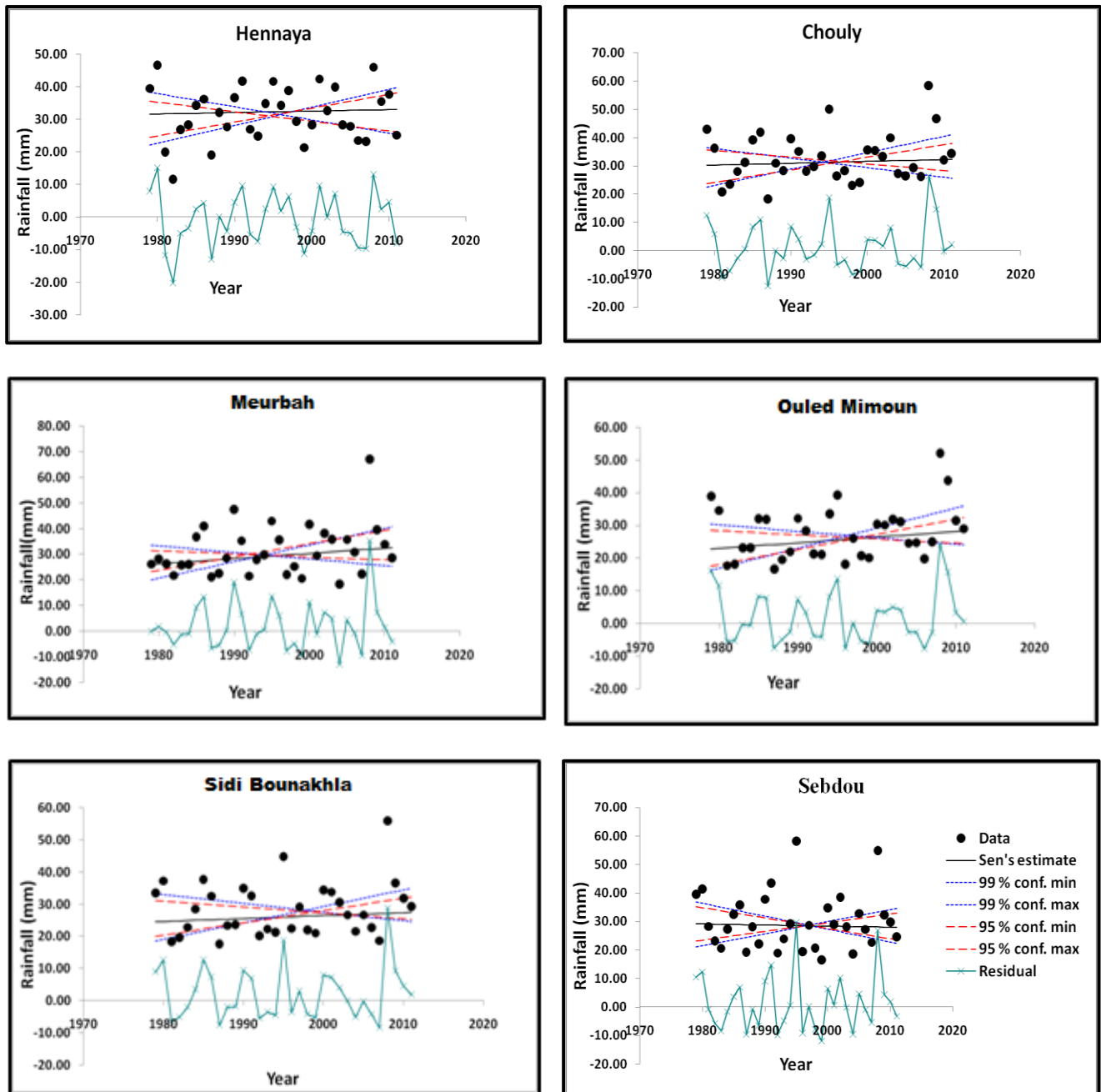


Figure III.46. Annual time series and significant trend statistics of rainfall.

Monthly rainfall has statistically significant increasing trends for Sebdou, Khemis, Meurbah, Ouled Mimoun, Sidi Bounakhla, Chouly and Hennaya stations. Sebdou station shows significant increasing trend for the months August (1.71 mm/month at $p=0.1$) September (2.56 mm/month at $p=0.05$) and October (2.17 mm /month at $p=0.05$), whereas Khemis station for the months September (2.93 mm/month at $p=0.01$) and October (2.59 mm/month at $p=0.01$). Ouled Mimoun and Sidi Bounakhla stations feature also significant increasing trend for the months September (1.83 mm/month at $p=0.1$, 1.94 mm/month at $p=0.1$, respectively) and October (2.47 mm/month at $p=0.05$, 2.73 mm/month at $p=0.01$, respectively). Meurbah station shows significant increasing trends for the month of August (2.29 mm/month at $p=0.05$), September (2.08 mm/month at $p=0.05$) and October (3.04 mm/month at $p=0.01$). Chouly and Hennaya station show significant increasing trend for the month of October (1.77 mm/month at $p=0.1$, 2.53 mm/month at $p=0.05$, respectively). We

conclude that most of the stations with significant increasing trends, this increase is occurring in the months of August, September and October. Furthermore, the maximum number of significant increasing trends of rainfall in these months (August, September and October) was found at Sebdoou and Meurbah stations. In contrast, no significant trend was detected at Djebel Chouachi station. The results are shown in table III.24 and appendix .2.

Table III.24. Results of Mann-Kendall test and Sen's method on monthly rainfall.

Test	Time series	Sebdoou	Khemis	Djebel Chouachi	Hennaya	Chouly	Meurbah	Ouled Mimoun	Sidi Bounakhla
Test Z	January	0.39	0.37	-0.26	1.27	0.99	0.84	0.34	0.81
	February	0.00	0.06	0.96	-1.05	0.02	0.26	-0.03	0.50
	March	-0.70	-0.29	0.22	-0.56	-0.15	-0.88	-0.22	-0.85
	April	0.88	1.27	-0.56	0.67	1.10	1.63	1.46	1.08
	May	-0.50	0.96	1.32	-0.48	0.23	0.82	-0.19	-0.28
	June	-0.03	0.29	0.00	0.48	0.03	0.06	-1.00	-0.21
	July	0.14	0.81	/	0.79	0.31	0.57	0.26	0.43
	August	1.71+	0.53	/	-1.20	1.55	2.29*	1.52	1.58
	September	2.56*	2.93**	/	1.36	1.63	2.08*	1.83+	1.94+
	October	2.17*	2.59**	/	2.53*	1.77+	3.04**	2.47*	2.73**
	November	-0.64	0.11	/	1.27	0.08	1.24	0.98	0.67
	December	-1.53	-0.48	/	-0.67	-0.88	-0.91	-1.19	-0.98
Q	January	0.211	0.182	-0.060	0.513	0.622	0.420	0.162	0.440
	February	0.009	0.064	0.654	-0.602	0.000	0.139	-0.021	0.313
	March	-0.403	-0.165	0.108	-0.329	-0.123	-0.489	-0.103	-0.275
	April	0.267	0.646	-0.135	0.388	0.589	0.800	0.593	0.485
	May	-0.131	0.317	0.403	-0.229	0.097	0.260	-0.031	-0.083
	June	0.000	0.000	0.000	0.009	0.000	0.000	0.000	0.000
	July	0.000	0.000	/	0.000	0.000	0.000	0.000	0.000
	August	0.200	0.000	/	-0.019	0.024	0.181	0.020	0.005
	September	0.677	0.633	/	0.389	0.416	0.653	0.496	0.466
	October	1.119	1.116	/	1.238	0.811	1.534	1.062	0.961
	November	-0.340	0.077	/	0.743	0.071	0.702	0.553	0.275
	December	-0.702	-0.194	/	-0.363	-0.709	-0.438	-0.331	-0.460

Z: Mann-Kendall test, Q: Sen's slope estimator, + if trend at ≤ 0.1 level of significance, * if trend at ≤ 0.05 level of significance, ** if trend at ≤ 0.01 level of significance.

Similar to the monthly time series, increasing trends were also detected at seasonal scale (tab.III.25). Autumn season (September, October, November) indicated an increasing rainfall trend for Khemis (2.43mm/month at $p=0.05$), Chouly (2.06 mm/month at $p=0.05$), Ouled Mimoun (2.56 mm/month at $p=0.05$), Sidi Bounakhla (2.25 mm/month at $p=0.05$), Hennaya (2.68 mm/month at $p=0.01$) and Meurbah (2.76 mm/month at $p=0.01$). However, as an exception, Sebdoou has no significant trend. For the other seasons: spring (March, April and May), summer (June, July and August) and winter (December, January and February) no statistically significant trend was revealed. We validated the results that show increasing trend of Mann-Kendall test with Sen's method which confirmed near-zero or positive slopes that displays an increasing trend almost for all the stations for the months (August, September and October) and the autumn season. Rainfall trend seems to be rising at the end of the time series as depicted in figure III.47, III.48, III.49, III.50, III.51, III.52, III.53, and III.54.

Table III.25. Results of Mann-Kendall test and Sen's method on seasonal rainfall.

Test	Time series	Sebdou	Khemis	Djebel Chouachi	Hennaya	Chouly	Meurbah	Ouled Mimoun	Sidi Bounakhla
Test Z	Spring	-0.60	0.85	/	-0.67	0.26	0.43	0.02	-0.54
	Summer	0.60	0.30	/	0.03	-0.03	0.48	-0.06	0.25
	Autumn	0.85	2.43*	/	2.68**	2.06*	2.76**	2.56*	2.25*
	Winter	-0.45	-0.17	/	-0.51	-0.26	-0.45	-0.29	0.00
Q	Spring	-0.265	0.427	/	-0.353	0.071	0.104	0.010	-0.110
	Summer	0.059	0.000	/	0.000	0.000	0.033	0.000	0.003
	Autumn	0.320	0.858	/	0.959	0.574	0.895	0.755	0.611
	Winter	-0.265	-0.118	/	-0.233	-0.081	-0.187	-0.134	-0.001

Z: Mann-Kendall test, Q: Sen's slope estimator, + if trend at ≤ 0.1 level of significance, * if trend at ≤ 0.05 level of significance, ** if trend at ≤ 0.01 level of significance.

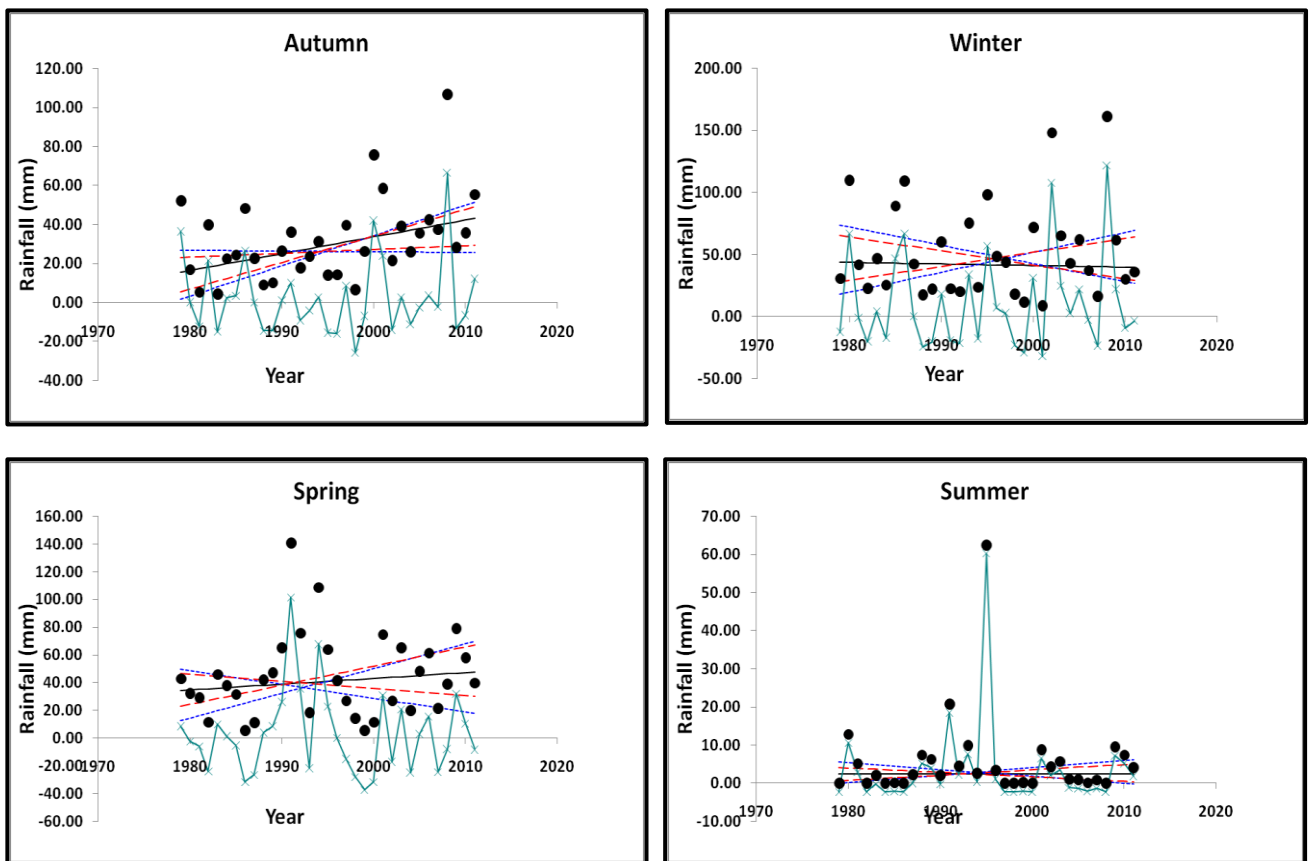


Figure III.47. Seasonal time series and significant trend statistics of rainfall at Khemis.

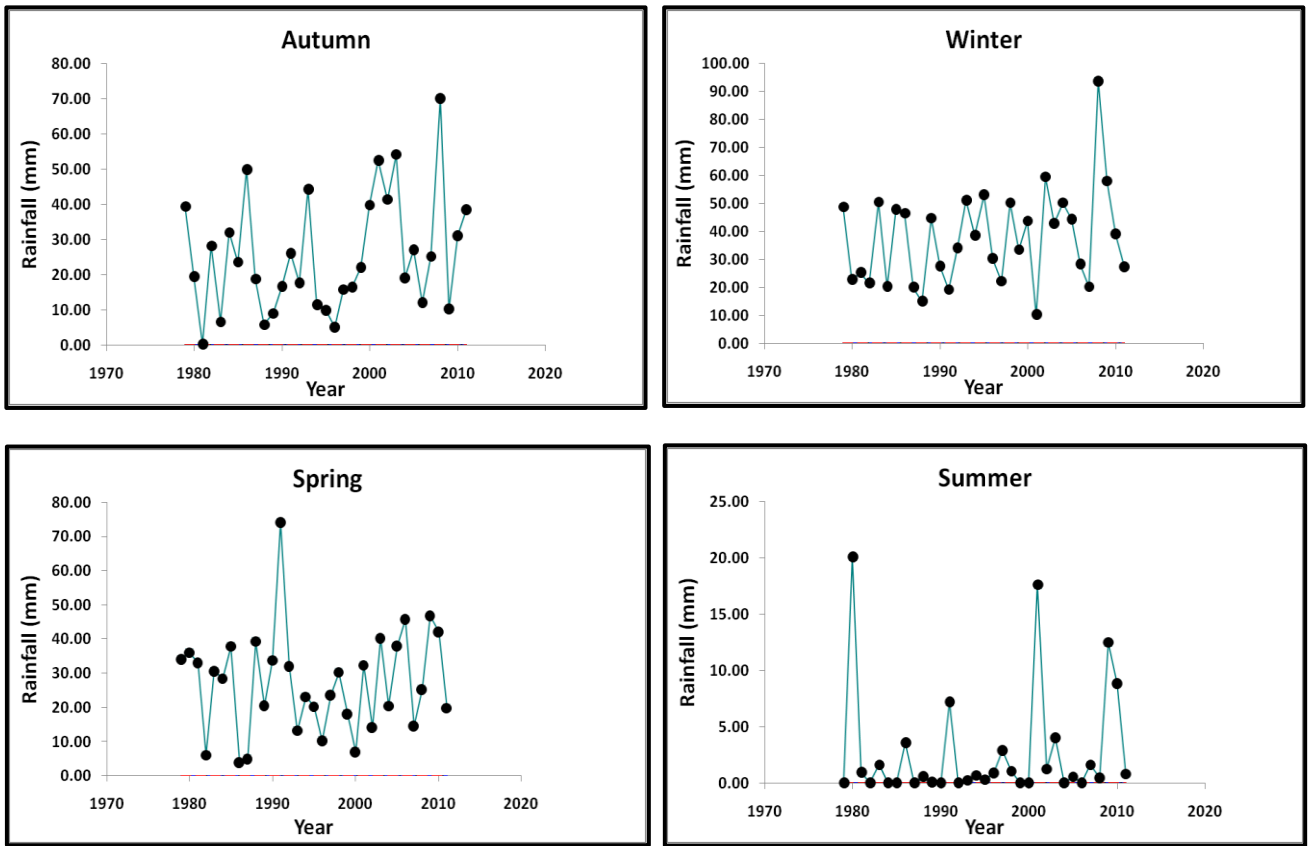


Figure III.48. Seasonal time series and significant trend statistics of rainfall at Djebel Chouachi station.

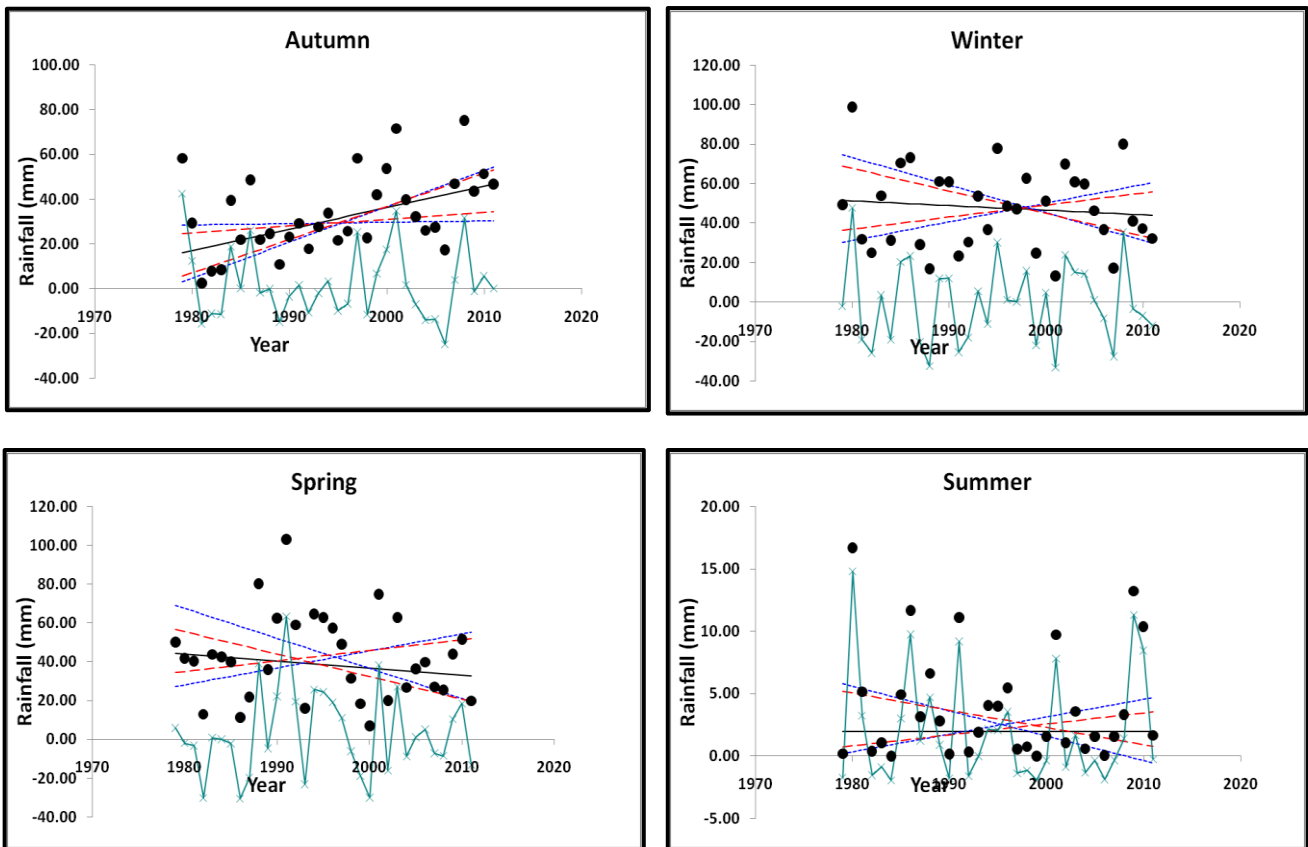


Figure III.49. Seasonal time series and significant trend statistics of rainfall at Hennaya station.

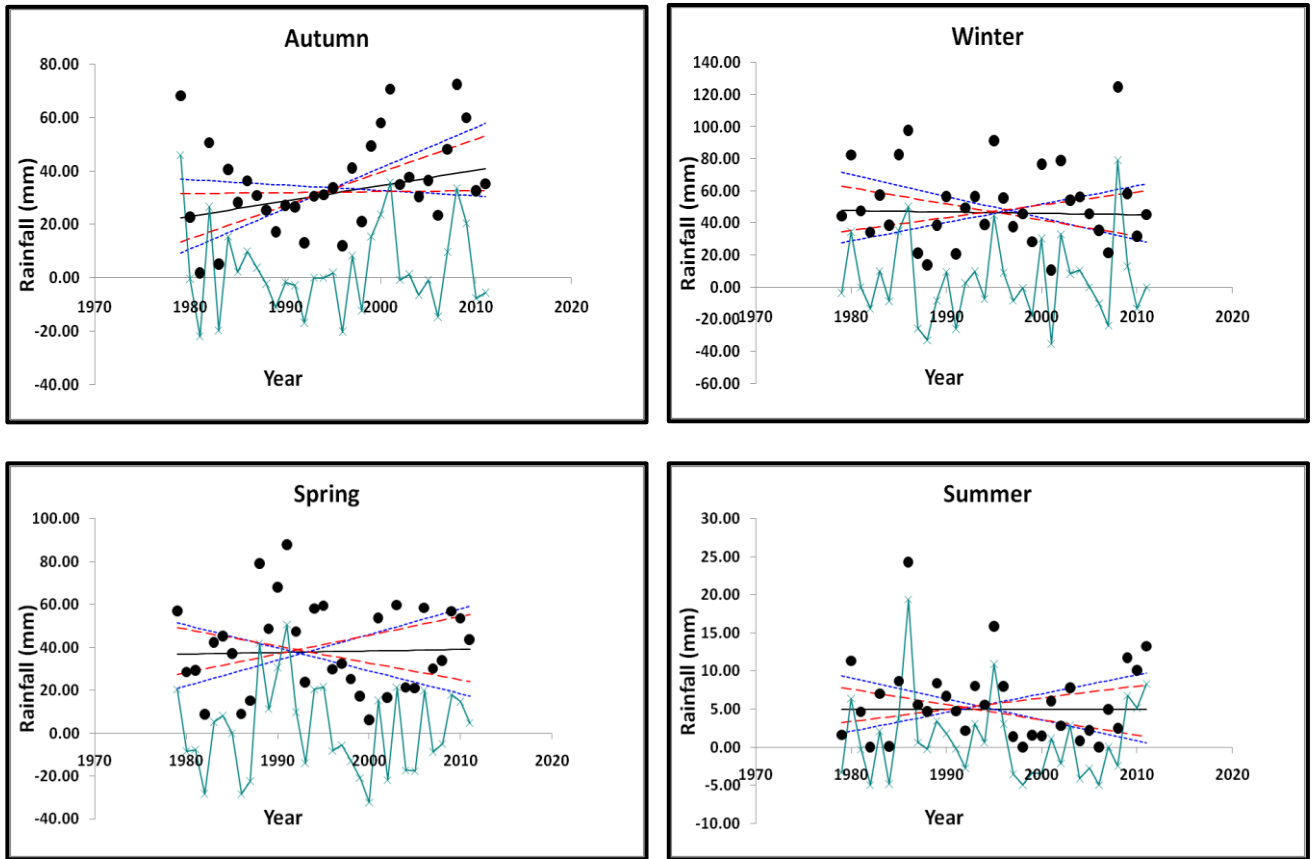


Figure III.50. Seasonal time series and significant trend statistics of rainfall at Chouly station.

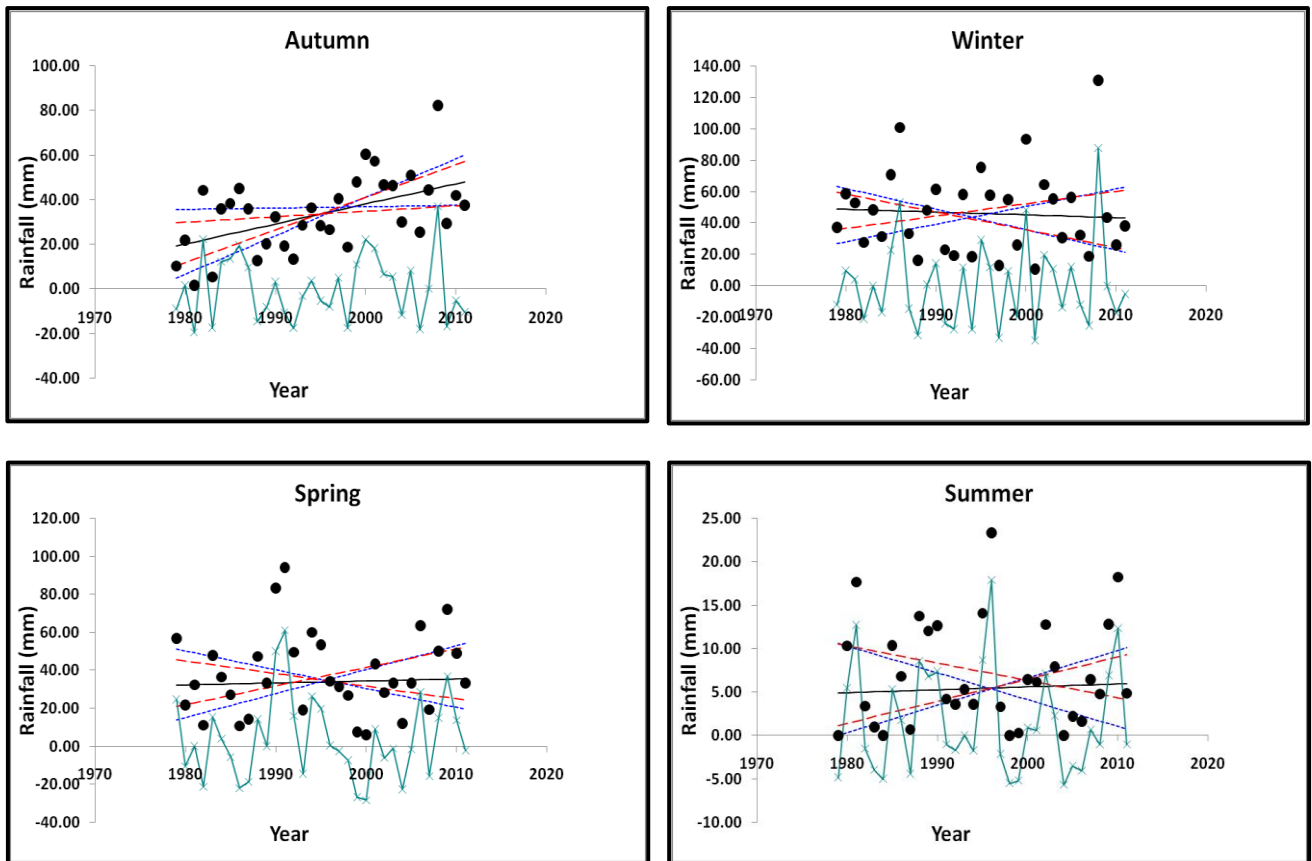


Figure III.51. Seasonal time series and significant trend statistics of rainfall at Meurbah station.

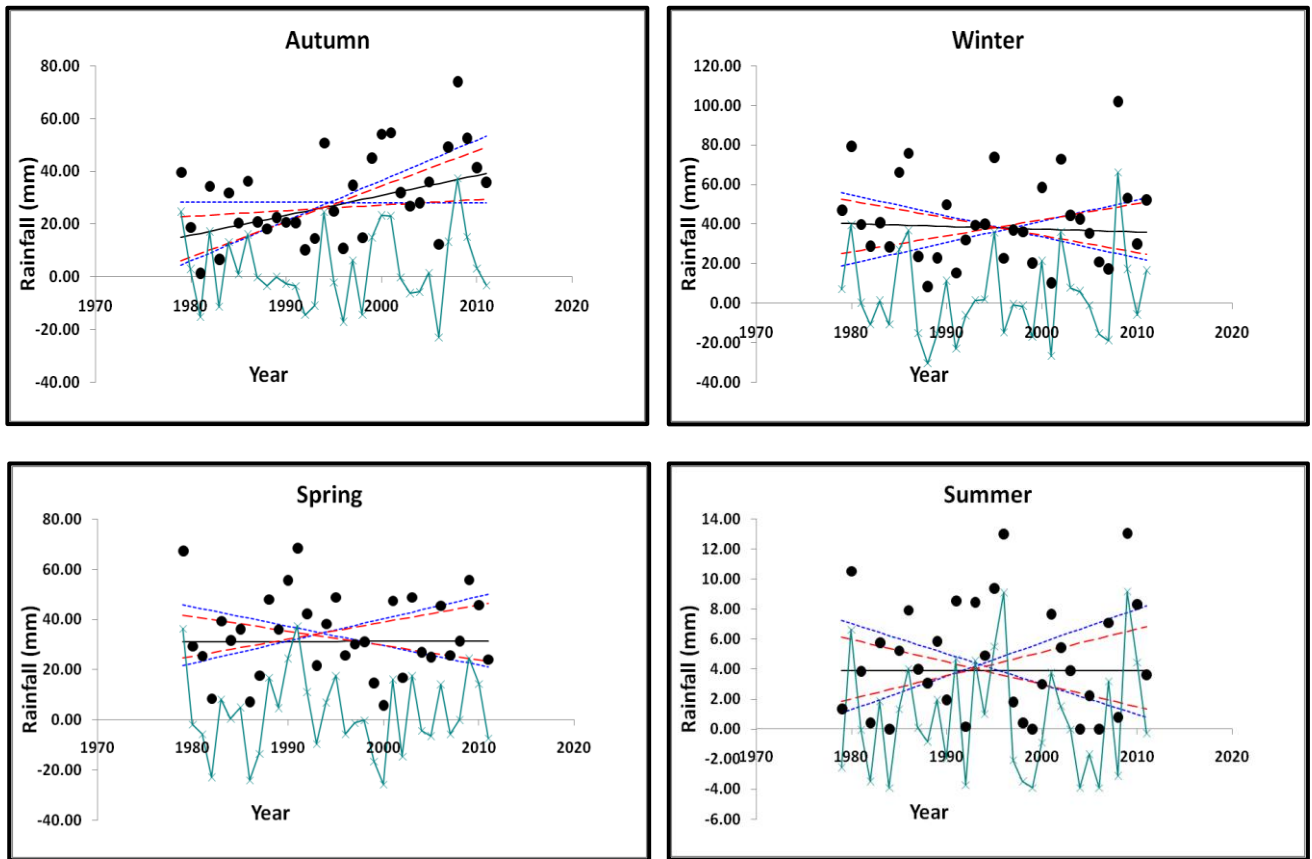


Figure III.52. Seasonal time series and significant trend statistics of rainfall at Ouled Mimoun station.

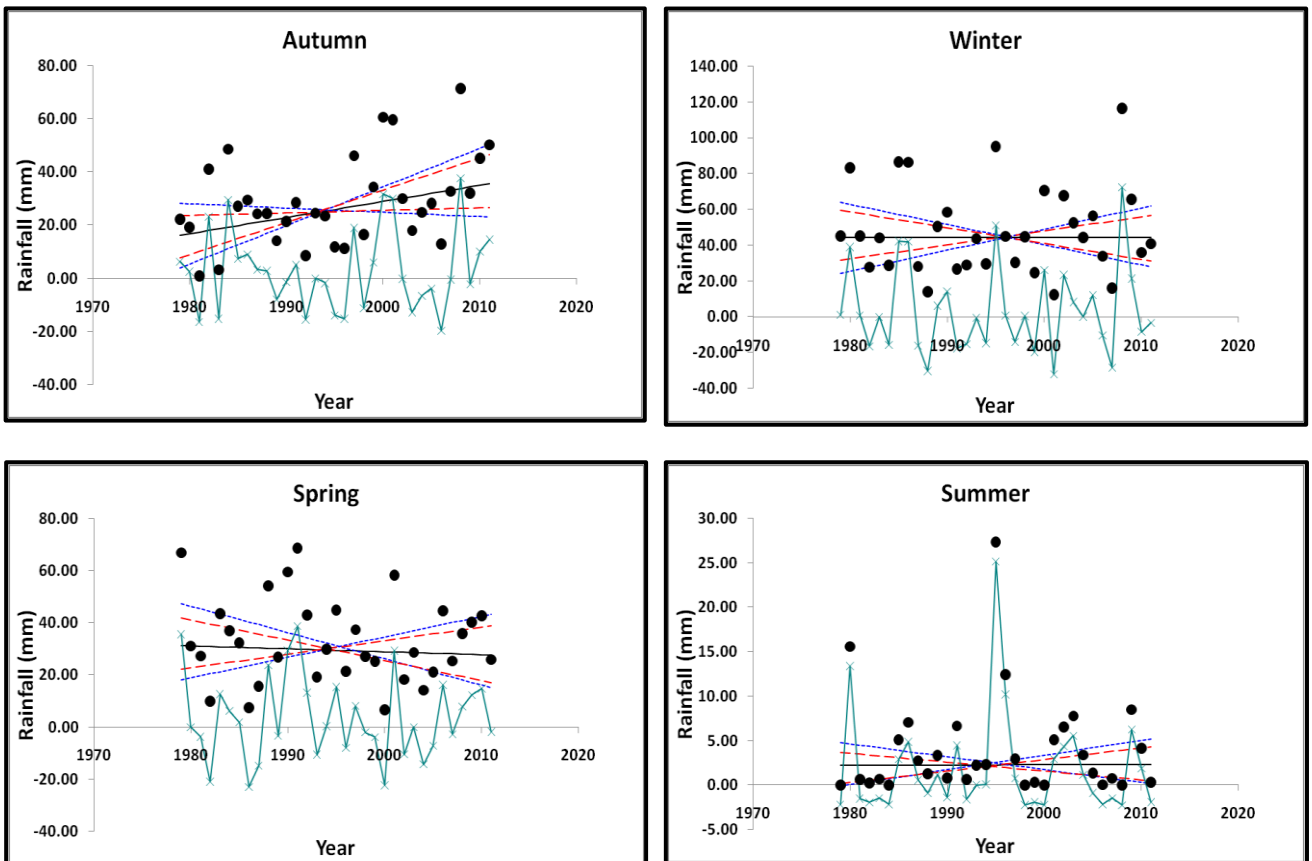


Figure III.53. Seasonal time series and significant trend statistics of rainfall at Sidi Bounakhla station.

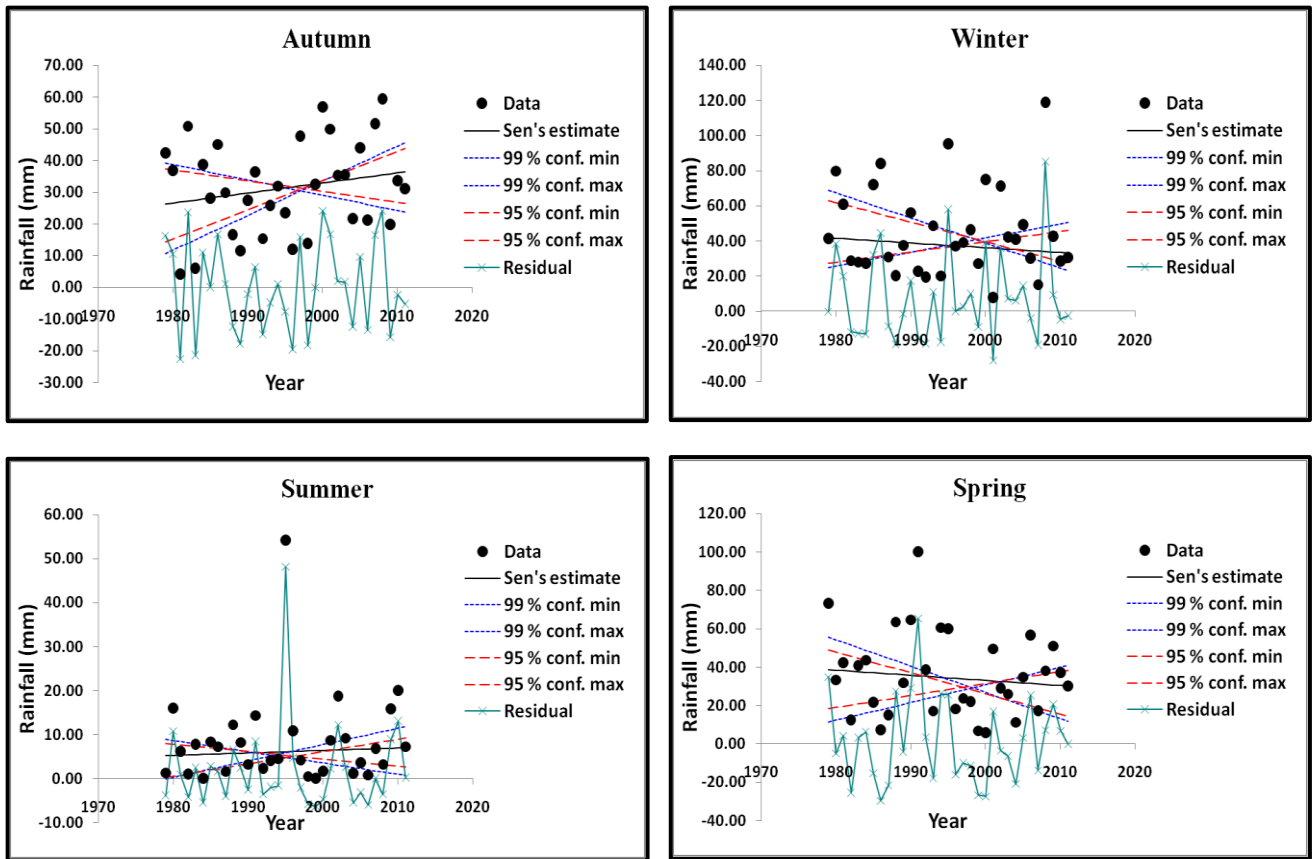


Figure III.54. Seasonal time series and significant trend statistics of rainfall at Sebdou station.

Results of the MK test for annual trends of runoff for the period 1985 to 2010 are shown in table III.26. All the stations exhibit no statistically significant trends with the exception of Zahra showed significant negative trend ($Z= -2.51 \text{ m}^3/\text{s}$) at $p=0.05$, which indicate the decreasing tendency of annual runoff which reveal the presence of dry periods in the time series. The significant magnitudes of Sen's estimator at Zahra were determined negative slope -0.018 that displays a decreasing trend, where it seems to be decline at the end of the time series (fig.III.55).

Table III.26. Results of Mann-Kendall test and Sen's method on annual runoff.

Test	Time series	Sebdou	Zahra	Zenata	Chouly	Sidi Aissa
Test Z	Annual	0.18	-2.51*	-0.42	-1.28	-1.52
Q	Annual	0.001	-0.018	-0.001	-0.002	-0.006

Z: Mann-Kendall test, Q: Sen's slope estimator, * if trend at ≤ 0.05 level of significance.

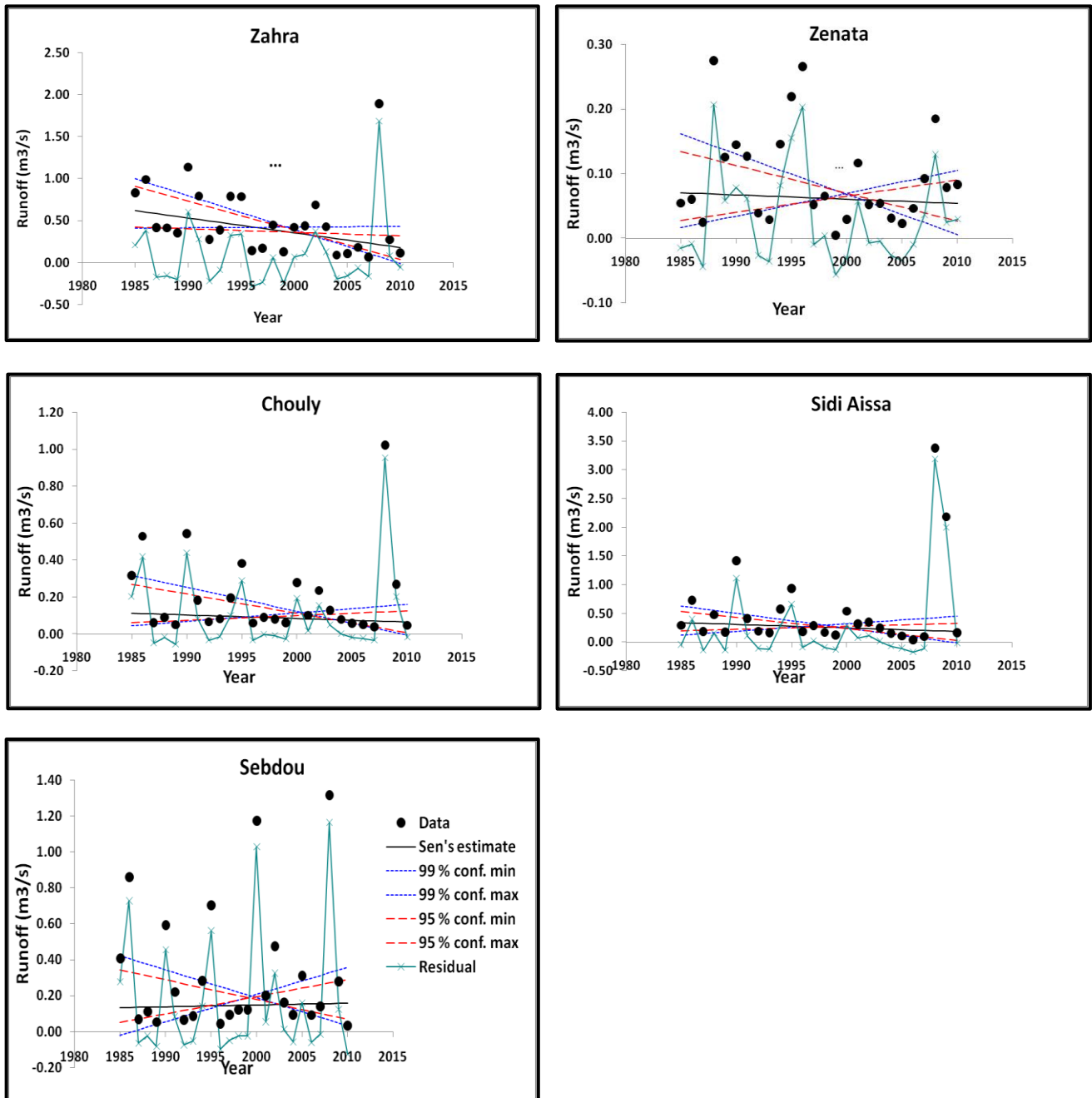


Figure III.55. Annual time series and significant trend statistics of runoff.

In the analysis of trend runoff by month, 3 stations of the 5 stations show statistically significant trends (tab.III.27), where Zahra station shows significant decreasing trend for the months November, December, January, June, July, and August at 0.01 level of significance with values of -3.25, -3.38, -3.18, -3.23, -4.60, -4.57 m³/s respectively, while at 0.05 level of significance with the values of -2.52, -2.54, -2.05, -2.34, -2.50 m³/s for months September, October, February, April, and May respectively, only the month of March showed significant decreasing trend of -1.79 m³/s at 0.1 level of significance. Whereas Chouly and Sidi Aissa were the only two stations indicating significant increasing trend, the first station in the months September (1.68 m³/s), and the second one in October (1.70 m³/s) at 0.1 level of significance. The rest of the runoff stations Sebdou, and Zenata showed no significant trends of runoff. Sen's monthly trend test presents the estimation of magnitudes slopes for

significance trends (per month), displays the downward the trend in monthly time series for the stations that showed the significant decreasing trends, and the upward trends of the stations that showed the significant increasing trends in appendix .3.

Table III.27. Results of Mann-Kendall test and Sen's method on monthly runoff.

Test	Time series	Sebdou	Zahra	Zenata	Chouly	Sidi Aissa
Test Z	January	-0.42	-3.18 **	0.86	-0.49	0.24
	February	-0.27	-2.05 *	0.40	-0.67	-0.60
	March	-0.53	-1.79 +	-0.93	-0.84	-0.09
	April	-0.71	-2.34*	0.15	-0.75	0.15
	May	-0.31	-2.50*	0.20	-0.16	0.00
	June	-0.65	-3.23**	-0.02	-0.35	0.82
	July	-0.43	-4.60**	-1.00	0.45	-0.42
	August	0.97	-4.57**	-0.97	1.12	0.78
	September	1.11	-2.52*	-0.39	1.68 +	0.62
	October	1.48	-2.54*	0.61	0.38	1.70 +
	November	0.42	-3.25**	0.55	0.38	1.39
	December	0.58	-3.38**	1.49	0.16	0.46
Q	January	-0.001	-0.014	0.001	0.000	0.001
	February	-0.001	-0.017	0.001	-0.001	-0.004
	March	-0.002	-0.029	-0.003	-0.002	-0.002
	April	-0.001	-0.016	0.000	-0.001	0.001
	May	0.000	-0.009	0.000	0.000	0.000
	June	0.000	-0.008	0.000	0.000	0.000
	July	0.000	-0.006	0.000	0.000	0.000
	August	0.000	-0.005	0.000	0.000	0.000
	September	0.001	-0.005	0.000	0.000	0.000
	October	0.004	-0.007	0.000	0.000	0.005
	November	0.000	-0.013	0.001	0.000	0.008
	December	0.000	-0.017	0.002	0.000	0.003

Z: Mann-Kendall test, Q: Sen's slope estimator, + if trend at ≤ 0.1 level of significance, * if trend at ≤ 0.05 level of significance, ** if trend at ≤ 0.01 level of significance.

The seasonal trends in runoff time series as depicted in (tab.III.28) showed all the stations did not have any significant trend, there exist both insignificant negative trend (~ 58 %) and insignificant positive trend (~ 42 %), displays insignificant increasing and decreasing trends as shown in (fig.III.56, III.57, III.58), except Zahra station which indicates significant negative trends in summer, autumn, and winter at 0.01 level of significance with values -3.95, -2.82, and -3.09 m³/s, respectively, while at 0.05 level of significance with value -1.98 m³/s in spring, displays the downward of runoff trend in season time series (fig.III.56) with the magnitudes slopes (per month) estimated between -0.006 (in summer) and -0.025 (in spring). The only significant increasing trend was defined in autumn at Sidi Aissa station with a value

of 1.70 at a 0.1 level of significance with a magnitude slope estimated at 0.009, showing increasing trend at the end of the autumn time series (fig.IV.64).

Table III.28. Results of Mann-Kendall test and Sen's method on seasonal runoff.

Test	Time series	Sebdou	Zahra	Zenata	Chouly	Sidi Aissa
Test Z	Spring	-0.18	-1.98*	-1.41	-0.64	-0.42
	Summer	0.04	-3.95**	-0.30	0.67	0.02
	Autumn	1.46	-2.82**	1.24	0.86	1.70+
	Winter	-0.02	-3.09**	0.15	-0.93	-1.17
Q	Spring	-0.001	-0.025	-0.003	-0.003	-0.003
	Summer	0.000	-0.006	0.000	0.000	0.000
	Autumn	0.003	-0.008	0.002	0.000	0.009
	Winter	0.000	-0.016	0.001	-0.001	-0.008

Z: Mann-Kendall test, Q: Sen's slope estimator, + if trend at ≤ 0.1 level of significance, * if trend at ≤ 0.05 level of significance, ** if trend at ≤ 0.01 level of significance.

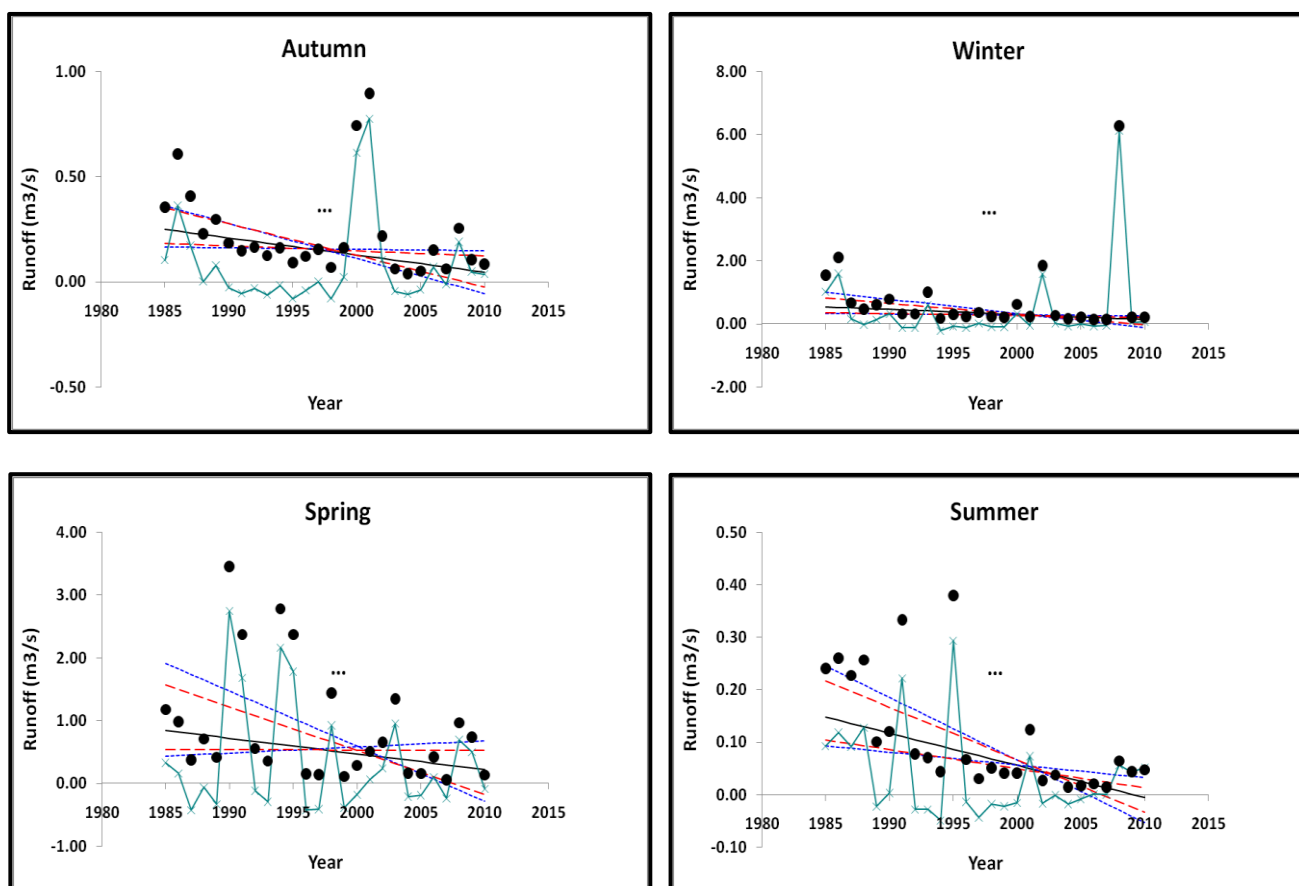


Figure III.56. Seasonal time series and significant trend statistics of runoff at Zahra station.

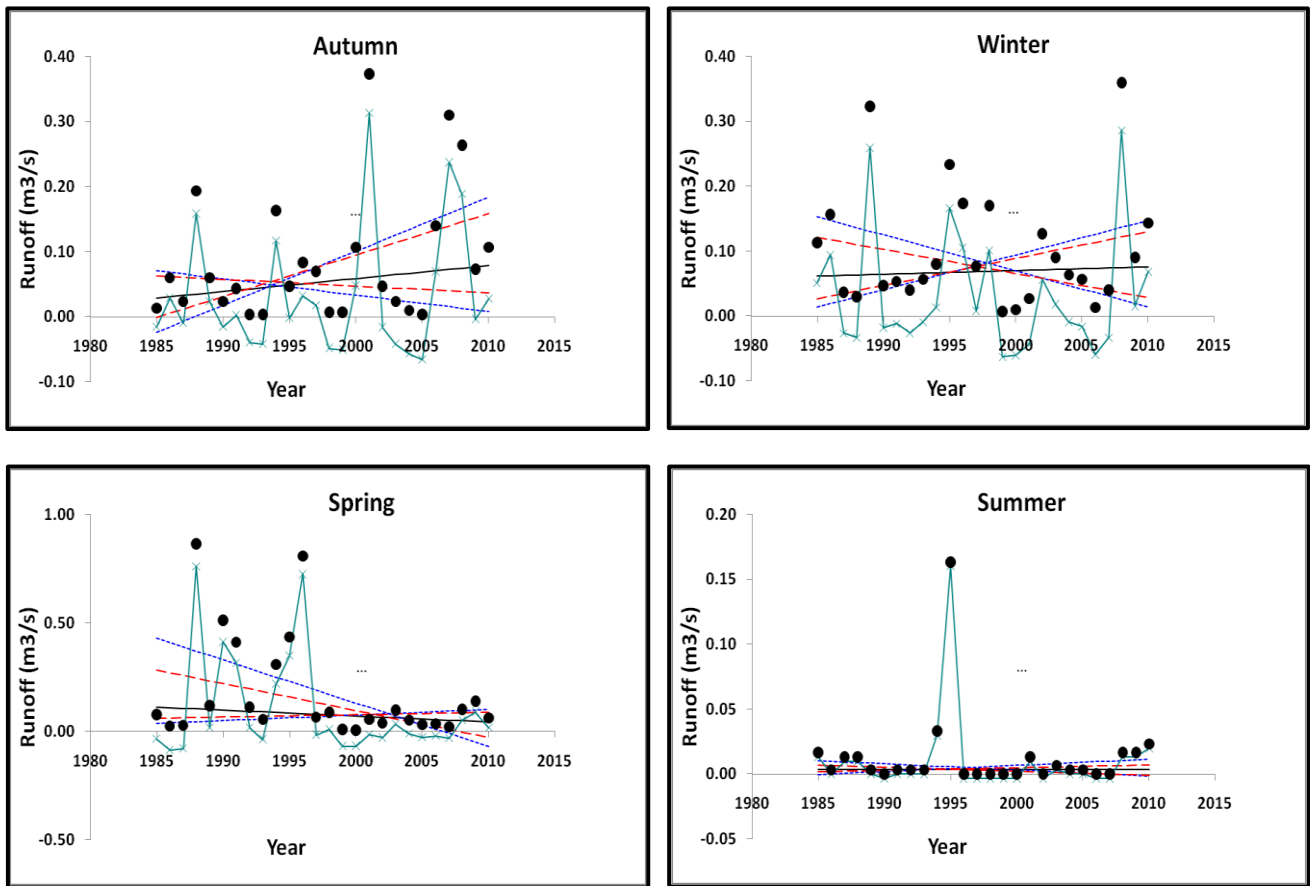
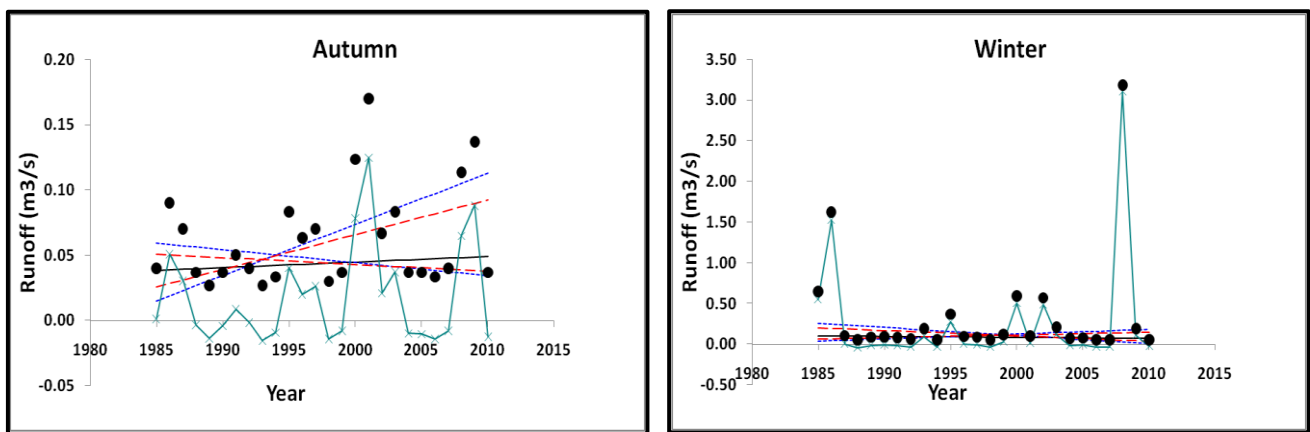


Figure III.57. Seasonal time series and significant trend statistics of runoff at Zenata station.



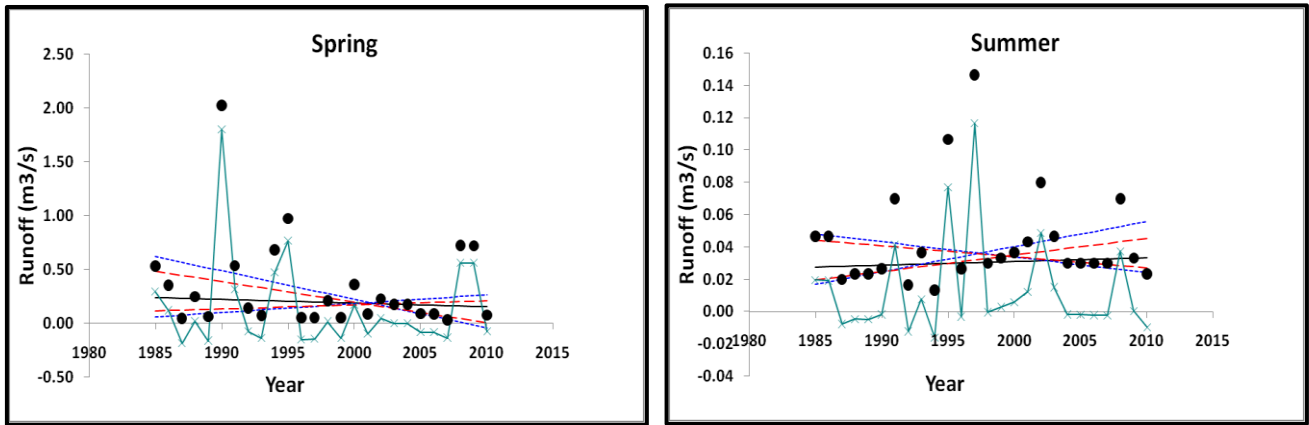


Figure III.58. Seasonal time series and significant trend statistics of runoff at Chouly station.

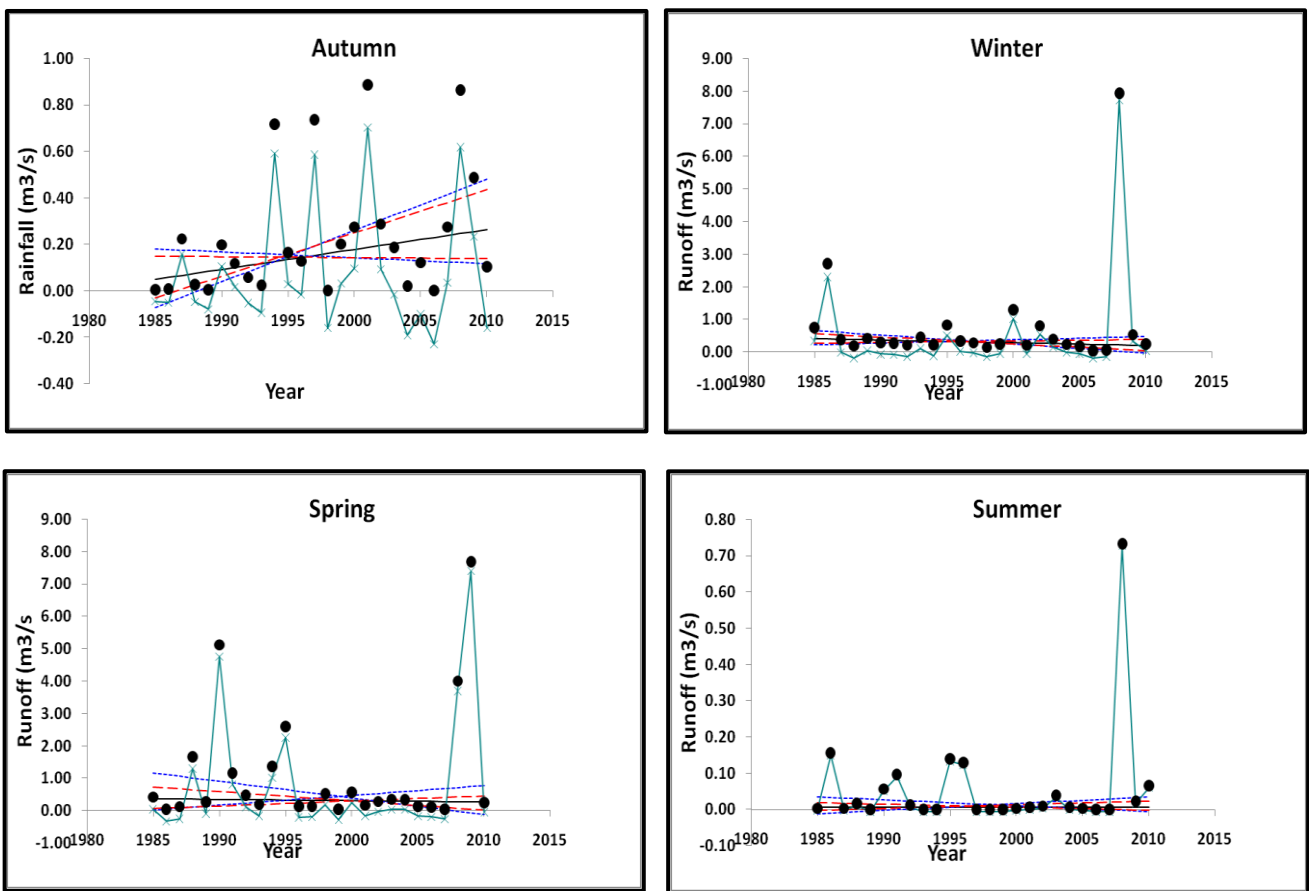


Figure III.59. Seasonal time series and significant trend statistics of runoff at Sidi Aissa station.

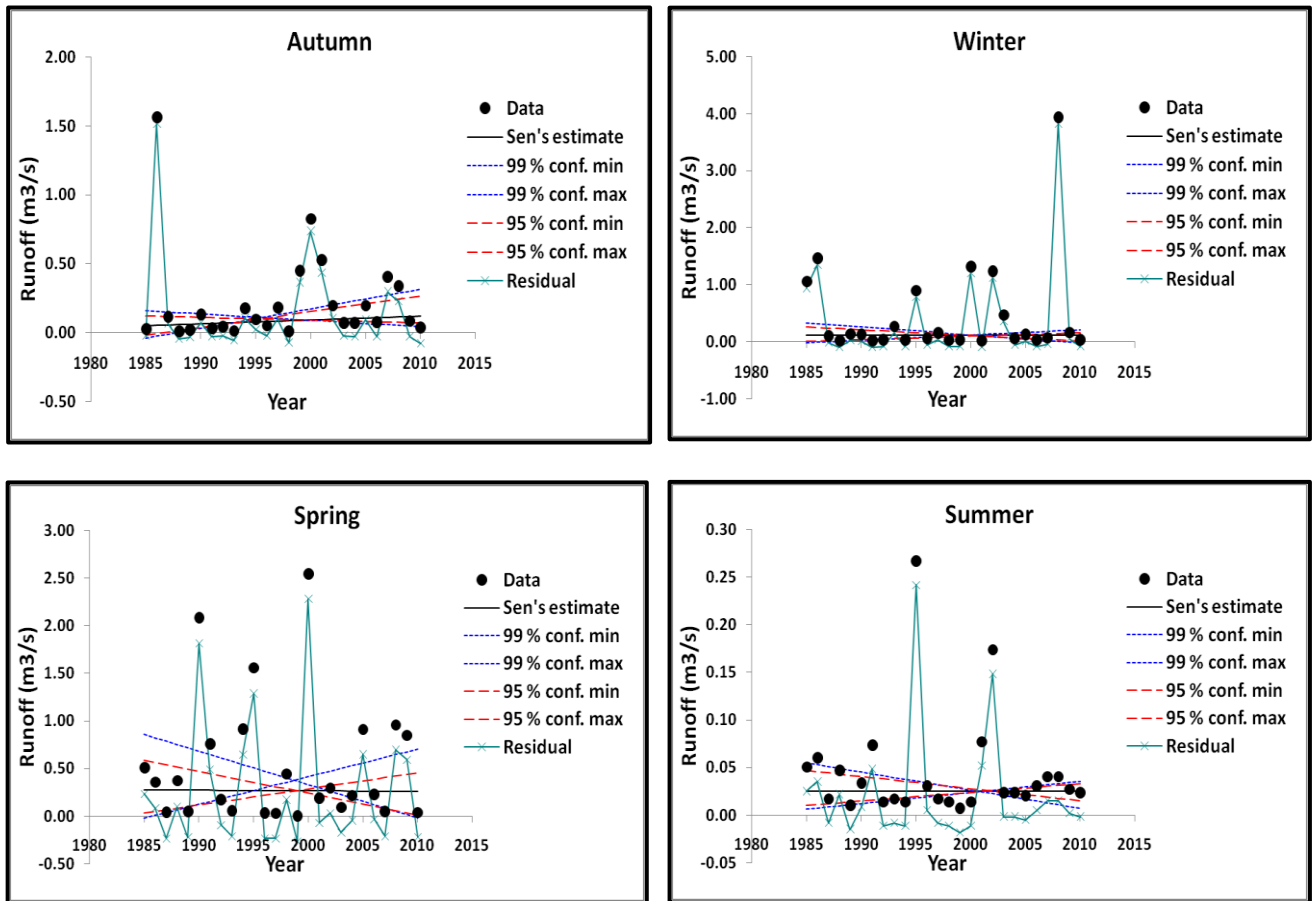


Figure III.60. Seasonal time series and significant trend statistics of runoff at Sebdu station.

The trend analysis of annual temperature was summarized in (tab.III.29) between 1979 and 2010. Positive trends were found at both temperature stations (Beni Bahdel, Zenata), and are considered statistically significant at $p= 0.1$ confidence level at Beni Bahdel station with a value of $1.93\text{ }^{\circ}\text{C}$, and at statistically significant $p= 0.05$ confidence level at Zenata station with the value of $2.55\text{ }^{\circ}\text{C}$. The two stations were dominated by the increasing trend of annual temperature. The magnitude of the slope for the positive trend in annual temperature (fig.III.61) found for Beni Bahdel station ($0.096\text{ }^{\circ}\text{C}$ per year) is greater than Zenata station ($0.036\text{ }^{\circ}\text{C}$ per year).

Table III.29. Results of Mann-Kendall test and Sen's method on annual temperature.

Test	Time series	Beni Bahdel	Zenata
Test Z	Annual	1.93+	2.55*
Q	Annual	0.096	0.036

Z: Mann-Kendall test, Q: Sen's slope estimator, + if trend at ≤ 0.1 level of significance, * if trend at ≤ 0.05 level of significance, ** if trend at ≤ 0.01 level of significance.

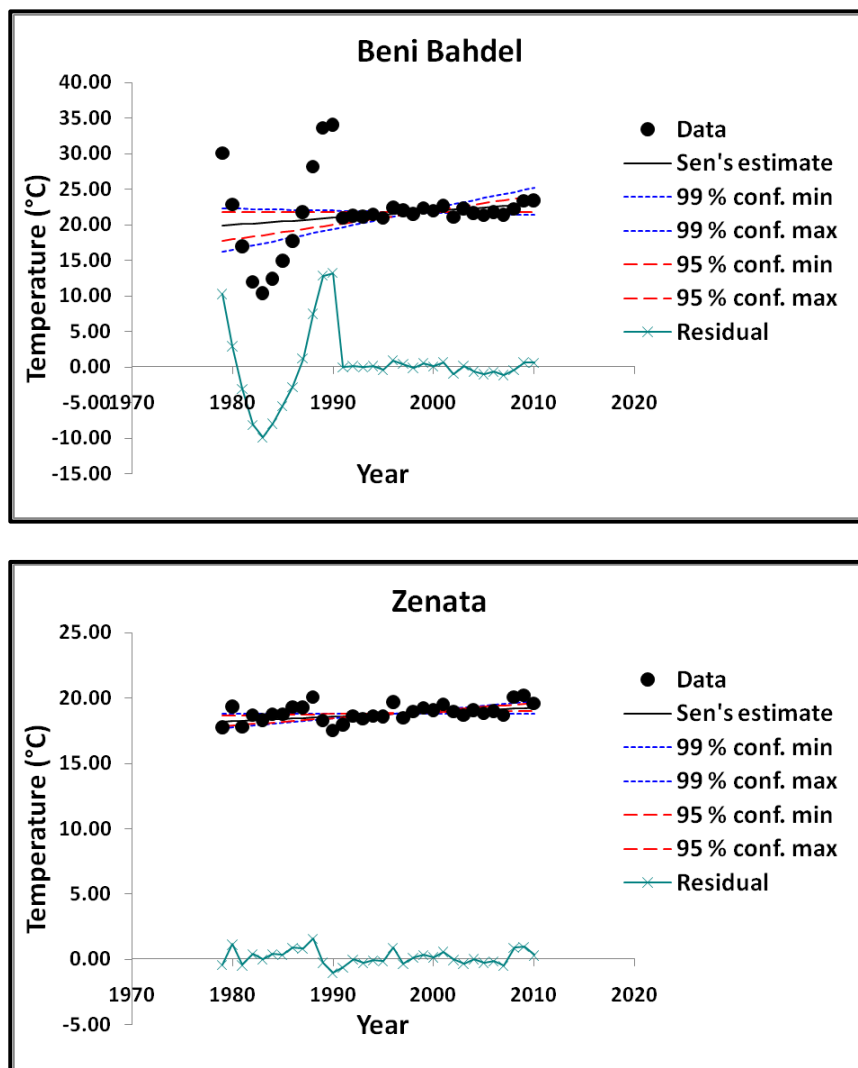


Figure III.61. Annual time series and significant trend statistics of temperature.

The results of the trend on monthly temperature (tab.III.30) for Beni Bahdel station illustrate significant positive and negative trends which were mostly positive ($\sim 71\%$) in July, August, and September (4.32 , 4.67 , and 3 $^{\circ}\text{C}$, respectively) at a statistically significant level $p=0.01$, and in June and October (3.02 , and 1.72 $^{\circ}\text{C}$, respectively at a statistically significant level $p=0.05$ and $p=0.1$, respectively), for significant negative trends, were observed in December and January (-1.98 and -2.11 $^{\circ}\text{C}$, respectively at a statistically significant level $p=0.05$). While Zenata station showed only significant positive trends in March and April (1.95 and 1.67 $^{\circ}\text{C}$) at a statistically significant level $p=0.1$, and in May, June (2.08 and 1.96 $^{\circ}\text{C}$) at a statistically significant level $p=0.05$. The rest of the months showed insignificant positive (~ 40 , 75 % at Beni Bahdel and Zenata respectively), and negative trends. The significant magnitude of slopes was estimated between -0.217 to 0.579 at Beni Bahdel station, and between 0.046 to 0.085 at Zenata station. The results were similar to the annual trend pattern, where the two stations dominated by the increasing trend. The upward trends of the stations that showed the significant increasing trends are presented in appendix .4.

Table III.30. Results of Mann-Kendall test and Sen's method on monthly temperature.

Test	Time series	Beni Bahdel	Zenata
Test Z	January	-2.11*	1.38
	February	-1.52	0.58
	March	-0.37	1.95+
	April	1.05	1.67+
	May	1.39	2.08*
	June	3.02*	1.96*
	July	4.32**	1.64
	August	4.67**	1.46
	September	3.00**	-1.35
	October	1.72+	1.14
	November	-0.81	-0.75
	December	-1.98*	0.78
Q	January	-0.191	0.055
	February	-0.116	0.026
	March	-0.029	0.046
	April	0.087	0.051
	May	0.142	0.085
	June	0.300	0.066
	July	0.416	0.060
	August	0.579	0.048
	September	0.302	-0.042
	October	0.194	0.052
	November	-0.050	-0.026
	December	-0.217	0.020

Z: Mann-Kendall test, Q: Sen's slope estimator, + if trend at ≤ 0.1 level of significance, * if trend at ≤ 0.05 level of significance, ** if trend at ≤ 0.01 level of significance.

On the seasonal time series (tab.III.31), Beni Bahdel station showed a significant positive trend in summer and autumn (4.10, 2.21 °C at $p=0.01$, $p=0.05$ respectively) with the magnitude of slopes 0.39 and 0.117, respectively, display increasing in temperature in these seasons (fig.III.62), the only season of winter showed a decreasing trend (-1.78 °C) at statistically significant level $p=0.1$. Zenata station indicates a significant positive trend in spring and summer (3 and 2.14 °C at $p=0.01$ and $p=0.05$, respectively) with slopes of 0.062 and 0.053, respectively, display rising at the end of time series (fig.III.63).

Table III.31. Results of Mann-Kendall test and Sen's method on seasonal temperature.

Test	Time series	Beni Bahdel	Zenata
Test Z	Spring	1.25	3.00**
	Summer	4.10**	2.14*
	Autumn	2.21*	-0.45
	Winter	-1.78+	1.25
Q	Spring	0.094	0.062
	Summer	0.390	0.053
	Autumn	0.117	-0.011
	Winter	-0.142	0.035

Z: Mann-Kendall test, Q: Sen's slope estimator, + if trend at ≤ 0.1 level of significance, * if trend at ≤ 0.05 level of significance, ** if trend at ≤ 0.01 level of significance.

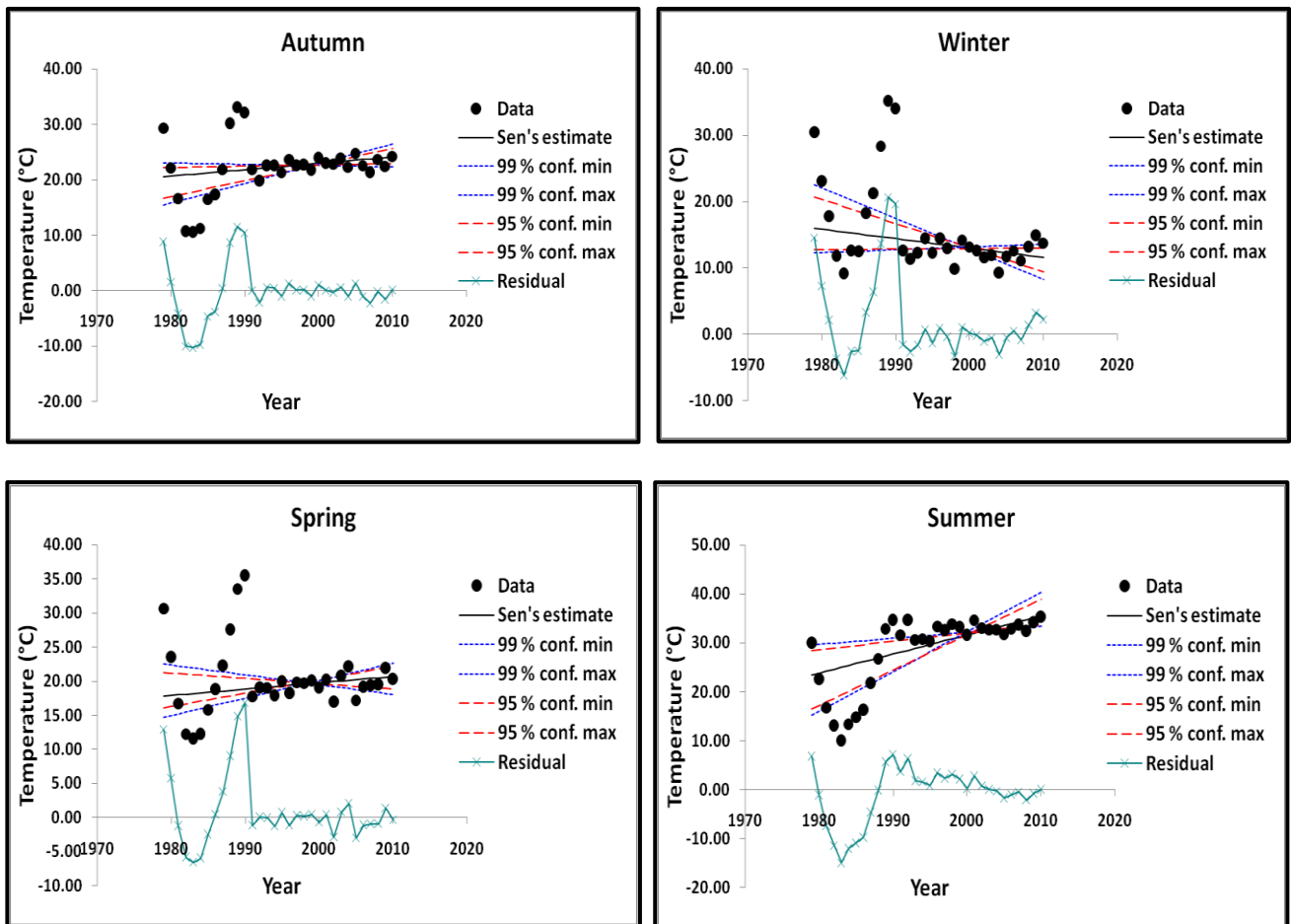


Figure III.62. Seasonal time series and significant trend statistics of temperature at Beni Bahdel station.

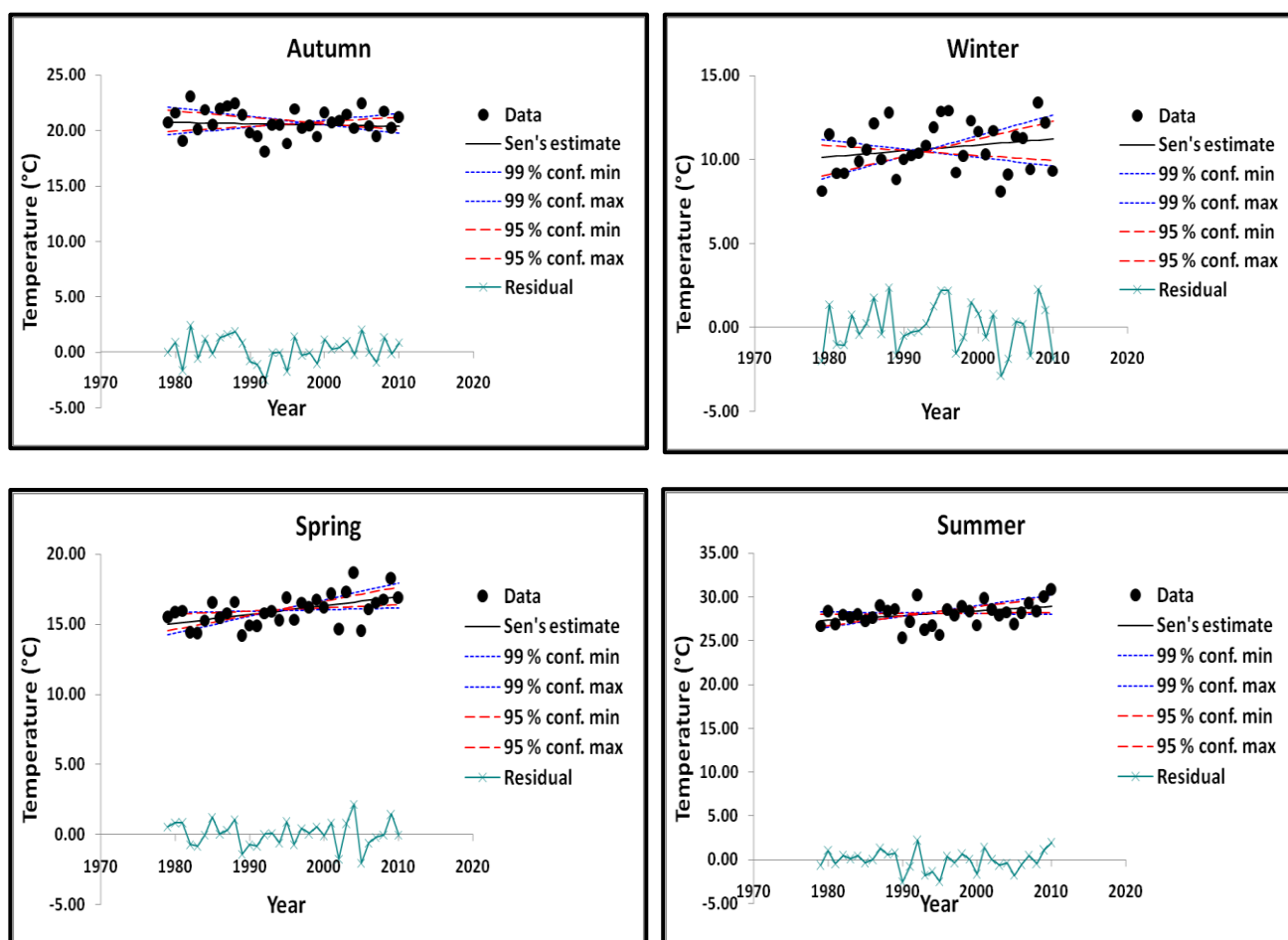


Figure III.63. Seasonal time series and significant trend statistics of temperature at Zenata station.

The occurrence toward showing a positive trend of rainfall in autumn can be explained by the positive anomalies in the rainfall amount that was experienced in areas of North Africa (Düneloh and Jacobeit, 2003; Philandras et al., 2011; Donat et al., 2014; Trambly et al., 2012) which is related to the influence of a negative trend of the North Atlantic oscillation (NAO) (Rimbu et al., 2001), the cyclones entering the basin from the North Atlantic are, together with regional cyclogenesis, one of the main sources of winter rainfall (Ulbrich et al., 1999; Rogers, 1997), and increased the occurrence of catastrophic torrential rains tend to occur in the rainy period (October–March) along coastlines with heavy orography, of the last few decades and especially becoming stronger during the 1980s and 1990s (Düneloh and Jacobeit, 2003). This negative phase is related to storm tracks represented in the pressure associated with the lower Azores height compared to the normal value and, at the same time, the Icelandic Low is formed. Contributing to the creation of a depression traffic mode corresponds to drawing further south and, thus, affects the Mediterranean regions of the south shore, which gets wetter (Nouaceur and Mursrescu, 2016a). This is described by an increase in the amount of rainfall. The NAO index is found to be stronger, which affects the Southwestern Mediterranean region than the El Nino Southern Oscillation ENSO index that was found to be more significant toward the eastern parts of the Mediterranean. This is to be expected considering the relative proximity of the areas in which

these two modes of variability act (Donat et al., 2014). The increase of rainfall is corresponding with temperature extremes, which are found to be strongly connected to the NAO index, where the negative period of this index is associated with higher temperature extremes (Donat et al., 2014, Báez et al., 2019), and that, in general, affect West Africa in the Mediterranean region. While the study of (Pozo Vazquez et al 2001) found influence of NAO on the Mediterranean temperature was weak, especially in the cold season was affected by extra tropical atmospheric circulation patterns with poor correlation than for rainfall, whereas showed a negative correlation between temperatures and the WeMOI index (Western Mediterranean Oscillation) which is a measure of pressure variation in the western part of the Mediterranean basin reflecting the movement of tropical (Azores anticyclone) and temperate (Central European anticyclone) air, that was confirmed with study of (Zeroual et al., 2017) which found negative correlation indicates that the positive phase of WeMOI corresponds with relatively high temperatures, and this what has monitored in study time series, where were observed an increase in temperature after the breakpoints in 1996 and 2008 due to increase in temperature in the summer season which caused by blocking conditions, subsidence, stability, a warm lower troposphere and positive Mediterranean SSTs (Xoplaki et al., 2003; Lionello et al., 2004; Luterbacher et al., 2004), and the predominance of warm tropical air associated with the Azores anticyclone (Martin-Vide and Lopez-Bustins, 2006). This increase of temperature was confirmed with previous studies (Fontaine et al., 2013, Donat et al., 2014; Baahmed et al., 2015).

The heavy floods of the Tafna catchment located in the western part of Algeria are generally occurring in autumn and spring. This is due to the north-westerly rainy winds loaded with moisture from the Mediterranean. Since the 1980s, the NAO index shows an opposite sign indicating that the negative phase of this index is associated with the increase in the number of rainy days (the probability for wet months is around 42-52% for a negative NAO) (Muñoz-Díaz, D.; Rodrigo, 2003), which can be understood as the result of warming over the Northern Atlantic Ocean, which draws rains, especially in the wet season in the region (October–March) (Philandras et al., 2011). The significantly negative correlations between NAO index and rain days appear only within the Western Mediterranean. This is in line with the study of Reference (Ketrouci et al., 2012) that reported most of the seasonal floods recorded in Upstream Sebdoou sub basin were during the autumn and spring seasons with the largest recording of these floods in September by (22%). Records from the Isser sub basin reveal that more than 55% of its floods in autumn and spring are concentrated in the two months, i.e., September and March, respectively, the results confirmed with our study, there was an observed increase of runoff in autumn with Sidi Aissa station following an increased runoff in September. Topographic features consisting of steep slopes and a discontinuous vegetal cover create an environment conducive to high floods by intense rain in autumn for flushing the sediment accumulated on the exposed soils after the dry summer season (Megnounif et al., 2007). The decreases in runoff were observed in Zahra station with a downward trend of runoff at different time scale (annual, monthly, seasonal) detected by the Mann-Kendall test and Sen's method which was also detected with the Pettitt test after breakpoint 2007. The decline in runoff was observed in several studies was applied in our regions such as the study of (Baahmed et al., 2015; Boulariah et al., 2017; Hallouz et al., 2019; Charifi Bellabas et al., 2020; Khedimallah et al., 2020), and (Zettam et al., 2017) which

showed the decrease in a runoff with a rate of 18 % of the basin surface, could be attributed to increase in the temperature, which were observed rising in temperature in study time series with decrease of runoff, also was found in the study of (Baahmed et al., 2015). While other study of (Laborde et al. 2010) in northern Algeria, was found a decrease in 15% in rainfall resulted in 40% reduction in runoff, while the study of (Khedimallah et al.,2020) in northwestern of Algeria, where the change a 10% in rainfall ensues in around 16–25% variation in runoff, and a considerable reduction in the quantity of water arriving at the outlet of the Tafna between 2003 and 2013 may affect the irrigated agricultural zone which mostly depends on the water of the basin (Zettam et al., 2017).

The previous studies on rainfall variability in the northwestern region of Algeria reported the drought in the forties of the last century and revealed a decrease in spring rain as a potential reason (Belarbi et al., 2016; Matari and Douguedroit, 1995). 1944 is characterized as a wet year and the two wettest decades follow in the 1950s and 1960s (Meddi et al., 2010). Drought decade in the 1970s was detected by (Belarbi et al., 2016, Meddi et al., 2010, Ghenim et al., 2010) in the Tafna basin. This decreasing trend is also evident in the Mediterranean region of northern Morocco (Meddi et al.,2010, Knippertz et al., 2003) and can be explained by a change in atmospheric circulation (Meddi et al.,2010; Wang et al.,2009). The situation is changing with having the wet year 1975, followed by a dry year in 1976 (Ghenim et al., 2010), and then the occurrence of the two driest decades 1980's and 1990s (Belarbi et al., 2016, Meddi et al., 2010, Bouragba, 2006). Especially in the 1980s, the dry level is due to a decrease in winter rainfall (Belarbi et al., 2016, Matari and Douguedroit, 1995) and back the fluctuation again to the wet years after the break date at 2007 which is driven by an increase of rainfall trend in autumn generating runoff leading to the heavy floods which can be qualified as moderate to high compared with the results found in the major rivers of Europe and Africa (Ketrouci et al., 2012). This is confirmed by our study results with the Mann-Kendall test and Sen's method that indicated a significant increasing trend for rainfall in September and October (representing autumn season). In contrast, Meurbah station, located at a high altitude (1100 m), showed a significant increasing trend of monthly rainfall in August, September, and October and featured an upward trend in the total mean of rainfall, Flood events are accompanied by erosion and suspended loads leading to sedimentation in riverbeds and siltation in reservoirs and in turn causing serious problems by affecting the manageable storage as well as the service life of dams. Thus, we should consider re-thinking of flood management structures, strengthening options to adapt to drought periods and water conservation practices in the basin. In order to provide sound information for designing and operating these structures, monitoring networks need to be improved.

The Mann-Kendall test did not show any significant trend for the Djebel Chouachi station in the time series of annual, monthly, and seasonal rainfall data and these results do not interpret any specific regional behavior.

In general, the majority of the change point detection tests showed that the Djebel Chouachi station has a significant change while the trend test showed no statistical significant trend. This is likely due to the low location of the station (110 m), where the results of the

study of (Bakreti et al.,2013) showed a relationship between the altitude and the rainfall amount. It was explained that the spatial rainfall was affected by the altitude gradient, where the lower stations have a lower amount of rainfall in the Tafna basin. Thus, it does not show an increase or decrease in the region.

III.12. Conclusion

The presented study is based on Hydro-climatic data collected from five sub basins of the Tafna basin and covers for rainfall the time period between 1979/1980 and 2011/2012, and a runoff between 1985/1986 and 2010/2011, temperature between 1979/1980 and 2010/2011, to analyze the characteristics on different time steps: annual, seasonal and monthly, starting with preliminary analysis (We include in this section the time step daily for the hydro-climatic variables, in addition to the evapotranspiration analyse), change points detection tests, trend analysis.

The Lee and Heghinian test detected two significant break dates for an annual time scale in rainfall, i.e., in 1980 for Sebdu, and Hennaya stations and the rest of the stations in 2007. For the single station Djbel Chouachi, a break date was revealed in 1999 with Pettitt and Buishand tests, whereas the trend test showed no significant trend at the same station, which can be explained by the multi breakpoint at the rainfall time series not indicating any increase or decrease of a rainfall trend. According to the Hubert test, the break date for Djebel Chouachi, Ouled Mimoun, and Sidi Bounakhla station was in 2007. The same year of 2007 was detected in runoff time series at Zahra station showing downward, was confirmed with Mann-Kendall test and Sen's method on monthly and seasonal time steps, this decrease in runoff is likely to be due to an increase in temperature, where the temperature quietly raised after breakpoint of 2008. It was likely that the break point in 1999 appeared only in the Djebel Chouachi station due to the unsuitable quality of data, where the station location in an isolated area made the observation of the data and reliability of the measurement difficult. This caused difficulty in providing an explanation for any specific behavior. While the appearance of the break point in 2007 at nearly all stations indicated a difference of the data distribution in rainfall time series (before and after the break point date) where the rainfall trend seems to be rising at the end of 2000s because of the increase of rainfall in the autumn season, which has been confirmed with the trend analysis, similar to the increase in runoff time series which was observed at Sidi Aissa station in autumn related to the increase of runoff in October. These are similar results to the study of Nouaceur and Mursrescu (2016a), which showed that the regional analysis of rainfall indicate the last years of 2000s, which are distinguished by rainy years (Nouaceur, 2011; Nouaceur and Murarescu, 2016b) recorded with a percentage of 55.72% from 2007–2013 in Algeria, while the rainy years recorded with a percentage of 85.71% from 2008 to 2010 in Morocco. This hypothesis was supported by the teleconnections with positive signs between the North Atlantic Oscillation (NAO), as it is the climate model dominant in the North Atlantic region and EL Nino Southern Oscillation (ENSO) with a low impact of the ENSO index in this region (Hasanean, 2004; Nouaceur et al.,2017). The monthly time series featured irregular results regarding the break point in the time series. The temperature has been increasing worldwide with a strong correlation of the Western Mediterranean Oscillation (WeMOI) climate index in the Mediterranean basin

(Northwestern of Algeria) that characterizes atmospheric circulation and the predominance of warm tropical air associated with the Azores anticyclone (Zeroual et al., 2017). The study of (Zamrane et al. 2016) has found a relationship between the runoff with the NAO climate index in Morocco, and suggest further research to explore the relationships between hydrological variability and the NAO signal, in order to check if there are clear boundaries between the influences of the Atlantic, the Mediterranean, and the Sahara.

These appear in terms of incompatibility of the results for each month with homogeneity tests or results of one test with different months. There are exceptional cases of some stations indicating the heterogeneity of the dataset. Rainfall analysis with the month of summer (June, July, and August) have not affirmed the exception or the rejection results of the hypothesis for both the Buishand and Lee and Heghinian test, which is plausible due to the similar approach of the two tests and due to the minimal amount of rainfall close to zero in this period (extreme values). Hence, it can be concluded that there is no distribution of the rainfall time series for lack of the values, which express the variability and fit the assumption of the tests.

The correlation demonstrate the rainfall-runoff relationship, and it should not be considered as final conclusion, in practically at daily scales. Thus, the intervention of rainfall-runoff modeling could improve the quality of the relationship that are used in this study.

The significant positive values of rainfall were identified by trend analysis after the break year in time series, and those were evidenced by an increasing rainfall tendency in the wet period. In the next section, we will evaluate temporal characteristics of meteorological and hydrological drought, as parallel analyses for detecting the wet/dry periods with the above results of homogeneity and trend analyses.

CHAPTER FOUR

**COMPARISON OF DIFFERENT INDICES OF
METEOROLOGICAL DROUGHT AND
HYDROLOGICAL DROUGHT**

IV. 1. Introduction

Drought is an inevitable and recurring feature of the global water cycle (Farahmand and Aghakouchak, 2019), and it is expected to affect as many as one-third of the world's population (Swetalina and Thomas, 2016), and a large proportion of the agricultural sector, especially in arid and semi-arid regions in Mediterranean (Kumar, 1998; Tigkas and Tsakiris, 2014), which is already suffering from stress and water availability (Ma et al., 2015) due to irregularity of rainfall in time and space (Shahabfar and Eitzinger, 2013) and expected to be worsen in future due to climate change (IPCC, 2014).

Drought is one of the most damaging natural hazards, which characterizes a broad range of climatic situations related to either low rainfall consequent to the high temperature and the evapotranspiration which all it is considered as significant factors of controlling the formation and persistence of the condition of drought (meteorological drought), besides the low soil moisture (agricultural drought), low levels of water in streams and lakes (hydrological drought), or a shortage of water for society at large (socio-economic drought) (Vogt and Somma, 2000; Lloyd-Hughes and Saunders, 2002; Soo Jun et al., 2011; Marengo et al., 2011; Bazrafshan and Khalili, 2013; IPCC, 2014; Swetalina and Thomas, 2016).

Drought is a frequent climate that determines its precision and the difficulty of studying the various dimensions of it, It can be described by three factors: severity, duration, and frequency of occurrence (Wilhite and Donald, 2000; Tsakiris et al., 2007; Soleimani Sardou and Bahremand, 2014). It has been observed that droughts have increased in magnitude and frequency, over the last few decades around the world. Droughts affect almost all the components of the hydrological cycle beginning with the precipitation factor that experienced a long period of the deficit, which has negative influence in hydrological drought of the streamflow and resulted in deficit in storage for surface water and groundwater (Beran and Rodier, 1985; Tsakiris et al., 2013; Sahnoune et al., 2013). Several studies have used drought indices as drought monitoring tools at different parts of the world to describe the droughts quantitatively and make the decision on estimations of the characteristics of a drought period and their consequences upon the hydrological cycle (Dogan et al., 2012; Tsakiris et al., 2013; Asefjah et al., 2014; Shah et al., 2015; Al-Timimi and Osamah, 2016; Afzali et al., 2016; Bagheri, 2016). There are indicators disaggregated by the type of drought (Wilhite and Glantz, 1985; Guttman, 1998), and classified into four main types: (a) meteorological drought, related to precipitation deficit which cause decreases in water supplies of a region over a period of time. (b) hydrological drought, defined as a deficit in surface water storage or groundwater causing reductions in water uses and effect to water resources management system. (c) agricultural drought, deficit in soil moisture and the consequent to crop failure at a particular period; and has no reference to stream flow, Meteorological drought, hydrological drought and agricultural drought are also considered as environmental droughts whereas, (d) socio-economic drought is deficit of water supply for socio-economic purpose, and it can be considered as water resources droughts (Wilhite and Glantz, 1985; WMO, 2006; Passioura, 2007; Azarakhshi et al., 2011). However, several of the drought indices have limitations in the application in order to monitor the drought condition due to climate conditions as well as the time step, and thus must addressing more than one index (Morid et

al., 2006; Jain et al., 2015). There is no single definition for drought, its onset and termination are difficult to determine. However, identify various indicators of drought, and tracking these indicators provides the assimilation for thousands of data on rainfall, streamflow, and other water supply indicators, more useful than raw data for decision making and crucial means of monitoring drought. Drought indices are usually calculated, either by applying manually the corresponding equations, or by using tools, that provide a comprehensive assessment and give a better perspective for outputs (Tigkas et al., 2015).

Algeria is one of the countries which has experienced several drought years, with high variability in annual rainfall (Habibi et al., 2018) with a reduction of 10% since the end of the 1970s (Sahnoune, 2013) this may affect the water mobilized in dams and groundwater. Particularly affected is the western north region (Meddi and Hubert, 2003; Meddi.M and Meddi. H, 2009), where experienced deficits in rainfall from 12% to 20% (Medjerab and Henia, 2005). This region suffered by drought years (Meddi et al., 2013) with the return of rising in rainfall between 2001 and 2007 (Khoualdia et al., 2014) and it is expected that the severity and frequency of droughts will change in the future (Mccarthy, 2001; Halwatura et al., 2017) and probability of occurrence of a severe drought in 2041 (Lazri et al., 2015).

Numerous studies have been conducted to analyse and identify drought condition from different parts of the world as for example (Pathak et al., 2016; Morid et al., 2006; Zarei et al., 2017; Akbari et al., 2015; Kanellou et al., 2008; Lorenzo-Lacruz and Morán -Tejeda, 2016; Boudad et al., 2018). Similar researches in northern of Algeria studied the drought behavior in the time series and the results showed that the severe/extreme drought increases considerably rising from the probability of 0.2650 in 2005 to a stable probability of 0.5756 in 2041(Lazri et al., 2015). While in the northeast region of the country were studied for the variability and trends in annual rainfall data for the period between 1970 and 2011 and it was found that the important fluctuation where experienced a long dry period with a moderate severity followed by a long wet period and a significant increasing rainfall trend (Khezazna et al., 2017). The studies in northwest of Algeria identified that the region had suffered from a severe drought especially after 1970's and multi-year drought, and this information may provide scientific support for managing drought situations (Meddi et al., 2013; Djellouli et al., 2016; Habibi et al., 2018).

The main objective of this study is a comparative analysis of four meteorological drought indices: (i) the Standardized Precipitation Index (SPI), (ii) the Percent of Normal Index (PN), (iii) the Declie Index (DI), and (iv) Rainfall Anomaly Index (RAI), and one of hydrological drought indices: Streamflow drought index (SDI). No index is ideal and/or universally suitable. The choice of indices for drought monitoring in a specific area should eventually be based on how commonly used these indices to determine the drought and the quantity of data availability (Azarakhshi et al., 2011; Morid et al., 2006). A common feature of the selected indices is that they all are calculated using only rainfall data at different time scales and allows the analysis of different drought categories. in order to assess the performance of these indices in the Tafna Basin the northwest of Algeria, where the assessment of the drought indices in this region represents the amount of rainfall and runoff, which reflects water resources availability and carrying capacity of the ecosystems and its relation to the economic

activities, human lives, and the environment (Tabari et al., 2012; Bayissa et al., 2015). Furthermore, SPI found as a highly valuable estimator of drought severity (Keyantash and Dracup, 2002) and was proven superior to Palmer Drought Severity Index (PDSI) (Guttman, 1998; Paulo and Pereira, 2006), and other rainfall based indices (Van Rooy, 1965; Mckee et al., 1993; Morid et al., 2006; Dogan et al., 2012; Hänsel et al., 2016). While the DI index defined as able to quantify both dry and wet cycles (Morid et al., 2006) and may assessing droughts when used with many timesteps in arid/semi-arid regions. The analysis of the study of (Barua et al., 2011) showed that SPI had the same raw score for the transparency criterion and were less transparent than PN or DI, with PN having the highest transparency score and was also found as the most irrelevant DI to other indices (Dogan et al., 2012). The RAI offers a higher degree of transparency and tractability and demands a lower degree of sophistication than the SPI with regard to the evaluation criteria for drought indices as proposed by (Keyantash and Dracup, 2002). In principle, the RAI may be calculated on the same timescales as the SPI and is similarly robust. and the streamflow Drought Index (SDI) (Nalbantis and Taskris, 2008), which is very simple in calculation and data demanding, powerful in predicting drought onset and duration using cumulative streamflow volumes (Arabzadeh et al., 2015). SDI is analogous to the standardized precipitation index (SPI) (WMO 2009; Rimkus et al., 2013).

IV.2. Methodology

The methodology applied in this study is based on four meteorological indices, and one hydrological index selected for drought monitoring in the Tafna Basin in order to:

(1) Classify the frequency of the drought severity categories (or humidity) using the drought thresholds method that based on the values of the drought indices for three-time scales (Annual, Seasonal, and Monthly).

(2) Determine the correlations between SPI and other indices (RAI, DI, PN), using the correlation coefficients of Pearson and Spearman. The better identification and monitoring of the drought is to compare the correlation between several drought indices and how they respond to the drought categories during the time series of the study for different time steps. Therefore, to evaluate the dependability in determining the correlation between them, the Pearson coefficient and the Spearman's rho correlation will be used, which are well known and widely used internationally. SPI is considered for analysing its correlation with other three indices because SPI as the index that has been often used as the measure in the drought analysis and it has statistical consistency advantages through different time scales of rainfall (Guttman, 1998; Hayes et al., 1999), and it is the most applied index to analyze meteorological drought in the northwest region of Algeria (Djellouli et al., 2016; Djellouli et al., 2018; Adjim and Djedid, 2018). This proves the applicability of the comparison of SPI with the rest of the indices that have not yet received much attention in the region as a primary step in the analysis.

(3) Investigate the relationship between the results of each meteorological drought index from all stations at a different time scale using the correlation coefficients of Pearson and Sp-

earman to assess the sensitivity and robustness for each index.

(4) Indicating the trend directions of the drought indices selected in the time series, using Mann-Kendall test, one of the most widely applied test (Jain and Kumar, 2015; Kumar et al., 2019; Khezazna et al., 2017; Bari Abarghouei et al., 2011; Boudad et al., 2018; Deo, 2011; Hänsel et al., 2015; Rahman et al., 2016) to detect whether the trend is upward or downward of the data during a time period while considering the level of statistical significance (Kisi and Ay, 2014; Da Silva et al., 2015; Gedefaw et al., 2018; Mrad et al., 2018).

(5) Investigate the relationship between the SDI for different study stations, and relationship between SDI and meteorological drought index at a different time scale using the correlation coefficients of Pearson and Spearman.

IV.2.1. Meteorological drought index

IV.2.1.1. Standardized Precipitation Index (SPI)

SPI is a widely recognized tool for characterizing and monitoring meteorological droughts (Mckee et al., 1993). Positive SPI values indicate above mean precipitation and negative values indicate below mean precipitation. It is a simple index which allows equally checking of wet periods and the dry periods and is based on the long-term precipitation record (longer than 30 years) (Edwards et al., 1997; Boudad et al., 2018). The available long-term rainfall data is fitted to a probability distribution (e.g. gamma distribution) to calculate SPI, which is then transformed to a normal distribution so that the mean SPI period is zero (Mckee et al., 1993; Jain et al., 2015). The equations to calculate SPI are as follows, the rainfall data are calculated using the gamma probability density function, which is defined as the equation IV.1:

$$g(x) = \frac{1}{\beta^\alpha \Gamma(\alpha)} x^{\alpha-1} e^{-x/\beta} \text{ for } x > 0 \quad \text{Eq.IV.1}$$

Where α is a shape parameter, β is a scale parameter and x is the rainfall amount as the equation IV.2:

$$\alpha = \frac{1}{4A} \left(1 + \sqrt{1 + \frac{4A}{3}} \right) \text{ and } \beta = \frac{\bar{x}}{\alpha} \quad \text{Eq.IV.2}$$

Where \bar{x} represents the sample statistic, A the rainfall average as the equation IV.3:

$$A = \ln(\bar{x}) - \frac{\sum \ln(x)}{n} \quad \text{Eq.IV.3}$$

And n is number of rainfall observations. The obtained parameters are then used to find the cumulative probability function as the equation IV.4:

$$G(x) = \int_0^x g(x) dx = \frac{1}{\beta^\alpha \Gamma(\alpha)} \int_0^x x^{\alpha-1} e^{-x/\beta} dx \quad \text{Eq.IV.4}$$

The rainfall dataset may contain zero values since the gamma distribution is undefined for zero rainfall, then the cumulative, $H(x)$, was calculated as the equation IV.5:

$$H(x) = q + (1 - q)G(x) \quad \text{Eq.IV.5}$$

q: Probability of zero rainfall.

The cumulative probability is then transformed to the standardized normal distribution random variable Z with mean zero and variance of one, which is the value of the SPI.

IV.2.1.2. Percent of Normal Index (PN)

PN is a simple index to measure the rainfall deficit for a location. The value 'normal' of the index may be calculated for a month, a season or a year, and is considered to be 100%. Analyses using the percent of normal are very effective when applied for a single region or a single season. It is calculated by dividing actual precipitation (P_i) by normal precipitation and multiplying by 100% (Dogan et al., 2012; Morid et al., 2006; Shahabfar and Eitzinger, 2013).

IV.2.1.3. Decile index (DI)

The decile index was developed by (Gibbs and Maher, 1967). This is based on ranking the monthly rainfall from the long-term series to construct a cumulative frequency distribution. This distribution is divided into 6 decile parts. The first decile value is the lowest than 10%, while the second decile is between the lowest 10% and 20%, the two above deciles are determined as considerably below normal, and the deciles 3 to 4 (20% to 40%) as below-normal rainfall, while the deciles 5 to 6 (40% to 60%) as near-normal rainfall, and the deciles 7 and 8 (60% to 80%) as above-normal rainfall and the deciles 9 and 10 (80% to 100%) indicate above-normal rainfall (Asefjah et al., 2014).

IV.2.1.4. Rainfall Anomaly Index (RAI)

RAI was developed by (Van Rooy, 1965), it is based on ranking the rainfall value to calculate the positive and negative magnitudes of the indices which are computed by using the mean of ten extremes. This index can be analysed on the frequency and intensity of the dry and rainy period (Al-Timimi and Osamah, 2016). The RAI offers a higher degree of transparency and a lower degree of complexity than the SPI with regard to the evaluation criteria for drought indices (Keyantash and Dracup, 2002; Hänsel et al., 2016). The function is defined as the equations IV.6 and IV.7:

$$RAI = 3 \frac{P - \bar{P}}{\bar{M} - \bar{P}} \text{ if } P > \bar{P} \quad \text{Eq.IV.6}$$

$$RAI = -3 \frac{P - \bar{P}}{\bar{m} - \bar{P}} \text{ if } P < \bar{P} \quad \text{Eq.IV.7}$$

\bar{M} : Mean of the ten highest rainfall records for the time series of the study,

\bar{m} : Mean of the ten lowest rainfall records for the time series of the study,

\bar{P} : Mean rainfall of the time series, and P the rainfall for the specific year.

The classification based on the above meteorological four drought indices are given in (tab.IV.1).

Table IV.1. Classification of meteorological drought indices range (Van Rooy, 1965; Mckee et al.,1993; Morid et al., 2006; Dogan et al., 2012; Hänsel et al., 2016).

State	Class description	SPI	PN	DI	RAI
1	Extremely Wet	≥ 2.0	–	1	≥ 3.00
2	Very Wet	[1.50;1.99]	–	2	[2.00;2.99]
3	Moderately Wet	[1.00;1.49]	≥ 110	3	[1.00;1.99]
4	Normal	[-0.99;0.99]]80;110[[4;7]	[-0.99;0.99]
5	Moderately Dry	[-1.49;-1.00]]55;80[8	[-1.99;-1.00]
6	Severely Dry	[-1.99;-1.50]]40;55[9	[-2.99;-2.00]
7	Extremely Dry	≤ -2.00	≤ 40	10	≤ -3.00

IV.2.2. Hydrological drought index

SDI (Streamflow Drought Index) is generally used for the analysis of hydrological drought (Bao et al., 2011), and has been developed by (Nalbantis and Tsakiris, 2009), if a time series of monthly streamflow volumes $Q_{i,j}$ is available, in which i denotes the hydrological year and j the month within that hydrological year ($j = 1$ for September et $j = 12$ for August), $V_{i,k}$ is described in the equation IV.8 as follow:

$$V_{i,k} = \sum_{j=1}^{3k} Q_{i,j} \quad i = 1,2, \dots \quad j = 1,2, \dots, 12 \quad k = 1,2,3,4 \quad \text{Eq.IV.8}$$

Where:

$V_{i,k}$: The monthly streamflow volumes for the i -th hydrological year and the k -th reference period, $k = 1$ for September-November, $k = 2$ for September-February, $k = 3$ for September-Mai, et $k = 4$ for September-August. Based on the cumulative streamflow volumes $V_{i,k}$, SDI is defined for each k reference period of the i -th hydrological year as equation IV.9 follows:

$$SDI_{i,k} = \frac{V_{i,k} - \overline{V}_k}{S_k} \quad i=1, 2, \dots, \quad k=1,2,3,4 \quad \text{Eq.IV.9}$$

Where, \overline{V}_k and S_k are respectively the mean and standard deviation of SDI for the k reference periods estimated for a long period.

Generally, for small basins, streamflow may follow a log-normal distribution. The distribution is then transformed into normal taking simple and the natural logarithms of streamflow, the SDI index is defined as equations IV.10 and IV.11 follows:

$$SDI_{i,k} = \frac{y_{i,k} - \overline{y}_k}{S_{y,k}} \quad i=1,2, \dots, \quad k=1,2,3,4 \quad \text{Eq.IV.10}$$

$$y_{i,k} = \ln(V_{i,k}) \quad i=1,2,\dots, \quad k=1,2,3,4 \quad \text{Eq.IV.11}$$

Where \bar{y}_k and $S_{y,k}$ are the mean of cumulative streamflow and standard deviation over a long period of time. Five hydrological drought conditions are considered which are denoted by an integer number ranging from 0 (non-drought) to 4 (extreme drought)(Nalbantis, 2008), and defined in (tab.IV.2).

Table IV.2. Definition of states of hydrological drought based on the SDI classes (Nalbantis, 2008).

State	Description	Criterion
1	Non-drought	$SDI \geq 0.0$
2	Mild drought	$-1.0 \leq SDI < 0.0$
3	Moderate drought	$-1.5 \leq SDI < -1.0$
4	Severe drought	$-2.0 \leq SDI < -1.5$
5	Extreme drought	$SDI < -2.0$

IV.3. Results and discussion

IV.3.1. Comparison of meteorological drought categories

At annual scale, figure IV.1 shows that PN detected the highest range of normal droughts categories approximately (30-50%) for Sebdu, and Khemis stations, while the rest of the stations indicated similarity of ranges between moderate droughts, normal and moderate wet categories (15-20%). Extreme droughts categories range was found (100%) on a seasonal time scale for Sebdu station. For the rest of the stations, the percentage of moderately wet categories indicated the highest range approximately (25-40%) compared to other categories. At monthly scale, extreme dry and moderate wet categories were found in similar range (35%).

On an annual scale, RAI detected a range of Normal categories (30%) for Djebel Chouachi, Several droughts approximately (20-30%) for Ouled Mimoun, Sidi Bounakhla, Chouly and Khemis, and Moderate droughts (20%) for the other stations. Extreme, Several droughts and Normal range were found approximately (15-20%) on a seasonal time scale for all stations, in addition to observation of a significant range of Several droughts categories approximately (10-20%) for Djebel Chouachi, Hennaya, and Sidi Bounakhla.

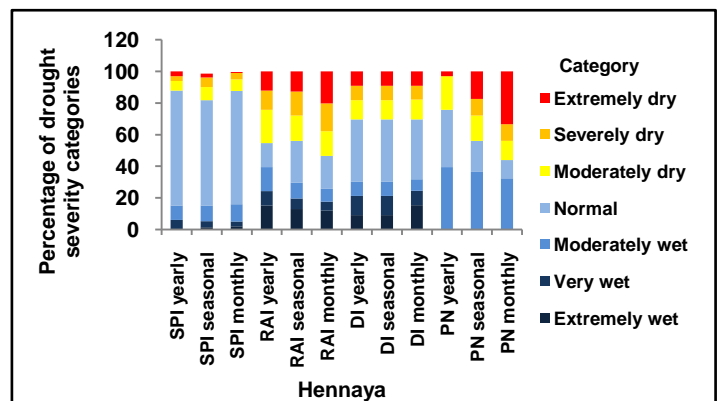
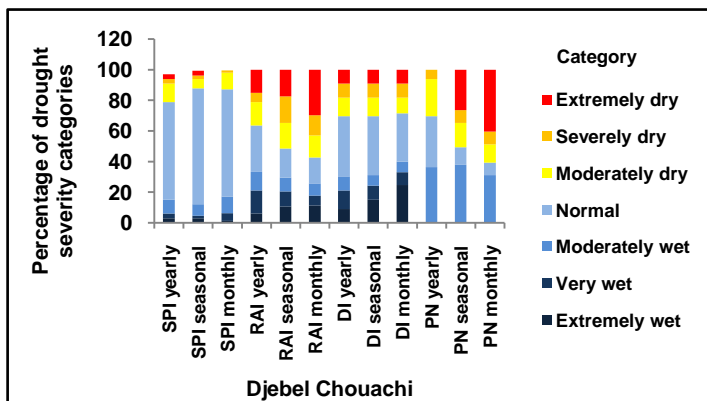
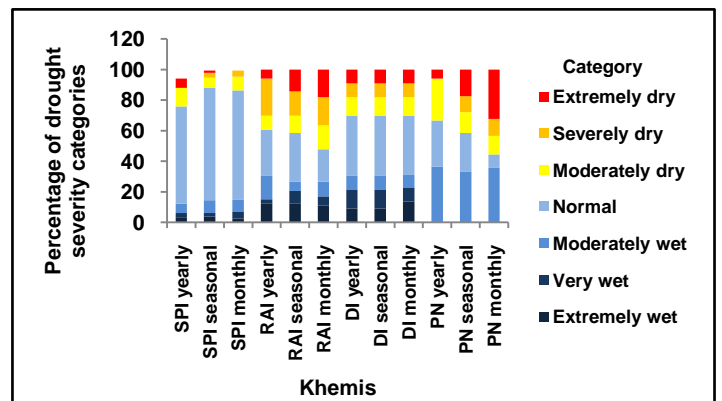
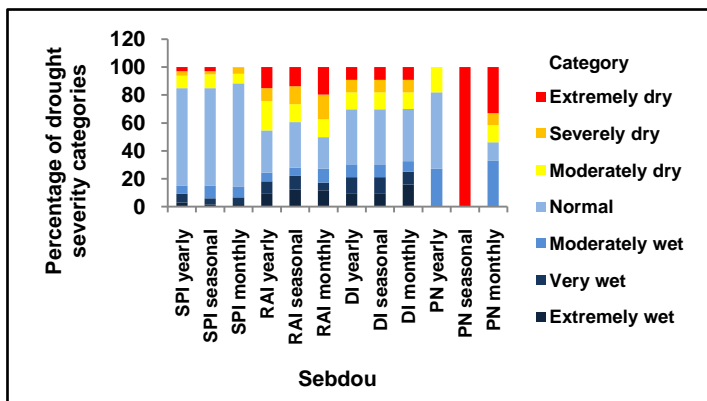
Extreme, several droughts, and Normal categories were found similarity ranges with approximation (15-20%) for all stations, expect Djebel Chouachi which has the highest range of Extreme droughts with (30%) on a monthly scale.

SPI and DI indices detected higher ranges of only Normal categories for all stations and on all timescales, whereas SPI detected approximately range (65-75%). DI indicated

approximately ranges 40%, 40-45%, 30-40% on annual, seasonal, and monthly time scale respectively.

As concluded: SPI and DI have responded in more consistent on all timescales for all stations. SPI has the most similar response to DI (normal categories), although DI underestimated the range of normal categories than SPI did on all timescale, where SPI has a much large rate of ‘normal categories’, while the rest of the categories of drought have less rate in SPI compared to DI. This indicates high sensitivity on the part of DI to rainfall amount, whereas the SPI is the worst in detecting the extreme, severe drought(<5 %).

PN, RAI resulted in values indicating more drought categories than SPI, DI, where they were able to detect gradual categories in droughts that cannot be detected by the SPI and DI. This analysis indicates that the application of RAI and PN allowed leading to a detailed assessment of the drought situation in the study area. Extreme droughts had also been overestimated by PN and RAI on seasonal and monthly scale but underestimated on annual scale.



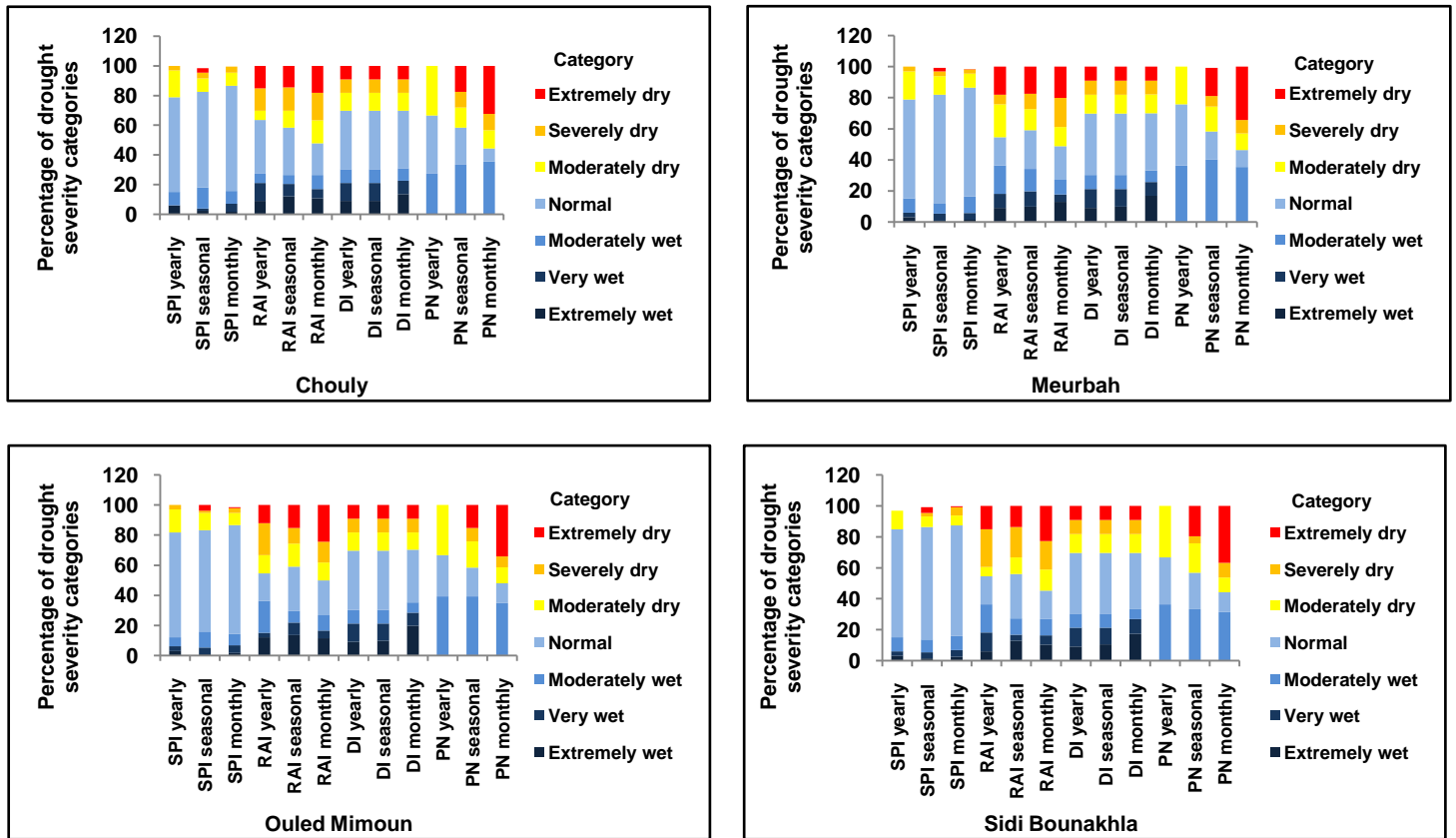


Figure IV.1. Drought categories percentage for SPI, RAI, DI, PN for different time scale (annual, seasonal, and monthly).

IV.3.2. Meteorological indices temporal evolution

The four indices (SPI, RAI, DI, PN) at the annual time scale were compared and displayed in figure IV.2, IV.3, IV.4, IV.5. The variance of two indices SPI and RAI is characterized by the same consistency change in wet and dry periods; it can be seen from the figure V.2 that the SPI time series of the curve is close to that of RAI. The period between 2000-2004 and 2008-2011 shows a recovery from drought. The highest values of the SPI, RAI and, PN are (3, 8, 230 respectively) in 2008 correspond Sidi Bounakhla station for SPI and RAI, and Khemis station for PN which representing the 'wet extremes categories and the lowest values are (-3, -6, 36 respectively) in 1982 correspond Hennaya station which representing the 'dry extremes'. While DI results showed that the highest and the lowest values (10,1 respectively) on the annual scale are the same for some stations (Sidi Bounakhla, Ouled Mimoun, Djebel Chouachi, Hennaya) which representing the 'wet and dry extremes' respectively.

The results of SPI and RAI showed that the estimates of droughts experienced a difference in terms of values; however, they are consistent in duration in terms of the start and end of the drought.

In the early 2000s, all stations showed mostly positive SPI, RAI, PN, and DI values which are often greater than (2, 4, 152, 10 respectively) with the exception years (2004, 2006, and

2007). Negative values are less than (-2, -4, 55, 1 respectively) observed between 1981-1999. The year 1982 was one of the driest years, and 2008 was the wettest year in the study area.

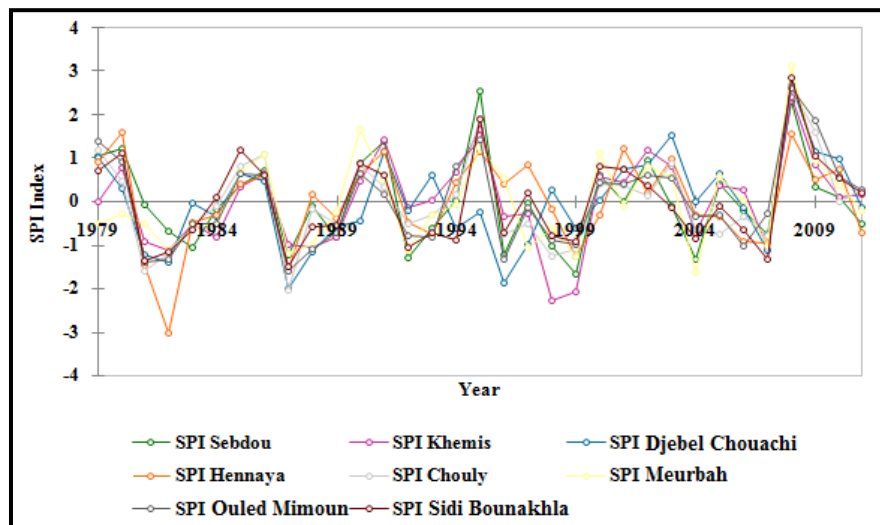


Figure IV.2. SPI index at annual scale for all stations.

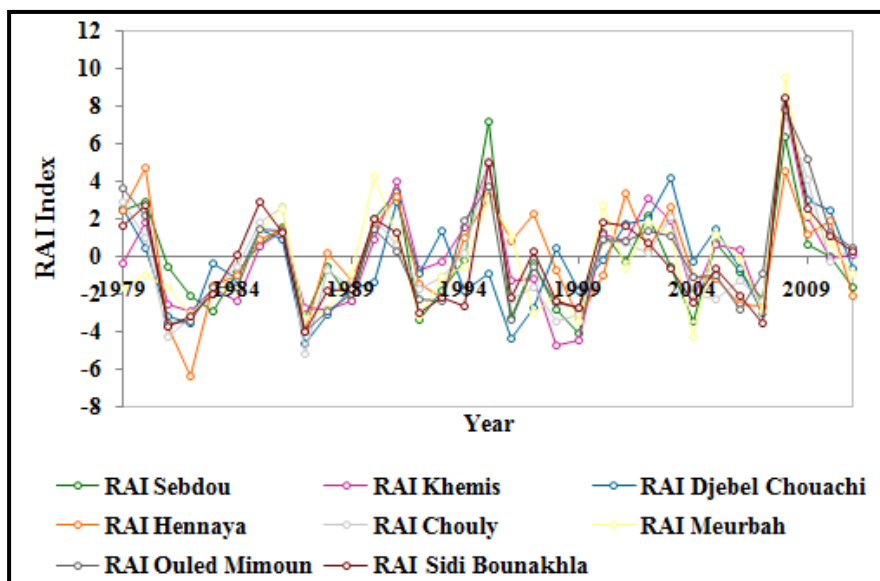


Figure IV.3. RAI index at annual scale for all stations.

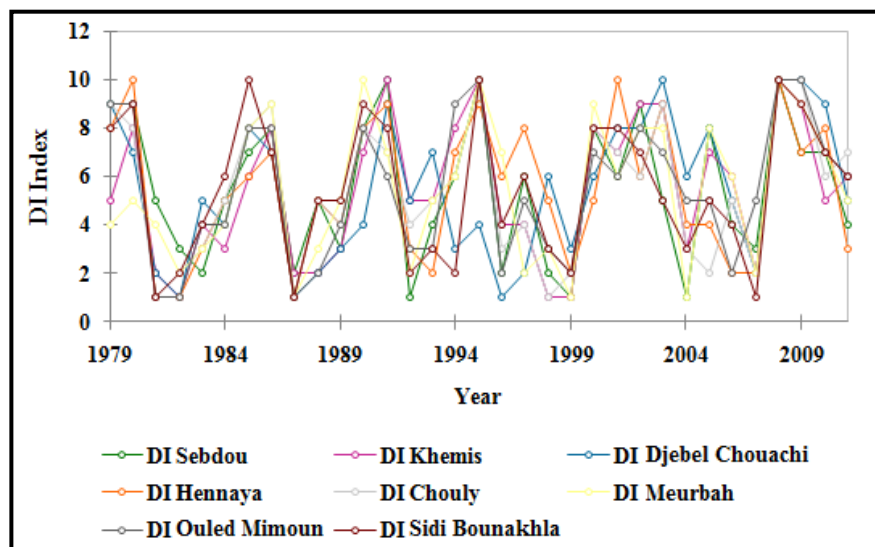


Figure IV.4. DI index at annual scale for all stations.

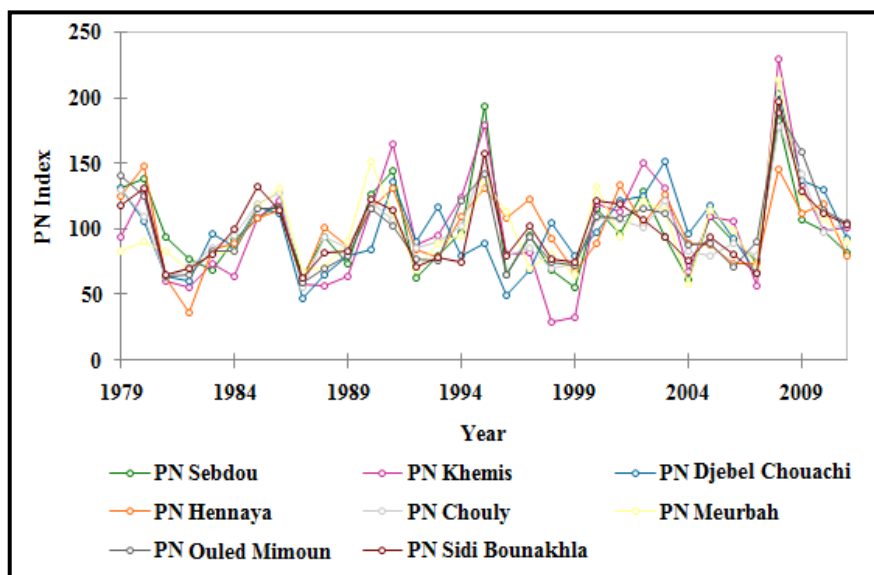


Figure IV.5. PN index at annual scale for all stations.

IV.3.3. Relationship between SPI AND RAI, DI, PN

In table IV.3, the relationship between SPI and the indices (RAI, DI and, PN) were determined with the coefficient of Pearson and Spearman correlation tests on the different time scale (annual, seasonal, monthly). The results showed that the relationship for the SPI versus the RAI, DI and, PN are highly correlated (> 0.6) for all time scale. The relationship has a strong positive correlation on an annual scale (≥ 0.94) and even higher with Spearman correlation tests (≥ 0.99) for all stations.

The highest Pearson correlation (0.99) was observed in several stations on annual scale, and the lowest (0.61) was observed between SPI and PN in Djebel Chouachi on a monthly scale.

The highest Spearman correlation (1.00) was observed between SPI and the indices PN and RAI for all stations on annual scale, and the lowest (0.59) was observed between SPI and PN in Djebel Chouachi on a monthly scale. For both correlation tests, RAI showed that it has the greatest correlation with SPI on all time scale. Overall, it is noted that the correlation of SPI with other indices increases with the long term in the time step and decrease with the short term.

Figure IV.6, IV.7 demonstrate the visualization results of table IV.3, it is showed with Pearson correlation that Khemis station has the lowest correlation between SPI and each of the other indices at annual and seasonal scale except the correlation between SPI and DI on annual scale and between the SPI and RAI on seasonal scale, on another hand, the correlation between SPI and other indices was the lowest at Djebel Chouachi. While the lowest Spearman's correlation between SPI and each one of the indices was indicated at Khemis station at all-time scale except between the indices SPI, PN and DI on the monthly scale and RAI on the annual scale.

The higher correlation coefficient between 0.99 and 1 for the indices and the stations and timescales signifies that these indices are well suited and adapted in the study area. The close similarity in coefficient values in different stations can be due to the indices values, which include zero or a small number for the entire time period.

Table IV.3. The correlation coefficients between SPI and DI, PN, and RAI respectively at different time scale.

Correlation Test	Station	Annual			Monthly			Seasonal		
		DI	PN	RAI	DI	PN	RAI	DI	PN	RAI
Pearson correlation	SPI Vs									
	Sebdou	0.96	0.99	0.99	0.94	0.85	0.94	0.96	0.86	0.96
	Khemis	0.96	0.97	0.98	0.7	0.64	0.72	0.79	0.74	0.83
	Djebel Chouachi	0.99	0.98	0.96	0.68	0.61	0.76	0.9	0.72	0.92
	Hennaya	0.95	0.99	0.99	0.91	0.8	0.92	0.97	0.88	0.97
	Chouly	0.96	0.99	0.99	0.9	0.76	0.92	0.95	0.91	0.97
	Meurbah	0.94	0.99	0.99	0.9	0.84	0.94	0.95	0.93	0.97
	Ouled Mimoun	0.97	0.99	0.99	0.81	0.76	0.88	0.96	0.93	0.97
	Sidi Bounakhla	0.95	0.99	0.99	0.88	0.76	0.89	0.95	0.81	0.96
Spearman's correlation	Sebdou	0.99	1	1	0.96	0.94	0.98	0.99	0.98	0.99
	Khemis	0.99	1	1	0.7	0.66	0.71	0.8	0.78	0.81
	Djebel Chouachi	0.99	1	1	0.64	0.59	0.75	0.96	0.87	0.95
	Hennaya	0.99	1	1	0.93	0.89	0.95	0.99	0.97	0.99
	Chouly	0.99	1	1	0.92	0.89	0.94	0.99	0.99	0.99
	Meurbah	0.99	1	1	0.91	0.89	0.94	0.98	0.99	0.99
	Ouled Mimoun	0.99	1	1	0.81	0.78	0.86	0.99	0.98	0.99
	Sidi Bounakhla	0.99	1	1	0.91	0.84	0.91	0.99	0.95	0.99

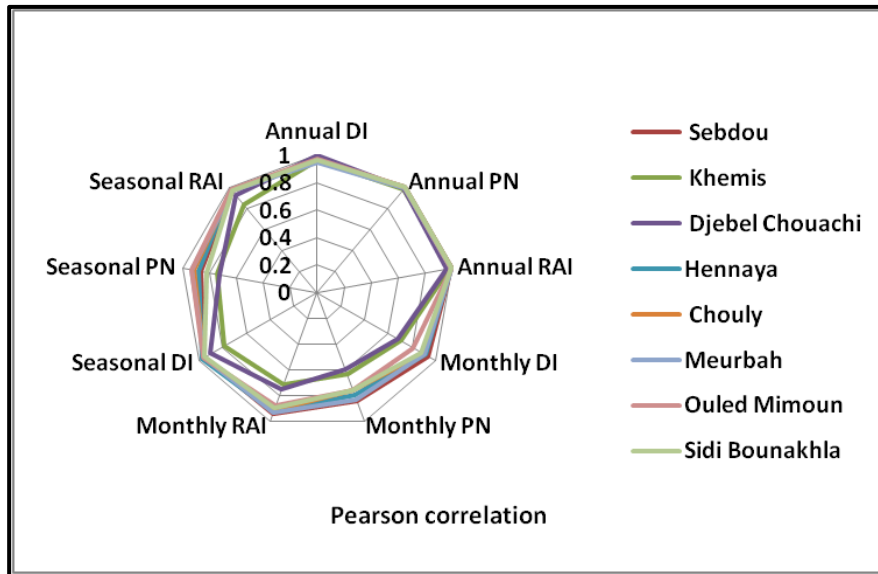


Figure IV.6. The spider chart displays the timescale variations of Pearson correlation between SPI and other indices.

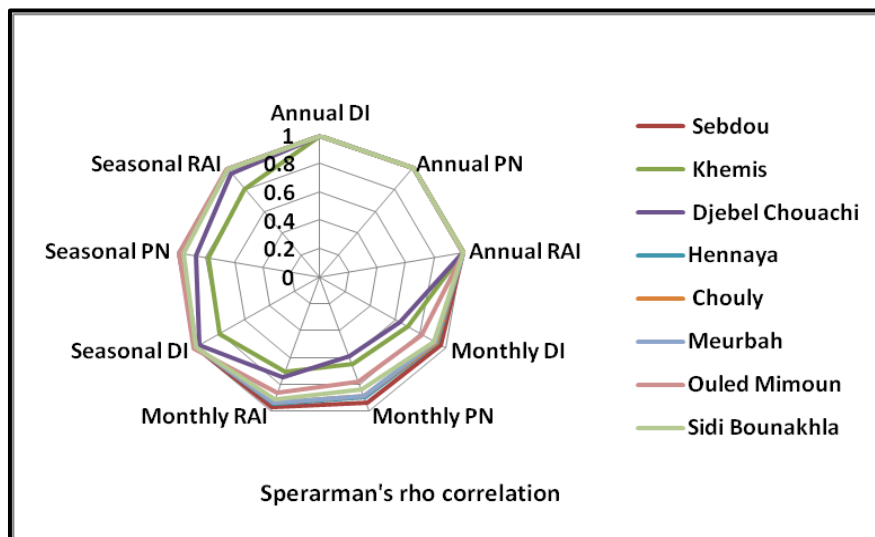


Figure IV.7. The spider chart displays the timescale variations of Spearman's correlation between SPI and other indices.

IV.3.4. Comparative evaluation of meteorological drought indices

The figures IV.8, IV.9, and IV.10 represent the average of SPI, RAI, DI, and PN for annual, seasonal, and monthly time steps compared with average rainfall on each time scale.

On an annual scale, the analysis of the results indicated that extremely dry category was detected in 1982 with RAI, DI and, PN, where had been a significant decrease in annual average rainfall, in addition to 1987 and 1999 that were also shown as extremely dry with RAI, where the period between 1984-1999 experienced a fluctuation in the deficit rainfall time series. On seasonal scale, this category was obvious in the spring of 1982 (fig IV.9), and

in April of 1983 on a monthly scale due to a decrease in rainfall both of them were determined with RAI.

While the severely dry category was determined in 1987, 1999 with SPI and DI. This category on the seasonal scale was detected in the Spring of 1982 with DI and PN, and in the Spring (1987, 1999) with SPI, DI, and PN, where this season of these years showed mostly the deficit in seasonal rainfall. As well as this category was indicated on a monthly scale in March of 1983 and May of 1983 with RAI, and February of 1983 to May of 1983 with PN, whereas April of 1983 with DI, and March and April of the two years of 1987 and 1999 with the DI, and PN.

The moderate dry category was indicated in 1987, 1999, and 2007 with PN, and the same index determined the year 1995 as the moderate wet category. Otherwise, this year was represented under the extreme wet category with RAI, and as very wet with SPI and DI due to the excess of rainfall in this year.

The category of extreme wet was appropriately detected in 2008 with all four indices, where the highest rainfall occurred throughout the study period. The period between 2000-2011 defined a slight raising of average rainfall(except 2004, and 2007), The same category was indicated on a seasonal scale in the Autumn of 2008 with RAI, DI, and PN, it is seen and confirmed also as extremely wet in the months September of 2008 to November of 2008. While SPI defined this season as severely wet as well as the month of October of 2008.

Overall, all indices indicated similar droughts categories when it was the highest and lowest of rainfall on annual time scale. It is noted that RAI was more appropriate compared to other indices in the detection of drought in the long term and short term. When the average rainfall was lower than normal, the RAI index showed an extreme dry situation, especially in 1987, 1999 and the worst dry period was reported in 1982. The deficit and fluctuation of rainfall detected the drought situation, and that showed a positive relationship between the drought indices and average rainfall.

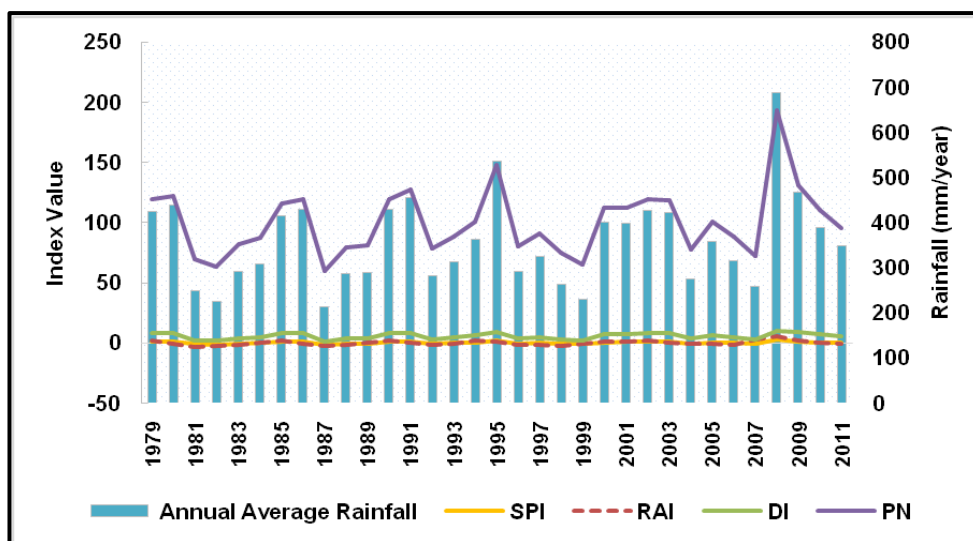


Figure IV.8. Average time series of all indices and Rainfall at annual scale.

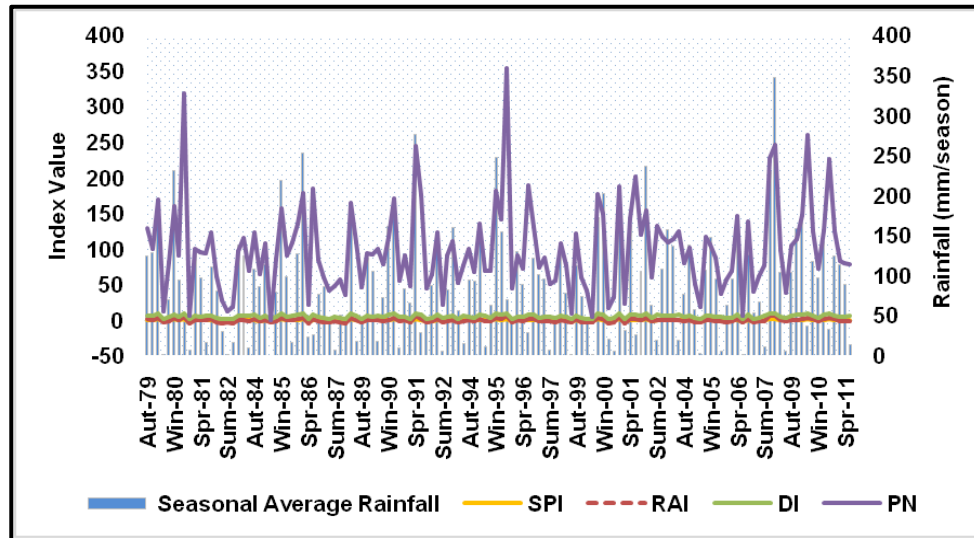


Figure IV.9. Average time series of all indices and rainfall at seasonal.

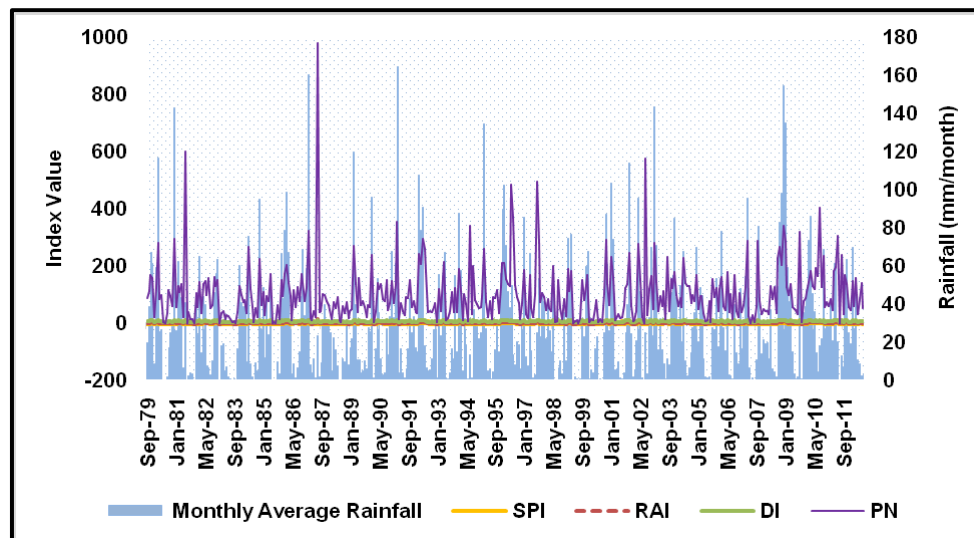


Figure IV.10. Average time series of all indices and rainfall at monthly scale.

Several studies have indicated the same results in line with our research (Adjim and Djedid, 2018; Khezazna et al., 2017; Medejerab and Henia, 2005; Hamlaoui-Moulai et al., 2013; Hammar et al., 2014), as these studies showed that the 1980s experienced a decrease in the rainfall, and considered as a dry sequence, it was observed mostly that drought index is often less than -1 . While the period from 1999 to 2011 of the study was considered as a wet sequence with a drought index range from 0.06 to 0.85, and it was pointed out that 2008 as the mostly wettest in this period that was confirmed with the studies that was mentioned above.

IV.3.5. Correlations between drought indices

In order to assess the sensitivity and robustness of the indices at a different timescale, we adopt the correlation coefficient method for choosing the better relationship between the one drought indexes for different stations (the study stations). For this section, the correlation

coefficient values are obtained by taking the average of the correlation coefficient (Pearson, Spearman's rho) to obtain one value for each index from all the stations at different timescales (annual, seasonal, monthly) to consider which time steps of the indices may have better correlation coefficients. The obtained results of RAI for Pearson and Spearman's rho correlation between different stations had the best correlation on all time steps (annual, seasonal, monthly), the average coefficients for these time steps were (0.99, 0.94, 0.87, and 1, 0.96, 0.88, respectively). Whereas DI, PN were significantly higher (0.7). The results of correlation test between drought indices are represented in table IV.4 and figure IV.11, IV.12.

In conclusion, DI and RAI were highly correlated on short-term (monthly) and medium (seasonal), while SPI and RAI were highly correlated on long-term (annual), is better suited for understanding and assessment of drought analysis in the study area, they were able to detect the period of drought which they found reasonable results of the drought performance reflecting the real situation of climate for this area without underestimated or overestimated the drought categories and their period.

Almost all indices reached a high correlation between the stations (0.82) may due to the fact that drought is strongly affected by rainfall, the low variation of rainfall amount led to this similarity of the strong correlation where the geographical coverage (distance) between the stations was small.

Table IV.4. Average correlation coefficients of indices from all stations with different time scale.

Correlation Test	Annual				Seasonal				Monthly			
	SPI	RAI	DI	PN	SPI	RAI	DI	PN	SPI	RAI	DI	PN
Pearson	0.98	0.99	0.96	0.99	0.91	0.94	0.93	0.85	0.82	0.87	0.84	0.75
Spearman's rho	0.99	1	0.99	1	0.95	0.96	0.96	0.94	0.85	0.88	0.85	0.81

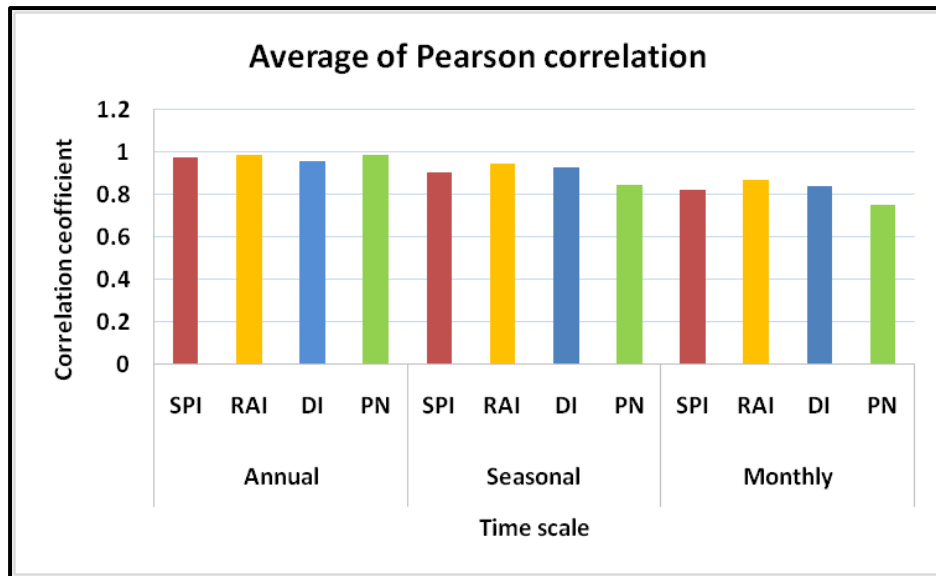


Figure IV.11. Average Pearson correlations of all indices with a different time scale from all stations.

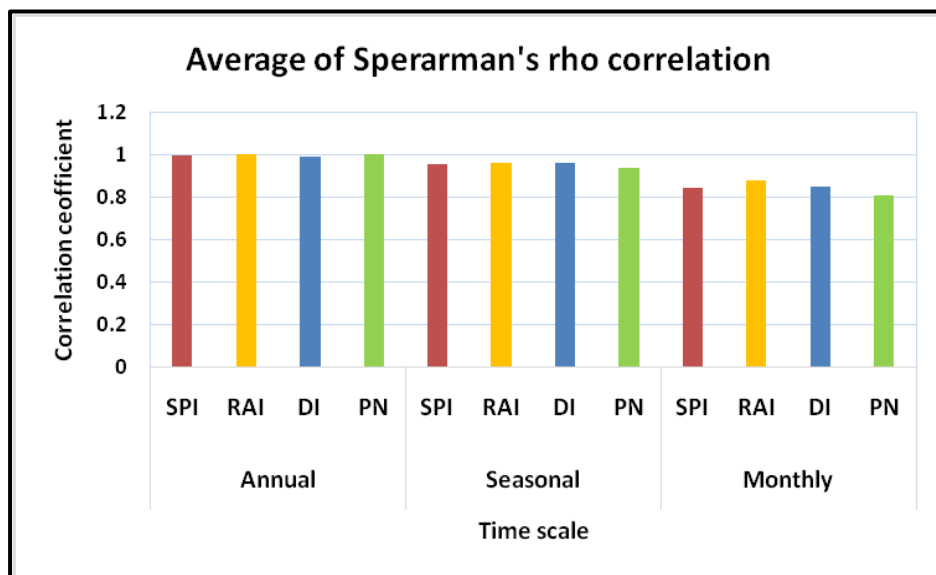


Figure IV.12. Average Spearman's rho correlations of all indices with a different time scale from all stations.

IV.3.6. Trend analysis of meteorological drought indices

The results of trend analysis Mann–Kendall (MK) test on different time series of drought indices for a period of 1979–2011 are presented in table IV.5. Overall, all the indices exhibited no considerably significant trend at the various stations on annual and seasonal scale except Djbel Chouachi station that were recorded significant positive trend (0.13 at $P=0.05$ level of statistical significance) on seasonal scale for RAI, and DI. Whereas, for Monthly scale, the trend provided by indices were significantly positive in Djebel Chouachi and Meurbah station, and the same result for Sidi Bounakhla station except RAI index that showed no significant trend, while the stations Khemis, Chouly, and Ouled Mimoun detected

positive trend with one of this indices SPI, DI, and RAI respectively. The rest of stations showed positive but not significant trend, and indicated almost similar positive values for all stations on Monthly scale, that display wet event means that the positive of the indices are considerable in the sequence of the indices values.

The positive trend of meteorological indices in monthly scale may demonstrated by the positive trend of rainfall in this region (Dünkeloh and Jacobeit, 2003; Philandras et al., 2011; Donat et al., 2014; Tramblay et al., 2012; Bendjema et al., 2019). The study area experienced a significance raising of rainfall during the period 2000-2011 which was due the North Atlantic Oscillation (NAO) index describing the NAO phenomenon. This phenomenon is a pressure difference between Azores and Iceland, and its negative correlation with rainfall (Lopez et al., 2010), and that affect West Africa in the Mediterranean region (Nouaceur and Murărescu, 2017). whereas the negative phase of NAO index have impacts on increasing of rainfall in north Africa (Hamlaoui-Moulai et al., 2013; Meddi et al., 2010; Brandimarte et al., 2011), the probability for wet months (October–March) is around 42%–52% for a negative NAO (Philandras et al., 2011; Muñoz-Díaz and Rodrigo, 2003). While from the middle of 1970 to 2000, the NAO represented a positive phase caused a decreasing trend of rainfall (Hamlaoui-Moulai et al., 2013), it has been confirmed with our study results, where the meteorological indices indicated a drought situation between 1980-1999, and it was strong in 1982 for the study period.

Table IV.5. Mann Kendall test results of all indices at all stations in different time sale.

Station	Mann Kendall Test											
	Annual				Seasonal				Monthly			
	SPI	DI	PN	RAI	SPI	DI	PN	RAI	SPI	DI	PN	RAI
Sebdou	-0.03	-0.01	-0.03	-0.03	0.01	0.02	0.01	0.01	0.04	0.03	0.04	0.04
Khemis	0.17	0.18	0.17	0.17	0.11	0.02	0.01	0.01	0.08*	0.03	0.04	0.04
Djebel Chouachi	0.22	0.23	0.22	0.22	0.12	0.13*	0.11	0.13*	0.09*	0.10*	0.09*	0.09*
Hennaya	0.03	0.07	0.03	0.03	0.05	0.06	0.03	0.04	0.04	0.04	0.04	0.04
Chouly	0.05	0.07	0.05	0.05	0.05	0.05	0.05	0.06	0.06	0.08*	0.05	0.06
Meurbah	0.16	0.17	0.16	0.16	0.09	0.11	0.08	0.10	0.09*	0.10*	0.10*	0.09*
Ouled Mimoun	0.13	0.14	0.13	0.13	0.07	0.07	0.07	0.07	0.06	0.06	0.07	0.07*
Sidi Bounakhla	0.07	0.05	0.07	0.07	0.06	0.05	0.06	0.05	0.07*	0.08*	0.07*	0.07

* if trend at ≤ 0.05 level of significance

IV.3.7. Comparison of hydrological drought categories

As shown in figure IV.13, the majority of the stations detected with SDI the highest range of Mild drought category approximately (25-55%) on all time scales, with high peak at Chouly station, in addition that the highest range to this category were observed at monthly scale at Sebdou, Zahra, and Chouly, means these stations showed consistently response with SDI on monthly scale. This category followed in term of height range of values by the Non-drought category approximately (55%) on annual scale at Zahra stations, noted that with higher values of this category were observed at Sebdou, Zahra, and Chouly on annual scale

clarified similar response in this category for this scale, and at Zenata and Sidi Aissa on monthly scale. Moderate drought category was found between ranges approximately (5-15%). Severe drought and Extreme drought categories range were the lower on all categories of the SDI approximately (0%) in Extreme drought category for all stations.

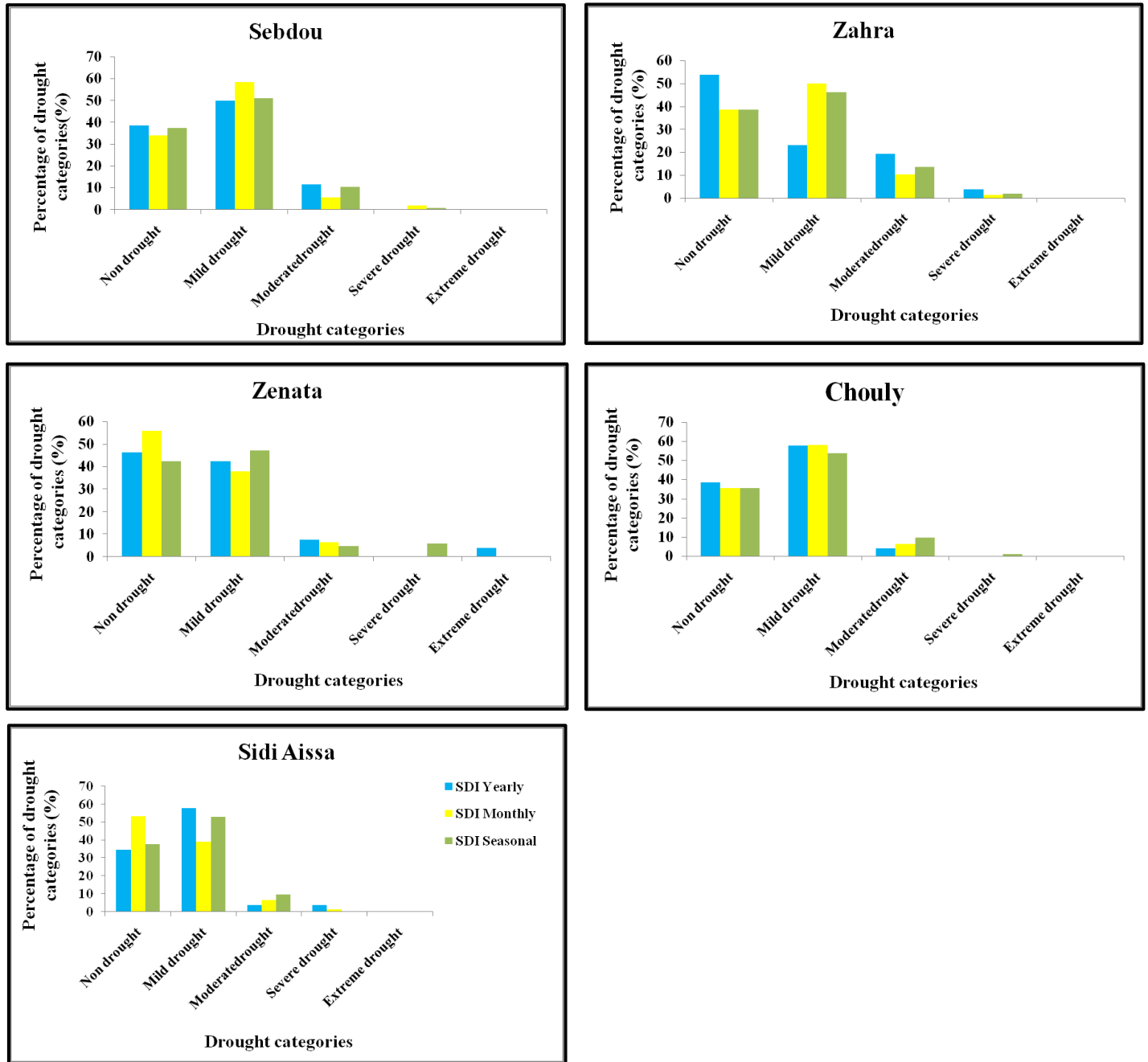


Figure IV.13. Drought categories percentage for SDI for different time scale (annual, seasonal, monthly).

IV.3.8. Comparative evaluation of hydrological drought index

The hydrological drought variation for all stations is shown in figure IV.14. As seen on annual scale, the similarities of positive values were obtained with the SDI at four stations

Sebdou, Zenata, Chouly, and Sidi Aissa in 2008 which indicate wet year, only Zahra station showed negative value. The similarities of negative values were observed in 2009 with all stations which indicated that drought occurred in the basin at this year. The extreme drought was experienced in 1999 for all stations; the annual SDI results indicate that the drought events tend to follow each other with an average duration of more than one year. The longest dry period occurred between 1996 and 1999, and between 2003 and 2007.

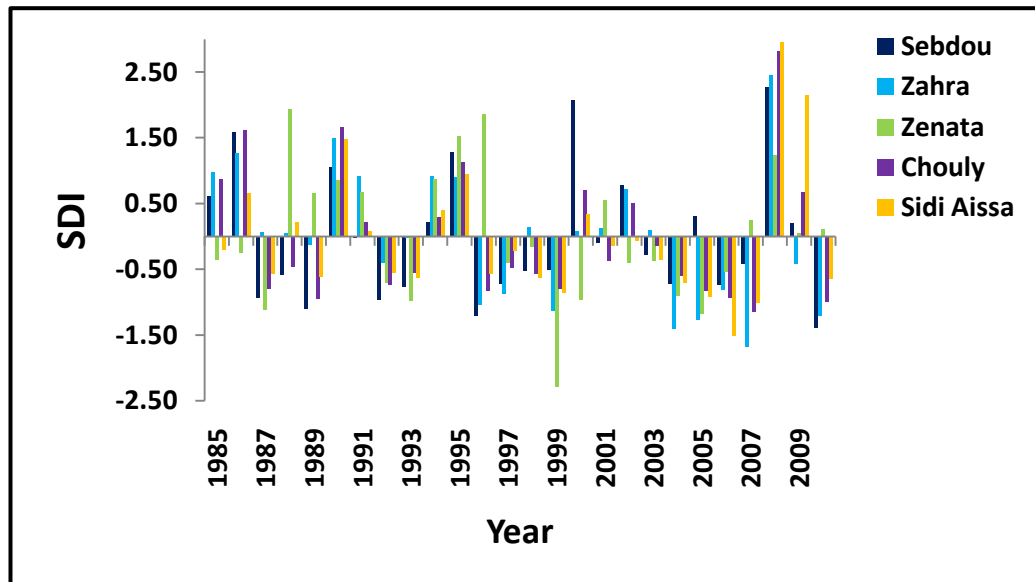


Figure IV.14. Evaluation of SDI on annual scale.

On monthly scale, SDI index shows with the majority of the stations drought condition during the period February to August, as seen in (fig.IV.15), all stations had negative values which identified the drought months for this period of time. Between the month of September and January, the two station Zenata and Sidi Aissa showed highest of positive values approximately (0.2) for September, approximately (0.8, 1, respectively) for October and November, approximately (0.4, 0.5, respectively) for December, and approximately (0.2, 0.3, respectively) for January which identified the wettest months for this period of time, while the rest of stations showed negative values of SDI.

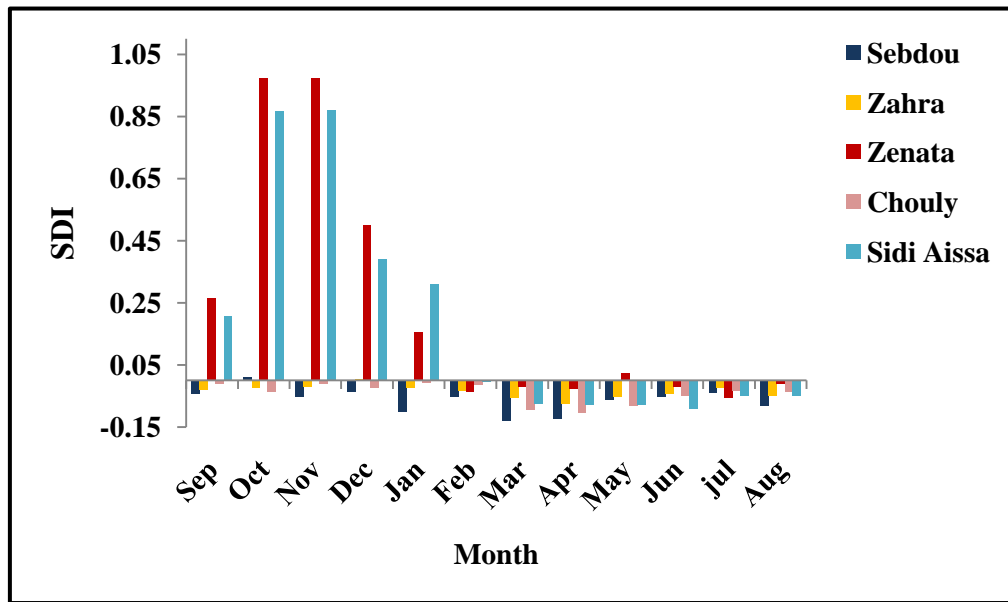


Figure IV.15. Evaluation of SDI on monthly scale.

According to the variation of SDI for seasonal scale (fig.IV.16), the wet period in autumn for almost all stations was observed between 2000 and 2002, and between 2007 and 2009. The year 1986 in autumn was the wettest year at Sebdou station, where this year is not part of the detected wetter period (2000-2009). The driest period was observed between 1987 and 1993, and between 2003 and 2007 for almost all stations. Winter season (fig.IV.17) showed wet period between 1985 and 1986 and 2008 which is considered as the wettest year in this period of time for all stations. The dry period in winter was defined as the longest period in time series between 1987 and 2007 (1999 at Zenata was the driest year), with the exclusive of wet years were defined along time series. In the successive years, 1990 and 1991, 2008 and 2009, wet condition was recorded in spring (fig. IV.18), the longest dry period occurred between 1996 and 2007, with highest value of drought in 1999 at Sebdou (-2). Very dry conditions for all stations were in summer season (fig. IV.19). with exclusive of wet years were defined clearly in 1995 and 2008.

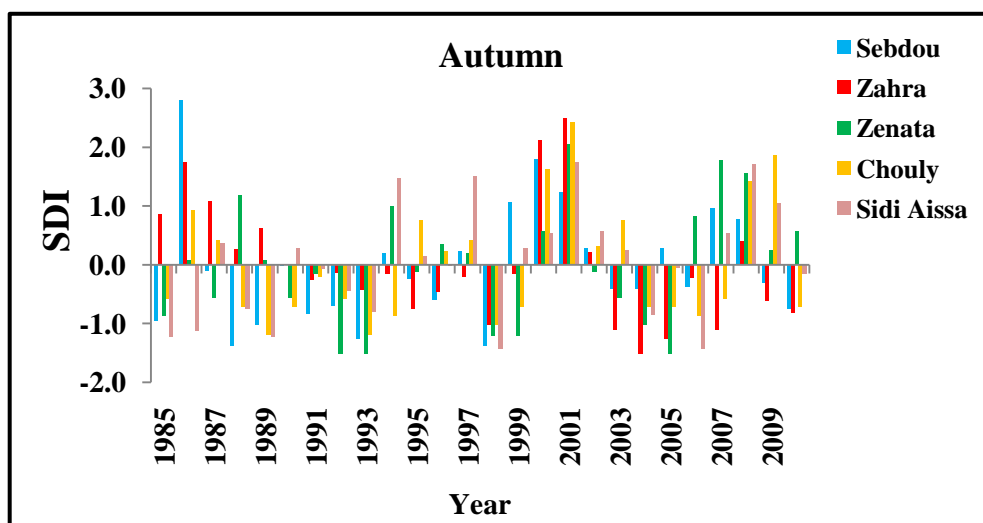


Figure IV.16. Evaluation of SDI on autumn season.

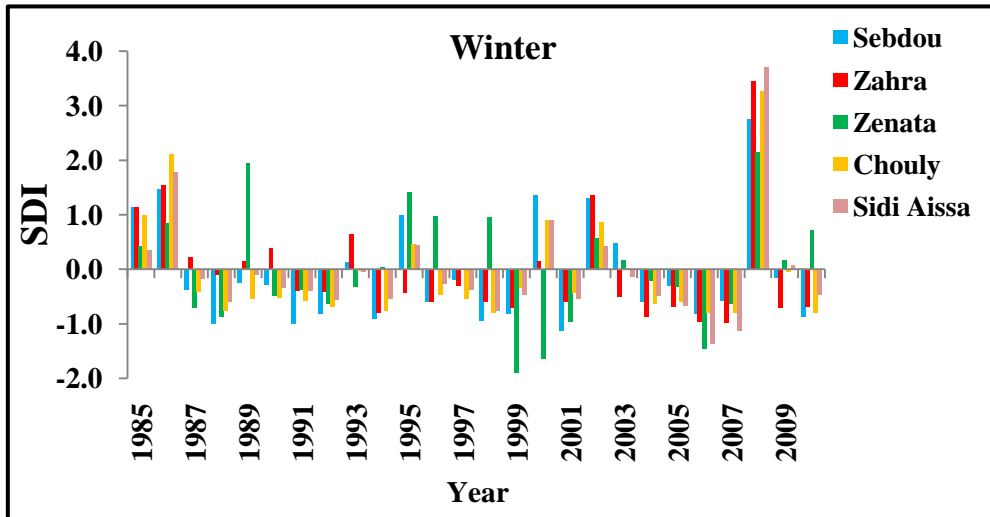


Figure IV.17. Evaluation of SDI on winter season.

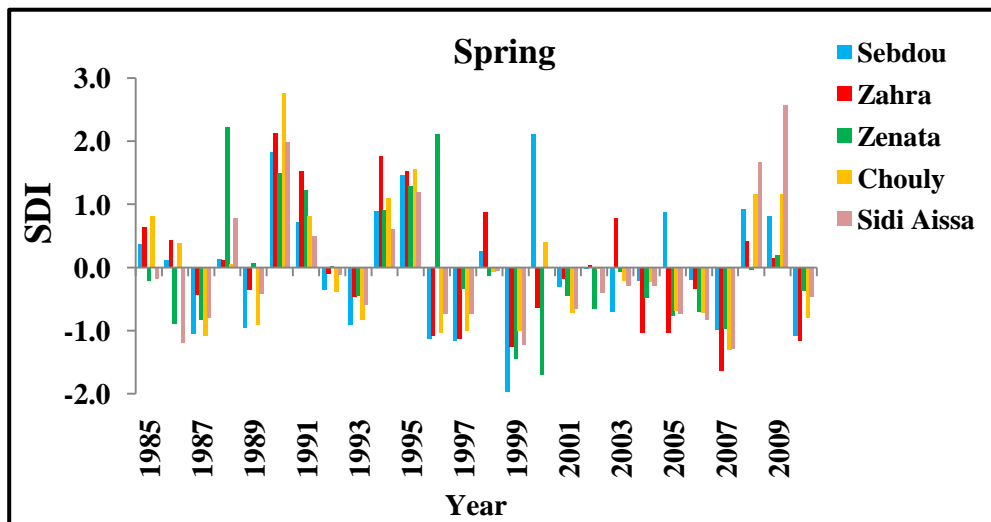


Figure IV.18. Evaluation of SDI on spring season.

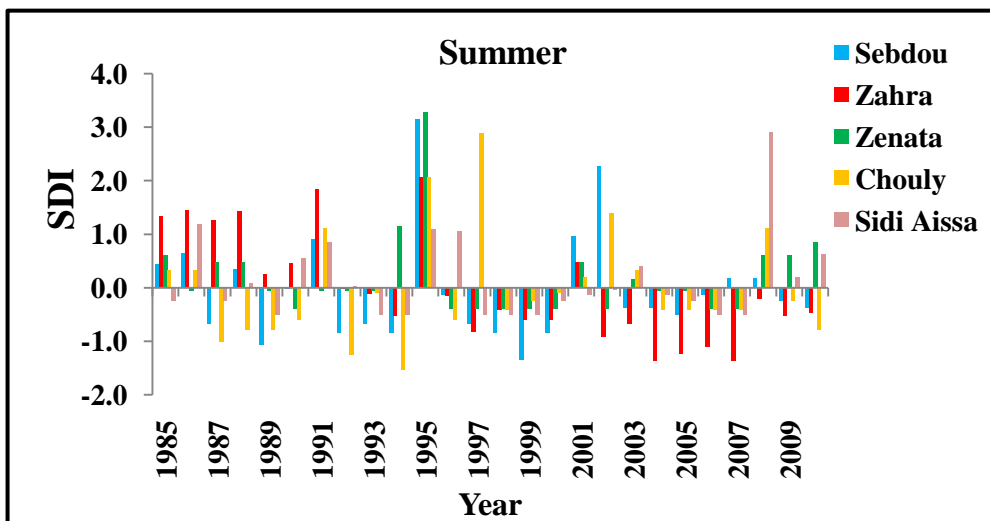


Figure IV.19. Evaluation of SDI on summer scale.

IV.3.9. Relationship of SDI between the study stations

The relationship of the values of SDI between stations was determined with the coefficient of Pearson and Spearman correlation tests on the different time scale (annual, seasonal, monthly). The results showed that Chouly and Sidi Aissa stations indicate high correlation on annual scale (tab. IV.6) with Spearman correlation tests, the station of Chouly (0.82, 0.83, 0.89), while Sidi Aissa (0.66, 0.76, 0.89), and with Pearson correlation of Chouly (0.89, 0.86, 0.87), and Sidi Aissa (0.71, 0.71, 0.87), with Sebdo, Zahra, (Sidi Aissa/Chouly) stations respectively, except Zenata stations (≤ 0.52) showed lowest correlation with other study stations for both tests. The highest correlation on monthly scale were observed (tab. IV.7) at Chouly station with Pearson (0.69, 0.64), and Spearman (0.64, 0.59) with Sebdo and Sidi Aissa stations, respectively, while Sidi Aissa station showed that highest correlation with Zenata station, (0.63, 0.69) with Pearson and Spearman, respectively. Zahra and Zenata stations showed the lowest correlation compared to other stations on monthly scale.

Table IV.6. The correlation coefficients between SDI for all stations at annual time scale.

Annual	Correlation	Station			
		Zahra	Zenata	Chouly	Sidi Aissa
Sebdo	Pearson Correlation	0.70	0.13	0.89	0.71
	Spearman's rho	0.64	0.14	0.82	0.66
Station	Correlations	Sebdo	Zenata	Chouly	Sidi Aissa
Zahra	Pearson Correlation	0.70	0.39	0.86	0.71
	Spearman's rho	0.64	0.39	0.83	0.76
Station	Correlations	Sebdo	Zahra	Chouly	Sidi Aissa
Zenata	Pearson Correlation	0.13	0.39	0.31	0.45
	Spearman's rho	0.14	0.39	0.29	0.52
Station	Correlations	Sebdo	Zahra	Zenata	Sidi Aissa
Chouly	Pearson Correlation	0.89	0.86	0.31	0.87
	Spearman's rho	0.82	0.83	0.29	0.89
Station	Correlations	Sebdo	Zahra	Zenata	Chouly
Sidi Aissa	Pearson Correlation	0.71	0.71	0.45	0.87
	Spearman's rho	0.66	0.76	0.52	0.89

Table IV.7. The correlation coefficients between SDI for all stations at monthly time scale.

Monthly	Correlation	Station			
		Zahra	Zenata	Chouly	Sidi Aissa
Sebdo	Pearson Correlation	0.59	0.44	0.69	0.56
	Spearman's rho	0.49	0.36	0.64	0.52
Station	Correlations	Sebdo	Zenata	Chouly	Sidi Aissa
Zahra	Pearson Correlation	0.59	0.41	0.55	0.47
	Spearman's rho	0.49	0.30	0.45	0.39

Station	Correlations	Sebdou	Zahra	Chouly	Sidi Aissa
Zenata	Pearson Correlation	0.44	0.41	0.42	0.63
	Spearman's rho	0.36	0.30	0.37	0.69
Station	Correlations	Sebdou	Zahra	Zenata	Sidi Aissa
Chouly	Pearson Correlation	0.69	0.55	0.42	0.64
	Spearman's rho	0.64	0.45	0.37	0.59
Station	Correlations	Sebdou	Zahra	Zenata	Chouly
Sidi Aissa	Pearson Correlation	0.56	0.47	0.63	0.64
	Spearman's rho	0.52	0.39	0.69	0.59

On seasonal scale (tab.IV.8), the coefficient of Pearson test indicated good correlation at Chouly station (0.72, 0.69) with Sebdou and Sidi Aissa, respectively, while Spearman test indicated good correlation at Sidi Aissa station (0.66, 0.69) with Chouly, and Sebdou stations, and at Chouly station (0.72) with Sebdou station. Zahra station showed average correlation for both tests (≤ 0.60 , ≤ 0.45) with all station. Zenata showed lowest correlation for both tests (≤ 0.51 , 0.48) with other stations.

Table IV.8. The correlation coefficients between SDI for all stations at seasonal time scale.

Seasonal	Correlation	Station			
		Zahra	Zenata	Chouly	Sidi Aissa
Sebdou	Pearson Correlation	0.60	0.37	0.72	0.61
	Spearman's rho	0.48	0.31	0.71	0.69
Station	Correlations	Sebdou	Zenata	Chouly	Sidi Aissa
Zahra	Pearson Correlation	0.60	0.45	0.59	0.52
	Spearman's rho	0.48	0.36	0.45	0.45
Station	Correlations	Sebdou	Zahra	Chouly	Sidi Aissa
Zenata	Pearson Correlation	0.37	0.45	0.38	0.48
	Spearman's rho	0.32	0.36	0.28	0.48
Station	Correlations	Sebdou	Zahra	Zenata	Sidi Aissa
Chouly	Pearson Correlation	0.72	0.59	0.38	0.69
	Spearman's rho	0.72	0.47	0.28	0.66
Station	Correlations	Sebdou	Zahra	Zenata	Chouly
Sidi Aissa	Pearson Correlation	0.60	0.52	0.48	0.69
	Spearman's rho	0.69	0.45	0.48	0.66

IV.3.10. Relationship between hydrological drought (SDI) and meteorological drought (SPI, RAI, DI, PN)

In this section, the relationship between hydrological drought (SDI) and meteorological drought (SPI, RAI, DI, PN) with the coefficient of Pearson and Spearman

correlation tests have been applied to explore the relationships between meteorological and hydrological droughts based on the annual, monthly, seasonal drought series (tab. IV.9,IV.10,IV.11,IV.12,IV.13), respectively for all stations in five sub basins. The results showed that the highest correlation between SDI and meteorological drought (SPI, RAI, DI, PN) on annual scale is related in Upstream Sebdou, and Chouly sub basins (≥ 0.68) for both tests, where SPI was more suitable to SDI than other indices. While Khemis sub basin showed average correlation ($0.59 \leq$ Pearson coefficient ≤ 0.66 , $0.57 \leq$ Spearman coefficient ≤ 0.59) on annual scale.

From low to average correlation ($0.34 \leq$ Pearson coefficient ≤ 0.48 , $0.32 \leq$ Spearman coefficient ≤ 0.39 at Khemis, and Chouly sub basins), and ($0.43 \leq$ Pearson coefficient ≤ 0.54 , $0.40 \leq$ Spearman coefficient ≤ 0.43 at Khemis, and Chouly sub basins) was observed on a monthly and seasonal scale, respectively. Upstream Sebdou showed an average to good correlation (≥ 0.59) on the monthly scale, and good (≥ 0.64) on seasonal scale.

Wadi Boumessaoud sub basin showed a lower correlation of SDI and meteorological drought (SPI, RAI, DI, PN) between Zenata (runoff station) and Djebel Chouachi (rainfall station) compared to Hennaya station (rainfall station), where this latter station showed an average correlation on an annual and seasonal scale.

On annual scale, Isser sub basin showed the lowest correlation (≤ 0.23) between SDI and meteorological drought for Ouled Mimoun (rainfall station) and Sidi Aissa (runoff station) compared to Sidi Bounakhla (rainfall station) and Sidi Aissa (runoff station) (≥ 0.67), while the opposite on monthly and seasonal scale, Ouled Mimoun (rainfall station) showed low to average correlation with Sidi Aissa (runoff station) but higher than Sidi Bounakhla (rainfall station).

Table IV.9. The correlation coefficients between SDI and meteorological drought indices for Upstream Sebdou sub basin at different time scale.

SDI Sebdou		SPI Sebdou	RAI Sebdou	DI Sebdou	PN Sebdou
Annual	Pearson Correlation	0.78	0.78	0.74	0.77
	Spearman's rho	0.79	0.79	0.76	0.79
Monthly	Pearson Correlation	0.64	0.70	0.59	0.66
	Spearman's rho	0.59	0.59	0.60	0.57
Seasonal	Pearson Correlation	0.67	0.71	0.65	0.66
	Spearman's rho	0.67	0.66	0.67	0.64

Table IV.10. The correlation coefficients between SDI and meteorological drought indices for Khemis sub basin at different time scale.

SDI Zahra		SPI Khemis	RAI Khemis	PN Khemis	DI Khemis
Annual	Pearson Correlation	0.60	0.66	0.66	0.59
	Spearman's rho	0.59	0.59	0.59	0.57
Monthly	Pearson Correlation	0.48	0.45	0.41	0.40
	Spearman's rho	0.36	0.38	0.39	0.36
Seasonal	Pearson Correlation	0.51	0.54	0.47	0.48
	Spearman's rho	0.42	0.41	0.40	0.41

Table IV.11. The correlation coefficients between SDI and meteorological drought indices for Wadi Boumessaoud sub basin at different time scale.

SDI Zenata		SPI Djebel Chouachi	RAI Djebel Chouachi	PN Djebel Chouachi	DI Djebel Chouachi	SPI Hennaya	RAI Hennaya	PN Hennaya	DI Hennaya
Annual	Pearson Correlation	-0.051	-0.011	-0.001	-0.134	0.61	0.60	0.60	0.56
	Spearman's rho	-0.058	-0.058	-0.058	-0.081	0.59	0.59	0.59	0.59
Monthly	Pearson Correlation	0.49	0.29	0.22	0.25	0.58	0.49	0.45	0.40
	Spearman's rho	0.51	0.21	0.18	0.12	0.54	0.41	0.44	0.34
Seasonal	Pearson Correlation	0.31	0.29	0.25	0.20	0.60	0.59	0.60	0.49
	Spearman's rho	0.30	0.25	0.27	0.19	0.64	0.62	0.64	0.59

Table IV.12. The correlation coefficients between SDI and meteorological drought indices for Chouly at different time scale.

SDI Chouly		SPI Chouly	RAI Chouly	PN Chouly	DI Chouly	SPI Meurbah	RAI Meurbah	PN Meurbah	DI Meurbah
Annual	Pearson Correlation	0.85	0.86	0.87	0.79	0.82	0.83	0.85	0.72
	Spearman's rho	0.82	0.82	0.82	0.80	0.69	0.69	0.69	0.69
Monthly	Pearson Correlation	0.43	0.44	0.34	0.34	0.46	0.48	0.37	0.44
	Spearman's rho	0.39	0.34	0.34	0.32	0.43	0.37	0.37	0.36
Seasonal	Pearson Correlation	0.44	0.50	0.44	0.43	0.47	0.51	0.45	0.44
	Spearman's rho	0.40	0.40	0.40	0.37	0.43	0.41	0.42	0.39

Table IV.13. The correlation coefficients between SDI and meteorological drought indices for Isser sub basin at different time scale.

SDI Sidi Aissa		SPI Ouled Mimoun	RAI Ouled Mimoun	PN Ouled Mimoun	DI Ouled Mimoun	SPI Sidi Bounakhla	RAI Sidi Bounakhla	PN Sidi Bounakhla	DI Sidi Bounakhla
Annual	Pearson Correlation	0.20	0.22	0.23	0.15	0.77	0.78	0.79	0.67
	Spearman's rho	0.17	0.17	0.16	0.13	0.67	0.67	0.67	0.68
Monthly	Pearson Correlation	0.52	0.42	0.31	0.38	0.47	0.41	0.32	0.36
	Spearman's rho	0.52	0.31	0.29	0.24	0.46	0.30	0.33	0.23
Seasonal	Pearson Correlation	0.55	0.60	0.56	0.54	0.53	0.55	0.49	0.44
	Spearman's rho	0.58	0.57	0.58	0.53	0.54	0.53	0.54	0.50

IV.3.11. Trend analysis of hydrological drought indices

The annual trends of Mann Kendall indicate that the SDI values have statistically insignificant negative trend, represented insignificant decreasing trend for all stations, except the SDI of Zahra station which indicates significant negative trends at 0.05 level of significance with value -0.3 in annual, monthly, and seasonal scale, this finding of the negative trend was seen in annual, monthly, and seasonal runoff at Zahra station, which indicate the downward trend of annual runoff which reveal the presence of dry periods in the time series. For the rest of stations on monthly and seasonal scale showed insignificant positive trend at Sebdou, Chouly, and Sidi Aissa stations, while Zenata station showed insignificant positive trend on monthly scale, and insignificant negative trend on seasonal scale.

The evolution of SDI values of the hydrological stations did not coincide with or correspond to meteorological drought indices, this result is particularly evident at Khemis sub basin (between Khemis and Zahra station). The results are shown in table IV.14.

Table IV.14. Mann Kendall test results of SDI at all stations in different time sale.

Scale		Station				
		Sebdou	Zahra	Zenata	Chouly	Sidi Aissa
SDI	Annual	-0.03	-0.3*	-0.06	-0.18	-0.2
	Monthly	0.01	-0.3*	0.03	0.02	0.05
	Seasonal	0.03	-0.3*	-0.009	0.006	0.02

* if trend at ≤ 0.05 level of significance.

IV.4. Conclusion

A comparative assessment of drought for the Tafna basin allowed discussing the performance of the indices during the period 1979-2011. The following conclusions can be drawn from this research:

- The SPI and DI have performed similar response to the drought categories. Where the similarity of data level (rainfall input), and the simplicity of calculations of these indices led to removing the difference between the indices.
- The RAI and PN were found to be more able to detect more drought categories and describe the drought conditions well compared with the SPI and DI.
- All indices indicated similar categories droughts when it was the highest and lowest of rainfall.
- Providing a figure for the average indices with involving also the average rainfall for each scale may help better for drought identification and also analyse characteristics.
- SPI is recommended for use in comparison studies since it has good correlations with various time steps of other indices.
- Tafna basin was characterized by a moderate to extreme severity drought periods determined by the four indices during 1982, 1987, 1999. While the extremely wettest was in 2008 during the wet period 2000-2011.
- The best correlation for the four indices at different time scales reflected the similarity between the durations of drought and well adapted to the study area.
- The results of trends based on the Mann-Kendall test showed generally no tendency of the indices series on annual and seasonal scale except Djebel Chouachi station that has an upward trend with RAI, DI on a seasonal scale. On the other hand, the significantly positive trend in the indices was mostly detected on the monthly scale.
- The assessment of the influence of NAO (North Atlantic Oscillation) on drought revealed that the dry and wet events during the period of the study are associated with the positive or negative phase of NAO, where the positive phase of NAO matched with the dry period 1980-1999, and the negative phase with wet period 2000-2011.
- The results of SDI have shown that the frequency of drought category varies according to the time scale considered.
- Hydrologic drought shows a more drought (wet) condition when the meteorological drought exhibits a deficit (excess).
- The hydrologic drought is not matched the meteorological indices. It could be noted that SDI time series show higher variability over series than the meteorological drought. This indicates different of representing the drought or wet conditions in the sub basins.
- As for the correlation results, they showed that relations between meteorological and hydrological (SDI) droughts are strongly on the annual scale.
- The current research recommended for orienting into the detection of drought indices based on the availability of more input data such as evapotranspiration (Gocić and Trajković, 2013) for assessment of drought characteristics and monitoring of drought conditions.

- The drought analysis showed that hydrological drought is associated with a shortfall in the surface water supply (runoff), rather than with a direct shortfall in rainfall, however, hydrological drought may be the result of long-term meteorological droughts.
- According to the drought trends and their frequency, the water resource management strategies should be adjusted, especially in the rainfall seasons (September - May months), where the deficit of water resources may affect agricultural activities in semi-arid regions. It is noted that the drought trend basically related to rainfall trends. Focusing on these trends is inevitable during the decision making of strategies for water resources related to agricultural production.

The analyse of the drought temporal evolution showed different climates conditions (dry/wet), this separation of wet and dry periods was used for hydrological modeling to evaluate the simulation efficiency and if the models selected are capable of simulating runoff during the different periods.

CHAPTER FIVE

**COMPARISON OF THE PERFORMANCE OF
TWO HYDROLOGICAL MODELS:
(GR4J and HBV LIGHT)**

V.1. Introduction

The hydrological modeling analysis reflects part from the impact of climate variability on available water quantities in the studied basin, where describes the rainfall relationship with flow. Rainfall-runoff modeling aims to reproduce the flow response of a watershed to rainfall observations at a daily time step. The objective of this chapter is to analyses the water balance performance of the response results provided using hydrological modeling by comparing the performance of two hydrological models (GR4J, and HBV light), with a global approach for the simulation of daily flows with five sub-basin of Tafna. The sufficient number of models is necessary to represent the compromise and managing the possible dispersion. The GR4J model considers the precipitation of the sub-basins as an average, while the HBV light takes into account the snow influence on the hydrological regime with showing interesting performances.

The chapter will be divided into three parts. The first part will be dedicated to a show the simulation results obtained by the two models (the calibration and validation) to judge the suitability. The second is for the comparison of the performances of the models in different sub basin of the study area to understand the uncertainties linked to hydrological modeling, and to analysis the assessment of the model, and the third part will expose the comparison between the results of the hydrological response of these models in different climates conditions and different sub basins.

The application of hydrological models provides a proper estimation of the water quantity. This approach could give confidence to decision-makers to develop water resource strategies and provision which their dimensions must be adapted to different climate conditions, and potentially transferable to other Mediterranean regions for the sustainable management of water resources.

V.2. Data used for the application of GR4J and HBV light models

V.2.1. Input data

The input data for the GR4J model of the simulation process is the observed daily rainfall (mm), observed depth of runoff(mm), daily potential evapotranspiration (mm) which is calculated by the Oudin method (2004) to obtain better results than all the formulations tested, in terms of restitution of runoff rates, and daily runoff is expressed in depth of runoff in mm. For defining the average rainfall over each sub basins, such as Upstream Sebdou, and Khemis sub basins have been expressed by the only one existing rainfall station in the area. And for Wadi Boumessaoud, and Chouly sub basins, the Arithmetic mean method was used, to sum up, all the rainfall values from the rainfall stations of the sub basins , and then divide them by the number of stations in that basin (two stations for each sub basins). For sub basin that has an area is more than 500 km², is the case of Isser sub basin, the average rainfall was obtained by the Thiessen polygon method, which made each station has endowed a weight based on its influence on the basin.

And for the HBV light model require observed daily rainfall (mm), depth of runoff (mm), daily temperature (°C), long term average monthly evapotranspiration (mm) as inputs.

V.2.2. Output data

The output of the model is simulated runoff which will be compared with the observed runoff.

V.3. Modeling methodology

V.3.1. GR4J daily model

- **Start-up period**

Before starting the rainfall-runoff simulation in GR4J model, the initial phase set as mandatory which is determining the initial values for the model parameters before moving on to the optimization phase. This initial phase is considered as a physical necessity, and the problem of arbitrary choice of initial tank levels at the start of the test period in this phase can influence the optimal set of parameters of the model as well as its performance, and the solution is to choose a start-up period. It consists of taking into account that the results after an observation period are fixed in advance (Saidi, 2011).

- **Calibration period**

Calibration phase is used for the optimization of the set of parameters manually through a certain number of simulations under an evaluation criterion (until the optimum values of the coefficient of the Nash-Sutcliffe quality criterion and of the coefficient of determination R^2), and adjustment of 4 parameters (X1, X2, X3 and X4) with limited range to change, which is proposed by Cemagref (Saidi, 2011). This phase is done by comparison between the outputs (simulated runoff) of the model with the real observations (observed runoff).

V.3.2. HBV light daily model

- **Calibration period**

The calibration is done manually based on the expertise of the operator in diagnostic of the flow hydrographs with the assessment of certain performance indices of the model (Nash, coefficient of determination R^2) which is set as a criterion to optimize an number of parameters (catchment and vegetation parameters) to obtain simulated runoff that are as close as possible to the observed runoff. The operator tries to reconstruct the peaks, the delayed responses, low runoff rates and the classified runoff rate curve, while having a good balance sheet in water, as well as on the assessment of quantitative and qualitative criteria.

V.3.3. Validation period (GR4J, HBV light)

This is a control phase to validate and ensure the optimized parameters during the calibration period. The validation period must be different from that of the calibration in order to check that this set of parameters can be transposed from one period to another. The first criterion of estimate the functioning of model is only consider validated models with good performance.

V.4. Application of GR and HBV light models

Based on the runoff data availability, a data period from 1985 to 2010, and the summary results of the homogeneity and trend tests for mainly hydro-climatic variability which indicate the year break of 2007, and for trend analysis indicate an increase at the end of the rainfall time series. In addition the evaluation of drought indices (Meteorological and Hydrological index) concluded that the wet periods are in early 2000, and the dry periods are between 1990 to 1999. The period between 1990 to 2005 was determined to assess the model performance, the selection was taking account the minimum periods used for the applied models (HBV light). To reach the objective of the study, we divided the series into two periods of simulation (calibration, validation), the first period simulation consists of two phases: calibration over period 1990 to 1999 (dry period), and validation over the period 2002 to 2005 (wet period), and the second period of the simulation consists of two phases: calibration over period 1990-1996 (dry period), and validation over period 1997-1999 (dry period) for the rainfall-runoff modeling for five sub basins (Upstream Sebdou, Khemis, Wadi Boumessaoud, Chouly, Isser) in the Tafna basin.

✓ Two period is considering for both GR4J and HBV light:

- First simulation: 10 years, 1990 to 1999 (dry period) were chosen for calibration and 4 years for validation 2002 to 2005 (wet period). The selection of the last period from the wet period (2000-2007) was due to the irregularity of dataset distribution of time series in each station (ups and downs of exceptional values), we selected the most stable period.
- Second simulation: 7 years, 1990 to 1996 (dry period) was used for calibration, and 3 years for validation 1997 to 1999 (dry period).

V.4.1. GR4J

The GR4J version used was developed by Perrin in 2002 and improved by Perrin et al. 2003 to predict the daily runoff. The GR4J model contains two tanks, a routing tank and a ground tank (production). The entry data used in the model is P (mm), the ETP by the Oudin method (mm), Q (mm) in daily time step.

V.4.1.1. Simulation for first period (Dry/Wet)

- **Results of Calibration**

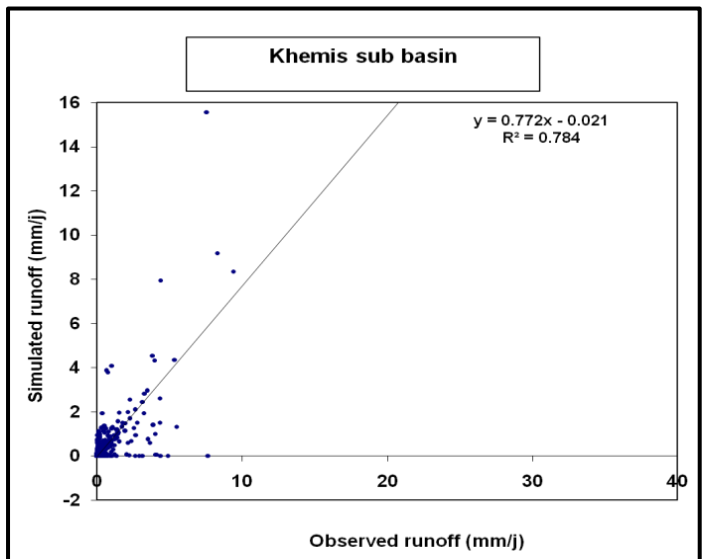
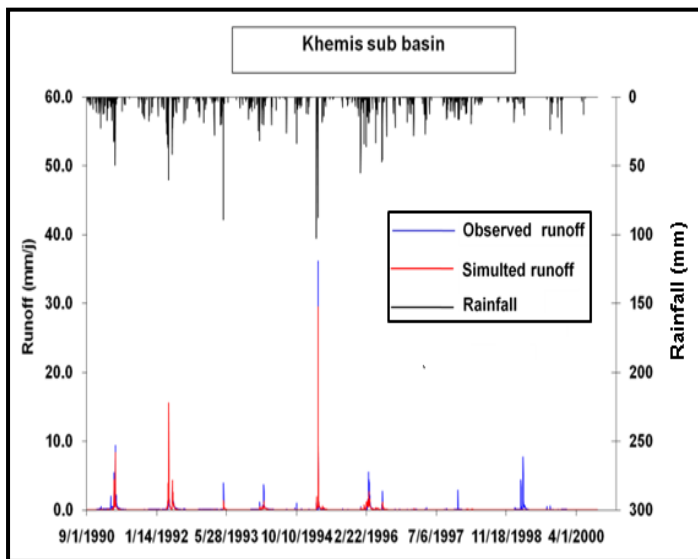
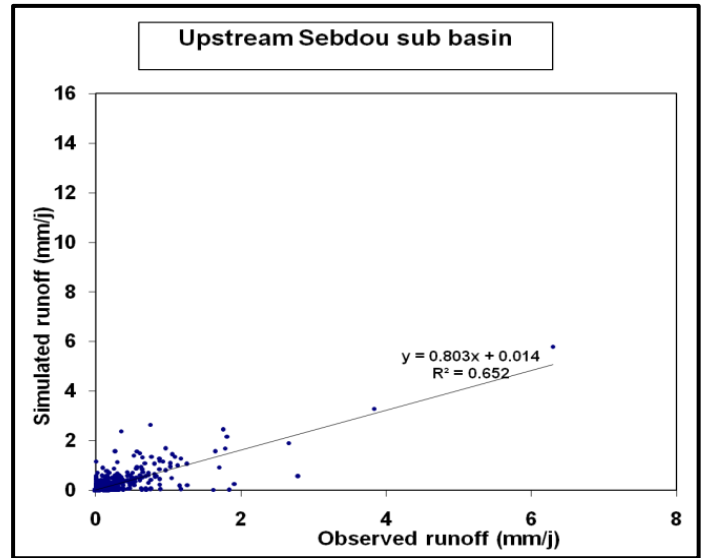
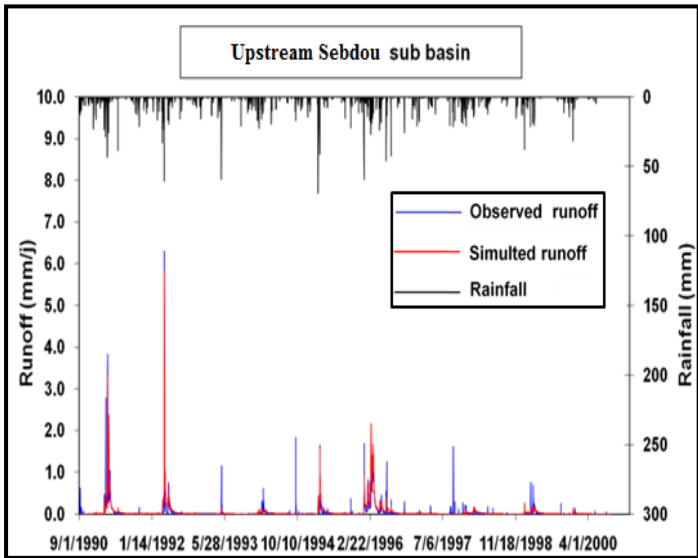
The calibration test period is applied over the period of (September 1, 1990 - August 31, 2000). The results of the calibration, coefficient of determination R^2 , and the performance criteria (Nash) are shown in the following table V.1:

Table V.1. Results of simulation and optimize parameters for the calibration during the period (1990-1999).

Sub basins	Calibration period (1990-1999)						
	Parameters				Optimization criterion		
	X ₁	X ₂	X ₃	X ₄	Nash (Q)%	Balance %	Coefficient of determination R ²
Upstream Sebdou	5.60	-1	3.5	-0.2	66.3	120.2	0.65
Khemis	5.59	-1.60	3.39	0.42	79.9	64	0.78
Wadi Boumessaoud	5.36	-2.29	3	-0.33	59.3	57.7	0.56
Chouly	4.89	-1.82	3.74	-0.39	80.6	86.1	0.79
Isser	4.90	-2.31	3	0.11	70.6	62.8	0.72

The calibration results obtained by the GR4J model for five sub basins of the Tafna basin over the period (1990-1999) of the simulation represent the ability of the model on making the response of the simulated runoff to be close as possible to observed runoff through optimizing calibration, and by taking consideration the interval limits of the parameters of the models, and the results showed adequation from average to good between simulated and observed according to the Nash criteria within the values of 66.3, 79.9, 59.3, 80.6, 70.6, while the coefficient of determination vary within 0.65, 0.78, 0.56, 0.79, 0.72 for Upstream Sebdou, Khemis, Wadi Boumessaoud, Chouly, and Isser sub basins respectively. The highest value was found at Chouly sub basin, this is appears by the compatibility between observed and modeled the hydrograph (fig.V.1) clarifying that the model is fairly well calibrated with the notice that the peak runoff are underestimated by the model and this might be due to the problem related to the identification of unit hydrographs for the massive runoff component in the narrow and very long basins. The representation of the distribution of points are important to detect the alignment of the observed and simulated points along the line $y = x$ which is useful to better appreciate the quality of the validation results, and it showed that the distribution are aligned harmoniously around the line of equation $y = x$ with the exception of a few points. And balance sheet showed low value at Wadi Boumessaoud sub basin (57.7%), while high value at Upstream Sebdou sub basin (120.2%), where the parameters are close to each other ($4.89 \leq X_1(\text{mm}) \leq 5.80$, $-2.31 \leq X_2(\text{mm}) \leq 1.20$, $3 \leq X_3(\text{mm}) \leq 3.74$, $-0.39 \leq X_4(\text{days}) \leq 0.42$), The different parameters sets for each sub basin may be assumed that the basins have different hydrological properties, and shows that the lumped calibration parameters reflect an intermediate level of these various properties. However, the most sensitive parameters turn out to be the groundwater recharge (X₂) and routing tank (X₃). It was by insisting on these two parameters that the best results came out for the Nash. Note that the negative value of (X₂) reflects groundwater recharge (Oddos, 2002), and the model simulates a loss of water (Gherissi, 2017) when the rain arrives on the ground is about to infiltrates and stored at the level of the production tank due to the karst formations and the depth losses by infiltration at the level of the fault network characterizing the basin. The time base of

unit hydrograph (x4) was fairly unresponsive during calibration, which shows no obvious correlation with physical phenomenon. The daily variability of the runoff is remarkable in the simulation period. This variability is reflected in the model by the level of the production tank which varies between 4.89 mm and 5.60 mm and the capacity of the routing tank which varies between 3 mm and 3.74 mm.



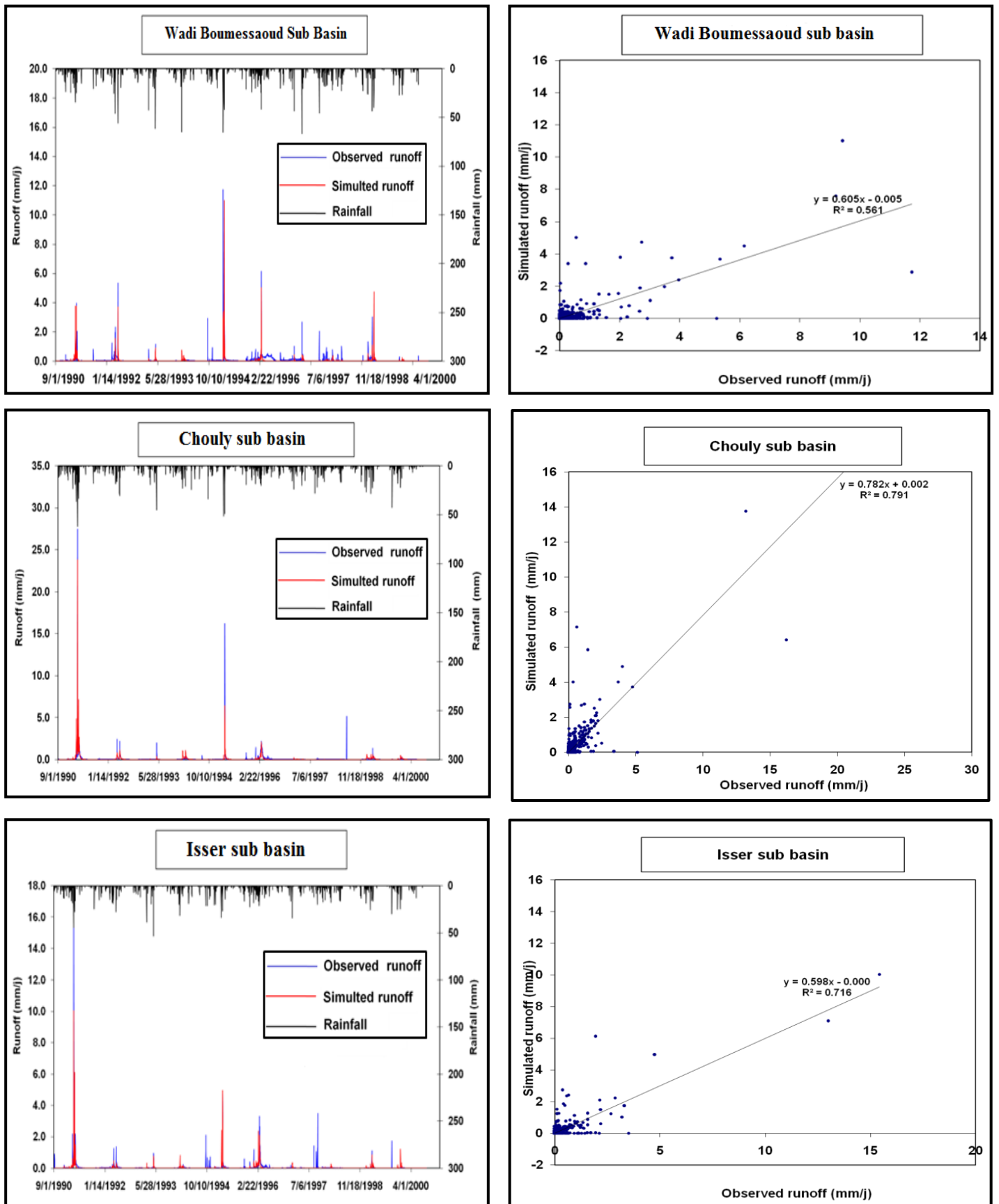


Figure V.1. Results of simulation and correlation for the calibration during the period (1990-1999).

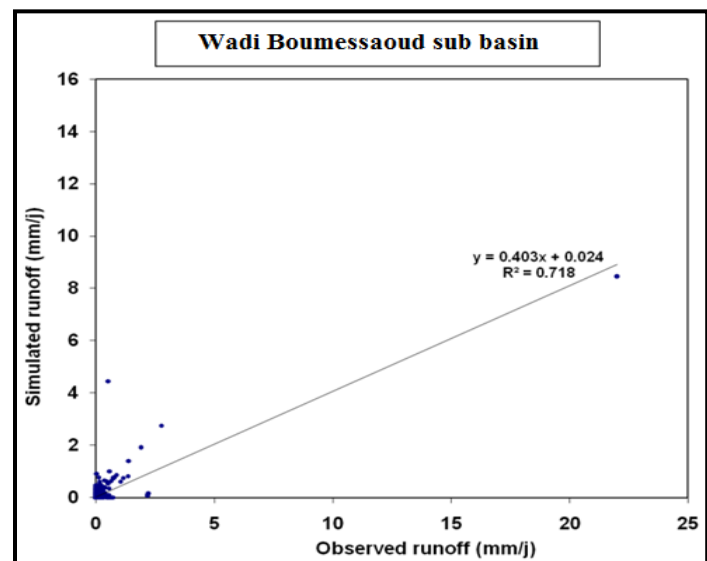
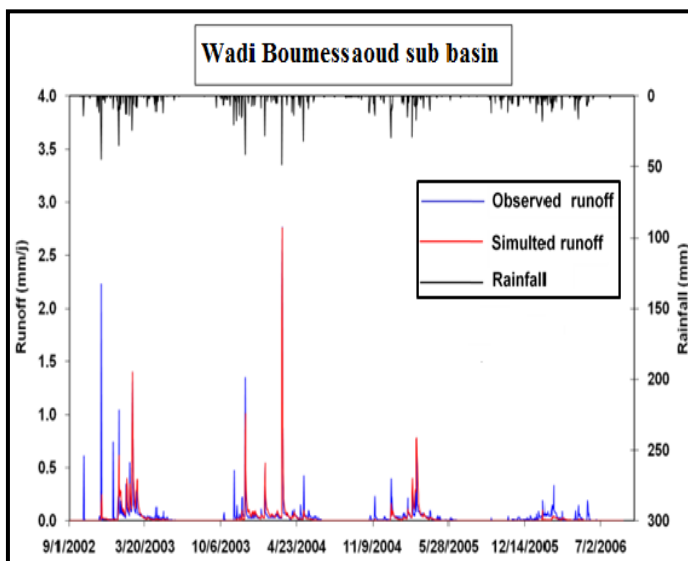
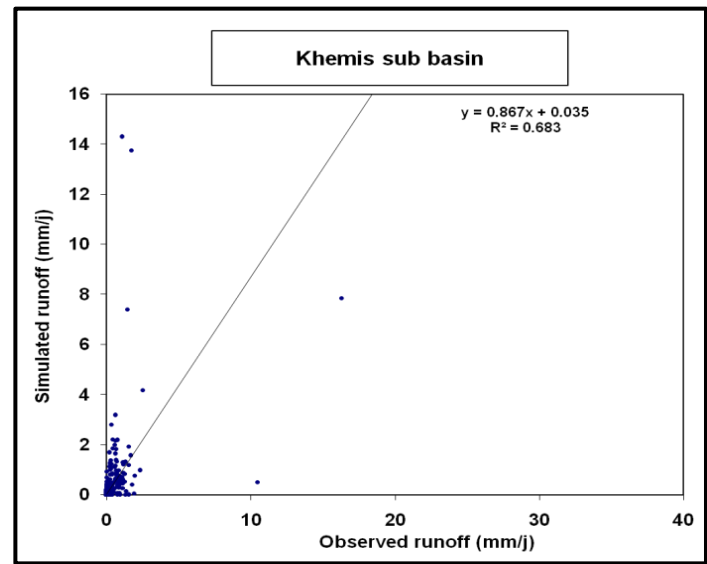
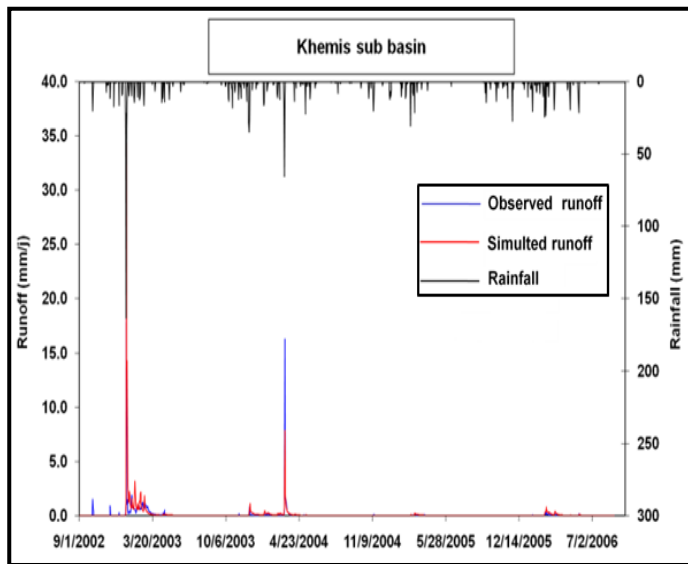
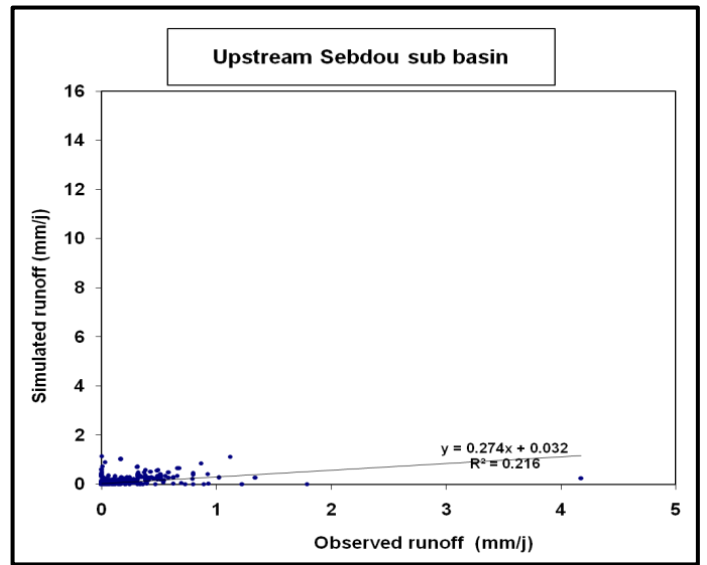
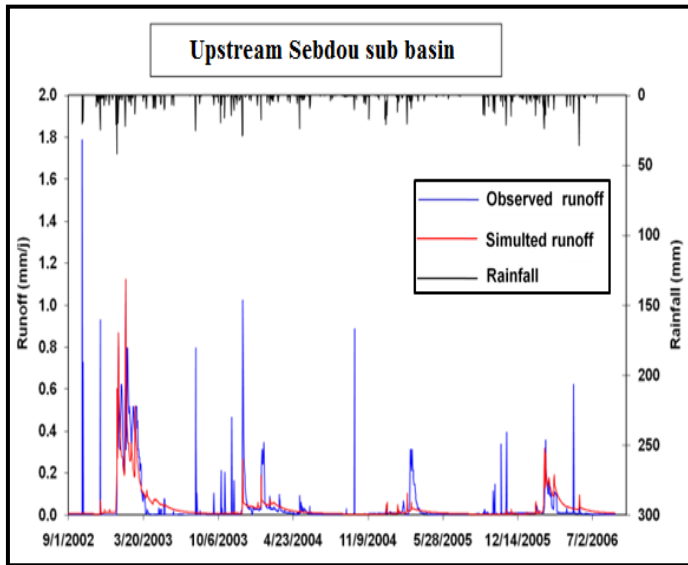
• **Results of validation**

The validation test period is applied over the period of (September 1, 2002 - August 31, 2006). The results of the validation, coefficient of determination R^2 , and the performance criteria are shown in the following table V.2:

Table V.2. Results of simulation for the validation during the period (2002-2005).

Five sub basins (Tafna basin)	Validation period (2002-2005)						
	Parameters				Optimization criterion		
	X_1	X_2	X_3	X_4	Nash (Q)%	Balance%	Coefficient of determination R^2
Upstream Sebdou	5.60	-1	3.5	-0.2	50.9	84.5	0.22
Khemis	5.59	-1.6	3.39	0.42	67.9	130.4	0.68
Wadi Boumessaoud	5.36	-2.29	3	-0.33	64.9	92.3	0.72
Chouly	4.89	-1.82	3.74	-0.39	62.5	100.2	0.55
Isser	4.90	-2.31	3	0.11	56.3	97.3	0.73

The results of the simulated hydrograph between the observed flows and those simulated of the GR4J model (fig.V.2) for the period (2002-2005) shows a significant variation of the validation results in terms Nash criteria and the coefficient of determination, which defines average Nash criteria at Khemis, Wadi Boumessaoud, Chouly, and Isser sub basins (67.9, 64.9, 62.5, 56.3 % respectively) and average Nash criteria at Upstream Sebdou which is (50.9% respectively) may due uncertainties resulting from uncertainties in the model structure, input data and parameter values. And good coefficient of determination found at Wadi Boumessaoud, Isser sub basins which clearly defines a similarity between the observed and simulated runoff with (0.72, 0.73 respectively), while as average values at Khemis and Chouly sub basins (0.68, 0.55 respectively), and the low value of correlation at Upstream Sebdou sub basins (0.22 respectively). The average performance with GR4J was considered in the two sub basins Wadi Boumessaoud and Isser although the good results of the coefficient of determination, because only the dispersion is quantified in this calculation, the coefficient of determination is a weak indicator of performance than the Nash; this issue is one of the major drawbacks of the coefficient of determination if it is considered alone (G. Tegegne et al. 2017). The instabilities of optimization criterion results may due to conceptual models structure, whose parameters cannot be deduced only from the physical properties of the basin and must be optimized against observational data (Sivapalan 2003), and which also confirming the variability and irregularity of the rainfall regime between the calibration phase (1990-1999), and the validation phase (2002-2005), and the simulation of validation is less satisfactory with parameters set of calibration.



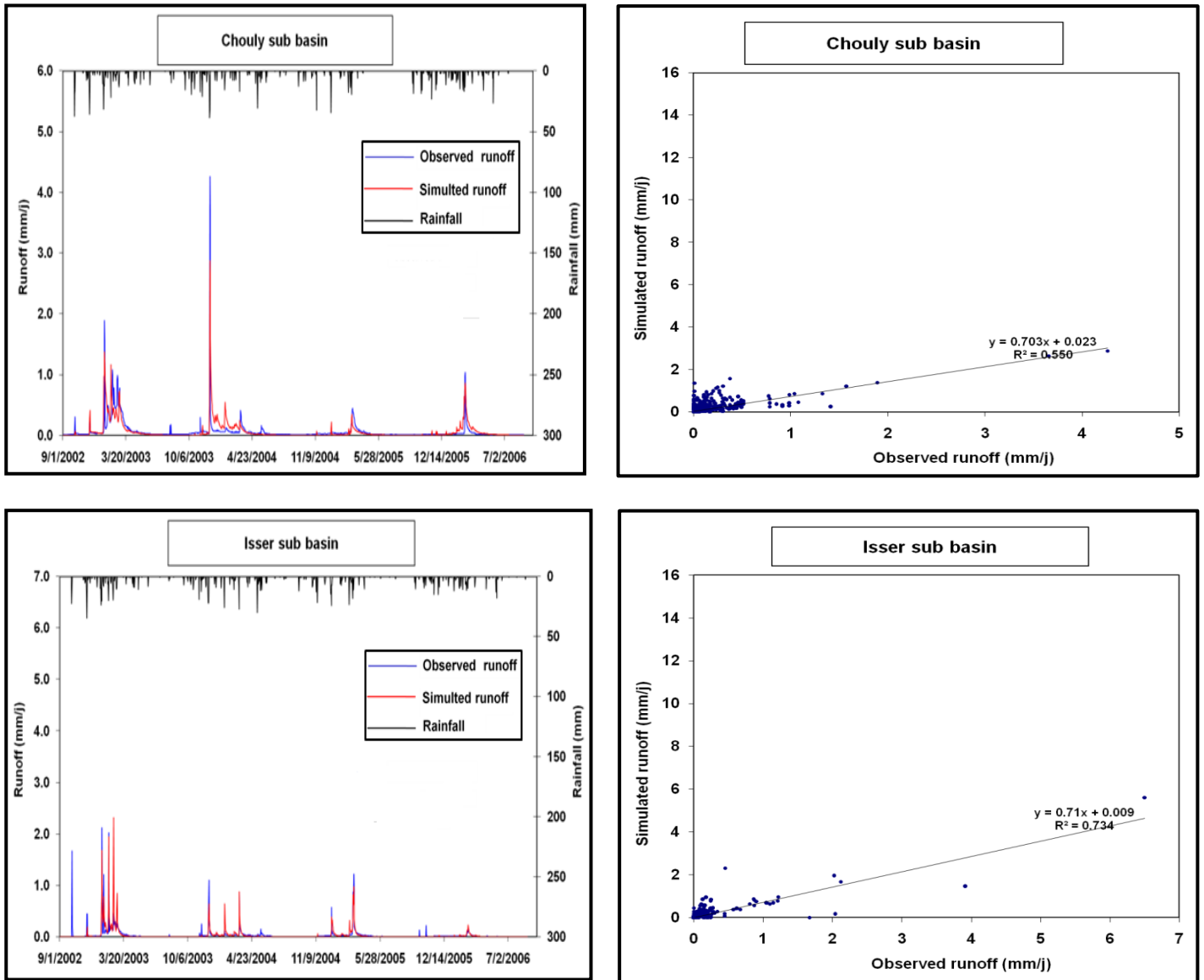


Figure V.2. Results of simulation and correlation for the validation during the period (2002-2005).

V.4.1.2. Simulation for second period (Dry/Dry)

- **Results of calibration**

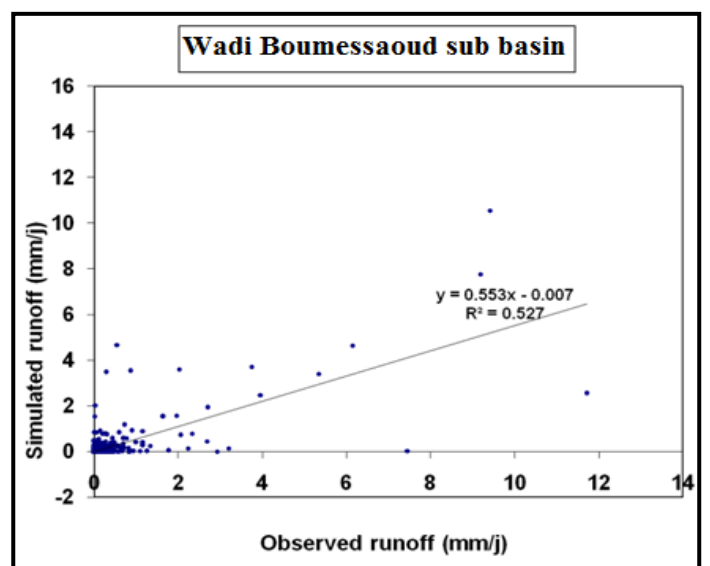
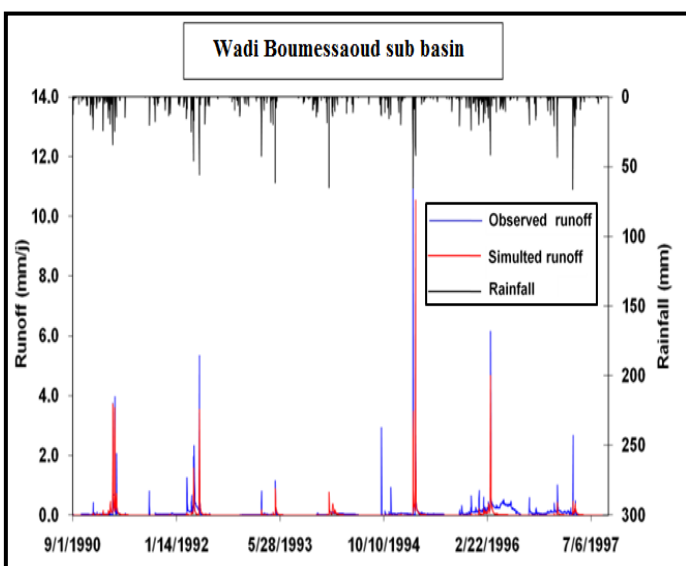
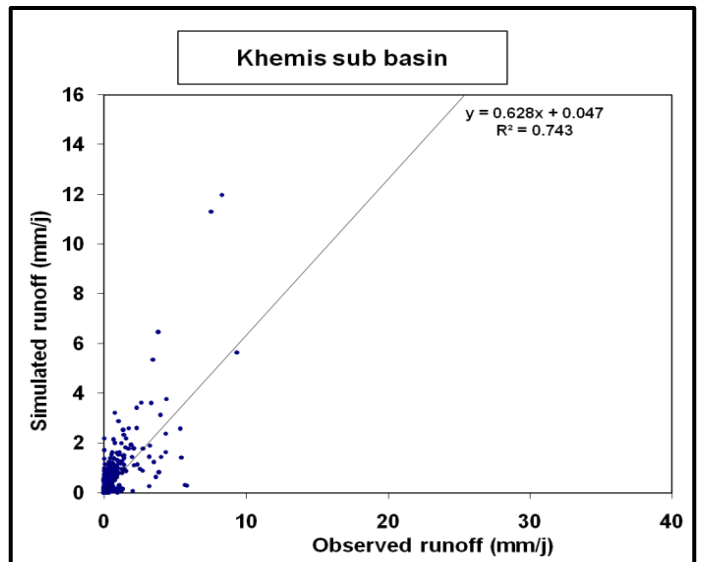
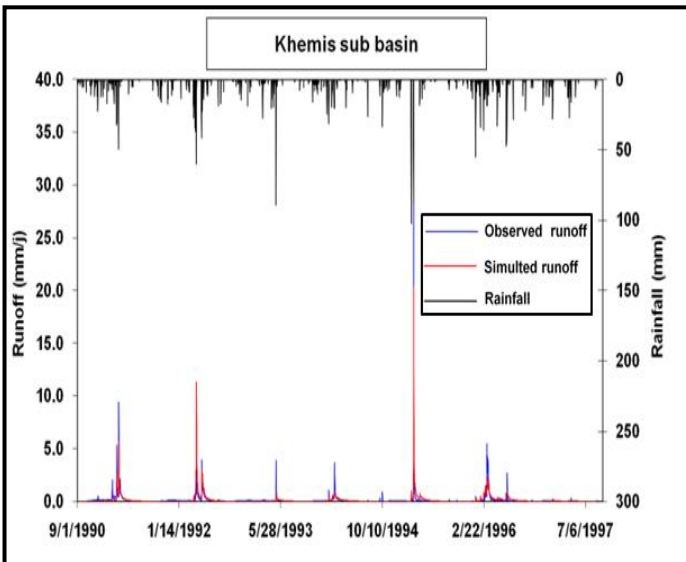
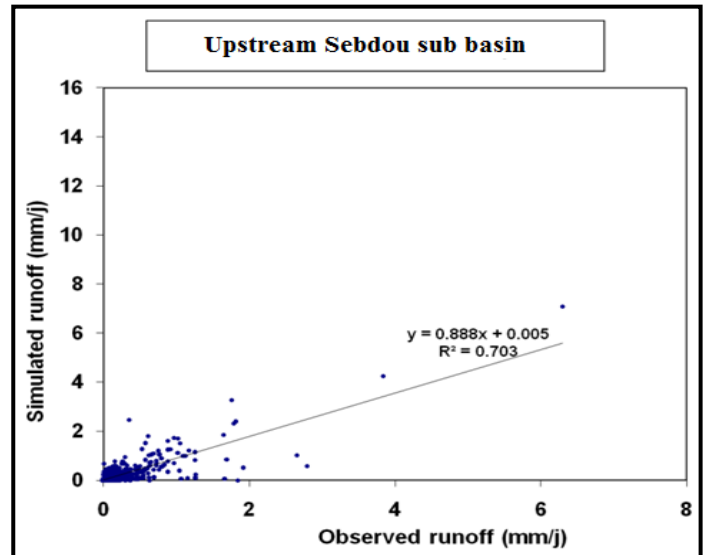
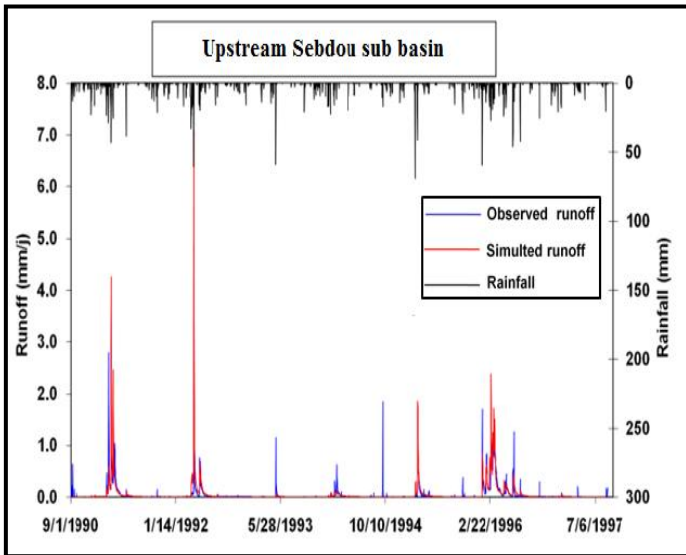
The calibration test period is applied over the period of (September 1, 1990 - August 31, 1997). The results of the validation, coefficient of determination R^2 , and the performance criteria are shown in the following table V.3:

Table V.3. Results of simulation and optimize parameters for the calibration during the period (1990-1996).

Five sub basins (Tafna basin)	Calibration period (1990-1996)						
	Parameters				Optimization criterion		
	X ₁	X ₂	X ₃	X ₄	Nash (Q)%	Balance%	Coefficient of determination R ²
Upstream Sebdu	5.65	-0.90	3	0.49	69.7	106.7	0.70
Khemis	5.64	-0.99	4.12	0.39	76.3	99.2	0.74
Wadi Boumessaoud	5.37	-2.30	3	-0.30	60	53.5	0.53
Chouly	5.10	-2	3.70	-0.38	76.3	67.2	0.76
Isser	5	-2.30	3.20	0.2	70.9	61	0.75

The results of simulation of GR4J for five sub basins in Tafna basin are showing in table V.3 and figure V.3 that the values of the optimization criterion (Nash) and coefficient of determination obtained in the calibration phase (1990-1996) are good at Upstream Sebdu, Khemis, Chouly, and Isser sub basins with Nash (69.7, 76.3, 76.3, 70.3% respectively), similar results were obtained for the coefficient of determination (0.70, 0.74, 0.76, 0.75, respectively), and average value of Nash (60 %) and coefficient of determination (0.53) for Wadi Boumessaoud sub basin. Overall, model described the runoff dynamics very well in this time phase (1990-1997), considering all of the parameter set up to calibrate model, the most sensitive parameters turn out to be the groundwater recharge (X2) and routing tank (X3) which showed best results. Note that the negative value of X2 indicate a loss of water to groundwater recharge (Oddos, 2002) due to karst formations which allows water to infiltrate in the level of the production tank. The daily variability of the runoff is remarkable in the simulation period. This variability is reflected in the model by the level of the production tank which varies between 5 mm and 5.64 mm and the capacity of the routing tank which varies between 3 mm and 4.12 mm.

According to the simulated diagrams of simulated and observed runoff, the simulated runoff model are underestimated by the GR4J in the peak of observed runoff in calibration period, this can be explained by the saturation of geological structure which is attributed to increase the amount of the observed runoff, while the model underestimated the runoff resulting in a high volume error and underestimated the high runoff peaks.



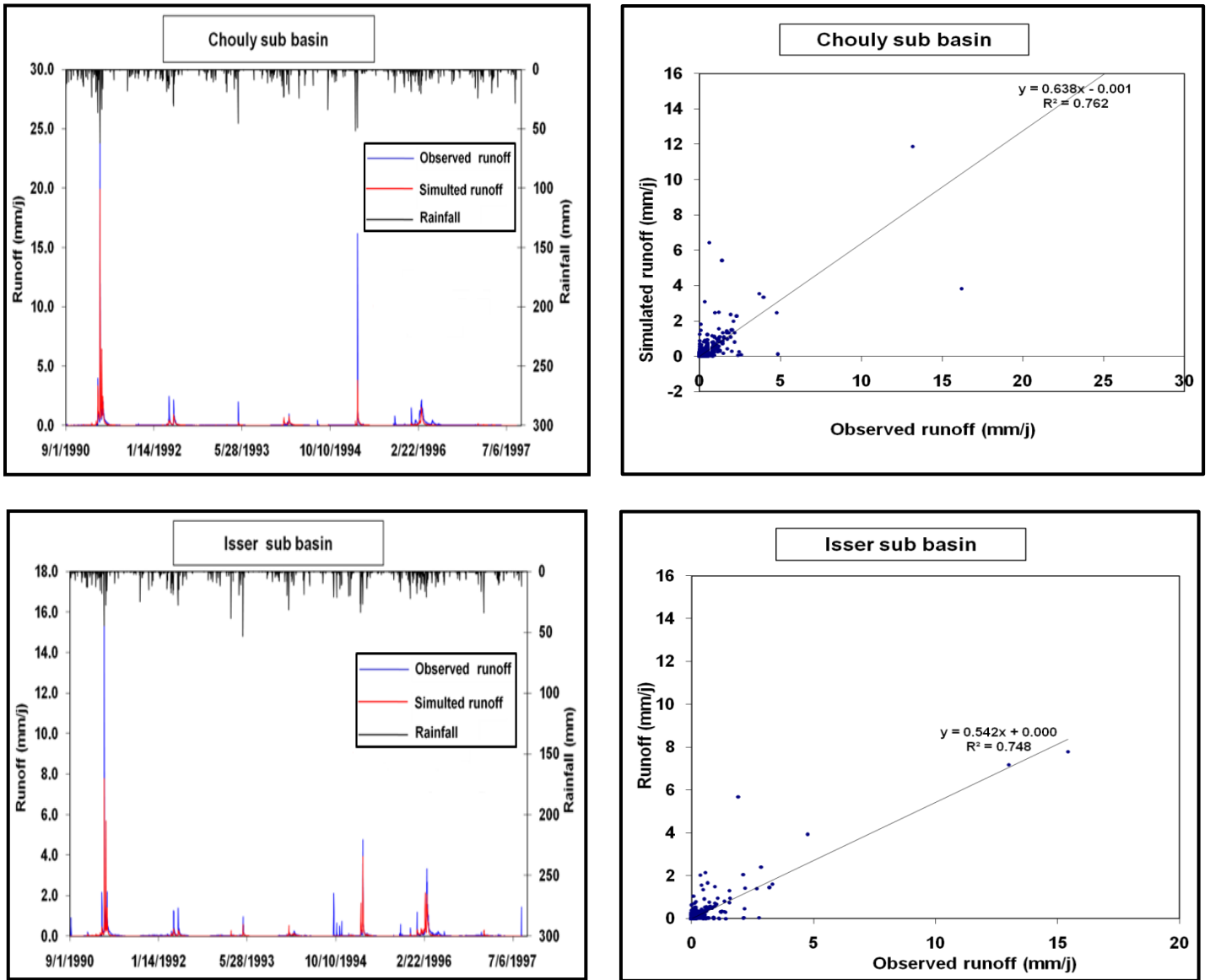


Figure V.3. Results of simulation and correlation for calibrating during the period (1990-1996).

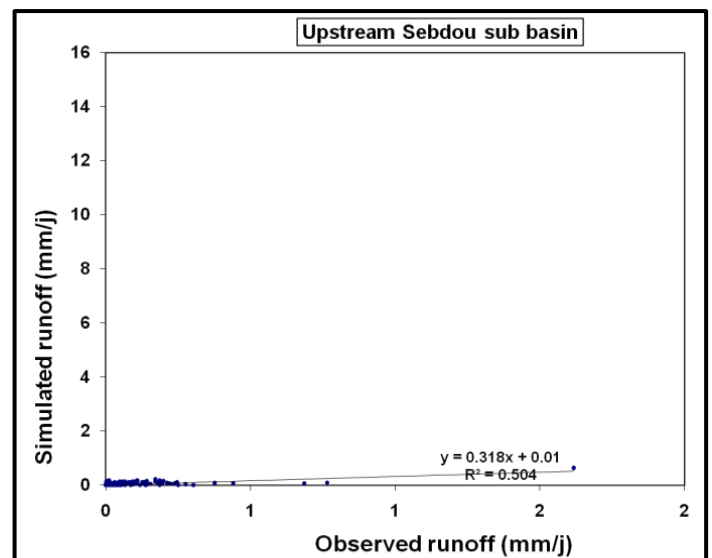
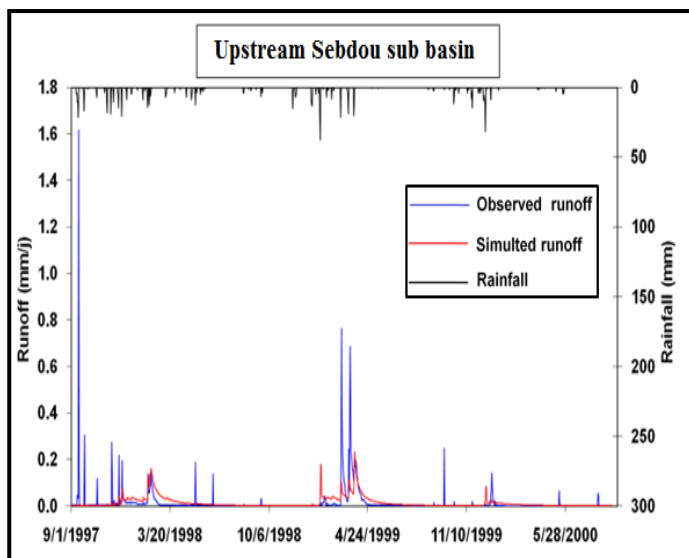
- **Results of validation**

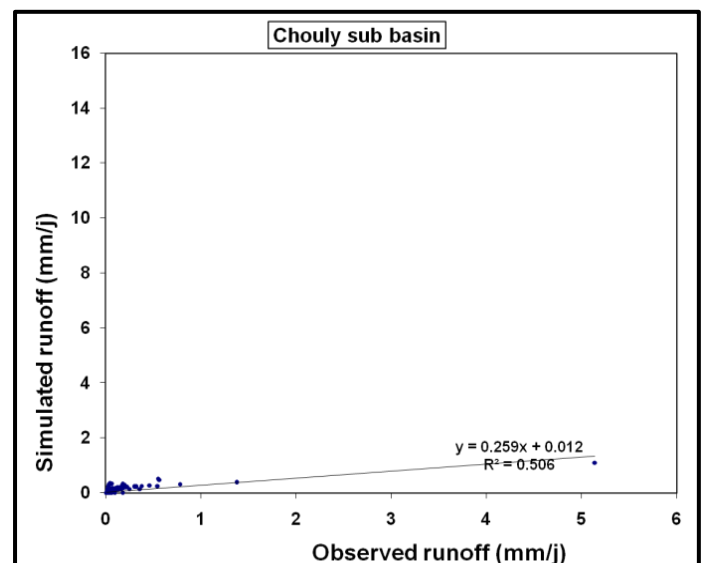
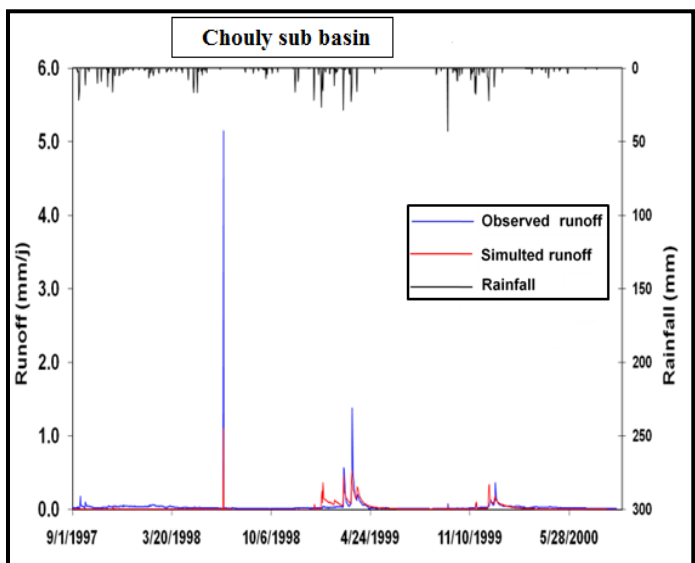
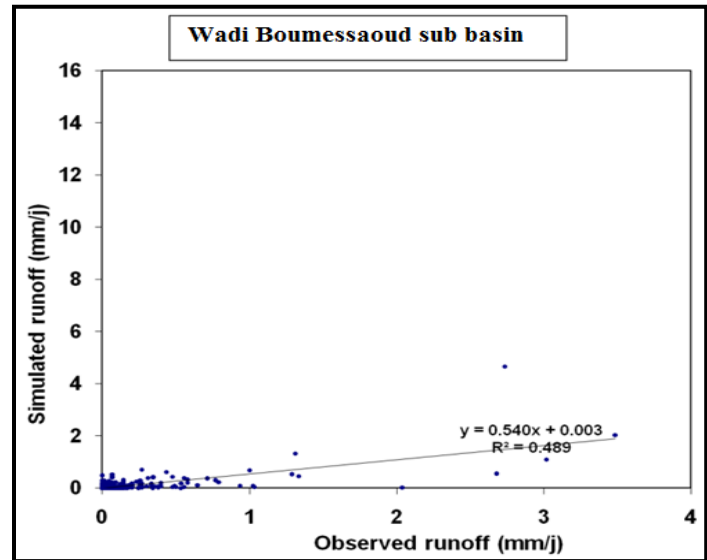
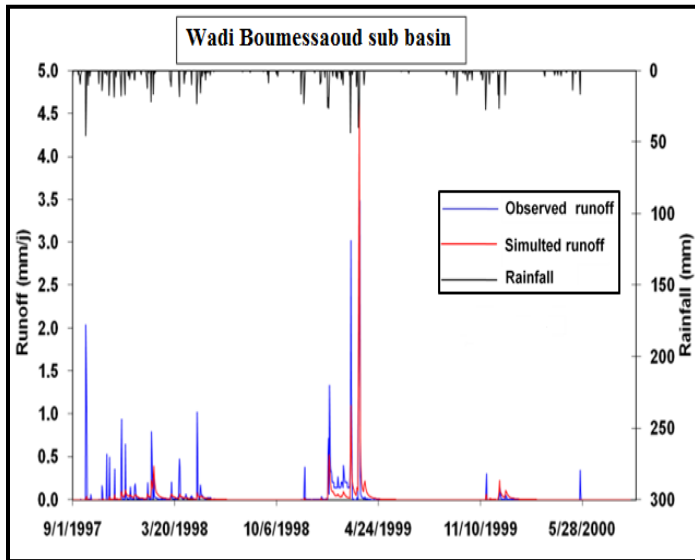
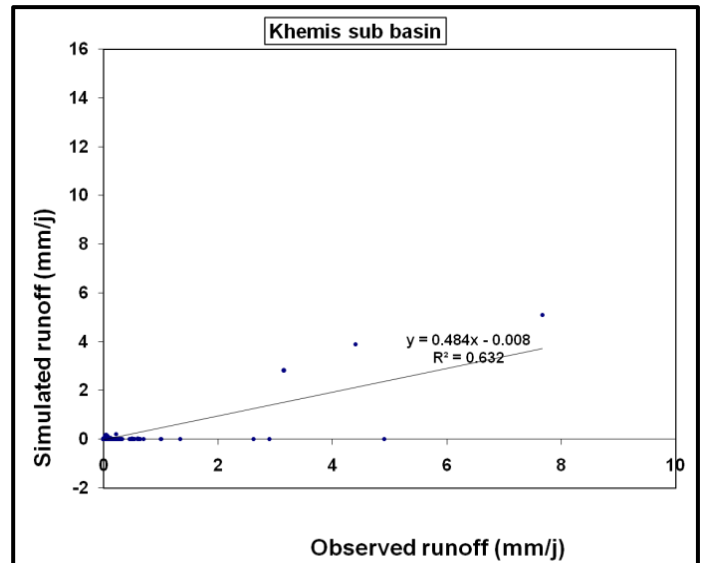
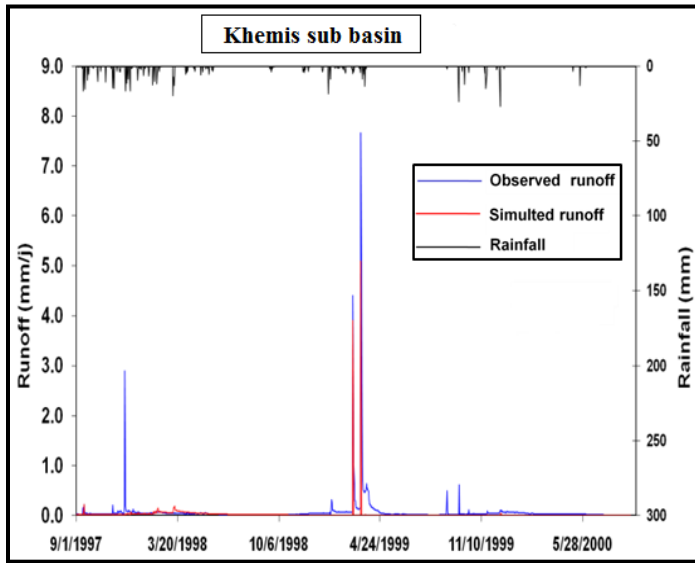
The validation test period is applied over the period of (September 1, 1997 - August 31, 2000). The results of the validation, coefficient of determination R^2 , and the performance criteria are shown in the following table V.4:

Table V.4. Results of simulation for the validation during the period (1997-2000).

Five sub basin (Tafna basin)	Validation period (1997-1999)						
	Parameters				Optimization criterion		
	X ₁	X ₂	X ₃	X ₄	Nash (Q)%	Balance%	Coefficient of determination R ²
Upstream Seb dou	5.65	-0.90	3	0.49	49.3	98.5	0.50
Khemis	5.64	-0.99	4.12	0.39	62.8	80.2	0.63
Wadi Boumessaoud	5.37	-2.30	3	-0.30	51.4	72.8	0.49
Chouly	5.10	-2	3.70	-0.38	58.1	55.5	0.51
Isser	5	-2.30	3.20	0.2	52.1	61.8	0.64

The results of the validation for the dry period (1997-1999) for five sub basins showed a weak value of Nash (49.3%), and an average value in a coefficient of determination (0.50) at the Upstream Seb dou sub basin, which may due to uncertainties in the input data (the relationship between observed rainfall and runoff), and defines average Nash (51.4, 58.1, 52.1%), and from average to good values of coefficient of determination (0.49, 0.51, 0.64) at Wadi Boumessaoud, Chouly, Isser sub basins, respectively, while good results of Nash and coefficient of determination (62.8%, 0.63, respectively) at Khemis, which clearly defines the similarity between the observed and simulated runoff (fig. V.4). Overall, the results showed clear improvement from the dry period (1997-1999) of Nash range between 49.3 and 62.8 % to the wet period (202-2005) of Nash range between 50.9 and 67.91%. However, the results of the two validation period were generally acceptable.





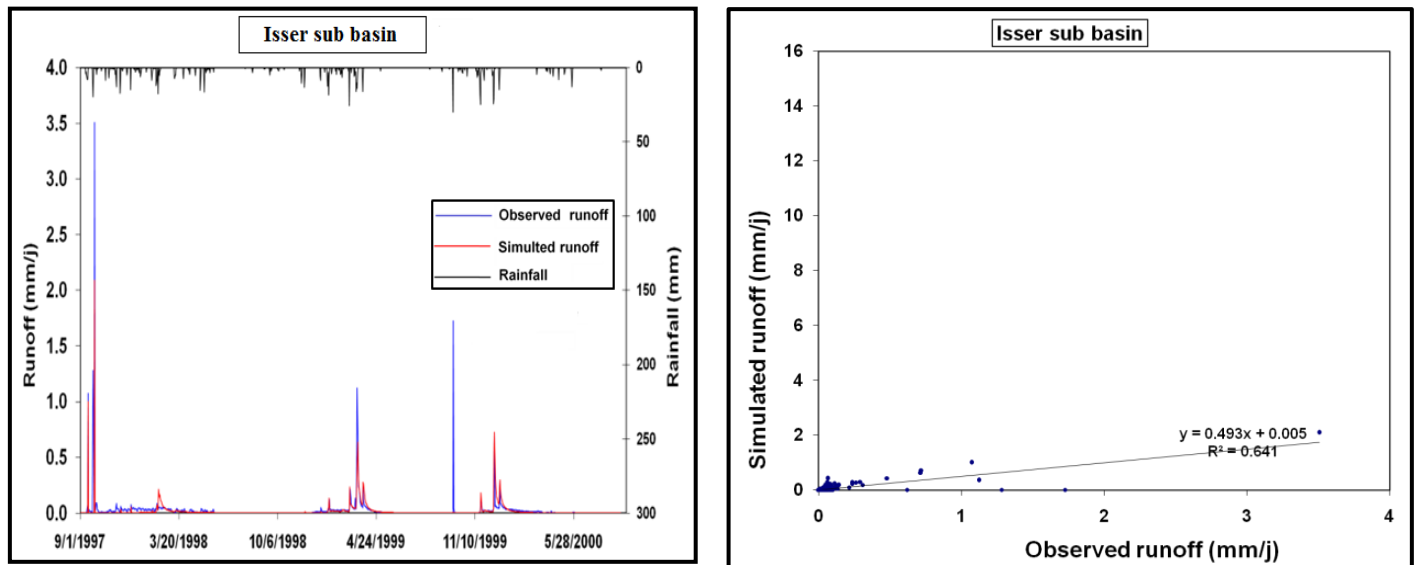


Figure V.4. Results of simulation and correlation for the validation during the period (1997-1999).

V.4.2. HBV light

V.4.2.1. Simulation for first period (Dry/Wet)

- **Results of calibration**

The calibration test period is applied over the period of (September 1, 1990 - August 31, 1997). The results of the validation, coefficient of determination R^2 , and the performance criteria are shown in the following table V.5:

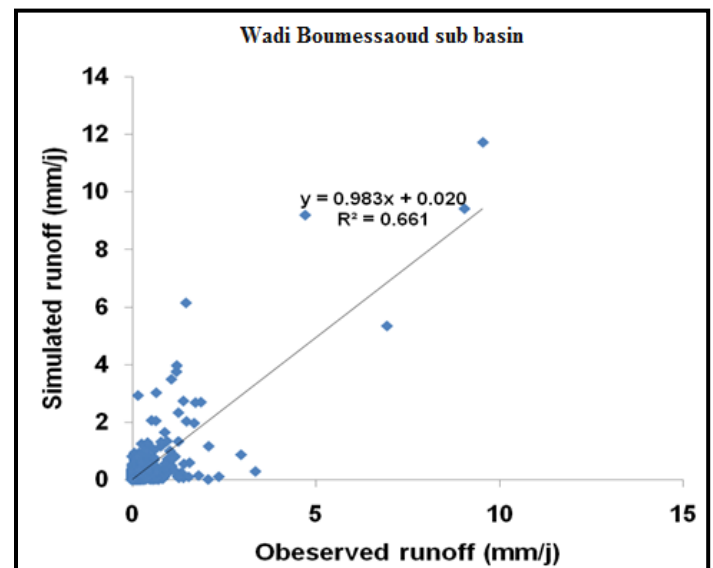
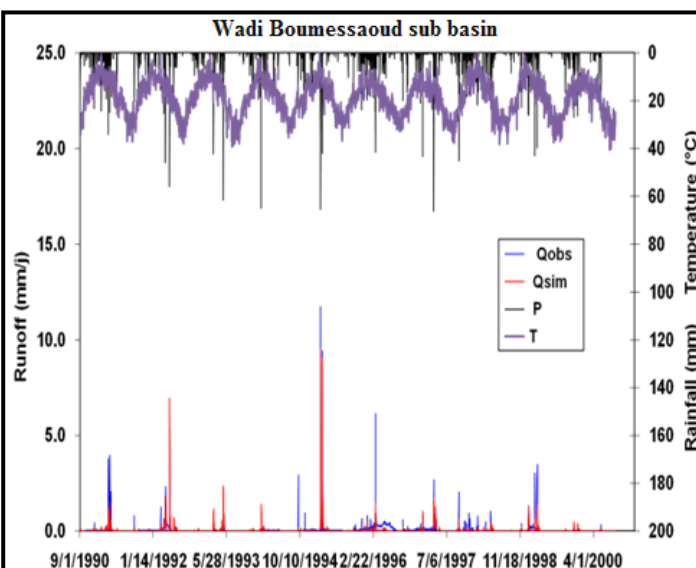
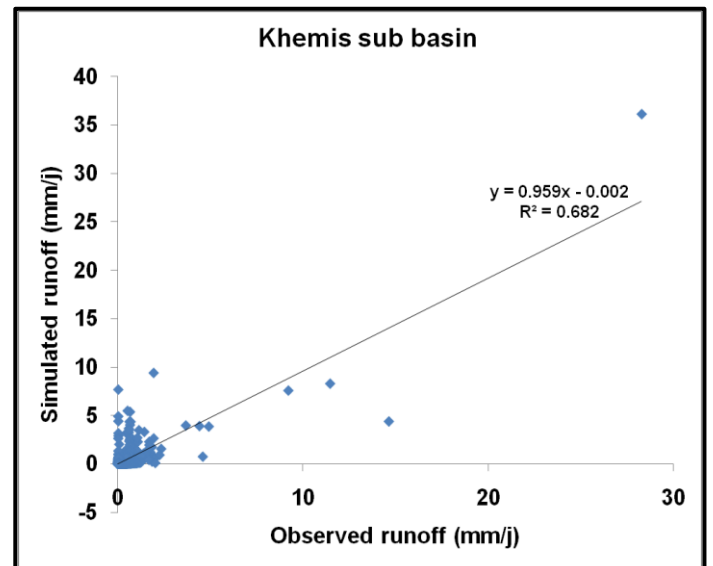
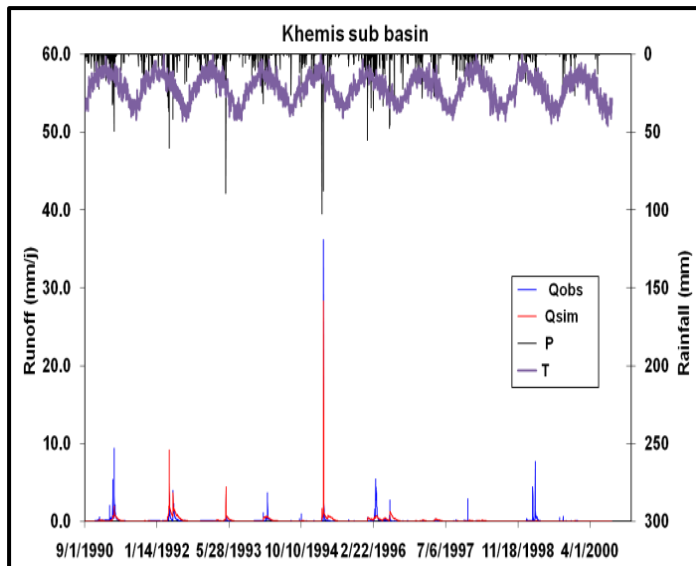
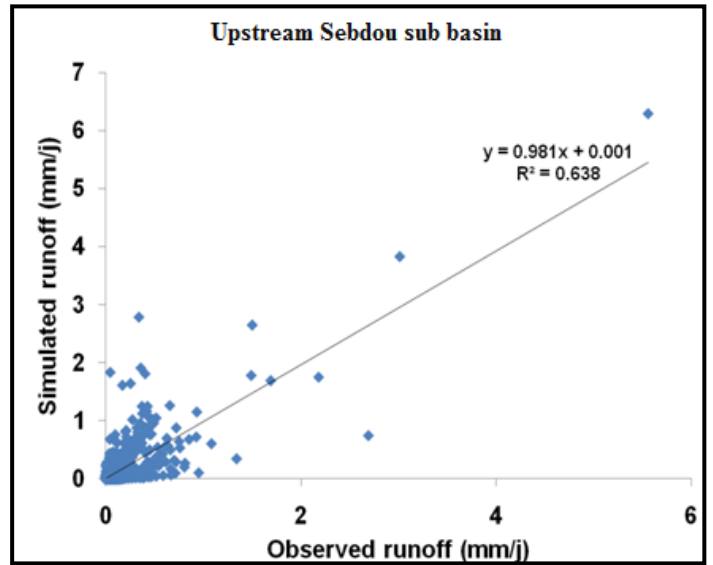
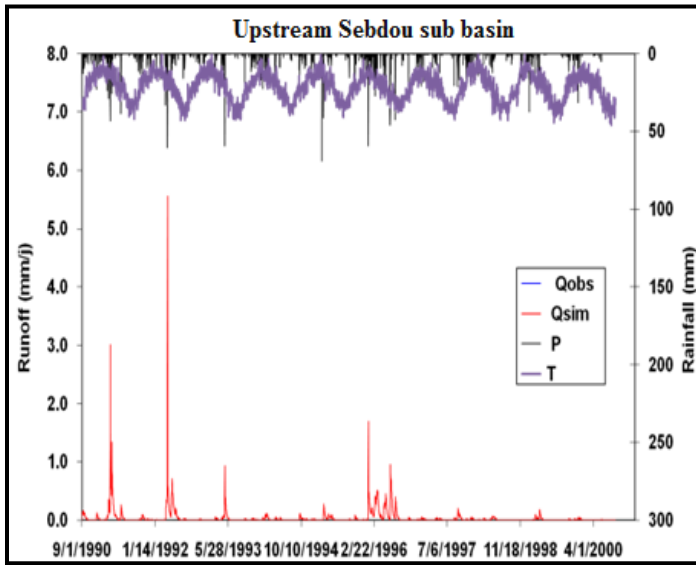
Table V.5. Results of simulation and optimize parameters for the calibration during the period (1990-1999).

Calibration period (1990-1999)		Five sub basin (Tafna basin)				
Parameters		Upstream Sebdou	Khemis	Wadi Boumessaoud	Chouly	Isser
Vegetation parameters	TT (°C)	11.1	8	-1	8.2	7.2
	CFMAX (mm/(d°C))	0.009	0.58	0.9	1.5	1
	SFCF [-]	0.01	1	0.1	0.47	0.05
	CFR [-]	0.4	0.01	6	0.8	0.5
	CWH [-]	0.05	0.01	1.5	15	1
	FC [-]	511	389	490	100	51
	LP [-]	0.151	0.17	0.03	0.68	0.01
	BETA [-]	1.13	1	0.97	2.4	80
Capture parameters	PERC [mm/d]	4.1	8.9	7	6.2	5.2
	UZL (mm)	5.13	11	0.01	11.1	7.8
	K0 [1/d]	0.99	0.99	0.99	0.99	0.99
	K1 [1/d]	0.99	0.7	0.99	0.54	0.63

	K2 [1/d]	0.12	0.05	0.39	0.26	0.1
	MAXBAS [d]	2.85	3	1.54	1.7	1.9
	Cet [1/°C]	2	1	2	1	2
Optimization criterion	Nash (Q)%	63.6	68.1	65	64.8	76.6
	Coefficient of determination R²	0.64	0.68	0.66	0.74	0.78

The calibration results with HBV light model over period (1990-1999) are provided in table V.5, summarizing the parameters (TT, CFMAX, SFCE, CFR, CWH, FC, LP, BETA, PERC, UZL, K0, K1, K2, MAXBAS...ect), Nash, and coefficient correlation estimates. The Nash value was reasonably good as 63.6, 68.1, 65, 64.8%, with four sub basins: Upstream Sebdou, Khemis, Wadi Boumessaoud, and Chouly respectively, with the exception of one sub basin Isser indicating very good value (76.6%). For coefficient correlation were also quite good with four out five sub basins were found to be 0.64, 0.68, 0.66, for Upstream Sebdou, Khemis, and Wadi Boumessaoud, respectively, while the very good value was at two sub basins Chouly and Isser (0.74, 0.78, respectively). Through examination of the hydrographs of the observed runoff and those of the simulated runoff for the calibration period (fig.V.5), the calibration results of the model showed satisfactory similarity between the observed and simulated runoff, depicting reasonably good performance, with generally a tendency to underestimate the peaks. Note that the shape of the curves of the simulated runoff of Isser sub basin produces well with HBV light closer to the observed runoff; these results reflect the ability of the model to represent runoff rates similar to the observed runoff in this time of period.

The performance of HBV light calibration showed that TT, LP, FC, and K0 are the most sensitive parameters to contribute a major change to simulation process, whereas the other parameters tend to have a moderate effect but the slight changes in these parameters values cause a change in one another. The lower values of CFMAX (0.009 mm/d°C) and SFCE(0.01) was defined in Upstream Sebdou sub basin, may due its location a mountainous and rainy area where the temperature is low that prevent melting snow in the elevated areas. The highest values of K1 (d⁻¹) and FC which all represented the storage in upper zone (mm) as shown in sub basin Upstream Sebdou (0.99, 511 resepectively), and Wadi Boumessaoud (0.99, 490 respectively), is related to the soil characteristics in sub basins which is constitute of calcareous-sandstone or marno-sandstone crusts as well as calcification clays which are characterized by reserving the amount of water in the upper part of the soil and decreasing the movement of water to downward. The lower value of FC (51) at Isser sub basin provide a much better optimization criterion between runoff observed and simulated (76.6% for Nash, 0.78 for coefficient of determination). The proportion of runoff through groundwater represented by the PERC parameter shows higher values at Khemis, and Wadi Boumessaoud sub basins (8.9, 7 mm/d) which are due to the karstic formations and the losses at depth by infiltration at the level of the groundwater network. Meanwhile, K0 remains constant at 0.99 for all the observation stations.



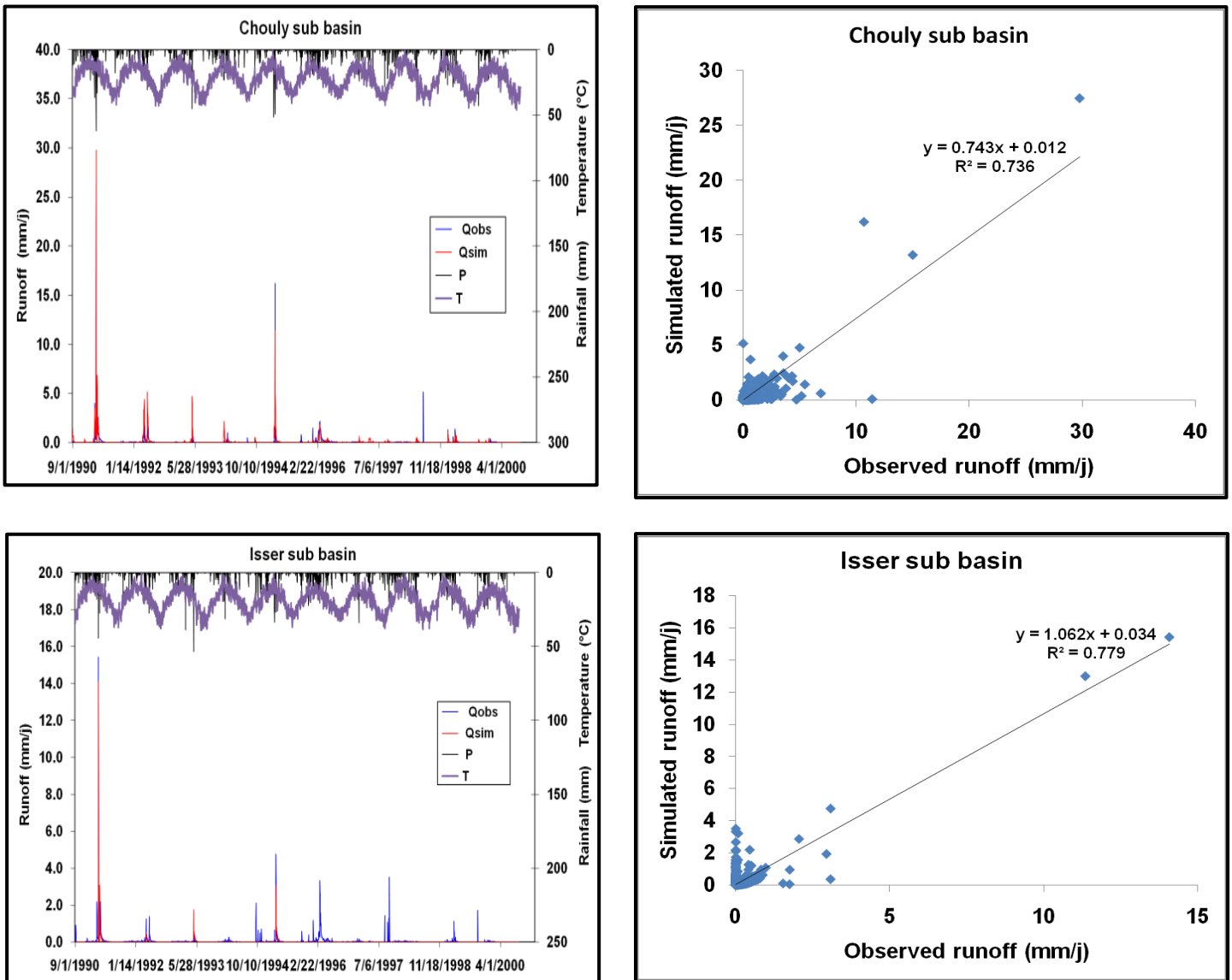


Figure V.5. Results of simulation and correlation for the calibration during the period (1990-1999).

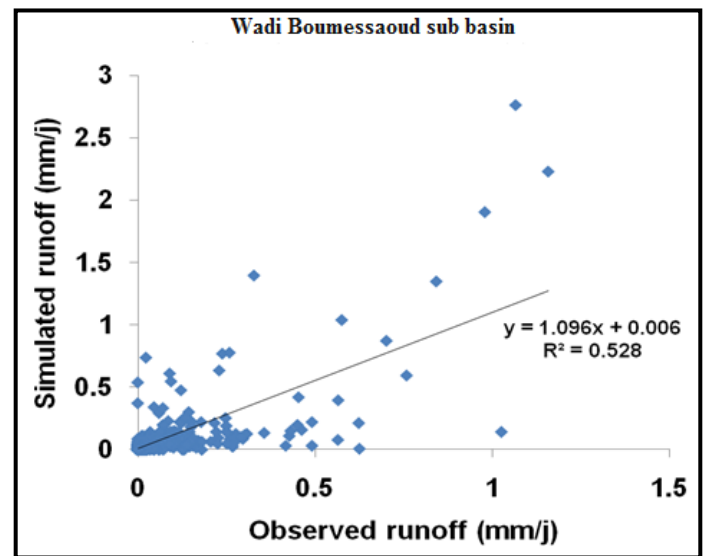
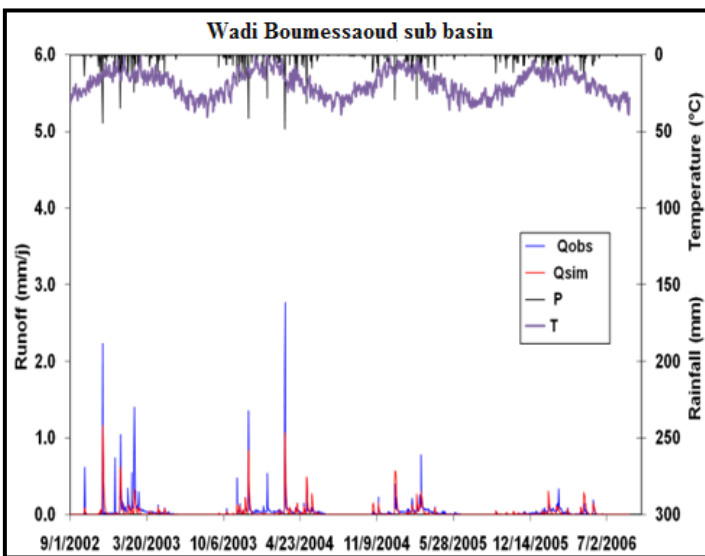
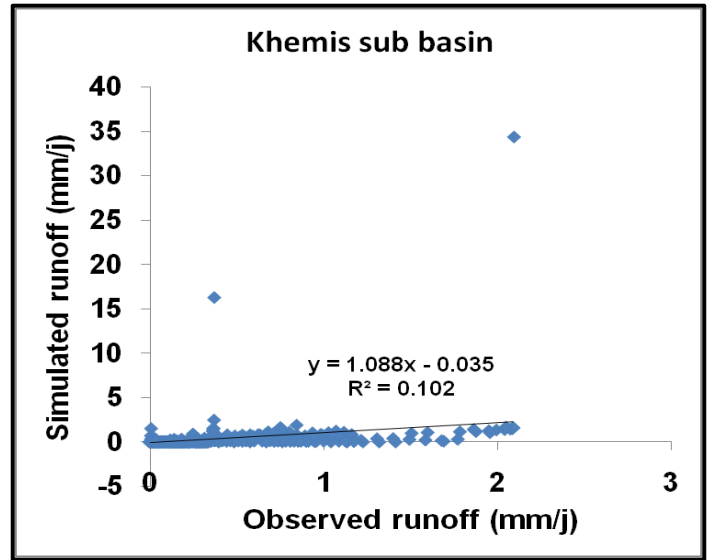
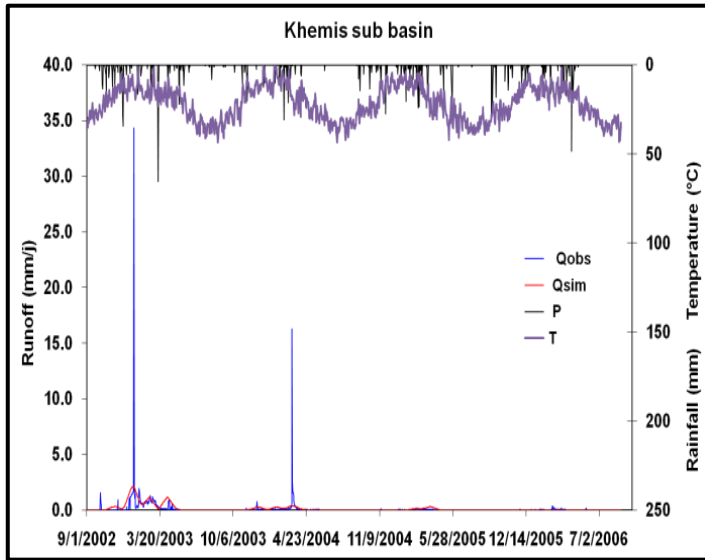
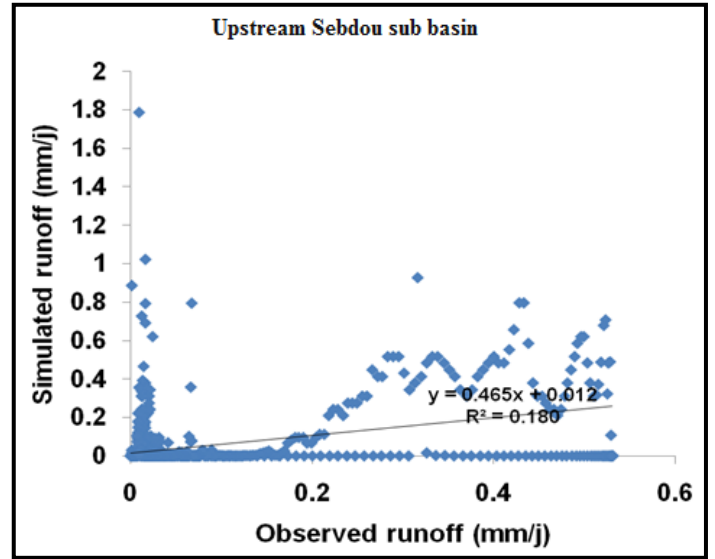
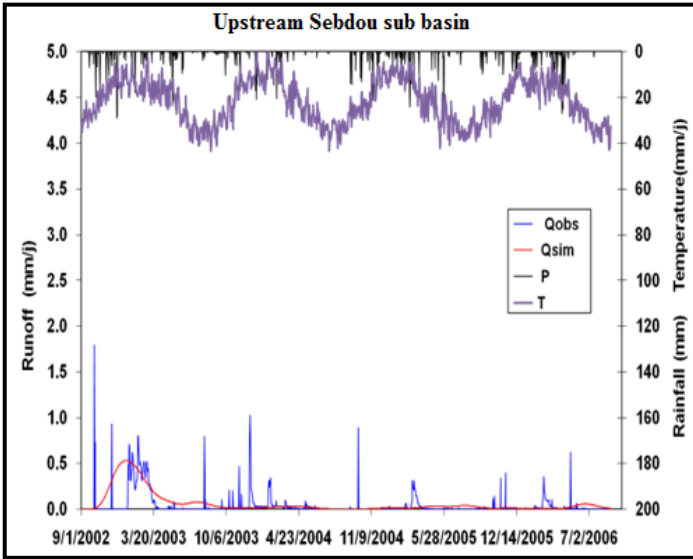
- **Results of validation**

The validation test period is applied over the period of (September 1, 2002 - August 31, 2006). The results of the validation, coefficient of determination R^2 , and the performance criteria are shown in the following table V.6:

Table V.6. Results of simulation for the validation during the period (2002-2005).

Validation period (2002-2005)		Five sub basins (Tafna basin)				
Parameters		Upstream Seb dou	Khemis	Wadi Boumessaoud	Chouly	Isser
Vegetation parameters	TT (°C)	11.1	8	-1	8.2	7.2
	CFMAX (mm/(d°C))	0.009	0.58	0.9	1.5	1
	SFCF [-]	0.01	1	0.1	0.47	0.05
	CFR [-]	0.4	0.01	6	0.8	0.5
	CWH [-]	0.05	0.01	1.5	15	1
	FC [-]	511	389	490	100	51
	LP [-]	0.151	0.17	0.03	0.68	0.01
	BETA [-]	1.13	1	0.97	2.4	80
Capture parameters	PERC [mm/d]	4.1	8.9	7	6.2	5.2
	UZL (mm)	5.13	11	0.01	11.1	7.8
	K0 [1/d]	0.99	0.99	0.99	0.99	0.99
	K1 [1/d]	0.99	0.7	0.99	0.54	0.63
	K2 [1/d]	0.12	0.05	0.39	0.26	0.1
	MAXBAS [d]	2.85	3	1.54	1.7	1.9
	Cet [1/°C]	2	1	2	1	2
Optimization criterion	Nash (Q)%	39.2	10.1	49.6	34.6	11.4
	Coefficient of determination R ²	0.18	0.10	0.53	0.38	0.14

For the model validation over the wet period (2002-2005), the values of the Nash are within the range of 10.1 and 49.6% and the coefficient of determination is within the range of 0.102 and 0.538. The validation results are not satisfactory and weaker than the calibration results, the degradation of the optimization criterion may due to the significant change between the calibration data (dry period) and the validation data (wet period). Comparing simulated with observed hydrograph (fig.V.6) shows significant fluctuations. The majority of peak runoff is underestimated in the model simulation, which made the optimization results less satisfactory for the validation period with the conclusion that the model is not well representing the runoff peaks.



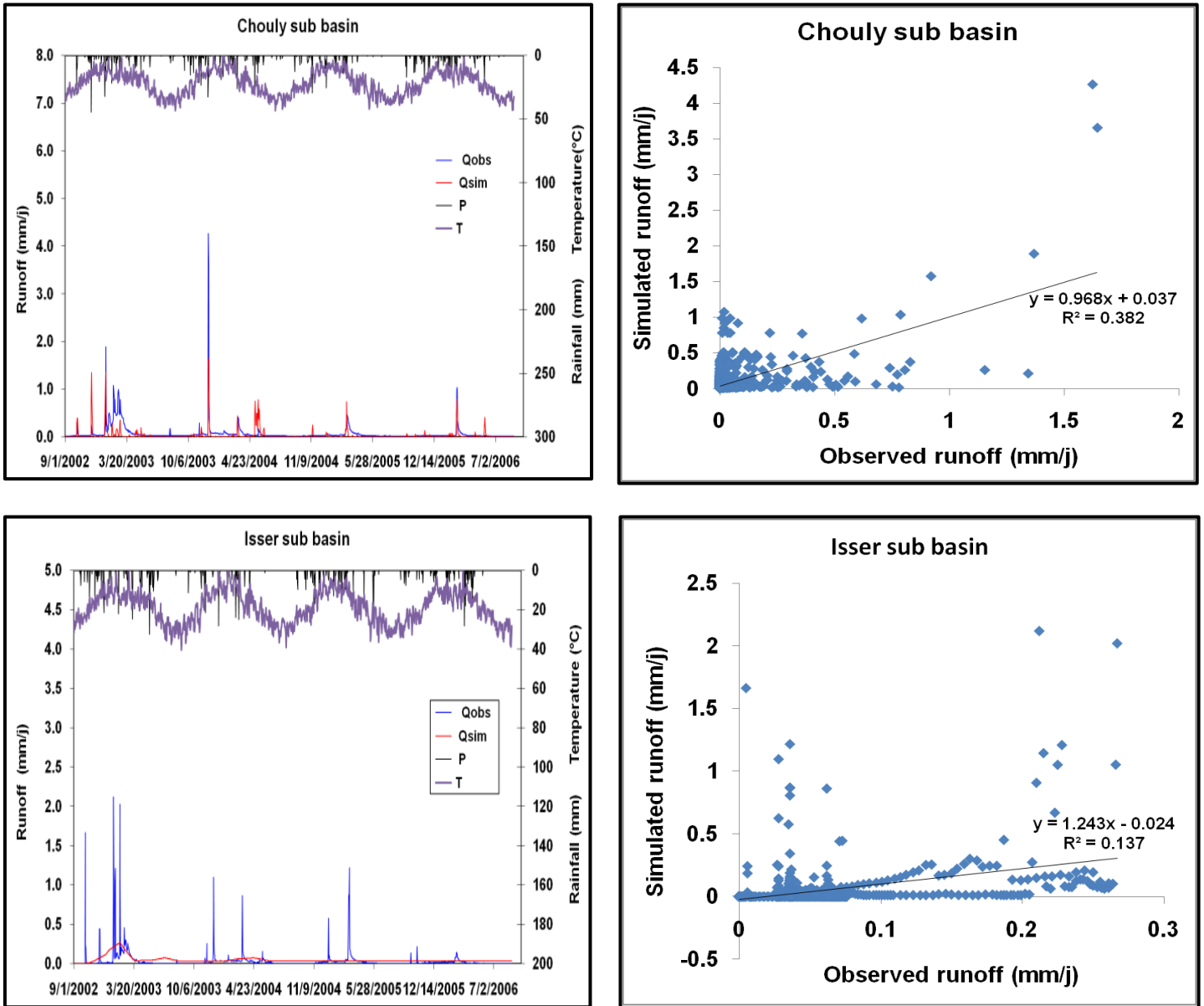


Figure V.6. Results of simulation and correlation for the validation during the period (2002-2005).

V.4.2.2. Simulation for second period (Dry/Dry)

- **Results of calibration**

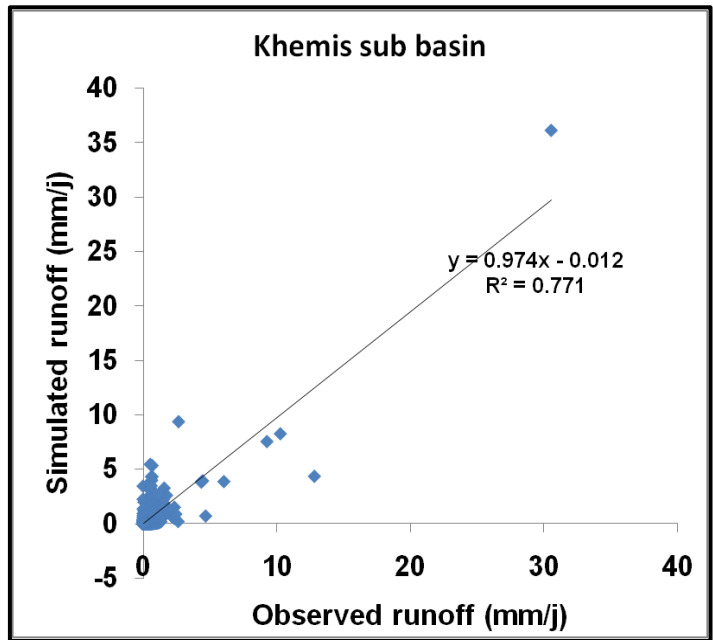
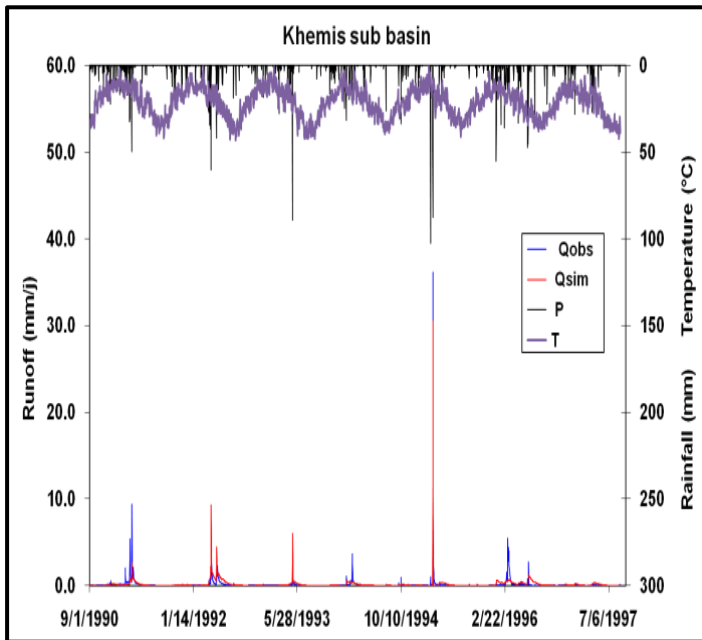
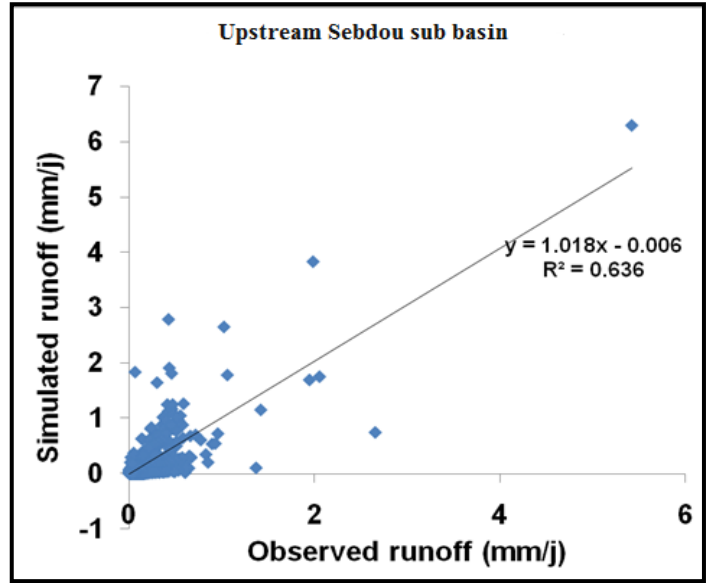
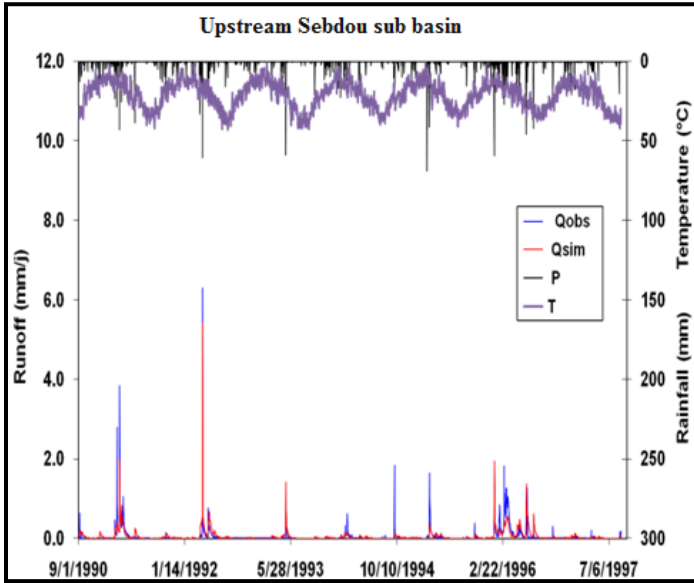
The calibration test period is applied over the period of (September 1, 1990 – August 31, 1997). The results of the validation, coefficient of determination R^2 , and the performance criteria are shown in the following table V.7:

Table V.7. Results of simulation and optimize parameters for the calibration during the period (1990-1996).

Calibration period (1990-1996)		Five sub basins (Tafna basin)				
Parameters		Upstream Sebdou	Khemis	Wadi Boumessaoud	Chouly	Isser
Vegetation parameters	TT (°C)	10.15	9.2	2.6	8.3	9.99
	CFMAX (mm/(d°C))	0.008	0.94	0.07	11.7	17
	SFCF [-]	0.008	0.3	0.3	0.7	0.43
	CFR [-]	1.84	1.3	0.1	11	0.55
	CWH [-]	0.34	21	0.1	12	1.3
	FC [-]	899	530	880	87	48
	LP [-]	0.1	0.05	0.001	0.02	0.02
	BETA [-]	0.9	0.71	0.76	15	33
Capture parameters	PERC [mm/d]	3.25	8.7	6.1	18.1	15.6
	UZL (mm)	4.44	13.2	0.04	0.4	0.6
	K0 [1/d]	0.99	0.99	0.99	0.99	0.99
	K1 [1/d]	0.99	0.99	0.99	0.99	0.99
	K2 [1/d]	0.12	0.5	0.38	0.4	0.07
	MAXBAS [d]	2.85	2.9	1.49	1.68	1.93
	Cet [1/°C]	2	0.4	0.9	1	2
Optimization criterion	Nash (Q)%	63.5	77.1	65.9	80.8	81.1
	Coefficient of determination R ²	0.64	0.77	0.67	0.82	0.82

The calibration performance of the HBV light model model at dry period(1990-1996) on five sub basins of the Tafna basin showed acceptable results, with the Nash ranging from (63.5 and 81.1%), and with the coefficient of the determination ranging from (0.64 and 0.82) (tab.V.7). The hydrographs of the observed runoff and the simulated runoff (fig.V.7) showed that the model is well calibrated in this time period, with the observation of proportion between the two runoffs and the rainfall variations, unless the tendency to underestimate the peaks of simulated runoff due to the contribution of underground water to the detriment of surface runoff. An increase in the optimized values with increasing altitudes is therefore reasonable (Seibert, 2000).

The low value of the SFCF (0.008) and higher values of FC (899) were defined at Upstream Sebdou due to characteristics of area (mountainous) and geology as explained in above section. The recession coefficients (K2) has low value (0.01 1/d) with large basin size (Isser sub basin, 696.1 km² due to a wetter and more uniform hydrograph in a larger basin, (Seibert et al., 2000), however also the geological differences with an extensive porous aquifer in the main valley of the basin has also main role in this basin.



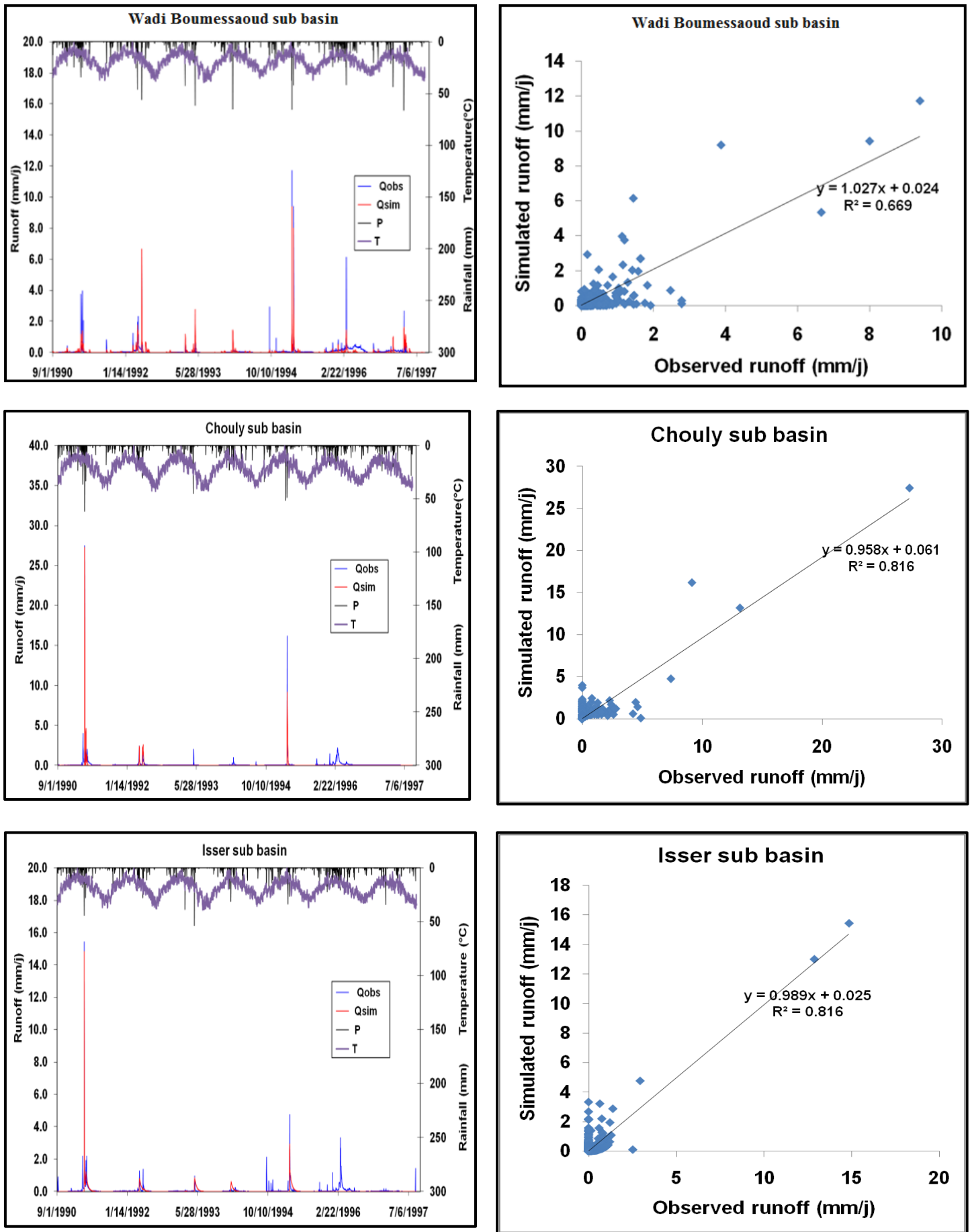


Figure V.7. Results of simulation and correlation for the calibration during the period (1990-1996).

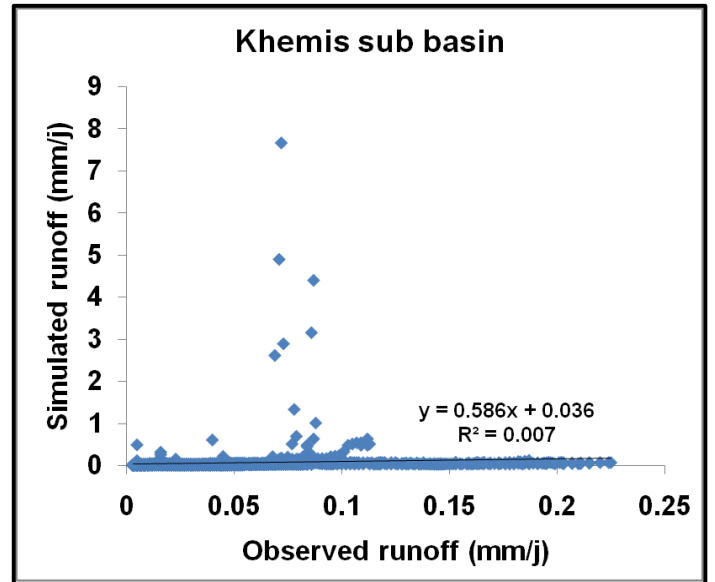
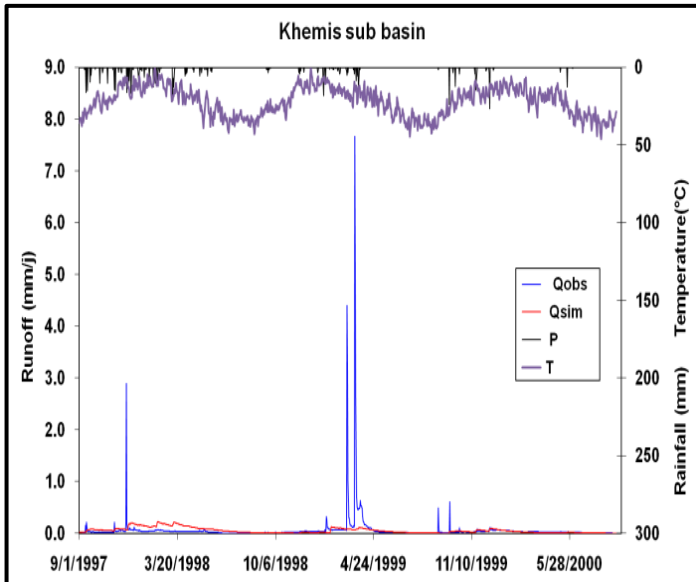
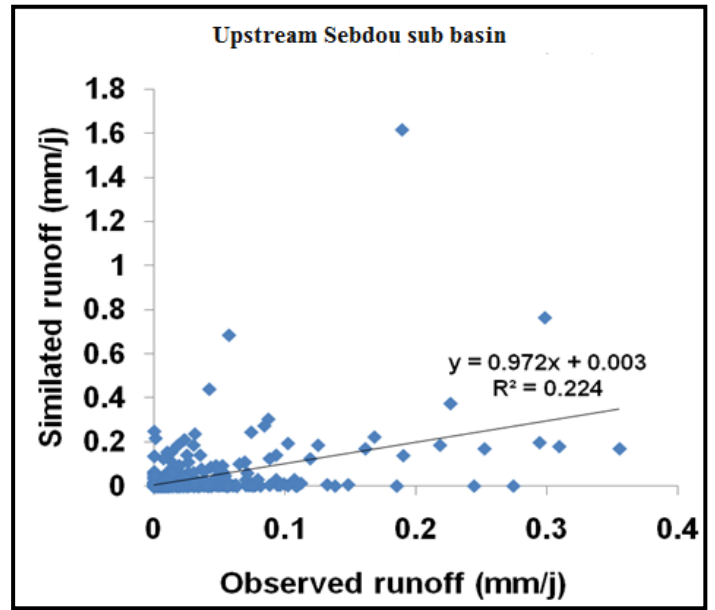
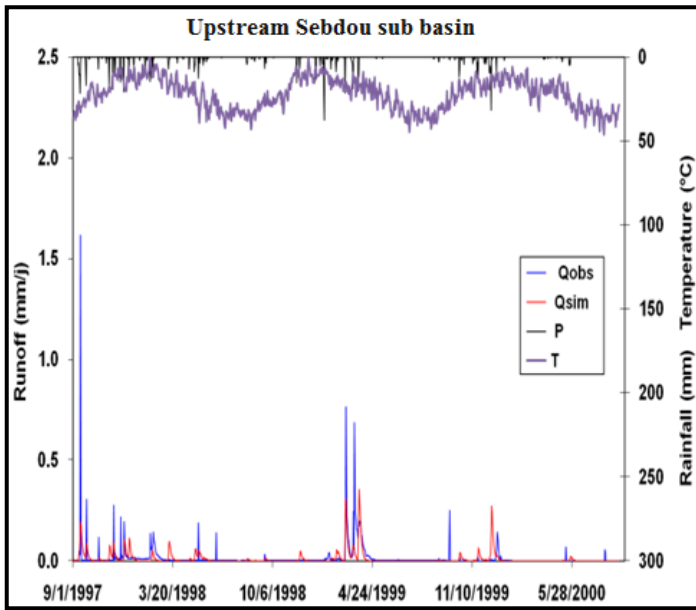
• **Results of validation**

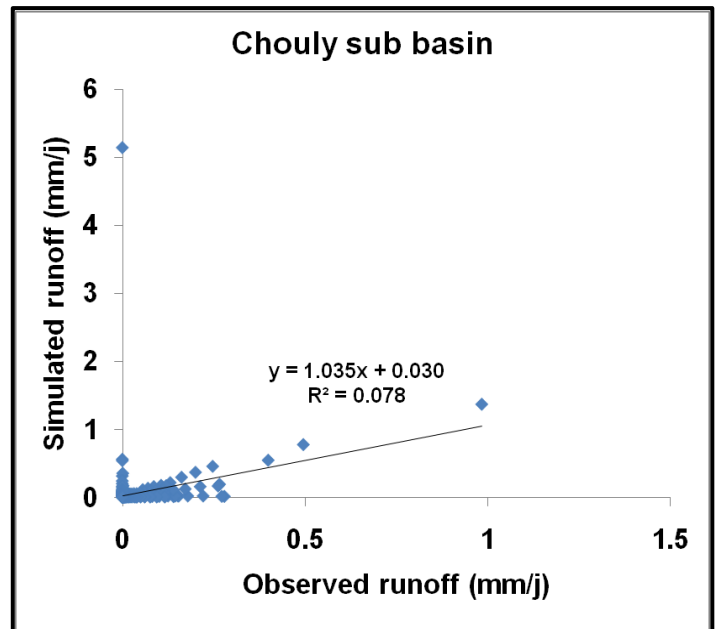
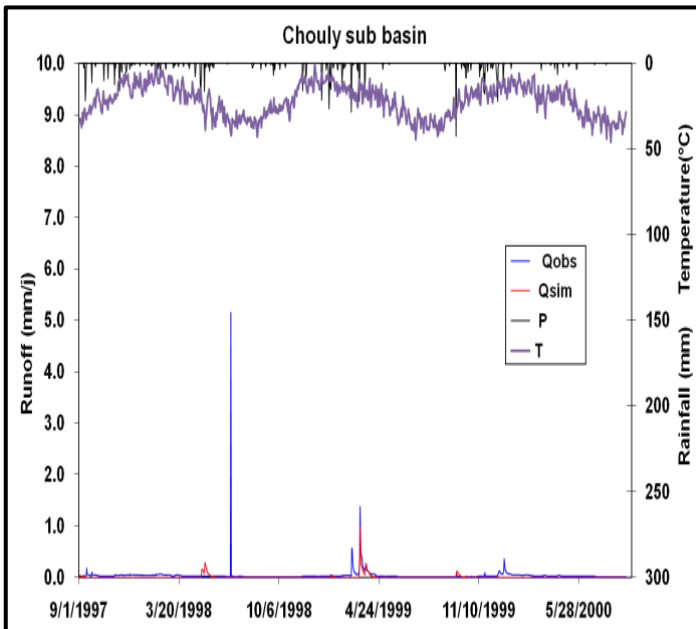
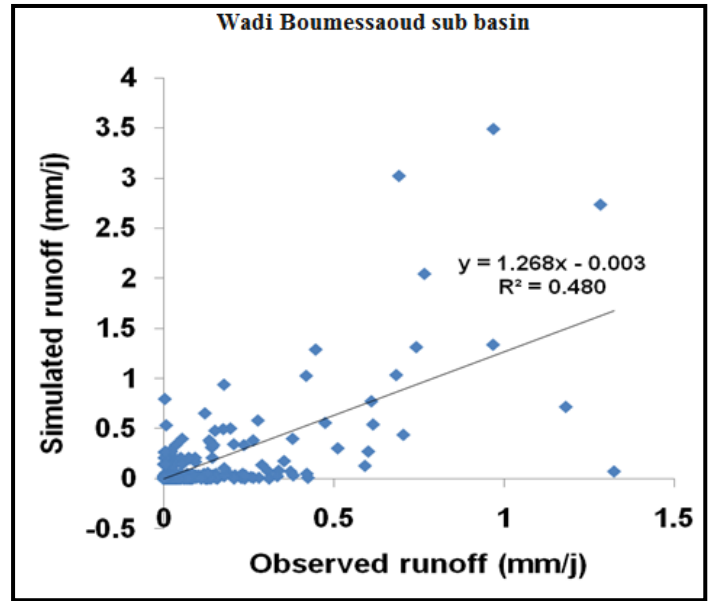
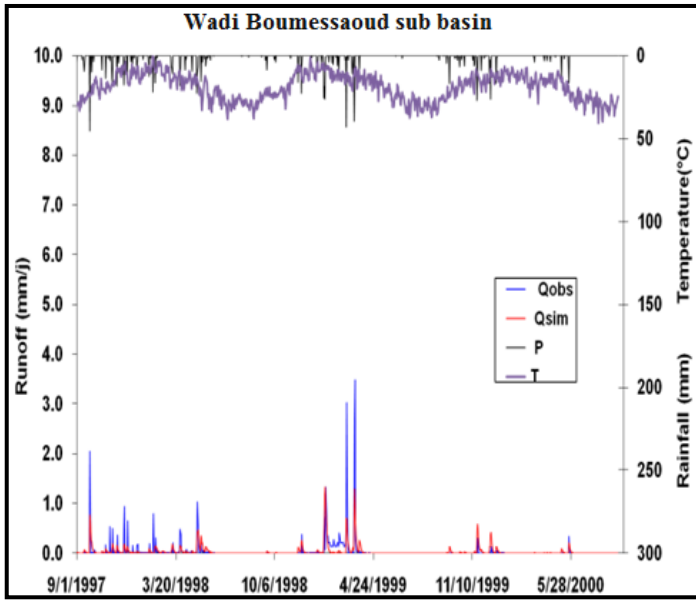
The validation test period is applied over the period of (September 1, 1997 - August 31, 2000). The results of the validation, coefficient of determination R², and the performance criteria are shown in the following table V.8:

Table V.8. Results of simulation for the validation during the period (1997-1999).

Validation period (1997-1999)		Five sub basins (Tafna basin)				
Parameters		Upstream Sebdou	Khemis	Wadi Boumessaoud	Chouly	Isser
Vegetation parameters	TT (°C)	10.15	9.2	2.6	8.3	9.99
	CFMAX (mm/(d°C))	0.008	0.94	0.07	11.7	17
	SFCF [-]	0.008	0.3	0.3	0.7	0.43
	CFR [-]	1.84	1.3	0.1	11	0.55
	CWH [-]	0.34	21	0.1	12	1.3
	FC [-]	899	530	880	87	48
	LP [-]	0.1	0.05	0.001	0.02	0.02
	BETA [-]	0.9	0.71	0.76	15	33
Capture parameters	PERC [mm/d]	3.25	8.7	6.1	18.1	15.6
	UZL (mm)	4.44	13.2	0.04	0.4	0.6
	K0 [1/d]	0.99	0.99	0.99	0.99	0.99
	K1 [1/d]	0.99	0.99	0.99	0.99	0.99
	K2 [1/d]	0.12	0.5	0.38	0.4	0.07
	MAXBAS [d]	2.85	2.9	1.49	1.68	1.93
	Cet [1/°C]	2	0.4	0.9	1	2
Optimization criterion	Nash (Q)%	21.0	0.2	42.8	4.3	11.3
	Coefficient of determination R ²	0.22	0.01	0.48	0.08	0.14

The analysis of the validation results at dry period (1997-1999) revealed that the values of the optimization parameters obtained are weak for Nash ($\leq 42.8\%$), and also for coefficient of determination (≤ 0.48) compared to those obtained in the calibration phase with the same calibrated parameters of the model. The degradation in the values of the optimization parameters can be explained by the irregularity of the rainfall during this period and the state of the soil, where the observed runoff are very high than the simulated runoff (fig.V.8), it showed that the model decrease the runoff degree for periods of the low rainfall.





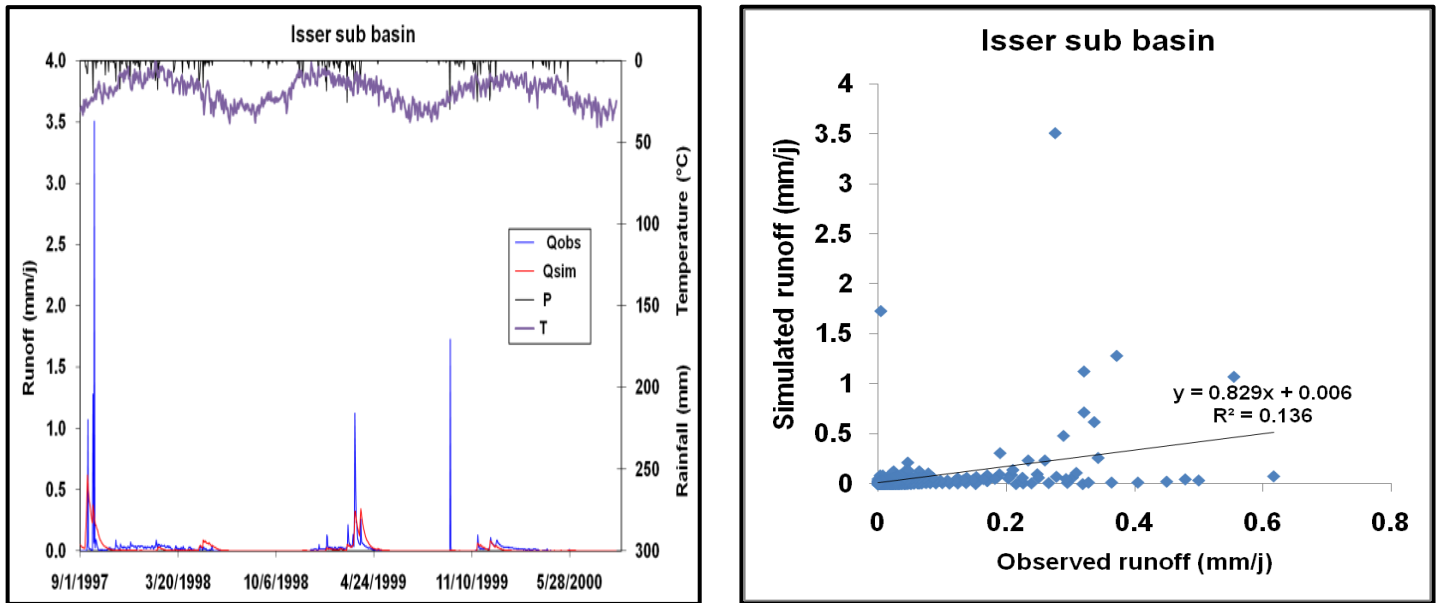


Figure V.8. Results of simulation and correlation for the validation during the period (1997-1999).

V.5. Comparison of models performance

The comparison of the performance of the two models in the two phases (dry/wet period, dry/dry period) for the five sub basins studied showed that the values of the Nash criteria and the coefficients of determination between the observed runoff and the runoff simulated during the calibration period have good results for both models at Khemis, and Isser sub basins within values (68.1, 76.6.1%), except Chouly (64.8%) for first calibration phase (1990-1999) with HBV light. That means the two models simulate the runoff well and indicate better performance despite the underestimation of runoff in peak values due to that these models don't consider the contribution of the groundwater in the excess of runoff (geology aspect). Although certain values in the simulation seem to compensate for each other which gave similarity of distribution between observed and simulated runoff.

Through both calibration phase, the HBV light showed in general good results than GR4J with improvement in the Nash between the simulated and observed that can be explained to the important of number of the optimizable parameters (HBV light with its 15 parameters), for example the snowmelt parameter shows the influence of the effectiveness on the simulation process, Where the hydrograph of simulated and observed runoff with temperature explains the null runoff during of the period of the study, which show the HBV light contribute in semi arid. It should be noted that these same observations have been described in the work of Dakhlaoui (2014).

The extension of the number of parameters on large basins made it possible to find good simulations (Seibert, 1999a), as shown in Isser, and Khemis sub basins (696.10, 342.22 km²) compared to Wadi Boumessaoud sub basin (108.76 km²). The low Nash results for calibration periods (1990-1999, 1990-1996) were observed at Wadi Boumessaoud sub basin (59.3, 60 %) for GR4J, and at Upstream Sebdou sub basin (63.6, 63.5%) for HBV light, this can be explained by the decrease in flows during the dry period experienced by the Tafna basin in 1990's.

The great results of Nash were defined with GR4J in wet period (2002-2005) with (62.5, 64.9 and 67.9%) at Chouly, Wadi Boumessaoud, and Khemis sub basins respectively. The average value of Nash (56.3%) was at Isser sub basin, while the lowest values were at Upstream Sebdo sub basin (50.9 %), and fairly acceptable results of simulation with dry period (1997-1999) within range of Nash (49.3 - 62.8 %). The HBV light showed weak results for both period of validation (<49.6%). We notice that simulation of HBV light gave a little improvement in wet period (2002-2005) within range (10.1- 49.6%) compared with dry period (2002-2005) within range (0.2 - 42.8 %) with same sub basins.

In general, the validation phase with HBV light models shows unacceptable results in both periods, this can be linked to the rainfall irregularity of the periods, or to the quality of the data which can influence the simulation phase and the output of the model, due to the precision errors of the measuring instruments, the precision problems of the extreme runoff.

V.6. Comparison between two validation periods for GR4J

The two validation periods (2002-2005, 1997-1999) of the GR4J model for the five studied sub basins of the Tafna basin, show that for the first period (wet period), the Nash values were good reaching to 7.9 %, the same case for the coefficient of determination reaching to 0.683. Although these values are lower than those of the calibration, the model gave good performances with most sub basins.

The performance of model at dry period showed a little decrease of the optimization criterion compared to the first period, They can also be explained by difficulty of the model producing the simulated runoff similar to the observed runoff which has low values (near to zero) in short period (3 years) compared to the calibration period (7 years) as it was enabled to achieve a fit between rainfall and observed runoff where the values compensates each other reflecting good performance. The results of two validation periods were shown in figure V.9.

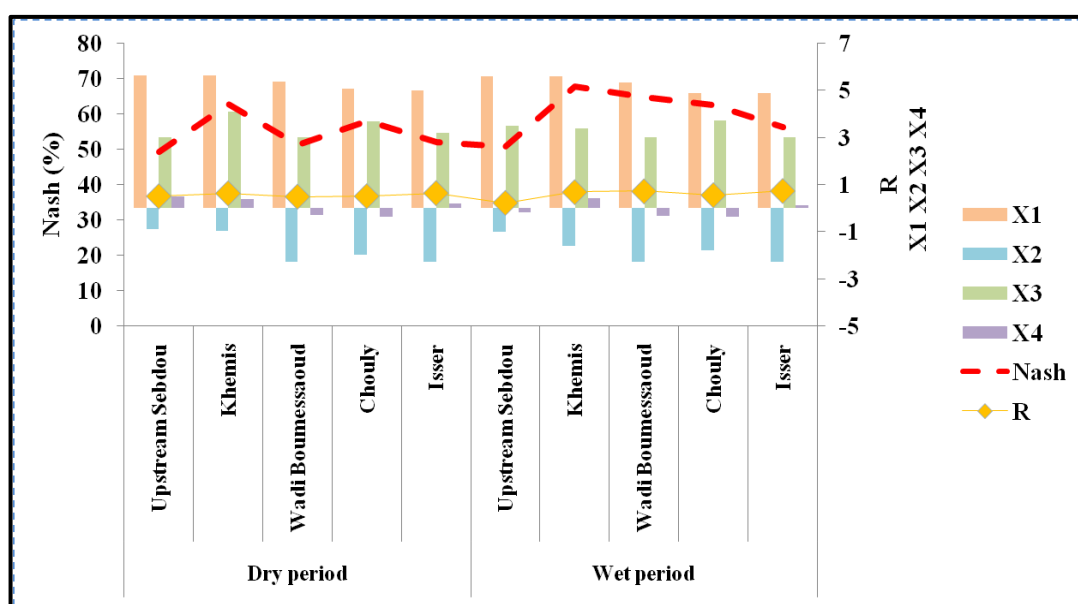


Figure V.9. Validation results for wet and dry periods for GR4J.

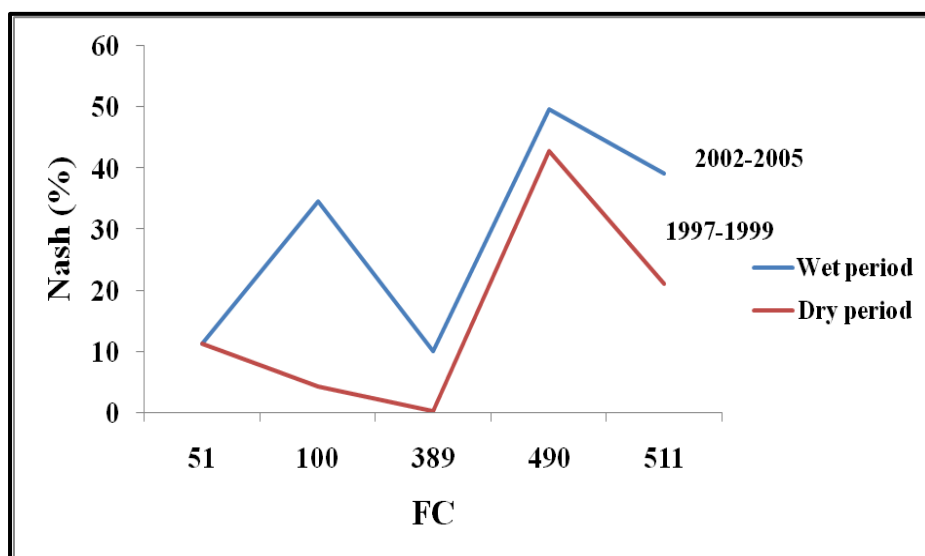
V.7. Comparison between parameters and performance of HBV light

In general, the HBV light is performing good in the both calibration period, this result indicated that the model generally was able to reproduce the observed runoff. However, it does show good improvement in validation for wet period (10.1-39.2%) compared to dry period which showed deteriorate in Nash values (0.2-21%), where the peak flows were not always simulated perfectly over this period, probably due to the calibration parameters that do not match the data distribution in the validation, i.e. the parameters values are specific to a certain period of time, in addition to the data quality caused by the errors in precision of measuring instruments, problems of precision in the extreme runoff, can influence the simulation and the model output, or may be due to the contribution of underground water at the expense of surface runoff.

The calibration procedure with HBV light reveal three important parameters (the snowfall correction factor (SFCF), the maximum soil moisture storage (FC), and the groundwater storage coefficient, (K2)). The lower and the higher values of the maximum soil moisture storages showed weak performance for the dry period compared to wet period, which is reflecting the decrease of the rainfall amount that recharging the upper zone of storage during the dry period, or the recharge from the groundwater to upper reservoir, which is difficult to conceptualized with model depending on the output data (rainfall, runoff, temperature, evapotranspiration), specially with parameter values (calibration period) representing different data and time series.

The improvement of performance of the model in the dry period are compatible with low values of K2 that is representing the low value of water in the ground, which contributed to the production the simulate runoff closer to observed runoff. The increase of K2 showed an improvement of the model performance in wet period, despite the decrease of water to ground. The model however retained the possibility of producing closer runoff to observed runoff (fig. V.10).

In general, the model showed weak improvement in performance. The minor differences between the two periods and between the sub basins could be related to the size and elevation, as well as their hydro-geological regimes.



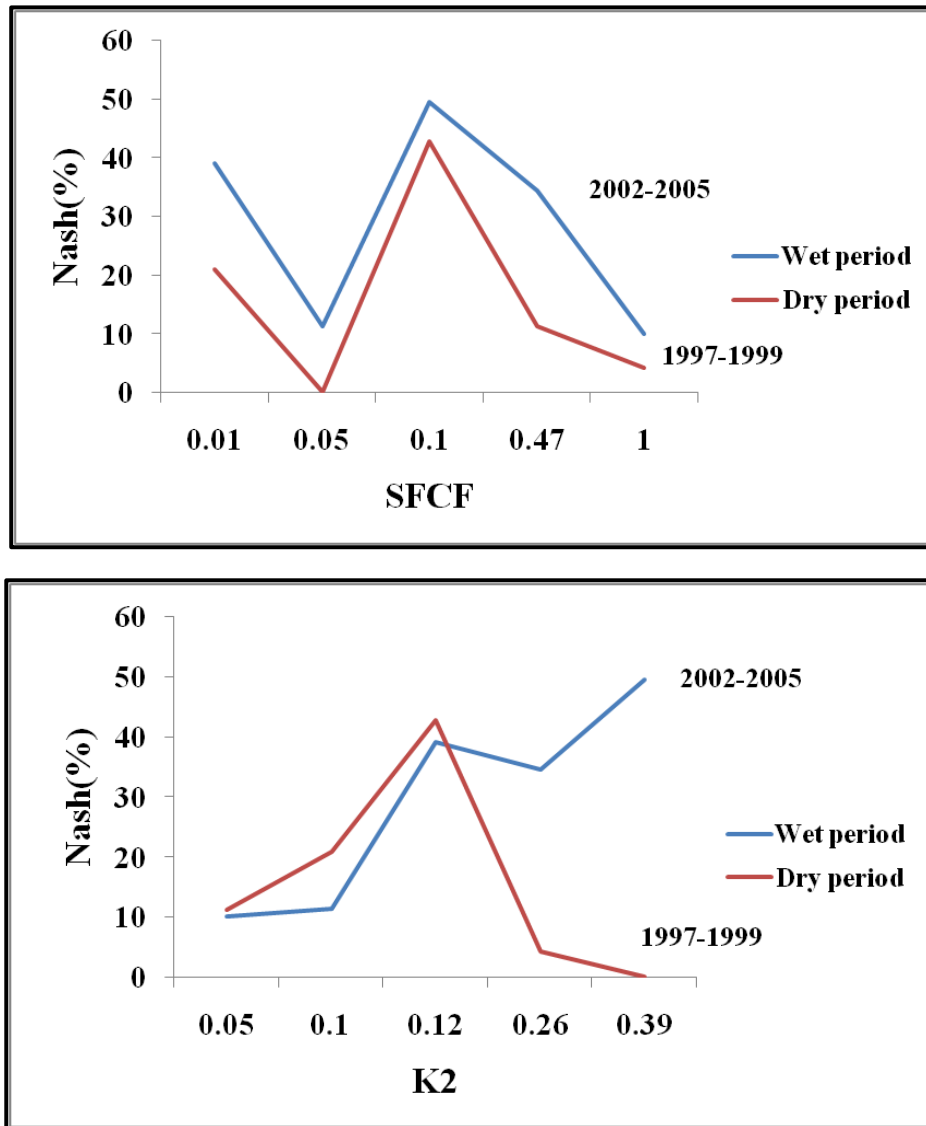


Figure V.10. Comparison of parameter FC, SFCF, K2 and Nash for the wet and the dry periods for HBV light.

V.8. Comparison between the simulated runoff of the GR4J and HBV light models

V.8.1. Comparison between the simulated runoff of the GR4J and HBV light models in the calibration phase

The coefficients of determination between the simulated runoff of the two models GR4J, and HBV light during calibration (1990-1999) and (1990-1996) showed a good correlation (> 0.6 , > 0.5 , respectively), the first period of calibration indicate a little improvement than the second phase, and it is clearly shown in Upstream Sebdu, Khemis, and Isser (0.75, 0.84, 0.73) for the calibration (1990-1999) compared to the period (1990-1996), which showed with the same sub basins the values (0.69, 0.75, 0.65), that can be explained by the difference of the length of the data series between the two periods.

The figures V.11, V.12 showed that the majority of the points surround the line with the exception of a few points. This means that the models have the similarity in terms of response to produce the simulated runoff with minor differences between the models may due to the snow parameter, where the ETP and temperature are used with HBV light.

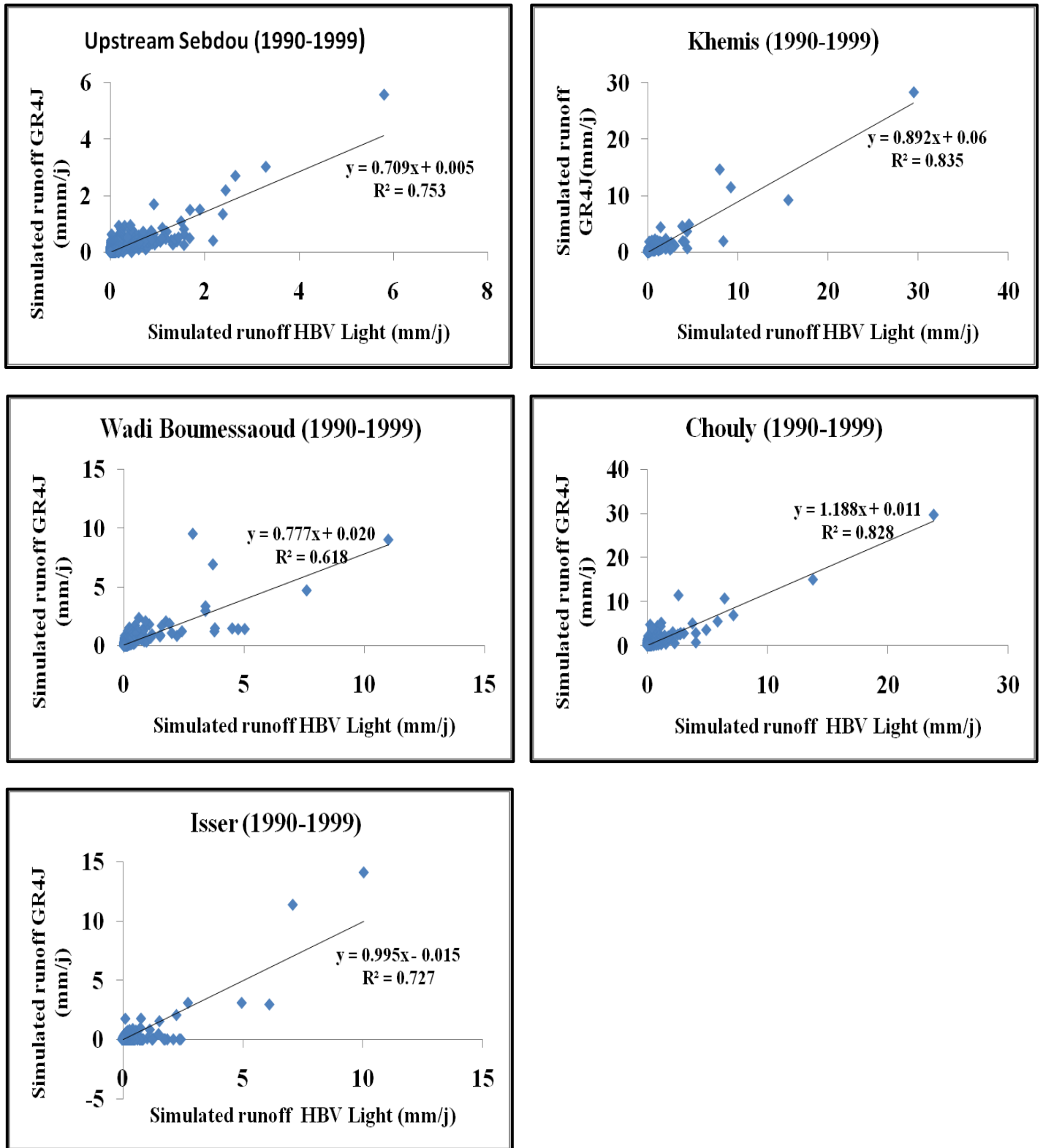


Figure V.11. Correlation between the simulated runoff of the two models in the calibration (1990-1999).

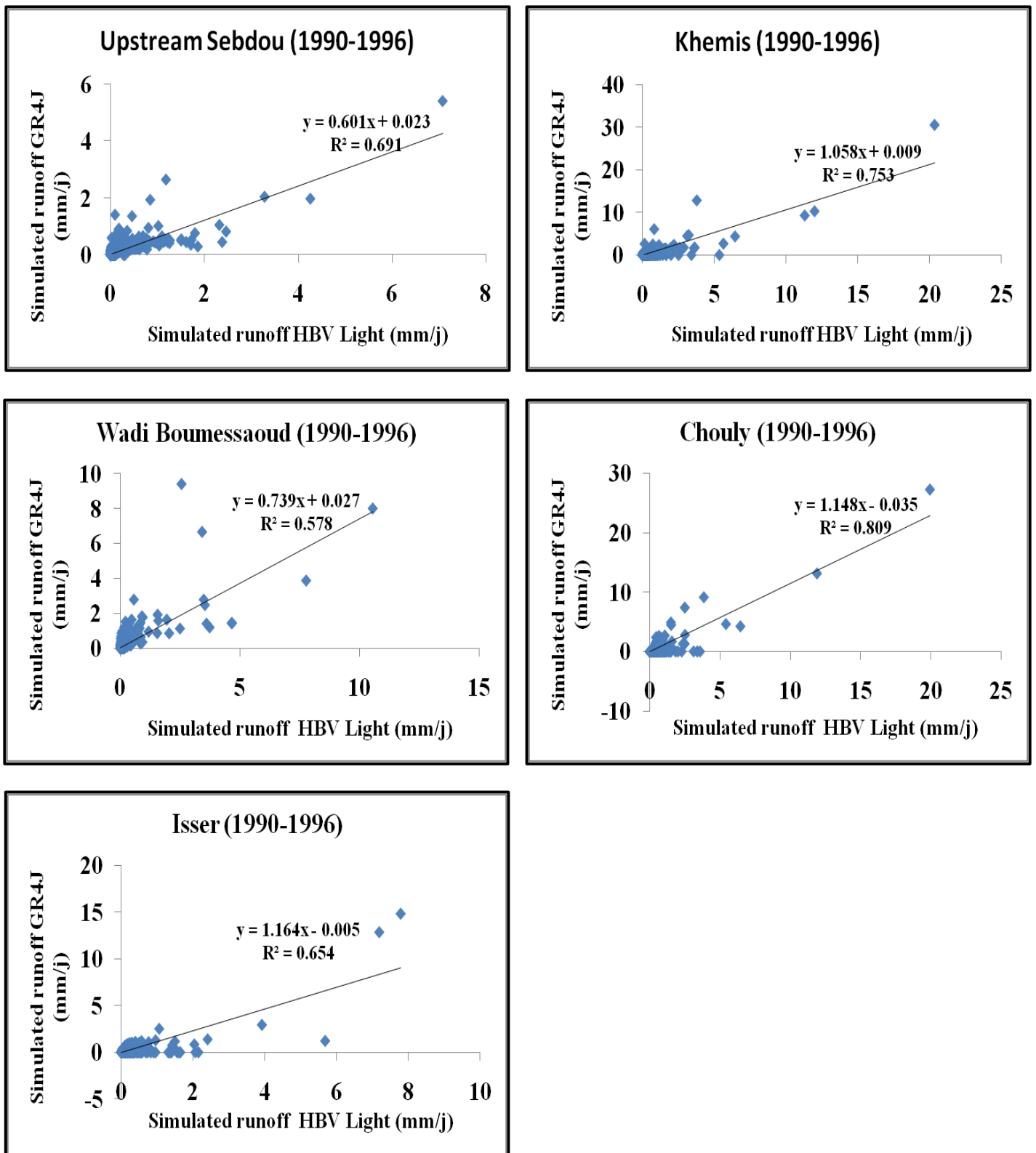
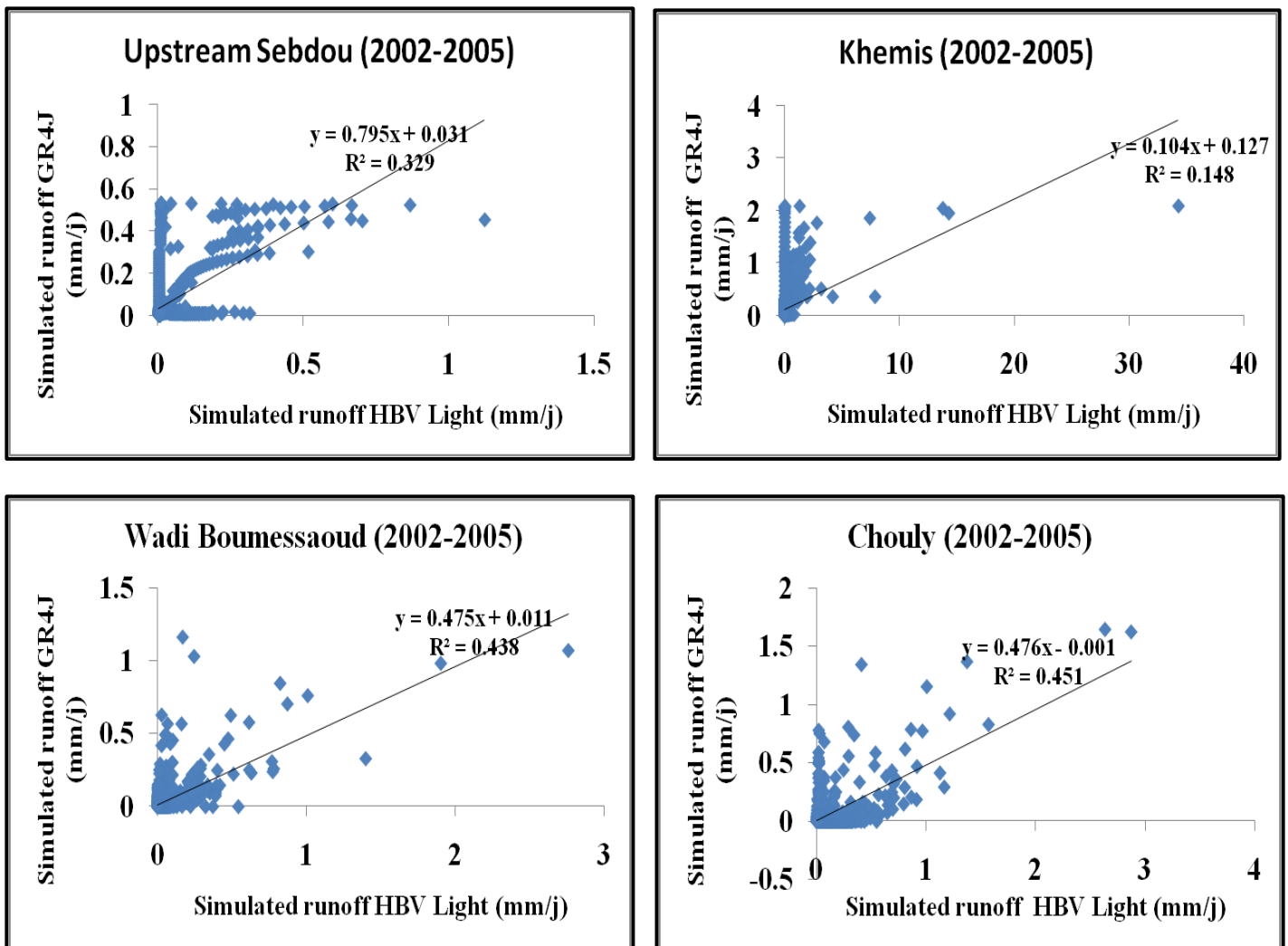


Figure V.12. Correlation between the simulated runoff of the two models in the calibration phase (1990-1996).

V.8.2. Comparison between the simulated runoff of the GR4J and HBV light models in the validation phase

The coefficients of determination during the two validation periods (2002-2005), (1997, 1999) (fig. V.13, V.14), showed deterioration, where the two models showed weak performance during these periods, this due to the difficulty of the two models in producing the simulated runoff similar to observed one with the values of calibration parameters, where these parameters are manually optimized fit certain period to give good results, and in addition to the difference of distribution of input data from period to other.



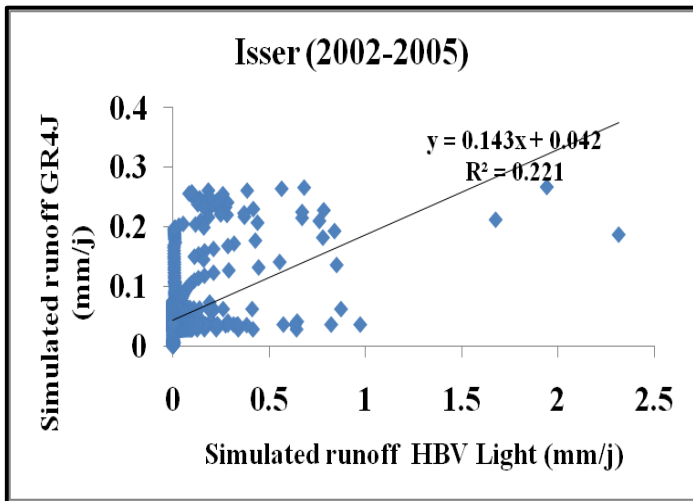
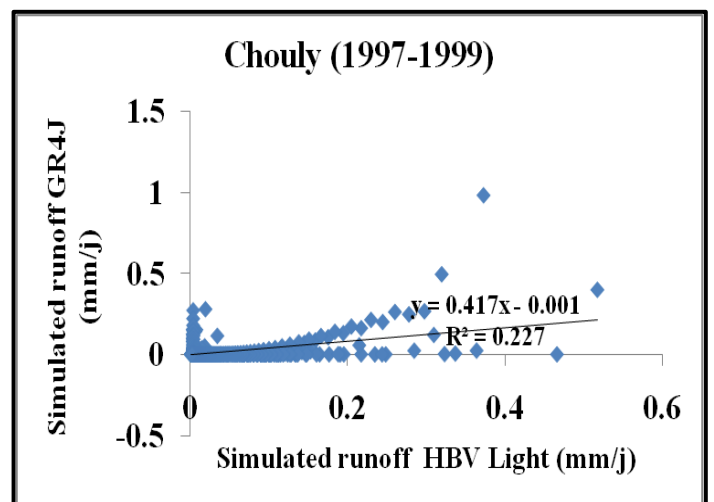
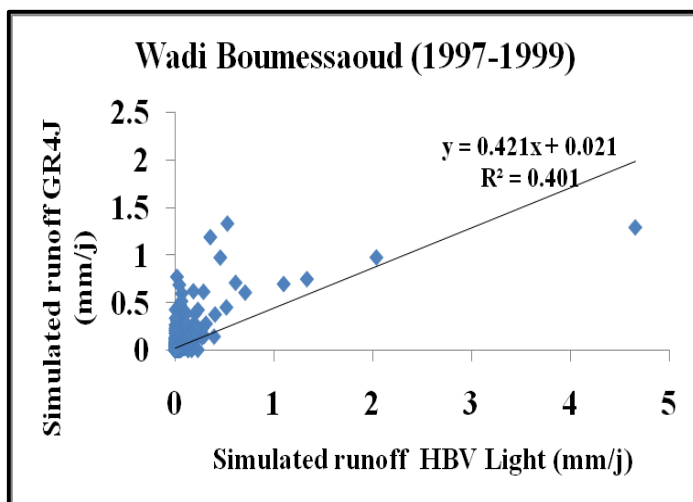
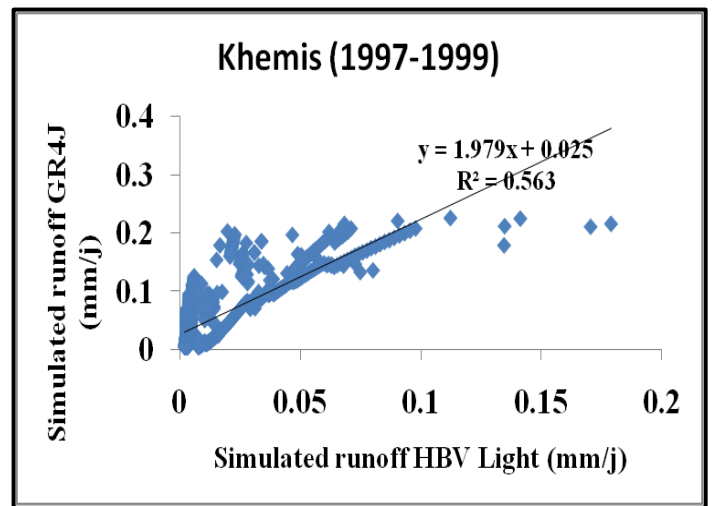
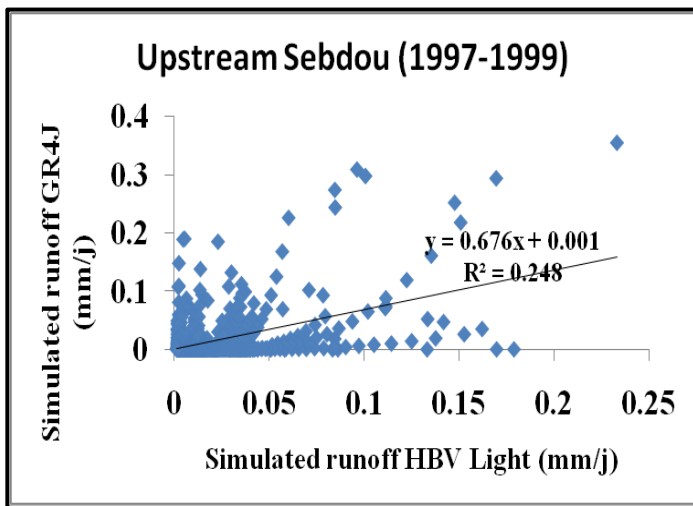


Figure V.13. Correlation between the simulated runoff of the two models in the validation phase (2002-2005).



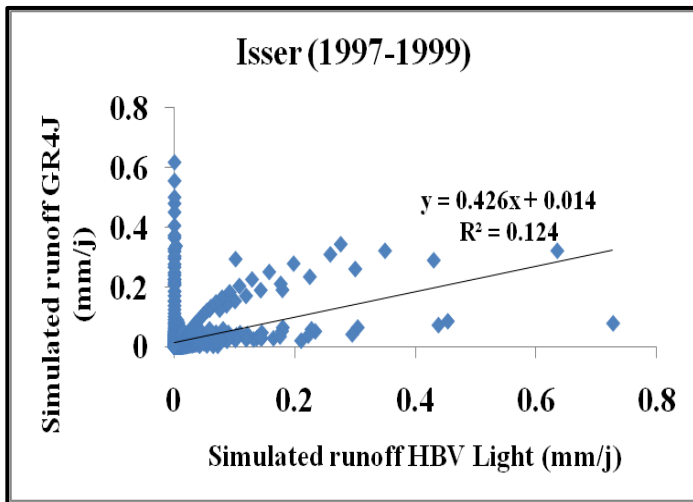
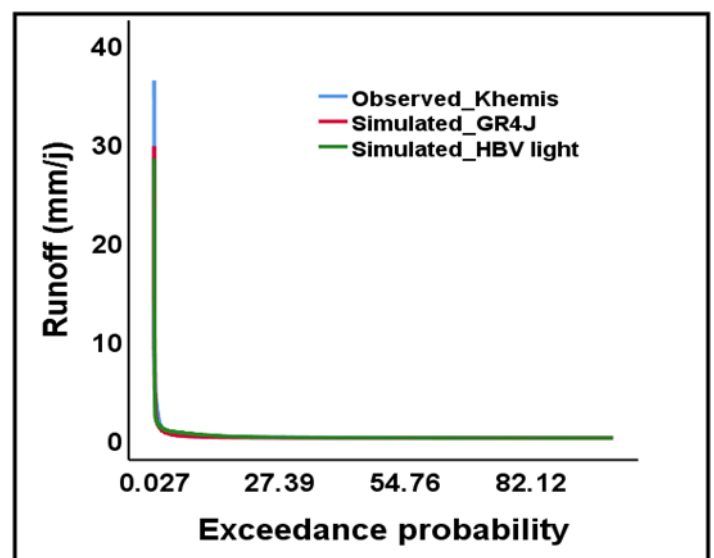
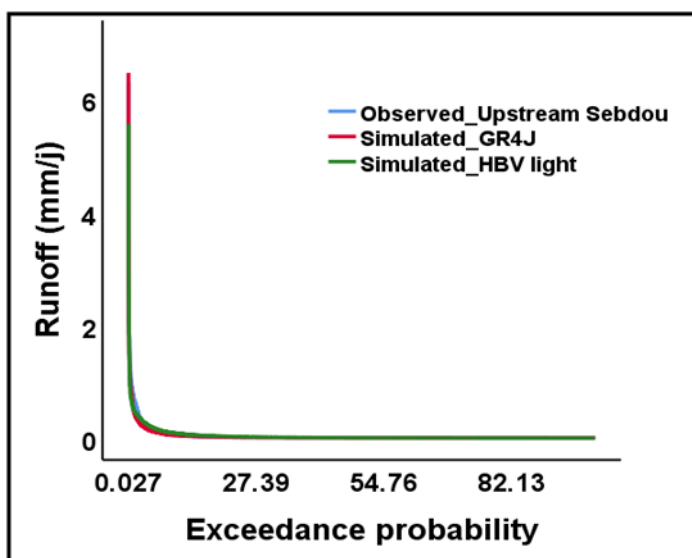


Figure V.14. Correlation between the simulated runoff of the two models in the validation phase (1997-1999).

V.9. Estimating the exceedance probability and cumulative observed runoff compared with simulated runoff from GR4J, HBV light

V.9.1. Estimating the exceedance probability and cumulative observed runoff compared with simulated runoff from GR4J, HBV light for both the calibration periods

Percent exceedance probability curve gave better explanation of how well the model produces the observed runoff during both calibration. The flow duration curve (fig.V.15, fig.V.16) plotted for all the study sub basins. GR4J performs better in the both calibration period in Upstream sebdou, and Wadi Boumessaoud sub basins, and only produces the runoff similar to observed for first period in Khemis sub basin. In Chouly sub basin, all the two models showed similar exceedance probability for the both calibration period. Where in Isser sub basin, HBV light showed exceedance plot close to observed runoff than GR4J for both calibration. GR4J and HBV light produce low runoff frequency closely.



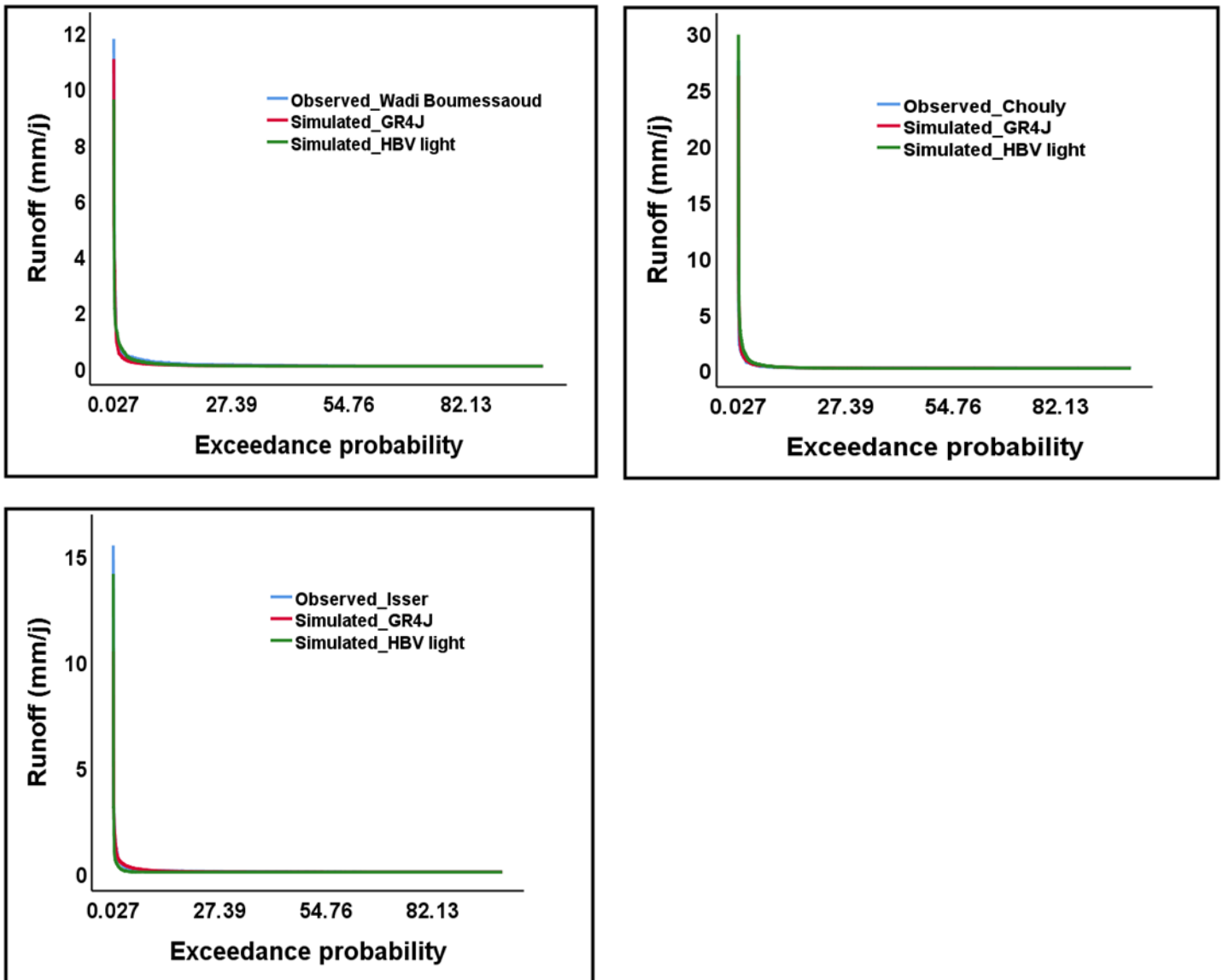
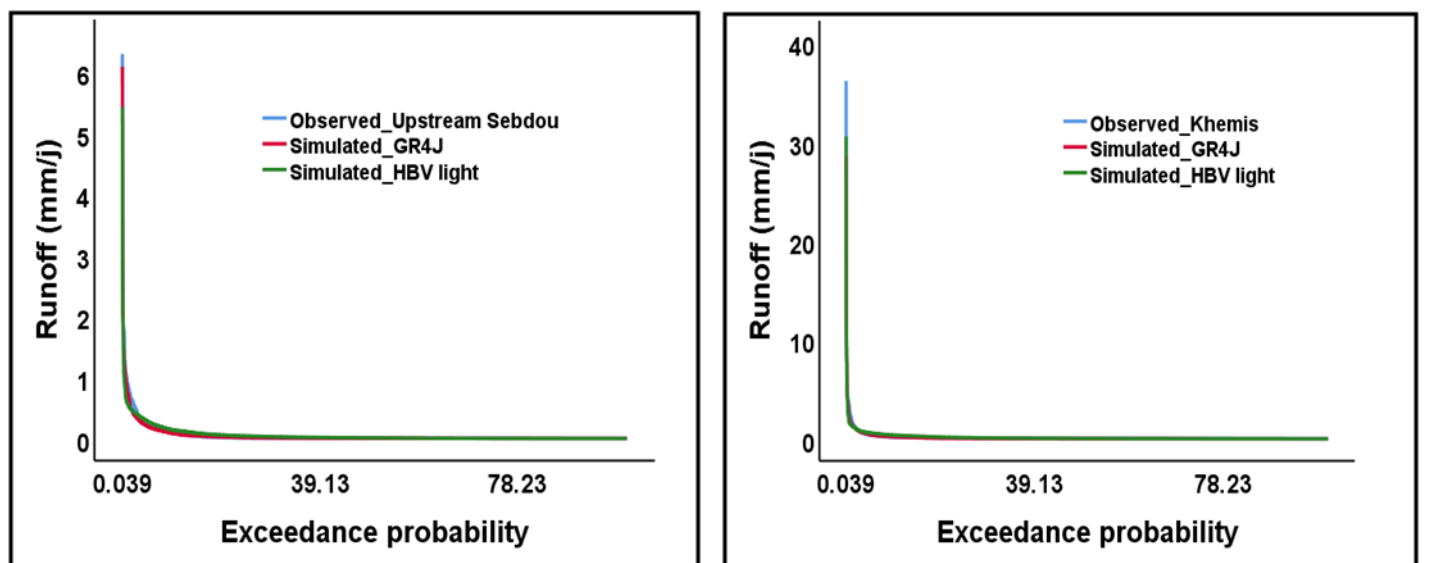


Figure V.15. Exceedance probability curve for observed and simulated runoff from GR4J, HBV light for calibration (1990-1999).



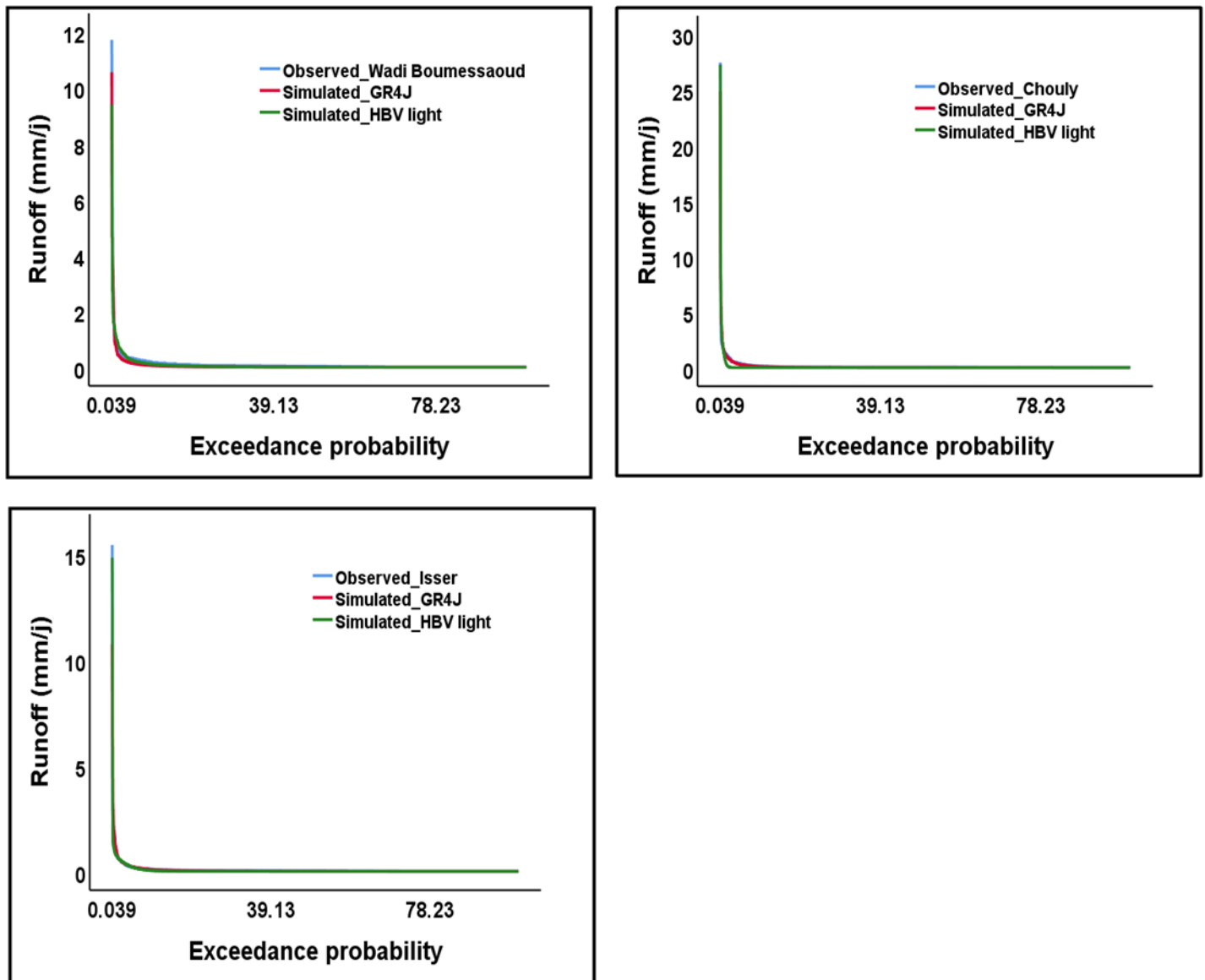


Figure V.16. Exceedance probability curve for observed and simulated runoff from GR4J, HBV light for calibration (1990-1996).

Cumulative runoff curve was plotted of two models for both calibration in all sub basins to understand the best-fit model to the observed runoff (fig.V.17, V.18). For both calibration 1990-1999, and 1990-1997 showed similarity results for cumulative analysis, it notice that HBV light fits well with observed runoff in the sub basin Upstream Sebdu, Khemis, and Wadi Boumessaoud. In Chouly, GR4J fitted well with observed runoff. However, the Isser sub basin results showed that HBV light underestimated values of the runoff which was reason for not fitting to the observed during the first calibration period, while in the second calibration, it showed improvement of this model than the GR4J estimation to runoff.

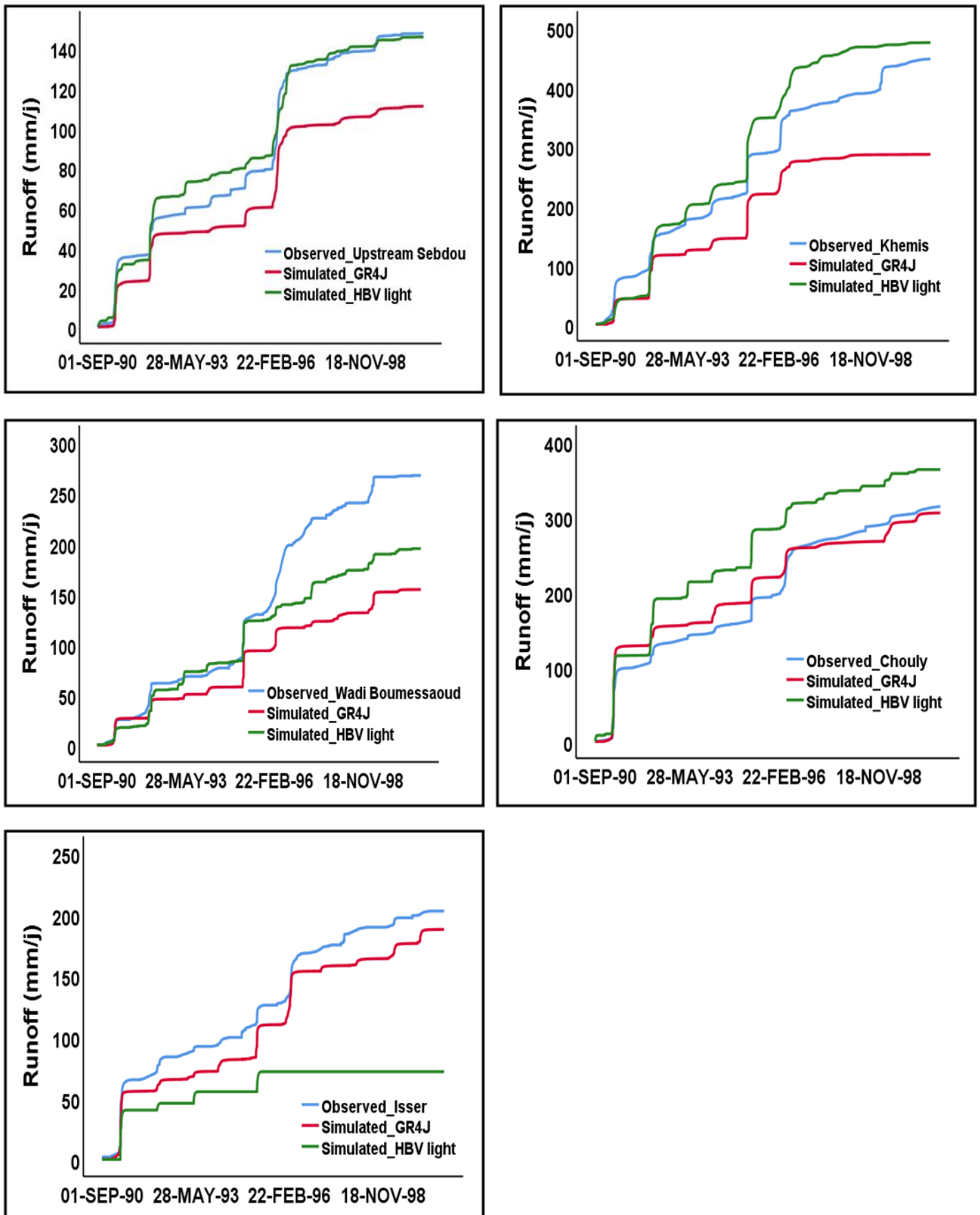


Figure V.17. Cumulative runoff for observed and simulated runoff from GR4J, HBV light for calibration (1990-1999).

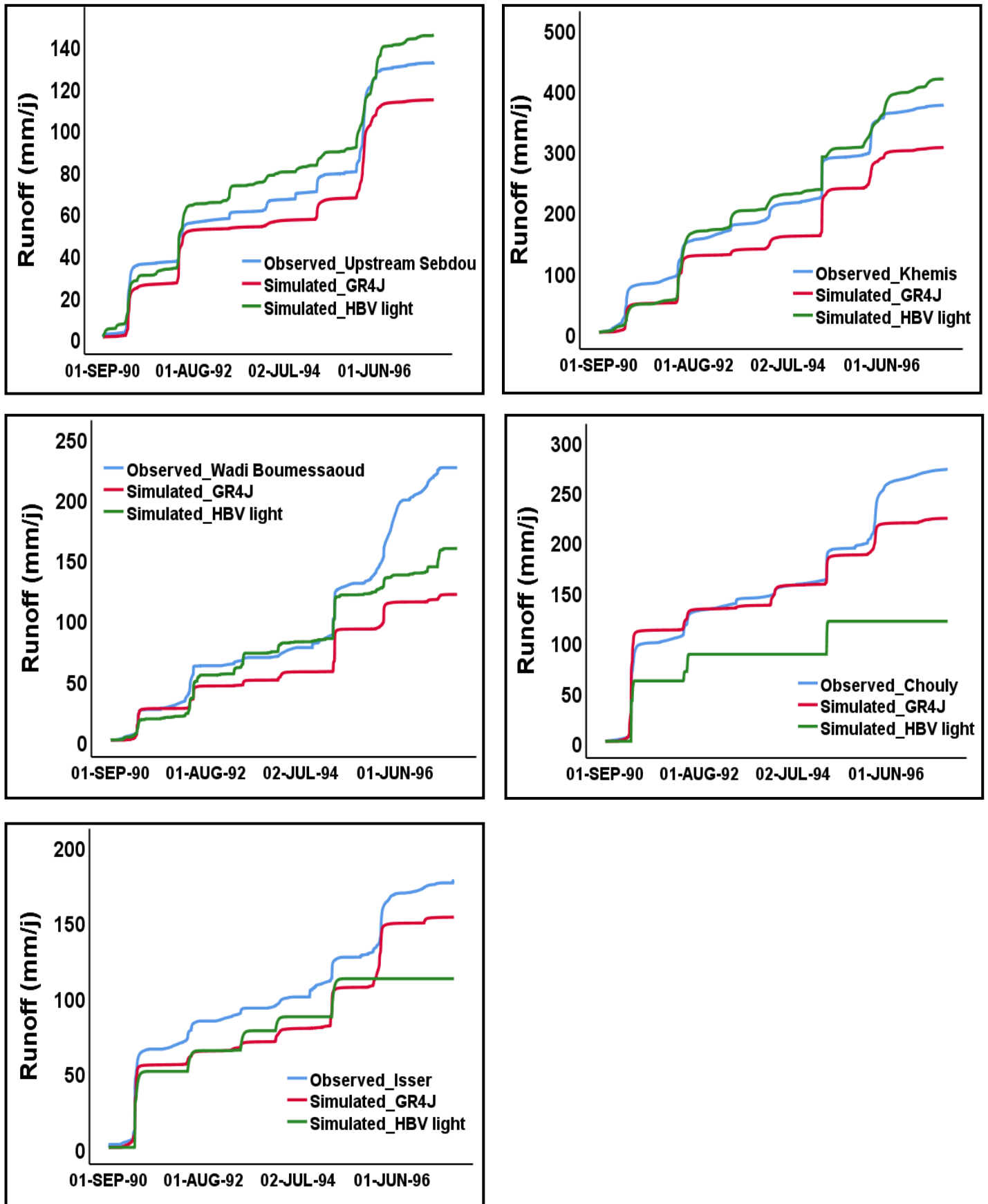
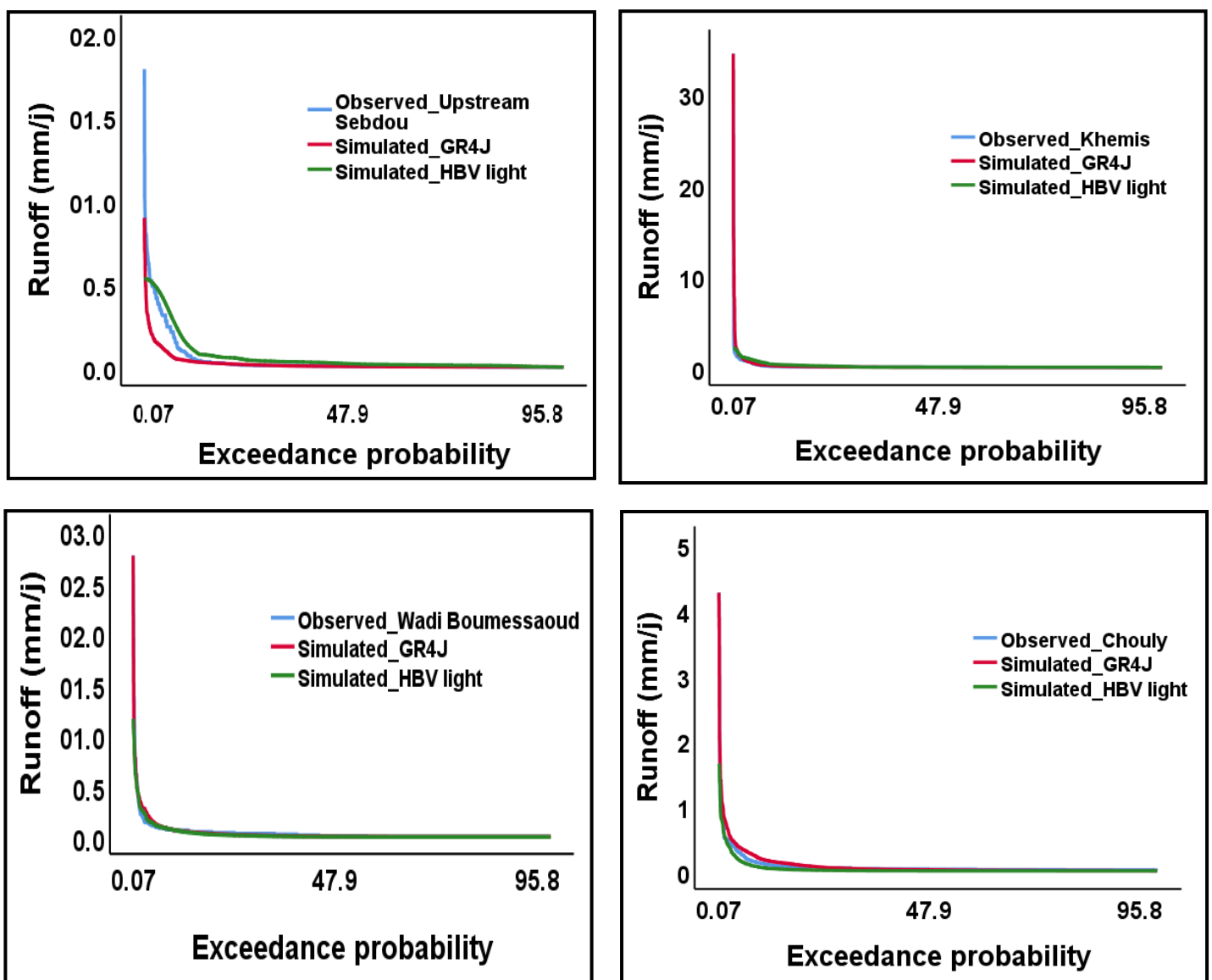


Figure V.18. Cumulative runoff for observed and simulated runoff from GR4J, HBV light for calibration (1990-1996).

V.9.2. Estimating the exceedance probability and cumulative observed runoff compared with simulated runoff from GR4J, HBV light for both the validation periods

Figures V. 19 and V.20 illustrate the exceedance probability during both validation periods. These figures show that the GR4J was producing the high runoff during the first validation period with all sub basins except Upstream Sebdou, but it was superior to HBV light which gave low runoff with all sub basins at the same period. Although, the exceedance probability showed some significant differences in computing runoff during the second validation period, where it notes that both models showed underestimation of extreme high runoff at all sub basins, except Wadi Boumessaoud sub basin which showed an overestimation of runoff with GR4J. The two models showed an unsimilarity of capturing well the timing and magnitude of high and low observed runoff.



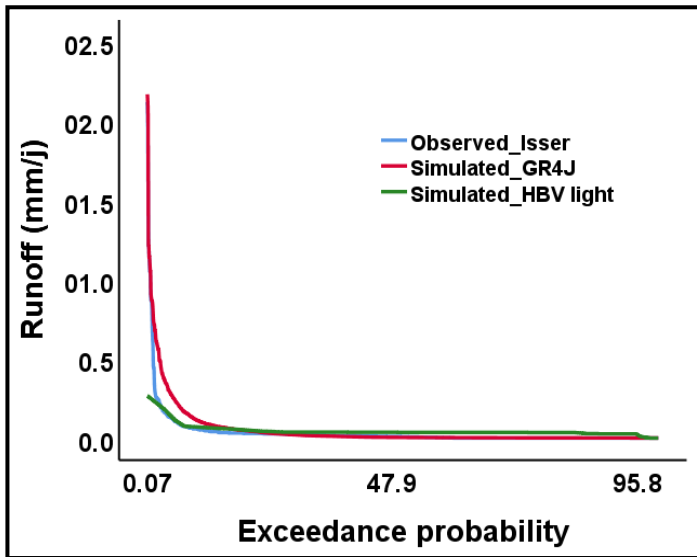
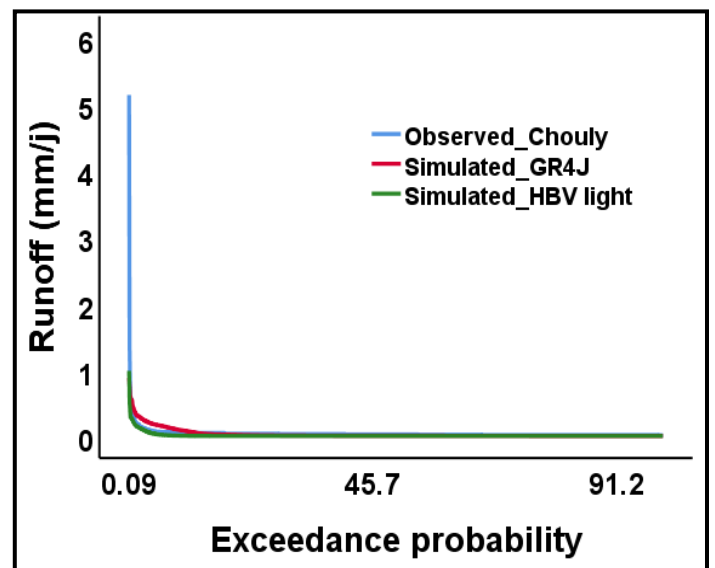
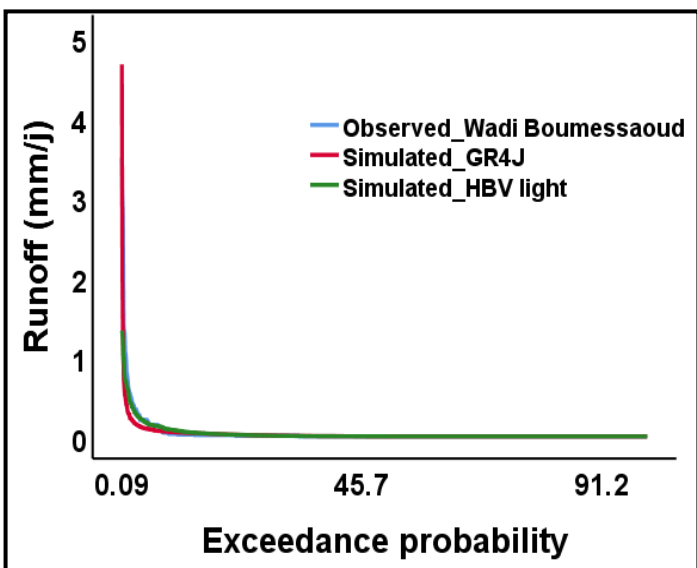
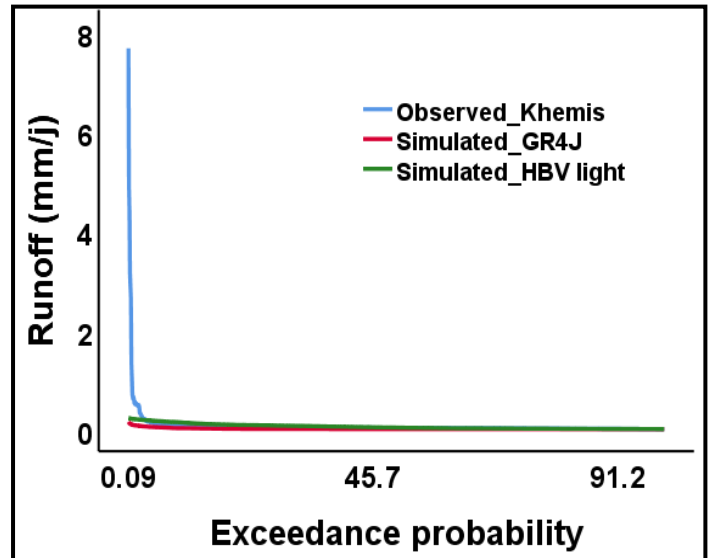
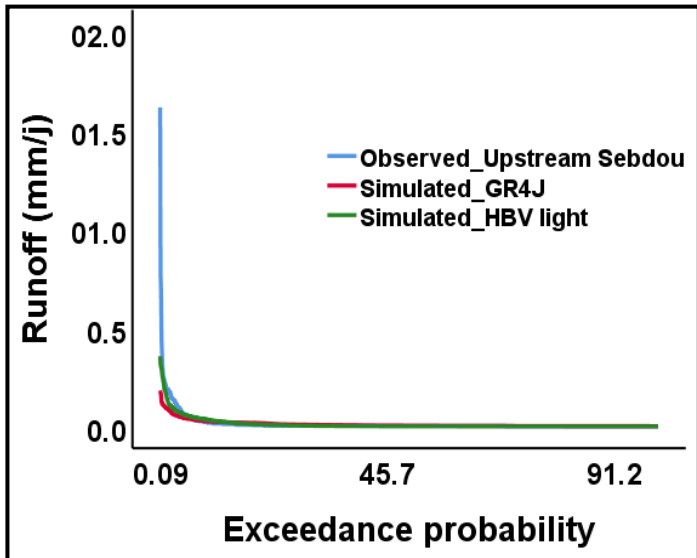


Figure V.19. Exceedance probability curve for observed and simulated runoff from GR4J, HBV light for validation (2002-2005).



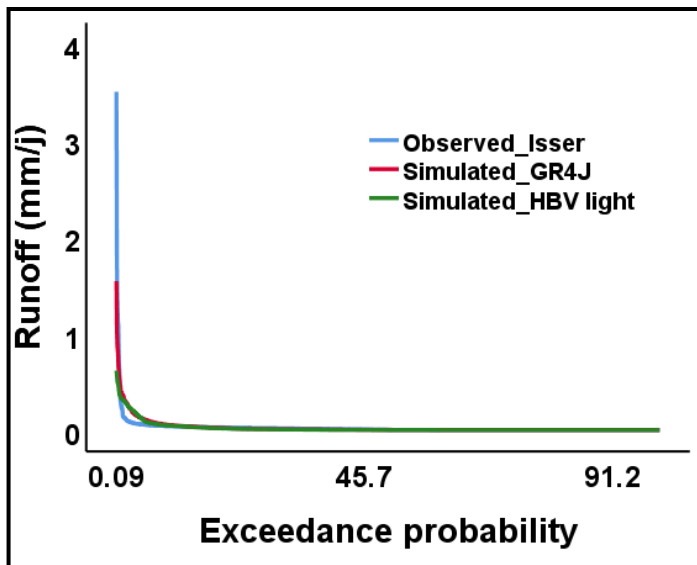
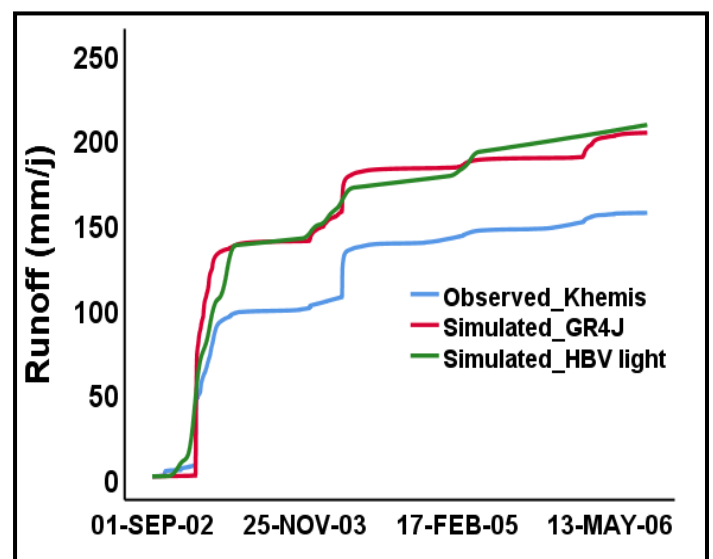
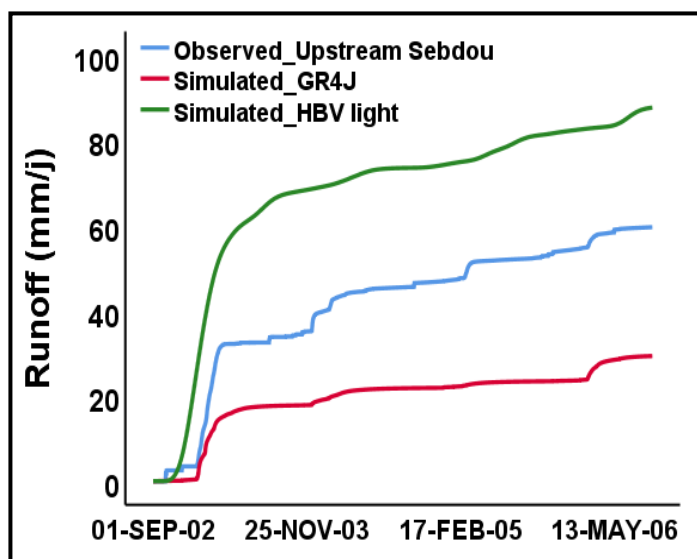


Figure V.20. Exceedance probability curve for observed and simulated runoff from GR4J, HBV light for validation (1997-1999).

By comparing the simulation with the observation from two validation periods (fig.V.21, fig.V.22), the cumulative curve for first validation showed that the high runoff was overestimated by GR4J and HBV light compared to the observed one in the case of Khemis, and Isser sub basins. Except for Upstream Sebdou sub basin showed an overestimation of runoff with HBV light, and underestimating the runoff with GR4J. In Chouly and Wadi Boumessaoud sub basin, both high and low runoff were simulated well with GR4J, the best fitting was particularly for the medium runoff simulation, while HBV light underestimated the runoff for both sub basins. For second validation, the three sub basins Upstream Sebdou, Wadi Boumessaoud, and Chouly underestimated the runoff for both models. In the case of Khemis and Isser sub basins, the cumulative runoff produced by the two models is not sufficiently similar to the observed runoff.



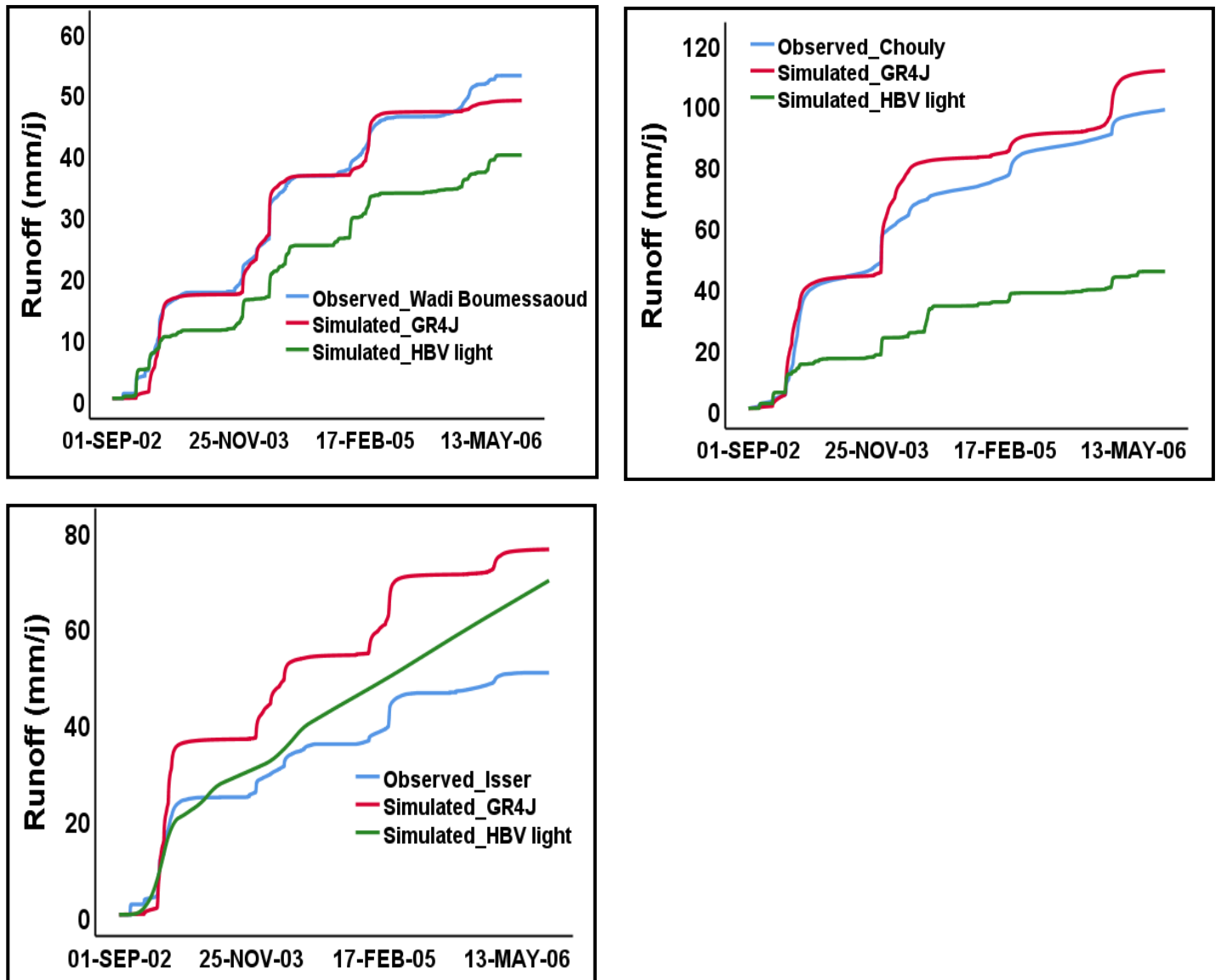


Figure V.21. Cumulative runoff for observed and simulated runoff from GR4J, HBV light for validation (2002-2005).

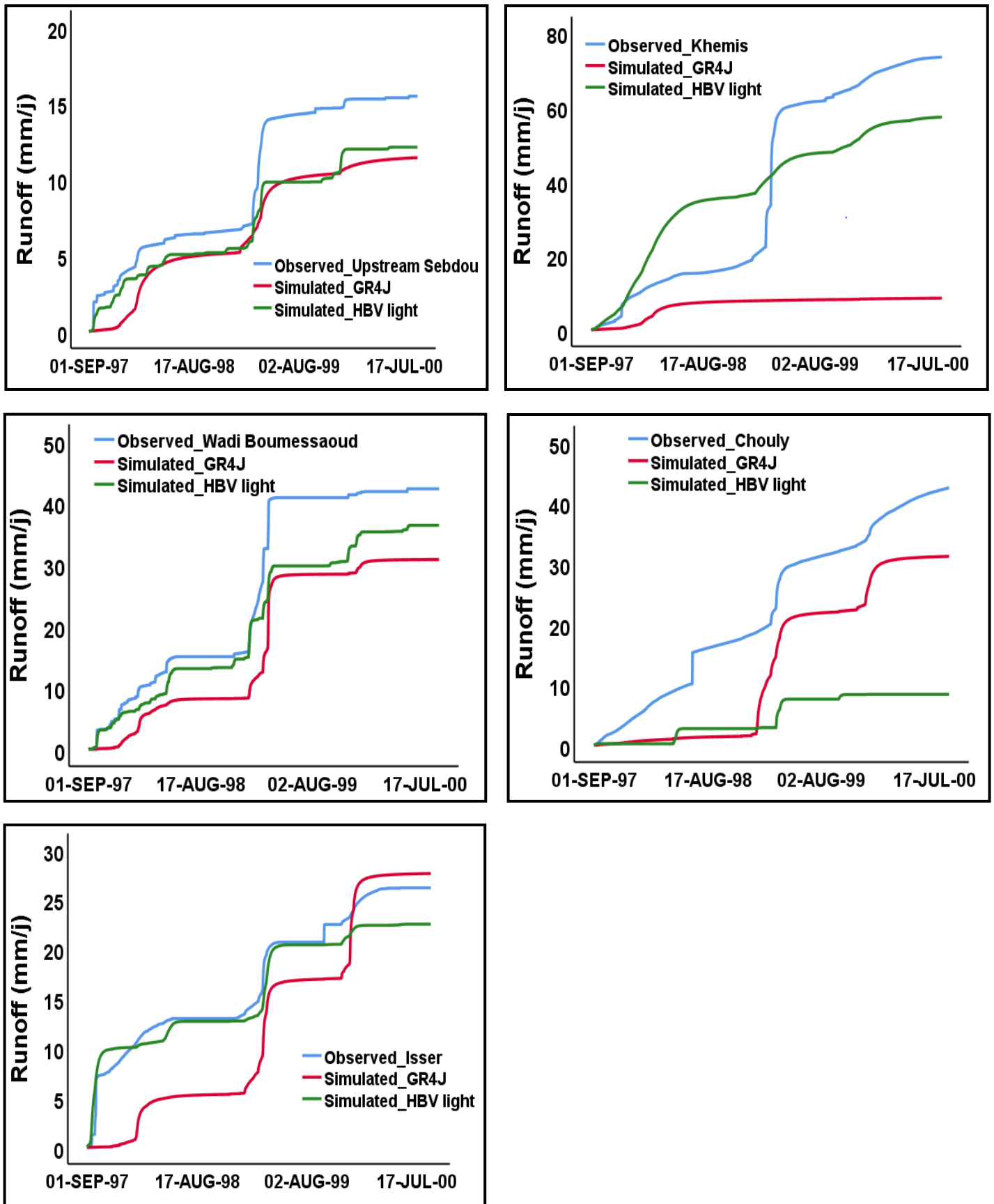


Figure V.22. Cumulative runoff for observed and simulated runoff from GR4J, HBV light for validation (1997-1999).

V.10. Conclusion

In this chapter, we have attempted to compare the response of the two models: the Rural Engineering (GR) developed by Cemagreff, and (HBV light) developed by the SMHI (Swedish Institute of Meteorology and Hydrology) on a daily time step for five sub basins of the Tafna (Upstream Sebdou, Khemis, Wadi Boumessaoud, Chouly, Isser) in the northwestern part of Algeria across periods with wet and dry conditions. The hydrological behavior for the models represented the response in terms of producing the simulated runoff close to observed runoff based on relationships between the input of the model (rainfall, runoff, temperature), and in addition the manual optimization of the parameters of the models. The criteria that were used to compare the efficiency of the models are the Nash coefficient (Nash), the coefficients of determination (R^2). In general, the results showed that the two models (GR4J, HBV light) gives a good performance (≥ 59 , ≥ 63 %, respectively) for the two calibration periods (1990-1999), and (1990-1996). The results of validation indicated showed less performance in HBV light (10.1-49.6%, 0.2-42.8%) compared to the GR4J (50.9-67.9 %, 49.3-62.8%) for both validation period (2002-2005, 1997-1999, respectively), it may due to the difficulty of producing simulated runoff similar to the observed runoff because of the irregularity of rainfall which is not fitting the distribution of observed runoff, where the model was decreasing the runoff based on the lower value of rainfall especially in the dry period (1997-1999), while the observed runoff was higher. In addition, the probability of the parameter being the optimal parameter for several periods (validation) is based on the sensitivity of the parameter over the calibration period, or the reason is likely due to the measurement of the error in the data inputs, parameter uncertainty, where the parameter set that was used for calibration has some limitations in terms of quality and is questioning the suitability for validation (Beven & Westerberg, 2011; Nauditt et al., 2017). Furthermore, to account, other factors such as the saturation of soil (contribution of underground water to the detriment of surface runoff) were not considered in the model, where the region is characterized by Karstified recharge area. Most probably the lower number of rainfall stations in the sub basins might be another reason for not well representing the spatial distribution of rainfall, which further reflected in the hydrological behavior.

GENERAL CONCLUSIONS AND RECOMMENDATIONS

The main objective of this thesis is the comparison of the performance between the two lumped conceptual hydrological models (GR4J, HBVLight) under different time periods representing climate conditions phases (wet, dry period) in diverse sub basins of the Tafna basin in Northwest of Algeria (Upstream Seb dou, Khemis, Wadi Boumessaoud, Chouly, and Isser). The comparison was based on exploring the hydrologic sensitivity of these sub basins to climate conditions (dry, wet period) through the analysis of the influence of the model parameters that are representing the hydrological process on runoff generation. The evaluation of the models performance was based on using different model performance criteria.

To reach this perspective, it requires a methodology for selecting periods to different climate conditions, we have tried to use several statistical approaches to analysis variability of hydro-climatic variables aims detecting the homogeneity, trend analysis (decrease or increase) of series, in addition, the estimation of droughts in terms of the quantification and characteristics, we have eight (8) rainfall stations and two (2) stations over a period extending from 1979 / 1980–2011 / 2012, and five (5) hydrometric series over the period 1979/1980–2010–2011.

The Tafna basin is a transboundary basin extending an area of 7245 km². It is characterized by the abrupt relief of the Tlemcen Mountains with slopes greater than 25% in the south, and in the north by the Mediterranean Sea, high Oran plains, and valley. And by the Moroccan Middle Atlas, Traras mountains, and Plain of Maghnia in the west, While in the east by the plain of Sidi Bel Abbes, and The plain of Tafna is crossed between the aquifers in north, and the high Oran plains in the south. The basin is characterized by a very complex geology and great tectonics, which was evaluated from Primary to Plio-Quaternary. The type of geological formations distribution may influence the hydrological response of the basin.

The hydrographic network of the basin is characterized by permanent or temporary wadis, and main stream with length is 170 km from Seb dou region. The length wadi varies between 20.47 km (Wadi Boumessaoued sub basin) to 53.97 km (Isser sub basin) associated in this case to the surface of the sub basin, with the density is relatively higher in small area. The drainage density is homogeneous over the whole of the Tafna basin. And the landscape experienced degradation by extensive small-scale agriculture due to the diversity of the natural sets which allows a diversity of activities according to the different climatic stages and the nature of the soils.

The statistical analysis of the variability of the hydro-meteorological series emphasized the presence of breaks mostly in the year 2007 with an significant trend of the rainfall time series that highlighted an upward trend at the end for all the stations in the autumn season, which is mainly due to an increase in rainfall in September and October. The increasing trend in rainfall may lead to a rise in streamflow and enhance potential floods risks in low-lying regions of the study area. Unlike, it has been indicated a decline in runoff time series could be attributed to an increase in the temperature.

Homogeneity, trend tests are an important basis for the quality and reliability testing of hydro- meteorological data and it should be noted that the data should represent a long-term series (at least more than 30 years) for detecting climate change. In addition, other factors such as the method for collection of data and reliability of the measurement should be considered as an important aspect in climate change studies. The analysis of trends based on statistical tests may be limited mainly because of data gaps, insufficient length of time series,

and other causes introducing uncertainty into the estimations. Liuzzo et al. 2017 presented the Bayesian procedure for estimating trends and uncertainty sources and, thereby, demonstrated the ability to provide a broader analysis of trends at the regional scale and is recommended for consideration in the follow up studies (Liuzzo et al., 2017).

The estimates of droughts are consistent in duration in terms of the start and end of the drought. The analysis of the long term changes between the period 1985 to 2010 showed that wet periods was indicated in the early 2000s, where the meteorological indices have a concurrence of the highest peak of wet year was 2008 with almost similar fluctuation of dry and wet phases which lead to conclusion that the rainfall amount is the most important factor for long term hydrological dry and wet periods identification as also confirmed by study of (Rimkus et al., 2013).

The meteorological drought indices considered in this study is based on only rainfall and might tend to underestimate the real drought risk. Thus it should be evaluated using indices that include temperature and evapotranspiration, where the rising of the temperatures potentially increases evapotranspiration rates, and may aggravate drought conditions, as (Hansel et al., 2016) suggested.

The advantage of the selected lumped conceptual hydrological rain-runoff models (GR4J, HBV light) is the simplicity, availability, and low computational costs, and it includes an interface where all parameters, inputs, and outputs easily could be controlled, and require available data on rainfall, potential evapotranspiration, and runoff. The models were calibrated using two periods of different climate conditions (wet, dry), with the parameter sets which are different for each simulation of the five sub basins related to the variability of the hydrological variables and characteristics data of each sub basins to obtain the model response. The comparison between the two models shows that these models are not representing satisfactorily the diversity of the hydrological behavior of the sub basins, it relatively explains the conceptions of the hydrological response through the models' parameters, alongside highlighted the limits of the models used and their producing the hydrological responses in different climate conditions (dry, wet period).

For the current work, which follows the performance comparison between these models in the five sub basins of the Tafna basin, we find that the GR model is more suitable in these sub basin in the wet period than the dry period due to the low-flow which likely corresponds to a change in the hydrological regime, thus accompanied with quite a low-performance level, where the more saturated basin, it will be obtain better performance of the lumped conceptual model. It is somewhat likely that should be highlighted the concept of how are functioning and reacting the models on the sub-periods in the series than the complete series of the time series during the calibration and validation phases, which highlighting climatic variability and its relation between the simulated runoff and those measured. However, The two models showed improvement from dry to wet conditions, where the rainfall-runoff modeling gives the best simulations with parameter sets for the wet period (Lidén and Harlin, 2000; Westra et al., 2014; Nauditt et al., 2017). This change in model performance is likely that hydrological systems are more closely related to the meteorological forcing under wet conditions, whereas in dry conditions runoff depends on the storage processes whose parameterization is highly uncertain (Gudmundsson et al., 2012). However, the assessments of the effects of climate conditions on hydrological model response are typically affected by a variety of uncertainties,

such as the hydrological model structure and parameter sets (Wilby and Dessai, 2010; Teutschbein et al., 2011; Teutschbein et al., 2015), in addition to the lack of input data (soil, groundwater) that was not provided to the model to recognizing how these sub basins transport and store water which is able to conceptualize the hydrological behavior of the sub basins and help to improve process understanding this complex environment in a more comprehensive way, especially further of mountain hydrology and highly varying hydro-climatic regimes, which need quality input data to reduce model uncertainty. The approach of this study is the impact of spatial and temporal on model performance which provides a view about water resources availability towards hydro-climatic variability and gives proper knowledge for future studies related to the impact of climate change and land-use changes on the hydrological system, and be can be transferred and applied to a similar setting in the Mediterranean region. The model may also be a useful tool for predictions of water availability on different climate conditions for further water management studies.

Outlook and recommendation of the study

This study is useful for conceiving complementary studies required to determine and understand the relationship between climate variability and the availability of the water resources of the Tafna basin. From the results obtained, we propose the following recommendation:

- The spatial and temporal scale analyses of various indices that monitor the intensity of drought and water stress in the area should be conducted regularly for better environmental monitoring and water management planning.
- Applying statistical methods can add interpretive conception when comparing model performance, where it can reflecting the conclusions that can be drawn from statistical hypothesis tests on analysing the performance criteria on the sub periods of the series.
- Modeling division into low and high flows and comparative analysis of parameter sets during low flows and high flows, and improve discharge simulations by additional efforts and testing complex models are required.
- Set up the parameters temporal transferability among different sub-periods of the original model and its modified version, in which the parameter was allowed to vary over time. This may provide new insights for improving the structure of existing hydrological models as the work of (Zeng et al., 2019) recommend.
- Recommend expanding gauge networks, and building an efficient process of data collection to support and enable quality research.
- Considering parameter uncertainty in the modeling approach to obtain reliable results.
- Application of the new version of GR with two add parameters (GR6J) which were developed by Pushpalatha (2011) to obtain a better simulation of water exchange between the river and groundwater, which is one of the most important processes for low flow simulations.

- In the aspect of choosing the right model for simulation, we should consider in the future studies, the modelling platforms as the study of (Kunnath-Poovakka and Eldho, 2019), where they worked in modelling interfaces such as Source, by eWater, Australia, are reducing that challenge by integrating all the information for water resources management and modelling tools in one platform.
- Using an approach to identify consecutive drought and predicting the return periods of droughts, and divided the series into homogenous sub periods under the same climate condition addressed to simulation rather than just indicating the rupture.
- The diverse data are needed in hydrological models which would support the process of ameliorating the simulation results.
- Proper knowledge of both subsurface flow and drainage basin characteristics is necessary otherwise it will create an adverse effect on model calibration, where the meteorological data and soil properties have got a large influence on the performance of each model.
- Preferred using the multi-variable calibration method to provide a reasonable evaluation of performance and applicability of the model in two different cases using more than a single variable in the basin.
- Taking into consideration the recommendation of (Sezen et al.2018 ; Van Esse et al. 2013) which stated that the better modeling results is in the larger basin compared to smaller area, where the hydrological processes are mixed and have smoother behavior at larger scales, which enable easier modeling by the conceptual model structure.
- Using several objective functions each focusing on a different aspect of the hydrograph (Specific streamflow characteristics) to evaluate different objective functions for their ability to produce simulated time series that adequately preserve the flow characteristics.
- Evaluation of more calibration approaches, more model structures, and extending the types of study areas.
- Application of models suitable for extremes and changes in flow conditions to be reliable and beyond the range of events during calibration and validation.
- Provide satellite rainfall product networks sparse and adequately distributed in the region (remote sensing data) may result in a perfect representation of rainfall spatial variability for future studies related to the conception of the relationship between rainfall and runoff, and including rapid advances in remote sensing technologies.
- Recommend further application of the lumped model for different types of basins (i.e., mountainous, urban, peri-urban, and rural) with low data availability for providing more comprehensive conclusions on land cover distribution, land use, and the intervention of human activity on the environment.
- Investigate how different process descriptions of the models respond to climate change scenarios and their impact on the runoff.

REFERENCES

- Abbott, M., J. Bathurst, J. Cunge, P. O'Connell, and J. Rasmussen. 1986. *An introduction to the european hydrological system - systeme hydrologique europeen, "she", 1 : History and philosophy of a physically-based distributed modelling system, and 2 : Structure of a physically-based distributed modelling system*. Journal of Hydrology, 87, 45–59 p.
- ABH(Agence De Bassin Hydrographique Oranie - Chott Chergui [Oranie Hydrographic Basin Agency - Chott Chergui]).2006.Cadastre Hydraulique Bassin Tafna. Document de synthese. Mission VI
- Abouabdillah, A. 2009. *Hydrological modeling in a data-poor Mediterranean catchment (Merguellil, Tunisia). Assessing scenarios of land management and climate change*. PhD Thesis, University of Tuscia, Italy.
- Abushandi, E. 2011. *Rainfall-Runoff Modeling in Arid Areas*. PhD Thesis, Freiberg Mining institute, Germany.
- Achamyelah, M.2019. *Application of SWAT Model To Evaluate The Water Balance Of An Arid Catchment*. PhD Thesis. University of the Free State. Bloemfontein, South Africa.
- Adjim, H. 2004. *Evolutions et Affectation des Ressources Hydriques Superficielles du Bassin Versant de la Tafna* (Developments and Allocation of Surface Water Resources of the Tafna Watershed). Magister Thesis, University of Tlemcen, Algeria.
- Adjim, H., Djedid, A.2018. *Drought and Water Mobilization in Semi-Arid Zone: The Example of Hammam Boughrara Dam (North-West of Algeria)*.” Journal of Water and Land Development. Vol. 37. N^o.1, 3-10. DOI:10.2478/jwld-2018-0019.
- Afzali, A., Keshtkar, H., Pakzad, S., Moazami, N., Farahani, E.A., Khosrojerdi, E., Yousefi, Z., Taghinaghilou, M. 2016. *Spatio-Temporal Analysis of Drought Severity Using Drought Indices and Deterministic and Geostatistical Methods (Case Study: Zayandehroud River Basin)*. Desert .Vol. 21. N^o.2, 165-172.
- Ajami, N K. Gupta, H., Wagener, T., Sorooshian, S.2004. *Calibration of a semi-distributed hydrologic model for streamflow estimation along a river system*. Journal of Hydrology, 298 . 112-135.
- Ahbari, A. 2013. *Le bassin versant Rhéraya : Modélisation pluie-débit et prédiction du comportement hydrologique* (The Rhéraya watershed: Rain-flow modeling and prediction of hydrological behavior). Master Thesis, University of Marrakech, Morocco. 101p.
- Allen, R. G., Pereira, L. S., Raes, D., Smith, M., 1998. *Crop evapotranspiration - guidelines for computing crop water requirements*. FAO Irrigation and drainage paper 56. Rome, Italy.
- Al-Timimi, Y.K., Osamaha, O.2016. *Comparative Study of Four Meteorological Drought Indices in Iraq*. Journal of Applied Physics. p. 10.e-ISSN: 2278-4861.Vol. 8. Iss.5 .Ver. III, 76-84.DOI: 10.9790/4861-0805037684
- Akbari, H., Rakhshandehroo, G.R., Sharifloo, A.H., Ostadzadeh, E. 2015. *Drought Analysis Based on Standardized Precipitation Index (SPI) and Streamflow Drought Index (SDI) in Chenar Rahdar River Basin, Southern Iran*. Proceedings of the Watershed Management Symposium. ISBN978-0-7844-7932-2, 11-22.DOI:10.1061/9780784479322.002

- Ambroise, B.1999. La dynamique du cycle de l'eau dans un bassin versant. Processus, facteurs, modèles (The dynamics of the water cycle in a watershed. Processes, factors, models). Center for Eco-Geographical Studies and Research. Louis Pasteur University in Strasbourg. Bucarest. 206 p.
- ANAT(Direction Régionale Ouest).2000. Actualisation du plan d'aménagement de la wilaya de Tlemcen, Bilan de la situation et problématique de l'aménagement (Update of the development plan for the wilaya of Tlemcen, Assessment of the situation and development issues).
- Anshuman, A., Kunnath-Poovakka, A., Eldho, T.I. 2019. *Towards the use of conceptual models for water resource assessment in Indian tropical watersheds under monsoon-driven climatic conditions*. Environmental Earth Sciences, 78, 282. Doi.org/10.1007/s12665-019-8281-5.
- Arabzadeh, R., Kholoosi, M. M, Bazrafshan, J. 2015.*Regional Hydrological Drought Monitoring Using Principal Components Analysis*. Journal of Irrigation and Drainage Engineering, 04015029-1- 04015029-20. DOI: 10.1061/(ASCE)IR.1943-4774.0000925.
- Asefjah, B., Fanian, F.,Feizi Z., Abolhasani, A., Paktinat, H., Naghilou, M., Atania, M., Asadollahi, M.,Babakhani, M., Kouroshniya, A.,Salehi, F.2014.*Meteorological Drought Monitoring Using Several Drought Indices (Case Study: Salt Lake Basin in Iran)*. Desert .Vol. 19. N^o.2,155-165.
- Audrey, B.2013. Conception de modèles de prévision des crues éclair par apprentissage artificiel (Design of flash flood forecasting models using machine learning). PhD Thesis, Pierre and Marie Curie University, Paris, France.
- Augustine, D., 2010. *Spatial versus temporal variation in precipitation in a semiarid ecosystem*. Landscape Ecology, 25(6), 913-925.
- Azarakhshi, M., Mahdavi, M., Arzani, H., Ahmadi, H.2011. *Assessment of the Palmer drought severity index in arid and semi-arid rangeland: (Case study: Qom province, Iran)*. Desert. Vol. 16.77-85.
- Baahmed, D., Oudin, L., Errih, M. 2015. *Current runoff variations in the Macta catchment (Algeria): is climate the sole factor?*, Hydrological Sciences Journal, 60:7-8, 1331-1339, DOI: 10.1080/02626667.2014.975708
- Baba- Hamed, K. 2001. Contribution à l'étude hydrologique de trois sous-bassins de la Tafna (bassin de Sebdou, de Mouilah et d'Isser)(Contribution to the hydrological study of three Tafna sub-basins (Sebdou, Mouilah and Isser basin). PhD Thesis, University of Oran, Algeria. 195 p.
- Báez, J.C., Enrique Salvo, A., García-Soto, C., Real, R., Márquez, A.L., Flores-Moya, A. 2019. *Effects of the North Atlantic Oscillation (NAO) and Meteorological Variables on the Annual Alcarria Honey Production in Spain*. Journal of Apicultural Research, 58, 788-791.
- Bagheri, F. 2016. *Mapping Drought Hazard Using SPI Index And GIS (A Case Study: Fars Province, Iran)*. International Journal of Environment and Geoinformatics. Vol. 3. N^o. 1, 22-28. DOI:10.30897/ijegeo.304419.

- Bakreti, A., Braud, I., Leblois, E., Benali, A. 2013. *Analyse conjointe des régimes pluviométriques et hydrologiques dans le bassin de la Tafna (Algérie Occidentale)* (Joint analysis of rainfall and hydrological regimes in the Tafna basin (Western Algeria)). *Hydrological Sciences Journal*. 58, 133-151.
- Bao, Y., Meng, C., Shen, S., Qiu, X., Gao, P., Liu, C., 2011. *Analysis on characteristics of a typical drought event in Jiangsu Province*. *Shengtai Xuebao*, 31 (22), 6853-6865.
- Bari, A, H., Zarch, M. A. A., Dastoranim, T., Kousarim, R., Zarchm, S. 2011. *The Survey of Climatic Drought Trend in Iran*. *Stochastic Environmental Research and Risk Assessment*. Vol. 25. N°. 6, 851- 63. DOI:10.1007/s00477-011-0491-7.
- Barua, S., Ng A.W.M., Perera, B.J.C. 2011. *Comparative evaluation of drought indexes: case study on the Yarra River catchment in Australia*. *Journal of Water Resources Planning and Management*. ISSN 0733-9496/2011/2-215–226. Vol. 137. N°. 2, 215–226.
- Bastidas, L., Gupta H., Sorooshian S., Shuttleworth W., Yang Z. 1999. *Sensitivity analysis of a land surface scheme using multicriteria methods*. *Journal of Geophysical Research*. 104 (D16), 19481-19490.
- Basist, A., Bell, G. and Meentemeyer, V., 1994. *Statistical relationships between topography and precipitation patterns*. *Journal of Climate*, 7(9), 1305-1315.
- Batelaan, O., Wang Z., De Smedt F. 1996. Hydrogis 96. In I. Publ (Ed.), *Application of Geographic Information Systems in Hydrology and Water Resources Management*, Volume 235, Vienna.
- Batisani, N.; Yarnal, B. 2010. *Rainfall Variability and Trends in Semi-Arid Botswana: Implications for Climate Change Adaptation Policy*. *Applied Geography*, 30, 483-489.
- Bayissa, Y.A., Moges, S.A., Xuan, Y., Van Andel, S.J., Maskey, S., Solomatined, P., Griensven, A., Van Tadesse, T. 2015. *Spatio-temporal assessment of meteorological drought under the influence of varying record length: The case of Upper Blue Nile Basin, Ethiopia*. *Hydrological Sciences Journal*. Vol. 60, 1927-1942.
- Bazrafshan J., Khalilia. 2013. *Spatial Analysis of Meteorological Drought in Iran from 1965 to 2003*. *Desert*. Vol. 18, 63-71.
- Beck, M. B. 1987. *Water Quality Modeling: A Review of the Analysis of Uncertainty*. *Water Resources Research* 2, 3 (8): 1393-1442.
- Bekele, A.A., Pingale, S.M., Hatiye, S.D., Tilahun, A.K. 2019. *Impact of climate change on surface water availability and crop water demand for the sub-watershed of Abbay Basin, Ethiopia*. *Sustainable Water Resources Management* 5:1859-1875. Doi.org/10.1007/s40899-019- 00339-w
- Belarbi, H., Touaibia, B., Boumechra, N., Amiar, S., Baghli, N. 2016. *Sécheresse et modification de la relation pluie-débit: Cas du bassin versant de l'Oued Sebdou (Algérie Occidentale)* (Drought and modification of the rain-flow relationship: Case of the Oued Sebdou watershed (Western Algeria)). *Hydrological Sciences Journal*, 62,1-13.
- Belouz, K. 2009. *Modélisation de l'évapotranspiration de référence et du déficit hydrique par les réseaux de neurones artificiels à différent pas de temps* (Modeling of reference

evapotranspiration and water deficit by artificial neural networks at different time steps). Magister thesis. ENSA - Alger. 137 p.

Benblidia, M., Thivet, G. 2010. Gestion des ressources en eau: Les limites d'une politique de l'offre (Water resources management: The limits of a supply policy). Les Notes D'Anal. CIHEAM 2010, 58, 15.

Bendjema, L. 2020. Contribution de la Modelisation Hydrologique a L'evaluation de L'impact De la Variabilite Climatique sur La Ressource en Eau. Cas du Bassin Versant d'oued Mellah (Ne Algérien). PhD Thesis. University of Tlemcen. Algeria.

Bendjema, L., Baba-Hamed, K., Bouanani, A. 2019. *Characterization of the climatic drought indices application to the Mellah catchment, North-East of Algeria*. Journal of Water and Land Development. No. 43 (X–XII), 28–40. DOI:10.2478/jwld-2019-0060.

Benhadji, N., Sartori, M., Abdellaoui Hassaine, K., Gattolliat, J-L. 2020. *Reports of Baetidae (Ephemeroptera) species from Tafna Basin, Algeria and biogeographic affinities revealed by DNA barcoding*. Biodiversity Data Journal 8: e55596.

Beran, M.A., Rodier, J.A. 1985. Hydrological aspects of drought. In: UNESCO–WMO Studies and Reports in Hydrology .ISBN 92-3-102288- 1 .N°.39.149 p.

Bergström, S., Forsman, A. 1973. *Development of a conceptual deterministic rainfall-runoff model*. Nordic Hydrology, 4, 147 -170.

Bergström, S. 1976. *Development and application of a conceptual runoff model for Scandinavian catchments*. SMHI RHO 7, Norrköping. 134 p.

Bergström, S. 1990. *Parametervärden för HBV-modellen i Sverige. Erfarenheter från modelkalibreringar under perioden 1975-1989* (Parameter values for the HBV model in Sweden. Experiences from model calibrations during the period 1975-1989). SMHI HYDROLOGI No 28, Norrköping. 35 p.

Bergström, S. 1992. *The HBV model - its structure and applications*. SMHI RH N°. 4, Norrköping. 32 p.

Bessière, H. 2008. Assimilation de données variationnelle pour la modélisation hydrologique distribuée des crues à cinétique rapide (Variational data assimilation for distributed hydrological modeling of fast-kinetic floods). PhD Thesis, University of Toulouse, France.

Beven, K. 2001. *Rainfall runoff modeling*. Number 2 in ISBN 978-0-470-71459-1. London, Angleterre : John Wiley & Sons.

Beven, K. Binley A. 1992. *The future of distributed models: model calibration and uncertainty prediction*. Hydrological Processes. 6, 279-298.

Beven, K. Westerberg, I, 2011. *On red herrings and real herrings: Disinformation and information in hydrological inference*. Hydrological Processes, 25(10), 1676-1680. DOI.org/10.1002/hyp.7963

Beven, K. J. 2012. *Rainfall-runoff models: The primer*, 2nd Ed., Wiley, Chichester, U.K.

- Bloschl, G., Montanari, A. 2010. *Climate change impacts—throwing the dice?*. Hydrological Processes, 24(3), 374-381, DOI:10.1002/hyp.7574.
- Boldetti, G. 2012. Estimation des paramètres des modèles hydrologiques sur des bassins versants non-jaugés : confrontation des approches directes et indirectes (Estimation of the parameters of hydrological models on ungauged watersheds: comparison of direct and indirect approaches). PhD thesis, Irstea (Antony), AgroParisTech, Paris, France. 206 p.
- Bormann, H., Breuer, L., Giertz, S., Huisman, J. A., Viney, N. R. 2009. *Spatially explicit versus lumped models in catchment hydrology—experiences from two case studies*. Uncertainties in environmental modeling and consequences for policy making, 3-26.
- Bouadila, A. 2015. *Elaboration D'un Modele Hydrometeorologique Sous Les Plateformes ATHYS et GR4J* (Development of a hydrometeorological model under the ATHYS and GR4J platforms). Master thesis. University of Sidi Mohamed Ben Abdellah. Fes, Morocco. 74p.
- Bouanani, R. 2010. Modélisation de la fonction pluie-débit. Application au bassin versant de la Tafna (NW-Algérien) (Modeling of the rain-flow function. Application to the Tafna watershed (NW-Algerian)). PhD Thesis, University of Tlemcen, 110 p.
- Boudad, B., Sahbi, H., Mansouri, I. 2018. *Analysis of Meteorological and Hydrological Drought Based in SPI and SDI Index in the Inaouen Basin (Northern Morocco)*. Journal of Materials and Environmental Sciences. Vol. 9.Nº. 1, 219-227. DOI:10.26872/jmes.2018.9.1.25.
- Boudhraa, H. 2007. Modélisation pluie-débit a base géomorphologique en milieu semi-aride rural Tunisien : Association d'approches directe et inverse (Rain-flow modeling on a geomorphological basis in semi-arid rural Tunisian environment: Association of direct and reverse approaches). PhD Thesis, National Agronomic Institute, Tunisia.
- Bouguerne, A. 2017. Relation pluie- débit et concentration des polluants dans les Oueds Boussalem et Rhumel. Est Algérien (Rain-flow relationship and concentration of pollutants in the Boussalem and Rhumel Oueds. East Algerian). PhD Thesis, University of Batna 2, 248 p.
- Boulariah, O., Longobardi, A., Meddi, M. 2017. *Hydroclimate temporal variability in a coastal Mediterranean watershed: the Tafna basin, North-West Algeria*. Geophysical Research Abstracts. Vol. 19, EGU2017-17462.
- Boulariah, O., Meddi, M., Longobardi, A. 2017. Statistical Comparison of nonlinear rainfall-runoff models for simulation in Africa North-West semi-arid areas. 15th International Conference on Environmental Science and Technology Rhodes, Greece, 31 August to 2 September 2017.
- Bouragba, N. 2006. Modélisation et Simulation des Changements Climatiques (Climate Change Modeling and Simulation). Mémoire Magister Mascara.
- Brandimarte, L., Di, Baldassarre, G., Bruni, G., D'odorico, P., Montanari, A. 2011. *Relation Between the North-Atlantic Oscillation and Hydroclimatic Conditions in Mediterranean Areas*. Water Resources Management. Vol. 25. No. 5, 1269- 1279. DOI:10.1007/s11269-010-9742-5.

- Burn, D. H., Fan, L., Bell, G. 2008. *Identification and quantification of streamflow trends on the Canadian Prairies*, Hydrological Sciences Journal, 53:3, 538-549, DOI: 10.1623/hysj.53.3.538
- Celleri, R., Willems, P., Buytaert, W., Feyen, J. 2007. *Space–Time Rainfall Variability in the Paute Basin, Ecuadorian Andes*. Hydrological Process., 21 (24), 3316-3327. DOI.org/10.1002/hyp.6575.
- Chakravarti, I. M. Laha, R. G. Roy, J. 1967. Handbook Methods of Applied Statistics. Volume I, John Wiley and Sons, 11-27.
- Chaponniere, A.2005. Fonctionnement hydrologique d'un bassin versant montagneux semiaride. Cas du bassin versant du Rehraya (Haut Atlas marocain)(Hydrological functioning of a semi arid mountainous watershed Case of the Rehraya watershed (Moroccan High Atlas)). PhD Thesis, National Agronomic Institute, Paris-Grignon, France.
- Charifi Bellabas, S., Benmamar, S., Dehni, A.2020. *Study and analysis of the streamflow decline in North Algeria*, Journal of Applied Water Engineering and Research. DOI: 10.1080/23249676.2020.1831974
- Chavan Madhukar Lombha.2017. Assessment of Area and Water Allocation in Canal Command of Purna Irrigation Project Using Swat. PhD thesis. College of Agricultural Engineering & Technology, Vasant Rao Naik Marathwada Krishi Vidyapeeth, Parbhani. India.
- Chkir, N. 1994. Mise au point d'un modèle hydrologique conceptuel intégrant l'état hydrique du sol dans la modélisation pluie-débit (Development of a conceptual hydrological model integrating the water state of the soil in rainfall-flow modeling). PhD Thesis, the National School of Ponts and Chaussées in Paris. 27 p.
- Chocat, B. 1997. *Encyclopédie de l'Hydrologie Urbaine* (Editions Lavoisier ed.). France.
- Chiew, F.H.S. McMahon, T.A. 1994. *Application of the daily rainfall-runoff model MODHYDROLOG to 28 Australian catchments*. Journal of Hydrology, 153, 383-416.
- Chow, V., Maidment, D., Mays, L.2005. *Applied Hydrology*. New York, USA : McGraw Hill
- Clarke, R.1973. *A review of some mathematical models used in hydrology, with observations on their calibration and use*. Journal of Hydrology, 19 (1), 1-20.
- Collignon, B. 1986. Hydrogéologie appliquée des aquifères karstiques des Monts de Tlemcen (Applied hydrogeology of karst aquifers in the Monts de Tlemcen). PhD Thesis, University of Avignon, France, Tomes 1 and 2, 282 p, 13 appendices.
- Conrad, V., Pollak, C. 1950. *Methods in Climatology*; Harvard University Press: Cambridge, MA.
- Cukur, H., 2011. *Daily precipitation variations of selected meteorological stations in Turkey*. Procedia-Social and Behavioral Sciences, Vol. 19, 617-626.
- Dakhlaoui, H., Bargaoui, Z., Bárdossy, A.2012. *Toward a more efficient Calibration Schema for HBV rainfall–runoff model*. Journal of Hydrology, 444-445, 161-179. <https://doi.org/10.1016/j.jhydrol.2012.04.015>

- Dakhlaoui, H. 2014. Vers une procédure de calage automatique plus efficiente du modèle HBV (Towards a more efficient automatic calibration procedure for the HBV model). PhD Thesis, University of Tunis El Manar. 249 p.
- Daly, C., 2006. *Guidelines for assessing the suitability of spatial climate data sets*. International journal of climatology, 26(6), 707-721.
- Dash, S.S., Kumar, H.V.H. 2017. *Statistical and Trend Analysis of Climate Data of Bapatla (A.P), India*. International Journal of Current Microbiology and Applied Sciences, 6, 4959-4969.
- Da Silva, R.M., Santos, C.A.G., Moreira, M., Corte-Real, J., Silva, V.C.L., Medeiros, I.C. 2015. *Rainfall and River Flow Trends Using Mann–Kendall and Sen’s Slope Estimator Statistical Tests in the Cobres River Basin*. Natural Hazards. 77, 1205-1221.
- De Lima, M. I. P., Carvalho, S. C. P., De Lima, J. L. M. P. 2010. *Investigating annual and monthly trends in precipitation structure: an overview across Portugal*. Natural Hazards and Earth System Sciences. 10, 2429-2440, 2010. DOI:10.5194/nhess-10-2429-2010
- Deo, R. C. 2011. *On Meteorological Droughts in Tropical Pacific Islands: Time-Series Analysis of Observed Rainfall Using Fiji as a Case Study*. Meteorological Applications. Vol. 18. No. 2 p. 171-80. DOI.:10.1002/met.216.
- Dilip, K. 2011. *Distributed rainfall Runoff modeling*. International journal of earth sciences and engineering, 270-275.
- Djellouli, F., Bouanani, A., Baba-Hamed, K. 2016. *Efficiency of Some Meteorological Drought Indices in Different Time Scales, Case Study: Wadi Louza Basin (NW-Algeria)*. Journal of Water and Land Development, 31, 33-41.
- Djellouli, F., Bouanani, A., Baba-Hamed, K. 2018. *Climate Change: Assessment and Monitoring of Meteorological and Hydrological Drought of Wadi El Hammam Basin (NW-Algeria)*. Journal of Fundamental and Applied Sciences. Vol. 8. N°. 3. 1037 p. DOI:10.4314/jfas.v8i3.20.
- Djikou, S.M. 2006. Calcul de l’ETP PENMAN-MONTEITH à différents pas de temps sur quatre sites du Haut Bassin de l’Ouémé. IRD. 34 p.
- Dogan, S., Berktaç, A., Singh, V. P. 2012. *Comparison of multi-monthly rainfall-based drought severity indices, with application to semi-arid Konya closed basin, Turkey*. Journal of Hydrology. Vol.470. 255-268. DOI:10.1016/j.jhydrol.2012.09.003
- Döll, P., Jiménez Cisneros, B., Oki, T., Arnell, N.W., Benito, G., Cogley, J.G., Jiang, T., Kundzewicz, Z.W., Mwakalila, S., Nishijima, A. 2015. *Integrating risks of climate change into water management*. Hydrological Sciences Journal, 60(1):3-14. DOI:10.1080/02626667.2014.967250
- Donald, A.E., Halcox, J.P., Charakida, M., Storry, C., Wallace, S.M., Cole, T.J., Friberg, P., Deanfield, J.E. 2008. *Methodological approaches to optimize reproducibility and power in clinical studies of flow-mediated dilation*. Journals of the American College of Cardiology. 51(20):1959-64. DOI: 10.1016/j.jacc.2008.02.044. PMID: 18482664.

- Donat, M.G., Peterson, T.C., Brunet, M., King, A.D., Almazroui, M., Kolli, R.K., Boucherf, D., Al-Mulla, A.Y., Nour, A.Y., Aly, A.A., et al. 2014. *Changes in extreme temperature and precipitation in the Arab region: long-term trends and variability related to ENSO and NAO*. International Journal of Climatology, 34 (3), 581-592.
- Donnelly-Makowecki, L. M., Moore, R.D.1999. *Hierarchical testing of three rainfall-runoff models in small forested catchments* . Journal of Hydrology, 219(3/4), 136-152.
- Dooge, J. 1977. *Mathematical Models for Surface Water Hydrology*, Chapter Problems and Methods of Rainfall-Runoff Modeling, 71–108. New York, USA : John Wiley & Sons.
- Dubreuil, P. 1966. Les caractéristiques physiques et morphologiques des bassins versants, leur détermination avec une précision acceptable(The physical and morphological characteristics of watersheds, their determination with an acceptable precision). ORSTOM notebooks, hydrology series, 3(5), 31.
- Düneloh, A., Jacobeit, J. 2003. *Circulation Dynamics of Mediterranean Precipitation Variability 1948-98: Circulation Dynamics of Mediterranean Precipitation Variability*. International Journal of Climatology, 23, 1843-1866.
- Dwarakish, G. S., Ganasri, B. P.2015. *Impact of land use change on hydrological systems: A review of current modeling approaches*. Cogent Geoscience.1(1) DOI.org/10.1080/23312041.2015.1115691
- Edijatno, C., Michel, C.1989. *Un modèle pluie-débit journalier à trois paramètres*(A three-parameter daily rainfall-flow model). La Houille Blanche. 2, 113-121.
- Edijatno, C., Nascimento, N.O., Yang, X., Makhlof, Z., Michel, C.1999. *GR3J : a daily watershed model with three free parameters*. Hydrology Sciences Journal, 44(2), 263-277.
- Edwards, D.C., Mckee, T.B. 1997. *Characteristics of 20th Century Drought in the United States at Multiple Times Scales*. Atmospheric Science Paper. Vol. 634, 1-30.
- Evans, J., Perlman H. 2015. The Water Cycle. U.S. Department of the Interior, U.S. Geological Survey.
- Eykhoff, P. 1974. "System Identification. Parameter and State Estimation, J. Wiley, London."
- Farahmand, A., Aghakouchak, A. 2019. *A generalized framework for deriving nonparametric standardized drought indicators*. Advances in Water Resources. Vol.76,140-145.
- Ficchi, A.2017. An adaptive hydrological model for multiple time-steps : diagnostics and improvements based on fluxes consistency. Hydrology. PhD Thesis, Pierre and Marie Curie University - Paris VI, France.
- Fischer, C. 2013. Automatische Kalibrierung hydrologischer Modelle. Entwicklung und Anwendung des Kalibrierungssystems OPTAS(Automatic calibration of hydrological models. Development and application of the calibration system OPTAS). Friedrich-Schiller University, Jena.
- Fniguire, F., Laftouhi, N.E., Saidi, M. E., Zamrane, Z., El Himer, H., Khalil, N. 2017. *Spatial and Temporal Analysis of the Drought Vulnerability and Risks over Eight Decades in a Semi-*

- Arid Region (Tensift Basin: Morocco)*. Theoretical and Applied Climatology. Vol. 130.No. 1-2. 321-30. DOI:10.1007/s00704-016-1873-z.
- Fontaine, B., Janicot, S., Monerie, P.A. 2013. *Recent changes in air temperature, heat waves occurrences, and atmospheric circulation in Northern Africa*. Journal of Geophysical Research: Atmospheres, 118, 1-17.
- Fortin, J.P., Moussa, R., Bocquillon, C., Villeneuve, J.P. 1995. *Hydrotel, un modèle hydrologique distribué pouvant bénéficier des données fournies par la télédétection et les systèmes d'information géographique*. Revue des Sciences de l'Eau. 8, 97-124.
- Fossou, R.M.N., Soro, N., Traore, V.B., Lasm, T., Sambou, S., Soro, T., Orou, R.K., Cisse, M.T. 2014. *Variabilité climatique et son incidence sur les ressources en eaux de surface: Cas des stations de Bocanda et de Dimbokro, Centre-Est de la Côte d'Ivoire en Afrique de l'Ouest* (Climate variability and its impact on surface water resources: The case of Bocanda and Dimbokro stations, Center-East of Côte d'Ivoire in West Africa). *Afrique Science*, 10, 118-134.
- Fouchier, C.2010. Développement d'une méthodologie pour la connaissance régionale des crues (Development of a methodology for regional knowledge of floods). PhD Thesis, University of Montpellier II Sciences Et Techniques Du Languedoc, France.
- Freezb, R. 1971. *Three-dimensional, transient, saturated-unsaturated flow in a groundwater basin*. Water Resources Research, 7 (2), 347-366.
- Furusho, C. 2008. Etude du fonctionnement hydrologique d'un bassin versant periurbain : La chezine (Study of the hydrological functioning of a periurban watershed: La chezine). Master Thesis, Ecole Nationale Supérieure des Techniques Industrielles et des Mines, Nantes, France.
- Garbrecht, J., Van Liew, M., Brown, G. O. 2004. *Trends in Precipitation, Streamflow, and Evapotranspiration in the Great Plains of the United States*. Journal of Hydrologic Engineering. Vol. 9, No. 5, 360-367.
- Gedefaw, M., Yan, D., Wang, H., Qin, T., Girma, A., Abiyu, A., Batsuren, D.2018. *Innovative Trend Analysis of Annual and Seasonal Rainfall Variability in Amhara Regional State, Ethiopia*. Atmosphere, 9, 326.
- Gerard, L.2010. Sensibilité des performances d'un modèle de prévision des crues au critère de calage (Sensitivity of the performance of a flood forecasting model to the calibration criterion). End of 2nd year internship, Institut National Polytechnique, Toulouse, France.
- Ghenim, A.N., Megnounif, A., Seddini, A., Terfous, A. 2010. *Fluctuations hydro-pluviométriques du bassin-versant de l'ouedTafna à BéniBahdel (Nord-Ouest algérien)* (Hydro-pluviometric fluctuations of the Tafna wadi watershed in Béni Bahdel (Northwest Algeria)). *Sécheresse*, 21, 115-120.
- Ghenim, A.N., Megnounif, A.2011. *Caractérisation de la sécheresse par les indices SPI et SSFI (Nord-Ouest de l'Algérie)* (Characterization of drought by the SPI and SSFI indices (North-West Algeria)). *Le Journal de l'Eau de de l'Environnement (LJEE)* 18, 59-77.
- Gherissi, R.2018. Modelisation Hydrologique D'un Bassin Versant En Climat Mediterranéen Par L'approche Conceptuelle Globale. Cas De L'oued Lakhdar (Ex : Chouly) (Tafna Nord Ouest Algerien) (Hydrological Modeling of a Watershed in a Mediterranean Climate Using

- the Global Conceptual Approach. Case Of Lakhdar Wadi (Ex: Chouly) (Tafna North West Algerian). PhD Thesis, University of Tlemcen, Faculty of Natural and Life Sciences and Earth and Universe Sciences, Algeria.
- Giandotti, M. 1934. Previsione delle pienee delle magre dei corsi d'acqua (Forecast of floods and lean streams), Ministry LL.PP, Memories hydrographic studies. Italian Hydrographic Service. Italy, 8(2), 107.
- Gibbs, W.J., Maher, J.V. 1967. Rainfall Deciles as Drought Indicators. Bureau of Meteorology bulletin No. 48. Commonwealth of Australia, Melbourne, VIC, Australia.
- Gilbert, R. O.1987.Statistical methods for environmental pollution monitoring, John Wiley & Sons, New York, USA.
- Gleick, P. 2003. Global freshwater resources: Soft path solutions for the 21st century. Journal of Science, 302: 1524-1528.
- Gocic, M., Trajkovic, S. 2013. *Analysis of Changes in Meteorological Variables Using Mann-Kendall and Sen's Slope Estimator Statistical Tests in Serbia. Global and Planetary Change*, 100, 172–182.
- Gocic, M., Trajkovic, S., 2013a. *Analysis of trends in reference evapotranspiration data in a humid climate. Hydrologic Sciences Journal*, 59:1, 165-180, DOI: 10.1080/02626667.2013.798659
- Götzinger, J.2007. Distributed conceptual hydrological modeling - simulation of climate, land use change impact and uncertainty analysis. PhD Thesis. University of Stuttgart. Stuttgart, Germany.
- Griensven, A. V., Meixner, T., Grunwald, S., Bishop, T., Diluzio, M. , Srinivasan, R. 2006. *A global sensitivity analysis tool for the parameters of multi-variable catchment models. Journal of Hydrology*, 324, 10-23.
- Grillakis, M.G., Tsanis, I.K., Koutroulis, A.G.2010. *Application of the HBV hydrological model in a flash flood case in Slovenia. Natural Hazards and Earth System Sciences*, 10, 2713-2725. DOI.org/10.5194/nhess-10-2713-2010
- Gudmundsson, L., Tallaksen, L. M., Stahl, K., Clark, D. B., Dumont, E., Hagemann, S., Bertrand, N., Gerten, D., Heinke, J., Hanasaki, N., Voss, F., Koirala, S.2012. *Comparing large-scale hydrological model simulations to observed runoff percentiles in Europe. Journal of hydrometeorology*,13,604-620. DOI: 10.1175/JHM-D-11-083.1
- Güntner, A., 2008. *Improvement of global hydrological models using GRACE data. Surveys in Geophysics*, 29(4-5): 375-397.
- Guo, Y., Huang, S., Huang, Q., Leng, G., Fang, W., Wang, L., Wang, H. 2020. *Propagation thresholds of meteorological drought for triggering hydrological drought at various levels. Science of the Total Environment*. 712:136502. DOI:10.1016/J.Scitotenv.2020.
- Gupta, V., Sorooshian, S., Yapo, P.1998. *Towards improved calibration of hydrological models: multiple and noncomensurable measures of information. Water Resources Research*, 34, 751-763.
- Guttman, N. B. 1998. *Comparing the Palmer Drought Index and the Standardized Precipitation Index. Journal- American Water Resources Association*. Vol.34, 113-122.

- Haan, C., Johnson, H., Brakensiek, D. 1982. Hydrologic modeling of small watersheds. ASAE Monograph 5, American Society of Agricultural Engineers, Michigan, USA.
- Habibi, B., Meddi, M., Torfs, P.J.J.F., Remaoun, M., Van Lanen, H. A.J. 2018. *Characterisation and Prediction of Meteorological Drought Using Stochastic Models in the Semi-Arid Chélif–Zahrez Basin (Algeria)*. Journal of Hydrology: Regional Studies. Vol. 16, 15-31. DOI:10.1016/j.ejrh.2018.02.005.
- Hallouz, F., Meddi, M., Mahe, G., Karahacane, H. Ali Rahmani, S. E. 2019. *Tendance des précipitations et évolution des écoulements dans un cadre de changement climatique : bassin versant de l'oued Mina en Algérie*. Revue des sciences de l'eau / Journal of Water Science, 32 (2), 83-114. <https://doi.org/10.7202/1065202ar>
- Halwatura, D., McIntyre, N., Lechner, A. M., Arnold, S. 2017. *Capability of meteorological drought indices for detecting soil moisture droughts*. Journal of Hydrology: Regional Studies. Vol.12, 396-412.
- Hamlaoui-Moulai, L., Mesbah, M., Souag-Gamane, D., Medjerab, A. 2013. *Detecting Hydro-Climatic Change Using Spatiotemporal Analysis of Rainfall Time Series in Western Algeria*. Natural Hazards, 65, 1293–1311.
- Hamlet, A.E.K. 2014. Contribution a la gestion des ressources en eau des bassins versants de l'ouest Algerien a l'aide d'un système informatisé (contribution to the management of water resources in the western Algerian watersheds using a computerized system). University of Mohamed Boudiaf-USTO-, Oran. 243 p.
- Hammar, Y., Djebbar, Y., Khoualdia, W. 2014. *Caractérisation de la Variabilité Climatique : Cas du Bassin Versant de La Medjerda (Nord-Est Algérien)* [Characterization of Climate Variability : Case of Watershed Medjerda (North East of Algeria)]. Synthèse : Revue des Sciences et de la Technologie. No. 29. 6-23. DOI:10.12816/0027871.
- Hänsel, S., Schucknecht, A., Matschullat, J. 2016. *The Modified Rainfall Anomaly Index (MRAI)—Is This an Alternative to the Standardised Precipitation Index (SPI) in Evaluating Future Extreme Precipitation Characteristics*. Theoretical and Applied Climatology. Vol. 123.No. 3–4, 827- 44. DOI:10.1007/s00704-015-1389-y.
- Hasanean, H.M. 2004. *Precipitation Variability Over the Mediterranean and Its Linkage with El Nino Southern Oscillation (ENSO)*. Journal of Meteorology. 29, 151-160.
- Hasanean, H.M. 2004. *Variability of the North Atlantic Subtropical High and Associations with Tropical Sea-Surface Temperature*. International Journal of Climatology. 24, 945–957.
- Hauke, J., Kossowski, T. 2011. *Comparison of Values of Pearson's and Spearman's Correlation Coefficients on the Same Sets of Data*. Quaestiones Geographicae. Vol. 30. No. 2, 87–93. DOI:10.2478/v10117-011-0021-1.
- Hawkins, D. M. 1977. *Testing a sequence of observations for a shift in location*. Journal of the American Statistical Association., 72, 180-186.
- Hayes, M.J., Svoboda, M., Wilhite, D.A., Vanyarkho, O. 1999. *Monitoring the 1996 drought using the SPI*. Bulletin of the American Meteorological Society. Vol. 80, 429-438.

- HEC.1998. *Flood Hydrograph Package* (User's Manual ed.). USA : Hydrologic Engineering Center. US Army Corps of Engineers.
- Hillel, D. 1977. *Computer simulation of soil-water dynamics: a compendium of recent work*. IDRC, Ottawa, Canada.
- Hillel, D.2004. *Introduction to environmental soil physics*. Academic Press, 1st ed. New York, USA.
- Hirsch, R.M., Slack, J.R., Smith, R.A. 1982. *Techniques of trend analysis for monthly water quality data*. Water Resource Research. Vol.18,107-121.DOI:10.1029/WR018i001p00107
- Horton, R.E. 1932. *Drainage basin characteristics*. Eos Transactions American Geophysical Union, 13(1), 350-361.
- Horton, R.E. 1945. *Erosional development of streams and their drainage basins; hydrophysical approach to quantitative morphology*. Bulletin of the Geological Society of America. 56(3), 275-370.
- Hsu, K., Gupta, V., Sorooshian, S.1995. *Artificial neural network modeling of the rainfall runoff process*. Water Resources Research, 31, 2517-2530.
- Hubert, P, Carbonnel, J.P, Chaouche, A.1989. *Segmentation of Hydrometeorological Series. Application to a Series of Precipitation and Flow of West Africa*. Journal of Hydrology, 110, 349-367.
- Hubert, P, Carbonnel, J.P.1993. *Segmentation Annual Series of Major African Rivers Flow. Bind. CIEH Bull, 3, 92*.
- Hubert, P.2000.*The Segmentation Procedure as a Tool for Discrete Modeling of Hydrometeorological Regimes. Stochastic Environmental Research and Risk Assessment*.14, 297-304.
- Huth, R., Pokorn, L. 2004.*Parametric versus Non-Parametric Estimates of Climatic Trends*. Theoretical and Applied Climatology.77, 107-112.
- IPCC: Climate Change .2014. Synthesis Report. Contribution of Working Groups I, II and III to the Fifth Assessment Report of the Intergovernmental Panel on Climate Change.
- Jain, V. K., Pandey, R. P., Jain, M. K., Byun, H.R. 2015. *Comparison of drought indices for appraisal of drought characteristics in the Ken River Basin*. Weather and Climate Extremes. Vol.8. 1-11.
- Jain, S. K., Kumar,V. 2012.*Trend Analysis of Rainfall and Temperature Data for India*. Current Science.Vol. 102. No. 1.13 p.
- Jeniffer, K., Su, Z., Woldai, T. and Maathuis, B., 2010. *Estimation of spatial-temporal rainfall distribution using remote sensing techniques: a case study of Makanya Catchment, Tanzania*. International Journal of Applied Earth Observation and Geoinformation, 12, 590-599.
- Jensen, M.E., Haise, H.R. 1963. *Estimating evapotranspiration from solar radiation*. Journal of Irrigation and Drainage Division, ASCE. Vol. 89 (LR4),15-41.

- Johansson, B., Chen, D. 2003. *The influence of wind and topography on precipitation distribution in Sweden: Statistical analysis and modeling*. International Journal of Climatology, 23(12), 1523-1535.
- Jovanovic, N., Israel, S., 2012. *Critical review of methods for the estimation of actual evapotranspiration in hydrological models*. In: Irmak, D.A., ed. *Evapotranspiration – remote sensing and modeling*. In Tech Open, 329-350.
- Jiang, H. 2004. Quantitative precipitation and hydrometeor content estimation in tropical cyclones from remote sensing observations. PhD Thesis. University of Utah, Salt Lake City, USA.
- Jiang, Y., Zhou, C. & Cheng, W.2007. *Streamflow trends and hydrological response to climatic change in Tarim headwater basin*. Journal of Geographical Sciences.17, 52-61, DOI: 10.1007/s11442-007-0051-8
- Kadir, M., Fehri, R., Souag, D.,Vanclooster, M.2020. *Exploring causes of streamflow alteration in the Medjerda river, Algeria*. Journal of Hydrology: Regional Studies, 32,100750
- Kale, S., Sönmez, A.Y. 2018. *Trend analysis of mean monthly, seasonally and annual streamflow of Daday Stream in Kastamonu, Turkey*. Marine Science and Technology Bulletin, 7(2): 60-67.
- Kanellou, E., Domenikiotis, C., Blanta, A., Hondronikou, E., Dalezios, N.R.2008.*Index-based Drought Assessment in Semi-Arid Areas of Greece based on Conventional Data*. European Water. Vol. 23/24, 87-98.
- Karimou Barké, M., Ousseini, I., Biolders, C., Jean-Marie, Ambouta, K., Tychon, B. 2017. *Caractérisation morphologique des cuvettes oasiennes du Centre-Est du Niger*(Morphological characterization of oasis basins in central-eastern Niger). Physio-Géo - Géographie Physique et Environnement, 11, 255-276. DOI: 10.4000/physio-geo.5607.
- Karlsen, R. H., Grabs, T., Bishop, K., Laudon, H., Seibert, J.2014, Landscape controls on spatiotemporal variability of specific discharge in a boreal region, Abstract #H52B-07 presented at 2014 Fall Meeting, AGU, San Francisco, Calif., 15-19 Dec. [Available at <http://adsabs.harvard.edu/abs/2014AGUFM.H52B.07K>, last accessed 21 Oct 2015.]
- Kay, A.L., Davies, H.N. 2008. *Calculating potential evaporation from climate model data: a source of uncertainty for hydrological climate change impacts*. Journal of Hydrology. Vol. 358. N°. 3-4, 221-239. Doi:10.1016/j.jhydrol.2008.06.005.
- Kauark Leite, L.A.1990. *Reflexions sur l'utilite des modeles mathematiques dans la gestion de la pollution diffuse d'origine agricole*(Reflections on the usefulness of mathematical models in the management of diffuse pollution of agricultural origin). Brief presented at the National School of Pontset Chaussees, CERGRENE, Paris, France.
- Ketrouci, K., Meddi, M., Abdesselam, B.2012. *Study of the extreme floods in Algeria: The case of the Tafna catchment area*. Sécheresse, 23, 297–305.

- Keyantash, J., Dracup, J.A. 2002. The quantification of drought: an evaluation of drought indices. *Bulletin of the American Meteorological Society*. Vol. 83.Issue.8. 1167-1180.DOI:10.1175/1520-0477-83.8.1167.
- Khedimallah, A., Meddi, M., Mahé, G. 2020. *Characterization of the interannual variability of precipitation and runoff in the Cheliff and Medjerda basins (Algeria)*. *Journal of Earth System Science*, 129(1). DOI:10.1007/s12040-020-01385-1
- Khezazna, A., Amarchi, H., Derdous, O., Bousakhria, F. 2017.*Drought monitoring in Seybouse Basin (Algeria) over the last decades*. *Journal of Water and Land Development*. No. 33, 79-88. DOI10.1515/jwld-2017-0022.
- Khoualdia, W., Djebbar, Y., Hammar, Y. 2014.*Caractérisation de la variabilité climatique: cas du bassin versant de La Medjerda (Nord-Est algérien)* [Climatic variability characterisation: Case of Medjerda watershed (Northeastern Algeria)]. *Synthèse: Revue des Sciences et de la Technologie*. Vol. 29. No. 1, 6–23.
- Kingumbi, A. 2006. Modélisation hydrologique d'un bassin affecté par des changements d'occupation. Cas du Merguellil en Tunisie centrale (Hydrological modeling of a basin affected by changes in occupation). Case of Merguellil in central Tunisia. PhD Thesis, El Manar University. 300 p .
- Kisi, O., Ay, M. 2014. *Comparison of Mann–Kendall and Innovative Trend Method for Water Quality Parameters of the Kizilirmak River, Turkey*. *Journal of Hydrology*. 513, 362–375.
- Kloosterman, P.2012. A comparison of the performance of lumped hydrological models in modeling a flash flood in the Hupsel Brook catchment. MSc thesis .Hydrology and Quantitative Water Management Group. Wageningen University, Wageningen.
- Knippertz, P., Ulbrich, U., Marques, F., Corte-Real, J. 2003. *Decadal Changes in the Link between El Niño and Springtime North Atlantic Oscillation and European-North African Rainfall: EL Niño, Nao, European-North African Rainfall*. *International Journal of Climatology*. 23, 1293-1311.
- Konz, M., Seibert, J. 2010. *On the value of glacier mass balances for hydrological model calibration*, *Journal of Hydrology*. 385, 238–246. DOI:10.1016/j.jhydrol.2010.02.025, 2010
- Krause, P., Boyle, D. P., Bäse, F. 2005. *Comparison of different efficiency criteria for hydrological model assessment*. *Advances in Geosciences*, 5, 89- 97.
- Kumar, N., Tischbein, B., Beg, M.K. 2019. *Multiple Trend Analysis of Rainfall and Temperature for a Monsoon-Dominated Catchment in India*. *Meteorology and Atmospheric Physics*. 131, 1019-1033.
- Kumar V. 1998. *An early warning system for agricultural drought in an arid region using limited data*. *Journal Arid Environments*. Vol. 40, 199–209.
- Kumar, P. 2011.*Typology of hydrologic predictability*. *Water Resources Research*, 47(4). DOI: 10.1029/2010WR009769

- Kunnath-Poovakka, A., Eldho, T.I. 2019. *A comparative study of conceptual rainfall-runoff models GR4J, AWBM and Sacramento at catchments in the upper Godavari river basin, India. Journal of Earth System Science, 128, 1-15.*
- Laborde, J. P., Assaba, M., Belhouli, L. 2003. *Les chroniques mensuelles de pluies de bassin: un préalable à l'étude des écoulements en Algérie* (Monthly basin rainfall chronicles: a prerequisite for the study of flows in Algeria). Colloque International Gestion du risque eau en pays semi aride. Tunis. 10 p.
- Lall, U. 2014, *Debates—The future of hydrological sciences: A (common) path forward? One water. One world. Many climes. Many souls*, Water Resources Research. 50, 5335–5341, DOI:10.1002/2014WR015402.
- Lappas, I., Tsioumas, I., Zorapas, V. 2017. *Spatial-Temporal Analysis, Variation and Distribution of Precipitation in the Water District of Central-Eastern Greece*. Bulletin de la Société Géologique. Greece, 47, 740.
- Lavabre, J., Fouchier, C., Gregoris, Y., Faure-Soulet, A. 2003. Mise en œuvre d'un modèle régional pour la prédétermination des crues (Implementation of a regional model for flood predetermination). Conférences SIRNAT-forum JPRN, Les journées pour la prévention des risques naturels, Orléans. 7 p.
- Lazri, M., Ameer, S., Brucker, J.M., Lahdir, M., Sehad, M. 2015. *Analysis of drought areas in Northern Algeria using Markov chains*. Earth System and Science. Vol.124, 61. DOI.org/10.1007/s12040-014-0500-6.
- Legates, D.R., McCabe G.J. 1999. *Evaluating the use of “goodness of fit” measures in hydrologic and hydroclimatic model validation*. Water resources research, 35(1): 233-241.
- L'Hôte, Y.; Mahé, G.; Somé, B.; Triboulet, J. P. 2002. *Analysis of a Sahelian Annual Rainfall Index from 1896 to 2000; the Drought Continues*. Hydrological Sciences Journal, 47 (4), 563–572. <https://doi.org/10.1080/02626660209492960>.
- Lidén, R., Harlin, J., 2000. *Analysis of conceptual rainfall– runoff modelling performance in different climates*. Journal of Hydrology. 238 (3–4), 231-247. DOI:10.1016/S0022-1694(00)00330-9
- te Linde, A. H., Aerts, J. C. J. H., Hurkmans, R. T. W. L., Eberle, M. 2008. *Comparing model performance of two rainfall-runoff models in the Rhine basin using different atmospheric forcing data sets*. Hydrology and Earth System Sciences, 12, 943-957.
- Lionello, P., Malanotte-Rizzoli, P., Boscolo, R., Luterbacher, J. 2004. *The Mediterranean Climate: Basic Issues and Perspectives*. White Paper on Mediterranean Climate Variability and Predictability Positioning MedCLIVAR as coordinated scientific activities under CLIVAR umbrella. International CLIVAR Project Office. Draft version 29th March 2004
- Liuzzo, L., Bono, E., Sammartano, V., Freni, G. 2016. *Analysis of Spatial and Temporal Rainfall Trends in Sicily during the 1921–2012 Period*. Theoretical and Applied Climatology, 126, 113–129.
- Liuzzo, L., Notaro, V., Freni, G. 2017. *Uncertainty Related to Climate Change in the Assessment of the DDF Curve Parameters*. Environmental Modelling & Software, 96, 1-13.

- Lloyd-Hughes, B., Saunders, M. 2002. *A drought climatology for Europe*. International Journal of Climatology. Vol. 22.Issue.13, 1571-1592.
- Lobligeois, F. 2014. Mieux connaître la distribution spatiale des pluies améliore-t-il la modélisation des crues ? Diagnostic sur 181 bassins versants français (Does better understanding the spatial distribution of rainfall improve flood modeling? Diagnosis on 181 French watersheds). PhD Thesis. L'Institut des Sciences et Industries du Vivant et de l'Environnement AgroParisTech. Paris, France.
- Longobardi, A., Villani, P. 2009. *Trend Analysis of Annual and Seasonal Rainfall Time Series in the Mediterranean Area*. International Journal of Climatology.30, 1538-1546. DOI.org/10.1002/joc.2001.
- Lopez-Bermudez, F., Romero-Diaz, A., Martinez-Fernandez, J., Martinez-Fernandez, J. 1998. *Vegetation and Soil Erosion under a Semi-Arid Mediterranean Climate: A Case Study from Murcia (Spain)*. Geomorphology, 24, 51-58.
- Lopez, J., Frances, F.2010. *Influence of the North Atlantic oscillation and the western Mediterranean oscillation in the maximum flow events in Spain*. International workshop advances in statistical hydrology, Taormina, Italy. May 23–25.
- Lorenzo-Lacruz, J., Morán-Tejeda, E.2016.*Spatio-Temporal Patterns of Meteorological Droughts in the Balearic Islands (Spain)*.Cuadernos de Investigación Geográfica. Vol. 42.No. 1, 49 p. DOI:10.18172/cig.2948.
- Loumagne, C.1988. Prise en compte d'un indice de l'état hydrique du sol dans la modélisation pluie-débit (Taking into account an index of the water state of the soil in the rainfall-flow modeling). PhD Thesis, University of Paris-Sud (Orsay), France.
- Luterbacher, J., Xoplaki, E., Gonzalez-Rouco, J. F., Herrera, R. G, Zorita, E., Jacobeit, J., Gonzalez-Hidalgo, J.C., Türkes, M., Gimeno, L., Ribera, P., Brunet-India, M., Crepon, M., Alpert, A.M.P. 2004. *Present Trends of Mediterranean Climate*. White Paper on Mediterranean Climate Variability and Predictability Positioning Med CLIVAR as coordinated scientific activities under CLIVAR umbrella. International CLIVAR Project Office. Draft version 29th March 2004.
- Lyon, S. W., Nathanson, M., Spans, A., Grabs, T., Laudon, H., Temnerud, J., Bishop, K. H., Seibert, J. 2012, *Specific discharge variability in a boreal landscape*, Water Resource Research, 48, W08506. DOI:10.1029/2011WR011073.
- Madsen, H., Wilson, G., Ammentorp, H. C. 2002.*Comparison of different automated strategies for calibration of rainfall-runoff models*. Journal of Hydrology, 261(1-4), 48-59.
- Maftai, C.P. 2002. Etude concernant les écoulements superficiels, modélisation spatialisée de l'écoulement sur le bassin versant de Voinesti, Roumani (Study concerning surface flows, spatialized modeling of the flow on the Voinesti, Roumani watershed). PhD Thesis. University of Ovidius. Roumanie. 208 p.
- Maftai, C., Barbulescu, A., Buta, C., Serban, C.2011. *Change Points Detection and Variability Analysis of Some Precipitation Series*. Recent Res. Comput. Tech. Non-Linear Syst. Control, 232-237.

- Mailhot, A., Rousseau, A. N., Salvano, E., Turcotte, R., Villeneuve, J. P. 2002. *Évaluation de l'impact de l'assainissement Urbain sur la qualité des eaux du bassin versant de la rivière Chaudière à l'aide du système de modélisation intégrée GIBSI (Assessment of the impact of Urban Sanitation on the water quality of the Chaudière River watershed using the GIBSI integrated modeling system)*. Revue des sciences de l'eau, 15, 149-172.
- Mailhot, A., Villeneuve, J.P. 2003. *Mean-value second-order uncertainty analysis method: application to water quality modeling*. Advances in water Resources, 26. 491-499.
- Ma, M., Ren, L., Singh, V.P., Yuan, F., Chen, L., Yang, X., Liu, Y. 2015. *Hydrologic model-based Palmer indices for drought characterization in the Yellow River basin, China*. Stochastic Environmental Research and Risk Assessment. Vol.30, 1401-1420. DOI:10.1007/s00477-015-1136-z.
- Marc, V., Knight, R., Pool, S., Wolfe, W., Seibert, J. 2015. *Model Calibration Criteria for Estimating Ecological Flow Characteristics*. Water, 7, 2358-2381, Doi:10.3390/w7052358
- Maref, N. 2019. Démarche méthodologique d'adaptation d'un système de prévision aux risques d'inondation en Algérie, cas du bassin versant de l'oued mekerra (N.W Algérien)(Methodological approach for adapting a forecasting system to flood risks in Algeria, case of the watershed of the Wadi Mekerra (Algerian N.W)). PhD Thesis. University of Tlemcen, Algeria.
- Marengo, J. A., Tomasella J., Alves, L.M., Soares, W. R., Rodriguez, D. A. 2011. *The drought of 2010 in the context of historical droughts in the Amazon region*. Geophysical Research Letters. Vol.38.Issue.12, L12703. DOI:10.1029/2011GL047436.
- Martin-Vide, J., Lopez-Bustins, J. A. 2006. *The western Mediterranean Oscillation and rainfall in the Iberian Peninsula*. International Journal of Climatology, 26, 1455-1475.
- Masih, I., Uhlenbrook, S., Maskey, S., Ahmad, M.D.2010. *Regionalization of a conceptual rainfall-runoff model based on similarity of the flow duration curve: A case study from the semi-arid Karkheh basin, Iran*. Journal of Hydrology, 391, 188-201.
- Matari, A., Douguedroit, A. 1995. *Chronologie des Précipitations et des Sécheresses dans l'ouest Algérien (Chronology of Precipitation and Drought in Western Algeria)*; Alger, Algeria, 1995.
- Mccarthy, J.J. 2001. *Climate Change 2001: Impacts, Adaptation, and Vulnerability: Contribution of Working Group II to the Third Assessment Report of the Intergovernmental Panel on Climate Change*. Cambridge University Press.
- Mcguinness, J.L., Bordne, E.F. 1972. *A comparison of lysimeter-derived potential evapotranspiration with computed values*. Technical Bulletin 1452, Agricultural Research Service, U.S. Department of Agriculture - Washington D.C. 71 p.
- Mckee, T.B., Doesken, N.J., Kleist, J.1993. *The relationship of drought frequency and duration to time scales*. Eighth Conference on Applied Climatology. Anaheim, California. No. 1 p. 179-184.
- Meddi, M.M., Assani, A.A., Meddi, H. 2010. *Temporal Variability of Annual Rainfall in the Macta and Tafna Catchments, Northwestern Algeria*. Water Resources Management, 24, 3817-3833.

- Meddi, M., Boucefiane, A., Belabbes, A.S. 2010 a. *Impact of climate change on runoff in the Chellif basin (Algeria)*. Global change. Facing Risks and Threats to Water Resources, 340, 95-102.
- Meddi, M., Hubert, P.2003. *Impact of a change in rainfall levels on water resources of northwestern Algeria*. Hydrology of Mediterranean and Semiarid Regions, 278, 229-235.
- Meddi, H., and Meddi, M.2004. *Sécheresse et spatialisation des précipitations dans le nord-ouest de l'Algérie*. *International Symposium (Terre et Eau)* (Drought and spatialization of precipitation in north-western Algeria. International Symposium (Land and Water)), Annaba, Algeria, November21-23.
- Meddi, H., Meddi, M.2009. *Variabilité des précipitations annuelles du Nord-Ouest de l'Algérie* (Variability of annual precipitation in North-West Algeria). *Sécheresse*, 20, 57- 65.
- Meddi, M., Toumi, S., Mehaiguen, M.2013. *Hydrological drought in Tafna Basin–Algeria*. Proceedings of the 13th International Conference of Environmental Science and Technology Athens. Greece, 5-7 September 2013.
- Medjerab, A., Henia, L. 2005. *Régionalisation Des Pluies Annuelles Dans L'algérie Nord-Occidentale* (Regionalization of Annual Rainfall In North-Western Algeria). *Revue Géographique De L'est*. Vol. 45. No. 2.
- Megnounif, A.; Terfous, A.; Ghenaim, A.; Poulet, J.-B. 2007. *Key Processes Influencing Erosion and Sediment Transport in a Semi-Arid Mediterranean Area: The Upper Tafna Catchment, Algeria/Processus Clefs Influençant l'érosion et Le Transport des Sédiments dans Une Région Semi-Aride Méditerranéenne: Le Bassin Versant de La Haute Tafna, Algérie*. *Hydrological Sciences Journal*, 52, 1271-1284.
- Mehta, A.V., Yang, S. 2008. *Precipitation Climatology over Mediterranean Basin from Ten Years of TRMM Measurements*. *Advances in Geosciences*, 17, 87- 91.
- Mekhloufi, N.2014. *Prédétermination et Prévision des étiages Des Oueds de l'Algérie Septentrionale* (Predetermination and forecasting of low water levels in the wadis of northern Algeria). Magister Thesis. University Kasdi Merbah. *Ouargla, Algeria*.
- Melching, C.S., Ben, C.Y., Harry, G., Wenzel, J. 1990. *A reliability estimation in modeling watershed runoff with uncertainties*. *Water Resources Research*, 26(10):2275-2286.
- Mengistu, A.G., Tesfahuney, W.A., Woyessa, Y.E., van Rensburg, L.D. 2020. *Analysis of the Spatio-Temporal Variability of Precipitation and Drought Intensity in an Arid Catchment in South Africa*. *Climate*, 8, No. 6, 70. <https://doi.org/10.3390/cli8060070>
- Michel, C., Perrin, C., Andréassian, V. 2003. *The exponential store: a correct formulation for rainfall–runoff modeling*. *Hydrology Science Journal*, 48(1),109-124.
- Mockus, V., 2004. Estimation of direct runoff from storm rainfall (Chapter 10). *In: National Engineering Handbook, Part 630-Hydrology*. USDA Soil Conservation Service, pp. 10.1-10.22 Washington, DC, USA.
- Moine, N.L. 2008. *Le bassin versant de surface vu par le souterrain : une voie d'amélioration des performances et du réalisme des modèles pluie-débit ?* (The surface watershed seen from

- underground: a way to improve the performance and realism of rain-flow models?). PhD Thesis. Pierre and Marie Curie University. 348 p.
- Mondal, A., Khare, D., Kundu, S. 2015. *Spatial and temporal analysis of rainfall and temperature trend of India*. Theoretical and Applied Climatology, 122, 143-158
- Morel-Seytoux, H. 1978. *Derivation of equations for variable rainfall infiltration*. Water Resources Research. 14 (4), 561- 568.
- Morid, S., Smakhtin, V., Moghaddasi, M. 2006. *Comparison of seven meteorological indices for drought monitoring in Iran*. International Journal of Climatology. Vol. 26. Iss. 8. 971-985.
- Mo, X., Liu, S., Lin, Z. Zhao, W., 2004. *Simulating temporal and spatial variation of evapotranspiration over the Lushi basin*. Journal of Hydrology. 285(1), 125-142.
- Moussu, F. 2011. *Prise en compte du fonctionnement hydrodynamique dans la modélisation pluie-débit des systèmes karstiques (Taking into account the hydrodynamic functioning in the rainfall-flow modeling of karst systems)*. PhD Thesis. University of Pierre and Marie Curie, Paris, France.
- Mrad, D., Djebbar, Y., Hammar, Y. 2018. *Analysis of Trend Rainfall: Case of North-Eastern Algeria*. Journal Water Land Deveplement, 36, 105-115.
- Muchuru, S., Botai, J. O., Botai, C. M., Landman, W. A., Adeola, A. M. 2016. *Variability of rainfall over Lake Kariba catchment area in the Zambezi river basin, Zimbabwe*. Theoretical and Applied Climatology. 124, 325-338. DOI 10.1007/s00704-015-1422-1
- Muleta, M. K., Nicklow, J.W. 2005. *Sensitivity and uncertainty analysis coupled with automatic calibration for a distributed watershed model*. Journal of Hydrology. 306, 127-145.
- Muñoz-Díaz, D., Rodrigo, F.S. 2003. *Effects of the North Atlantic Oscillation on the Probability for Climatic Categories of Local Monthly Rainfall in Southern Spain*. International Journal of Climatology. 23, 381-397.
- Musy, A., Higy, C. 1998. *Hydrologie appliquée*. Suisse : Ecole Polytechnique Fédérale de Lausanne. 61.
- Nalbantis, I. 2008. *Evaluation of a Hydrological Drought Index*. European Water, 23/24, 67-77.
- Nalbantis, I., Tsakiris, G. 2009. *Assessment of hydrological drought revisited*. Water Resource Management. 23, 881-897.
- Nash, J.E., Barsi, B.I. 1983. *A hybrid model for flow forecasting on large catchments*. Journal of Hydrology, 65, 125-137.
- Nash, J. E. Sutcliffe, J.V. 1970. *River flow forecasting through conceptual models, Part I - A discussion of principles*. Journal of Hydrology. 10, 282-290.
- Nauditt, A., Birkel, C., Soulsby, C., Ribbe, L. 2017. *Conceptual modeling to assess the influence of hydro-climatic variability on runoff processes in data scarce semi-arid Andean catchments*. Hydrological Sciences Journal. 62, 515-532. DOI/10.1080/02626667.2016.1240870

- Ndiaye, M.L., Toure, M.A., Diaw, A.T. 2016. *Contribution of Remote Sensing to The Study of Spatiotemporal Evolution of Rainfall in Senegal: Exploitation of TRMM 3B43 Low Spatial Resolution*. Journal of multidisciplinary engineering science studies, 2, 6.
- Normand, S., Konz, M., Merz, J.1970. *An application of the HBV model to the Tamor Basin in Eastern Nepal*. Journal Hydrology and Meteorology,7, 49-58. DOI.org/10.3126/jhm.v7i1.5616
- Nouaceur, Z. 2011.*Vers Un Retour des Pluies Sur La Rive Sud Du Bassin Mediterranéen Occidental: Analyse et Evaluation de la Tendence Pluviométrique sur plus d'un Demi – Siècle en Algérie* (Towards a Return of the Rains on the South Shore of the Western Mediterranean Basin: Analysis and Evaluation of the Rainfall Trend over More than Half a Century in Algeria). Annals of "Valahia" University of Târgoviște Geographical Series. 11, 6.
- Nouaceur, Z., Murarescu, O. 2016a. *Rainfall Variability and Trend Analysis of Annual Rainfall in North Africa*. International Journal of Atmospheric Sciences, 1-12.
- Nouaceur, Z., Murarescu, O. 2016b. *Trend of Rainfall Over Nearly Half a Century in North Africa*. Air. Water Components Of The Environment , 84, 9.
- Nouaceur, Z., Murărescu, O., Murătoreanu, G.2017.*Rainfall Variability and Trend Analysis of Multiannual Rainfall in Romanian Plain*. Annals of Valahia University of Targoviste Geographical Series.Vol.17, 124-144.DOI:10.1515/avutgs-2017-0012.
- Obled, C., Zin, I. ., Hingray, B.2009. *Choix des pas de temps et d'espace pour des modélisations parcimonieuses en hydrologie des crues (Choice of time and space steps for parsimonious modeling in flood hydrology)*. la Houille Blanche, 5, 81-87.
- Oddos, A. 2002. Intérêt d'une approche semi distribuée par rapport à une approche globale en modélisation pluie-débit(Interest of a semi-distributed approach compared to a global approach in rainfall-flow modeling). Thesis for the Engineering Diploma of ENGEES and DEA, Mechanics and Engineering option Water Sciences, University of Louis Pasteur Strasbourg.99 p.
- Otmane, A., Baba Hamed, K., Bouanani, A., Kebir, L.W.2018.*Mise en Évidence de la Sécheresse Par l'étude de La Variabilité Climatique Dans Le Bassin Versant de l'oued Mekerra (Nord-Ouest Algérien) (Highlighting drought by studying climate variability in the watershed of the Mekerra river (northwest of Algeria))*. Techniques sciences méthodes, 9, 23-37.
- Otmane, A., Baba-Hamed, K, Safa, A. 2015. *Prédétermination des valeurs de pluies et crues extrêmes dans le bassin versant d'Oued Mekerra (Predetermination of extreme rainfall and flood values in the Oued Mekerra watershed)*. Master Thesis, University of Oran 2, P .187.
- Ouachani, R. 2003. *Etude des ressources en eaux des bassins frontaliers de l'extrême nord ouest de la Tunisie (Study of the water resources of the border basins of the extreme northwest of Tunisia)*. Engineering graduation project, National Engineering School of Tunis (ENIT), Tunisia.
- Ouachani, R. 2004. *Implémentation d'une procédure de mise à jour pour le modèle HBV (Implementation of an update procedure for the HBV model)*. MSc Thesis, ENIT, Laboratory of modeling in hydraulics and environment (LMHE), Tunis, Tunisia.

- Oudin, L., Kay, A., Andreassian, V., Perrin, C. 2010, *Are seemingly physically similar catchments truly hydrologically similar?*. *Water Resource Research*. 46, W11558, DOI:10.1029/2009WR008887
- Oudin, L. 2004. Recherche d'un modèle d'évapotranspiration potentielle pertinent comme entrée d'un modèle pluie-débit global (Search for a relevant potential evapotranspiration model as an input to a global rainfall-discharge model). PhD Thesis. Cemagref. Ecole Nationale du Génie Rural, des eaux et des forêts, centre de Paris. 495 p.
- Oudin, L., Hervieu, F., Michel, C., Perrin, C., Andréassian, V., Anctil, F., Loumagne, C. 2005. *Which potential evapotranspiration input for a rainfall-runoff model, Part 2—towards a simple and efficient PE model for rainfall-runoff modelling*. *Journal of Hydrology*. 303, 290-306.
- Ouatiki, H., Boudhar, A., Ouhinou, A., Beljadid, A., Leblanc, M., Chehbouni, A. 2020. *Sensitivity and Interdependency Analysis of the HBV Conceptual Model Parameters in a Semi-Arid Mountainous Watershed*. *Water*. 12(9), 2440. <https://doi.org/10.3390/w12092440>
- Pal, A.B., Khare, D., Mishra, P.K., Singh, L. 2017. *Trend Analysis of Rainfall, Temperature and Runoff Data: A Case Study of Rangoon Watershed in Nepal*. *International Journal of Students' Research in Technology & Management*. 5, 21-38.
- Panda, A., Sahu, N. 2019. *Trend Analysis of Seasonal Rainfall and Temperature Pattern in Kalahandi, Bolangir and Koraput Districts of Odisha, India*. *Atmospheric Science Letters*, 20.
- Passioura, J. 2007. *The drought environment: physical, biological and agricultural perspectives*. *Journal of Experimental Botany*. Vol.58. No.2, 113-7.
- Pathak, A.A., Channaveerappa., Dodamani, B.M. 2019. *Comparison of two hydrological drought indices*. *Perspectives in Science*. Vol.8, 626-628.
- Paulo, A.A., Pereira, L.S. 2006. *Drought Concepts and Characterization*. *Water International*. 31, 37-49. <https://doi.org/10.1080/02508060608691913>
- Pearson, K. 1896. *Mathematical contributions to the theory of evolution. III. Regression, heredity, and panmixia*. *Philosophical Transactions of the Royal Society Series. A* 187, 253–318.
- Pearson, K. 1900. *Mathematical contributions to the theory of evolution. VII. On the correlation of characters not quantitatively measurable*. *Philosophical Transactions of the Royal Society Series. A* 195, 1- 47.
- Perrin, C. 2000. Vers une amélioration d'un modèle global pluie-débit au travers d'une approche comparative (Towards an improvement of a global rainfall-runoff model through a comparative approach). PhD Thesis, INPG (Grenoble) / Cemagref (Antony). 530 p.
- Perrin, C. 2002. *Vers une amélioration d'un modèle global pluie-débit au travers d'une approche comparative* (Towards an improvement of a global rainfall-runoff model through a comparative approach). *Houille Blanche*, EDP Science, No 6-7, 84-91.
- Perrin, C., Michel, C. 2002. Robustness of two flood estimation methods with data availability. In: Spreafico M, Weingartner R, Dobmann J, Hodel H, Hunziker S (eds)

- International conference on flood estimation. International commission for the hydrology of the rhine basin (CHR), Berne, 629-635.
- Perrin, C., Michel, C., Andréassian, V. 2003. *Improvement of a parsimonious model for streamflow simulation*. Journal of Hydrology, 279(1-4): 275-289.
- Peterson, T.C., Easterling, D.R., Karl, T.R., Groisman, P., Nicholls, N., Plummer, N., Torok, S., Auer, I., Boehm, R., Gullett, D., et al. 1998. *Homogeneity Adjustments of in Situ Atmospheric Climate Data: A Review* International Journal of Climatology. 18, 1493-1517.
- Pettitt A.N. 1979. *A Non-Parametric Approach to the Change Point Problem*. Applied Statistics. 25, 126.
- Philandras, C.M., Nastos, P.T., Kapsomenakis, J., Douvis, K.C., Tselioudis, G., Zerefos, C.S. 2011. *Long Term Precipitation Trends and Variability within the Mediterranean Region*. Natural Hazards and Earth System Sciences, 11, 3235-3250.
- Planos, E., Scatena, F., Servat, E. Climate Variability and Change Hydrological Impacts, Vol. 308. IAHS-AISH Publication. IAHS Press. Wallingford. UK. 122-127.
- Plate, E.J., Zehe, E. 2008. Wasser- und Stofftransport auskleinen ländlichen Einzugsgebieten (Water and material transport in small rural catchment areas). Schweizerbart, Stuttgart. Germany. 365 p.
- Pool, S. 2018. *Value of Hydrograph Characteristics or Single Discharge Observations in Hydrological Modeling*. University of Zurich. 177p. <https://doi.org/10.5167/UZH-169494>
- Pozo-Vázquez, D., Esteban-Parra, M. J., Rodrigo, F., Castro-Díez, Y. 2001. *A study of NAO variability and its possible non-linear influences on European surface temperature*. Climate Dynamics. 17, 701-715.
- Pushpalatha, R., Perrin, C., Le Moine, N., Mathevet, T., Andreassian, V. 2011. *A downward structural sensitivity analysis of hydrological models to improve low-flow simulation*. Journal of Hydrology. 411, 66-76.
- Qin, L., He, Y., Huang, W., Ma, G. 2017. *Analysis of the rainfall and runoff temporal variation of Jialing River during 1955-2006*. Advances in Materials, Machinery, Electronics I. AIP Conference Proceedings. 1820, 080008. <https://doi.org/10.1063/1.4977364>
- Rahman, A.S., Kamruzzama, M., Jahan, C.S., Mazumder, Q.H. 2016. *Long-Term Trend Analysis of Water Table Using 'MAKESENS' Model and Sustainability of Groundwater Resources in Drought Prone Barind Area, NW Bangladesh*. Journal of the Geological Society of India. Vol. 87. No. 2. 179-93. DOI:10.1007/s12594-016-0386-9.
- Ramos, M. C., Martínez-Casasnovas, J. A. 2006. *Trends in Precipitation Concentration and Extremes in the Mediterranean Penedès-Anoia Region, Ne Spain*. Climate Change, 74 (4), 457-474. <https://doi.org/10.1007/s10584-006-3458-9>.
- Ramos, M., Thielen, Del Pozo, J., De Roo, A. 2005. *Prévision Hydrologique d'Ensemble et Alerte avec le Système Européen d'Alerte aux Crues (EFAS): Cas des Cues du Bassin du Danube (Ensemble Hydrological Forecasting and Warning with the European Flood Warning System (EFAS): Case of the Danube Basin Cues) en Août 2005*. In: Jean Michel Tanguy,

- editor. De la goutte de pluie jusqu'à la mer, traite d'hydraulique d'environnementale. Paris (France): HERMES Sciences Lavoisier; 2009. 69-85. JRC47656
- Rasheed, H., Al-Anaz, H., Abid, K.1989. *Evaporation from soil surface in presence of shallow water tables*. IAHS Publishing, Baltimore, Maryland, USA.
- Reed, S., Schaake, J., Zhang, Z. 2007. *A distributed hydrologic model and threshold frequency-based method for flash flood forecasting at ungauged locations*. Journal of Hydrology. 337, 402-420. 61
- Refsgaard, J., Storm, B.1996. *Distributed Hydrological Modelling*, Chapter Construction, calibration and validation of hydrological models. 41-54. Netherlands : Kluwer Academic Publishers.
- Refsgaard, J.C.1991. *Parameterisation, calibration and validation of distributed hydrological models*. Journal of Hydrology.198, 69-97.
- Refsgaard, J. C. Henriksen, H. J.2004. *Modelling guidelines - Terminology and guiding principles*. Advances in Water Resources. 27(1), 71-82.
- Reynolds, J.E., Halldin, S., Xu, C.Y., Seibert, J., Kauffeldt, A.2017. *Sub-daily runoff predictions using parameters calibrated on the basis of data with a daily temporal resolution*. Journal of Hydrology. 550, 399- 411. <https://doi.org/10.1016/j.jhydrol.2017.05.012>
- Rimbu, N., Le Treut, H., Janicot, S., Boroneant, C., Laurent, C.2001. *Decadal precipitation variability over Europe and its relation with surface atmospheric circulation and sea surface temperature*. Quarterly journal of the royal meteorological society.Vol. 127, Iss. 572, 315-329.
- Rimkus, E., Stonevicius, E., Korneev, V., Kažys, J., Valiuškevičius, G., Pakhomau, A.2013. *Dynamics of meteorological and hydrological droughts in the Neman river basin*. Environmental Research Letters. 8, 045014.
- Roche, M. 1963. Hydrologie de surface (Surface hydrology). ORSTOM et Gauthier-Villars, Paris - France. 431 p.
- Rogers, J.C.1997. *North Atlantic storm track variability and its association to the North Atlantic Oscillation and climate variability of northern Europe*. Journal Climatology. 10:1635-1647
- Romero, R., Guijarro, J.A., Ramis, C., Alonso, S.1998. *A 30-Year (1964–1993) Daily Rainfall Data Base for the Spanish Mediterranean Regions: First Exploratory Study*. International Journal of Climatology.18, 541- 560.
- Rose, D., Konukcu, F., Gowing, J. 2005. *Effect of watertable depth on evaporation and salt accumulation from saline groundwater*. Soil Research. 43(5), 565-573.
- Roudi-Fahimi, F., Kent, M.M. 2007. *Challenges and Opportunities— The Population of the Middle East and North Africa*. Population Bulletin, 62(2).
- Rouissat, B. 2016. Analyse systémique appliquée aux aménagements hydrauliques (Systemic analysis applied to hydraulic installations). PhD Thesis, University of Abou Bekr Belkaid Tlemcen, Algeria.

- Rousseau, A.N., Lafrance, P., Lavigne, M.P., Savary, S., Konan, B., Quilbé, R., Jiapizian, P., Amrani, M. 2012. *A Hydrological modeling framework for defining achievable performance standards for pesticides*. Journal of Environmental Quality. 41, 5243.
- Rousseau, A.N., Savary, S., Hallema, D.W., Gumiere, S.J., Foulon, E. 2013. *Modeling the effects of agricultural BMPs on sediments, nutrients and water quality of the Beaurivage River watershed (Quebec, Canada)*. Canadian Water Resources Journal. 38 (2), 99-120.
- Rusli, S.R., Yudianto, D., Liu, J. 2015. *Effects of temporal variability on HBV model calibration*. Water Science and Engineering. 8(4), 291-300.
- Sahnoune, F., Belhamel, M., Zemat, M., Kerbachi, R. 2013. *Climate Change in Algeria: Vulnerability and Strategy of Mitigation and Adaptation*. Energy Procedia. Vol.36, 1286-1294.
- Saidi, H. 2011. *Impact des changements climatiques sur le régime des cours d'eau : cas de l'Oued Mina (W.Relizane) (Impact of climate change on the river regime: the case of Oued Mina (W. Relizane))*. Magister Thesis. National School of Hydraulics. 141 p.
- Scharffenberg, W., Flemin, M. 2010. *Hydrologic modeling system HEC-HMS v3.2 user's manual*. Davis, USA : USACE-HEC.
- Schilling, J., Freier, K.P., Hertig, E., Scheffran, J. 2012. *Climate change, vulnerability and adaptation in North Africa with focus on Morocco*. Agriculture, Ecosystems & Environment. 156, 12-26. <https://doi.org/10.1016/j.agee.2012.04.021>.
- Schumm, S.A. 1956. *Evolution of drainage systems and slopes in badlands at Perth Amboy*. Geological Society of America, 67:597-646.
- Seckler, D., Molden, D., Barker, R. 1999. *Water Scarcity in the Twenty-First Century*. International Journal of Water Resources Development. 15 (1/2): 29-42.
- Seibert, J. 1999. *Regionalisation of parameters for a conceptual rainfall-runoff model (Regionalization of parameters for a conceptual rainfall-runoff model)*. Agricultural and Forest Meteorology. 98-99, 279-293.
- Seibert, J. 2000. *Multi-criteria calibration of a conceptual runoff model using a genetic algorithm*, Hydrology and Earth System Science. 4(2), 215-224.
- Seibert, J. 2002. *HBV light version 2, user's manual (2002)*. environmental assessment, SLU. Oregon State University Department of Forest Engineering Corvallis, Oregon, USA; Uppsala University Department of Earth Sciences Hydrology.
- Seibert, J. 2005. *HBV light version 2, user's manual (2005)*. Stockholm University Department of Physical Geography and Quaternary Geology. SLU Department of Environmental Assessment Uppsala , Oregon State University Department of Forest Engineering Corvallis, Oregon, USA ,Uppsala University Department of Earth Sciences Hydrology.
- Seibert, J., Beven, K. J. 2009. *Gauging the ungauged basin: how many discharge measurements are needed?*. Hydrology and Earth System Science. 13, 883-892, DOI.10.5194/hess-13-883-2009.

- Seibert, J., Vis, M. J. P. 2012. *Teaching hydrological modeling with a user-friendly catchment runoff- model software package*. Hydrology and Earth System Sciences. 16(9), 3315-3325. DOI: <https://doi.org/10.5194/hess-16-3315-2012>
- Sellami, H., Benabdallah, S., La, I., Vanclooster, M., 2016. *Quantifying hydrological responses of small Mediterranean catchments under climate change projections*. Science of the Total Environment. 543, 924-936. <https://doi.org/10.1016/j.scitotenv.2015.07.006>.
- Sen, P.K. 1968. *Estimates of the Regression Coefficient Based on Kendall's Tau*. Journal of the American Statistical Association. 63, 1379-1389.
- Senarath, S.U.S., Ogden, F.L., Downer, C.W., Sharif, H.O. 2000. *On the calibration and verification of two dimensional, distributed, hortonian, continuous watershed models*. Water Resources Research. 36(6), 1495-1510.
- Sezen, C., Bezak, N., Šraj, M. 2018. *Hydrological modelling of the karst Ljubljana River catchment using lumped conceptual model*. ACTA hydrotechnica. 31, 87-100.
- Shahabfar, A., Eitzinger, J. 2013. *Spatio-Temporal Analysis of Droughts in Semi-Arid Regions by Using Meteorological Drought Indices*. Atmosphere. Vol.4.Iss.2.94-112.
- Shah, R. B., Nitin Manekar, V. 2015. *Drought Index Computation Using Standardized Precipitation Index (SPI) Method For Surat District, Gujarat*. Aquatic Procedia. Vol.4, 1243-49. DOI: 10.1016/j.aqpro.2015.02.162.
- Shapiro, S., Wilk, M. 1965. *An analysis of variance test for normality*. Biometrika. 52(3/4):591-611. <https://doi.org/10.2307/2333709>
- Sharma, S., Stark, T.F., Beattie, W.G., Moses, R.E. 1986. *Multiple control elements for the uvrC gene unit of Escherichia coli*. Nucleic Acids Research. 14:2301-2318.
- Sharma, C. S., Panda, S. N., Pradhan, R. P., Singh, A., Kawamura, A. 2016. *Precipitation and Temperature Changes in Eastern India by Multiple Trend Detection Methods*. Atmospheric Research. 180, 211- 225. <https://doi.org/10.1016/j.atmosres.2016.04.019>.
- Sharma, M.A., Singh, J.B. 2010. *Use of Probability Distribution in rainfall Analysis*. New York science Journal. 40-49.
- Singh, V. 1995. Watershed modeling. In *Computer models of watershed hydrology*, Colorado, USA. 1-22. Water Resources Publications, Highlands Ranch.
- Singh, P.V., Frevert, D.K. 2006. *Watershed Models*. CRC Press, Taylor & Francis Group: 1-42.
- Singh, V. P., Woolhiser, D.A. 2002. *Mathematical modeling of watershed hydrology*. Journal of Hydrologic Engineering. 7(4), 270-292.
- Sivapalan, M. 2003. *Prediction in ungauged basins: a grand challenge for theoretical hydrology*. Hydrological Processes. 17, 3163-3170.
- Sneyers, R. 1975. *Sur l'analyse Statistique des Séries d'observations; Organisation météorologique mondiale (On the Statistical Analysis of Series of Observations; World*

- Meteorological Organization), Note Technique N.143; Secrétariat de l'Organisations Météorologique Mondiale: Genève, Switzerland. 192 p.
- Soleimani Sardou, F., Bahremand, A.2014. *Hydrological Drought Analysis Using SDI Index in Halilrud Basin of Iran*. Environmental resources Research.Vol.2.No.1, 47-56. doi: 10.22069/ijerr.2014.1678
- Soo Jun, K., Chung, E.S., Sung, J.Y., Seong Lee, K. 2011.*Development of spatial water resources vulnerability index considering climate change impacts*. Science of the Total Environment.Vol.409.Iss.24, 5228-42.
- Sorooshian, S. 1983. *Contributions in Hydrology, U.S. National Report to International Union of Geodesy and Geophysics, 1979-1982*, Chapter Surface Water Hydrology : On-Line Estimation, 706-720. USA : American Geophysical Union.
- Sorooshian, S., Gupta, V. 1995. *Computer Models of Watershed Hydrology*, Chapter Model calibration. Highlands Ranch, USA : Water Resources Publications. 62,23-67.
- Spearman, C.E.1910. *Correlation calculated from faulty data*. British Journal of Psychology.Vol.3, 271- 295.
- Srivastava, A., Deb, P., Kumari, N.2020. *Multi-Model Approach to Assess the Dynamics of Hydrologic Components in a Tropical Ecosystem*. Water Resources Management. 34, 327-341. <https://doi.org/10.1007/s11269-019-02452-z>.
- Steele-Dunne, S., Lynch, P., McGrath, R., Semmler, T., Wang, S.Y., Hanafin, J., Nolan, P. 2008. *The impacts of climate change on hydrology in Ireland*. Journal of Hydrology. 356, 28-45, doi:10.1016/j.jhydrol.2008.03.025.
- Strahler, A.N.1952. *Hypsometric (area-altitude) analysis of erosional topography*. Geological Society of America Bulletin. 63:1117-1141
- Strahler, A.N.1957. *Quantitative analysis of watershed geomorphology*. Transactions, American Geophysical Union. 38(6), 913-920.
- Swetalina, N., Thomas, T.2016. *Evaluation of Hydrological Drought Characteristics for Bearma Basin in Bundelkhand Region of Central India*. Procedia Technology.Vol. 24.85-92.
- Tabari, H., Abghari, H., Hosseinzadeh Talaei, P.2012.*Temporal trends and spatial characteristics of drought andrainfall in arid and semi-arid regions of Iran*. Hydrological Processes. Vol. 26, 3351-3361.
- Tabari, H., Hosseinzadeh Talaei, P.2011. *Analysis of Trends in Temperature Data in Arid and Semi-Arid Regions of Iran*. Global and Planetary Change. 79, 1–10.
- Tegegne, G., Park, D. K., Kim, Y.O.2017. *Comparison of hydrological models for the assessment of water resources in a data-scarce region, the Upper Blue Nile River Basin*. Journal of Hydrology: Regional Studies. 14, 49-66. <https://doi.org/10.1016/j.ejrh.2017.10.002>.
- Teng, J., Chiew, F.H.S., Vaze, J., Marvanek, S., Kirono, D. 2012. *Estimation of climate change impact on mean annual runoff across continental Australia using budyko and fu equations and hydrological models*. Journal of Hydrometeorology. 13(3):1094-1106. DOI:10.1175/JHM-D-11-097.1, 2012.

- Terink, W., Immerzeel, W. W., Droogers, P. 2013. Climate change projections of precipitation and reference evapotranspiration for the Middle East and Northern Africa until 2050. *International Journal of Climatology*. 33_14, 3055-3072. DOI: 10.1002/joc.3650
- Teutschbein, C., Wetterhall F., Seibert, J. 2011, *Evaluation of different downscaling techniques for hydrological climate-change impact studies at the catchment scale*, *Climate Dynamics*. 37(9-10), 2087-2105, doi:10.1007/s00382-010-0979-8.
- Teutschbein, C., Grabs, T., Karlsen, R. H., Laudon, H., Bishop, K. 2015. *Hydrological response to changing climate conditions: Spatial streamflow variability in the boreal region*. *Water Resources Research*. 51. doi:10.1002/ 2015WR017337
- Theil, H .1950. A rank-invariant method of linear and polynomial regression analysis, I, II, III. *Ned Akad Wetensch Proc* 53:386-392, 521-525 and 1397-1412
- Thirel, G., Andréassian, V., Perrin, C. 2015. *On the need to test hydrological models under changing conditions*. *Hydrology Science Journal*. 60 (7e8), 1165e1173. <https://doi.org/10.1080/02626667.2015.1050027>.
- Tigkas, D., Tsakiris, G. 2014. *Early Estimation of Drought Impacts on Rainfed Wheat Yield in Mediterranean Climate*. *Environmental Processes*. Vol. 2.Iss.1, 97-114.
- Tigkas, D., Vangelis, H., Tsakiris, G. 2015. *DrinC: a software for drought analysis based on drought indices*. *Earth Science Informatics*. Vol.8.Iss.3, 697-709. DOI: 10.1007/s12145-014-0178-y.
- Todini, E., Wallis, J. 1977. *Mathematical Models for Surface Water Hydrology*, Chapter Using CLS for Daily or Longer Period Rainfall-Runoff Modeling, 149-168. New York, USA : John Wiley & Sons.
- Tossou, E.M., Ndiaye, M.L., Traore, V.B., Sambou, H., Kelome, N.C., SY, B.A., Diaw, A.T. 2017. *Characterisation and Analysis of Rainfall Variability in the Mono-Cou_o River Watershed Complex, Benin (West Africa)*. *Resources and Environment*. 1, 13-29.
- Touazi, M., Bhiry, N., Laborde, J.P., Achour, F. 2011. Régionalisation des débits moyens mensuels en Algérie du nord. *Revue des sciences de l'eau (Regionalization of monthly average flows in northern Algeria. Journal of Water Sciences)*. *Journal of Water Science*. 24 (2), 177-191. <https://doi.org/10.7202/1006110ar>
- Touazi, M., Laborde, J.P. 2004. *Modélisation pluie-débit à l'échelle annuelle en Algérie du nord (Rain-flow modeling on an annual scale in northern Algeria)*. *Revue des sciences de l'eau*. 17(4):503-516.
- Tramblay, Y., Badi, W., Driouech, F., El Adlouni, S., Neppel, L., Servat, E. 2012. *Climate Change Impacts on Extreme Precipitation in Morocco*. *Global and Planetary Change*. 82-83, 104-114.
- Traore, V. B. 2014. *Trends and Shifts in Time Series of Rainfall and Runoff in the Gambia River Watershed*. *International Journal of Environmental Protection and Policy*. 2 (4), 138. <https://doi.org/10.11648/j.ijep.20140204.13>.

- Traore, V.B., Ndiaye, M.L., Mbow, C., Malomar, G., Sarr, J., Beye, A.C., Diaw, A.T. 2017. *Khronostat Model as Statistical Analysis Tools in Low Casamance River Basin, Senegal*. World Environment. 1, 10-22.
- Tsakiris, G., Nalbantis, I., Vangelis, H., Verbeiren, B., Huysmans, M., Tychon, B., Jacquemin, I., Canters, F., Vanderhaegen s., Engelen, G., Poelmans, L., De Becker, P., Batelaan, O.2013. *A system-based paradigm of drought analysis for operational management*. Water Resources Management. Vol.27, 5281-5297.
- Tsakiris, G., Pangalou, D., Vangelis, H. 2007. *Regional Drought Assessment Based on the Reconnaissance Drought Index (RDI)*. Water Resources Management. Vol.21.Iss.5, 821-833.
- Turanyi, T., Zador, J., Zsély, I.G. 2006. *Local and global uncertainty analysis of complex chemical kinetic systems*. Reliability Engineering and System Safety 91, 1232-1240.
- Ulbrich, U., Christoph, M., Pinto, J.G, Corte-Real, J.1999. *Dependence of winter precipitation over Portugal on NAO and baroclinic wave activity*. International Journal Climatology. 19:379-390.
- Van Esse, W.R., Perrin, C., Booij, M.J., Augustijn, D.C.M., Fenecia, F., Kavetski, D., Lobligeois, F. 2013. *The influence of conceptual model structure on model performance: A comparative study for 237 French catchments*. Hydrology and Earth System Sciences, 17, 4227- 4239.
- Van Rooy, M.P. 1965. *A Rainfall Anomaly Index (RAI), Independent of the Time and Space*. Notos. Vol. 14, 43-48.
- Vogt, J., Somma, F. 2000. Introduction. Drought and Drought Mitigation in Europe.3-5.
- Wagener, T., McIntyre, N.2007. *Tools for teaching hydrological and environmental modeling*. Computers in Education Journal, 17(3).
- Wagener, T., Wheeler, H., Gupta, H.2004. *Rainfall-runoff modelling in gauged and ungauged catchments*. 1st edn. Imperial College Press, London, UK.
- Wagener, T., Sivapalan, M., Troch, P. A., McGlynn, B. L., Harman, C. J., Gupta, H., Kumar, V., P., Rao, P.S.C., Basu, N.B., Wilson, J. S. .2010, *The future of hydrology: An evolving science for a changing world*. Water Resource Research. 46, W05301, doi:10.1029/2009WR008906
- Wang, L., Chen, W., Zhou, W., Chan, J.C.L., Barriopedro, D., Huang, R. 2009. *Effect of the Climate Shift around Mid-1970s on the Relationship between Wintertime Ural Blocking Circulation and East Asian Climate*. International Journal Climatology. Vol.30.Iss.1.153-158. <https://doi.org/10.1002/joc.1876>
- Wang, S., Ancell, B.C., Huang, G.H., Baetz, B.W.2018. *Improving robustness of hydrologic ensemble predictions through probabilistic preand post-processing in sequential data assimilation*. Water Resource Research. 54, 2129e2151. <https://doi.org/10.1002/2018WR022546>
- Wenzhi, Z., Xibin, J.2016. *Spatio-temporal variation in transpiration responses of maize plants to vapour pressure deficit under an arid climatic condition*. Journal of Arid Land. 8(3), 409-421.

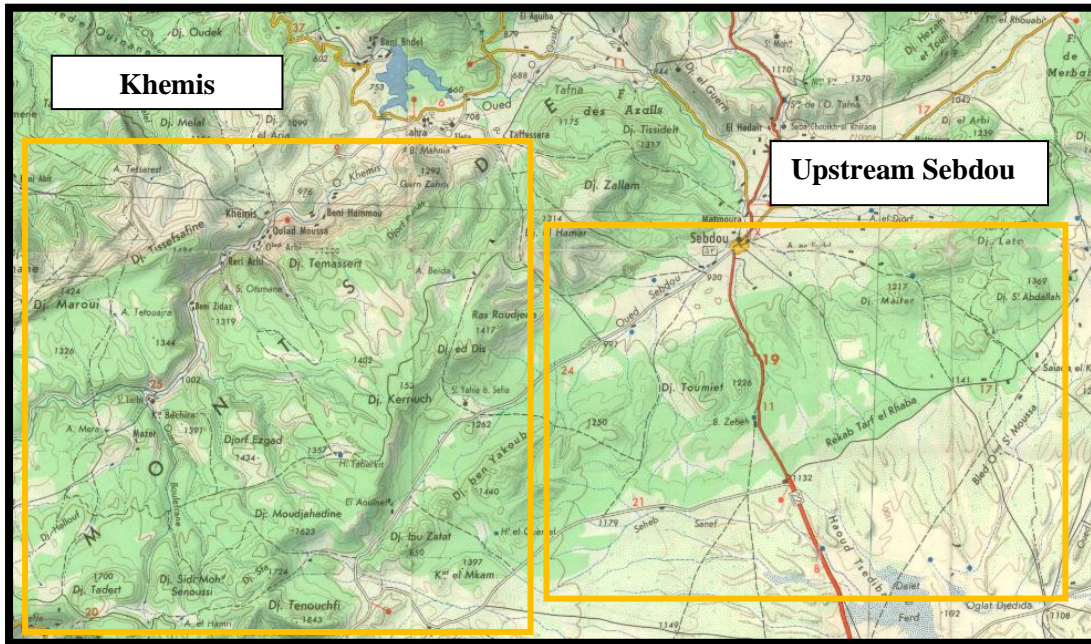
- Western, A.W., Zhou, S.L., Grayson, R.B., McMahon, T.A., Blöschl, G. and Wilson, D.J., 2004. *Spatial correlation of soil moisture in small catchments and its relationship to dominant spatial hydrological processes*. *Journal of Hydrology*. 286(1), 113-134.
- Westra, S., Thyer, M., Leonard, M., Kavetski, D., Lambert, M. 2014. *A strategy for diagnosing and interpreting hydrological model nonstationarity*. *Water Resources Research*.50 (6), 5090- 5113. doi:10.1002/ 2013WR014719
- Wijngaard, J. B., Klein Tank, A. M. G., Können, G. P. 2003. *Homogeneity of 20th Century European Daily Temperature and Precipitation Series: HOMOGENEITY OF EUROPEAN CLIMATE SERIES*. *International Journal Climatology*.23 (6), 679-692. <https://doi.org/10.1002/joc.906>.
- Wilby, R. L., Dessai, S. 2010. *Robust adaptation to climate change*. *Weather*. 65(7), 180-185, doi:10.1002/wea.543.
- Wilhite, D.A.2000.Chapter 1 Drought as a Natural Hazard: Concepts and Definitions. Drought Mitigation Center Faculty Publications. 69.
- Wilhite, D.A. Glantz, H.1985.*Understanding the drought phenomenon: the role of definitions*. *Water International*. Vol. 10.Iss.3,111-120.
- Wilk, J., Andersson, L., Plermkamon, V.2001. *Hydrological impacts of forest conversion to agriculture in a large river basin in northeast Thailand*. *Hydrological Processes*. 15, 2729-2748. DOI: 10.1002/hyp.229
- Willmott, C. J., Matsuura, K.2005. *Advantages of the mean absolute error (MAE) over the root mean square error (RMSE) in assessing average model performance*. *Climate Research*. 30, 79-82.
- WMO.2006. Drought monitoring and early warning: concepts, progress, and future challenges. Geneva. Switzerland. World Meteorological Organization.ISBN 978-92-63-11006-0.
- WMO.2009. Experts agree on a universal drought index to cope with climate risks WMO Press Release No. 872, 15 December 2009 (Geneva: World Meteorological Organization) (available at www.wmo.int/pages/mediacentre/press_releases/pr_872_en.html (accessed 2013))
- Wu, H., Qian, H. 2017. *Innovative Trend Analysis of Annual and Seasonal Rainfall and Extreme Values in Shaanxi, China, since the 1950s: Trend in Annual and Seasonal Rainfall and Extreme Values in Shaanxi*.*International Journal Climatology*. 37, 2582-2592.
- Yang, K., Wu, H., Qin, J., Lin, C., Tang, W., Chen, Y. 2014. *Recent Climate Changes over the Tibetan Plateau and Their Impacts on Energy and Water Cycle: A Review*. *Global and Planetary Change*. 112, 79-91.
- Yue, S., Hashimo, M. 2003. *Long term trends of annual and monthly precipitation in Japan*. *Journal of the American Water Resources Association*. 3(3): 587-596
- Yu, Z. 2015. *Hydrology, Floods and Droughts / Modeling and Prediction, in: Encyclopedia of Atmospheric Sciences*. Elsevier. 217-223. <https://doi.org/10.1016/B978-0-12-382225-3.00172-9>

- Xoplaki, E., González-Rouco, F.J., Gyalistras, D., Luterbacher, J., Rickli, R., Wanner, H. 2002. *Interannual summer air temperature variability over Greece and its connection to the large-scale atmospheric circulation and Mediterranean SSTs 1950–1999*. *Climate Dynamics*. 20(7), 723-739. DOI 10.1007/s00382-002-0291-3.
- Xu, C. 2002. *Hydrologic Models*. Department of Earth Sciences Hydrology, Uppsala University Uppsala.
- Zamoum, S., Souag-Gamane, D. 2019. *Monthly streamflow estimation in ungauged catchments of northern Algeria using regionalization of conceptual model parameters*. *Arabian Journal of Geosciences*. 12, 1-14. <https://doi.org/10.1007/s12517-019-4487-9>.
- Zamrane, Z., Turki, I., Laignel, B., Mahé, G., Laftouhi, N.E. 2016. *Characterization of the Interannual Variability of Precipitation and Streamflow in Tensift and Ksob Basins (Morocco) and Links with the NAO*. *Atmosphere*. 7, 84. <https://doi.org/10.3390/atmos7060084>
- Zarei, A., Asadi, E., Ebrahimi, A., Jafary, M., Malekian, A., Tahmoures, M., Alizadeh, E. 2017. *Comparison of meteorological indices for spatio-temporal analysis of drought in chahrmahal-bakhtiyari province in Iran*. *Hrvatski Meteoroloski Casopis*. Vol.52.No.52,13-26.
- Zeng, L., Xiong, L., Liu, D., Chen, J., Kim, J.S. 2019. *Improving Parameter Transferability of GR4J Model under Changing Environments Considering Nonstationarity*. *Water*. 11(10):2029. <https://doi.org/10.3390/w11102029>
- Zekouda, N., Meddi, M., LaVanchy, G.T., Remaoun, M. 2020. *The Impact of Human Activities on Flood Trends in the Semi-Arid Climate of Cheliff Basin, Algeria*. ISSN 0097-8078. *Water Resources*. Vol. 47.No. 3, 409-420.
- Zeroual, A., Assani, A.A., Meddi, M. 2017. *Combined Analysis of Temperature and Rainfall Variability as They Relate to Climate Indices in Northern Algeria over the 1972–2013 Period*. *Hydrology Resource*. 48, 584-595.
- Zettam, A., Taleb, A., Sauvage, S., Boithias, L., Belaidi, N., Sánchez-Pérez, J.M. 2017. *Modelling Hydrology and Sediment Transport in a Semi-Arid and Anthropized Catchment Using the SWAT Model: The Case of the Tafna River (Northwest Algeria)*. *Water*. 9, 216. <https://doi.org/10.3390/w9030216>
- Zhang, X., Srinivasan, R. 2010. *GIS-based spatial precipitation estimation using next generation radar and raingauge data*. *Environmental Modelling and Software*. 25(12), 1781-1788.

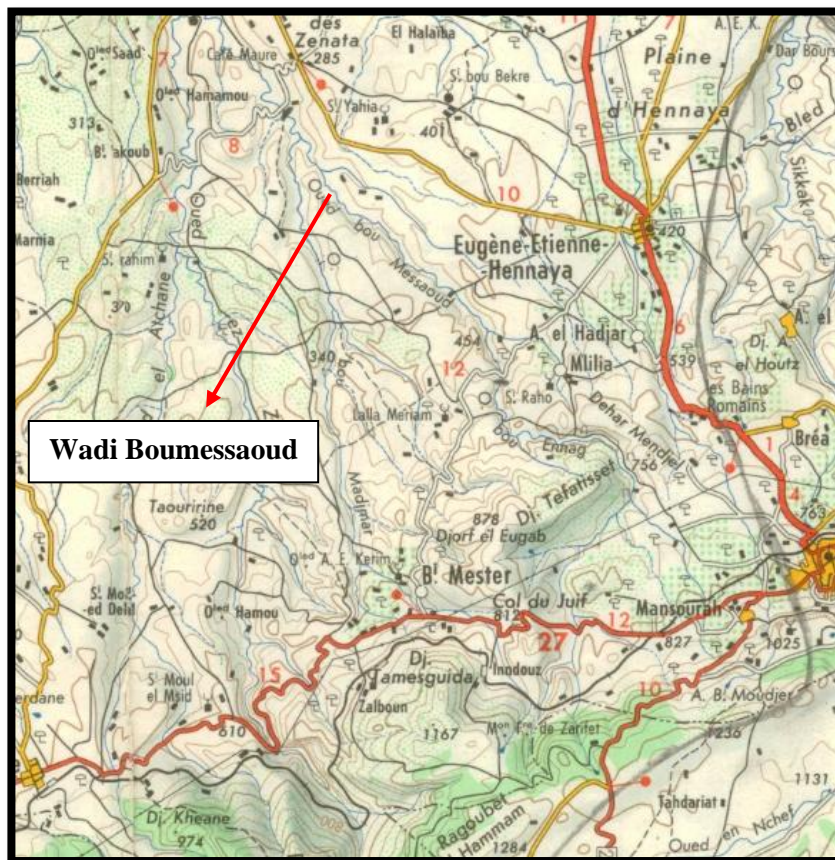
APPENDICES

Appendix .1. Presentation of mountains and tributary of the study area

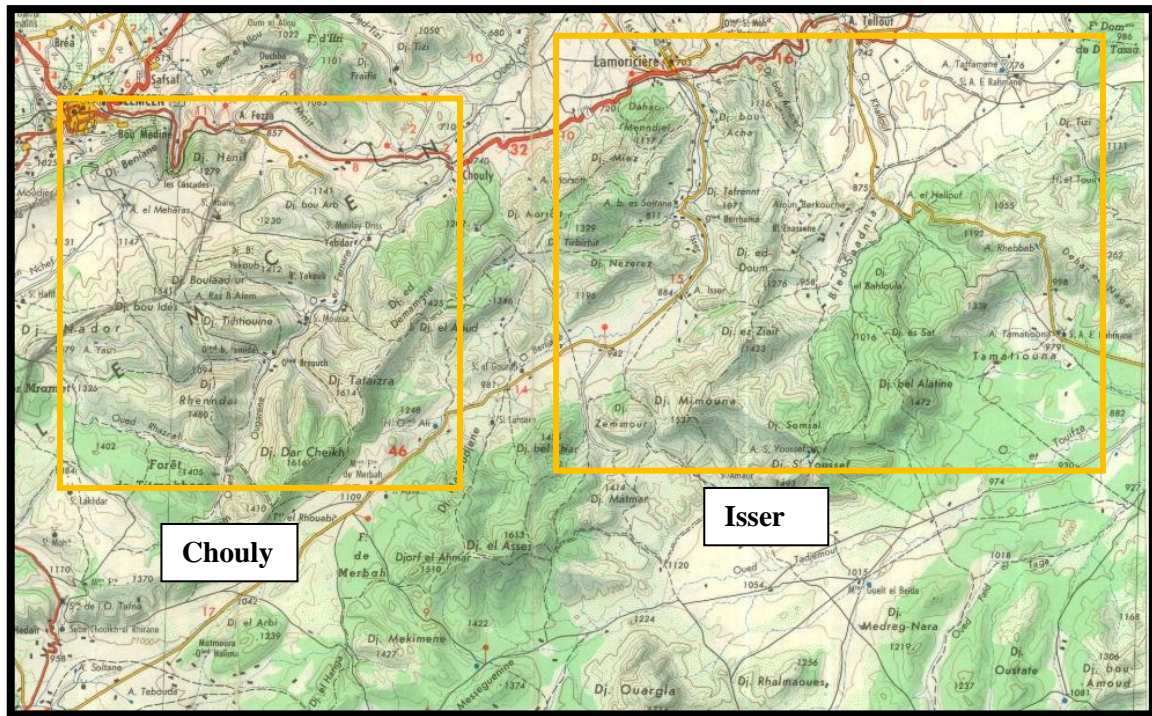
- Upper part of the Tafna basin (Upstram Seb dou, Khemis sub basins)



- The lower part of the Tafna basin (Wadi Boumessaoud)

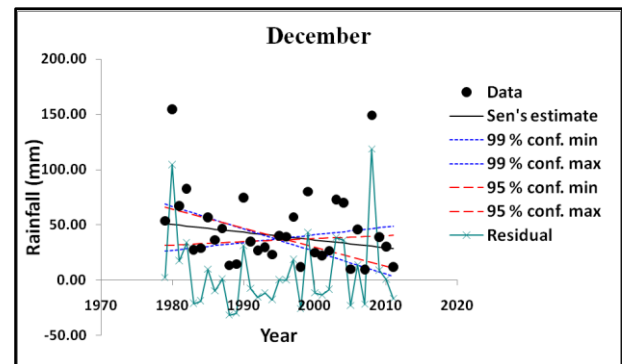
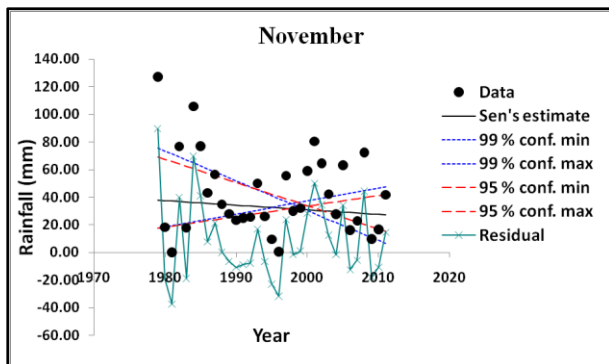
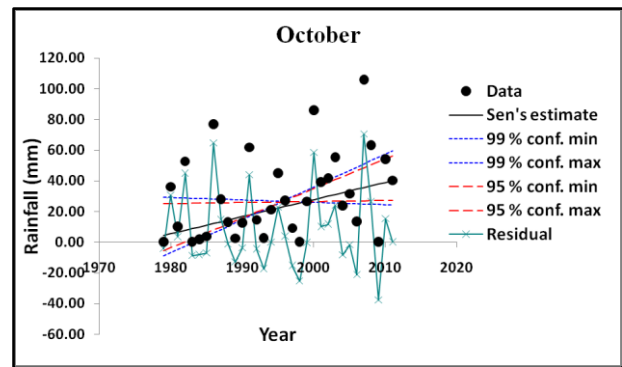
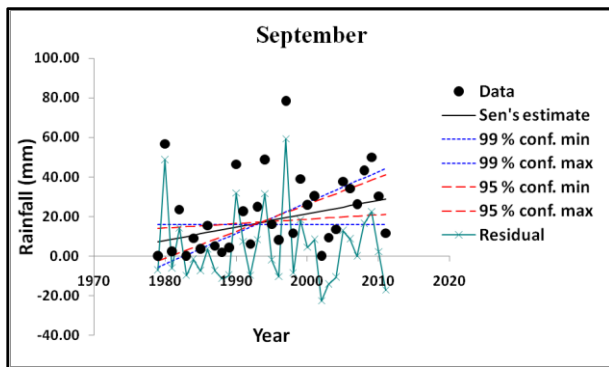


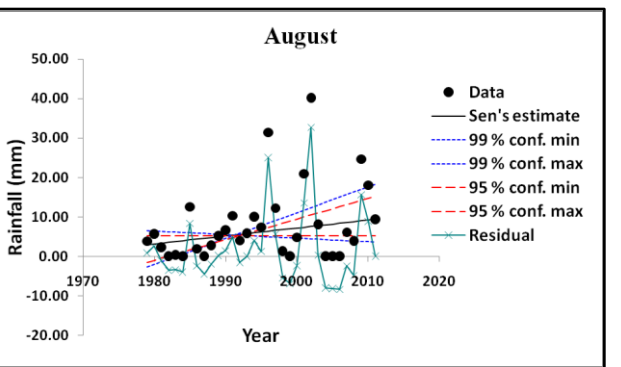
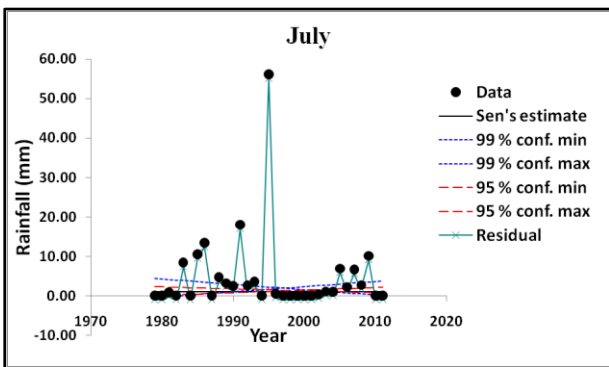
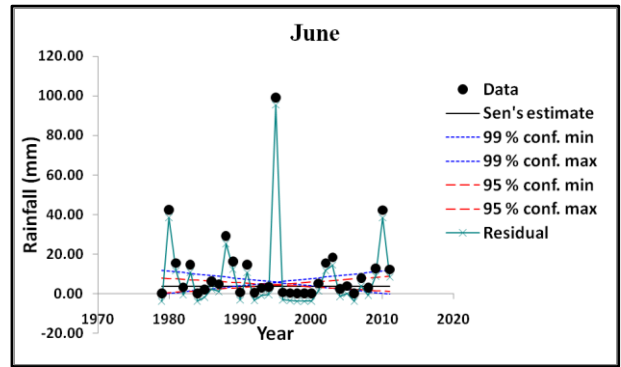
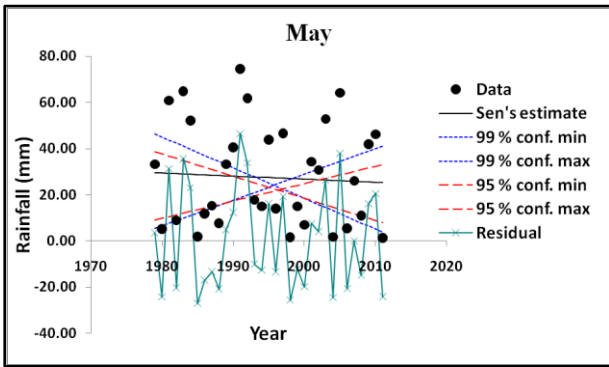
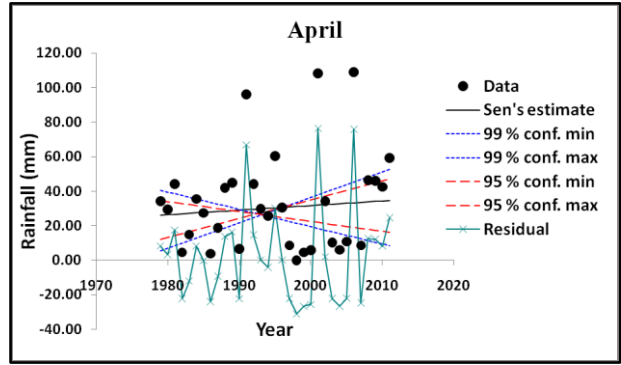
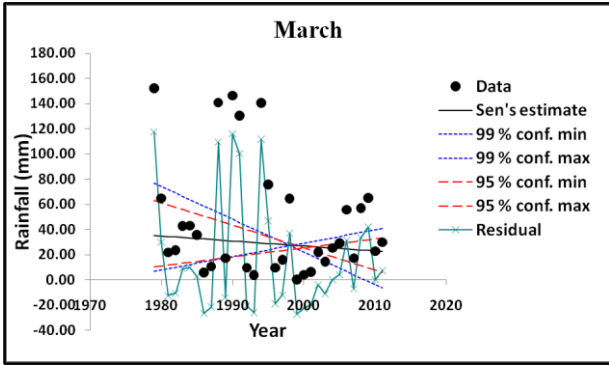
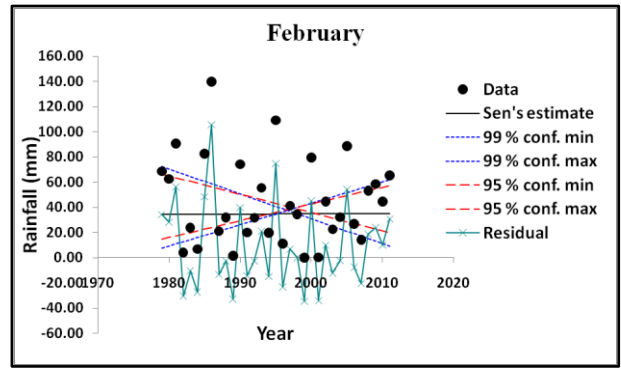
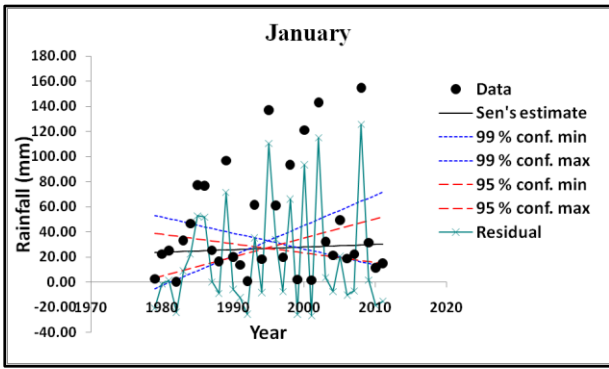
- Middle part of the Tafna basin (Chouly, Isser sub basin)



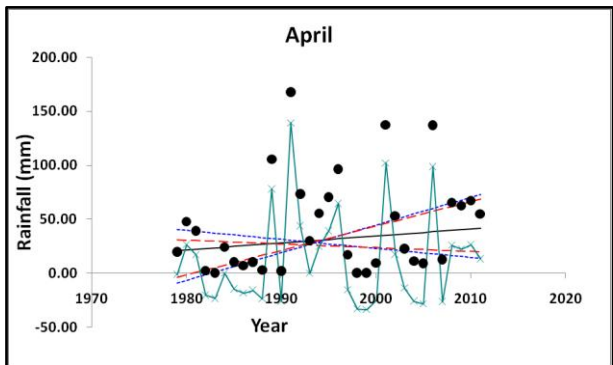
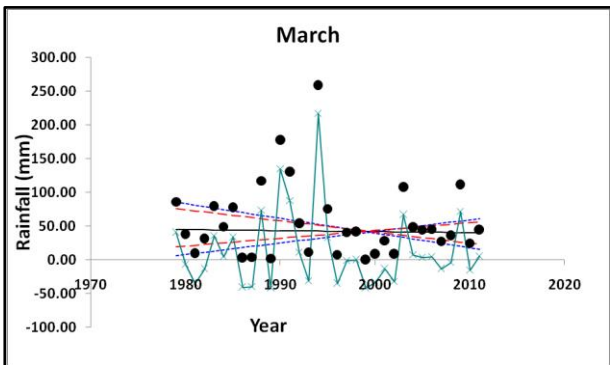
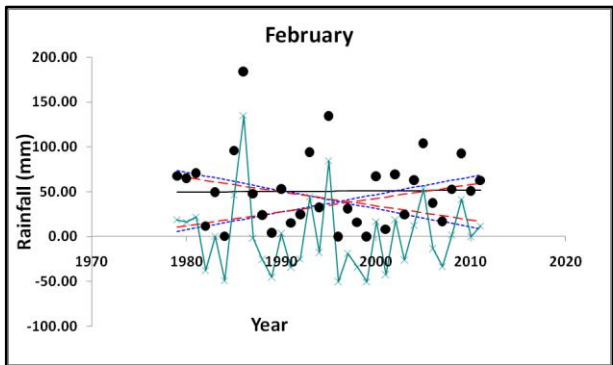
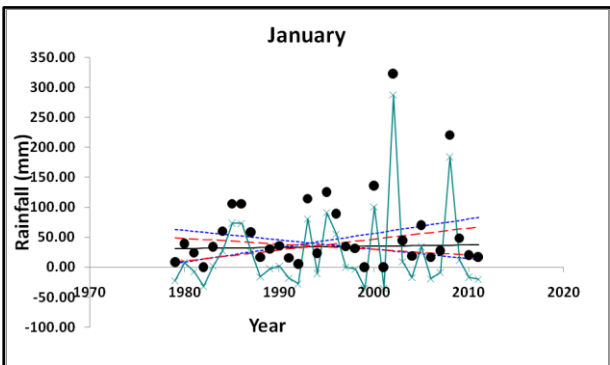
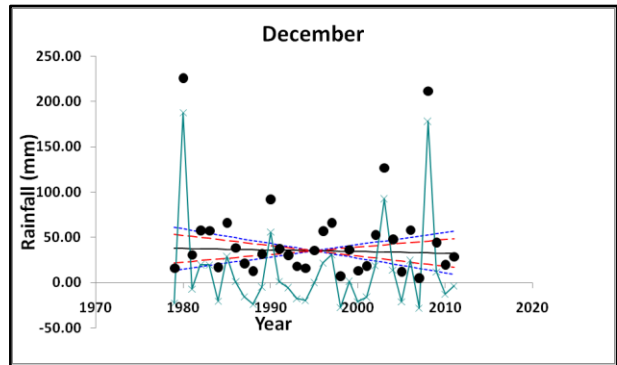
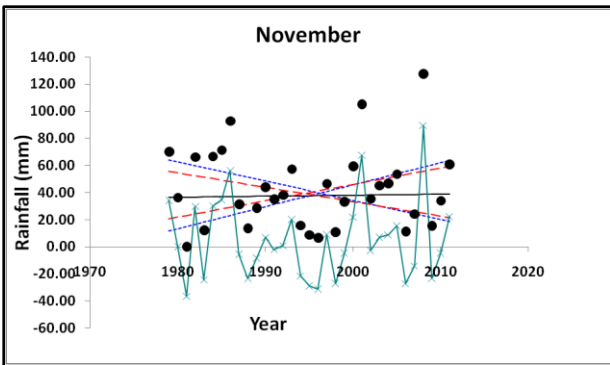
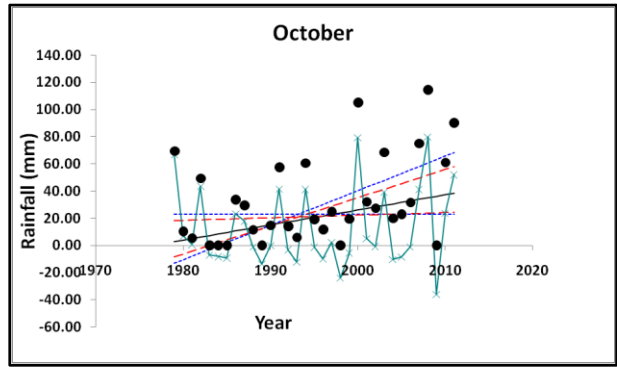
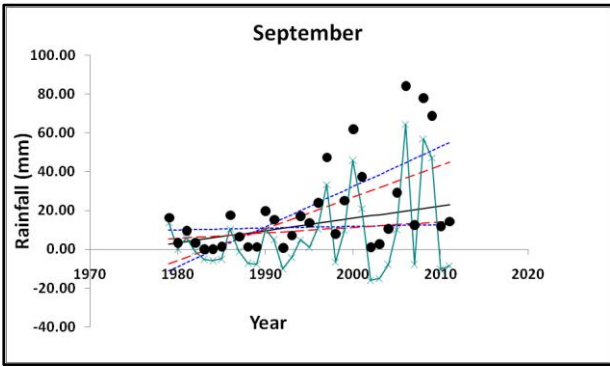
Appendix .2. Sen's Slope trend analysis for monthly rainfall

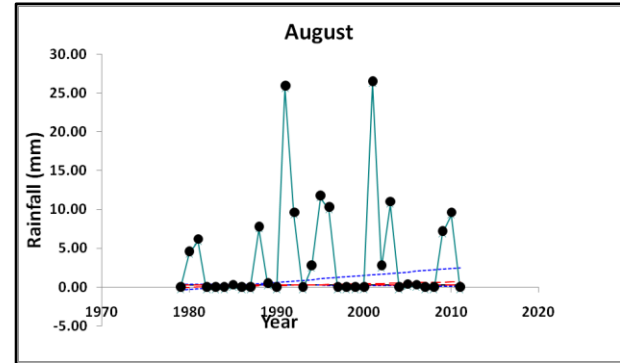
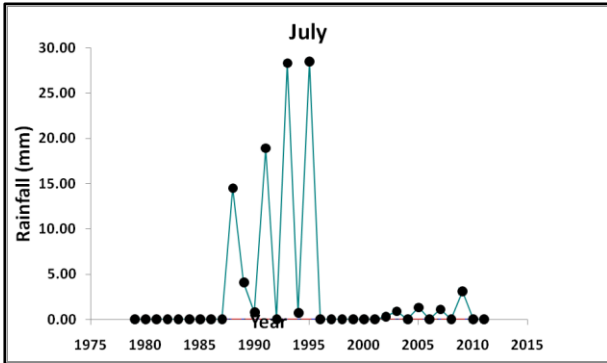
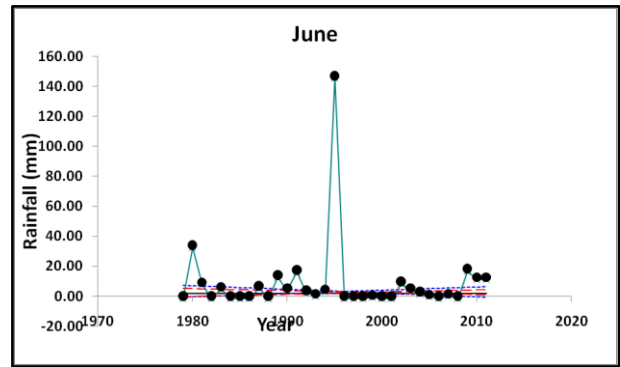
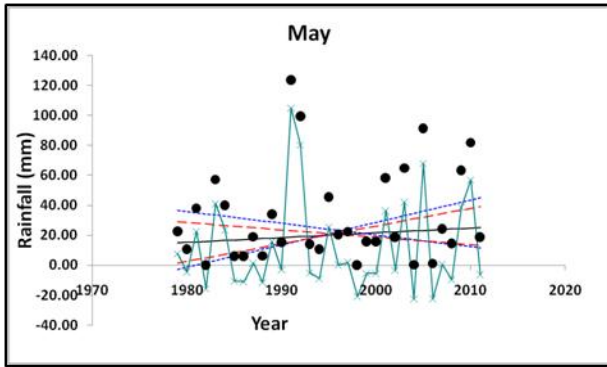
- Sebdou station



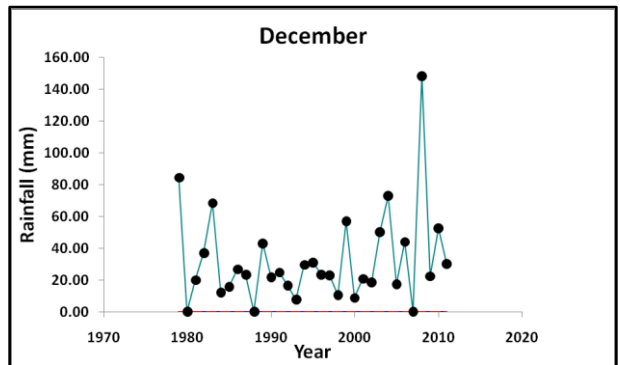
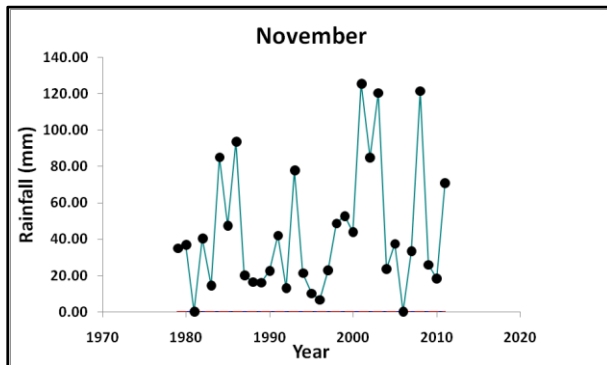
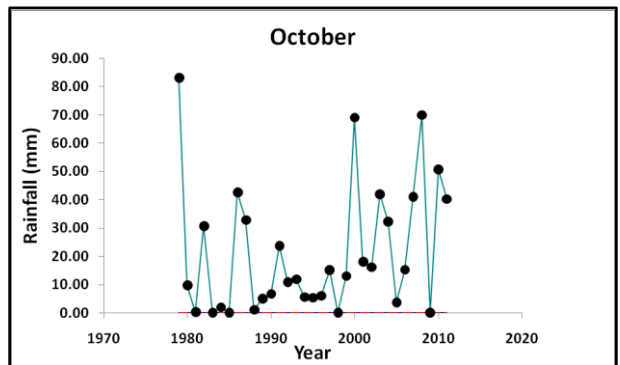
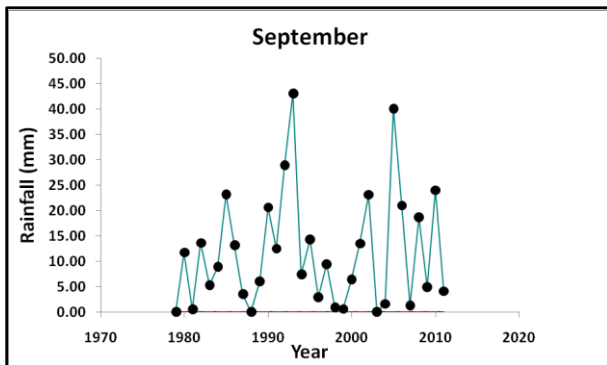


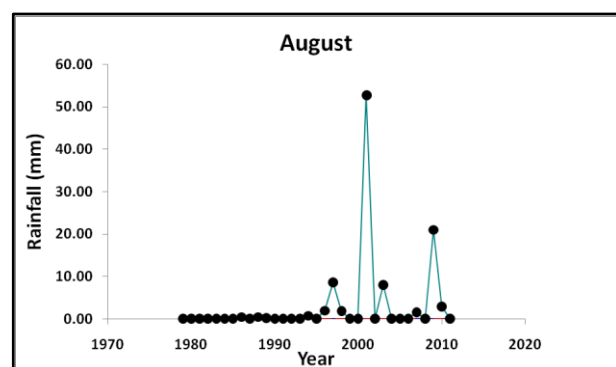
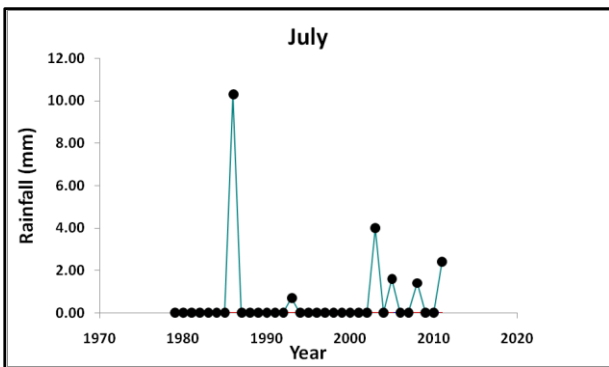
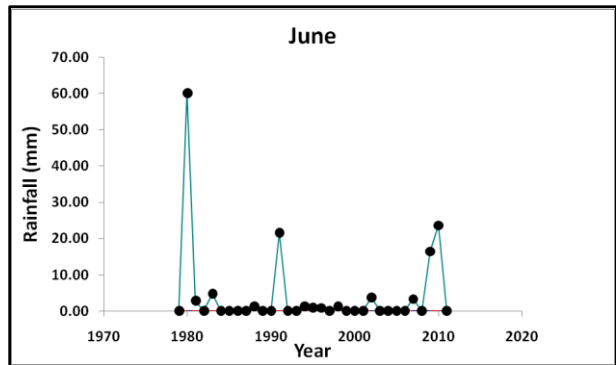
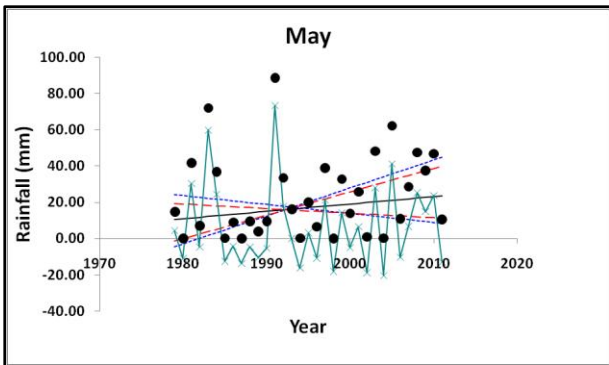
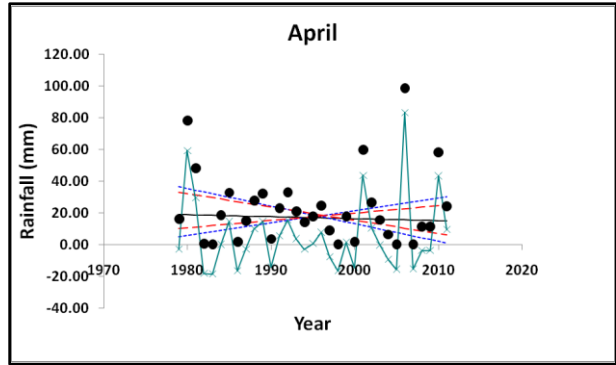
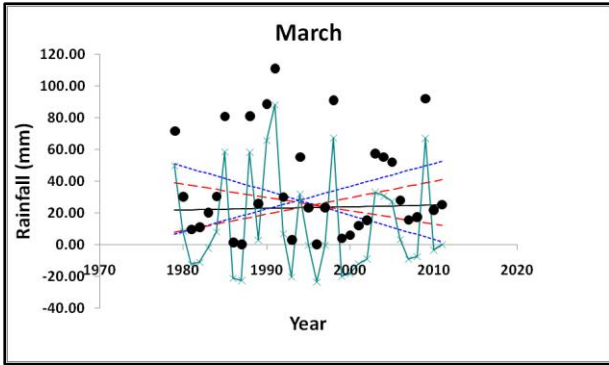
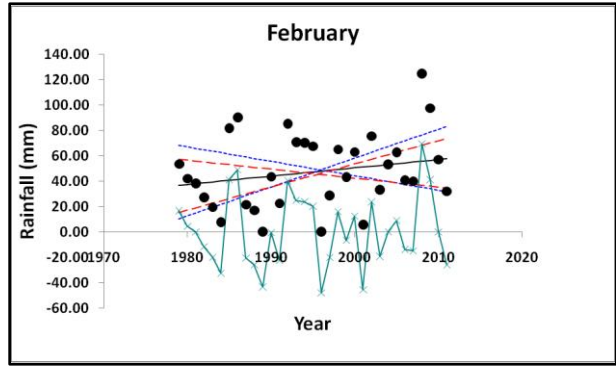
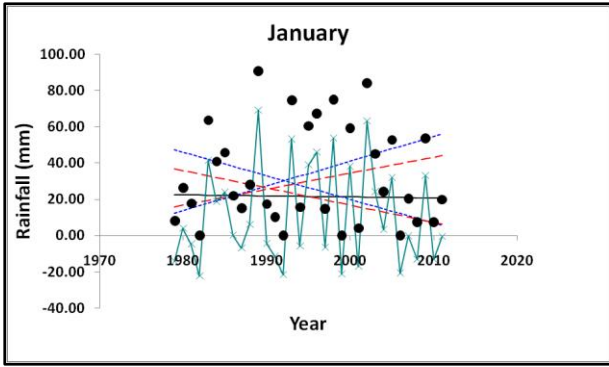
- Khemis station



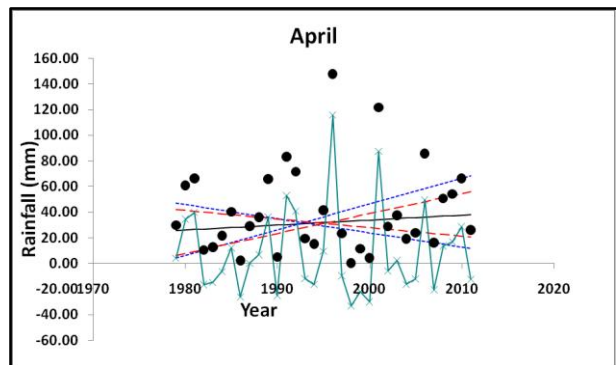
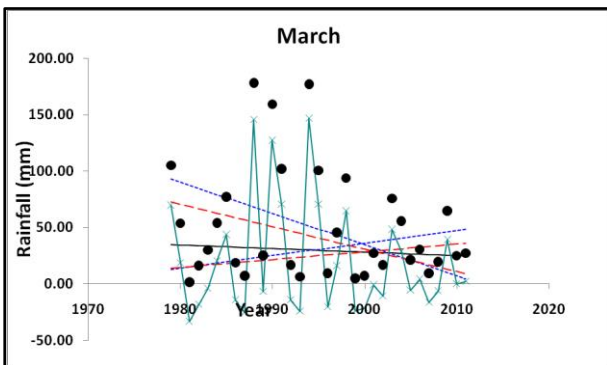
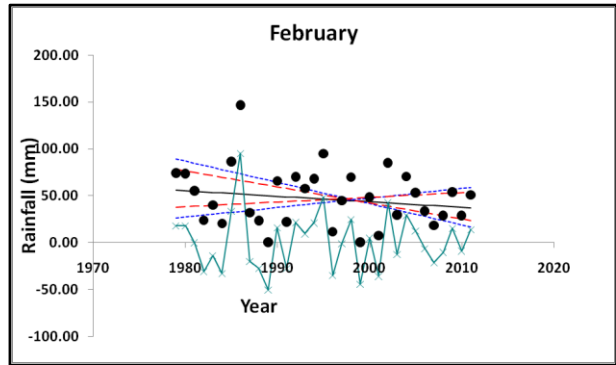
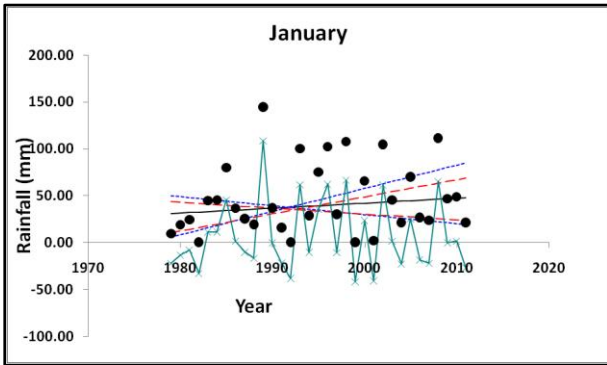
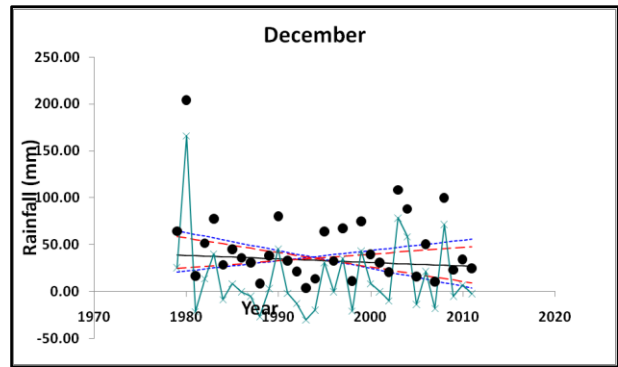
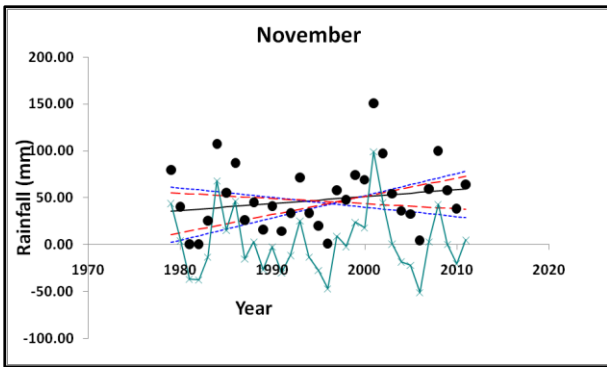
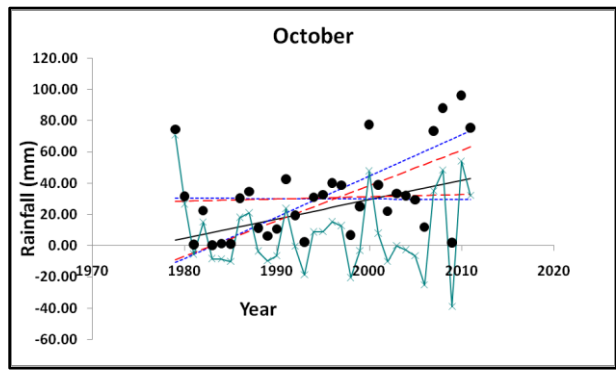
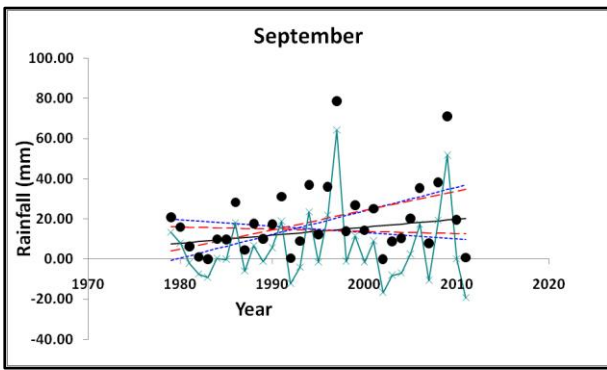


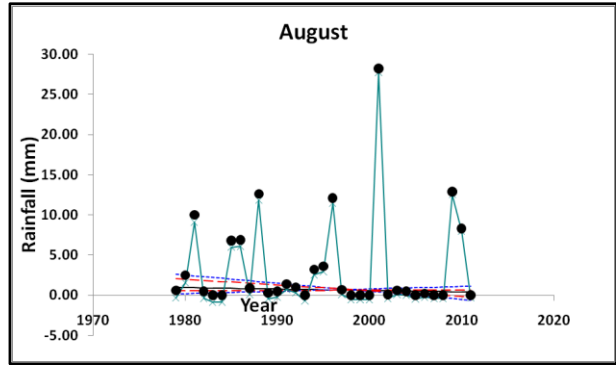
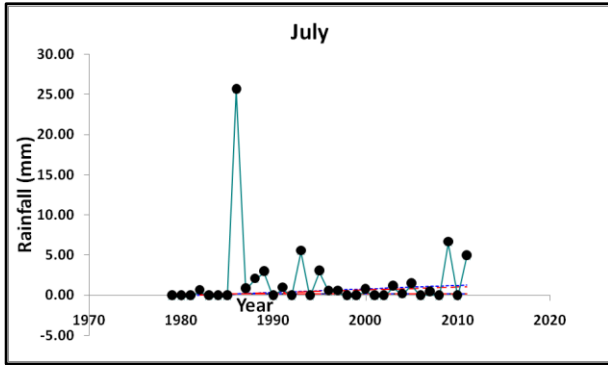
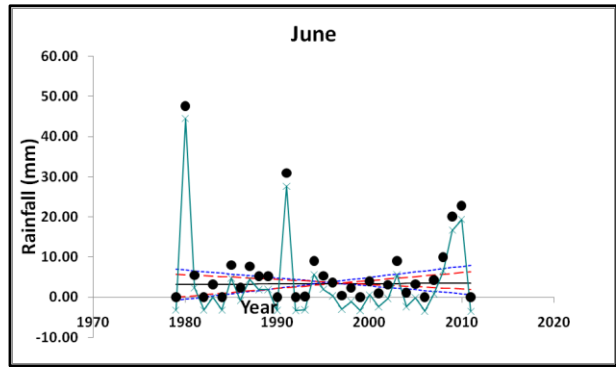
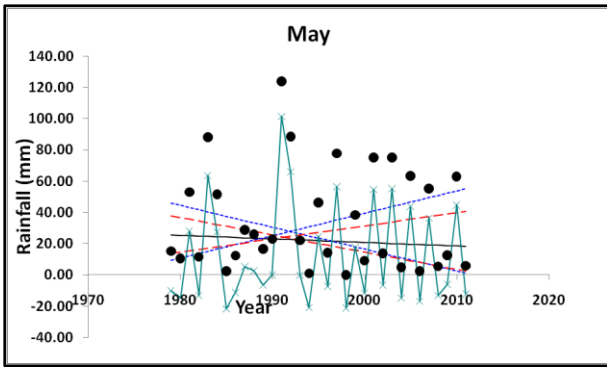
- Djebel Chouachi



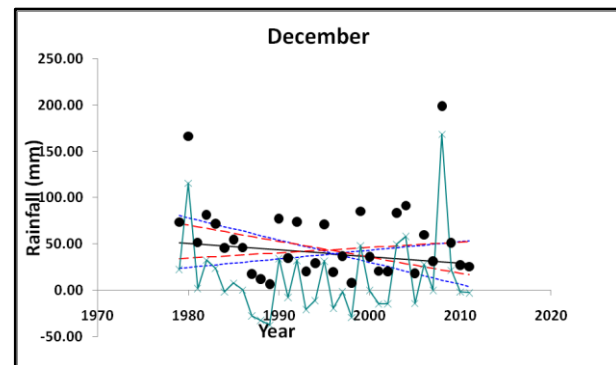
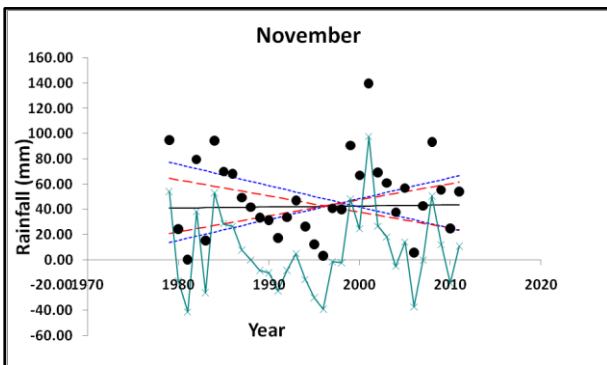
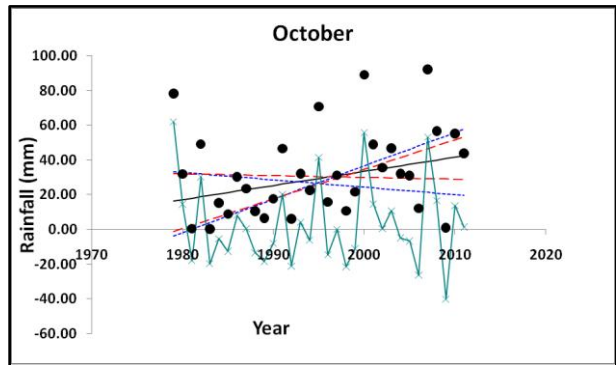
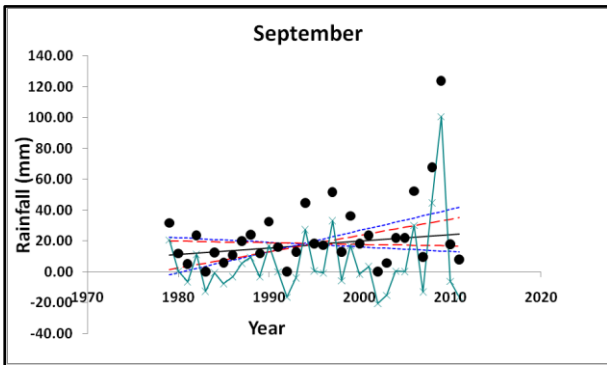


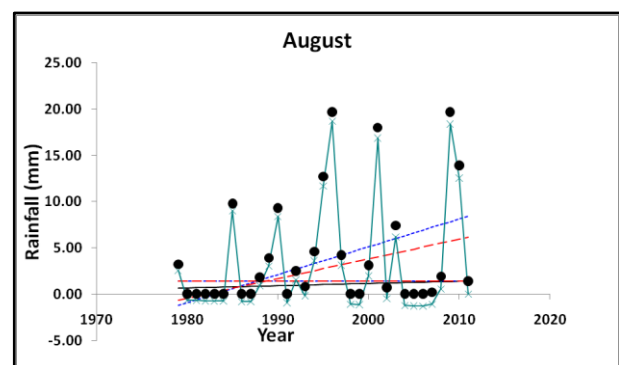
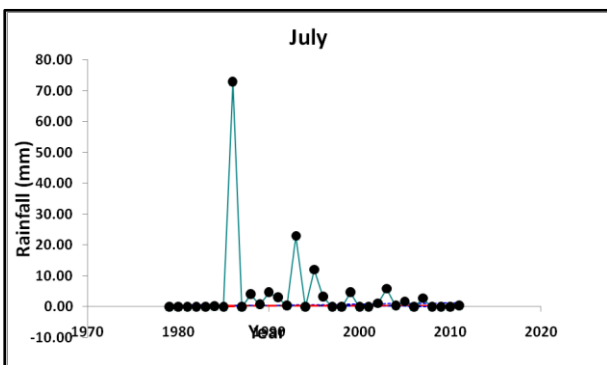
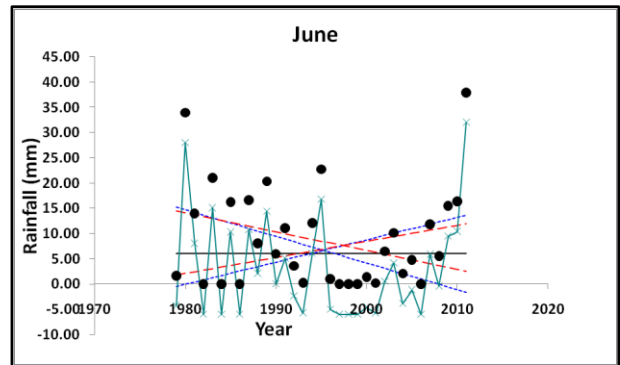
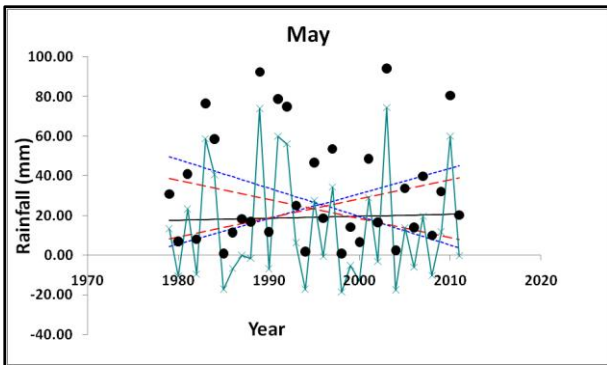
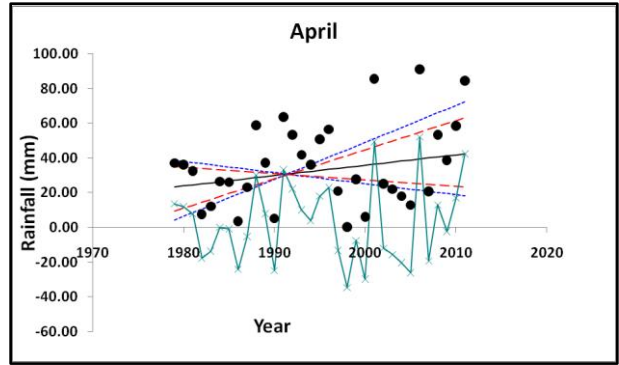
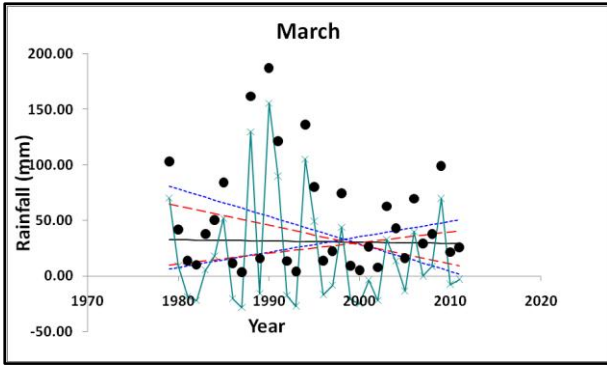
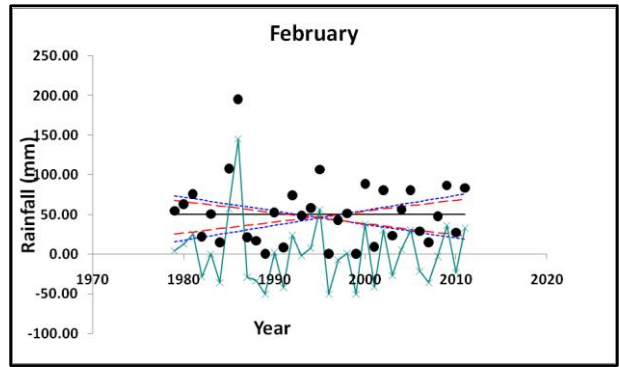
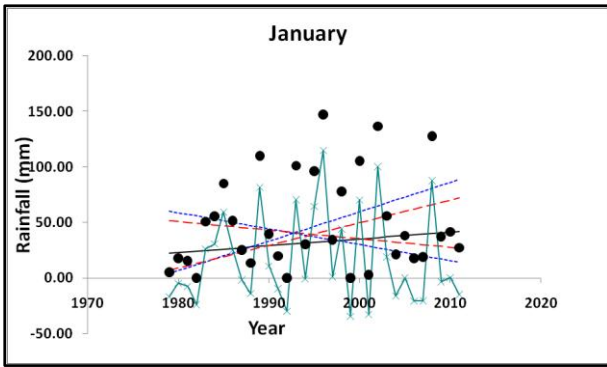
- Hennaya station



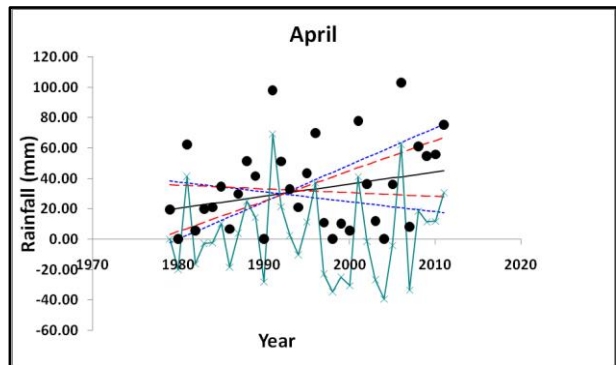
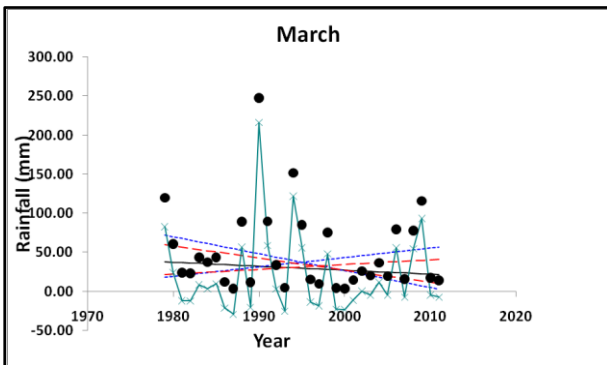
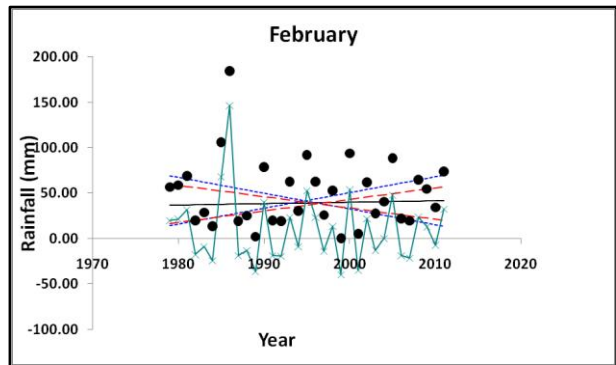
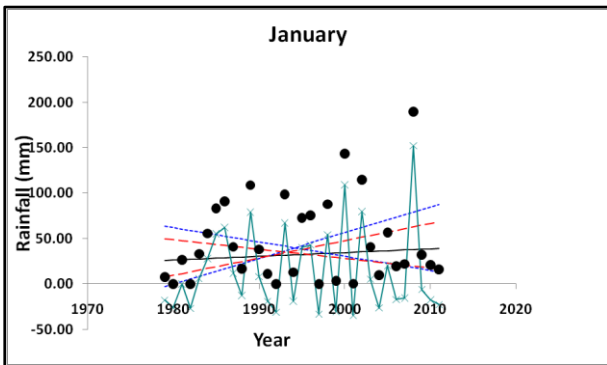
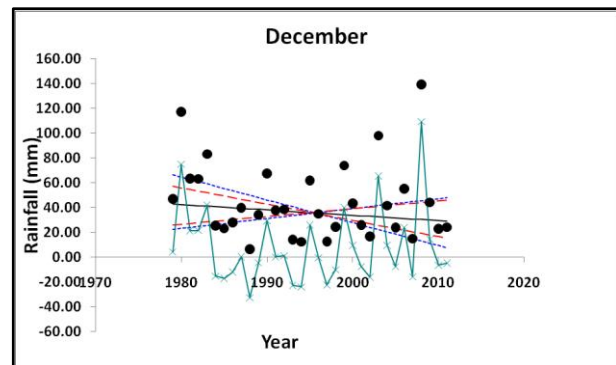
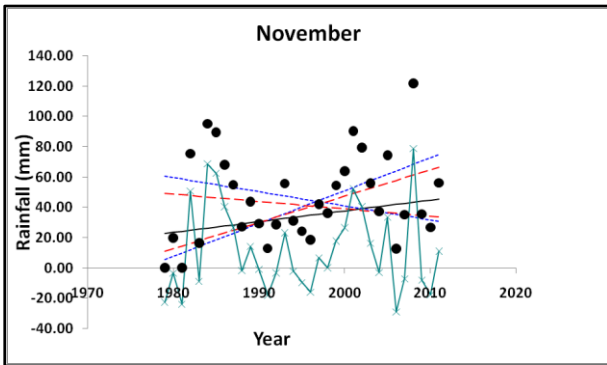
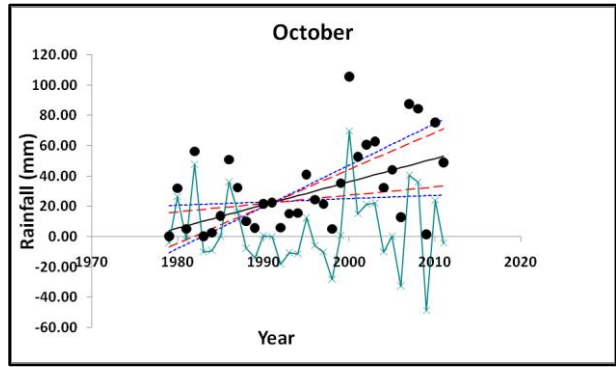
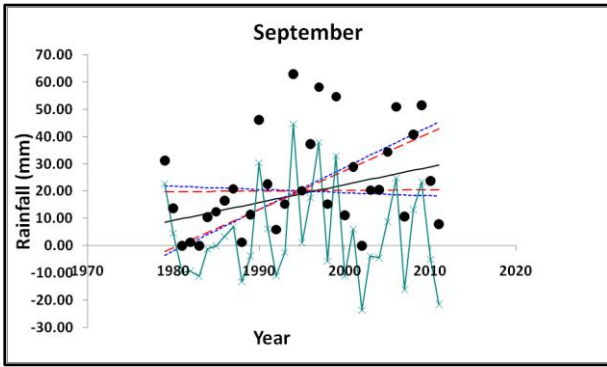


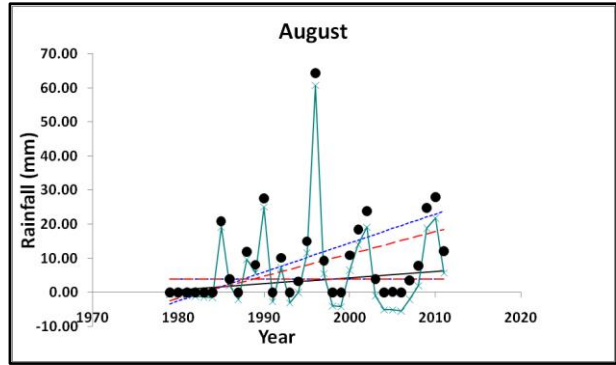
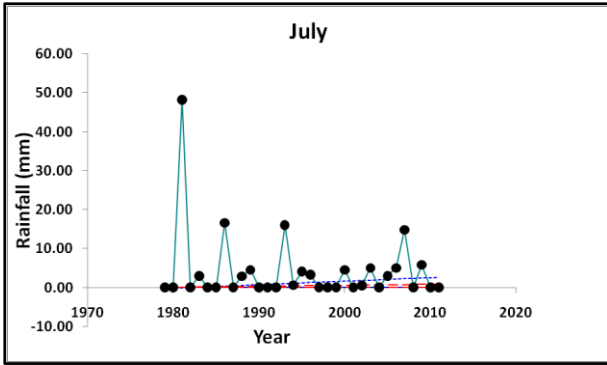
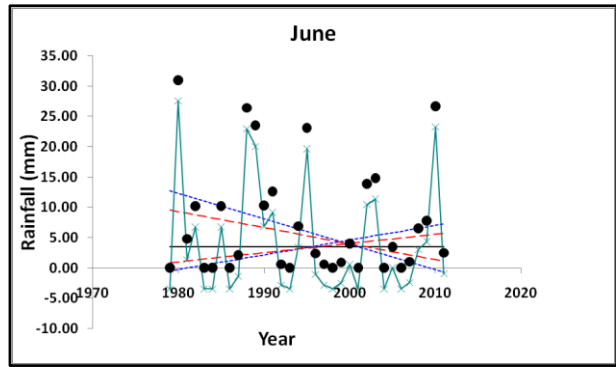
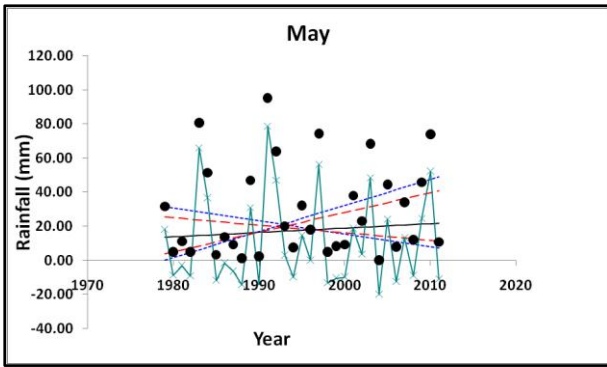
• Chouly station



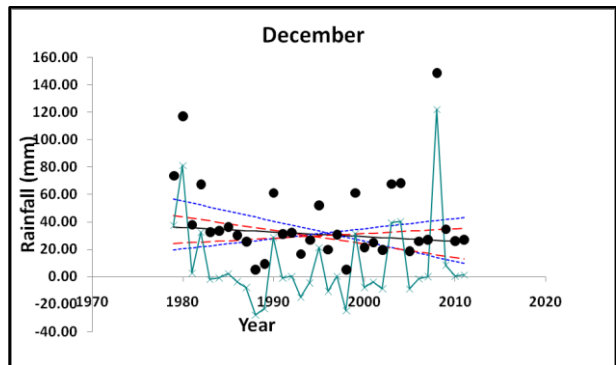
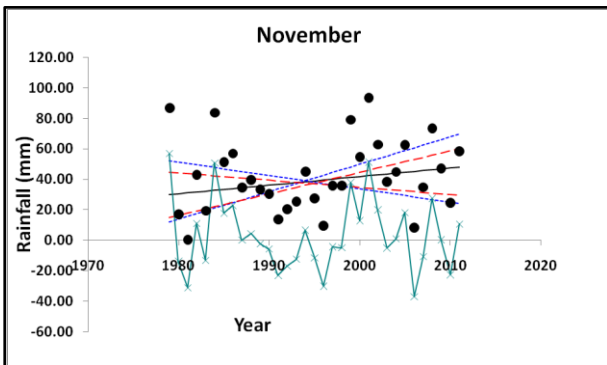
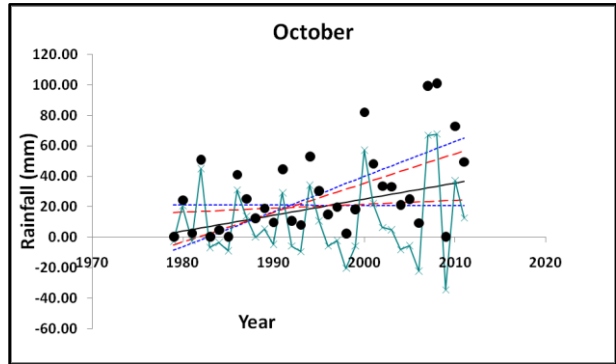
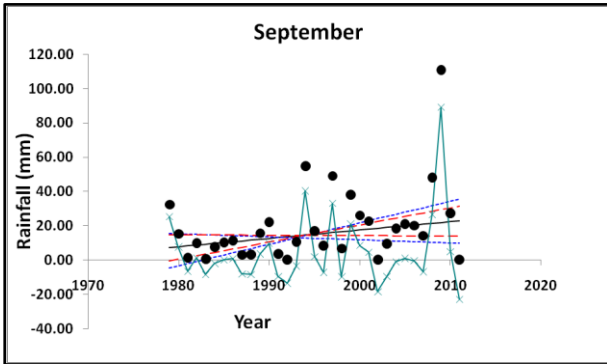


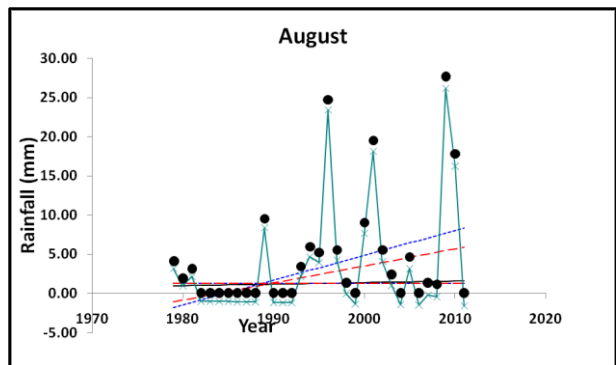
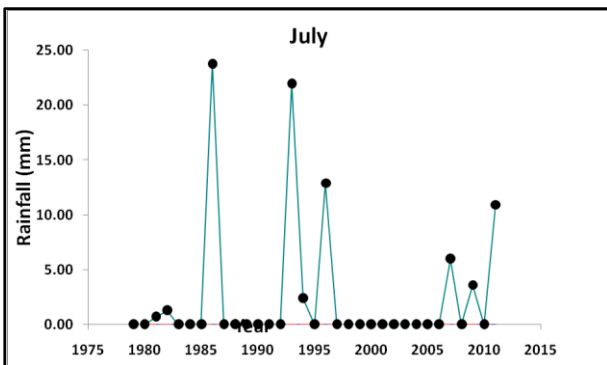
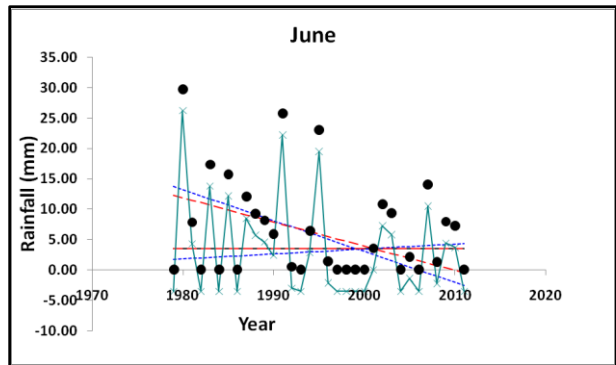
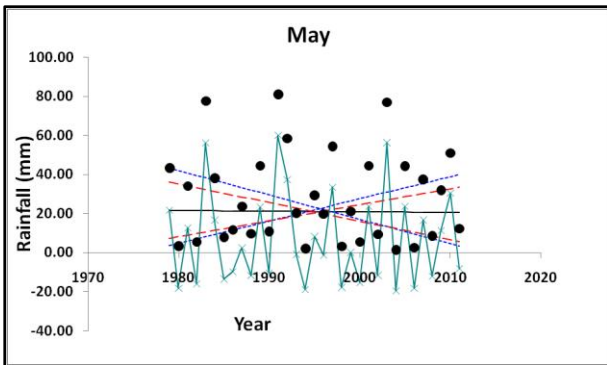
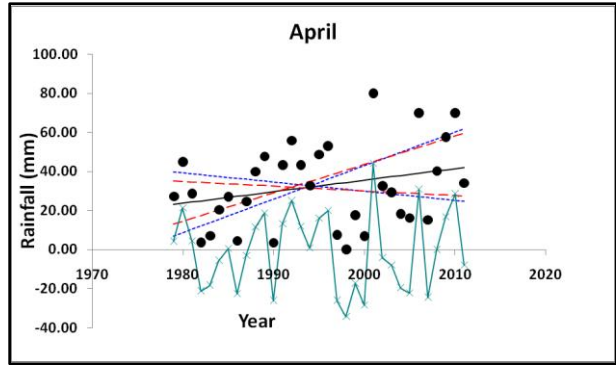
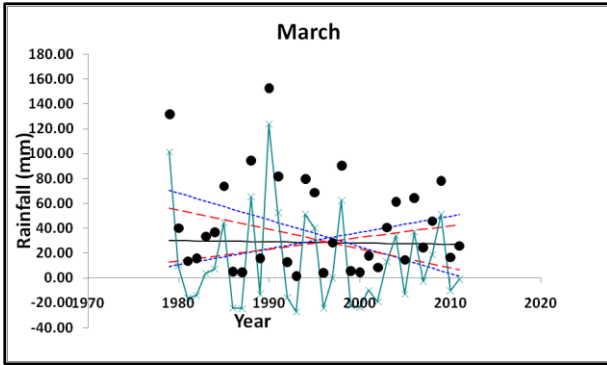
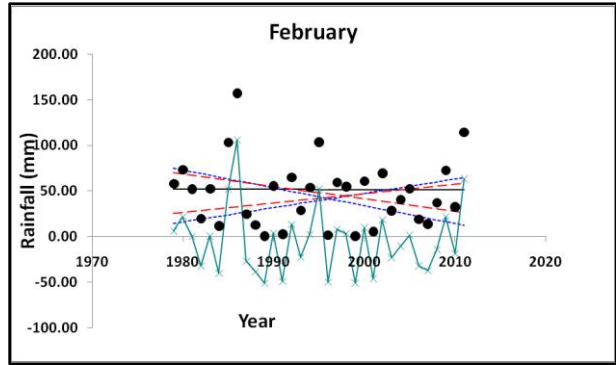
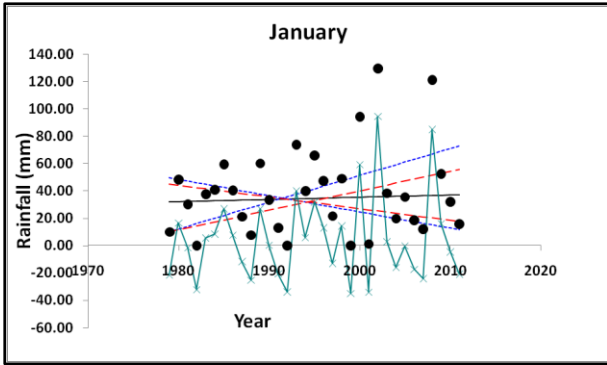
- Meurbah station



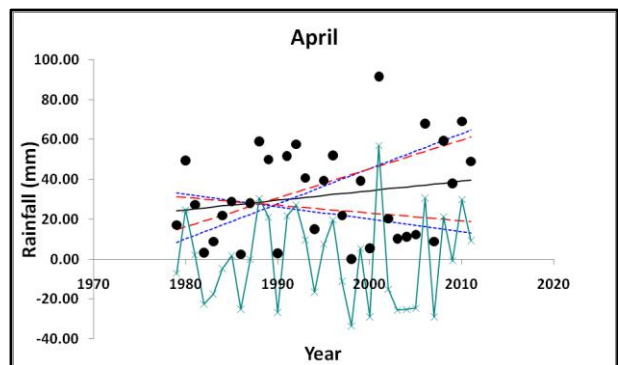
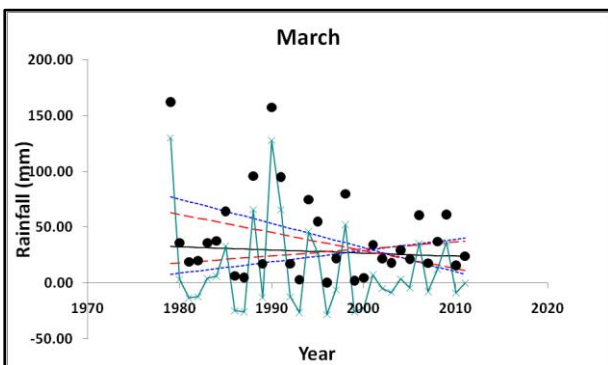
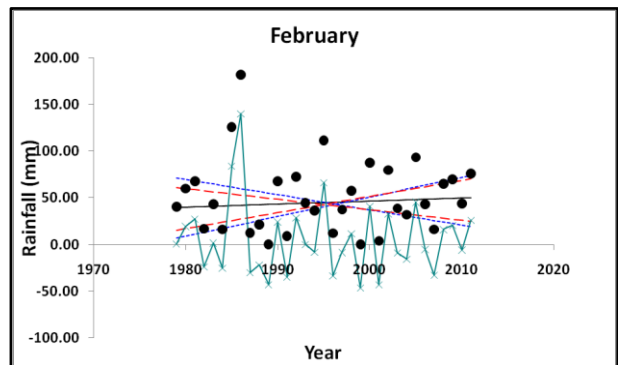
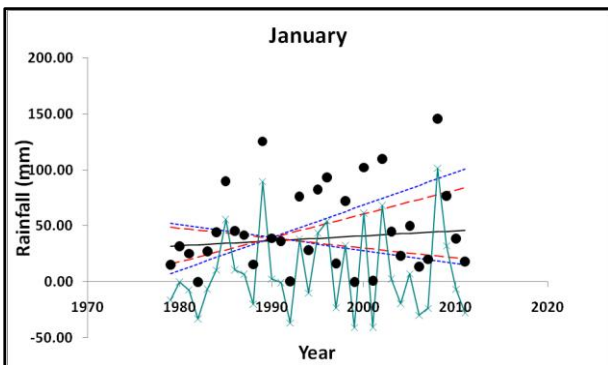
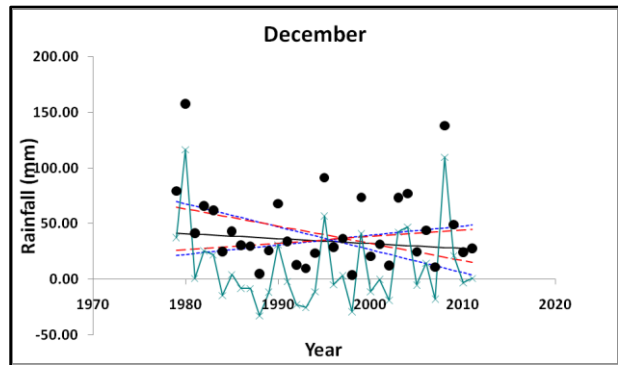
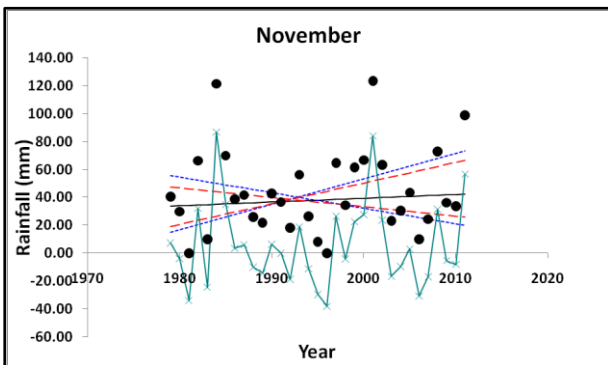
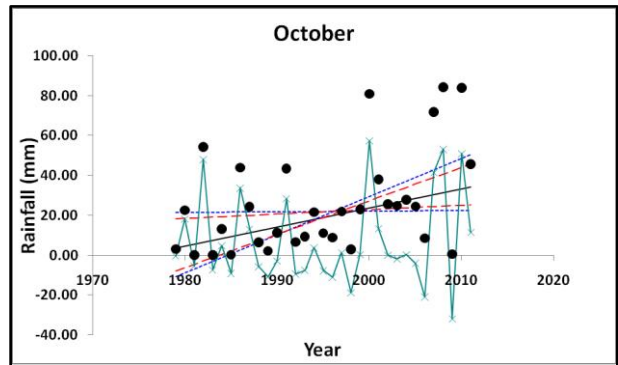
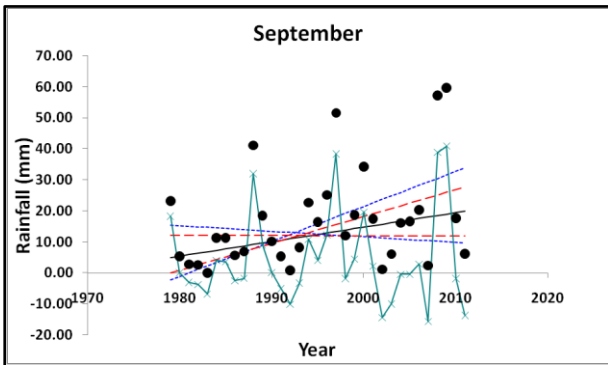


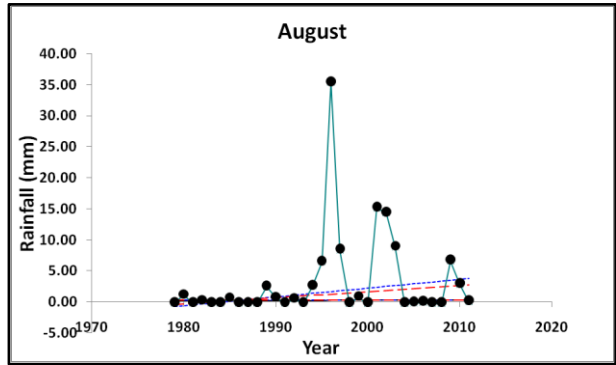
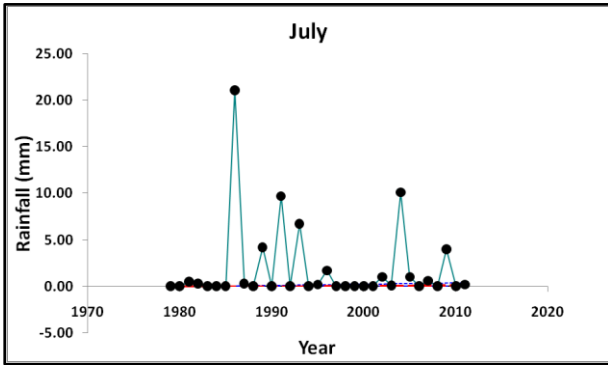
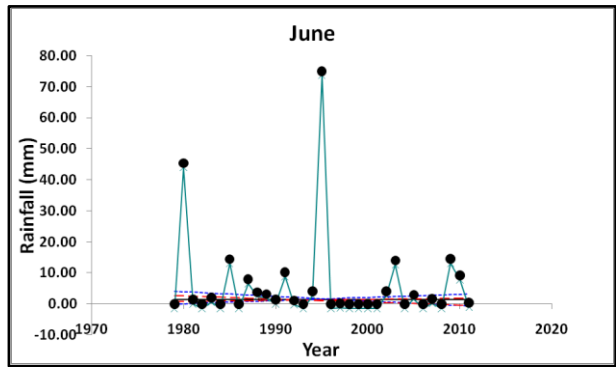
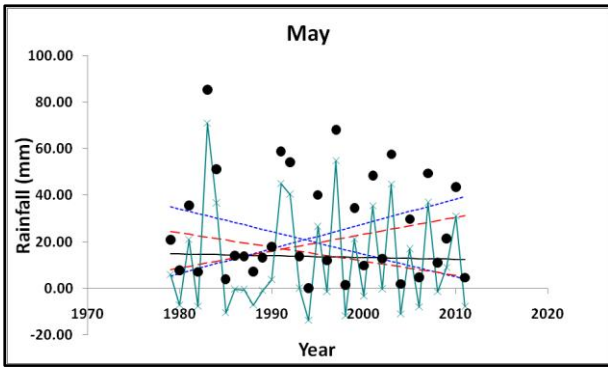
● Ouled Mimoun station





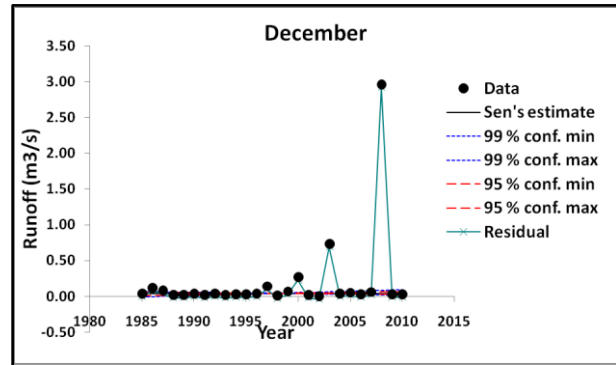
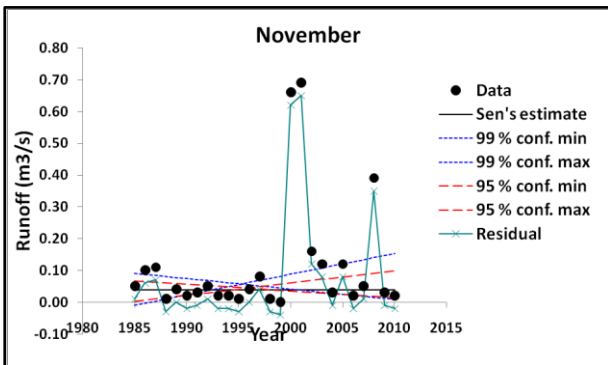
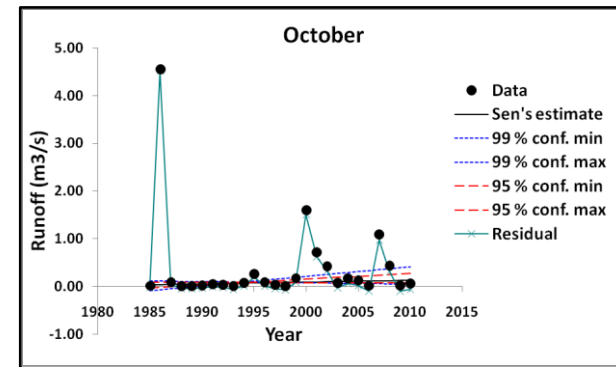
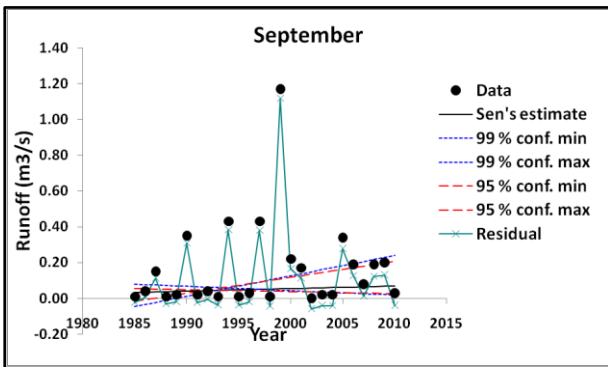
- Sidi Bounakhla

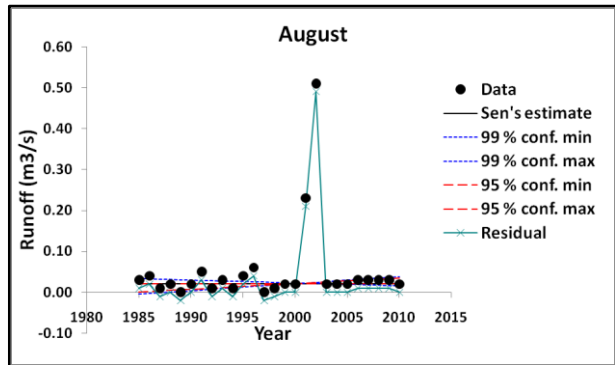
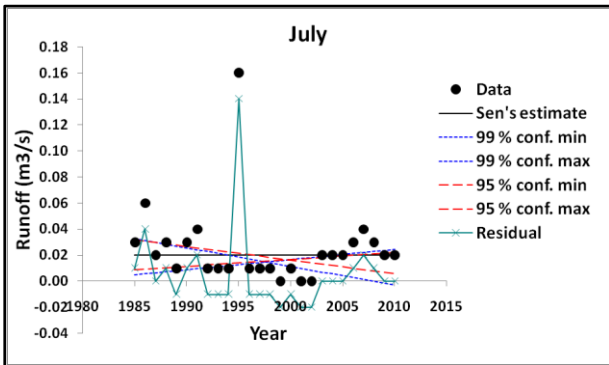
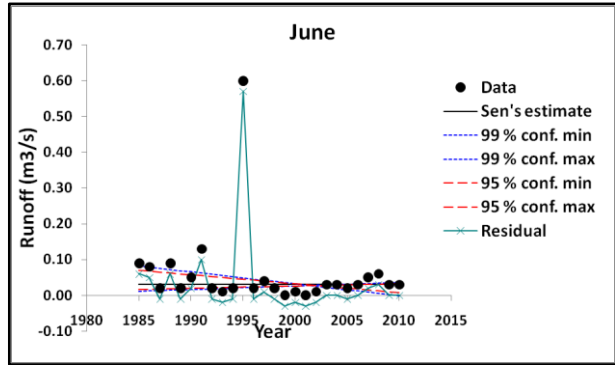
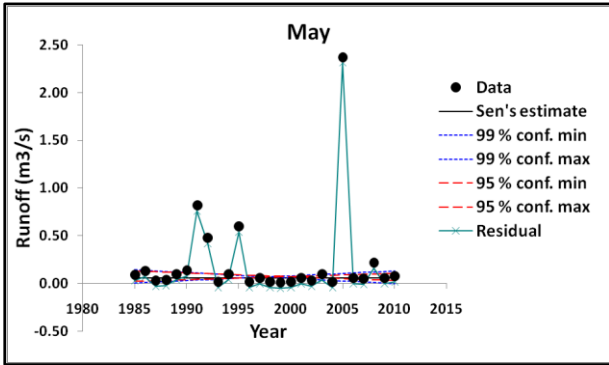
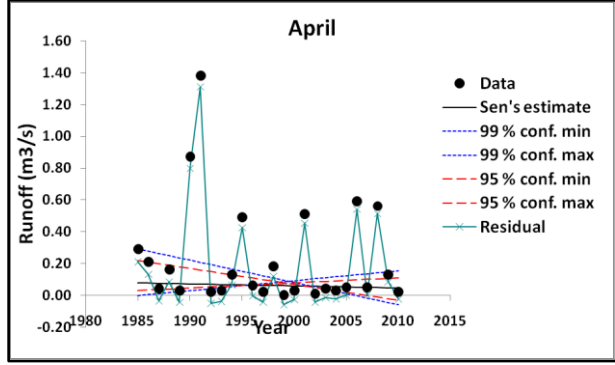
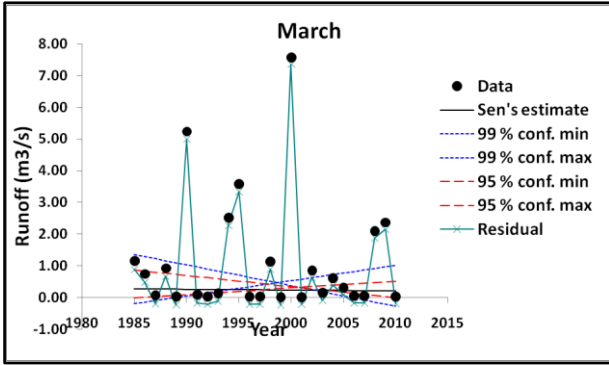
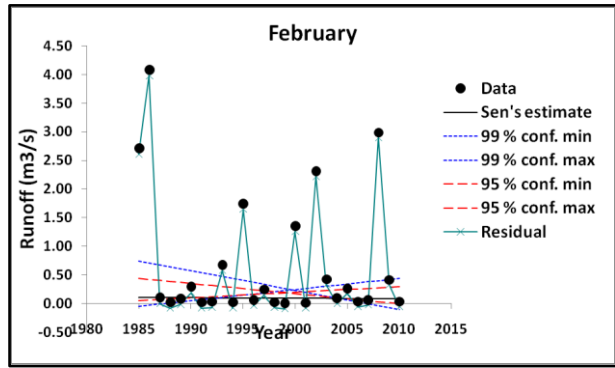
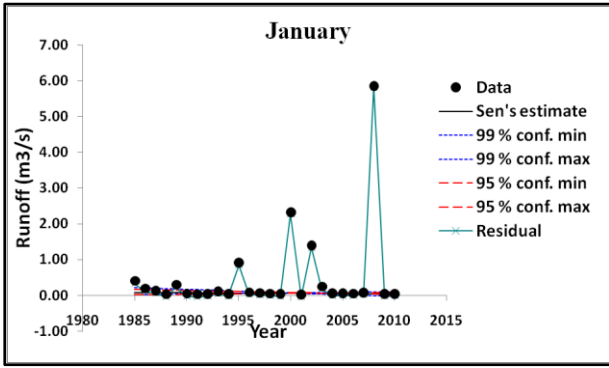




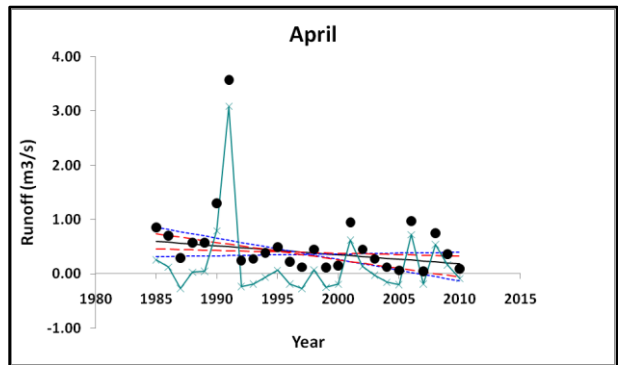
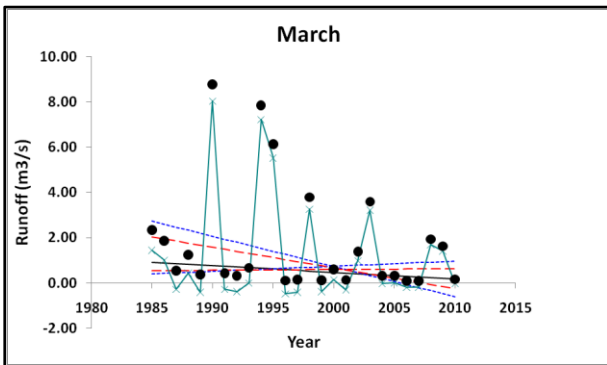
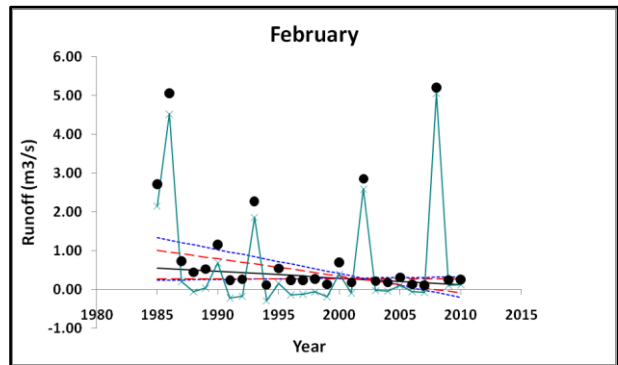
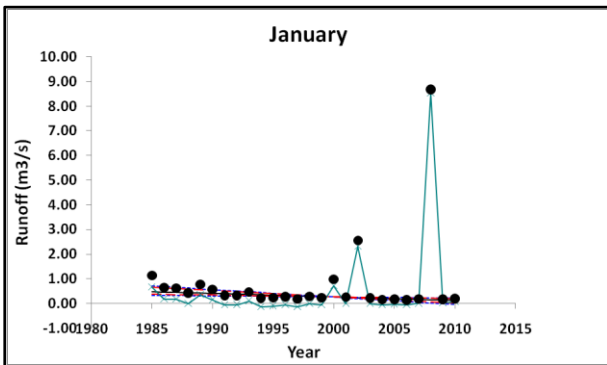
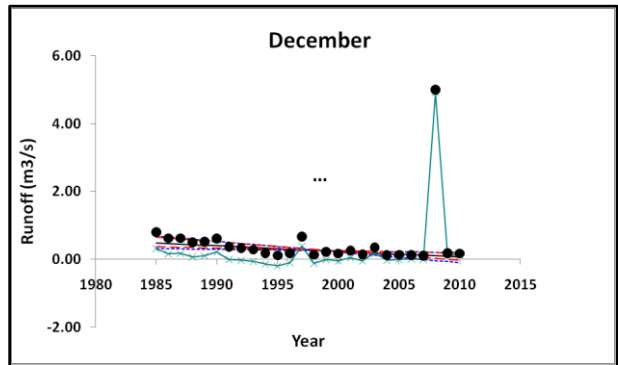
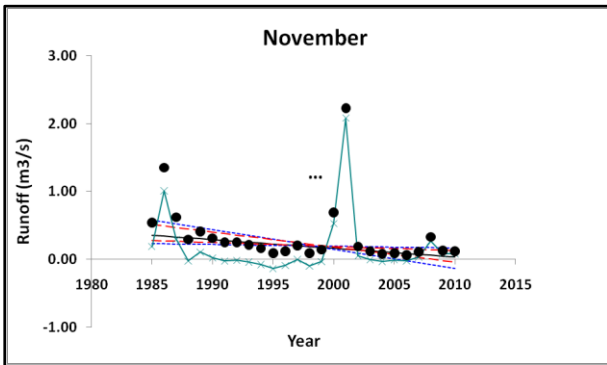
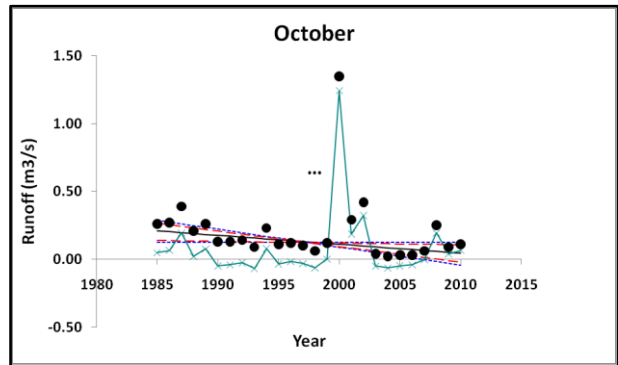
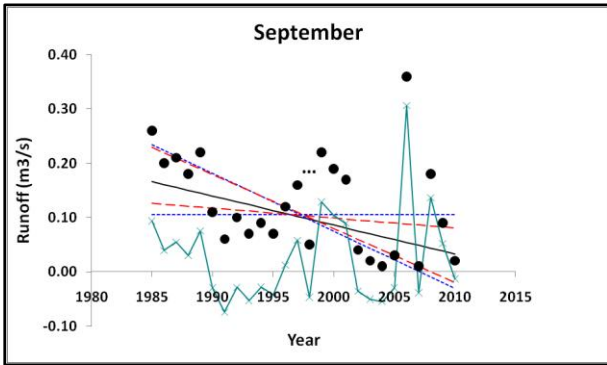
Appendix .3. Sen's Slope trend analysis for monthly runoff

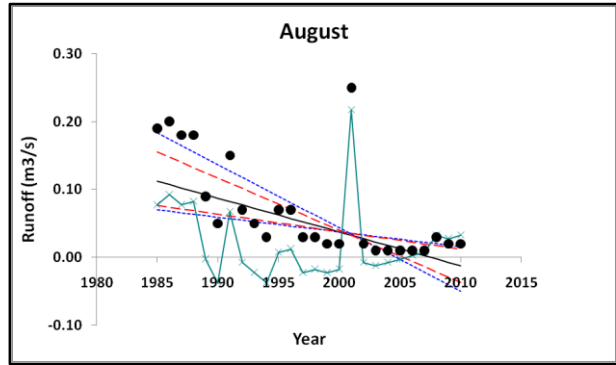
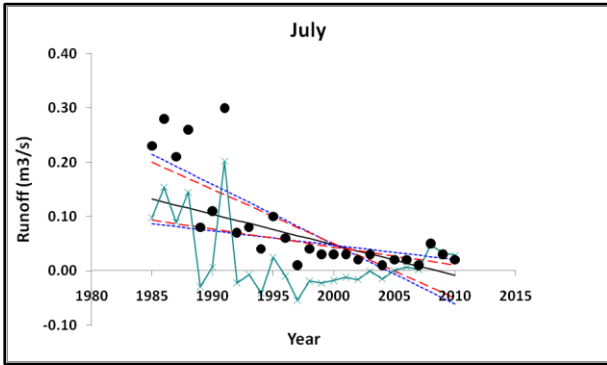
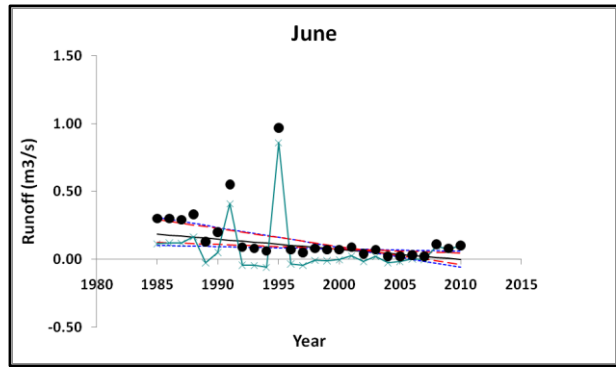
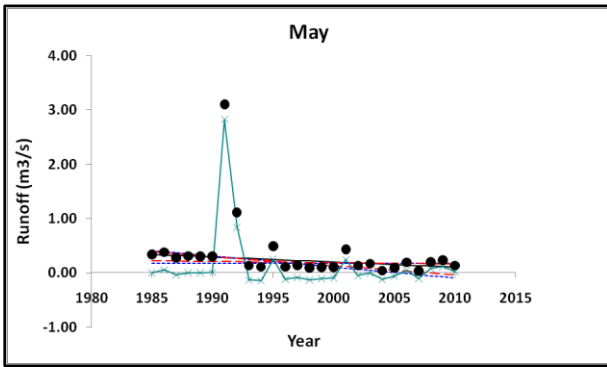
- Seb dou station



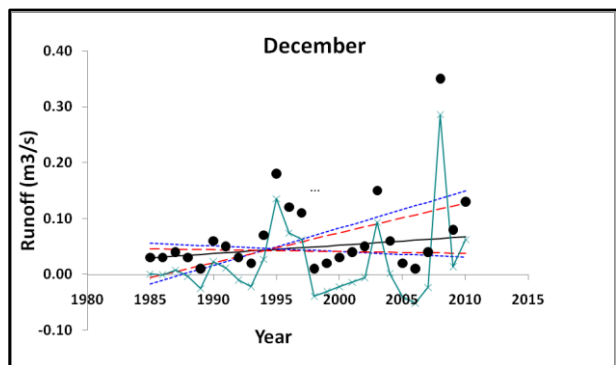
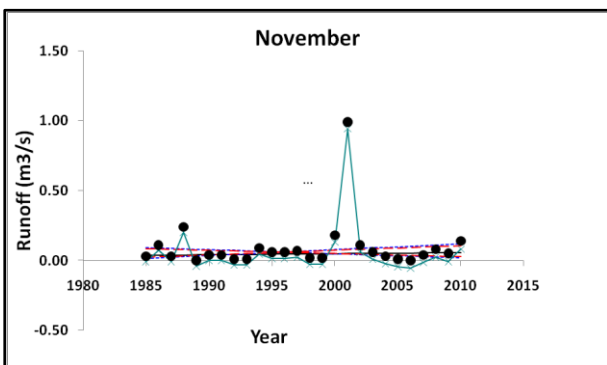
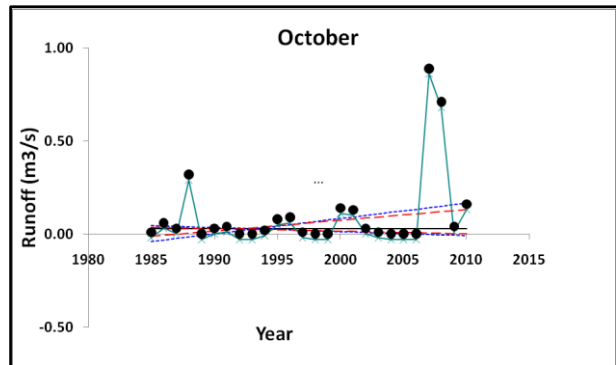
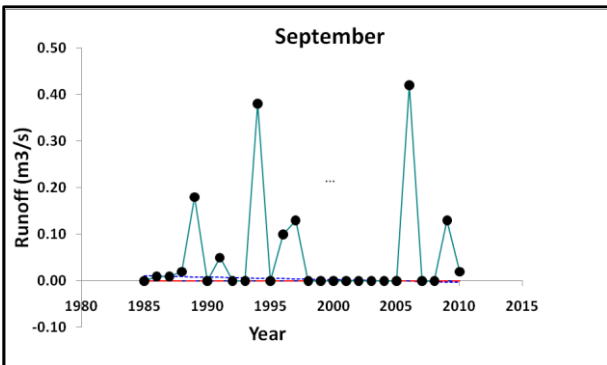


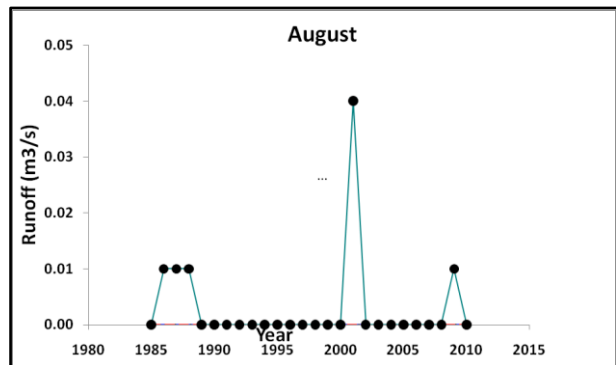
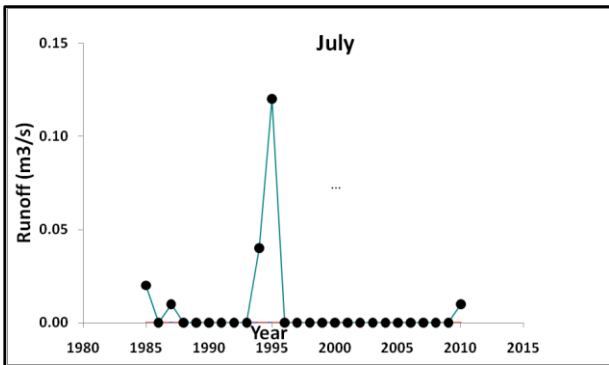
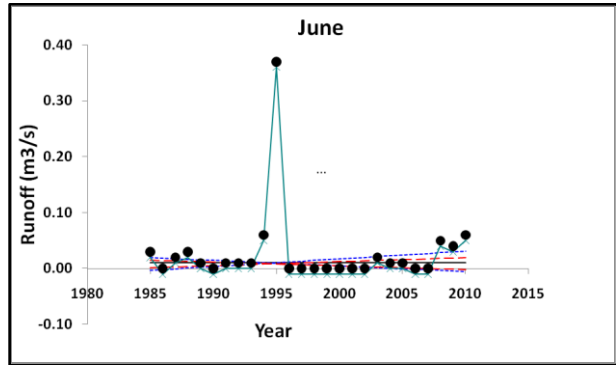
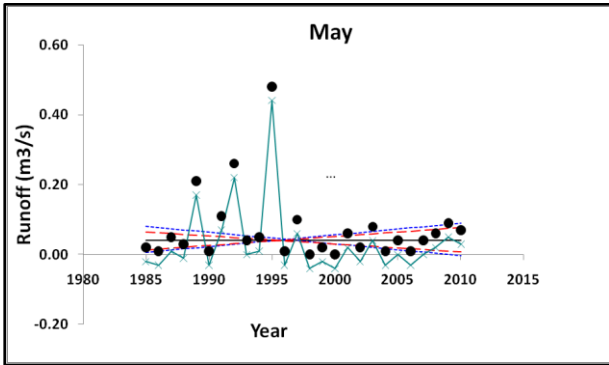
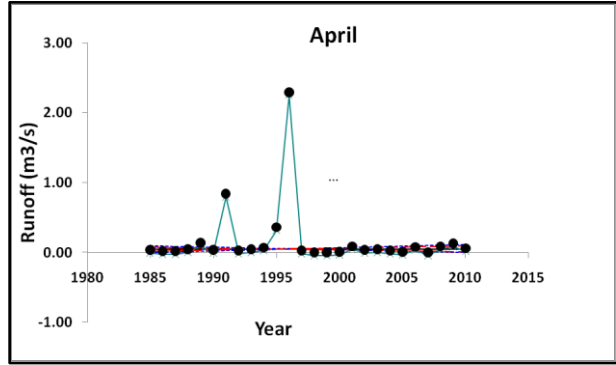
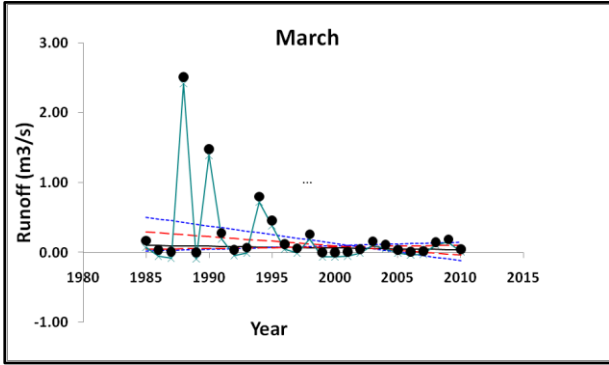
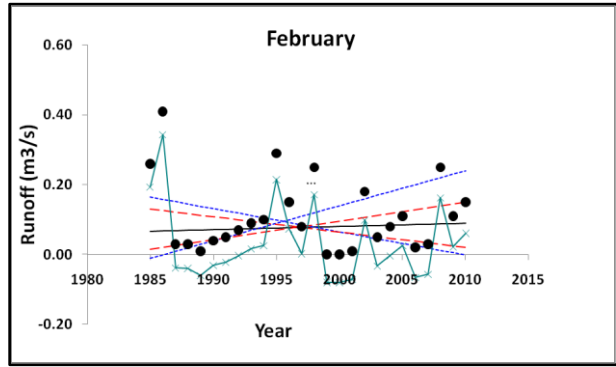
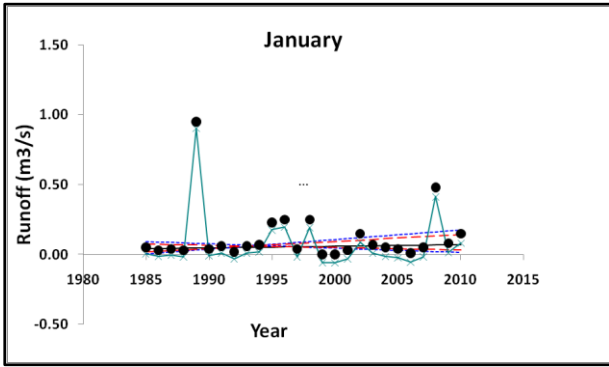
- Zahra station



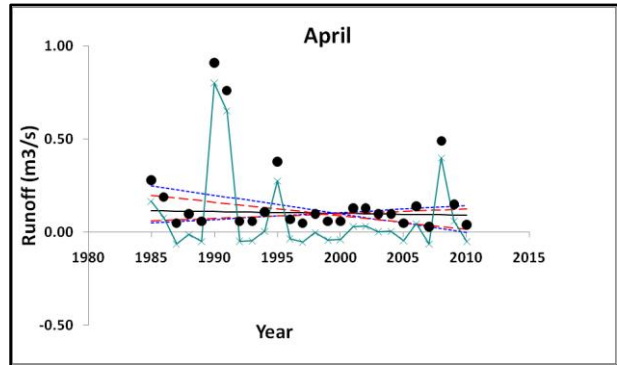
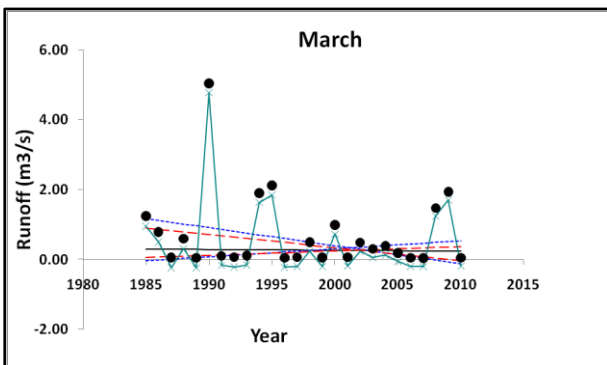
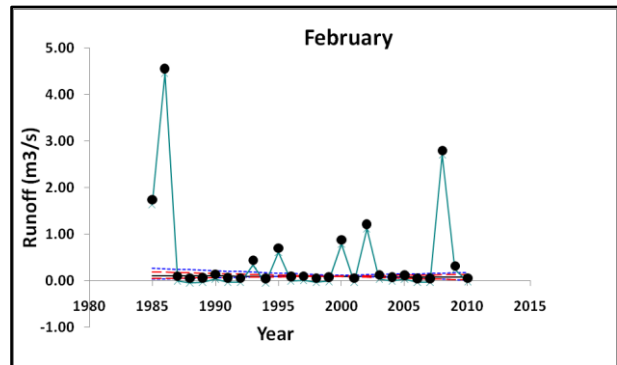
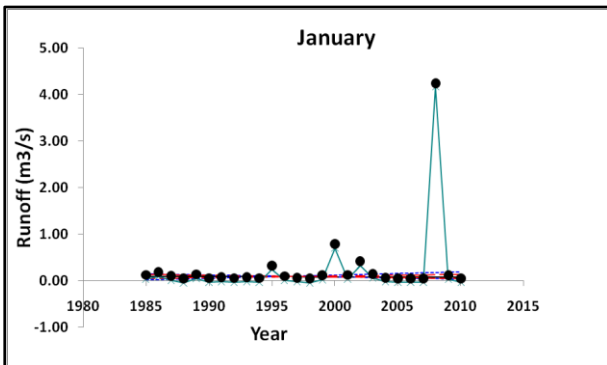
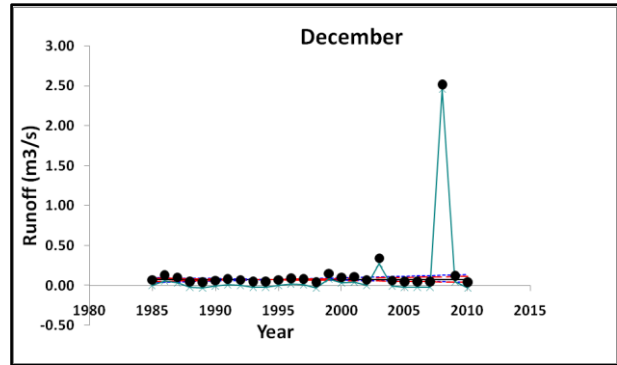
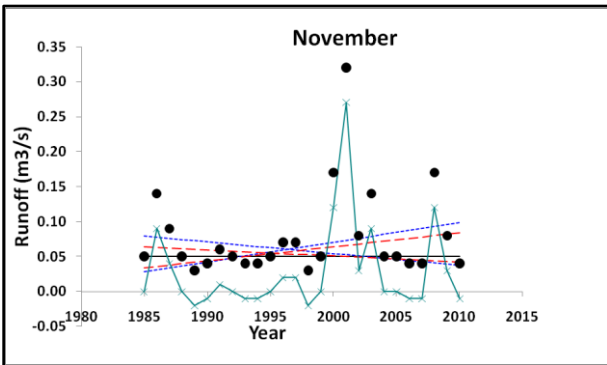
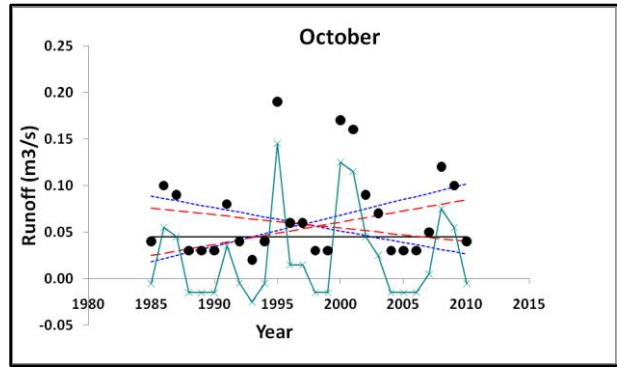
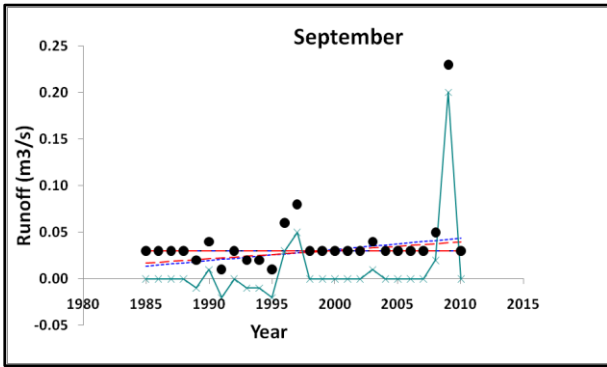


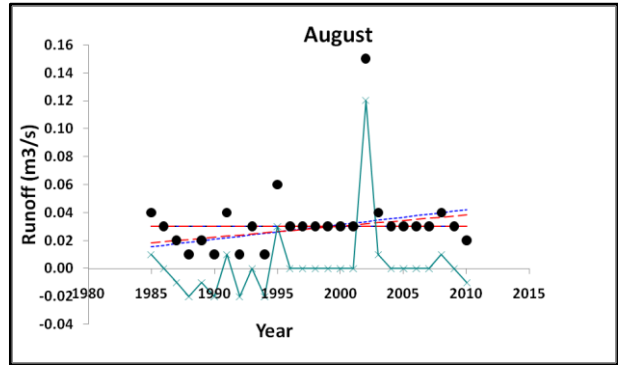
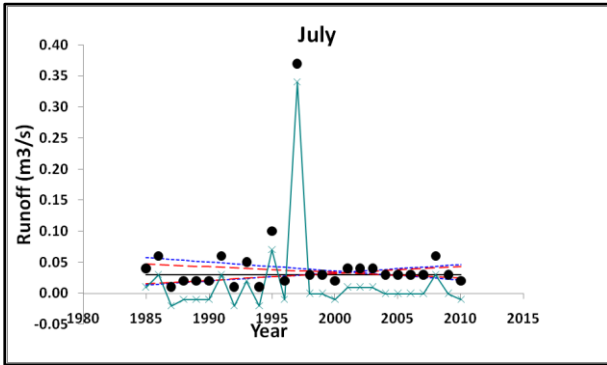
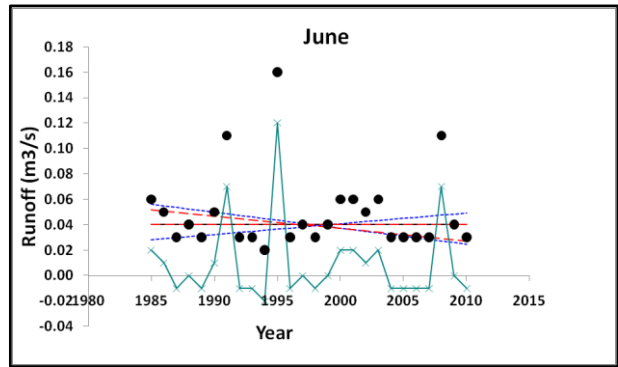
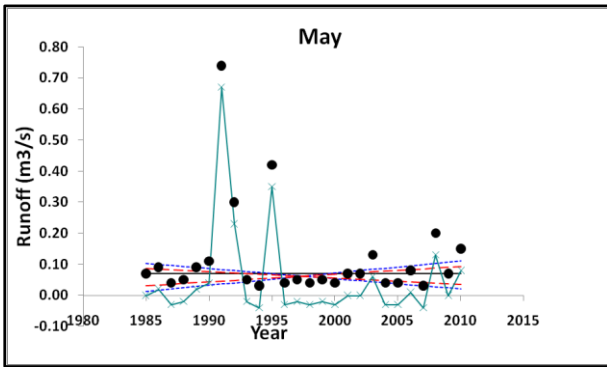
● Zenata station



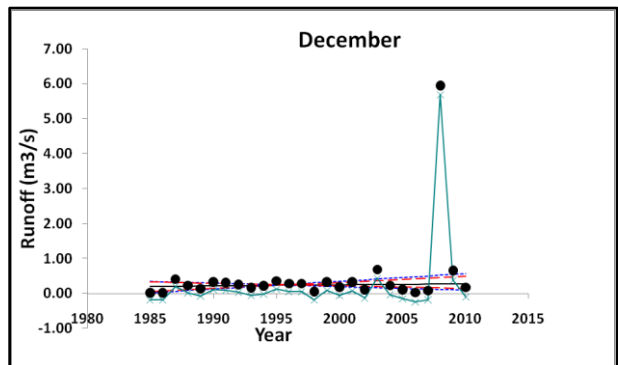
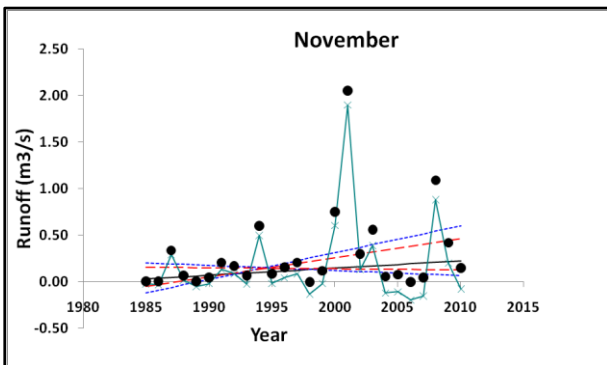
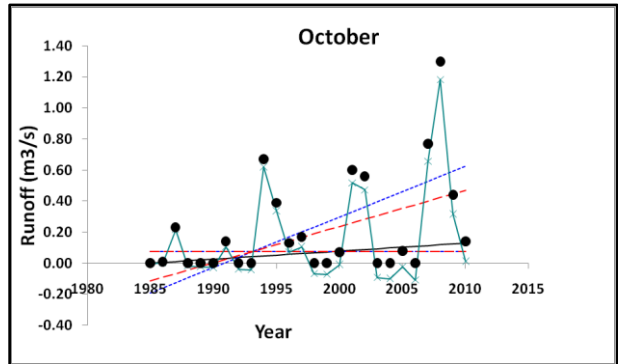
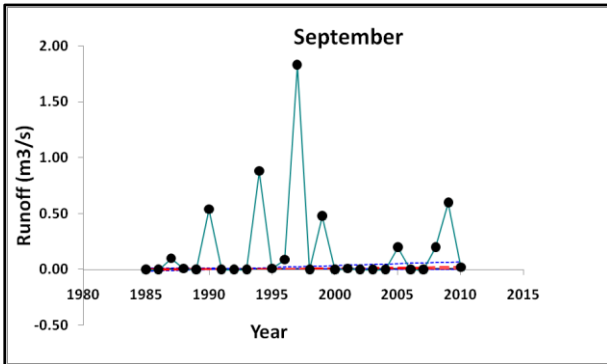


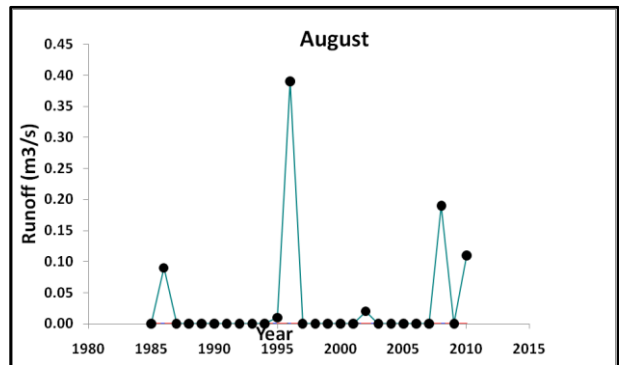
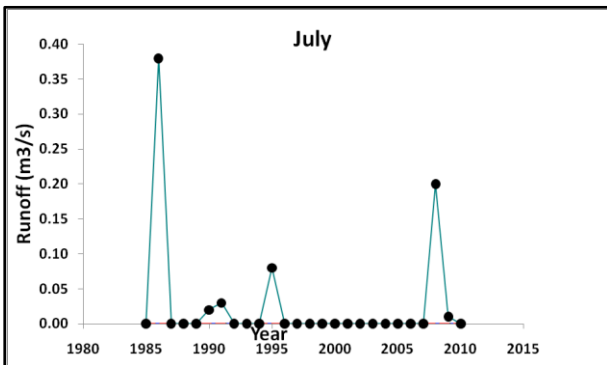
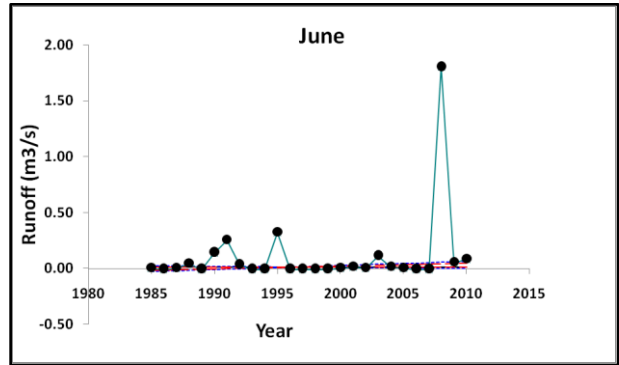
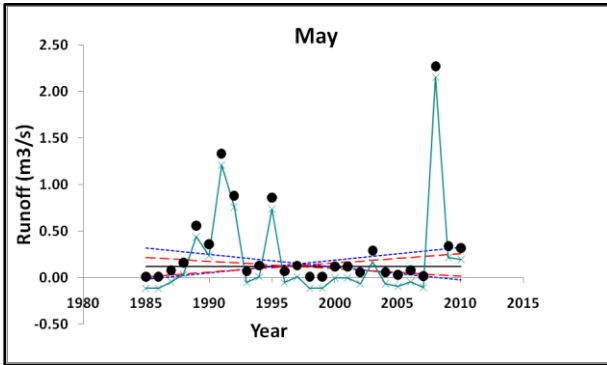
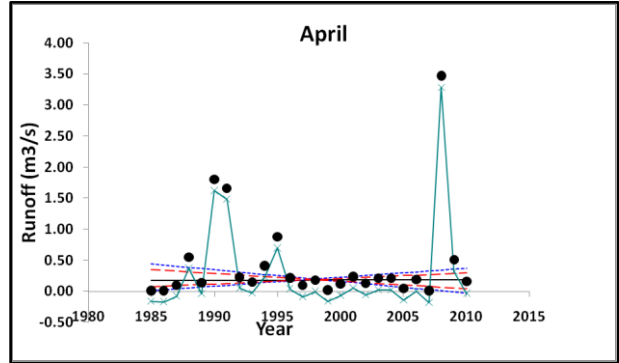
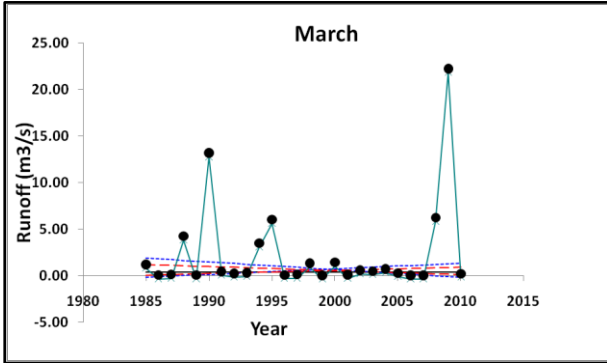
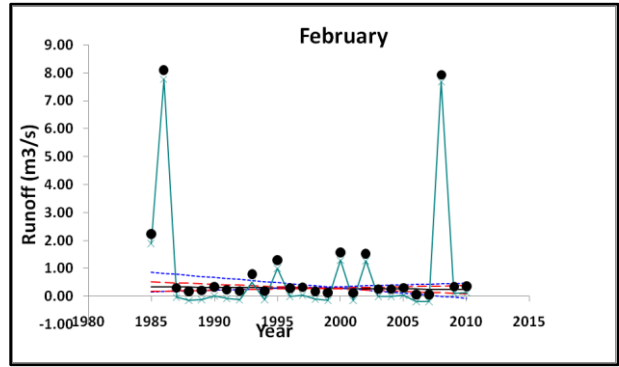
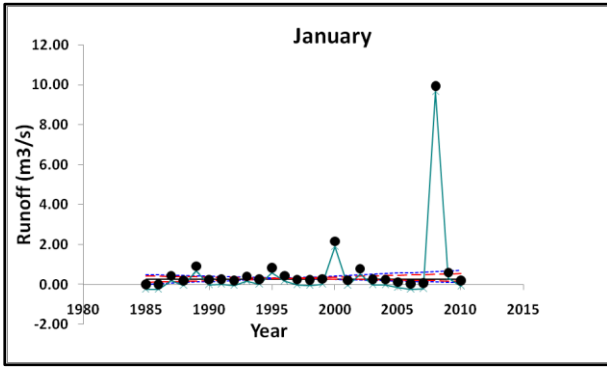
- Chouly station





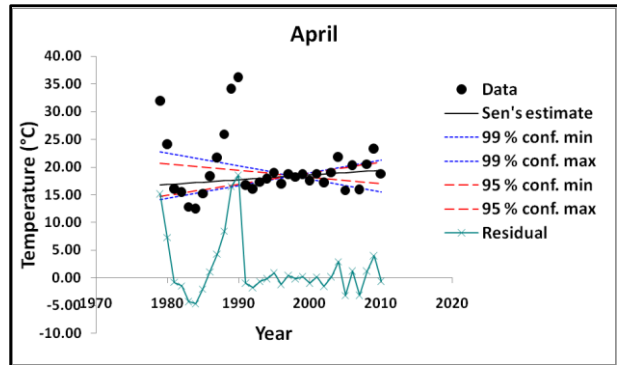
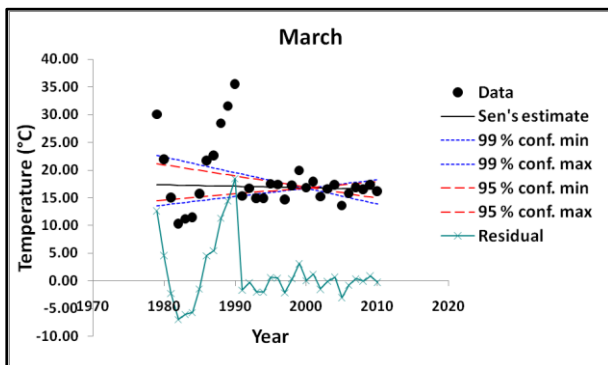
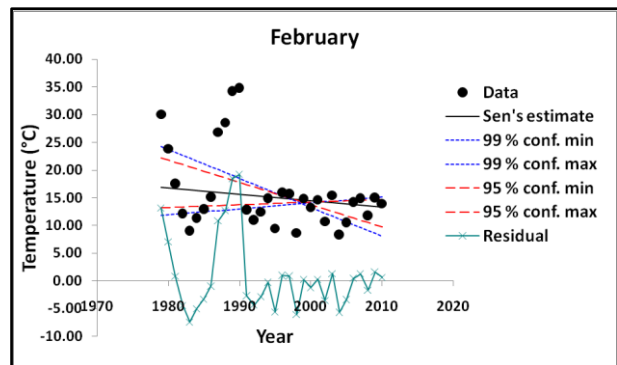
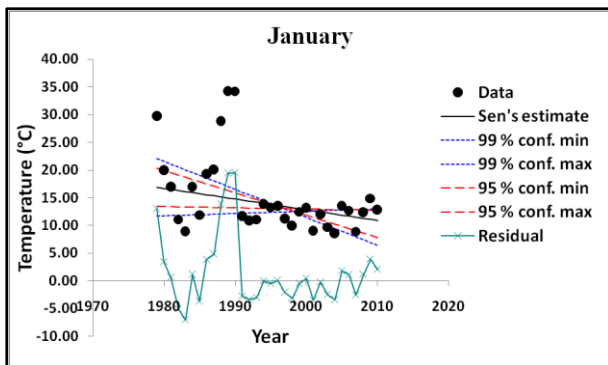
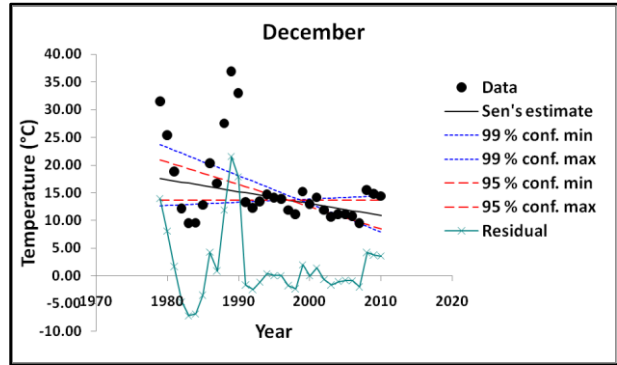
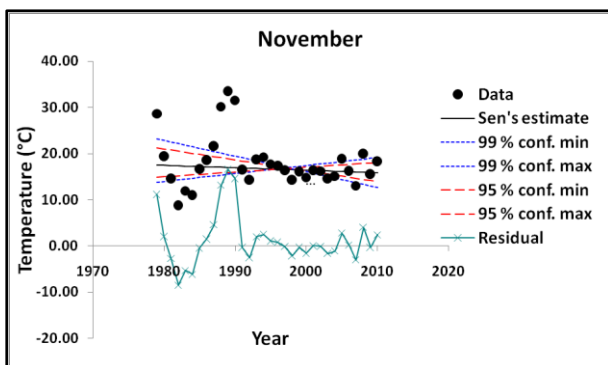
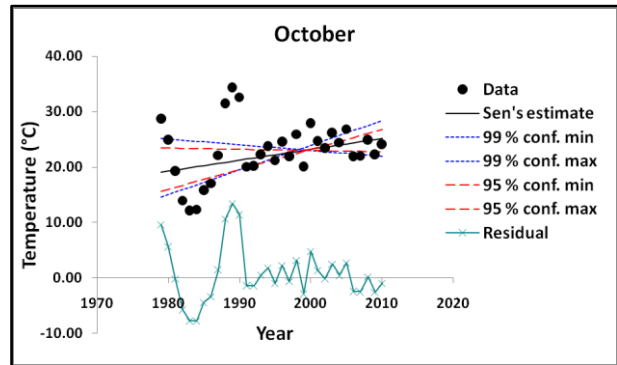
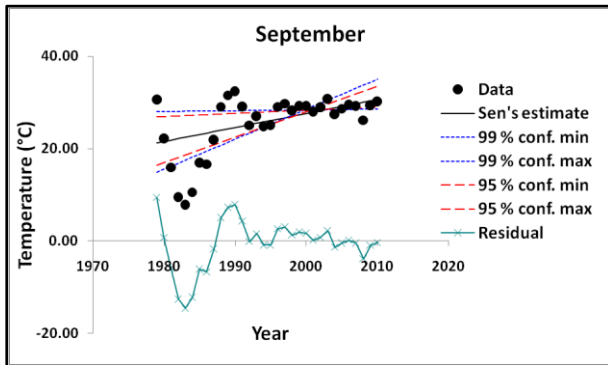
● Sidi Aissa station

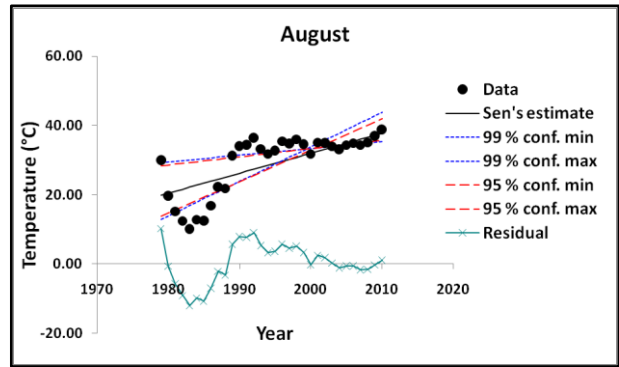
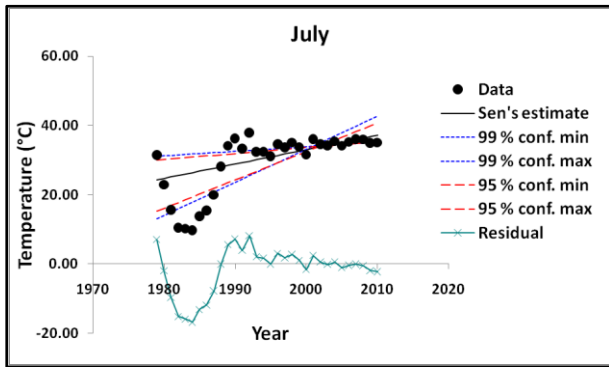
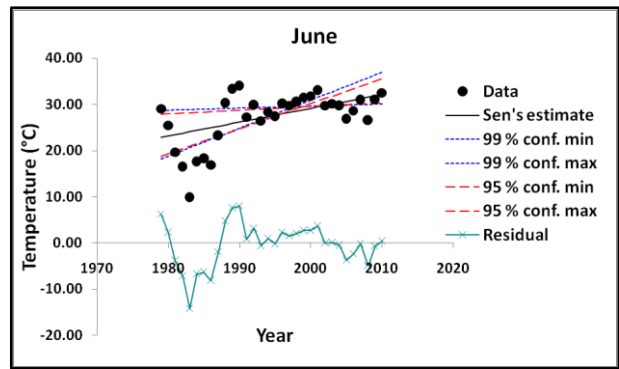
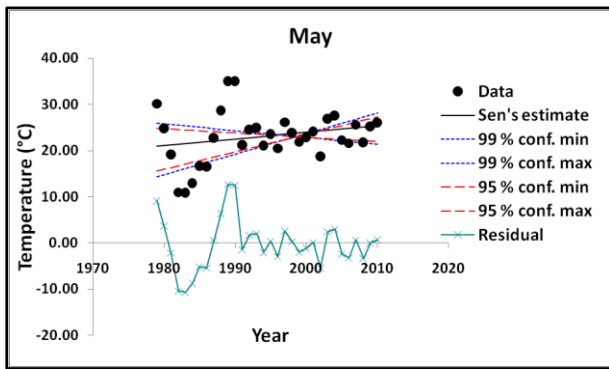




Appendix .4. Sen's Slope trend analysis for monthly temperature

- Beni Bahdel station





• Zenata station

